

Durham E-Theses

Phylogeography and Population Structure in Highly Mobile Marine Taxa in the Western Indian Ocean: Bottlenose Dolphins (Tursiops spp.) and Common Dolphins (Delphinus sp.)

GRAY, HOWARD,WILLEM,IAN

How to cite:

GRAY, HOWARD,WILLEM,IAN (2016) *Phylogeography and Population Structure in Highly Mobile Marine Taxa in the Western Indian Ocean: Bottlenose Dolphins (Tursiops spp.) and Common Dolphins (Delphinus sp.)*, Durham theses, Durham University. Available at Durham E-Theses Online: <http://etheses.dur.ac.uk/11542/>

Use policy

The full-text may be used and/or reproduced, and given to third parties in any format or medium, without prior permission or charge, for personal research or study, educational, or not-for-profit purposes provided that:

- a full bibliographic reference is made to the original source
- a [link](#) is made to the metadata record in Durham E-Theses
- the full-text is not changed in any way

The full-text must not be sold in any format or medium without the formal permission of the copyright holders.

Please consult the [full Durham E-Theses policy](#) for further details.

Academic Support Office, Durham University, University Office, Old Elvet, Durham DH1 3HP
e-mail: e-theses.admin@dur.ac.uk Tel: +44 0191 334 6107
<http://etheses.dur.ac.uk>

**Phylogeography and Population
Structure in Highly Mobile Marine
Taxa in the Western Indian Ocean:
Bottlenose Dolphins (*Tursiops* spp.)
and Common Dolphins (*Delphinus* sp.)**

Howard Willem Ian Gray

A thesis presented for the degree of
Doctor of Philosophy



School of Biological and Biomedical Sciences

University of Durham

2015

Abstract

In the marine environment, where barriers to dispersal are limited, taxa normally exhibit genetic homogeneity across large spatial scales. Extraordinarily, marine mammals regularly exhibit genetic differentiation within their cruising range. Furthermore, recent radiation in Delphininae has resulted in several closely related species that remain taxonomically unresolved, particularly bottlenose dolphins (BND) *Tursiops* spp. and common dolphins (CD) *Delphinus* spp., making these taxa interesting for studying evolutionary processes.

Using mitogenomes and a multi-locus dataset, BNDs from the northwest Indian Ocean (IO) were compared with other recognized species/eco-types around the world. A new (third) lineage of Indo-Pacific BND, *T. aduncus*, was identified from the region. Reconstructions of ancestral biogeography and divergence date estimates, suggest a divergence mechanism within *T. aduncus* that coincides with climate change over the Pleistocene. Reconstructions of ancestral morphology suggest a coastal ancestry for BNDs.

Significant population structure was exhibited between *T. aduncus* populations in the western IO based on mtDNA control region sequences and 14 microsatellite loci. Genetic subdivision appears to correlate with habitat heterogeneity across the study area, which may be driving differentiation through local adaptation.

Traditional and geometric morphometric techniques were used to investigate congruency between genetic and phenotypic differentiation of three BND lineages in the northwest IO. Strong differences were exhibited in morphology between common BNDs, *T. truncatus*, and *T. aduncus*. The *T. aduncus* lineages were similar, however significant differences in morphology were evident.

Significant genetic structure was evident between CD populations off Portugal, South Africa and Oman, based on mtDNA sequences and 14 microsatellites. Further analyses support the taxonomic designation of *D. capensis tropicalis* in the northwest IO.

Both genera exhibit significant population structure over spatial scales outdistanced by their dispersal abilities. Contemporary and historic environmental heterogeneity are suggested as drivers for this structure. Further evidence is provided for the northwest/northern IO as a region of evolutionary endemism, which will inform regional conservation initiatives.

Table of Contents

Abstract	ii
Declaration	xii
Acknowledgements	xiii
Chapter 1. General Introduction	2
1.1 Speciation and Population Differentiation.	2
1.2 Cetaceans as Candidates for the Study of Speciation and Population Structure	5
1.3 Environmental Heterogeneity in the Western and Northwestern Indian Ocean	7
1.3.1 Contemporary Oceanography of the Indian Ocean	7
1.3.2 Pleistocene Oceanography in the Indian Ocean	14
1.4 Cetaceans in the Northwest Indian Ocean and Conservation Concern	15
1.5 Bottlenose Dolphins.	18
1.5.1 Taxonomy.	19
1.5.2 Indo-Pacific Bottlenose Dolphins, <i>T. aduncus</i>	20
1.5.3 Common Bottlenose Dolphins <i>T. truncatus</i>	22
1.6 Common Dolphins	23
1.6.1 Taxonomy.	23
1.6.2 Common Dolphin Conservation Status, Distribution, Habitat and Ecology	24
1.7 Assessment of Taxonomy and Population Differentiation	26
1.7.1 Morphological Analysis of Population Structure.	26
1.7.2 Molecular Analysis of Population Structure	27
1.8 Rationale	28
1.9 Principal Hypotheses	30
1.9.1 Chapter 2 Phylogeography of Bottlenose Dolphins (<i>Tursiops</i> spp.) in the Northwest Indian Ocean: Evidence for a Cryptic Lineage.	30
1.9.2 Chapter 3 Population Structure of Bottlenose Dolphins (<i>Tursiops</i> spp.) in the Western Indian Ocean.	31
1.9.3 Chapter 4 Comparative Cranial Morphology of Three Bottlenose Dolphin Lineages, (<i>Tursiops</i> spp.), in the Northwest Indian Ocean Utilising Traditional and Geometric Morphometric Techniques.	31
1.9.4 Chapter 5 Population Structure of Common Dolphins (<i>Delphinus</i> spp.): Novel Insights from the Northwest Indian Ocean	32
1.9.5 Synopsis.	33

Chapter 2. Phylogeography of Bottlenose Dolphins (<i>Tursiops</i> spp.) in the North-west Indian Ocean: Evidence for a Cryptic Lineage.	34
2.1 Introduction.	34
2.2 Materials and Methods	38
2.2.1 Sample Acquisition	38
2.2.2 Biopsy Sampling, Oman	39
2.2.3 DNA Extraction	41
2.2.4 Mitogenome Sequencing and Assembly.	42
2.2.5 Library Preparation	42
2.2.6 Target Enrichment	44
2.2.7 Pooling and Sequencing.	44
2.2.8 Mitogenome Assembly	44
2.2.9 Amplification of mtDNA Markers	45
2.2.10 Amplification of nuDNA Markers	45
2.2.11 Estimation of Phylogeny	48
2.2.12 Reconstruction of Ancestral Distributions.	49
2.2.13 Estimation of Divergence Dates using Mitogenomic Data	50
2.2.14 Estimation of Ancestral Cranial Morphology	52
2.3 Results.	57
2.3.1 Estimation of Phylogeny	57
2.3.2 Estimation of Ancestral Distributions.	65
2.3.3 Estimation of Divergence Dates using Mitogenomic Data	68
2.3.4 Estimation of Ancestral Cranial Morphology	71
2.4 Discussion.	92
2.4.1 Phylogeography	93
2.4.2 Pattern of Divergence	94
2.4.3 Ancestral Reconstruction of Morphological Traits.	98
2.4.4 Limitations	99
2.4.5 Conclusion	101
Chapter 3. Population Structure of Bottlenose Dolphins (<i>Tursiops</i> spp.) in the Western Indian Ocean	103
3.1 Introduction.	103
3.2 Materials and Methods	109
3.2.1 Sample Acquisition	109
3.2.2 Biopsy Sampling, Oman	112
3.2.3 Bone Sampling	112

3.2.4	DNA Extraction from Tissue	112
3.2.5	DNA Extraction from Bone.	113
3.2.6	Microsatellite Analysis.	113
3.2.7	Mitochondrial DNA Analysis	120
3.2.8	Estimates of Population Divergence Times	121
3.2.9	Inference of Demographic History in the Western Indian Ocean	122
3.3	Results.	125
3.3.1	Microsatellites.	125
3.3.2	Mitochondrial DNA	143
3.3.3	Inference of Demographic History in the Western Indian Ocean	154
3.4	Discussion.	157
3.4.1	Phylogeography	157
3.4.2	Demographic History in the Western Indian Ocean	159
3.4.3	Population Structure	161
3.4.4	Migration Patterns, Identification of Migrants and Introgression	164
3.4.5	Consideration for an Isolating Mechanism in the Northwest Indian Ocean.	166
3.4.6	Implications for Management, Taxonomy and Future Research	167
Chapter 4. Comparative Cranial Morphology of Three Bottlenose Dolphin Lineages (<i>Tursiops</i> spp.) in the Northwest Indian Ocean Utilising Traditional and Geometric Morphometric Techniques		169
4.1	Introduction.	169
4.2	Materials and Methods	174
4.2.1	Specimen Acquisition	174
4.2.2	Lineage Assignment.	174
4.2.3	Assessment of Maturity	176
4.2.4	Traditional (Linear) Morphometric Analyses	176
4.2.5	Geometric Morphometric Analyses	184
4.3	Results.	191
4.3.1	Lineage Assignment.	191
4.3.2	Assessment of Maturity	191
4.3.3	Cranial Morphometrics	191
4.3.4	Geometric Morphometrics	221
4.4	Discussion.	241
4.4.1	Morphological differences between <i>T. truncatus</i> and <i>T. aduncus</i>	242
4.4.2	Morphological differences between <i>T. aduncus</i> (Hol-Ta) and <i>T. aduncus</i> (AS-Ta)	244

4.4.3	Comparison of Methodologies	246
4.4.4	Distribution of Samples and Evidence for Hybridization/Introgression	247
Chapter 5. Population Structure of Common Dolphins (<i>Delphinus</i> spp.): Novel Insights from the Northwest Indian Ocean		249
5.1	Introduction.	249
5.2	Materials and Methods	252
5.2.1	Sample Acquisition and DNA extraction	252
5.2.2	Microsatellite Loci	254
5.2.3	Mitochondrial DNA	256
5.3	Results.	257
5.3.1	Microsatellite Loci	257
5.3.2	Mitochondrial DNA	264
5.4	Discussion.	270
5.4.1	Population Structure	271
5.4.2	Demographic Expansion, Population Divergence and Genetic Diversity	274
5.4.3	Contemporary Gene Flow	275
5.4.4	Conclusions.	278
Chapter 6. General Discussion.		280
6.1	Summary of Key Findings.	280
6.2	A Case for the Conservation of Coastal Cetaceans in the Northwest Indian Ocean	281
6.3	Implications for Bottlenose Dolphin Taxonomy and Management	283
6.3.1	Contributions to the Resolution of Bottlenose Dolphin Taxonomy	283
6.3.2	Evidence for Hybridisation and Introgression Between <i>T. aduncus</i> Lineages.	286
6.3.3	Identification of Management Units	287
6.3.4	Estimates of Effective Population Size and Genetic Diversity	287
6.3.5	Population Dynamics	288
6.3.6	Identification of Migrants and Gene Flow.	288
6.4	Implications for Common Dolphin Taxonomy and Management.	289
6.4.1	Management Units, Genetic Diversity, Population Dynamics and Gene Flow	289
6.5	Towards the Study of Evolutionary Processes	290
6.6	Evolutionary History of Bottlenose Dolphins in the Northwest/Western Indian Ocean	290

6.6.1	Phylogeography and Evolutionary History	290
6.6.2	A Putative Barrier to Dolphin Dispersal in the Northwest Indian Ocean	292
6.6.3	A Putative Barrier to Dolphin Dispersal Across the Indo-Pacific Boundary	293
6.7	The Regional Context	294
6.8	Differentiation in Bottlenose and Common Dolphins: A Comparison . .	295
6.9	Recommendations for Further Research	297
6.10	Conclusions	298
	Appendices	300
	References	325

List of Figures

Figure 1	Seasonal mean values for major surface currents during the boreal winter (Dec-Feb), spring (Mar-May), summer (Jun-Aug) and autumn (Sept-Nov) months (1993-2010).	9
Figure 2	The East African coastline and the western Indian Ocean.	10
Figure 3	The coastlines of the Arabian Peninsula, Pakistan and India in the the northwest Indian Ocean	13
Figure 4	Bottlenose dolphin (<i>Tursiops</i> spp.) sample locations	41
Figure 5	Illustration of mitogenome (a) and partial mitogenome (b) used in the present study	46
Figure 6	Bayesian majority-rule consensus phylogeny estimated from the mitogenome dataset	60
Figure 7	Bayesian estimated phylogeny generated from concatenated mtDNA-nuDNA sequences	61
Figure 8	Maximum Likelihood phylogeny inferred from the mitogenome dataset.	62
Figure 9	Maximum Likelihood phylogeny inferred from the concatenated mtDNA/nuDNA datasety	63
Figure 10	Maximum parsimony tree and partitioned Bremer support indices for different loci	64
Figure 11	Statistical Dispersal Vicariance Analysis (S-DIVA) and b) Bayesian Binary MCMC Analysis (BBM) for mitogenome dataset	66
Figure 12	Statistical Dispersal Vicariance Analysis (S-DIVA) and b) Bayesian Binary MCMC Analysis (BBM) for the mtDNA/nuDNA dataset.	67
Figure 13	Estimation of divergence dates using the mitogenome dataset	69
Figure 14	Maximum parsimony estimation of GLPTF relative to CBL length (%) using the mitogenome phylogeny	78
Figure 15	Maximum parsimony estimation of RL relative to CBL length (%) using the mitogenome phylogeny	79
Figure 16	Maximum parsimony estimation of ZW relative to CBL length (%) using the mitogenome phylogeny	80
Figure 17	Maximum parsimony estimation of GLPTF relative to CBL length (%) for the concatenated mtDNA-nuDNA dataset.	81
Figure 18	Maximum parsimony estimation of RL relative to CBL length (%) for the concatenated mtDNA-nuDNA dataset	82
Figure 19	Maximum parsimony estimation of ZW relative to CBL length (%) for the concatenated mtDNA-nuDNA dataset	83

Figure 20	Trait values relative to condylobasal length (CBL); rostral width at mid-length (RWM), zygomatic width (ZW) and tip of rostrum to external nares (TREN), plotted against time as estimated from the mitogenome phylogeny.	86
Figure 21	Trait values relative to condylobasal length (CBL); greatest length of left posttemporal fossa (GLPTF), greatest width of left posttemporal fossa (GWPTF) and mandible height (MH), plotted against time as estimated from the mitogenome phylogeny	87
Figure 22	Trait values relative to condylobasal length (CBL); length of upper left tooth row (UTLTR), length of lower left tooth row (LTRL) and rostral length (RL), plotted against time as estimated from the mitogenome phylogeny.	88
Figure 23	Trait values relative to condylobasal length (CBL); rostral width at mid-length (RWM), zygomatic width (ZW) and tip of rostrum to external nares (TREN), plotted against time as estimated from the concatenated mtDNA and nuDNA phylogeny	89
Figure 24	Trait values relative to condylobasal length (CBL); greatest length of left posttemporal fossa (GLPTF), greatest width of left posttemporal fossa (GWPTF) and mandible height (MH), plotted against time as estimated from the concatenated mtDNA and nuDNA phylogeny	90
Figure 25	Trait values relative to condylobasal length (CBL); length of upper left tooth row (UTLTR), length of lower left tooth row (LTRL) and rostral length (RL), plotted against time as estimated from the concatenated mtDNA and nuDNA phylogeny	91
Figure 26	Two proposed mechanisms; a and b, for divergence events within <i>T. aduncus</i>	96
Figure 27	General hypotheses to explain the demographic history, and associated isolating mechanisms, of contemporary populations of coastal bottlenose dolphins in the western and northern Indian Ocean	108
Figure 28	Locations of bottlenose dolphin (<i>Tursiops</i> spp.) samples utilised in this study	110
Figure 29	Demographic scenarios tested in DIYabc	124
Figure 30	FCA plots for 14 microsatellites	134
Figure 31	FCA plots for seven microsatellites	135
Figure 32	FCA plots utilising genotype data from 16 microsatellite loci from the South African populations (F1 vs F2)	136
Figure 33	Patterns of migration between populations in the Western Indian Ocean.	137
Figure 34	Probability assignment of individuals based on 14 microsatellite loci	139
Figure 35	Probability assignment of individuals based on 7 microsatellite loci	140

Figure 36	Ancestry posterior probabilities for each individual in the Oman, South Africa and Zanzibar populations using the 14 loci dataset	141
Figure 37	Ancestry posterior probabilities for each individual in the Oman, South Africa, Zanzibar and Indian/Pakistan populations using the seven loci dataset	142
Figure 38	Distributions and frequencies of sampled bottlenose dolphin lineages.	145
Figure 39	Bottlenose dolphin median-joining haplotype network	153
Figure 40	Logistic regression of posterior probabilities for each demographic scenario (1-3) against the number of simulated datasets	155
Figure 41	Map showing locations of bottlenose dolphin specimens	175
Figure 42	Morphological measurements taken	179
Figure 43	Positioning of landmarks on a bottlenose dolphin (<i>Tursiops aduncus</i>) skull.	186
Figure 44	Neighbour-joining phylogenetic tree	192
Figure 45	Within-cluster sum of squares for different numbers of clusters (k) using meristic characters	197
Figure 46	Group-wise plots of TTU frequencies (%) illustrating the overlap of tooth counts	198
Figure 47	Screeplot showing the variance explained by each PC from a PCA on the ONHM Dataset	199
Figure 48	PCA on ONHM Dataset	201
Figure 49	Within-cluster sum of squares for different numbers of clusters under the k -means cluster algorithm for the ONHM Dataset	202
Figure 50	Average silhouette widths, considering different numbers of clusters, using the k -medoids algorithm on the ONHM Dataset.	203
Figure 51	Silhouette plot for most optimal number of clusters ($k = 2$) for ONHM Dataset using the k -medoids clustering algorithm	204
Figure 52	Hierarchical cluster analysis using ONHM Dataset.	205
Figure 53	DFA for the ONHM Dataset.	206
Figure 54	DFA considering only the most important characters for the ONHM Dataset	208
Figure 55	PCA screeplot illustrating the contribution of each PC to the total variance for the Combined Dataset	210
Figure 56	PCA on the Combined Dataset	211
Figure 57	Within-cluster sum of squares for different numbers of clusters under the k -means cluster algorithm using the Combined Dataset	212

Figure 58	Average silhouette widths, considering different numbers of clusters (k), using the k -medoids algorithm on the Combined Dataset	213
Figure 59	Silhouette plot for most optimal number of clusters ($k = 2$) for the Combined Dataset using the k -medoids clustering algorithm	214
Figure 60	Hierarchical cluster analysis using Combined Dataset	215
Figure 61	DFA considering the Combined Dataset	216
Figure 62	DFA considering only the most important characters for the Combined Dataset	218
Figure 63	Plot of RW60 against ZW	220
Figure 64	PCA screeplots for dorsal, ventral and lateral aspect	223
Figure 65	PCA in Dorsal aspect.	226
Figure 66	PCA in Ventral aspect.	227
Figure 67	PCA in Lateral aspect	228
Figure 68	Visualisation of shape changes along extreme values (-0.1 and +0.1) of principal components 1 and 2 in dorsal ventral and lateral aspect . . .	229
Figure 69	Visual comparisons of average group shapes, AS-Ta, Hol-Ta and Tt, for all aspects.	231
Figure 70	CVA for Dorsal aspect	234
Figure 71	CVA for Ventral aspect	235
Figure 72	CVA for Lateral aspect	236
Figure 73	Dorsal aspect CVA Plot with superimposed phylogeny.	239
Figure 74	Ventral aspect CVA Plot with superimposed phylogeny.	240
Figure 75	Lateral aspect CVA Plot with superimposed phylogeny.	240
Figure 76	Example specimens of Ta-type (SMNS 45-720) from Pakistan and a Tt (ONHM 3524) from Oman in lateral (left) aspect	247
Figure 77	Locations of common dolphin (<i>Delphinus</i> spp.) samples utilised . . .	253
Figure 78	FCA plots for 14 microsatellites	263
Figure 79	Probability assignment of individuals based on 14 microsatellite loci .	264
Figure 80	Ancestry posterior probabilities for each individual in the Oman, South Africa and Portugal populations using 14 microsatellite loci	264
Figure 81	Common dolphin minimum spanning tree	269
Figure 82	The coastlines of the Arabian Peninsula, Iran, Pakistan and India . . .	285

List of Tables

Table 1	Bottlenose dolphin species and ecotypes considered in the present study	40
Table 2	Details of primers used to amplify the mtDNA and nuDNA markers .	47
Table 3	Priors used to estimate divergence dates	52
Table 4	Morphological characters common to all populations for use in ancestral reconstruction	54
Table 5	Population averages for morphological characters	55
Table 6	Partitioning schemes detailed for the different datasets for each analysis	58
Table 7	Posterior values for parameters estimated from different models carried out in BEAST.	70
Table 8	Model comparison using pairwise log Bayes Factors	71
Table 9	Ancestral character estimation (ACE) using the mitogenome phylogeny.	72
Table 10	Ancestral character estimation (ACE) using the concatenated mtDNA-nuDNA phylogeny.	75
Table 11	Summary of sample locations and numbers, N , used for a) microsatellite and b) mitochondrial DNA markers	111
Table 12	Overview of microsatellite markers amplified in this study.	117
Table 13	Prior and hyperprior values for analyses conducted in MSVAR	119
Table 14	Number of alleles and expected (exp.) and observed (obs.) heterozygosities (Het) for each locus within each population	130
Table 15	mtDNA (control region) and microsatellite diversity statistics for each putative population, considering 14 loci and 7 loci (in parentheses). .	132
Table 16	Pairwise F_{ST} values for all populations considering 14 microsatellite loci (below diagonal) and 7 microsatellite loci (above diagonal)	133
Table 17	Posterior mean estimates for migration rates	138
Table 18	Posterior probabilities for N_0 , N_1 and ta	143
Table 19	Haplotype frequencies for each bottlenose dolphin population	146
Table 20	P -values in pairwise comparisons of π (below diagonal) and h (above diagonal) using Welch's t -test	149
Table 21	Mitochondrial DNA F_{ST} values below diagonal and Φ_{ST} above the diagonal.	150
Table 22	Neutrality tests and mismatch distribution analysis	151

Table 23	Values for θ , M and T , estimated for Oman, Zanzibar and South Africa	152
Table 24	Prior and posterior distributions of parameters across all scenarios	156
Table 25	Descriptions of measured cranial characters and whether they were measured for ONHM and SMNS specimens	177
Table 26	Landmark descriptions and summary of associated statistics	187
Table 27	Summary of measurements (mm) and associated statistics for <i>Tursiops truncatus</i> , <i>T. aduncus</i> (holotype lineage) and <i>T. aduncus</i> (Arabian Sea lineage)	194
Table 28	Principal Component loadings for PCA on the ONHM Dataset	200
Table 29	Group standardised coefficients of linear discriminants for all characters in the ONHM Dataset	207
Table 30	Stepwise-selection of characters for the ONHM Dataset	208
Table 31	Cross-validation scores for ONHM Dataset	209
Table 32	Principal Component loadings for the Combined Dataset	209
Table 33	Group standardised coefficients of linear discriminants for the Combined Dataset	217
Table 34	Stepwise-selection of characters for the Combined Dataset	217
Table 35	Pairwise DFA group standardised coefficients of linear discriminants for most important characters	219
Table 36	Cross-validation scores for the Combined Dataset	220
Table 37	Dorsal Principal Component (PC) Coefficients for each Landmark (LM)	224
Table 38	Ventral Principal Component (PC) Coefficients for each Landmark (LM)	224
Table 39	Lateral Principal Component (PC) Coefficients for each Landmark (LM)	225
Table 40	CVA pair-wise Mahalanobis and Procrustes distances between groups	237
Table 41	Discriminant Function Analysis pairwise Mahalanobis and Procrustes distances between groups for dorsal, ventral and lateral aspect	237
Table 42	DFA pairwise group allocation table and cross-validation scores for dorsal, ventral and lateral aspect	238
Table 43	Numbers of samples used for each population in analyses using (a) microsatellites and (b) mitochondrial DNA respectively	254
Table 44	Number of alleles and expected and observed heterozygosities for each locus within each population	260
Table 45	Mitochondrial DNA (control region) and microsatellite diversity statis-	

	tics for each putative population, considering 14 loci	262
Table 46	Pairwise F_{ST} values for all populations considering 14 microsatellite loci	263
Table 47	Posterior mean estimates for migration rates	263
Table 48	P -values in pairwise comparisons of π (below diagonal) and h (above diagonal) using Welch's t -test	266
Table 49	Mitochondrial DNA F_{ST} values below diagonal and Φ_{ST} above the diagonal	267
Table 50	Tajima's D and Fu's F_s values	268
Table 51	Values for θ , M and T	270

List of Appendices

Appendix I	GenBank accession numbers for bottlenose dolphin sequences used	300
Appendix II	Bayesian phylogeny from mitochondrial markers only (i.e. no nuclear markers)	306
Appendix III	List of bottlenose dolphin specimens.	307
Appendix IV	Haplotype frequencies for each common dolphin population.	314
Appendix V	Common dolphin median-joining network	324

Declaration

The work presented in this thesis has not been previously submitted for a degree at Durham University or any other institution. The author has conducted all original work unless stated otherwise in the acknowledgements or the main text.

Copyright © 2015 Howard Gray

The copyright of this thesis rests with the author. No quotation from it should be published without the author's prior written consent and information derived from it should be acknowledged.

Acknowledgements

Six years worth of work is now drawing to a close. As you might imagine, there are many people to thank who have helped me along the way.

My Supervisor

First of all, I would like to thank my supervisor, Rus Hoelzel, who took a risk on this project, and on me. The funding was hairy, to say the least, and the samples were difficult to work with. On top of this, my experience working with genetics was quite limited, so I am grateful to Rus for giving me the opportunity to conduct the research I wanted to do.

Provision of Samples and Materials

For samples, and access to skeletal specimens, there are several individuals and institutions to acknowledge: The Environment Society of Oman, its Whale and Dolphin Research Group, and affiliated scientists, generously provided samples from Oman to the project. In particular, I would like to thank Robert Baldwin, Tim Collins, Andrew Willson, Gianna Minton & Louisa Ponnampalam. I am also grateful to the Director and Staff at the Oman Natural History Museum for providing access to specimens for genetic and morphological analyses; especially, Saddiqa Al Lawati, Raiya Al Kindi & Hanan Al Nabhani. Authorization to collect biological samples and other documentation that permitted fieldwork to be carried out in Oman were provided by the Ministry of Transport and Communications and the Ministry of Environment and Climate Affairs. Samples from India were kindly provided by Tomohiko Isobe from the Environmental Specimen Bank (es-Bank) at the Center for Marine Environmental Studies, Ehime University of Japan. Samples from Zanzibar were provided by Per Berggren, Anna Särnblad-Hansson and Omar Amir. Samples collected in Pakistan were provided by Mauvis Gore, Ross Culloch, Muhammad Shoaib Kiani, Rupert Ormond, Umer Waqas and Babar Hussain. Further samples from Pakistan, Iran and Thailand were curated at the Museum am Löwentor, Staatliches Museum für Naturkunde, in Stuttgart and were collected by G. Pilleri and M. Gühr. Samples from South Africa were provided by Ada Natoli, Vic Peddemors and The Natal Shark Board. I would also like to acknowledge Luciana Möller (Flinders University), Elena Politi, Giovanni Bearzi, Caterina Fortuna (Tethys Research Institute), Alexei Birkun (CIESM, ACCOBAMS Scientific Committee), Iris Segura and André Moura (Durham University) for providing samples from other locations around the world.

Sources of Funding

I am thankful to the Environment Society of Oman for their assistance in securing funds from the Ford Middle East Environmental Grant and the Renaissance Whale and Dolphin project, which contributed towards lab expenses.

Labwork Assistance

For his help with amplifying and producing sequences for samples from India, I would like to extend my gratitude to Shin Nishida (Miyazaki University). Without his help I would never have been able to include such an interesting set of samples in my analyses. I also thank Ing(e) Chen for amplifying the microsatellites for these samples and transporting them to the UK. Many thanks to Inaê Guion for her generous help extracting DNA, and amplifying sequences, from samples that were difficult to work with. I would also like to thank Tom Gilbert, Andaine Seguire and the Danish National High-throughput DNA sequencing Centre for their assistance in generating a mitogenome sequence from an Oman sample.

Museum and Morphological Work

At the Oman Natural History Musuem, I would like to thank Hanan Al Nabhani for her assistance in accessing the skeletal material curated there, and an enormous thanks is also due to Mr. Mohammed for all of his careful work moving specimens around and kind assistance with the bone sampling.

Thank you to Doris Mörrike from the Museum am Löwentor for the time she gave up retrieving skulls from the collections and assisting with the back-breaking work of photographing, measuring and sampling them. I enjoyed our lunchtime chats about the collections at the museum and I am grateful for her hospitality.

Through the medium of e-mail, Koen Van Waerebeek managed to successfully train me in the art (and it really is an art) of measuring delphinid skulls. A non-trivial task which required a lot of time and patience. So, heel hartelijk bedankt, Koen!

I would like to thank Una Strand-Viðarsdóttir for her help with setting up a protocol for collecting Geometric Morphometric data. I am also very grateful to Joe Owen who guided me through the analysis stage of that work, and for coming in to Durham on occasion to see how I was getting on.

Logistical and Administrative Support

I am indebted to the staff at ESO for their assistance over the years. In particular, I would like to mention Nida El-Helou, Bashaar Zaitoon, Maïa Sarrouf Willson, Suaad Al Harthi, Asma Al Bulushi and Omar Al-Riyami for helping me overcome various obstacles, such as intercepting a biopsy crossbow at customs (!), chasing the paperwork for shipping samples and for attaining the necessary permissions for me to conduct fieldwork.

Fieldwork and Support ‘On the Ground’

I would like to express my gratitude to my ‘whale and dolphin’ teammates in Oman for their help on various fronts; from sourcing funding, to supporting me through my fieldwork endeavours, keeping me focussed, training me up, and for all the good discussions we have had over the years. Thank you to Robert Baldwin for welcoming me into the team, for backing me, and for all the help he gave me during, and on the lead up to, the PhD. I am thankful to Louisa Ponnampalam, and her spinner dolphins, for her encouragement and inspiration to pursue a PhD in the first place! Thanks to Andrew Willson for his support and being a good friend, but more on that later! Tim (Moth) Collins, please note that I am, hereby, grateful for all you have done to help me get here, including biopsy training, and various other bits of advice and support behind the scenes! Much appreciation also goes to Gianna Minton for her support and encouragement, particularly in those earlier years when I was sending her drafts of proposals (and similar things), which were in heavy need of good feedback.

In addition, thank you to everyone at Five Oceans Environmental Services Ltd. for their support and for continuing to find me bits of paid work to keep baked-beans in the cupboard! Of those not already mentioned elsewhere, a special thanks to Simon Wilson, Kris Vallancey, Iain Benson and Oli Taylor (who were all there ‘at the beginning’) for their words of encouragement over the years. I am also appreciative of the help received, from Umar Arshad and Haitham Al Wahaibi, with various bits of paperwork, visa extensions and car-rental arrangements over the course of my visits to Oman.

Begging, Borrowing and Stealing

Although he may not realize it, I owe a lot to the help, support and friendship of Andrew Willson. He has been my go-to guy for a great many things and we have shared in a number of marine adventures, which I have really enjoyed. Thanks are due in particular for making me sea-worthy, looking out for me, and looking after my things while I have been away, in-

cluding keeping the wrangler running and helping to sell it when the fieldwork finished. I look forward to our next adventure!

During my time of solitude in Hasik, a heartfelt thanks to Ali Tiwi, his friend Awoud and the people of Hasik for their outrageous hospitality and enthusiastic conversations about Oman's whales and dolphins. A particular thanks to Ali for taking me out on his fishing boat to conduct biopsy sampling and for his seemingly boundless generosity in the form of countless cups of tea, egg sandwiches, '*chips Oman*' and fish dinners! Caught by his hand, of course.

I am forever indebted to Bob, Margaret-Anne and Elayne Looker for letting me borrow *Ribbit* (the boat) for a Musundam adventure I will never forget. Without the samples I collected on that trip, sample representation from Oman would have been alarmingly low. Putting a boat on a boat would sound like a crazy idea to some, but not to the Lookers. Thanks for trusting me with *Ribbit* and for helping me with running paperwork around to make the impossible possible. An extra big thanks to Elayne for always being there to lend a hand and for her help in the field.

I would also like to thank Dave Mothershaw, who helped me in a number of ways, including getting *Ribbit* to the boat I was going to put it on, and to Darryl MacDonald for being a friend to call upon for help.

The generosity and support I received from the diving operator Extra-Divers in Musundam was astounding. I can't thank Kurt Bonami and Sandra de Munk enough for providing me with accommodation (and a shower) after many weeks camping, as the desert foxes (actually) started to close in! Thanks also to Ed Milman, Camilla Steffensen, Caren van Lente and Thorsten Sandmann for making me feel like I was part of their team and for their continuous support and interest in the work. Idris Mohammed Abdulrahman A'Shahee was my skipper for a number of biopsying days off Musundam, and I am eternally grateful for his time. An enormous thanks is due to skipper Yousef Abdullah Ali Al Kumzari, with whom I enjoyed working. We quickly became somewhat of a double act. While one could not necessarily rely on him to show up on time, one could rely on him to show up eventually! I thank him for all his hard work, patience, support and, most importantly, for being 'there' in a time of need.

Thank you to Major Salim Bin Mubarak Al Siyabi and the Musundam Coastguard for making me feel welcome, and for providing a berth and secure place for *Ribbit* and survey equipment. In particular, I would like to thank Major Salim, with whom I enjoyed many a cup of tea to discuss my progress, family and the awful weather (searing heat and *shamal* winds).

Thanks to Jim(bly) (Bru-min) Profit for joining me on my great Musundam escapade, for all of his help in the field, enthusiasm, sense of humour and positive outlook when the going got tough. I still crack up when I think of the things we got up to on *Ribbit* while searching, desperately, for the right kind of dolphin. Thanks also for sorting me out with a place to stay in Muscat for a while when plans fell through.

Many thanks to Traill Stocker for his help in the field and to Ada Natoli for the weekend she gave up with her family to come and help me chase dolphins around Musundam. I also appreciate Ada's continued support on the project, for tracking down samples in the UAE, and for her help finding volunteers.

Without a base in Muscat to plan and prepare for fieldwork, and work in the museum, this project would have been impossible. A big thanks to Kaveh Samimi and Mojdeh Zohari for kindly inviting me to stay at their house in the middle of a house move! If there were limits to their generosity I would have been pushing them, as I was there for a very long time. It would seem that measuring and photographing skulls can take a while. I would also like to thank Ann and Roger Mothershaw for kindly putting me up in their home, a lovely place to 'chill' while waiting for necessary paperwork to come through, and for letting me store all kinds of stuff while I was away chasing dolphins. Also, I am grateful to Andrew and Maïa Willson for letting me crash at their place and keeping me fed during various visits to Oman.

The Cathedral City

Over the course of the project, at the labs in Durham, I will have pestered many a post-doc, lab-tech and fellow student for help, thoughts and guidance on virtually every topic and analysis covered in this thesis. After much deliberation, I have decided not to mention everyone here by name, firstly because we are getting on for five pages now, and secondly, the risks of unwittingly forgetting someone over the six years worth of colleagues coming and going are too high. Therefore, please know that I am truly grateful to each and every person that has joined our labs at Durham for being the characters they are.

However, a special ‘thanks’ must go to the following people who have been particularly important to me. To begin with, I would like to thank Ratima Karuwanchaoen and Ing(e) Chen with whom it has been a pleasure to share in the PhD experience. It has been great to work alongside Kim Andrews who was a fun lab-bench neighbour and good friend, always happy to discuss a problem or just chat something through. I hope we continue to stay in touch. To Andreanna Welch, who must be the busiest person I know, thank you so much for patiently taking the time to answer my relentless questions on various phylogenetic analyses (which must have quickly faded to white noise), and for effectively carrying me through the ‘next-generation’ elements of the work presented here. Michelle Gaither has always been happy to calmly lend an ear, and be a voice of reason, to filter crazy ideas through. Her discussion and advice have been paramount to my progression, particularly towards the end of the project.

I am grateful to Laura Corrigan for welcoming me into the lab as part of the gang, for her lab-related guidance and for being a good friend. I suppose I must also extend my thanks to Laura for introducing me to Lois! A super ‘thank you’ to Karis Baker for all of her help, and support, as I ventured deeper into the PhD. She has been a red-thread throughout my time at the lab, and her no-nonsense attitude and advice have been valuable for getting me through some of the harder patches. Thanks Karis! André Moura was the first to show me how to set up a PCR (a skill for which, I suppose, I have mixed feelings) and was always happy to chat (at length) about dolphins, which has been awesome! I thank him for his friendship and continued efforts to get me through tricky analyses and I look forward to more dolphin-related chit-chat and collaboration in the near future.

To Fiona Bracken, thanks for being an awesome friend, lab-buddy and housemate! While we did enjoy chatting in depth about genetics related things, such as base pairs, we had good times watching David Attenborough, both on the TV and in real life, playing hockey, eating food and, well, quite frankly, partying! All the good things that get one through a PhD, so thanks for your friendship, Fiona B! Similarly to James Howard, a big ‘thanks’ for being a good friend and being part of those times too. I enjoyed our phase of scheduled afternoon breaks for a cup of coffee to chat about not very much at all and everything else in between. Looking forward to more of that soon!

Technically under this section, but from another time, I cannot thank my good friends Rory McCann and David Swingler enough for being a part of my support network and for continuing to include me in their lives and antics.

Last But Not Least

I would like to take this opportunity to extend my gratitude to the family Albin for their kind words of encouragement.

A big ‘thank you’ goes to the Bürgisser family; (Uncle) Heinz, (Auntie) Trudy and (cousins) Petra, Agnes and Emma for their support as well as general interest in the crazy things I get up to. To (Uncle) Dick Hupkes I am also thankful for the laughter and support he has given me. A special thank you must also go to my grandparents, Nancy and Geoff Gray, for their enthusiastic encouragement along the way.

All PhDs are different. However, I think we can all relate to a point where the daily routine turns into what feels more like a survival situation; and the only thing you can do is write your way out of it! I am grateful to those closest to me for helping me through this particular phase.

I am truly thankful to my parents, Cathy and Dave, for providing me with the opportunities to freely pursue my ambitions. Thanks for all the heartfelt support, and I look forward to celebrating in style! A super-massive ‘thanks’ to my brother and sister, Thomas and Sarah, for having my back and for being ‘there’ in times of need. An extra thanks to Thomas for his legendary help making the referencing a breeze! Of course, a shout-out is also due to Sofi for the part she played in maintaining my sanity.

I would like to finish with a ‘thank you’ to Lois for all the pep talks (which were always good-to-go), for the proof reading bits and for the practice presentations. Thanks for being so understanding about the things I had to do to complete this... although I appreciate we’re not ‘counting’ a year ;)! Thanks so much for getting me to the finish line.

Dedicated to

Mum & Dad



Bottlenose dolphin, *Tursiops aduncus*.
Musundam, Oman. July 2012
H. Gray

Chapter 1

General Introduction

1.1 Speciation and Population Differentiation

Differentiation may be considered at a variety of taxonomic levels e.g. the species level, inter-population level or intra-population level. The fundamental processes that govern differentiation at each level are mutation, genetic drift, gene flow and selection. Mutations introduce changes to DNA, which may or may not cause a phenotypic change. Genetic drift is the process where frequencies in variants (e.g. alleles) change by chance over time. This particularly applies to changes in DNA that are not under selective pressure i.e. 'neutral' markers such as microsatellites (but see Li *et al.* 2002). Gene flow is the process whereby alleles are exchanged between individuals or populations within a species, but cross-species gene flow may also occur through hybridisation or horizontal gene transfer (as frequently observed in bacteria). A variety of factors operating on a multitude of spatial and temporal scales can influence gene flow, such as: (i) behaviour e.g. assortative mating and variations in resource utilisation (Skúlason & Smith, 1995; Hoelzel, 1998a), (ii) demographic history e.g. male-mediated dispersal and female philopatry (Hoelzel, 1994), (iii) environmental parameters e.g. sea surface temperature, primary production and surface currents as barriers to dispersal (Fontaine *et al.* 2007; Mendez *et al.* 2011) and (iv) climatic history e.g. sea level fluctuations over the Pleistocene altering habitat availability (Moura *et al.* 2013a). If phenotypic changes occur, and are advantageous to the fitness of an individual, they may be selected for. The combined and cumulative effects of these processes facilitate population differentiation and/or speciation over time.

The most widely accepted mode of speciation is allopatric speciation (Dobzhansky, 1937; Mayr, 1942; Mayr, 1963; Mayr, 1970). Under this scenario, populations within a species are extrinsically separated, for example through the formation of a geographic barrier, such that gene flow is impeded or absent between them. Over time, processes of mutation, random genetic drift and/or adaptation to local environmental or ecological conditions, will drive population differentiation. Complete or partial reproductive isolation can result if the populations have differentiated sufficiently. If reproductive isolation is incomplete, this can give rise to hybridization zones and introgression between the diverged lineages upon secondary

contact (Poelstra, 2014), potentially resulting in homogenization (Servedio & Kirkpatrick, 1997; Servedio & Noor, 2003), speciation by reinforcement (Hoskin *et al.* 2005) or possibly hybrid speciation (Amaral *et al.* 2014).

By definition, the model of allopatric speciation was limited because it did not consider the controversial idea of divergence between sympatric populations. Even strict allopatry would be difficult to achieve in most circumstances because, at least initially, there would be some degree of gene flow between diverging populations (Futuyma & Mayer, 1980; Mallet *et al.* 2009). Indeed, speciation through a combination of allopatric (no gene flow) and sympatric (gene flow) mechanisms could be quite common (Bolnick & Fitzpatrick, 2007).

A series of experiments conducted on *Drosophila* (Thoday & Boam, 1959; Millicent & Thoday, 1960; Thoday & Gibson, 1962), in which reproductive isolation was achieved in two populations in the absence of geographic isolation, led Maynard Smith (1966) to address the question of sympatric speciation. Maynard Smith (1966) mathematically showed that the establishment of a stable polymorphism was possible in a population occupying a heterogeneous environment, where individuals adapted to different niches, for example, through utilising different resources (*cf.* ecological speciation) (Schluter, 2001; Rundle & Nosil, 2005). Establishment of a stable polymorphism could then lead to reproductive isolation and subsequent sympatric speciation, particularly in the presence of habitat selection and assortative mating (Maynard Smith, 1966). However, in order to establish a stable polymorphism, stringent conditions would need to be satisfied: Populations occupying different niches would need to remain approximately constant and the selective forces (disruptive selection) acting upon the polymorphism would need to be strong (Maynard Smith, 1966). There are multiple (over 70) models for sympatric speciation but they all share a similar framework. Whereby disruptive selection acts on a panmictic population to change mating patterns, such that reproductive isolation is the outcome (Bolnick & Fitzpatrick, 2007).

Empirical cases for sympatric speciation are few. A classic example can be found in the Hawthorn fly *Rhagoletis pomonella*, which seems to be undergoing incipient speciation, in sympatry, facilitated by adaptation to alternative host species (Feder *et al.* 1988). Two species of palm tree *Howea* sp. appear to have diverged sympatrically on an oceanic island in the presence of ancestral panmixia (Savolainen *et al.* 2006). Sympatric speciation has been documented in

cichlid fish in Nicaraguan crater lakes, facilitated by habitat selection and assortative mating (Barluenga *et al.* 2006). Divergence has also been reported in killer whales, *Orcinus orca* off Vancouver Island, where genetic differentiation between sympatric transient and resident populations has been attributed to behavioural isolating mechanisms, particularly foraging strategies (Hoelzel & Dover, 1991).

A problem with sympatric speciation is that it can be difficult to falsify historic allopatric divergence in distinct populations currently in sympatry (Berlocher, 1998; Coyne & Orr, 2004). After all, it is likely that current species distributions do not reflect those of conspecifics in the past if shifts in habitat availability have been driven by climate change. Indeed, populations may have experienced repeated range fluctuations in response to historic ecological changes generating complex population dynamics and genetic structure (Hofreiter & Stewart, 2009).

Another issue with sympatric speciation is that there has been some confusion over how to define it. Originally, sympatric speciation considered the divergence of populations that occupied the same geographical area (Mayr, 1942). This definition was later changed, in order to incorporate genetic concepts, specifically gene flow, to the divergence of populations occupying different ecological niches within the ‘cruising range’, i.e. the average dispersal distance of a single individual (Coyne & Orr, 2004), within an ancestral population (Mayr, 1947; Mallet *et al.* 2009). For the purpose of modelling evolutionary processes, this was simplified so that sympatric speciation was thought to occur when two populations diverged from a panmictic ancestral population, thus the spatial component of sympatric speciation was effectively lost (Mallet *et al.* 2009). However, under the pre-requisite of ancestral panmixia, sympatric speciation would be ‘almost impossible to demonstrate’ (Fitzpatrick *et al.* 2008; Mallet *et al.* 2009). In order to re-introduce the spatial component to the definition of sympatric speciation, Mallet *et al.* (2009) proposed that populations are said to be sympatric if conspecifics encounter each other with moderately high frequency (Futuyma & Mayer, 1980) i.e. within the normal ‘cruising range’ as proposed by Mayr (1947).

The question of speciation without geographic isolation, or in the presence of at least some degree of gene flow, is particularly pertinent in the marine environment, where there are apparently few barriers to dispersal, population sizes are generally large, and the ‘cruising range’

of many organisms and/or their larvae is large (Palumbi, 1994). Only mild genetic differentiation is expected and indeed regularly observed under these circumstances (e.g. Williams & Benzie, 1993; Mladenov *et al.* 1997), however unexpectedly high degrees of population structure have been documented in some marine taxa, such as echinoderms (e.g. O'Loughlin *et al.* 2011), squids (e.g. Shaw *et al.* 1999), fish (e.g. Knutsen *et al.* 2003. Bay *et al.* 2004), turtles (e.g. Encalada *et al.* 1996) and cetaceans (e.g. Tolley *et al.* 2001). Contemporary spatial and temporal heterogeneity in oceanographic conditions such as ocean currents (e.g. Muss *et al.* 2001; Mendez *et al.* 2011) and available habitat/niches such as different depths (e.g. Ingram, 2011) can limit gene flow between populations (even if only periodically or in particular directions) resulting in at least partial isolation of populations (Palumbi, 1994). Even in the presence of gene flow, the marine environment theoretically offers opportunities for species to diverge sympatrically, provided disruptive selection can drive reproductive isolation between two diverging populations.

1.2 Cetaceans as Candidates for the Study of Speciation and Population Structure

In the marine environment there are fewer opportunities for allopatric divergence to occur, particularly for highly mobile marine species where barriers to gene flow are relatively rare. Instead, speciation and population structure are more likely to occur in sympatry or parapatry driven by environmental heterogeneity across space and time. Cetaceans are able to disperse over relatively large distances and yet regularly show significant genetic differentiation over relatively small spatial scales (e.g. Tolley *et al.* 2001; Natoli *et al.* 2004; Hayano *et al.* 2004; Sellas *et al.* 2005; Fontaine *et al.* 2007; Natoli *et al.* 2008a; Andrews *et al.* 2010; Fernández *et al.* 2011; Hamner *et al.* 2012).

Adaptation to local habitat characteristics, or utilization of local resources, is reflected in cetacean population structure (Hoelzel, 1994). While Mysticetes (baleen whales) are generally solitary, several species of Odontocete (toothed whales) exhibit extreme social cohesion, probably related to foraging strategies (e.g. Natoli *et al.* 2005), and complex breeding systems (Ross, 2001), which also contribute to the population structure of many Odontocete species (Hoelzel, 1994; Pilot *et al.* 2010). Such social cohesion may also be associated with female philopatry and male-mediated dispersal (e.g. Lyrholm *et al.* 1999; Escorza-Treviño & Dizon, 2000; Möller & Beheregaray, 2004; Krützen *et al.* 2004; Oremus *et al.* 2007; Särnblad *et al. in review*), although this is not always the case (e.g. Andrews *et al.* 2010, Natoli *et al.* 2005).

Therefore, both environmental and social processes are implicated in shaping the genetic structure observed in several Odontocete species. Examples include spinner dolphins, *Stenella longirostris* in the Hawaiian Archipelago, which show genetic structure consistent with habitat and resource availability associated with different islands (Andrews *et al.* 2010). Social cohesion and high relatedness between females within groups of striped dolphins, *Stenella coeruleoalba*, contributes to significant genetic structure in the Mediterranean (Gaspari *et al.* 2007). The social cohesion and breeding system seen in North Pacific killer whales, *Orcinus orca*, enhances the genetic structure observed between killer whale populations (Pilot *et al.* 2010).

In an attempt to understand the interaction between environmental factors and genetic structure in two Odontocete species (franciscana dolphins, *Pontoporia blainvillei* in the southwest Atlantic Ocean and Indo-Pacific humpback dolphins, *Sousa* spp. in the western Indian Ocean), Mendez *et al.* (2010; 2011) analysed remote sensing data (e.g. chlorophyll concentration and sea surface temperatures) alongside genetic data to test for isolation by environmental distance (IBED). Testing for IBED checks for correlations between genetic and environmental differentiation (Mendez *et al.* 2010; 2011). Significant genetic differentiation was observed in both franciscana and humpback dolphin populations, consistent with environmental heterogeneity and discontinuities. Mendez *et al.* (2010) showed evidence for IBED in franciscana microsatellite data but not mtDNA data and explain that a high degree of female philopatry could be the cause. In humpback dolphins Mendez *et al.* (2011) did not find evidence for IBED, despite a consistent overlap between environmental heterogeneity and genetic differentiation. Among alternative hypotheses, Mendez *et al.* (2011) suggest that the presence of environmental discontinuities (breaks) may be of higher biological significance than their magnitude.

Many cetacean species are long-lived, feed at high trophic levels and can exhibit long-term residency in coastal areas (Wells *et al.* 2004). Therefore, cetaceans are particularly vulnerable to environmental change, such that the health and status of a population, as well as the lower trophic levels it depends on, reflect the natural and anthropogenic pressures on an ecosystem (Wells *et al.* 2004). Because of this, cetaceans have been proposed as sentinels for marine ecosystem health, variability, and degradation (Ross, 2000; Simmonds & Isaac, 2007; Moore, 2008; Bossart, 2011). Environmental changes, particularly those associated with habitat

availability/distribution in space and time, are likely to impact on cetacean population structure. Indeed, genetic differentiation attributed to climate changes over the Pleistocene has been documented in several delphinid species (e.g. Amaral *et al.* 2012a; Moura *et al.* 2013a; Louis *et al.* 2014; Moura *et al.* 2014).

1.3 Environmental Heterogeneity in the Western and Northwestern Indian Ocean

1.3.1 Contemporary Oceanography of the Indian Ocean

This thesis is particularly focused on the study area that encompasses the coastal biomes of East Africa, the Arabian Peninsula and the Indian subcontinent. The oceanographic characteristics across these areas are complex and well described in Longhurst (2006). I will endeavour to summarise their properties here. In general, the contemporary oceanography of the Indian Ocean is governed by the seasonal reversal of the wind regime and its interaction with the ocean basin (see Figure 1) (Longhurst, 2006).

1.3.1.1 East Africa

The continental shelf along the East African coastline from the Cape of Good Hope (South Africa) to Zanzibar (Figure 2) is relatively narrow and steep, extending to ~150 km at its widest point off Mozambique. The Agulhas Bank is also a large shelf area off the South African coast, reaching ~180 km offshore (Longhurst, 2006).

During the boreal winter months, the Intertropical Convergence Zone (ITCZ) lies in the southern hemisphere over the Mozambique Channel at ~15°S. Consequently, winds from the Arabian northeast monsoon are able to extend down to ~15°S and the southern Indian Ocean winds dominate south of this latitude. During the boreal summer months, the ITCZ migrates to the northern hemisphere and the southern Indian Ocean winds become continuous with the southwest monsoon winds of the Arabian Sea (Figure 1) (Longhurst, 2006).

The westward flowing South Equatorial Current meets the African continent at ~10°S where it diverges northwards as the East African Current (EAC) and southwards into the Mozambique Channel (Figure 1). During the boreal summer months and the southwest monsoon, the northbound EAC is continuous with the Somali Current. During the boreal winter months and the northeast monsoon, the Somali Current is reversed and diverges offshore where it meets the northbound EAC ~2°S - 3°S off southern Kenya (Figure 1). This process may be accompanied by coastal upwelling (Longhurst, 2006). During the boreal winter,

productivity in the East African Bight (0°S - 10°S) maximizes and is at its minimum in the period just prior to the northeast monsoon. During the southwest monsoon productivity is also increased but it is the northeast monsoon that dominates (Longhurst, 2006). The end of the northeast monsoon sees a maximal increase in mesozooplankton biomass and fish and large invertebrate reproductive effort (Longhurst, 2006).

Circulation through the Mozambique Channel is a complex southern flow of eddies and mesoscale gyres with a resultant northward flowing current along the Mozambican coast (Saetre & da Silva, 1984; Quartly & Srokosz, 2004). Upwellings are strongest at the Natal Bight, Delagoa Bight and Banco de Sofala (Quartly & Srokosz, 2004). For many months of the year, high chlorophyll concentrations are reported moving in a west-southwest direction from southern Madagascar (Quartly & Srokosz, 2004).

The Agulhas Current originates in the Mozambique Channel and flows continuously along the South African coast, becoming wider at the southern extremity of the continent where it undergoes retroflexion as it encounters the eastward flowing circumpolar zonal currents (Lutjeharms *et al.* 1989; Longhurst, 2006). Seasonal changes in the depth of the mixed layer over the Agulhas Bank are suggestive of periodic coastal upwellings, particularly during the austral summer.

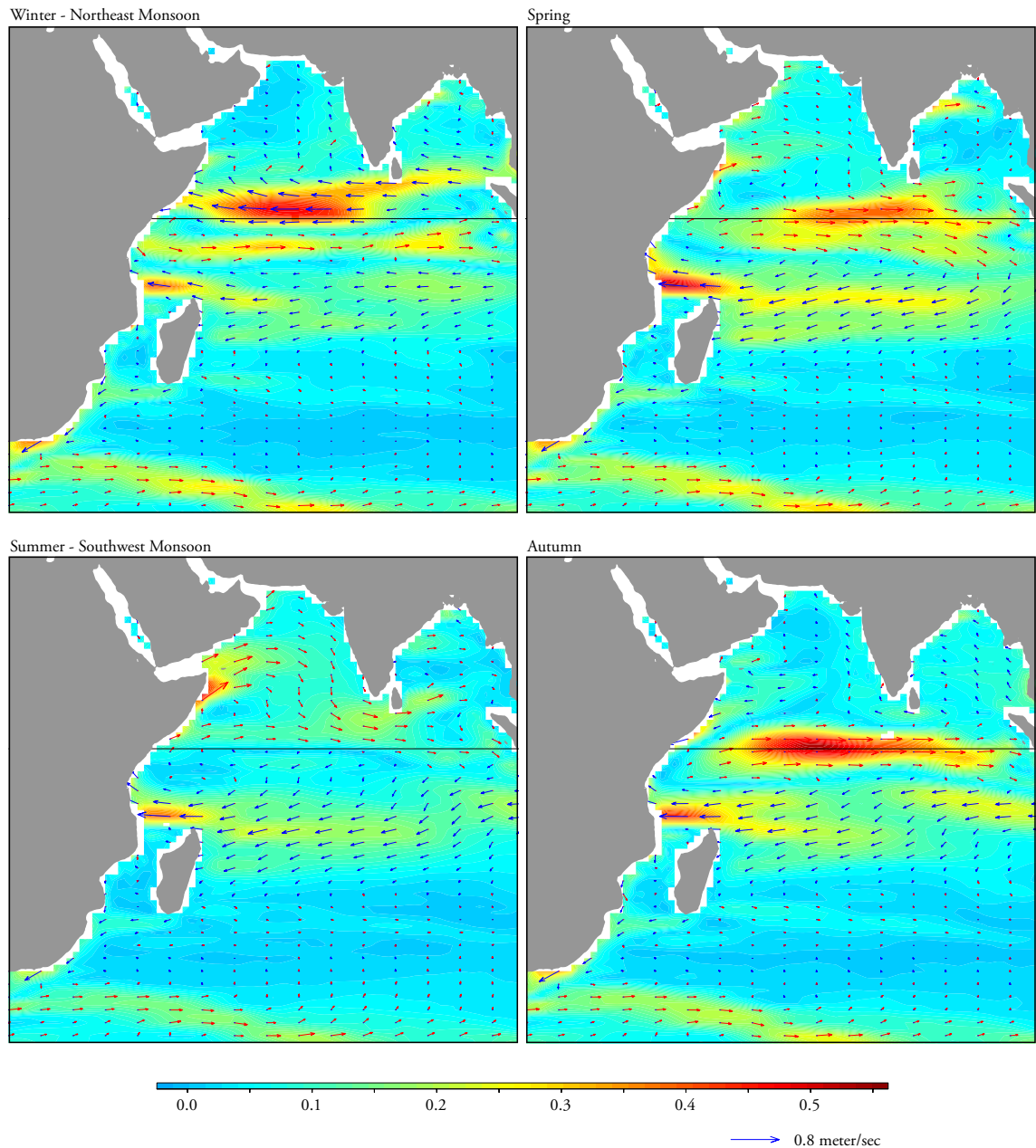


Figure 1: Seasonal mean values for major surface currents during the boreal winter (Dec-Feb), spring (Mar-May), summer (Jun-Aug) and autumn (Sept-Nov) months (1993-2010). Figures generated using the Ocean Surface Current Analyses – Real Time (OSCAR) online platform (www.oscar.noaa.gov) (Bonjean & Lagerloef, 2002). Colours and vector sizes correspond to current speeds (meters/second). Blue vectors indicate westbound currents and red vectors indicate eastbound currents.



Figure 2: The East African coastline and the western Indian Ocean. Colour change = 200m isobath.

1.3.1.2 Northwest Arabian Sea

The continental shelf extending from Zanzibar and throughout the Arabian Peninsula is narrow and steep with the exception of a few broad shelf areas along the Arabian Sea coast of Oman, such as the Gulf of Masirah and between Ras Madrakah and the Hallaniyat Islands (Figure 3).

The Somali Current moves northwards during the boreal summer months, i.e. during the southwest monsoon and continues along the Arabian Sea coast and towards the Indian sub-continent, generating significant upwelling (Figure 1). During the boreal winter, i.e. during the northeast monsoon, the flow of this current reverses and converges with the EAC (Elliott & Savidge, 1990; Sheppard *et al.* 1992; Burkill, 1999; Kindle & Arnone, 2001). During this time, upwelling along the eastern Oman coastline is intermittent (Banse, 1987; Longhurst, 2006).

The seasonal reversal of atmospheric circulation over the northwest Indian Ocean influences the primary productivity in the region, making it one of the most fertile areas in the world (Banse & McClain, 1986; Bauer *et al.* 1991; Burkill, 1999; Kindle & Arnone, 2001 Singh *et al.* 2011). The southwesterly monsoon is the dominant feature and it generates strong upwelling along the Arabian Sea coast leading to a ten-fold increase in productivity off Oman and Somalia (Brock & McClain, 1992; Almogi-Labin *et al.* 2000) and a five-fold increase in nitrate and phosphate concentrations (Savidge *et al.* 1990). It is postulated that the conditions resulting from the seasonal reversal provides nutrients and food to a variety of cetacean species in the region throughout the year (Sheppard *et al.* 1992; Papastavrou & Van Waerebeek, 1997)

1.3.1.3 Arabian/Persian Gulf and Red Sea

Both the Red Sea and Arabian/Persian Gulf (hereafter referred to as the Arabian Gulf) are extreme environments with high salinities due to high evaporation and low precipitation and river influx. In the Red Sea, influx through the Strait of Bab-el-Mandeb is higher during the northeast monsoon than the southwest monsoon (Longhurst, 2006). The Arabian Gulf exhibits a slow cyclonic circulation. Primary productivity in both basins is generally low due to the high salinities, which are lethal to plankton, but there are significant blooms in coastal areas of the southern Red Sea and Gulf of Aqaba. The Arabian Gulf also experiences high

coastal phytoplankton blooms, which are particularly high during the southwest monsoon (Longhurst, 2006).

1.3.1.4 Pakistan and India

The continental shelf is narrow off the coast of Pakistan and begins to broaden around Karachi. The shelf is at its broadest in the Gulf of Khambhat reaching ~300 km (Longhurst, 2006) and progressively narrows moving southwards towards the southernmost extremity of the Indian subcontinent. The continental shelf along the eastern coast of India is also narrow but broadest around the mouth of the Brahmaputra-Ganges delta (Figure 3).

Coastal currents seasonally reverse off Pakistan and western India such that currents move eastwards during the southwest monsoon and westwards during the northeast monsoon. The coastline is characterised by high chlorophyll concentrations even during inter-monsoonal periods, but this could also be due to terrestrial run-off from the Indus delta (Longhurst, 2006). Productivity peaks towards the end of the southwest monsoon and declines rapidly to a minimum in December (Longhurst, 2006). Along the eastern coast of India and the Bay of Bengal there is a seasonal reversal of the coastal current moving westwards during the northeast monsoon and eastwards during the southwest monsoon (Longhurst, 2006). Phytoplankton blooms occur during both the northeast and southwest monsoons but to a much weaker degree in comparison to the Arabian Sea. The southwest monsoon also generates a stronger bloom than the northeast monsoon but this might also be due to river discharges from the Irrawady and Ganges. These river discharges are also responsible for low salinity waters around this coastline.

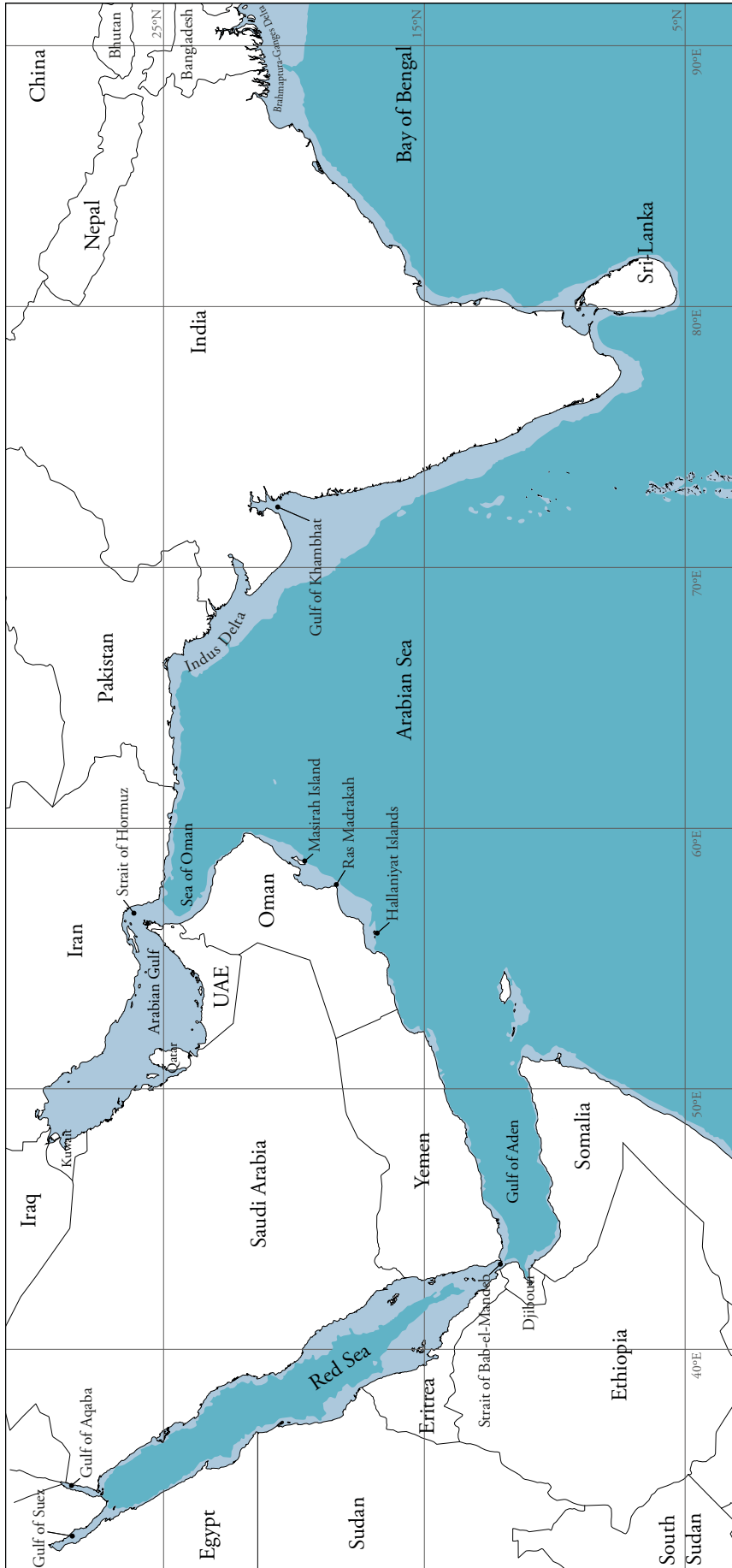


Figure 3: The coastlines of the Arabian Peninsula, Pakistan and India in the the northwest Indian Ocean. Colour change = 200m isobath.

1.3.1.5 Potential Boundaries Generated by Contemporary Oceanography

There is evidently considerable environmental heterogeneity in the study area. Most oceanographic processes are governed by the seasonal reversal of the Asian Monsoon system, which generates particularly high levels of productivity in the northwest Indian Ocean compared to the waters of East Africa and India. The difference in productivity off the Arabian Peninsula from East Africa has been noted elsewhere as a putative environmental break for humpback dolphins (Mendez *et al.* 2011). The Indian coastline, with its terrestrial influx of organic material from rivers, such as the Indus river delta, generates a possibly unique, brackish environment with reduced visibility that is different to that observed in the Arabian Sea and off East Africa. Off East Africa, Mendez *et al.* (2011) note a putative environmental break where the South Equatorial Current meets the African continent at $\sim 10^{\circ}\text{S}$ where it diverges into northward and southward-flowing coastal currents. These habitat differences provide a potential arena for local adaptation and population differentiation to take place in cetaceans, particularly coastal dolphins.

1.3.2 Pleistocene Oceanography in the Indian Ocean

Palaeoclimate data suggest great variability in the Asian Monsoon systems during the Pleistocene. In contrast to today, palaeoproductivity data from the northern Indian Ocean and South China Sea suggest the northeast and East-Asian monsoons intensified, generating strong upwellings, during certain glacial events, while the southwest monsoon weakened (Fontugne & Duplessy, 1986; Wang *et al.* 1999a Almogi-Labin *et al.* 2000, Sun *et al.* 2003). Off Pakistan and India, glacial periods were associated with higher turbidite deposits from the Indus delta, suggesting the environment may have been particularly turbid (von Rad & Tahir, 1997).

The coastal topography during the Pleistocene was also subject to dramatic change. Sea levels were considerably lower than they are today during glacial periods and were sometimes higher during interglacials (Shackleton 1987; Glennie 1996). The northern and southern extremities of the Red Sea are particularly sensitive to sea-level fluctuations, with the southern opening to the Indian Ocean, the Bab al-Mandab Straits, being very narrow or closed during low sea-level stands (Bailey, 2009). Also of particular note is the emptying of the Arabian Gulf during low sea-level stands (Kassler, 1973). Furthermore, it is interesting to make reference to the repeated exposure of the Indo-Pacific Barrier, formed as the Sunda and Sahul

shelves were exposed during low sea level stands (Voris, 2000). This barrier is thought to play a role in the mechanisms that have generated great species diversity (a 'biodiversity hotspot') in the Indo-Malay-Phillipine region (Gaither & Rocha, 2013).

Such changes in oceanographic characteristics have the potential to influence the population genetics of cetaceans in the region e.g. through allopatric divergence possibilities in the Red Sea and on either side of the Indo-Pacific barrier. Additionally, changes in primary productivity in favour of the northeast monsoon during glacial periods may have had an effect on the distribution and inter-connectedness of cetacean populations in the region at that time.

1.4 Cetaceans in the Northwest Indian Ocean and Conservation Concern

The International Whaling Commission (IWC) was set up in 1946 to manage whaling stocks and regulate the whaling industry (Donovan, 2009). In 1979, the Indian Ocean Sanctuary was established, thereby banning commercial whaling in the Indian Ocean. In 1982, a 'moratorium' on commercial whaling was implemented, but this did not put forward management regulations for direct (hunting) and indirect (incidental catch in fisheries) takes on small cetaceans (Donovan, 2009). Nevertheless, the IWC Scientific Committee continues to review the conservation status of small cetaceans and advises governments accordingly on their management (Donovan, 2009). In the northwest Indian Ocean, only Oman and India are members of the IWC. Across the broader region encompassed in this thesis, Egypt, Eritrea, South Africa, Tanzania and Kenya are also member states.

Other international treaties and organisations have a presence in the region with the aim of directly or indirectly protecting regional marine habitats and wildlife. For instance, the Convention on Biological Diversity (CBD), which sets out to promote sustainable development, and the Convention on the Conservation of Migratory Species of Wild Animals (CMS), which sets out to conserve species that cyclically/predictably cross multiple national jurisdiction boundaries. Oman, the United Arab Emirates and Iraq are the only states that are not currently parties to CMS in the northwest and western Indian Ocean region. All countries in the region are parties to the Convention on International Trade in Endangered Species of Wild Fauna and Flora (CITES), which regulates the international trade of endangered species. The International Convention for the Prevention of Pollution from Ships (MARPOL 73/78) also has a presence in the northwest Indian Ocean (Oman, Iran, Pakistan and India) and sets out to minimise the pollution of the marine environment from ships.

On a regional scale, the Regional Organization for the Protection of the Marine Environment (ROPME) is an organization that was established to implement the 'Kuwait Regional Convention for Cooperation on the Protection of the Marine Environment from Pollution' across the eight member states: Bahrain, Iran, Iraq, Kuwait, Oman, Qatar, Saudi Arabia and the United Arab Emirates. The objective of this convention is to promote sustainable coastal development in the region.

Across the northwest Indian Ocean, most (but not all) countries, have issued national legislation, some in response to fulfilling obligations to conventions to which they are party (such as the CBD), that specifically or indirectly protect marine mammals. However, 'enforcement is often weak' (Anderson, 2014).

In 1998, concerns were raised at an IWC meeting in Oman about the impacts of anthropogenic activities on small cetaceans in the Indian Ocean and Red Sea (IWC, 1999). These concerns were fourfold: (i) a paucity of data and information on fisheries effort in the region, particularly given the increasing number of strandings with evidence of fisheries interaction (see Collins *et al.* 2002); (ii) pollution in the Arabian Gulf, due to a poor turnover rate of water (3-5 years) and high pollution rate; (iii) directed hunting; and (iv) habitat degradation and loss. These concerns led the committee to put forward recommendations for further study and investigation. Amongst others, these included the stock assessment of coastal dolphins in the region, with an initial focus on humpback dolphins, *Sousa* spp., common dolphins, *Delphinus* spp. and bottlenose dolphins, *Tursiops* spp.. The assessment of the conservation status and systematics of these species was also encouraged and is generally regarded as a priority within the scientific community (see Reeves *et al.* 2004).

There is a good framework of international agreements and conventions, as well as national legislation, in place in the region. These broadly protect cetacean species from direct hunting and/or protect the marine environment from pollution and other stressors that results from coastal development and anthropogenic activities. However, the design and implementation of site-specific management of small cetaceans in the region is largely non-existent (Ponnampalam, 2009). Information on taxonomic affinities (and uniqueness), population size estimates and demographic trends can be estimated using genetic data and will be important contributions in the identification of management units and prioritise conservation efforts in the northwest Indian Ocean.

Since the IWC meeting, several studies and reviews have incorporated the use of morphometric data from small cetacean skeletal remains from Oman. Cetaceans examined have included humpback dolphins (Baldwin *et al.* 2004; Jefferson & Van Waerebeek, 2004; Mendez *et al.* 2013) spinner dolphins, *Stenella longirostris*, rough toothed dolphins, *Steno bredanensis*, melon-headed whales, *Peponocephala electra* (Van Waerebeek *et al.* 1999) and common dolphins (Jefferson & Van Waerebeek, 2002). One can find further general and specific aspects of small cetaceans of the region in reviews by Leatherwood (1986), de Silva (1987) and Baldwin *et al.* (1999). Genetic analyses have been focused on humpback whales, *Megaptera novaeangliae* (Rosenbaum *et al.* 2002; Rosenbaum *et al.* 2004; Rosenbaum *et al.* 2006; Rosenbaum *et al.* 2009; Pomilla *et al.* 2010; Pomilla *et al.* 2014), common dolphins (Amaral *et al.* 2012a), humpback dolphins (Mendez *et al.* 2011; 2013) and bottlenose dolphins (Särnblad *et al. in review*). Although taxonomic studies of cetaceans in the region have been limited, work conducted to date reveals some degree of endemism in Odontocetes and Mysticetes (reviewed briefly below).

The taxonomy of spinner dolphins in the region is limited to a morphological study on eight skeletal specimens collected in Oman (Van Waerebeek *et al.* 1999). Although virtually indistinguishable from the eastern spinner dolphin (Perrin, 1999) based on cranial measurements, Oman spinner dolphins have slightly longer rostra (Van Waerebeek *et al.* 1999). Two colouration morphotypes (CM) of spinner are also reported, CM1 exhibiting the typical tripartite pattern associated with Gray's spinner dolphins, the other CM2, characterised by a dark dorsal overlay, obscuring most of the tripartite pattern, and by a pinkish or white ventral field and supragenital patch (Van Waerebeek *et al.* 1999). It is conceivable that these morphological differences are a result of local adaptation to the oceanographic conditions in the northwest Indian Ocean.

Notable work on Oman's humpback whales has shown that they are genetically isolated and distinct from other humpback whale populations (Rosenbaum *et al.* 2002; Rosenbaum *et al.* 2004; Rosenbaum *et al.* 2006; Rosenbaum *et al.* 2009; Pomilla *et al.* 2010; Pomilla *et al.* 2014) and have been designated as a subpopulation of non-migratory Arabian Sea humpbacks (IWC, 2010), now recognised by the IUCN Red List as endangered (Minton *et al.* 2008). The mechanism by which these individuals have become non-migratory and adherent to a northern hemisphere breeding cycle (southern hemisphere ancestry) is not known. How-

ever, it is assumed that local adaptation to the high productivity of the Arabian Sea, driven by the seasonal reversal of the Asian Monsoon, is an important factor (Pomilla *et al.* 2014).

Mendez *et al.* (2011) showed that genetic differentiation in humpback dolphin populations along the western and northwest Indian Ocean coincided with environmental heterogeneity in the region. Again, this is suggestive of local adaptation of populations to different habitats. Furthermore, Mendez *et al.* (2013) suggest that a transition from *S. plumbea* to *S. chinensis* occurs in the northern Indian Ocean.

To date, with the exception of a small number of samples included in Särnblad *et al.* (*in review*), work on the taxonomy and population genetics of bottlenose dolphins in this region has been limited. Assessment of the population structure and phylogeography of bottlenose dolphins in the northwest Indian Ocean is a particular focus of this thesis (see below).

The presence of the common dolphin sub-species *D. capensis tropicalis* has been described from both morphological assessment of dolphins in the region (Jefferson & Van Waerebeek, 2002) and from phylogenetic analysis (Amaral *et al.* 2012a) (see below). To date, only a limited number of samples from the northwest Indian Ocean have been used in analyses, particularly utilizing nuclear markers, on population differentiation and taxonomy of common dolphins in the region (Natoli *et al.* 2006; Amaral *et al.* 2012a). Work presented in this thesis endeavours to utilize further samples from the northwest Indian Ocean to investigate the population structure and taxonomy of common dolphins in the region using both nuclear and mitochondrial loci (see below).

1.5 Bottlenose Dolphins

Observations of bottlenose dolphins in the northwest Indian Ocean suggest that both *T. truncatus* and *T. aduncus* types are present, based on external morphology (Minton *et al.* 2010) and limited genetic identification (see Curry, 1997; Ballance & Pitman, 1998; Särnblad *et al.* *in review*). Below I review the current taxonomy and conservation status of bottlenose dolphins and briefly summarise general aspects of their distribution, habitat preferences and ecology, particularly as they may pertain to driving population structure in these taxa. I focus here on *T. aduncus* and to a lesser extent *T. truncatus*. The Burrunan dolphin, *T. australis* is not wholly considered here, as its distribution is peripheral to the focus of this thesis. For more information on *T. australis* see Charlton-Robb *et al.* (2011).

1.5.1 Taxonomy

Although bottlenose dolphins *Tursiops* sp. have received a large amount of taxonomic attention over recent decades (e.g. Mead & Potter 1990; Ross & Cockcroft, 1990; Hoelzel *et al.* 1998; Wang *et al.* 1999b; Möller & Beheregaray, 2001; Natoli *et al.* 2004; Kemper, 2004; Charlton-Robb *et al.* 2011; Moura *et al.* 2013a) there are still gaps in our knowledge (see Reeves *et al.* 2004) and the taxonomy remains confused. Most studies agree on the polyphyly of *Tursiops* sp. with *Delphinus* and *Stenella* genera (e.g. LeDuc *et al.* 1999, McGowen, 2011; Moura *et al.* 2013a), with the genus encompassing at least two species: the common bottlenose dolphin, *T. truncatus* (Montagu, 1821) and the Indo-Pacific bottlenose dolphin, *T. aduncus* (Ehrenberg, 1832) (LeDuc *et al.* 1999; Wang *et al.* 1999b; Wang *et al.* 2000). There is also accumulating evidence for a third species: the Burrunan dolphin, *T. australis*, from southern Australia (Charlton-Robb *et al.* 2011). Within the *T. aduncus* clade there is support for further division into at least two lineages, whereby *T. aduncus* populations off South Africa and Australasia are reciprocally monophyletic (Natoli *et al.* 2004; Moura *et al.* 2013a). Mitochondrial DNA sequences from the *T. aduncus* holotype specimen, collected from the Red Sea, were a match for the South African lineage (Perrin *et al.* 2007), suggesting that it is the Australasian lineage that would require reclassification (in the interest of nomenclature) if these lineages were recognised as distinct species. Further division can be made within the *T. truncatus* lineage into regional ecotypes occupying coastal or pelagic habitat (Mead & Potter, 1995; Hoelzel *et al.* 1998; Torres *et al.* 2003). In addition, the Black Sea is inhabited by a recognised sub species of bottlenose dolphin, *T. truncatus ponticus* (Viaud-Martinez *et al.* 2008).

Moura *et al.* (2013a) confirmed the presence of these lineages in a phylogeographic analysis utilizing entire mitochondrial genomes. Furthermore, ancestral biogeographic reconstructions and divergence date estimation suggest that the *Tursiops* lineages originated in Australasian coastal waters (Moura *et al.* 2013a) with divergence patterns throughout the genus coinciding with glacial termination events or the periods of global warming that followed them (Moura *et al.* 2013a).

Taxonomic and population genetic studies of bottlenose dolphins in the western and north-west Indian Ocean have been limited to a study on coastal bottlenose dolphins off Zanzibar (Särnblad *et al.* 2011; *in review*), which included only four *T. aduncus* samples from Oman.

These were a genetic match for the South African lineage and therefore belonged to the *T. aduncus* holotype lineage.

1.5.2 Indo-Pacific Bottlenose Dolphins, *T. aduncus*

1.5.2.1 Conservation Status

The Indo-Pacific bottlenose dolphin, *T. aduncus* is listed as ‘Data Deficient’ under the IUCN Red List of Threatened Species, which means ‘there is inadequate information to make a direct, or indirect, assessment of its risk of extinction based on its distribution and/or population status’ (Hammond *et al.* 2012a). The species is also considered under Appendix II of CITES, which lists species that may not be currently threatened but may become so if trade is not closely controlled.

1.5.2.2 Distribution, Habitat and Ecology

The presence of *T. aduncus* has been recorded throughout the tropical to warm-temperate waters of the Indo-Pacific, including cooler waters around Japan, northern China, southern Australia and South Africa (e.g. Pilleri & Gahr, 1972; Lal Mohan, 1982; Gallagher, 1991; Baldwin *et al.* 1999; Kemper, 2004; Preen, 2004; Jayasankar *et al.* 2008; Wang & Yang, 2009; Braulik *et al.* 2010; Minton *et al.* 2010). *T. aduncus* largely occupy coastal habitat, over continental shelf waters in areas with coral reefs, sandy bottoms or sea-grass beds or around oceanic islands (Wang & Yang, 2009; Hammond *et al.* 2012a). In the northwest Indian Ocean, based on work in Oman, *T. aduncus* sightings were predominantly made in shallow waters (< 1 km of shore), averaging 9.4 m depth in the Dhofar region (Minton *et al.* 2010).

Broadly overlapping distributions with other species have been documented around the world, including *T. truncatus*, *Sousa* spp., *S. longirostris*, pantropical spotted dolphins, *S. attenuata*, finless porpoise, *Neophocaena phocaenoides* and snubfin dolphins *Orcaella* spp. (Wang & Yang, 2009). In the northwest Indian Ocean, *T. aduncus* has overlapping distributions with *Sousa plumbea*, *Delphinus capensis tropicalis* and humpback whales, *Megaptera novaeangliae* (Minton *et al.* 2010). Mixed species assemblages have been recorded with *Delphinus* sp. and *Sousa* sp. (Minton *et al.* 2010).

Worldwide, there is significant variability in *T. aduncus* diet and they prey primarily on benthic and reef-dwelling fish as well as cephalopods (Wang & Yang, 2009). In the northwest

Indian Ocean, preliminary analysis of stomach contents of *Tursiops* spp. ($n = 11$) in Oman revealed they were feeding on a variety of prey, including reef-fish and species associated with muddy/sandy substrates as well as near-shore/continental shelf cephalopod species (Ponnampalam *et al.* 2012). Throughout the species' range a variety of foraging strategies have been developed (Wang & Yang, 2009). Some of these are unique to the populations that use them and must either be socially learned through vertical transmission (parent-offspring) or horizontally from one individual to another. For example, in Shark Bay, western Australia, *T. aduncus* individuals exhibit 'beach hunting'; a potentially dangerous foraging tactic which involves chasing prey onto beaches (Sargeant *et al.* 2005). Expression of unique foraging strategies may also carry a genetic component (Wang & Yang, 2009). Such resource polymorphisms may result in assortative mating, or habitat-specific specialisations (e.g. Rosel *et al.* 2009), which may physically separate groups, such that they become genetically differentiated.

Individuals live in small fission-fusion societies with group sizes commonly between 20 and 50 individuals (Wang & Yang, 2009). Males form a hierarchical system of alliances consisting of two or three individuals that cooperate, against other male alliances, to 'herd' females in order to gain or maintain mating access (Connor *et al.* 1992; Möller *et al.* 2001). There is conflicting evidence over whether kin-selection is important in the formation and maintenance of these alliances as alliance members for some populations are closely related whereas those in other populations are, on average, only randomly related (Möller *et al.* 2001; Krützen *et al.* 2003; Möller *et al.* 2012). Females also form cooperative coalitions, with some evidence for frequent associates to have elevated levels of genetic relatedness (Möller *et al.* 2006). These groups may cooperate against shark predation, to help rear calves and obstruct male coercion (Möller *et al.* 2006; Wang & Yang, 2009). Genetic studies have shown that female *T. aduncus* exhibit philopatry while dispersal is male-biased (e.g. Möller & Behrergaray 2004), however, other studies have shown that males also exhibit a degree philopatry by incorporating their natal range into their home range (Krützen *et al.* 2003; Krützen *et al.* 2004; Möller *et al.* 2012; Tsai & Mann, 2013). In some areas, populations of *T. aduncus* exhibit strong year-round site-fidelity with males expanding their ranges during breeding excursions (Tsai & Mann, 2013). Seasonal changes in prey distributions can affect the seasonal movements of *T. aduncus*, for example, a population off South Africa follows the annual migration of sardines into coastal waters in June-August (Peddemors, 1999; Natoli *et al.* 2008).

Although *T. aduncus* has high dispersal capabilities, conspecifics exhibit bisexual philopatric behaviour and, in some populations, form alliances with close relatives. Location philopatry may be due to the fitness benefits from familiarity with habitats/resources (e.g. foraging) as well as associates to form alliances with (Tsai & Mann, 2013). Such restrictions in dispersal would be expected to generate population genetic differentiation if populations become physically isolated.

1.5.3 Common Bottlenose Dolphins *T. truncatus*

1.5.3.1 Conservation Status

The common bottlenose dolphin, *T. truncatus* is listed as ‘Least Concern’ on the IUCN Red List (Hammond *et al.* 2012b) and is also considered under Appendix II of CITES.

1.5.3.2 Distribution, Habitat and Ecology

T. truncatus is found in tropical and temperate waters around the world and includes all bottlenose dolphins outside the Indo-Pacific and all offshore variants, including those in the Indo-Pacific. *T. truncatus* has been recorded as far north as Nova Scotia, Norway and Iceland in the Atlantic (Wells & Scott, 1999). In the Pacific, *T. truncatus* are documented off California in the east and the Okhotsk Sea in the west (Wells & Scott, 1999). The species’ range also extends into the Mediterranean Sea and Black Sea, where the subspecies *T. t. ponticus* is recognised (Viaud-Martinez *et al.* 2008). The species’ range extends as far south as Tierra del Fuego, South Africa, Australia and New Zealand (Wells & Scott, 2009).

In the northwest Indian Ocean, *T. truncatus* have been reported in offshore waters off Oman (Minton *et al.* 2010), Pakistan (Gore *et al.* 2012) and India (Jayasankar *et al.* 2008). Biopsies collected by Ballance & Pitman (1998) of bottlenose dolphins in the western Indian Ocean were genetic matches for *T. truncatus* (Curry, 1997; Ballance & Pitman, 1998). Some anecdotal evidence suggests the presence of two morphotypes of *T. truncatus* in the region. *T. truncatus* types generally encountered in offshore waters of Oman are approximately 3 m in length, however, occasionally sightings off the Sea of Oman (OMCD; *pers. obs.*) and observations of *T. truncatus* in the Red Sea, are exceptionally large, 4 m or more in length (Beaton, 1991).

T. truncatus inhabits both offshore and coastal waters around the world, but are only found offshore in the Indian Ocean (Wells & Scott, 2009). It has been suggested that pelagic populations act as a pool from which coastal populations are founded (Natoli *et al.* 2004). The diets of *T. truncatus* include a variety of fish and cephalopods and reflect the coastal or pelagic habitats they occupy (Wells & Scott, 2009). In the northwest Indian Ocean preliminary stomach contents analysis suggest *T. truncatus* in the Gulf of Oman are feeding on pelagic and epipelagic fish (Ponnappalam *et al.* 2012). Similar to *T. aduncus*, a variety of foraging strategies have been reported in *T. truncatus* (e.g. Rossbach & Herzing, 1997; Connor *et al.* 2000; Gazda *et al.* 2005). Differences in resources (e.g. prey) and associated use (foraging strategies) could facilitate genetic differentiation or speciation between populations (e.g. Hoazel *et al.* 1998a; Hoazel *et al.* 1998).

Coastal ecotypes of *T. truncatus* exhibit varied ranging patterns, from long-term residency to long-range movements and seasonal migrations (Wells & Scott, 2009). The movements of offshore variants are not well known (Wells & Scott, 2009), although genetic studies have revealed high levels of gene flow across large distances (Qu erouil *et al.* 2007). As with *T. aduncus* (see above), *T. truncatus* live in fission-fusion societies (Connor, 2000) and are typically observed in group-sizes of 2-15 individuals, although group sizes of over 1000 individuals have been reported (Wells & Scott, 2009). Social strategies appear to be varied across the *T. truncatus* distribution, where strong male-male and female-female alliances are found in some populations and not in others (Connor, 2000). Male-biased dispersal is not the norm, with many studies reporting philopatry in both sexes (Natoli *et al.* 2005; Parsons *et al.* 2006; Martien *et al.* 2012).

1.6 Common Dolphins

Below I review the taxonomy and conservation status of common dolphins, with a focus on those in the northwest Indian Ocean, and briefly outline general aspects of their distribution, habitat preferences and ecology.

1.6.1 Taxonomy

As with bottlenose dolphins, the taxonomy of common dolphins, *Delphinus* spp., has been subject to a great deal of ambiguity within the last few decades. Substantial morphological variation is observed across the genus' range (e.g. Bell *et al.* 2002; Jefferson & Van Waerebeek,

2002; Stockin & Visser, 2005; Murphy *et al.* 2006; Westgate, 2007; Tavares *et al.* 2010), with some 30 putative species previously described (Hershkovitz, 1966). Despite this, only two species are currently recognised, namely the short-beaked, *D. delphis* and long-beaked, *D. capensis* common dolphin (Heyning & Perrin, 1994; Rosel *et al.* 1994). The distinction between the two species was made in the northeast Pacific, where they occur in sympatry, based on morphological characteristics (Heyning & Perrin, 1994). This distinction was corroborated by genetic analyses in a parallel study where long-beaked and short-beaked morphotypes were reciprocally monophyletic (Rosel *et al.* 1994). In a study on delphinid phylogenetic relationships conducted by LeDuc *et al.* (1999), *Delphinus* were seen to be paraphyletic with *Tursiops* and *Stenella* genera.

Further genetic studies in other parts of the world showed long and short beaked morphotypes to be polyphyletic outside the northeast Pacific (Natoli *et al.* 2006; Amaral *et al.* 2012a). Failure to genetically resolve between the morphotypes in other regions suggested that populations were adapting to particular habitat characteristics or prey compositions and independently converging on a similar long-beaked morphotype (Natoli *et al.* 2006; Amaral *et al.* 2012a). In a phylogeographic analysis, Amaral *et al.* (2012a) propose a northeast Pacific origin for the *Delphinus* genus. They suggest that climate change over the Pleistocene facilitated the movement of common dolphins into the southern hemisphere followed by a westward expansion into the Indian and Atlantic Oceans.

Although two species were identified in the northeast Pacific, the proposed species *D. tropicalis* van Bree (1971) remained controversial (Jefferson & Van Waerebeek, 2002). This putative species was later described as a subspecies, *D. capensis tropicalis* based on morphological analyses (Jefferson & Van Waerebeek, 2002). Amaral *et al.* (2012a) also showed *D. c. tropicalis* to form a separate lineage to other populations, diverging basally with populations outside the northeast Pacific.

1.6.2 Common Dolphin Conservation Status, Distribution, Habitat and Ecology

1.6.2.1 Conservation Status

The short-beaked common dolphin, *D. delphis* is listed as 'Least Concern' on the IUCN Red List (Hammond *et al.* 2008a) while the long-beaked common dolphin *D. capensis* (including *D. c. tropicalis*) is listed as 'Data Deficient' (Hammond *et al.* 2008b). Both *D. delphis* and *D.*

capensis are considered under Appendix II of CITES.

1.6.2.2 *Distribution, Habitat and Ecology*

Although long-beaked morphotypes of *D. delphis* have been reported in other parts of the world, for example off South Africa (Jefferson & Van Waerebeek, 2002), the long-beaked common dolphin, *D. capensis* appears to be endemic to the northeast Pacific (Heyning & Perrin, 1994; Rosel *et al.* 1994; Natoli *et al.* 2006; Amaral *et al.* 2012a; Cunha *et al.* 2015). Short-beaked common dolphins, *D. delphis*, are found offshore throughout warm-temperate waters in the Atlantic and Pacific. In coastal waters, in several parts of the world, *D. delphis* appears to have converged on a long-beaked coastal morphotype (see Natoli *et al.* 2006; Amaral *et al.* 2012a) in a similar fashion to *T. truncatus* (see above). The recognised lineage *D. c. tropicalis* (Jefferson & Van Waerebeek, 2002; Amaral *et al.* 2012a) appears to be endemic to the Indian Ocean. Encounter rates of common dolphins in the Arabian Sea and Sea of Oman were highest along the continental shelf edge (50 - 200 m depth) (Minton *et al.* 2010). Seasonal migrations have been reported and may be closely linked to movement of prey (e.g. Cockcroft & Peddemors, 1990). Long-term residency of individuals has also been reported (Bernal *et al.* 2003; Perrin, 2009).

The diet of common dolphins varies with region/habitat and season, suggestive of flexible foraging strategies, feeding on a diversity of prey species, including small mesopelagic fishes and squids as well as epipelagic schooling fishes (Perrin, 2009). In the northwest Indian Ocean, stomach contents examined from individuals in Pakistan (Pilleri & Gühr, 1972) and India (James *et al.* 1987; Krishnan *et al.* 2008) revealed they were feeding on a variety of demersal and pelagic prey species. Although these studies were limited to a few individuals ($n = 3$), the target prey species are not unusual for common dolphins (*cf.* Pusineri *et al.* 2007; Meynier *et al.* 2008a; Meynier *et al.* 2008b).

As with bottlenose dolphins (see above), common dolphins live in fission-fusion societies (Bruno *et al.* 2004) with varied group sizes. In some cases, hundreds or thousands of individuals have been reported, but these are believed to comprise of smaller groups of 20-30 individuals (Perrin, 2009). In the northwest Indian Ocean, group sizes as large as 3,000 have been reported (Minton *et al.* 2010). There is limited documentation of the social structure of common dolphins although genetic analyses suggest individuals within a group are no more

closely related than individuals between groups (Viricel *et al.* 2008), however, individuals do appear to associate non-randomly (Bruno *et al.* 2004). Cooperative care giving (amongst adults) has also been reported (Park *et al.* 2013). Common dolphins do not appear to exhibit sex-biased dispersal (Natoli *et al.* 2006; Möller *et al.* 2011).

Association with particular habitats or prey compositions can be precursors to population structure and speciation if they lead to populations being physically or ecologically separated from one another. Indeed population structure of common dolphins has been shown to coincide with oceanographic parameters (e.g. Möller *et al.* 2011).

1.7 Assessment of Taxonomy and Population Differentiation

1.7.1 Morphological Analysis of Population Structure

Traditionally, systematists and biometricians studied inter- and intra-species relationships through comparative analyses of morphological characteristics. Such characteristics were either qualitative i.e. descriptions of morphological features e.g. whether a character was present or absent, or quantitative i.e. measurements of the size (e.g. lengths, areas) or shape (e.g. angles, ratios) of a character (continuous data) or counts of meristic characters (discrete data) such as tooth and vertebrae counts (see Thiele, 1993). Quantitative morphological data were subject to multivariate analyses, such as Principal Components Analysis (PCA), Canonical Variates Analysis (CVA), and Discriminant Function Analysis (DFA) (Bookstein, 1998; Adams *et al.* 2004). Through these analyses, assessment could be made of the inter- and intra-sample variation in the measured characters (Adams *et al.* 2004).

Although quantitative assessment of morphology was possible utilizing these traditional methods, there were problems with the methodology. In particular, there were difficulties, and disagreements over, how to account for allometric effects in the datasets (Adams *et al.* 2004). Ways around this problem included removing juvenile individuals from a dataset or standardizing all measurements as a ratio to a size proxy e.g. skull length (Sundberg, 1989). The traditional methodology had other problems, including uncertainty in the homology of measured traits and a loss of shape information (Adams *et al.* 2004). All of these problems were largely to do with the inadequacy of linear measurements to quantify the geometry of morphology.

In the 1980s, geometric morphometric techniques were developed to assess variation in morphological shape based on two- or three-dimensional landmark coordinates (Rohlf & Marcus, 1993; Bookstein, 1998; Mitteroecker & Gunz, 2009). In order to perform statistical analyses on the coordinates, all non-shape variation i.e. size and orientation, is to be removed from the dataset. This is done through a superimposition method, usually a Generalized Procrustes Analysis (GPA) (Rohlf, 2003; Adams *et al.* 2004; Zelditch *et al.* 2012). Although size variation is eliminated, size information, in terms of scale, can be re-introduced. The measure that captures this information is the centroid size of each configuration of landmarks and is calculated as the square root of the summed squared distances from the centroid to each landmark in the configuration (Zelditch *et al.* 2012). Once configurations have been superimposed, multivariate analyses can be conducted on the coordinates. Other analyses can also be conducted using geometric morphometric data to visualize shape differences and changes. Such analyses include the generation of deformation grids through thin-plate spline interpolation (see Bookstein, 1989; 1991; Mitteroecker & Gunz, 2009).

Although useful to investigate congruence between the two, there are several advantages and disadvantages to using morphological analyses over molecular analyses to infer inter- and intra-species differentiation (see Hillis, 1987). For instance, both techniques utilize different methods, which rely on different assumptions. Morphological data is a measure of an individual's phenotype where there is some degree of uncertainty over whether variation is heritable (and therefore phylogenetically informative) or shaped by the environment (through phenotypic plasticity, gene-environment interactions, or environmental effects on development). Amongst other evolutionary and ecological questions, assessment of taxonomic and population structure is increasingly carried out using molecular techniques, particularly in the advent of high-throughput next-generation sequencing technologies where an enormous amount of data can be collected. Although this is the case, morphological assessment of museum and fossil specimens can be the only way to measure inter- and intra-population relationships when DNA is not preserved (Hillis, 1987).

1.7.2 Molecular Analysis of Population Structure

Molecular analysis of populations, as we know it today, began in the 1960s with gel electrophoretic separation of allozymes (see Lewontin & Hubby, 1966). These methods were widely used for several years until the invention of the Polymerase Chain Reaction (PCR) by

Kary Mullis in 1983, which allowed for the amplification of a specific region of DNA using a thermo-stable DNA polymerase and site-specific primers. This reaction, and its derivatives, revolutionized the development of powerful DNA analyses. Further advances in the field came with DNA sequencing techniques, which enabled us to ‘read’ DNA sequences of interest. Several types of molecular marker have been developed, and are used to address a variety of questions on population structure, evolutionary history, population dynamics and behaviour (Hoelzel *et al.* 2002). More recently, next generation sequencing technology has provided us with an ability to answer a great number of evolutionary and ecological questions on genomic, transcriptomic and epigenetic levels (Mardis, 2008; Reis-Filho, 2009). Next generation sequencing technologies are largely peripheral to this thesis and so will not be reviewed further (but see Chapter 2).

Utilising markers with high levels of variation allows for better resolution of differentiation at the species, population and individual level. Such genomic regions are found in: (i) non-coding markers, such as nuclear DNA (nuDNA) introns, or ‘neutral’ markers such as variable number tandem repeat loci e.g. microsatellites, (ii) genomic regions with high mutation rates, e.g. mitochondrial DNA (mtDNA) which is also generally utilised as a ‘neutral’ marker, and with a reduced effective population size ($\frac{1}{4}$ nuDNA N_e) due to haploidy and uniparental inheritance, mtDNA is more affected by genetic drift than nuDNA, (iii) or functional genomic regions which have high variation due to a selective pressures e.g. the Major Histocompatibility Complex (MHC) gene family (see Hedrick, 1994). For many population genetic analyses, for example STRUCTURE (Pritchard, *et al.* 2000), neutral theory is assumed, (i.e. no selection) such that loci are not linked and exhibit Hardy-Weinberg equilibrium.

1.8 Rationale

As the coastlines develop in the northwest Indian Ocean, fisheries activities, areas of construction, shipping and oil exploration continue to overlap with identified habitat for coastal cetacean species (IWC, 1999; Collins *et al.* 2002; Anderson, 2014). Arguably, the expanding fisheries industry is the greatest cause for concern to coastal cetacean populations in the region. Preliminary investigations into the causes of mortality in beach cast specimens off Oman revealed that 78% of cases, where a cause of death could be determined ($n = 90$), had evidence for interaction with fisheries (Collins *et al.* 2002). Furthermore, the remains of *Tursiops* spp. were the most frequently encountered ($n = 112/317$) (Collins *et al.* 2002). In the

western and central Indian Ocean, there could be as many as 60,000 small cetaceans killed per year as bycatch in the tuna gillnet fisheries industry (Anderson, 2014).

Currently, little is known about the effects of these anthropogenic activities on regional populations. In order to prioritise and design effective conservation strategies for coastal cetaceans in the region, which are duly needed (IWC, 1999; Ponnampalam, 2009), management units and evolutionary significant units need to be identified (IWC, 1999; Mace, 2004; Morin & Dizon, 2009). These can be inferred utilising multiple lines of evidence based on genetic, morphological, ecological and behavioural data (see Dizon *et al.* 1992; Mortiz, 1994; Fraser & Bernatchez, 2001; Reeves *et al.* 2004; Palsbøll *et al.* 2007). Furthermore, estimates of effective population sizes and other demographic parameters (e.g. dispersal rates among populations and signals of decline/expansion) will have implications for management (e.g. Palsbøll *et al.* 2007).

Assessment of the conservation status and taxonomy of *Tursiops* spp. in the northwest Indian Ocean has been limited. Furthermore, broad-scale phylogenetic and population-genetic analyses of *Tursiops* to date (e.g. Natoli *et al.* 2004; Moura *et al.* 2013) do not include samples from the region. Assessment of *Delphinus* spp. taxonomy in the region has included morphological (Jefferson & Van Waerebeek, 2002) and genetic (Amaral *et al.* 2012a) studies. Nevertheless, population genetic studies on *Delphinus* spp. in the northwest Indian Ocean using microsatellite markers and mtDNA control region sequences have not been carried out and should provide further insight into the demography (e.g. expansion signals, dispersal) and taxonomy of common dolphins in the northwest Indian Ocean to inform future management.

This thesis also sets out to investigate putative drivers of sympatric population differentiation and speciation in top predators inhabiting a heterogeneous marine environment (Longhurst, 2006; Mendez *et al.* 2011). Despite the high dispersal ability observed in coastal dolphins, they regularly show high site-fidelity (e.g. Tsai & Mann, 2013) and population/taxonomic structure repeatedly coincides with environmental discontinuities (e.g. Bilgmann *et al.* 2007; Natoli *et al.* 2008a; Mendez *et al.* 2011) or historic climate change (e.g. Moura *et al.* 2013). Furthermore, because of the recent radiation in Delphininae (McGowen *et al.* 2011), and associated incipient speciation experienced by multiple genera (e.g. *Tursiops* spp. and *Delphi-*

nus spp.), taxonomic resolution between taxa is limited (e.g. LeDuc *et al.* 1999; McGowen *et al.* 2011). The distributions of dolphins are frequently associated with the distribution of foraging habitat and prey (Hastie *et al.* 2004; Torres *et al.* 2008), making them susceptible to changes in their environment (Simmonds & Elliott, 2009). These attributes make delphinids interesting candidates for the study of evolutionary processes that give rise to population structure and speciation (often in apparent sympatry) in response to historic climate change and contemporary environmental heterogeneity. Furthermore, such inference may be used to predict how delphinid populations may respond to future climate change or other anthropogenic stressors (Hoelzel, 2010).

1.9 Principal Hypotheses

1.9.1 Chapter 2 Phylogeography of Bottlenose Dolphins (*Tursiops* spp.) in the Northwest Indian Ocean: Evidence for a Cryptic Lineage.

Utilising bottlenose dolphin mitogenomic data presented in Moura *et al.* (2013a) I include further data from the northwest Indian Ocean in a phylogeographic study. Further analyses are also performed utilising additional samples from the region and multiple loci from mtDNA and nuDNA, testing for congruence between the loci.

From the inferred phylogenies, I estimate divergence times and perform reconstructions of ancestral distributions in order to test whether divergence events, particularly within the *T. aduncus* lineage, coincide with spatio-temporal changes driven by climate change during the Pleistocene. Changes in climate over the Pleistocene have been attributed to delphinid taxonomic structure elsewhere (e.g. Amaral *et al.* 2012a; Moura *et al.* 2013a; Louis *et al.* 2014; Moura *et al.* 2014). Such inference may indicate whether divergence in a marine predator with high dispersal ability is occurring in sympatry or in allopatry. Furthermore, these analyses may permit speculation over putative mechanisms for divergence in coastal delphinids across the Indo-Pacific.

Moura *et al.* (2013a) proposed a coastal origin for the *Tursiops* lineage. I test this hypothesis by estimating ancestral values for morphological characters using morphological data for all populations represented in the phylogeny, including published and novel data (Chapter 4). A morphological resemblance for extant *T. aduncus* over *T. truncatus* in ancestral traits would suggest the *Tursiops* ancestor was coastal and that traits associated with the pelagic variant were derived.

Coastal cetaceans in the region are under threat from an expanding fisheries industry (IWC, 1999; Collins *et al.* 2002; Anderson, 2014), pollution (Preen, 1991; IWC, 1999; Freije, 2015) and habitat fragmentation (IWC, 1999; Baldwin *et al.* 2004). Although taxonomic assessment has been carried out for a number of delphinids in the region, this is still due for bottlenose dolphins. I will endeavour to elucidate this information here, which will be of use to local conservation efforts.

1.9.2 Chapter 3 Population Structure of Bottlenose Dolphins (*Tursiops spp.*) in the Western Indian Ocean.

Habitat heterogeneity across the western Indian Ocean may be expected to generate population structure in delphinids (e.g. Bilgmann *et al.* 2008; Natoli *et al.* 2008a; Andrews *et al.* 2010; Mendez *et al.* 2011). Mendez *et al.* (2011) investigate correlations between population structure in humpback dolphins and oceanographic parameters. They suggest environmental breaks are responsible for the population differentiation and contemporary migration patterns exhibited in humpback dolphin populations between South Africa and Oman. Because the habitat of Indo-Pacific bottlenose and humpback dolphins overlap (Wang & Yang, 2009), I test the hypothesis that they exhibit similar patterns of population genetic structure and migration. Mendez *et al.* (2011) do not consider samples from India/Pakistan, however, given the discontinuities in habitat between the western and eastern Arabian Sea (Longhurst, 2006), I test the hypothesis that populations off Pakistan/India are also significantly differentiated from populations in the western Indian Ocean. Populations are also tested for evidence of hybridisation and introgression.

Approximate Bayesian Computation analyses are used to explore the sequence of population colonisation events along the western Indian Ocean coastline and determine whether reproductive isolation between diverged lineages in the region was maintained or driven by the presence of a barrier (or habitat gap) in the Arabian Sea. These inferences may reveal how homogenisation between diverged lineages is prevented during periods of apparent secondary contact.

1.9.3 Chapter 4 Comparative Cranial Morphology of Three Bottlenose Dolphin Lineages, (*Tursiops spp.*), in the Northwest Indian Ocean Utilising Traditional and Geometric Morphometric Techniques

Cranial morphological analyses utilizing both traditional and geometric morphometric techniques is performed on *T. aduncus* specimens from Oman and Pakistan and *T. truncatus*

specimens from Oman. I test the hypothesis that strong, species level, morphological differentiation is exhibited between *T. aduncus* and *T. truncatus* types, thus providing further evidence for the presence of both forms in the northwest Indian Ocean. Furthermore, I test whether the genetic differences identified between *T. aduncus* lineages in the northwest Indian Ocean (Chapters 2 and 3) are reflected in their morphology. If genetic and morphological differentiation patterns are congruent, this could suggest local adaptation to specific environments or assortative mating are maintaining reproductive isolation between lineages. Conversely, where morphological differences are incongruent with the genetic data, differences in morphology may be indicative of phenotypic plasticity, gene-environment interactions, or environmental effects on development.

Due to the habitat differences between Pakistan and Oman, we might expect to see evidence of local adaptation in cranial morphology, particularly if it is linked to prey composition or foraging strategy. For instance, *D. c. tropicalis* in the India-Pakistan region have longer rostra compared to adjacent populations (Jefferson & Van Waerebeek, 2002). Although not formally demonstrated, longer rostra are often associated with species that occupy regions of high turbidity e.g. river dolphins.

1.9.4 Chapter 5 Population Structure of Common Dolphins (Delphinus spp.): Novel Insights from the Northwest Indian Ocean

Population genetic analyses of common dolphins sampled off Oman, *D. c. tropicalis*, long-beaked morphotypes off South Africa, *D. delphis* and short-beaked morphotypes in the northeast Atlantic, *D. delphis*, utilising microsatellite markers, are performed to test whether the populations are significantly differentiated. These analyses will be the first to use microsatellite markers on the *D. c. tropicalis* population as part of a broad-scale comparison. I shall test whether the results provide support for the taxonomic status of *D. c. tropicalis* off Oman. Furthermore I investigate whether any individuals show signs of mixed-ancestry in their genotype data and I test for migration bias as observed in humpback dolphins in the region (Mendez *et al.* 2011).

Novel mtDNA control region sequences of *D. c. tropicalis* from Oman/Pakistan are included as part of a broader analysis using published sequences from *Delphinus* populations around the world. I conduct tests for population expansions, as have been reported for *D. c. tropicalis*

and other populations elsewhere based on mtDNA (e.g. Amaral *et al.* 2012a) and discuss these in light of historic climate change.

1.9.5 Synopsis

Overall, I test whether populations of bottlenose and common dolphins in the region exhibit population differentiation in sympatry (*cf.* parapatry) that correlates with historic climate events or environmental heterogeneity. In particular, results presented here will provide insight into the evolutionary history of bottlenose dolphins, and the mechanisms that drive population differentiation and speciation in coastal dolphins across the Indo-Pacific. Additionally, results presented on population structure and taxonomy of both common and bottlenose dolphins will be informative to conservation initiatives in the region.

Chapter 2

Phylogeography of Bottlenose Dolphins (*Tursiops* spp.) in the Northwest Indian Ocean: Evidence for a Cryptic Lineage

2.1 Introduction

Insights from phylogeographic studies include the identification of regions, and historical processes, associated with species richness and evolutionary endemism (Ricklefs & Schluter, 1993; Bermingham & Moritz, 1998). Such information can advise conservation initiatives (Moritz & Faith, 1998) and contribute to predictions over species responses to contemporary and future environmental changes (Hoelzel, 2010). This is especially pertinent in the advent of climate change and other anthropogenic threats, such as habitat fragmentation and loss (e.g. Vandergast *et al.* 2007). In addition, phylogeographic studies provide a means of answering questions about evolutionary processes and mechanisms of speciation (Bermingham & Moritz, 1998).

Advances in molecular genetic techniques have resulted in the recognition of many new species in cryptic taxonomies (Mace, 2004). Although there is contention around what defines a cryptic taxon, Bickford *et al.* (2007) define them as two or more species that are, at least superficially, indistinguishable from one another based on morphology. Such cryptic taxa are of particular concern where they exist within species complexes already regarded as endangered. This is because the risk of extinction is often greater in these cryptic taxa due to reductions in distribution and population size. Different management strategies may also be required of novel cryptic species (Bickford *et al.* 2007). For example, the threatened Malagasy lemur, *Lepilemur septentrionalis* was divided into two cryptic species based on mitochondrial DNA markers (Ravaoarimanana *et al.* 2004) and cytogenetic data (Rumpler *et al.* 2001). This reduced one lineage down to a small, endangered population in a heavily fragmented habitat, unprotected by legislation (Ravaoarimanana *et al.* 2004). In a meta-analysis Pfenninger & Schwenk (2007) showed that cryptic species were evenly distributed across taxa and biogeographical regions.

Assumptions about the presence of gene flow, based on dispersal ability, or whether populations occur in sympatry, can contribute to whether cryptic species are expected. Therefore,

cryptic species are often morphologically similar taxa that either diverged in allopatry (and are currently free to disperse and come into secondary contact) (e.g. Stewart *et al.* 2010), or in sympatry (e.g. Jones & Van Parijs, 1993).

The contemporary distributions of species may not reflect those of conspecifics in the past if shifts in habitat availability have been driven by climate change. Indeed, populations may have experienced repeated range fluctuations in response to historic ecological changes generating complex population dynamics and genetic structure (Hofreiter & Stewart, 2009). During periods of isolation, populations can diverge in allopatry such that reproductive isolation impedes gene flow upon secondary contact. Reproductive isolation may manifest itself through resource polymorphisms, although these can also emerge in sympatry (Skúlason & Smith, 1995; Hoelzel, 1998a; Niemiller *et al.* 2008). Reproductive isolation between diverged populations may be incomplete upon secondary contact, giving rise to hybridization zones and introgression between the diverged lineages (Poelstra, 2014), potentially resulting in homogenization (Servedio & Kirkpatrick, 1997; Servedio & Noor, 2003), speciation by reinforcement (Hoskin *et al.* 2005), or possibly hybrid speciation (Amaral *et al.* 2014).

The Pleistocene was subject to rapid and dramatic climatic fluctuations generating extensive environmental changes, which would have influenced the temporal and spatial distribution of taxa over glacial cycles (Hofreiter & Stewart 2009; Stewart *et al.* 2010). In the marine environment such changes will have contributed to the spatial genetic structure and taxonomic variation in marine species. Fluctuations in sea level changed coastal topography and caused patterns of isolation between areas of available habitat (e.g. Gaither & Rocha, 2013). Furthermore, oscillations in climate had dramatic effects on oceanographic processes such as the reduction and intensification of monsoon systems associated with upwelling (Wang *et al.* 1999a).

The Delphinidae (oceanic dolphins) are an excellent group for phylogeographic study of marine speciation. Recent radiation within this widely distributed group began approximately 10 Ma (McGowen *et al.* 2009) resulting in approximately 36 extant species (McGowen *et al.* 2012). Species within the sub-family Delphininae radiated even more recently, making genetic resolution difficult due to incomplete lineage sorting (retention of ancestral polymorphisms in a given gene/locus, resulting in probable incongruence between the gene-tree

and true species tree) and other confounding phenomena (e.g. Amaral *et al.* 2012b). Species within this group have high dispersal ability yet often exhibit taxonomic structure over unexpectedly small spatial scales (e.g. Natoli *et al.* 2004; Natoli *et al.* 2008a; Andrews *et al.* 2010; Fernández *et al.* 2011). Various studies have shown that genetic sub-division within delphinids is often associated with environmental heterogeneity (e.g. Bilgmann *et al.* 2008; Natoli *et al.* 2008a; Andrews *et al.* 2010; Mendez *et al.* 2011) and/or historical climate or geologic events. Indeed, several studies attribute delphinid taxonomic structure to changes in climate during the Pleistocene (e.g. Amaral *et al.* 2012a; Moura *et al.* 2013a; Louis *et al.* 2014; Moura *et al.* 2014). Delphinids are highly adapted to their environment and, as top predators, rely upon healthy ecosystems for survival (Moore, 2008). This makes them useful as putative sentinels for ecosystem health and change (e.g. Ross, 2000; Wells *et al.* 2004; Moore, 2008) while also being of conservation concern due to habitat loss and climate change (e.g. Simmonds & Elliott, 2009).

Within the Delphininae, the taxonomy of bottlenose dolphins, *Tursiops* spp. has been subject to much confusion. Although more work is needed (see Reeves *et al.* 2004), resolution is drawing closer, with the genus receiving much taxonomic attention over the last few decades (e.g. Mead & Potter, 1990; Ross & Cockcroft, 1990; Hoelzel *et al.* 1998; Wang *et al.* 1999b, Möller & Beheregaray, 2001; Kemper, 2004; Natoli *et al.* 2004, Charlton-Robb *et al.* 2011; Moura *et al.* 2013a). The majority of studies support the paraphyly of *Tursiops* spp. (LeDuc *et al.* 1999; McGowen, 2011; Moura *et al.* 2013a), with the genus encompassing at least two species, the common bottlenose dolphin, *T. truncatus* and the Indo-Pacific bottlenose dolphin, *T. aduncus* (LeDuc *et al.* 1999; Wang *et al.* 1999b; 2000). There is recent support for a third species, the Burrunan dolphin, *T. australis*, from southern Australia (Charlton-Robb *et al.* 2011) and further division within the *T. aduncus* group to include distinct lineages off South Africa and Australasia (Natoli *et al.* 2004; Moura *et al.* 2013a). Analysis of mtDNA from the *T. aduncus* holotype specimen (Red Sea) revealed it to be a match for the South African *T. aduncus* (Perrin *et al.* 2007), suggesting reclassification of the Australasian lineage is required. Within the *T. truncatus* lineage, further division can be made into regional ecotypes occupying coastal or pelagic habitat (Mead & Potter, 1995, Hoelzel *et al.* 1998; Torres *et al.* 2003). Also of note is the recognised sub-species *T. t. ponticus* from the Black Sea (Viaud-Martinez *et al.* 2008).

Moura *et al.* (2013a) confirmed the distinction of these described species, putative species and ecotypes of bottlenose dolphin based on a phylogeographic analysis using mitogenomic sequences. Divergence patterns inferred from dating nodes and reconstructing ancestral biogeography suggest the *Tursiops* lineage originated in Australasian coastal habitats. The South African *T. aduncus*, hereafter referred to as the holotype lineage, diverged from the Australasian lineage ~327 Ka, following an expansion across the region. This divergence time, along with several other nodes differentiating pelagic from coastal populations within the *T. truncatus* lineage, was consistent with glacial terminations, or the periods of global warming that followed them (Moura *et al.* 2013a).

The coastline of the northwest Indian Ocean is environmentally heterogeneous (Longhurst, 2006), characterised by high productivity off the Arabian Peninsula (Singh *et al.* 2011; Banse & McClain, 1986; Bauer *et al.* 1991; Burkill, 1999; Kindle & Arnone, 2001). The coastal waters off India are characterised by freshwater influx from rivers carrying large quantities of organic material (Longhurst, 2006). This, unique, heterogeneous environment has the potential to drive taxonomic structure in dolphin species through resource specialisations (Hoelzel, 1998a). Indeed the evolutionary endemism of other marine mammals is already recognized in the region (e.g. Jefferson & Van Waerebeek, 2002; Mendez *et al.* 2011; Minton *et al.* 2011; Amaral *et al.* 2012a; Mendez *et al.* 2013; Pomilla *et al.* 2014). Analysis of bottlenose dolphin taxonomy in the northwest Indian Ocean using genetic techniques has been limited to an east African study on bottlenose dolphins (Särnblad *et al.* 2011; *in review*), which showed coastal bottlenose dolphins off Oman ($n = 4$) to be a genetic match for *T. aduncus* off South Africa and, therefore, the holotype lineage. Sightings data from the region suggest the presence of both coastal and pelagic *Tursiops* species; the latter being *T. truncatus* based on morphology (Minton *et al.* 2010) and limited genetic data ($n = 13$) (Ballance & Pitman, 1996; Curry, 1997; Ballance & Pitman, 1998).

In the present study I incorporate novel mitogenomic data from the northwest Indian Ocean with the dataset used by Moura *et al.* (2013a). Further analyses are also performed, using multiple loci from mtDNA and nuDNA, while including additional samples from both *T. aduncus* and *T. truncatus*-types to improve representation from the region.

Delphinid population genetic structure appears to be correlated, at least in part, with either contemporary environmental heterogeneity, for example, through environmental breaks (Natoli *et al.* 2008a; Mendez *et al.* 2011) and the establishment of resource polymorphisms (e.g. Moura *et al.* 2015), or historic environmental change, such as adaption to new environments or changes to the permeability of dispersal corridors (e.g. Amaral *et al.* 2012a; Moura *et al.* 2013a). I will investigate whether ancestral distributions and divergence times at key nodes, particularly within the *T. aduncus* lineage, corroborate with historic climatic events over the Pleistocene. As top predators, changes to delphinid population structure should provide insight into the broader ecological changes happening in the Indian Ocean during this time (e.g. Fontaine *et al.* 2007). Furthermore, these analyses may shed light on whether cryptic taxonomic structure in a highly mobile marine taxon is being driven by divergent evolution in sympatry or allopatry.

Moura *et al.* (2013a) proposed a coastal origin for the *Tursiops* lineage based on ancestral biogeographic reconstructions. Using morphological data for all populations represented in the phylogeny, including published and novel data (Chapter 4), I perform ancestral character estimations to determine whether coastal traits, as seen in *T. aduncus*, are ancestral or derived.

Assessment of coastal bottlenose dolphin taxonomy in the northwest Indian Ocean has been a priority for some time (IWC, 1999; Reeves *et al.* 2004), particularly in the presence of increasing fisheries related mortalities (IWC, 1999; Collins *et al.* 2002; Anderson, 2014), pollution (Preen, 1991; IWC, 1999; Freije, 2015) and habitat fragmentation (IWC, 1999; Baldwin *et al.* 2004). I attempt to elucidate this information here, which will be valuable for regional conservation initiatives.

2.2 Materials and Methods

2.2.1 Sample Acquisition

Samples of bottlenose dolphins (*Tursiops* spp.) were collected in Oman, from strandings ($n = 1$) or free-ranging ($n = 3$) individuals, by the Environment Society of Oman (ESO) and affiliates. Further biopsy samples ($n = 4$) were collected off Oman by the author in collaboration with ESO (see below). All samples from Pakistan ($n = 2$) were collected from strandings provided by Cetacean Conservation Pakistan (CCP). Indian samples ($n = 11$) were provided by the Environmental Specimen Bank at the Center for Marine Environmental Studies, Ehime

University of Japan. Additional laboratory work was carried out on a subset of samples used in Moura *et al.* (2013a), available at Durham University, representing a number of well-described regional populations, species and/or ecotypes worldwide (Table 1). All *Tursiops* mitogenome sequences generated by Moura *et al.* (2013a) and two *Tursiops* sequences generated by Xiong *et al.* (2009), available on GenBank, were also utilised in this study (see Table 1 for locations and Appendix VI for Accession numbers). Figure 4 shows the geographic locations of samples.

2.2.2 Biopsy Sampling, Oman

Biopsy sampling was conducted off the town of Hasik, in the southern region of Dhofar, in February and October, 2012. Dolphins were approached in a 6.5 m Rigid-hulled Inflatable Boat (RIB) with twin 75 hp HONDA four-stroke engines. On two occasions, biopsy sampling was successfully conducted onboard a fibreglass fishing skiff.

For biopsy, Finn Larson bolts and tips (70 mm diameter, 25 mm length) were fired from a 40 lbs/18 kg draw-weight PETRON recurve crossbow. Shooting protocols were adapted from Wenzel *et al.* (2010). Dolphins were approached slowly, traveling at approximately 4 kts, when pre-biopsy behaviour was deemed appropriate. If animals were observed as feeding or socialising, biopsy was delayed until the behaviour of the group changed. Animals were shot aiming high on the lateral side, just below the dorsal fin, at a perpendicular angle to the survey vessel. Individuals approaching head-on were not permissible targets. As the crossbow draw-weight was low, it was considered acceptable to shoot the dolphins at close range (e.g. bow-riding individuals) without excessive wounding (*cf.* Patenaude & White, 1995). The ideal range for shooting was considered to be within 5-6 m from the vessel. Biopsy of cow-calf pairs was avoided. Animals were only shot when their surfacing behaviour was predictable. Biopsy attempts were not made in the presence of other vessels, particularly dolphin watching vessels and fishermen. Samples were preserved in a salt-saturated 20% DMSO solution or in > 90% ethanol.

Table 1: Bottlenose dolphin species and ecotypes considered in the present study. Following Moura *et al.* (2013a), T=*Tursiops truncatus*; Ta=*Tursiops aduncus*; GC=Gulf of California; WNAC=northwest Atlantic (coastal ecotype); WNAP=northwest Atlantic (pelagic ecotype); SCO=Scotland; EMED=eastern Mediterranean; BSEA=Black Sea; OM=Oman; PAK=Pakistan; IND=India; SA=South Africa; SABD=Burrunan dolphin, *T. australis*; AUS=Australasian Indo-Pacific bottlenose dolphin; CHINA=Australasia (China). Two datasets are considered, one composed of mitogenomes the other composed of a subset of concatenated mtDNA and nuDNA markers. Sample numbers contributing to each dataset also presented below. * = identification of dolphins as *T. truncatus* based on phylogenetic analysis as opposed to field-based observation.

Code	Location	Species/Ecotype	Reference	N (Total)	N (Mitogenomes)	N (mtDNA + nuDNA)
WNAP-Tt	Western North Atlantic	<i>T. truncatus</i> (pelagic)	Hoelzel <i>et al.</i> (1998)	10	10	3
WNAC-Tt	Western North Atlantic	<i>T. truncatus</i> (coastal)	Hoelzel <i>et al.</i> (1998)	9	9	2
SCO-Tt	Scotland	<i>T. truncatus</i> (coastal)	Reid <i>et al.</i> (2003); Natoli <i>et al.</i> (2005)	8	8	0
EMED-Tt	Eastern Mediterranean	<i>T. truncatus</i> (coastal)	Natoli <i>et al.</i> (2005)	10	10	3
BSEA-Tt	Black Sea	<i>T. truncatus ponticus</i> (coastal)	Natoli <i>et al.</i> (2005)	10	10	2
SA-Ta	South Africa	<i>T. aduncus</i> (coastal)	Natoli <i>et al.</i> (2005)	10	10	2
AUS-Ta	Eastern Australia/Australasia	Indo-Pacific <i>T. aduncus</i> (coastal)	Wang <i>et al.</i> (1999b); Möller & Beheregaray (2001)	10	10	3
GC-Tt	Gulf of California	<i>T. truncatus</i> (coastal)	Segura <i>et al.</i> (2006)	1	1	1
SABD	Southern Australia	Southern Australian/Burrunan Dolphin <i>T. australis</i> (coastal)	Charlton <i>et al.</i> (2006); Möller <i>et al.</i> (2008)	7	7	2
CHINA-Tt	China (Polar and Oceanic Park, Shandong Province)	<i>T. truncatus</i> (unknown)	Xiong <i>et al.</i> (2009)	1	1	0
CHINA-Ta	China (Dongshan, Fujian Province)	Indo-Pacific <i>T. aduncus</i> (coastal)	Xiong <i>et al.</i> (2009)	1	1	0
PAK-Ta	Pakistan	<i>T. aduncus</i> (coastal)	This Study	2	2	2
IND-Ta	India	<i>T. aduncus</i> (coastal)	This Study	10	0	10
IND-Tt	India	<i>T. truncatus</i> (unknown)*	This Study	1	0	1
OM-Ta	Oman	<i>T. aduncus</i> (coastal)	This Study	6	1	6
OM-Tt	Oman	<i>T. truncatus</i> (pelagic)	This Study	2	0	2

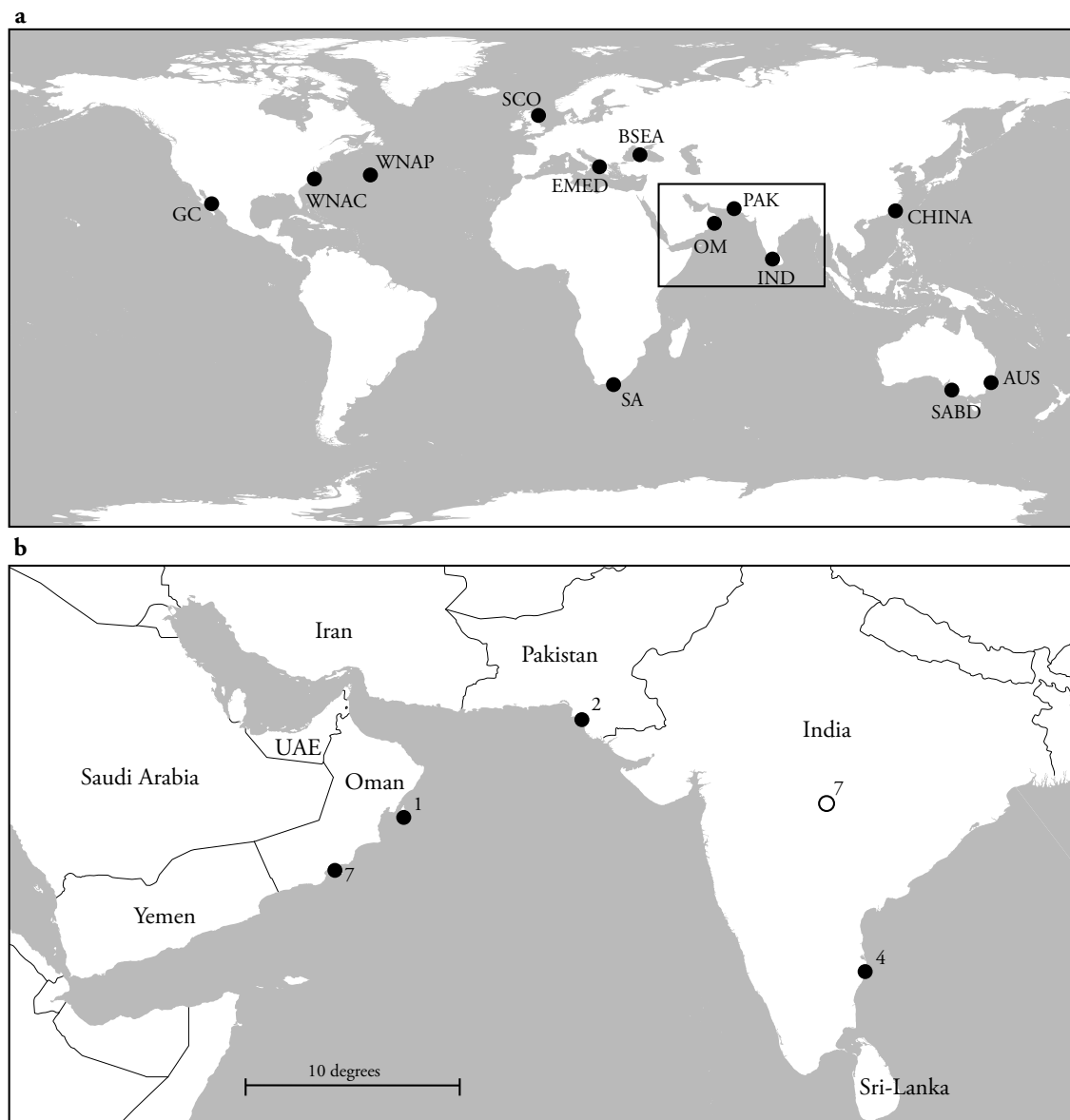


Figure 4: Bottlenose dolphin (*Tursiops* spp.) sample locations. Box a) Sample locations from worldwide populations. GC = Gulf of California; WNAC = northwest Atlantic (coastal ecotype); WNAP = northwest Atlantic (pelagic ecotype); SCO = Scotland; EMED = eastern Mediterranean; BSEA = Black Sea; OM = Oman; PAK=Pakistan; IND = India; SA = South Africa; SABD = Burrnunan dolphin, *T. australis*; AUS = Australasian Indo-Pacific bottlenose dolphin; CHINA = Australasia (China); Rectangle delineates study area. Box b) Approximate locations of novel samples analysed in the present study. Shaded circles = known sample locations; Clear circles = unknown sample locations from respective country; numbers = sample numbers associated with each circle.

2.2.3 DNA Extraction

Phenol-chloroform DNA extraction protocols, as adapted from Hoelzel (1998b), were carried out on tissue samples. Approximately 100 mg of tissue were finely chopped and added to 500 μ l of extraction buffer (50 mM Tris pH 7.5, 1 mM EDTA, 100 mM NaCl, 1% (w/v) SDS). A further 45 μ l of proteinase-K was added to the solution and the tissues were left to digest overnight in a water-bath at 37°C with occasional agitation. 500 μ l of phenol was added to

the digestions, mixed thoroughly, and then centrifuged for 5 min at 7000 x g to separate the phases. The aqueous phase was pipetted off and transferred to a new tube while the organic layer was either kept for future 'back' extractions or appropriately discarded. This process was repeated a second time with phenol, followed by a mixture of phenol:chloroform:isoamyl-alcohol (25:24:1 by vol.), then using chloroform:isoamyl alcohol (24:1 by vol.) and the final separated aqueous phase was transferred to a new tube. A 0.1 vol. (~45 μ l) of 3M sodium acetate was added and mixed. 1 ml of chilled 100% ethanol was then added to precipitate the DNA and put in a freezer to incubate at -20°C for approximately 1 hr. The solution was centrifuged at 7000 x g for 15 min to pellet the DNA. The supernatant was removed and replaced with chilled 70% ethanol and centrifuged again to clean the DNA pellet. The supernatant was removed and the DNA pellets were dried in a centrifugal evaporator. DNA was resuspended in an appropriate volume (~200 μ l) of TE buffer (10 mM Tris pH 8.0, 1 mM EDTA pH 8.0).

2.2.4 Mitogenome Sequencing and Assembly

For one Oman sample (OM64) a mitogenome sequence was generated following the protocols in Moura *et al.* (2013a). For two Pakistan samples (PAK5 and PAK6) mitogenome libraries were prepared for Illumina sequencing following Meyer & Kircher, (2010) with modifications (see below).

2.2.5 Library Preparation

DNA extractions were quantified using a QUBIT (Life Technologies Inc.) Fluorometer. Subsequently, 50 μ l aliquots were made to a concentration of 10 ng/ μ l and were randomly sheared to a range of 100-600 base pairs (bp) using a sonicator (Diagenode Biopruptor Pico) for eight cycles of 7 min with an 'on/off' interval of 30 sec. Fragment size distributions were checked on a BIOANALYSER (Agilent Technologies) and samples were concentrated down to 20 μ l using a centrifugal evaporator.

Repair of blunt ends was carried out using a reaction mix (New England BioLabs) of 7 μ l 10x NEBuffer 2, 2 μ l T4 Polynucleotide Kinase (10 U/ μ l), 1.3 μ l of T4 DNA Polymerase (3 U/ μ l), 9.7 μ l of Ultrapure Water and 20 μ l of DNA sample. Incubation was carried out on a heat block for 15 min at 25°C and then for 5 min at 12°C . Blunt-end repair was followed by a speed bead clean-up step (ThermoScientific).

Both P5 and P7 adapters were ligated using the following reaction mix (New England BioLabs), 0.5 µl of dsAdapter P5 (50 µM) and 0.5 µl dsAdapter P7 (50 µM), 4 µl 10x T4 Ligase Buffer, T4 Ligase (5 U/µl), 4 µl of 50% PEG-4000 and 10 µl of Ultrapure Water. The reaction mix was incubated at 22°C for 1 hr followed by a bead clean-up step and a streptavidin bead clean-up step (MyOne C1, Dynabeads) to remove extra adapters. Libraries remained immobilised to the beads at the end of this clean-up.

Adapter fill-in was carried out by resuspending the libraries in 50 µl of the reaction mix (New England BioLabs) of 5 µl of 10x ThermoPol buffer, 6.25 µl of dNTPS (2 mM), 2 µl of Bst Polymerase (8 U/µl) and 36.75 µl of Water. The reaction mix was then incubated at 37°C for 20 min and the beads were cleaned again. Libraries were then eluted in 20 µl of elution buffer.

Quantitative PCR (qPCR) was carried out on the libraries to determine the optimal number of cycles for PCR amplification i.e. keeping the reaction in the exponential phase of PCR, while avoiding the plateau phase, thus limiting errors due to PCR instability. A total reaction volume of 25 µl composed of 2.5 µl 10x PCR Buffer, 2.5 µl MgCl₂ (25 mM), 2.5 µl dNTPs (2 mM), 1 µl P5 primer (10 µM), 1 µl P7 primer (10 µM), 0.6 µl of 1:2000 SYBR Green, 0.1 µl Taq Gold (5 U/µl) (Life Technologies Inc) and 1 µl of library. Temperature profile for the qPCR was as follows, 94°C denaturation for 8 min, 55 cycles of 94°C for 30 sec, 58°C annealing for 30 sec and 72°C extension for 1 min and a final extension of 72°C for 7 mins.

PCR amplification was carried out to extend the adapters and to amplify the libraries. A total reaction volume of 50 µl comprised of 25 µl of 2x Phusion Master Mix (New England BioLabs) and 2.5 µl of P5 primer (10 µM), 2.5 µl of P7 primer (10 µM) and 20 µl of adapter-filled library. The PCR profile was, 98°C denaturation for 1 min, followed by 98°C for 30 sec, 58°C annealing for 30 sec and 72°C extension for 1 min for the most optimal number of cycles as determined by the previous qPCR, and then a final extension of 72°C for 10 min.

After PCR, the libraries were purified using a bead clean-up step and eluted in 20 µl of elution buffer. Libraries were checked on a BIOANALYSER for shift in fragment size (due to adapter attachment) and quantified on a plate reader (Fluoroscanner Ascent, LabSystems) using a Quant-it PicoGreen kit (Life Technologies Inc.).

2.2.6 Target Enrichment

Capture of mitogenomic DNA was performed on the libraries (500 ng) using a target-enrichment kit (MYbaits, MYcroarray Inc.). Bait probes were synthesised (20,000 probes, 100 bp each, 2x coverage) based on an alignment of killer whale, *Orcinus orca* mitogenomes available on GenBank (Accession Numbers GU187171, GU187200, GU187194, GU187181, GU187209). Captured libraries were subjected to a qPCR followed by a PCR step and then a clean-up (as above).

2.2.7 Pooling and Sequencing

Before pooling, captured libraries were quantified using qPCR by running it against 'home-made' standards consisting of 180 bp PCR product made into a library and calibrated against a KAPA Library Quant kit (KAPA Biosystems). Libraries were pooled in equimolar concentrations and a final qPCR was run to verify the concentration of the pooled libraries. These were then run on a 2200 TAPESTATION (Agilent Technologies) to verify fragment sizes. Pooled libraries were sequenced on an ILLUMINA HiSEQ 2500 in rapid run mode using 150 bp paired-end reads, TruSeq v3 chemistry.

2.2.8 Mitogenome Assembly

De-multiplexing of the raw Illumina output, removal of adapters, and trimming for quality was carried out post-sequencing. Reads for each individual were then transferred to GENEIOUS v. 7.1.2 (<http://www.geneious.com>, Kearse *et al.* 2012) for assembly. For PAK5, 836,934 paired reads were generated with an average trimmed length of 90 bp and for PAK6, 784,583 paired reads were generated with an average trimmed length of 83 bp. Reads were paired and mapped to a *Tursiops aduncus* mitogenome reference sequence available on GenBank (accession number EU557092). Mapping was set to 'medium-low sensitivity/fast' with up to five iterations, whereby the reads were mapped to the consensus of the previous iteration. Reads for PAK5 were mapped to 100% of the reference sequence with an average coverage of 69 reads (min = 2x, max = 198x). Reads for PAK6 were mapped to 95.4% of the reference sequence with an average coverage of 9.6 reads (min = 0x, max = 53x). Consensus sequences were generated using the '50% - Strict' threshold whereby bases had to match at least 50% of sequences at that position to be called unambiguously. Consensus quality scores were assigned as the difference in quality between contributing bases and non-contributing bases. A minimum depth of coverage threshold of 5x was used.

2.2.9 Amplification of mtDNA Markers

A total of 4,301 bp of mtDNA were sequenced for 21 individuals from Oman ($n = 8$), Pakistan ($n = 2$) and India ($n = 11$). PCR amplifications were performed for five mtDNA fragments spanning five loci, the control region, cytochrome-*b*, 12S rRNA, 16S rRNA and ND6 (see Figure 5). Primers ($n = 9$) were designed in PRIMER3 v. 2.3.4 (Untergasser *et al.* 2012) as implemented in GENEIOUS v. 7.1.2 (<http://www.geneious.com>, Kearse *et al.* 2012) and used in conjunction with published primers to amplify the fragments. All amplifications were performed in a 20 μ l final reaction volume containing 1.0 μ l of template DNA, 1.25 U of GoTaq Flexi DNA polymerase (Promega), 1x GoTaq Flexi buffer (Promega), 0.2 mM dNTP, 1-2 mM MgCl₂ and 0.16-0.2 μ M of each primer (PCR details for each fragment are detailed in Table 2). The PCR temperature profile for each fragment included an initial heating step at 95°C for 2 min, followed by 45 cycles of 95°C for 30 sec, annealing temperature for 40 sec and 72°C for 1 min, and a final extension of 72°C for 10 min. PCR products were purified with QIAGEN PCR purification columns (Qiagen, GmbH, Germany) and sequenced using an ABI automated sequencer. Primer sequences, annealing temperatures and product sizes are summarised in Table 2.

2.2.10 Amplification of nuDNA Markers

Two nuclear loci were chosen that showed good resolution in a multi-species tree presented in Banguera-Hinestroza (2008) (also see Banguera-Hinestroza *et al.* 2014). A segment of 995 bp from intron 1 from the Actin gene and 472 bp from intron 2 from the α -Lactalbumin gene were amplified for all individuals, including a subset of individuals also included in Moura *et al.* (2013a) (see Table 1). The Actin gene codes for a muscle protein and the α -Lactalbumin gene codes for a mammary secretory protein. A final reaction volume of 20 μ l contained 1.0 μ l of template DNA, 1.25 U of GoTaq Flexi DNA polymerase (Promega), 1x GoTaq Flexi buffer (Promega), 0.2 mM dNTP, 2 mM MgCl₂ and 0.16 μ M of each primer. The PCR temperature profile began with an initial denaturation step at 94°C for 2 min, followed by 45 cycles at 92°C for 30 sec, and annealing temperature for 30 sec and an extension at 72°C for 30 sec. A final extension time of 72°C for 5 min was also given. PCR products were purified with QIAGEN PCR purification columns (Qiagen, GmbH, Germany) and sequenced using an ABI automated sequencer. Primer sequences, annealing temperatures and product sizes are summarised in Table 2.

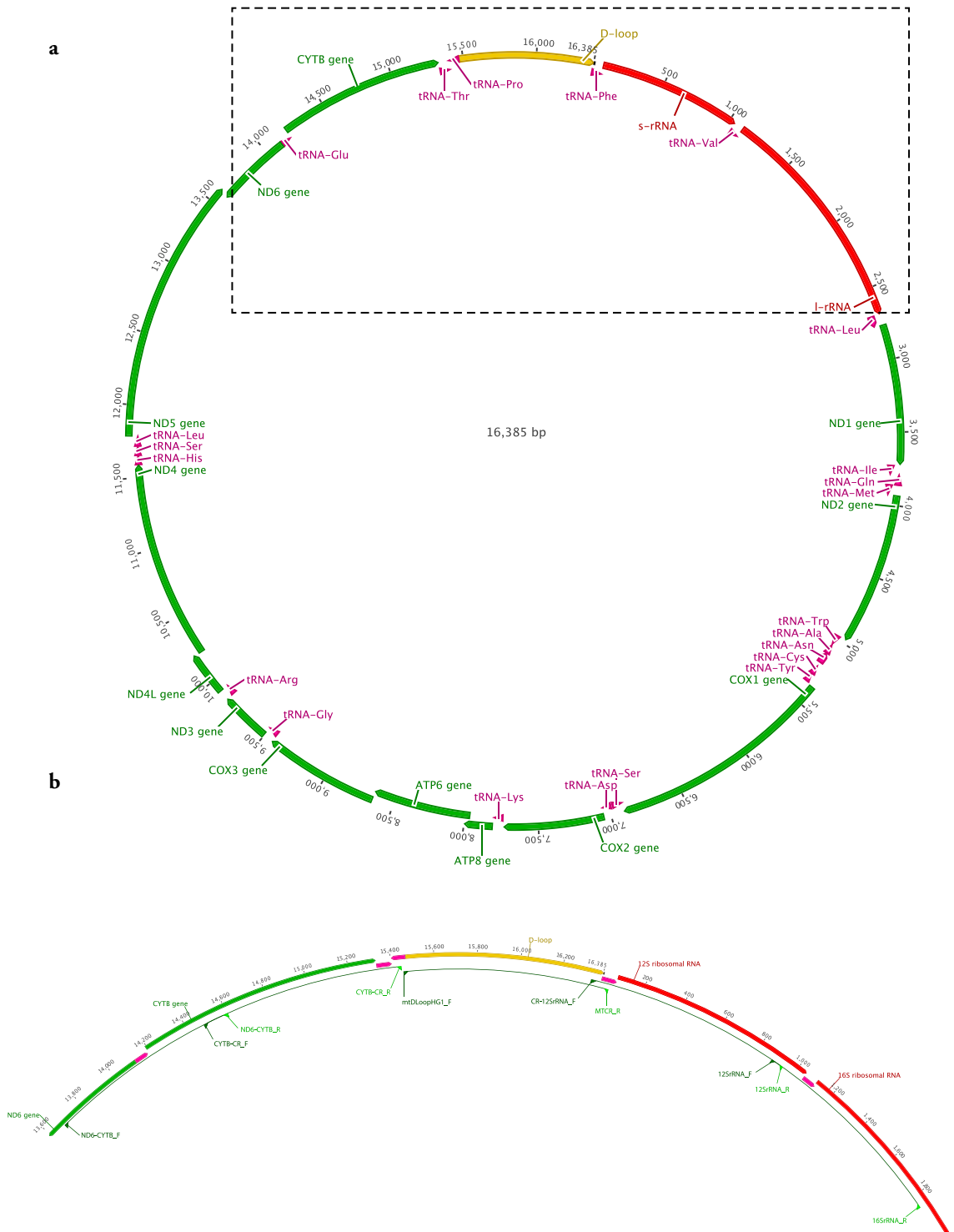


Figure 5: Illustration of mitogenome (a) and partial mitogenome (b) used in the present study. Figure generated in GENEIOUS v 7.1.2 (<http://www.geneious.com>, Kearse *et al.* 2012). Binding locations for the primer-pairs used to amplify the five fragments are illustrated in the partial figure.

Table 2: Details of primers used to amplify the mtDNA and nuDNA markers. Anneal Temp. = annealing temperature (°C); Frag. Size = size of amplified fragment (bp).

Locus	Code	Oligonucleotide	Anneal Temp. (°C)	Frag. Size (bp)	Source
mtDNA	ND6	F ACTGTACAAGCGCAGCAATCCCC	70	882	This study
		R CCTCAGGGCAGGACGTAGCC			This study
	Cytochrome-<i>b</i>	F ACGCCACATTTGGACCTGGC	57	928	This study
		R CCAGCTTTGGGTGTTGGTGGTGA			This study
	Control Region	F TTCTACATAAACTATTC	44	941	This study
		R ATTTTCAGTGTCCTTGCTTT			Hoelzel <i>et al.</i> (1991)
	12S rRNA	F ACAAGCCCCCATAATGAAATCATACA	59	923	This study
		R AGGAGGGTGACGGGCGGT			This study
	16S rRNA	F AAGAATAGAATGCTTAATTG	46	900	This study
		R AATAGTTTAGTGTAGGTTAT			This study
nuDNA	Actin	F GATTGGTCCCCTCTATGTCICT	58	995	Harlin-Cognato & Honeycutt (2006)
		R TACTTTTGAACCTTGCCACCCTAC			Harlin-Cognato & Honeycutt (2006)
	α-Lactalbumin	F GGGTCTGTACCGTATTTTCATA	54	665	Milinkovitch <i>et al.</i> (1998)
		R GACTCACCCAGTAGGTAATTC			Milinkovitch <i>et al.</i> (1998)

2.2.11 Estimation of Phylogeny

2.2.11.1 Alignment

Mitogenomes sequences from Oman and Pakistan were aligned with all bottlenose dolphin mitogenomes available on GenBank generated in Moura *et al.* (2013a) (Appendix VI). Also included were the mitogenomes of harbour porpoise, *Phocoena phocoena*, narwhale, *Monodon monoceros*, and four river dolphins, Franciscana, *Pontoporia blainvillei*, Indus river dolphin, *Platanista minor*, Amazon river dolphin, *Inia geoffrensis* and Yangtze river dolphin, *Lipotes vexilifer*, as outgroups (see Appendix VI for sample details and GenBank Accession numbers). The alignment was carried out using the MUSCLE algorithm (Edgar, 2004) as implemented in GENEIOUS v. 7.1.2 (<http://www.geneious.com>, Kearse *et al.* 2012).

Each nuDNA locus was phased using the PHASE algorithm (Stephens *et al.* 2001; Stephens & Donnelly, 2003) as implemented in DNASP v. 5 (Librado & Rozas, 2009). Assuming no linkage between the loci, haplotype duplexes for one locus were randomly concatenated with the other for each individual. Sequences of mtDNA for each individual were assigned to their respective nuDNA haplotypes and concatenated together. Where not amplified in this study, homologous mtDNA regions were excised from mitogenomes, available on GenBank. A dusky dolphin, *Lagenorhynchus obscurus*, outgroup was generated from sequences available on GenBank (See Appendix VI). All sequences were aligned using the MUSCLE algorithm (Edgar, 2004) as implemented in GENEIOUS v. 7.1.2 (<http://www.geneious.com>, Kearse *et al.* 2012).

2.2.11.2 Bayesian Inference of Phylogeny

MRBAYES v. 3.2.2 (Huelsenbeck & Ronquist, 2001) was implemented online using the CIPRES (Cyberinfrastructure for Phylogenetic Research) Scientific Gateway v. 3.3 (Miller *et al.* 2010) to estimate phylogeny from the mitogenome dataset and the concatenated mtDNA/nuDNA dataset. Four independent chains were run over 22,000,000 generations with a burn-in period of 2,200,000 generations and a sample frequency of 4000 generations. Three of the four chains were heated and the analysis was run twice. The best partitioning scheme was inferred using the 'greedy' algorithm as implemented in PARTITIONFINDER v. 1.0.1 (Lanfear *et al.* 2012; 2014) considering the evolutionary models available to MRBAYES. Model and partitioning selection was carried out using the Bayesian Information Criterion (BIC) metric.

2.2.11.3 *Maximum Likelihood Estimation of Phylogeny*

A maximum likelihood (ML) phylogenetic tree was generated for both the mitogenome dataset and the mtDNA/nuDNA dataset using RAXML (Randomized Axelerated Maximum Likelihood) v. 8.0.24 (Stamatakis, 2014) as implemented on CIPRES v. 3.3 (Miller *et al.* 2010). The alignments were partitioned following the best partitioning scheme identified in PARTITIONFINDER v. 1.0.1 (Lanfear *et al.* 2012; 2014) considering the evolutionary models available to RAXML. Bootstrap node support values were generated over 5000 iterations.

2.2.11.4 *Congruence Between mtDNA and nuDNA Markers*

Partitioned Bremer support indices (PBSIs) (Baker & DeSalle, 1997) were calculated for each node in a phylogeny generated from the concatenated mtDNA/nuDNA dataset in PAUP* v. 4.0b10 (Swofford, 2011). This was conducted to examine congruence between the mtDNA and nuDNA markers. PBSIs are a measure of the contribution of each locus to the estimated topology and can be positive, negative or zero, whereby positive values indicate support for a node and negative values indicate the contrary in a combined analysis (Baker *et al.* 1998). The sum of all PBSIs at a node is equal to the total Bremer support value for that node (Baker *et al.* 1998). A heuristic maximum parsimony analysis was performed with Tree-Bisection-Reconnection branch swapping and 1000 random-addition-sequence replications. The maximum number of saved trees 'maxtrees' was set to automatically increase by 100. Support for nodes were obtained from 500 bootstrap replicates. Outgroups were defined as dusky dolphin and harbour porpoise using sequences available on GenBank (Appendix VI). All characters were unordered and equally weighted and a strict consensus phylogeny was generated from the tree output. This phylogeny was used to generate a PAUP* (Swofford, 2011) command file in TREEROT v. 3 (Sorenson & Franzosa, 2007), which was subsequently run. PBSI values were parsed from the PAUP* output in TREEROT and plotted on a majority-rule consensus phylogeny based on the heuristic analysis.

2.2.12 *Reconstruction of Ancestral Distributions*

To reconstruct the biogeographic state of ancestral nodes and to determine whether divergence events occurred through vicariance (speciation through subdivision of an ancestral distribution range) or dispersal, statistical dispersal-vicariance analysis (S-DIVA) (Ronquist, 1997) was implemented in RASP (Reconstruct Ancestral State Phylogenies) v. 2.2 (Yu *et al.*

2010). 10,000 trees were sampled at random from a Bayesian phylogenetic Markov Chain Monte Carlo (MCMC) analysis generated from a mitogenome alignment comprised of all *Tursiops* individuals with a rough-toothed dolphin, *Steno bredanensis* (Accession Number JF339982) as an outgroup. S-DIVA analysis was run on all trees and ancestral nodes were plotted on a majority-rule consensus tree, generated from the MCMC output in RASP. Sampling locations were used to provide populations with unique distributions (see Figure 4). Following Moura *et al.* (2013a), a further distinction was made between ecotypes (coastal or pelagic) where either genetic or survey data were available for respective populations. Both the Australasian *T. aduncus* (including individuals from China) and the Burrunan dolphin *T. australis* were considered as occupying Australasia. The maximum number of areas considered for each node was constrained to four in order to limit the number of distributions assigned to the ancestral nodes. This is because optimization of ancestral areas becomes less reliable as we approach the root node (Ronquist, 1996). The out-group was assigned a null distribution by using a location unique to it.

A Bayesian Binary MCMC (BBM) analysis was also performed in RASP using the same dataset. A 'null' root distribution was assigned to the outgroup and a maximum of four areas for each node was configured. The BBM analysis was run for 5,000,000 generations with a burn-in of 5,000. The sampling frequency was set to 100 and 10 chains were run with a temperature of 0.1. The Fixed Jukes-Cantor model for state frequencies was applied with the gamma shape parameter for among-site rate variation. The analysis was run twice under the same conditions to check estimations were converging on similar distributions. Both S-DIVA and BBM analyses were repeated on a Bayesian phylogeny derived from the concatenated mtDNA and nuDNA dataset.

2.2.13 Estimation of Divergence Dates using Mitogenomic Data

Divergence dates were estimated using BEAST (Bayesian Evolutionary Analysis Sampling Trees) v. 1.8 (Drummond & Rambaut, 2007) on CIPRES (Miller *et al.* 2010) from the mitogenome dataset, which was partitioned based on results generated in PARTITIONFINDER v. 1.0.1 (Lanfear *et al.* 2012; 2014). The initial tree was generated at random and the Yule-branching model was set as the tree prior (see Moura *et al.* 2013a). The two terminal clades including Eastern Mediterranean and Black Sea groups were each constrained to monophyly with the same time to most recent common ancestor (TMRCA) priors. The TMRCA priors

for these nodes were given a uniform distribution set between 3 and 10 Ka, defined according to the opening of the Bosphorous strait, following Moura *et al.* (2013a). Two fossil calibration points were also used. These were the TMRCA for Delphinoidea (McGowen *et al.* 2009; Steeman *et al.* 2009; Xiong *et al.* 2009) and the TMRCA for the clade that includes all *Tursiops* species (Barnes, 1990; Fitzgerald, 2005). The ancestor to Delphinoidea was defined by constraining the clade that includes Monodontidae and Delphinidae to monophyly and the *Tursiops* ancestor was defined by constraining the clade that included all *Tursiops*, and other delphinids nested within that group, to monophyly. Normal distributions were assigned to both fossil TMRCA priors, with means of 10 Ma for the Delphinoidea ancestor and 5 Ma for the *Tursiops* ancestor, each with a standard deviation of 1.5 Ma (see Table 3). The exponential distribution of mutations model was used for the uncorrelated relaxed clock model, following Moura *et al.* (2013b). MCMC analyses were run with 150,000,000 iterations and 10% burn-in, sampling every 5000 generations. Four independent runs were performed and outputs combined in LOGCOMBINER v. 1.7.5 (Drummond & Rambaut, 2007). Trees were resampled in LOGCOMBINER at a lower frequency of 60,000 runs, yielding 9000 trees, which were summarised in TREEANNOTATOR v. 1.7.5 (Drummond & Rambaut, 2007).

Divergence dates were estimated using a further two models that included only fossil calibration points and biogeographic calibration points respectively (see Table 3). Models were compared using stepping-stone sampling (Xie *et al.* 2011), which is the most reliable means available of estimating marginal likelihoods for model comparison (Baele *et al.* 2013). For each model, four independent runs were performed in BEAST v. 1.8 (Drummond & Rambaut, 2007) on CIPRES (Miller *et al.* 2010) with 100 power-posteriors run for 1,000,000 iterations. Stepping-stone sampling was then used to estimate the log-marginal likelihoods from the combined outputs (Baele *et al.* 2012; 2013). Log Bayes factors were generated from the log-marginal likelihoods for model comparison. To check that an appropriate number of iterations had been performed, the runs were carried out again for twice the number of iterations (2,000,000). Log-marginal likelihood calculations were then inspected for convergence.

Table 3: Priors used to estimate divergence dates. Analysis conducted in BEAST v. 1.8 (Drummond & Rambaut, 2007). TMRCA = Time to Most Recent Common Ancestor. BSEM = Black Sea-Eastern Mediterranean calibrated divergence (based on opening of Bosphorous Strait, see Moura *et al.* 2013). Fossil = Fossil calibration times. BSEM1 and 2 = BSEM divergences 1 and 2.

Parameter		BSEM & Fossil	BSEM only	Fossil only
TMRCA	<i>Distribution</i>	Uniform	Uniform	n/a
(BSEM1 & BSEM2)	<i>Lower-Upper</i>	0.003-0.01	0.003-0.01	n/a
TMRCA	<i>Distribution</i>	Normal	n/a	Normal
(<i>Tursiops</i>)	<i>Mean, Stdev</i>	5, 1.5	n/a	5, 1.5
TMRCA	<i>Distribution</i>	Normal	n/a	Normal
(Delphinoidea)	<i>Mean, Stdev</i>	10, 1.5	n/a	10, 1.5
Molecular clock		exponential	exponential	exponential

2.2.14 Estimation of Ancestral Cranial Morphology

Cranial measurements of continuous traits (Table 4) were obtained from Chapter 4 and published sources for all populations represented in the mitogenomic dataset (see Table 5). Where available, measurements for other Delphinidae represented in the dataset, and outgroups, were also incorporated. Only those characters where measurements were available across all major clades were used in analyses. Average measurements for each population were standardized as a percentage of average condylobasal length (CBL) for each population. Only population-averages were available in several cases. Therefore, in order to test whether such standardization was appropriate, regression analyses were conducted for each character against CBL using data where measurements were available for each specimen (Ross, 1977, Viaud-Martinez *et al.* 2008, This Study). Where a character had an isometric relationship with CBL, such standardization was deemed appropriate. The ancestral states of fifteen continuous cranial characters (Table 5) were estimated for all analyses, using a Bayesian phylogeny, inferred from the mitogenomic dataset, pruned of outgroups as required where character data were not available.

Several methods were implemented to estimate ancestral character states so that comparisons between the methodologies could be made. Methods included (i) Maximum Parsimony (MP), (ii) Phylogenetic Independent Contrasts (PIC) (Felsenstein, 1985), (iii) Generalised Least Squares (GLS) (Martins & Hansen, 1997) and (iv) MCMC Bayesian inference (Pagel *et al.* 2004).

Maximum parsimony is a widely used method for reconstructing ancestral states, which at-

tempts to keep evolutionary events to a minimum (Cunningham *et al.* 1998). Maximum parsimony reconstruction was implemented in MESQUITE v. 2.75 (Maddison & Maddison, 2015). Both PIC and GLS methods assume a model of Brownian motion for character state change. The methods also both consider branch lengths, which is in contrast to the MP method. The PIC method corrects for the non-independence of closely-related taxa (Felsenstein, 1985) and the GLS method reconstructs ancestral states as an average of the values of all extant species, weighted according to the phylogenetic relationships and evolutionary distances between ancestors and terminal nodes (Martins & Hansen, 1997). Both PIC and GLS methods were implemented using the *ace* function in the *ape* package (Paradis *et al.* 2004) in R v. 3.0 (R Core Team, 2013).

Bayesian inference of ancestral states was conducted in BAYESTRAITS v. 2.0 (Pagel *et al.* 2004). Using the Bayesian phylogenetic tree and terminal node data for a character, a distribution of models was generated. An initial MCMC was configured with 10,000,000 iterations with a burn-in of 10,000, sampling every 1000 generations. The continuous random-walk model (Model A) was used and assumes a GLS Brownian motion model of evolution (Pagel, 1997; 1999). Tuning of the transition rate parameters was performed automatically so that the rate deviation parameter (RateDev) fell between 20-40% at convergence. The generated models were then used to estimate ancestral character states at internal nodes by re-running the MCMC chain under the continuous random walk model, with 10,000,000 iterations, 10,000 burn-in, sampling every 1000 iterations. The ancestral state was estimated for nodes defined by key species or ecotype divergence events within *Tursiops*. Analyses were run three times with different random starting seeds to confirm ancestral state estimations were converging on similar values.

All ancestral reconstruction analyses were repeated using a Bayesian phylogeny inferred from the concatenated mtDNA and nuDNA dataset. The dusky dolphin was used as an outgroup and *D. capensis* was included as an ingroup.

Table 4: Morphological characters common to all populations for use in ancestral reconstruction. Descriptions from Perrin (1975).

Character	Description (Perrin, 1975)
RL	Rostrum length, from tip to line across hindmost limits of antorbital notches
RWM	Rostrum width at mid-length
PRW	Width of premaxillaries at mid-rostral length
TREN	Tip of rostrum to external nares, to mesial end of anterior transverse margin of right naris
TRIN	Tip of rostrum to internal nares, to mesial end of posterior margin of right pterygoid
GPRW	Greatest preorbital width
GPOW	Greatest postorbital width
ZW	Greatest width across zygomatic process of squamosal
GWPX	Greatest width of premaxillaries
GLPTF	Greatest length of left posttemporal fossa, measured to external margin of raised suture
GWPTF	Greatest width of left posttemporal fossa, at right angles to greatest width
UTLTR	Length of upper left tooth row, from hindmost margin of hindmost alveolus to tip of rostrum
LTRL	Length of lower left tooth row, from hindmost margin of hindmost alveolus to tip of mandible
ML	Greatest length of left ramus
MH	Greatest height of left ramus at right angles to greatest length

Table 5: Population averages for morphological characters. Values taken from the literature to represent recognized species, populations and ecotypes considered in this study. Condylobasal lengths (CBL) are presented in millimetres (mm) and all other measurements are presented as percentages of CBL. For the concatenated mtDNA and nuDNA dataset, measurements for IND-Tt were not available, therefore IND-Tt individuals were assigned the same character values as OM-Tt because as these populations are likely to be morphologically similar. Sources are: 1) Hersh & Duffield, 1990; 2) Viaud-Martinez *et al.* 2008; 3) Ross, 1977; 4) Charlton-Robb *et al.* 2011; 5) Perrin *et al.* 2011; 6) Wang *et al.* 2000; 7) This Study, Chapter 4; 8) Lal Mohan, 1988; 9) Ort & Danilewicz, 1996; 10) Jefferson & Van Waerebeek, 2004; 11) Perrin, 1975; 12) Jefferson & Van Waerebeek, 2002; 13) Paul, 1968; 14) Zerbini & Santos, 1997; 15) Pardo *et al.* 2009.

Population/ Species/ Ecotype (DNA)	Source	CBL	RL	RWM	PRW	TREN	TRIN	GPRW	GPOW	ZW	GWPX	GLPTF	GWPTF	UTLTR	LTRL	ML	MH
WNAP-Tt	1	500.5	54.85	16.28	8.59	65.13	65.23	46.65	53.05	53.05	17.78	21.68	16.78	46.85	45.75	84.02	18.28
WNAC-Tt	1	452	55.11	16.59	8.56	66.13	65.8	44.27	51.81	51.75	19.27	22.77	17.92	47.94	48.67	84.07	18.85
SCO-Tt	2	536.29	55.4	17.64	9.63	65.72	67.28	45.83	51.67	52.81	19	22.48	17.57	47.92	47.47	86.63	19.41
EMED-Tt	2	519.44	56.29	16.42	8.76	66.56	67.66	44.2	50.12	50.68	18.6	22.8	17.61	46.8	47.01	85.27	18.78
BSEA-Tt	2	452.35	55.51	14.36	7.92	66.18	66.07	43.57	50.75	50.29	19.56	23.09	16.76	46.27	44.26	83.69	18.28
SA-Ta	3	472	57.3	13.9	7.3	67.1	66.6	42.9	48.7	48.5	17.7	22.5	16.5	47.7	47.8	84.9	17.8
AUS-Ta	4	441	57.66	14.2	7.55	66.94	67.39	43.97	48.3	46.37	17.56	21.7	17.43	47.41	49.86	84.63	18.2
GC-Tt	5	509.4	53.49	17.03	9.48	64.52	na	45.42	51.86	52.77	19.11	23.46	16.22	47.05	46.34	85	18.99
SABD	4	493.58	56.8	16.09	9.82	66.45	67.55	43.23	48.41	46.3	19.19	23.22	16.81	47.93	47.18	85.76	18.59
CHINA-Tt	6	506.2	56.06	16.59	na	66.22	na	45.79	50.3	50.83	18.47	na	na	48.12	48.08	85.8	18.06
CHINA-Ta	6	485.1	58.13	13.23	na	67.72	na	41.62	46.05	47.54	17.77	na	na	48.84	50.26	85.55	17.03
PAK-Ta	7	468.4	57.25	13.72	7.72	66.96	66.64	39.91	44.15	47.26	18.27	21.44	15.24	47.37	49.27	84.98	17.62
IND-Ta	8	454	61.34	na	na	na	na	40.48	42.82	46.63	17.2	20.09	na	50.9	51.16	85.67	na
OM-Ta	7	464.87	57.44	14.42	7.64	67.25	65.41	43.01	48.43	48.73	18.55	22.31	15.82	47.24	48.43	83.37	17.75
OM/IND-Tt	7	515.24	56.72	16.79	9.19	66.87	70.17	45.18	49.64	50.37	17.79	20.96	15.75	48.53	48.98	87.92	18.45
<i>S. bredanensis</i>	9	554.5	59.47	11.93	7.65	68.64	71.29	34.62	43.35	44.34	15.64	21.88	18.64	49.68	50.31	84.48	18.14
<i>S. coeruleoalba</i>	9	438.2	57.61	14.18	6.56	68.15	71.27	43.19	51.64	50.92	19.4	17.38	12.06	50.1	50.01	86.65	16.42
<i>S. chinensis</i>	10	502.3	61.52	9.18	5.89	na	na	37.53	42.21	42.33	16.01	22	17.56	54.23	na	84.55	na
<i>S. attenuata</i>	11	413.4	59.66	10.82	5.88	69.5	70.05	37.16	41.63	41.68	16.52	18.24	14.3	52.09	50.92	84.77	14.84

Population/ Species/ Ecotype (DNA)	Source	CBL	RL	RWM	PRW	TREN	TRIN	GPRW	GPOW	ZW	GWPX	GLPTF	GWPTF	UTLTR	LTRL	ML	MH
<i>D. capensis</i>	12	486	64.28	10.66	4.69	na	na	35.21	39.84	39.32	14.86	14.98	11.46	55.31	na	86.6	14.53
<i>G. griseus</i>	13	494	46.15	22.06	14.78	76.11	na	60.12	65.59	na	20.85	28.14	15.99	12.35	na	81.38	na
<i>F. attenuata</i>	14	378.3	47.21	23.71	16.36	61.91	63.79	59.19	62.36	63.07	24.85	23.13	na	8.35	36.93	79.3	na
<i>P. crassidens</i>	15	618	43.96	28.37	20.42	54.05	54.81	53.62	59.27	67.73	22.38	34.64	23.62	40.78	71.88	35.7	19.74

2.3 Results

2.3.1 Estimation of Phylogeny

Phylogenies were estimated from the mitogenome sequence data and the concatenated mtDNA/nuDNA sequence data using both Bayesian and ML methodologies. Partitioning schemes, and associated evolutionary models, for each method were identified in PARTITION-FINDER v. 1.0.1 (Lanfear *et al.* 2012; 2014) (see Table 6 for partitions and associated evolutionary models). For all Bayesian phylogenetic analyses, convergence was confirmed through examination of various diagnostic outputs, particularly the ESS (Effective Sample Size) and PSRF (Potential Scale Reduction Factor) values. All ESS values were greater than 100 (minimum values ranged from 1727.87 - 4951.00) and all PSRF values approached one, indicative of convergence and that a sufficient number of generations had been implemented. For the ML analysis, a general-time-reversible (GTR) model with gamma substitution rate heterogeneity was applied across all partitions (see Table 6). Individual alpha-shape parameters, GTR-rates, and empirical base frequencies were optimized for each partition during analysis.

The Bayesian (Figure 6 and Figure 7) and ML (Figure 8 and Figure 9) phylogenies, inferred from both datasets, showed similar topologies. Some clades within the *T. truncatus* lineage remained unresolved in the ML phylogenies. The phylogenies generated from the different datasets (concatenated mtDNA/nuDNA and mitogenomes) also had similar topologies.

The maximum parsimony tree for the mtDNA/nuDNA dataset exhibited a similar topology as presented in the Bayesian and ML trees (see Figure 10). PBSIs (Baker & DeSalle, 1997) were calculated for all nodes in TREEROT v. 3 (Sorenson & Franzosa, 2007) and the values for key nodes are presented in Figure 10. The majority of loci were supportive of these nodes and where they were not, PBSI values were > -2 (Figure 10). The nuDNA loci were largely uninformative with four and 10 segregating sites for Actin and α -Lactalbumin respectively, and PBSIs between -0.76 and 2.22. This indicates that, in the combined analysis, all loci were either congruent or uninformative in their support for key divergence events within the *T. aduncus* lineage.

Estimated phylogenies agreed with those generated in Moura *et al.* (2013a). The focus of this study is on the novel sequence data collected from the northwest Indian Ocean, particularly *T. aduncus*. The presence of a new lineage within the *T. aduncus* clade is revealed, closely

related to the Australasian lineage (Wang *et al.* 1999b). This new lineage is supported in the mitogenome and mtDNA/nuDNA phylogenies. Greater sample representation from the northwest Indian Ocean for the latter shows the new lineage occurs off Oman, Pakistan and India (Figure 7 and Figure 9, also see Appendix VII).

From the mtDNA/nuDNA phylogeny, novel sequences from Oman and India are placed within the *T. truncatus* lineages, confirming the presence of *T. truncatus* in the northwest Indian Ocean. These individuals are spread throughout the Eastern Mediterranean, Black Sea and Western North Atlantic (pelagic) lineages, which is either indicative of incomplete lineage sorting or dispersal. As argued by Moura *et al.* (2013a), dispersal is less likely given the apparent low dispersal rates among European individuals (Natoli *et al.* 2005).

Table 6: Partitioning schemes detailed for the different datasets for each analysis. c1-3 = codon positions 1-3.

Partition	Partition Composition	Model of Evolution
Mitogenome Dataset		
MRBAYES		
1	ATP6_c1 ATP8_c1 ATP8_c2 ND2_c2 ND3_c1 ND6_c1 ND6_c3 tRNA_Arg tRNA_Gln tRNA_His tRNA_Lys tRNA_Phe tRNA_Pro tRNA_Ser2	HKY+I+G
2	12SrRNA COX1_c3 COX2_c1 CYTB_c1 ND1_c1 ND4L_c1 ND4_c1 ND5_c1 tRNA_Thr	GTR+I+G
3	16SrRNA tRNA_Ala tRNA_Cys tRNA_Glu tRNA_Gly tRNA_Ser1 tRNA_Trp tRNA_Val	GTR+I+G
4	COX3_c1 tRNA_Asp tRNA_Leu1 tRNA_Leu2 tRNA_Met tRNA_Tyr tRNA_ile	HKY+I+G
5	COX1_c1 COX2_c2 COX3_c2 CYTB_c2 ND1_c2 ND4_c2 tRNA_Asn	HKY+I+G
6	ATP6_c3 ATP8_c3 COX2_c3 COX3_c3 CYTB_c3 ND1_c3 ND2_c1 ND3_c3 ND4L_c3 ND4_c3 ND5_c3 ND6_c2	GTR+I+G
7	ATP6_c2 ND2_c3 ND3_c2 ND4L_c2 ND5_c2	HKY+I+G
8	COX1_c2	HKY+I+G
9	D_LOOP (control region)	HKY+G
RaxML		
1	ATP6_c1 ATP8_c1 ATP8_c2 ND2_c2 ND4_c1 ND5_c1 ND6_c1 ND6_c3 tRNA_Arg tRNA_Gln tRNA_His tRNA_Leu1 tRNA_Lys tRNA_Phe tRNA_Pro tRNA_Ser2	GTR+I+G
2	12SrRNA 16SrRNA tRNA_Ala tRNA_Cys tRNA_Glu tRNA_Gly tRNA_Met tRNA_Ser1 tRNA_Thr tRNA_Trp tRNA_Tyr tRNA_Val	GTR+I+G
3	COX1_c3 COX2_c1 COX3_c1 CYTB_c1 ND1_c1 ND3_c1 ND4L_c1	GTR+I+G
4	COX1_c1 COX3_c2 CYTB_c2 ND1_c2 ND2_c3 ND3_c2 ND4L_c2 ND4_c2 ND5_c2	GTR+I+G
5	ATP6_c3 ATP8_c3 COX2_c3 COX3_c3 CYTB_c3 ND1_c3 ND2_c1 ND3_c3 ND4L_c3 ND4_c3 ND5_c3 ND6_c2	GTR+I+G
6	ATP6_c2 COX2_c2 tRNA_Asn tRNA_Asp tRNA_Leu2 tRNA_ile	GTR+I+G

Partition	Partition Composition	Model of Evolution
7	COX1_c2	GTR+I+G
8	D_LOOP (control region)	GTR+G
BEAST		
1	ATP6_c1 ATP8_c1 ATP8_c2 ND2_c2 ND6_c1 ND6_c3 tRNA_Arg tRNA_Asp tRNA_Gln tRNA_His tRNA_Leu1 tRNA_Lys tRNA_Phe tRNA_Pro tRNA_Ser2	HKY+I+G
2	12SrRNA 16SrRNA COX3_c1 tRNA_Ala tRNA_Cys tRNA_Glu tRNA_Gly tRNA_Leu2 tRNA_Met tRNA_Ser1 tRNA_Thr tRNA_Trp tRNA_Tyr tRNA_Val tRNA_ile	GTR+I+G
3	COX1_c3 COX2_c1 CYTB_c1 ND1_c1 ND3_c1 ND4L_c1 ND4_c1 ND5_c1	GTR+I+G
4	COX1_c1 COX2_c2 COX3_c2 CYTB_c2 ND1_c2 ND4_c2 tRNA_Asn	HKY+I+G
5	ATP6_c3 ATP8_c3 COX2_c3 COX3_c3 CYTB_c3 ND1_c3 ND2_c1 ND3_c3 ND4L_c3 ND4_c3 ND5_c3 ND6_c2	GTR+I+G
6	ATP6_c2 ND2_c3 ND3_c2 ND4L_c2 ND5_c2	HKY+I+G
7	COX1_c2	Tn+I+G
8	D_LOOP (control region)	HKY+G
Concatenated mtDNA & nuDNA Dataset		
MRBAYES		
1	ND6_c1	HKY
2	12SrRNA 16SrRNA CYTB_c1 ND6_c2 tRNA_Glu tRNA_Phe	HKY+I
3	CYTB_c2 CYTB_c3 ND6_c3	HKY+G
4	D_LOOP (control region)	HKY+I+G
5	Act_in1 Lac_ex2_c1 Lac_ex2_c2 Lac_ex2_c3 Lac_ex3_c1 Lac_ex3_c2 Lac_ex3_c3 Lac_in2 tRNA_Val	HKY+I+G
RAXML		
1	CYTB_c2 CYTB_c3 ND6_c1 ND6_c3	GTR+G
2	12SrRNA 16SrRNA CYTB_c1 Lac_ex2_c1 ND6_c2 tRNA_Glu tRNA_Phe tRNA_Val	GTR+I+G
3	D_LOOP (control region)	GTR+I+G
4	Act_in1 Lac_ex2_c2 Lac_ex2_c3 Lac_ex3_c1 Lac_ex3_c2 Lac_ex3_c3 Lac_in2	GTR+I+G

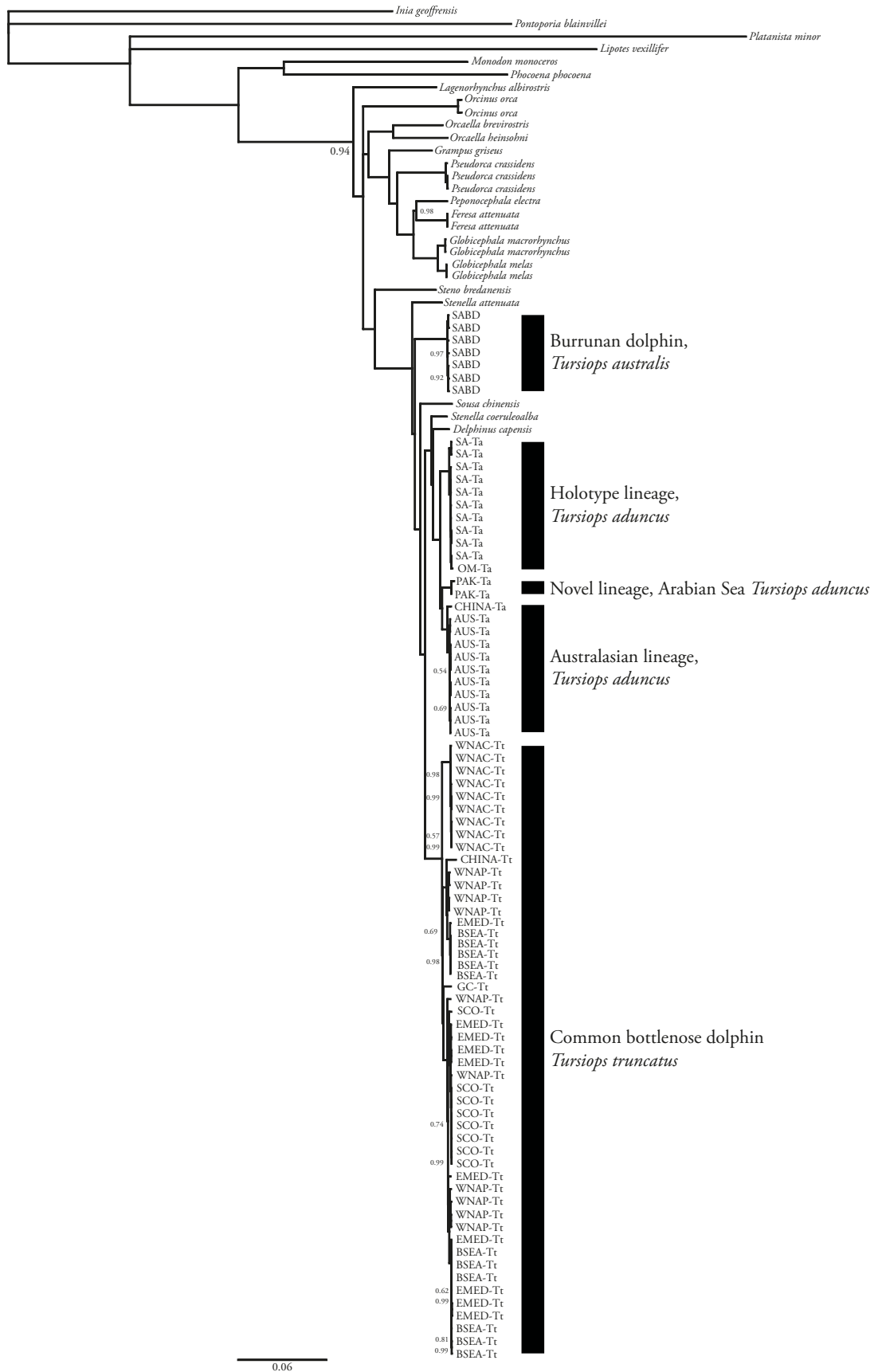


Figure 6: Bayesian majority-rule consensus phylogeny estimated from the mitogenome dataset. Generated in MRBAYES v. 3.2.2 (Huelsenbeck & Ronquist, 2001). Scale bar represents 0.06 substitutions/site. Posterior probabilities below 1 are shown.

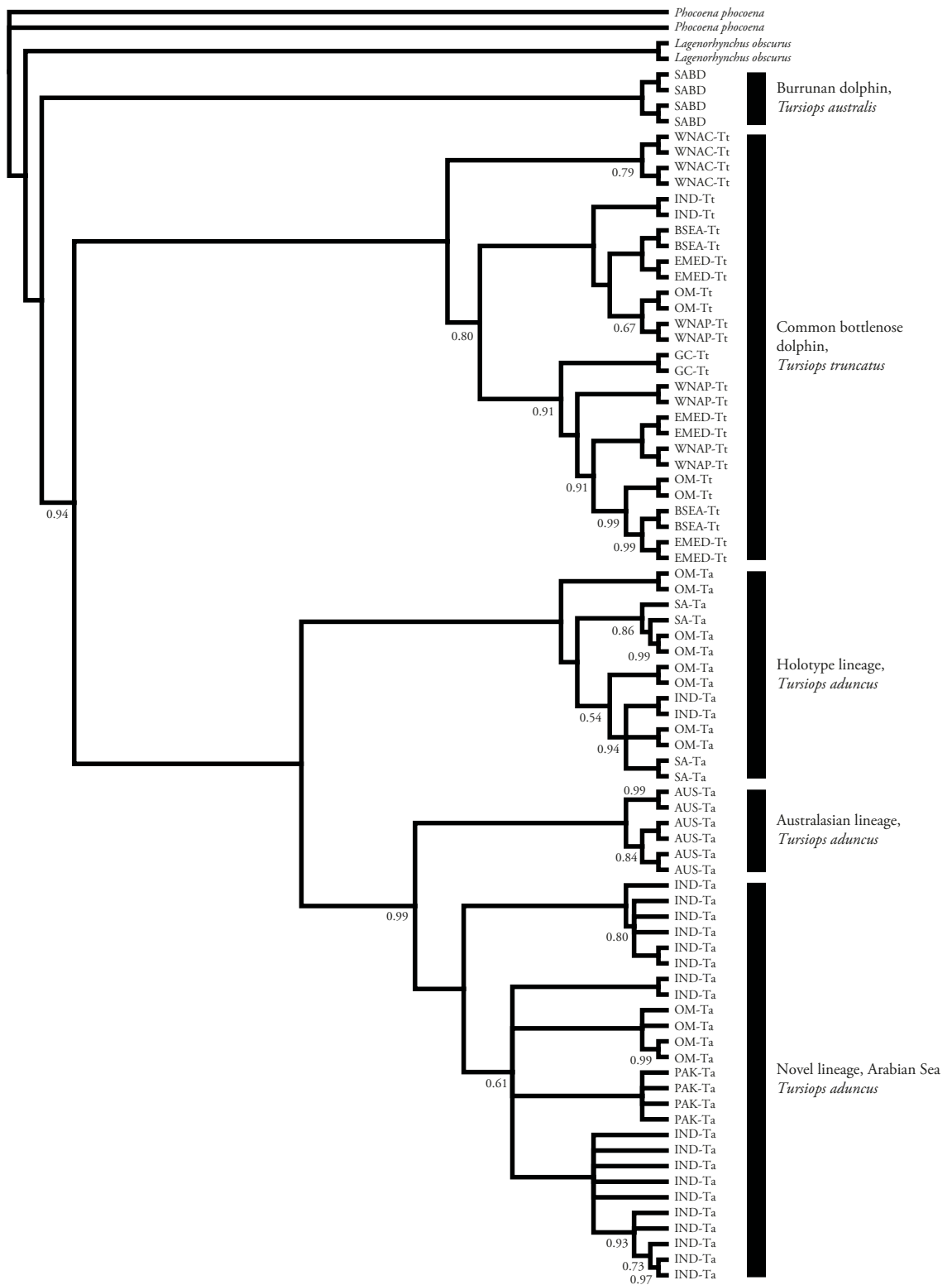


Figure 7: Bayesian estimated phylogeny generated from concatenated mtDNA-nuDNA sequences. Generated in MRBAYES v. 3.2.2 (Huelsenbeck & Ronquist, 2001). Posterior probabilities less than 1 are displayed. Branch-lengths not to scale to enhance topology.

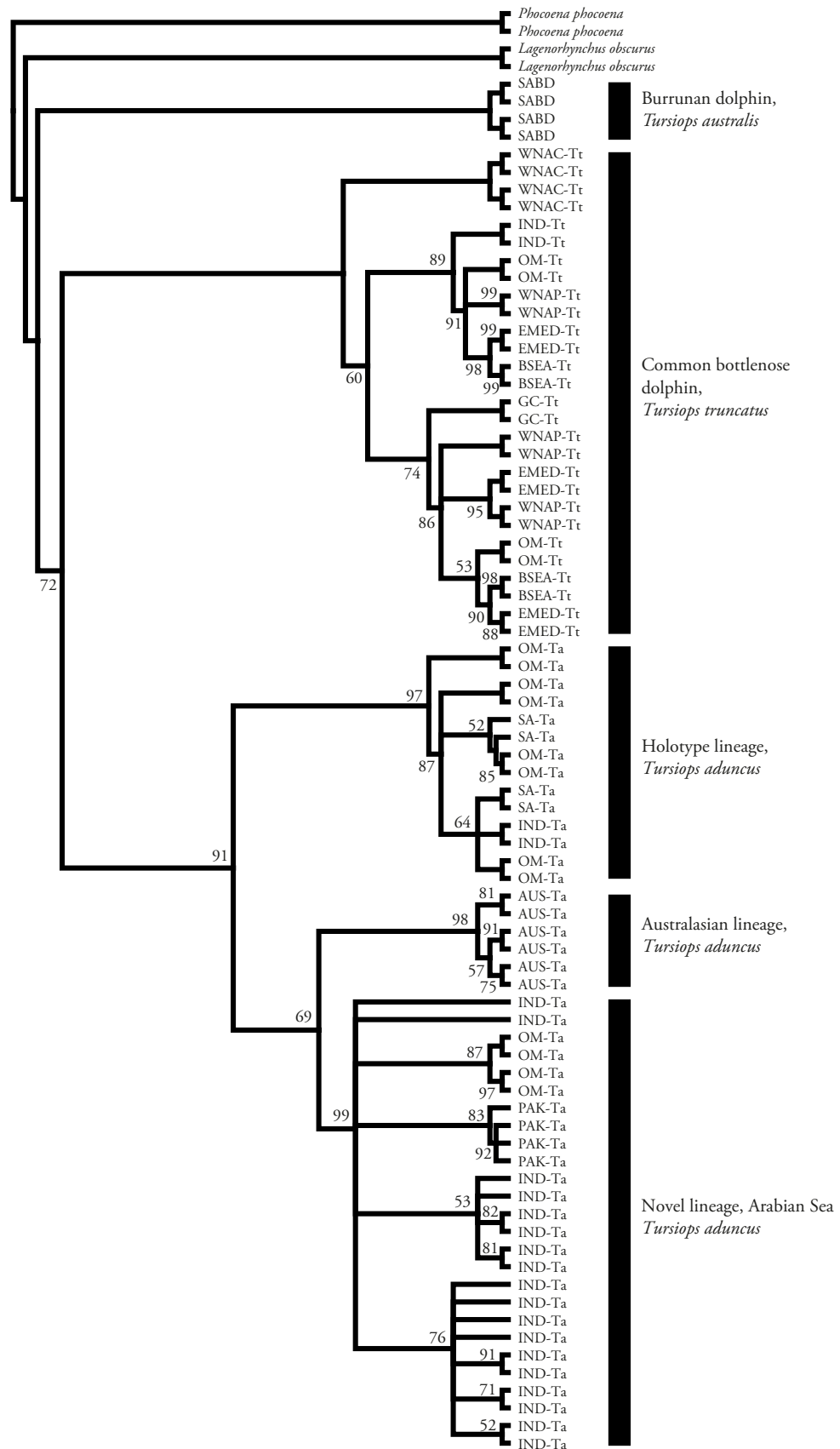


Figure 9: Maximum Likelihood phylogeny inferred from the concatenated mtDNA/nuDNA dataset. Generated in RAXML v. 8.0.24 (Stamatakis, 2014). Bootstrap support values less than 100 are indicated next to respective nodes. Proportional transformation applied to the branch lengths to emphasise tree topology.

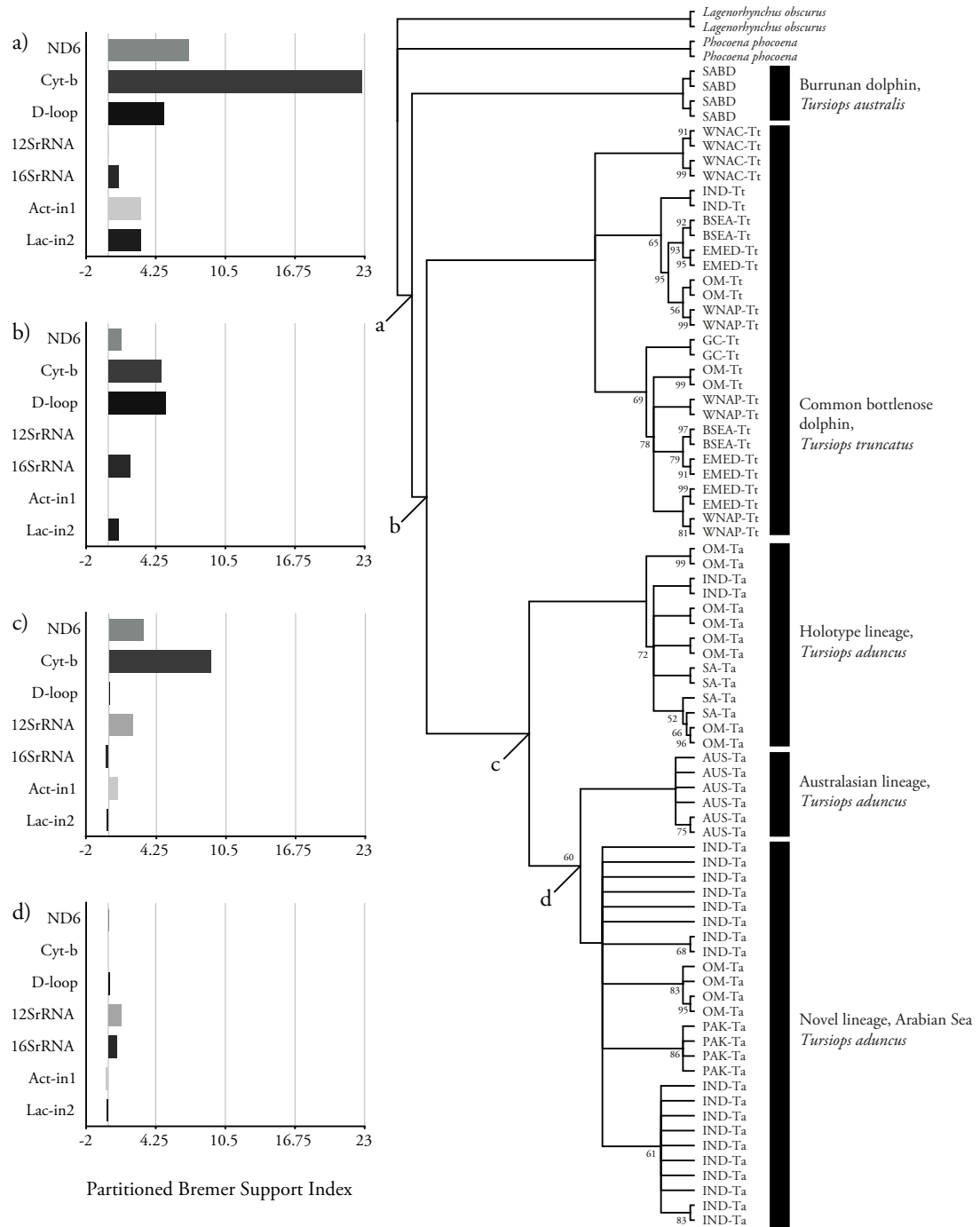


Figure 10: Maximum parsimony tree and partitioned Bremer support indices for different loci. Mitochondrial markers: ND6, Cytochrome-*b*, D-loop, 12S rRNA and 16S rRNA. Nuclear DNA markers: Actin intron 1 and α -Lactalbumin intron 2. Nodes and charts: a) divergence of *T. australis* from other *Tursiops* species; b) divergence of *T. truncatus* and *T. aduncus* lineages; c) divergence of *T. aduncus* holotype lineage from other *T. aduncus* lineages; d) divergence of Australasian and novel, Arabian Sea *T. aduncus* lineages. Bootstrap support values less than 100 are indicated at respective nodes.

2.3.2 *Estimation of Ancestral Distributions*

The general ancestral biogeographic patterns observed across the *Tursiops* genus are similar to those described in Moura *et al.* (2013a). The biogeographic distribution of the ancestor to *T. aduncus* and *T. truncatus* (Node 157, Figure 11a) is unresolved based on the S-DIVA analysis, however Australasia is most likely (55.97%) based on the BBM analysis (Node 157, Figure 11b). The origin of the *T. aduncus* lineage (Node 109) remains unresolved in the S-DIVA analysis (Figure 11a), however the BBM analysis (Figure 11b) suggests Australasia as most likely (47.47%). The ancestral origin of the Australasian and new, Arabian Sea lineage (Node 108) is Australasia/Pakistan from the S-DIVA analysis (100% support) (Figure 11a) and is Australasia from the BBM analysis (77.59% support) (Figure 11b).

From reconstructions generated from the concatenated mtDNA-nuDNA sequences, the S-DIVA (Figure 12a) and BBM (Figure 12b) results are largely congruent with those derived from the mitogenome dataset (Figure 11). An Australasian origin for the ancestor to all extant *Tursiops* species and ecotypes is supported. Furthermore, an Australasian distribution is supported for the ancestors common to all extant *T. aduncus* (Nodes 108 and 109) and the ancestor to *T. aduncus* and *T. truncatus* (Node 157). BBM reconstructions using the concatenated mtDNA-nuDNA phylogeny support the hypothesis that *T. truncatus* ancestors were a coastal eco-type, which is consistent with Moura *et al.* (2013a).

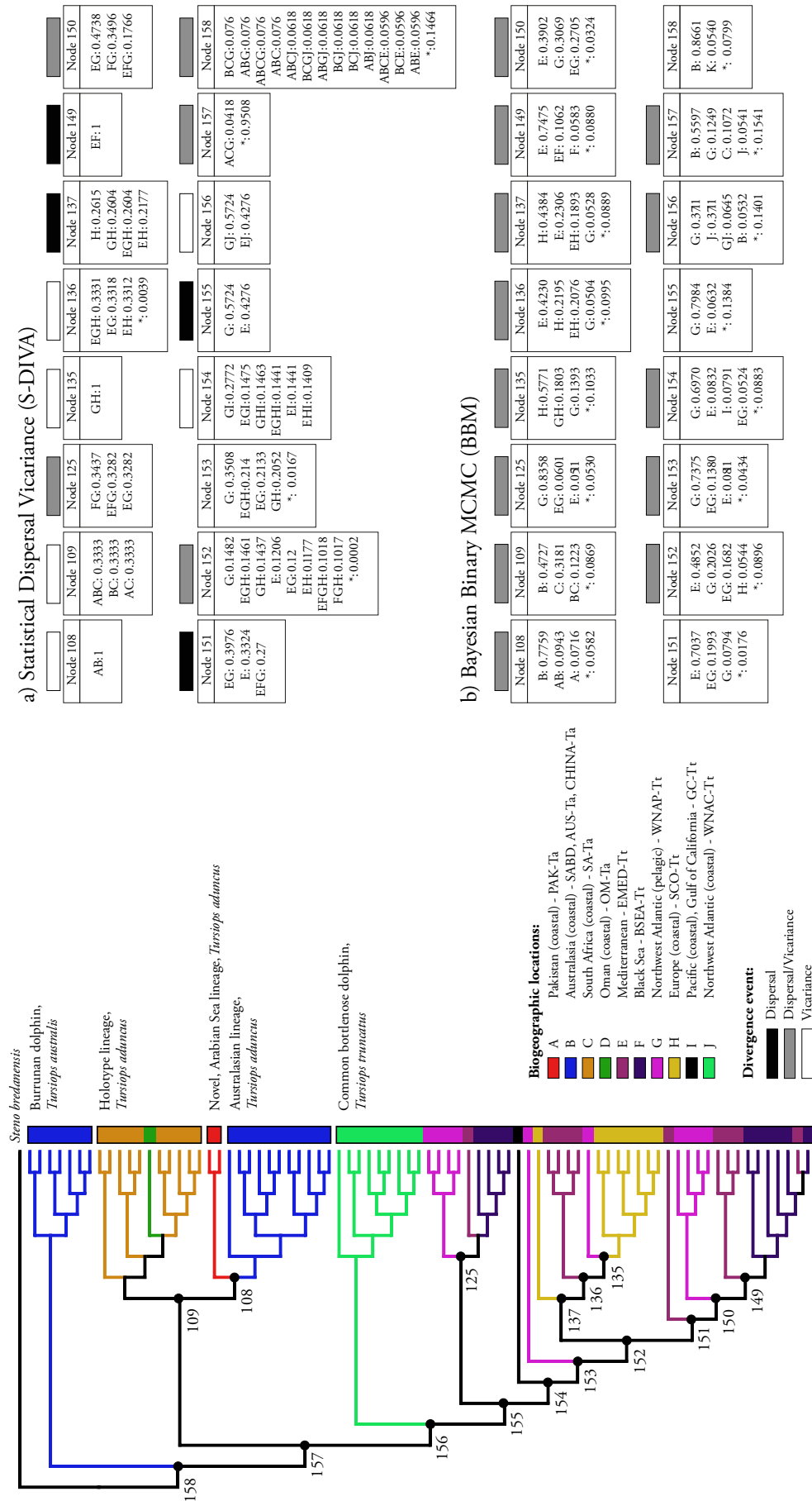


Figure 11: Statistical Dispersal Vicariance Analysis (S-DIVA) and b) Bayesian Binary MCMC Analysis (BBM) for mitogenome dataset. Implemented in RASP v. 2.2 (Yu et al., 2010). Nodes of interest are indicated by a small black circle with a unique number. Colours and letters correspond to the locations of the various populations, ecotypes and species represented in the tree. Black bars = divergence by dispersal; white bars = divergence by vicariance; grey bars = divergence by both dispersal and vicariance. Under each analysis, each node of interest has its own table showing the likely biogeographic reconstructions.

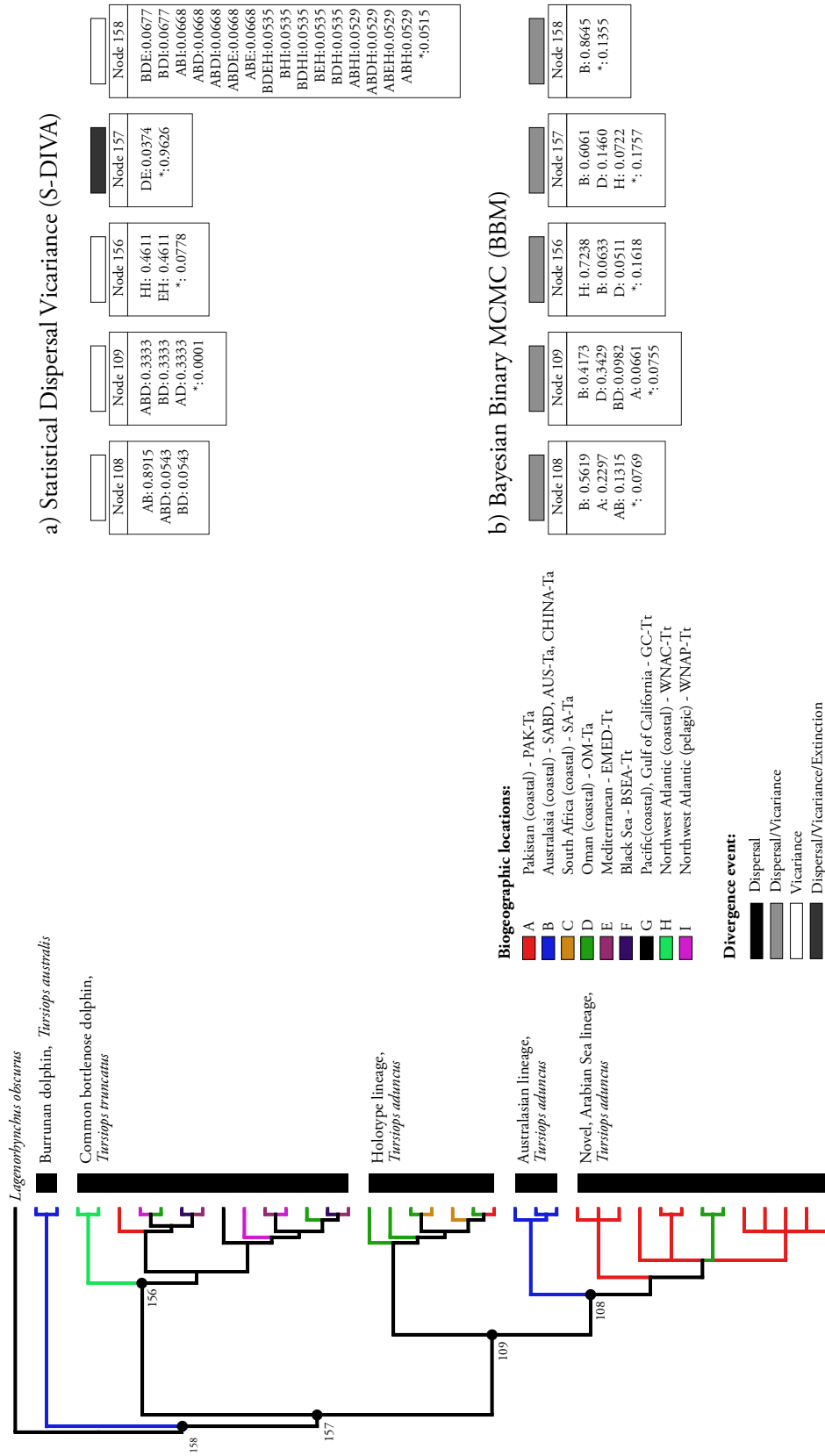


Figure 12: Statistical Dispersal Vicariance Analysis (S-DIVA) and b) Bayesian Binary MCMC Analysis (BBM) for the mtDNA/nuDNA dataset. Implemented in RASP v. 2.2 (Yu et al. 2010). Nodes of interest are indicated by a small black circle with a unique number. Colours and letters correspond to the locations of the various populations, ecotypes and species represented in the tree. Black bars = divergence by dispersal; white bars = divergence by vicariance; light grey bars = divergence by both dispersal and vicariance; dark grey bars = divergence by dispersal, vicariance and extinction. Under each analysis, each node of interest has its own table showing the likely biogeographic reconstructions.

2.3.3 Estimation of Divergence Dates using Mitogenomic Data

Bayesian inference of divergence times was performed in BEAST v. 1.8 (Drummond & Rambaut, 2007). PARTITIONFINDER v. 1.0.1 (Lanfear *et al.* 2012; 2014) identified eight partitions in the data (see Table 6 for details and evolutionary models). A total of 486,018,000 iterations, were performed after burn-in and the marginal density plots for each parameter were examined in TRACER v. 1.6 (Rambaut *et al.* 2014) to confirm that the runs had converged on the same stationary distributions. Runs were combined resulting in ESS values for all parameters above 200, indicating an appropriate number of iterations had been performed. Inferred node dates were congruent with those estimated in Moura *et al.* (2013a) (see Figure 13 and Table 7). Within *T. aduncus*, the holotype lineage diverged from other *T. aduncus* ~342 Ka (95% HPD: 143, 630 Ka) and divergence of the new, Arabian Sea lineage and Australasian lineage was estimated to have occurred ~ 261 Ka (95% HPD: 111, 509). Log Bayes factors generated from the marginal likelihoods calculated using stepping-stone sampling (Baele *et al.* 2012; 2013) suggested the model including both fossil and biogeographic calibrations outperformed the others (see Table 8). This is consistent with the model testing performed in Moura *et al.* (2013a).

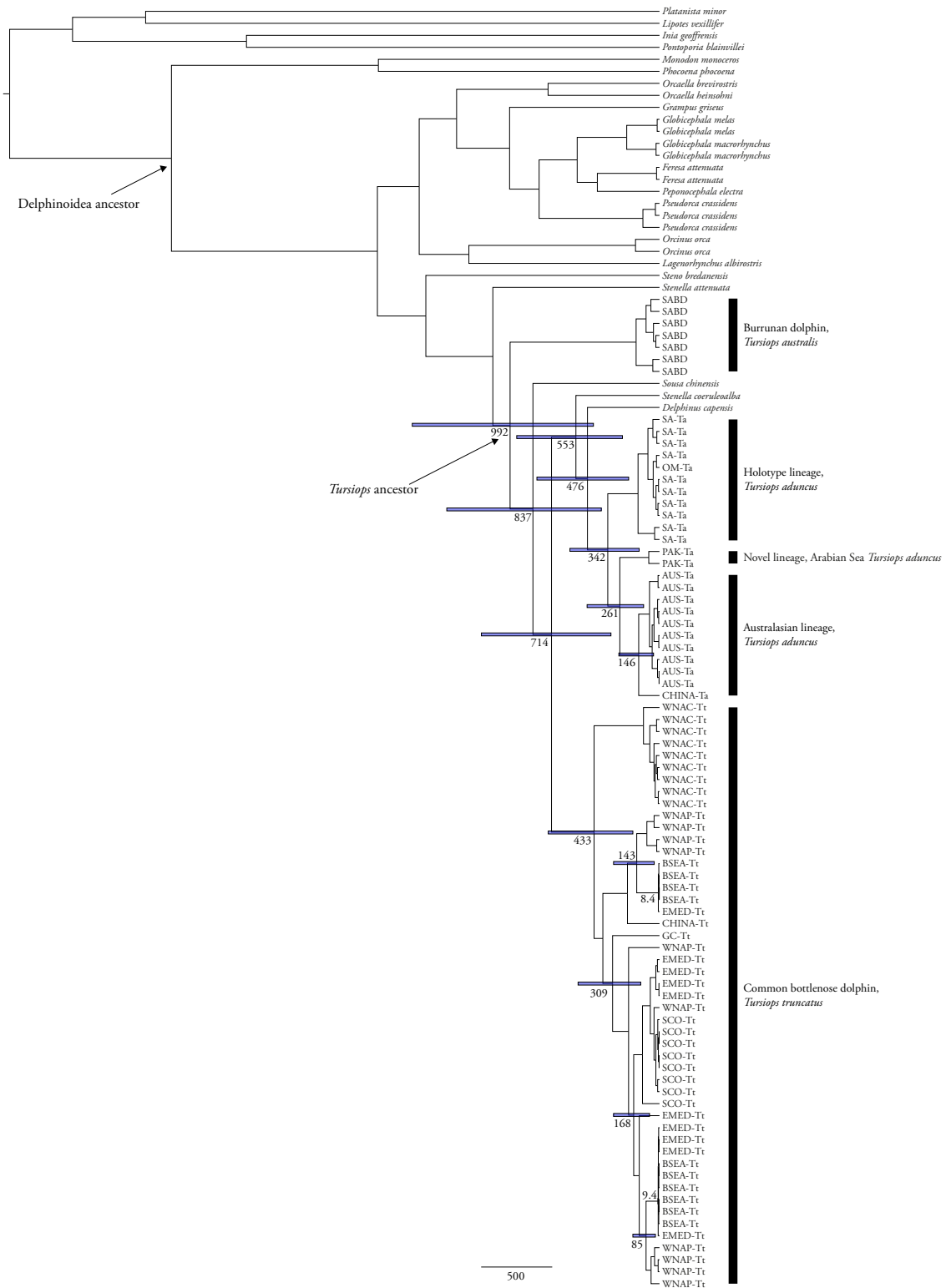


Figure 13: Estimation of divergence dates using the mitogenome dataset. Analysis conducted in BEAST v. 1.8 (Drummond & Rambaut, 2007). Divergence times indicated next to respective nodes. Grey bar indicates 95% highest posterior densities. Branch lengths are in Ka units according to the scale bar.

Table 7: Posterior values for parameters estimated from different models carried out in BEAST. Models are as outlined in Moura *et al.* (2013). BSEM = Biogeographic calibration using Black Sea/Eastern Mediterranean clade; uced = uncorrelated exponential distribution for the relaxed clock.

Model	Statistic	Posterior probability	Root Height	TMRCa BSEM1	TMRCa BSEM2	TMRCa <i>Tursiops</i>	TMRCa Delphinoidea	uced mean
BSEM & Fossil	<i>Mean</i>	-98506.069	4.5619	8.10E-03	9.18E-03	1.0495	3.4139	0.048
	<i>Median</i>	-98508.6385	4.355	8.42E-03	9.39E-03	0.9914	3.205	0.0466
	<i>Geometric Mean</i>	n/a	4.3816	7.95E-03	9.15E-03	0.9953	3.2343	0.0464
	<i>95%</i>	-98562.4087,	2.3007,	5.2339E-03,	7.7153E-03,	0.4653,	1.5197,	0.0253,
<i>HPD Interval</i>	-98455.8755	7.2253	1E-2	1E-2	1.7592	5.7279	0.0733	
<i>ESS</i>	852	724	16342	31652	533	472	910	
BSEM only	<i>Mean</i>	-98443.042	2.675	7.59E-03	8.93E-03	n/a	n/a	0.0745
	<i>Median</i>	-98442.531	2.6045	7.86E-03	9.17E-03	n/a	n/a	0.0733
	<i>Geometric Mean</i>	n/a	2.6184	7.38E-03	8.88E-03	n/a	n/a	0.0731
	<i>95%</i>	-98485.1172,	1.6831,	4.4822E-3,	7.0943E-3,	n/a	n/a	0.0472,
<i>HPD Interval</i>	-98401.0217	3.8124	9.9999E-3	1E-2	n/a	n/a	0.1038	
<i>ESS</i>	4768	1336	22386	24686	n/a	n/a	2292	
Fossil only	<i>Mean</i>	-98640.3987	15.867	n/a	n/a	3.7011	9.867	0.0119
	<i>Median</i>	-98640.7459	15.6077	n/a	n/a	3.6642	9.8609	0.0116
	<i>Geometric Mean</i>	n/a	15.5717	n/a	n/a	3.6238	9.7606	0.0117
	<i>95%</i>	-98682.6328,	10.0288,	n/a	n/a	2.2727,	6.9811,	7.7115E-03,
<i>HPD Interval</i>	-98598.5502	22.002	n/a	n/a	5.1883	12.5832	0.0167	
<i>ESS</i>	1020	369	n/a	n/a	657	52256	299	

Table 8: Model comparison using pairwise log Bayes Factors. Values generated from log marginal likelihoods calculated from 100 power posteriors for 1,000,000 iterations in BEAST v. 1.8 (Drummond & Rambaut, 2007) using stepping-stone sampling (Xie *et al.* 2011; Baele *et al.* 2012;2013). Log marginal likelihoods for each model and the log Bayes factors are presented in a pairwise comparison. Where log Bayes factors are positive, the model in the column header is better supported. Overall, the combined BSEM & Fossil calibration model outperforms the others *cf.* Moura *et al.* (2013).

Model	Log Marginal Likelihood	BSEM & Fossil	BSEM only	Fossil only
BSEM & Fossil	-99319.068	-	-65.914	-70.362
BSEM only	-99387.803	65.914	-	-4.449
Fossil only	-99390.598	70.362	4.449	-

2.3.4 Estimation of Ancestral Cranial Morphology

Where individual data were available for several specimens (SA, OM, PAK, EMED, SCO, BSEA), regression analysis was performed on fifteen cranial measurements to test for isometry with condylobasal length (CBL). Because only population averages for trait measurements were available in some cases (WNAP, WNAC, GC, AUS-Ta, SABD) it was important to identify this relationship in a given trait as it is assumed when using population averages to calculate relative measures of a trait to CBL. The variation in all measurements can be explained by skull length, all with R^2 values > 0.5 ($P < 0.001$), including a subset of seven characters with R^2 values > 0.8 ($P < 0.001$) (Table 9).

Ancestral traits were estimated for all nodes in the mitogenome and concatenated mtDNA-nuDNA phylogenies, but only five nodes of interest are presented in Table 9 and Table 10. These represent (i) the *Tursiops* ancestor, (ii) the ancestor to *T. truncatus* and *T. aduncus*-type dolphins (iii) ancestor to all *T. truncatus* ecotypes (iv) ancestor to all extant *T. aduncus*-type dolphins and (v) ancestor to the new, Arabian Sea lineage *T. aduncus* and Australasian *T. aduncus*.

The branches of the phylogenies used in the Maximum Parsimony ancestral character estimation were coloured using MESQUITE v. 2.75 (Maddison & Maddison, 2015) based on extant trait values and estimated ancestral states (mitogenomes, Figure 14 - Figure 16; concatenated mtDNA and nuDNA, Figure 17 - Figure 19). Presented here are trees illustrating changes in GLPTF, RL and ZW over the phylogeny. These characters represent measurements of length (RL), width (ZW) and a dimension of the temporal fossae (GLPTF) (see discussion).

Table 9: Ancestral character estimation (ACE) using the mitogenome phylogeny. Results of regression analyses (R^2 value) of each trait against condylobasal length (CBL) are presented ($P < 0.001$). Estimations of ancestral states were carried out using various methods. These were, Bayesian (Bayes), Phylogenetic Independent Contrasts (PIC), Generalised Least Squares (GLS) and Maximum Parsimony (MP). Estimated values are percentages of CBL in all cases. 95% Highest Posterior Densities (HPD) (MCMC Bayesian inference) and Confidence Intervals (CI) for PIC and GLS, are also presented with each estimation. Confidence Intervals are calculated based on variation under the Brownian motion model. Node 1 = most recent common ancestor (MRCA) to Arabian Sea and Australasian *T. aduncus*, Node 2 = MRCA of holotype-*T. aduncus* and other *T. aduncus*, Node 3 = MRCA of *T. truncatus* and *T. aduncus*, Node 4 = MRCA of all extant *Tursiops*, Node 5 = MRCA to northwest Atlantic coastal *T. truncatus* and other *T. truncatus*.

Cranial Trait	R^2	ACE Method	Node 1		Node 2		Node 3		Node 4		Node 5	
			Est.	95% HPD/CI	Est.	95% HPD/CI	Est.	95% HPD/CI	Est.	95% HPD/CI	Est.	95% HPD/CI
RL (%CBL)	0.88	Bayes	57.871	56.641 - 59.063	57.91	56.614 - 59.204	57.816	56.175 - 59.423	57.209	55.168 - 59.207	55.77	55.432 - 56.098
		PIC	57.596	57.392 - 57.801	57.485	57.281 - 57.689	57.68	58.24 - 58.809	58.153	58.234 - 58.932	54.966	57.024 - 57.367
		GLS	57.867	57.833 - 57.997	58.013	58 - 58.174	58.023	58.498 - 58.727	57.942	58.123 - 58.387	55.3	57.279 - 57.421
		MP	57.869		58.015		58.019		57.932		55.298	
RWM (%CBL)	0.72	Bayes	13.708	11.499 - 15.682	13.501	11.16 - 15.597	13.443	10.568 - 16.493	12.434	8.932 - 15.846	16.002	14.071 - 18.064
		PIC	13.779	13.575 - 13.984	13.825	13.621 - 14.029	14.369	14.084 - 14.653	13.889	13.54 - 14.238	16.442	16.271 - 16.614
		GLS	13.681	13.599 - 13.763	13.628	13.541 - 13.715	13.79	13.676 - 13.905	13.711	13.579 - 13.843	16.153	16.082 - 16.224
		MP	13.679		13.625		13.781		13.675		16.172	
PRW (%CBL)	0.66	Bayes	7.315	6.111 - 8.453	7.166	5.951 - 8.452	7.051	5.615 - 8.442	7.262	5.475 - 9.131	8.567	7.48 - 9.514
		PIC	7.626	7.416 - 7.837	7.5	7.294 - 7.706	7.309	7.025 - 7.594	7.789	7.44 - 8.138	8.753	8.581 - 8.925
		GLS	7.374	7.29 - 7.458	7.248	7.16 - 7.336	7.424	7.309 - 7.538	7.849	7.716 - 7.981	8.607	8.535 - 8.678
		MP	7.373		7.246		7.416		7.823		8.615	
TREN (%CBL)	0.92	Bayes	67.066	65.882 - 68.202	67.071	65.858 - 68.301	66.626	64.853 - 68.402	66.736	64.754 - 68.677	65.76	64.704 - 66.729
		PIC	67.126	66.921 - 67.33	67.116	66.912 - 67.32	66.76	66.468 - 67.051	66.65	66.287 - 67.013	65.582	65.411 - 65.754
		GLS	67.15	67.067 - 67.234	67.164	67.074 - 67.253	66.986	66.863 - 67.11	67.272	67.133 - 67.412	65.735	65.664 - 65.807
		MP	67.154		67.169		67.021		67.354		65.734	
TRIN (%CBL)	0.94	Bayes	67.187	64.895 - 69.278	67.022	64.749 - 69.356	67.188	64.221 - 70.31	66.75	63.519 - 70.161	66.144	64.24 - 67.914
		PIC	67.054	66.843 - 67.264	66.877	66.671 - 67.083	67.671	67.377 - 67.964	67.628	67.265 - 67.991	65.96	65.785 - 66.136
		GLS	67.229	67.144 - 67.315	67.317	67.227 - 67.408	67.793	67.669 - 67.917	67.947	67.807 - 68.086	66.187	66.111 - 66.263
		MP	67.234		67.325		67.817		67.997		66.193	

Cranial Trait	R	ACF Method	Node 1		Node 2		Node 3		Node 4		Node 5	
			Est.	95% HPD/CI	Est.	95% HPD/CI	Est.	95% HPD/CI	Est.	95% HPD/CI	Est.	95% HPD/CI
GPRW (%CBL)	0.7	Bayes	41.657	39.823 - 43.522	41.546	39.788 - 43.576	41.305	38.783 - 43.656	40.121	37.325 - 42.821	44.81	43.288 - 46.566
		PIC	41.745	41.541 - 41.949	42.179	41.975 - 42.383	42.415	42.131 - 42.7	41.722	41.373 - 42.071	45.277	45.106 - 45.449
		GLS	41.717	41.635 - 41.799	41.702	41.615 - 41.789	41.664	41.549 - 41.778	41.25	41.118 - 41.382	44.883	44.812 - 44.954
		MP	41.714		41.698		41.671		41.26		44.906	
GPOW (%CBL)	0.69	Bayes	46.608	44.634 - 48.589	46.787	44.751 - 49.134	47.1	44.464 - 49.585	45.456	42.186 - 48.812	51.269	49.511 - 53.129
		PIC	46.06	45.856 - 46.265	47.051	46.847 - 47.255	48.653	48.369 - 48.938	47.344	46.995 - 47.693	51.863	51.692 - 52.034
		GLS	46.585	46.503 - 46.668	46.868	46.781 - 46.955	47.503	47.389 - 47.618	46.699	46.567 - 46.831	51.387	51.316 - 51.458
		MP	46.582		46.863		47.523		46.747		51.399	
ZW (%CBL)	0.71	Bayes	47.077	45.461 - 48.781	47.048	45.244 - 48.913	46.949	44.334 - 49.511	45.458	42.477 - 48.268	50.547	50.025 - 51.031
		PIC	47.007	46.802 - 47.211	47.568	47.363 - 47.772	48.635	48.35 - 48.919	46.726	46.377 - 47.075	52.11	51.938 - 52.281
		GLS	47.113	47.03 - 47.195	47.17	47.082 - 47.257	47.378	47.263 - 47.492	46.375	46.243 - 46.507	51.593	51.522 - 51.664
		MP	47.109		47.163		47.369		46.344		51.61	
GWPX (%CBL)	0.57	Bayes	17.808	16.719 - 18.886	17.652	16.421 - 18.92	17.547	15.924 - 19.14	17.091	15.09 - 19.093	19.16	18.832 - 19.486
		PIC	17.903	17.699 - 18.108	17.828	17.624 - 18.032	17.992	17.708 - 18.277	17.971	17.622 - 18.32	18.679	17.653 - 17.747
		GLS	17.777	17.695 - 17.859	17.709	17.622 - 17.796	17.799	17.684 - 17.913	17.813	17.681 - 17.945	17.7	17.679 - 17.722
		MP	17.775		17.706		17.782		17.78		18.565	
GLPTF (%CBL)	0.6	Bayes	21.201	19.896 - 22.302	20.953	19.663 - 22.145	20.16	18.736 - 21.603	20.506	18.741 - 22.361	23.077	22.972 - 23.182
		PIC	21.583	21.373 - 21.794	21.938	21.732 - 22.144	20.046	19.761 - 20.33	21.372	21.023 - 21.721	22.11	21.998 - 22.221
		GLS	21.222	21.138 - 21.307	21.042	20.954 - 21.13	20.577	20.462 - 20.692	21.118	20.986 - 21.251	22.158	22.109 - 22.207
		MP	21.218		21.035		20.565		21.096		22.315	
GWPTF (%CBL)	0.59	Bayes	15.906	14.654 - 17.163	15.725	14.577 - 16.908	15.376	13.713 - 16.891	15.347	13.464 - 17.239	16.784	16.675 - 16.891
		PIC	16.448	16.238 - 16.658	16.468	16.262 - 16.673	14.942	14.657 - 15.226	16.004	15.655 - 16.353	17.101	16.93 - 17.273
		GLS	15.991	15.906 - 16.075	15.762	15.674 - 15.85	15.489	15.375 - 15.604	15.947	15.815 - 16.079	16.924	16.853 - 16.995
		MP	15.988		15.758		15.479		15.919		16.926	

Cranial Trait	R	AF Method	Node 1		Node 2		Node 3		Node 4		Node 5	
			Est.	95% HPD/CI	Est.	95% HPD/CI	Est.	95% HPD/CI	Est.	95% HPD/CI	Est.	95% HPD/CI
UTLRL (%CBL)	0.88	<i>Bayes</i>	48.256	46.077 - 50.465	48.506	46.229 - 50.809	48.872	46.034 - 51.726	47.468	43.82 - 50.699	46.516	45.946 - 47.068
		<i>PIC</i>	47.719	47.514 - 47.923	47.711	47.507 - 47.915	49.281	48.997 - 49.566	49.826	49.477 - 50.175	47.208	47.037 - 47.379
		<i>GLS</i>	48.268	48.186 - 48.35	48.563	48.476 - 48.65	49.454	49.339 - 49.568	48.909	48.777 - 49.041	47.453	47.382 - 47.524
		<i>MP</i>	48.268		48.564		49.426		48.83		47.456	
LTRL (%CBL)	0.8	<i>Bayes</i>	49.051	46.163 - 52.284	48.796	45.521 - 52.05	47.535	43.096 - 51.934	46.89	42.1 - 52.221	45.323	44.54 - 46.076
		<i>PIC</i>	49.705	49.501 - 49.91	48.991	48.786 - 49.195	48.358	48.067 - 48.65	47.942	47.579 - 48.305	46.793	46.622 - 46.964
		<i>GLS</i>	49.252	49.169 - 49.336	49.009	48.919 - 49.098	48.678	48.554 - 48.802	49.081	48.941 - 49.22	46.999	46.928 - 47.07
		<i>MP</i>	49.255		49.012		48.673		49.056		47.017	
ML (%CBL)	0.96	<i>Bayes</i>	85.114	82.432 - 87.756	85.053	82.214 - 88.128	84.546	80.706 - 88.397	82.209	78.479 - 87.351	84.297	83.563 - 85.063
		<i>PIC</i>	84.985	84.781 - 85.19	84.952	84.748 - 85.156	85.416	85.131 - 85.7	85.353	85.004 - 85.702	84.51	84.338 - 84.681
		<i>GLS</i>	85.092	85.01 - 85.174	85.15	85.063 - 85.237	84.936	84.822 - 85.051	84.297	84.164 - 84.429	84.556	84.485 - 84.627
		<i>MP</i>	85.096		85.155		84.963		84.36		84.569	
MH (%CBL)	0.81	<i>Bayes</i>	17.48	16.597 - 18.345	17.364	16.395 - 18.373	16.995	15.802 - 18.308	16.619	15.268 - 18.099	18.451	18.221 - 18.672
		<i>PIC</i>	17.692	17.488 - 17.897	17.733	17.529 - 17.937	17.27	16.986 - 17.555	17.726	17.365 - 18.087	18.642	18.47 - 18.813
		<i>GLS</i>	17.494	17.412 - 17.576	17.387	17.3 - 17.474	17.234	17.114 - 17.354	17.184	17.045 - 17.322	18.488	18.417 - 18.559
		<i>MP</i>	17.492		17.384		17.225		17.163		18.489	

Table 10: Ancestral character estimation (ACE) using the concatenated mtDNA-nuDNA phylogeny. Estimations of ancestral states were carried out using Bayesian (Bayes), Phylogenetic Independent Contrasts (PIC), Generalised Least Squares (GLS) and Maximum Parsimony (MP) methods. Estimated values are percentages of CBL in all cases. 95% Highest Posterior Densities (HPD) (MCMC Bayesian inference) and Confidence Intervals (CI) for PIC and GLS, are also presented with each estimation. Confidence Intervals are calculated based on variation under the Brownian motion model. Node 1 = most recent common ancestor (MRCA) to Arabian Sea and Australasian *T. aduncus*, Node 2 = MRCA of holotype-*T. aduncus* and other *T. aduncus*, Node 3 = MRCA of *T. truncatus* and *T. aduncus*, Node 4 = MRCA of all extant *Tursiops*, Node 5 = MRCA to northwest Atlantic coastal *T. truncatus* and other *T. truncatus*.

Cranial Trait	Method	Node 1		Node 2		Node 3		Node 4		Node 5	
		Est.	95% HPD/CI	Est.	95% HPD/CI	Est.	95% HPD/CI	Est.	95% HPD/CI	Est.	95% HPD/CI
RL (%CBL)	Bayes	58.495	55.119 - 61.899	58.377	54.851 - 61.699	57.278	52.777 - 61.651	55.249	49.932 - 60.585	55.584	52.551 - 58.692
	PIC	58.738	58.552 - 58.923	58.227	58.05 - 58.404	58.798	58.565 - 59.032	58.048	57.771 - 58.325	55.279	55.114 - 55.443
	GLS	58.659	58.584 - 58.735	58.605	58.527 - 58.684	58.393	58.293 - 58.494	57.887	57.765 - 58.01	55.77	55.701 - 55.838
	MP	58.651		58.592		58.328		57.741		55.76	
RWM (%CBL)	Bayes	13.923	12.328 - 15.638	13.884	12.169 - 15.623	13.943	11.752 - 16.088	13.739	11.18 - 16.466	16.034	14.521 - 17.524
	PIC	13.973	13.784 - 14.162	14.132	13.954 - 14.311	14.054	13.82 - 14.287	14.819	14.541 - 15.096	16.482	16.318 - 16.646
	GLS	13.991	13.915 - 14.067	14.003	13.924 - 14.082	14.466	14.365 - 14.566	14.98	14.857 - 15.102	16.164	16.095 - 16.233
	MP	13.992		14.005		14.473		14.997		16.165	
PRW (%CBL)	Bayes	7.5	6.6 - 8.41	7.402	6.425 - 8.327	7.447	6.2 - 8.637	7.683	6.231 - 9.172	8.579	7.712 - 9.39
	PIC	7.63	7.441 - 7.82	7.602	7.424 - 7.78	7.25	7.017 - 7.483	8.215	7.938 - 8.493	8.819	8.655 - 8.983
	GLS	7.529	7.452 - 7.605	7.461	7.382 - 7.54	7.723	7.622 - 7.823	8.313	8.19 - 8.435	8.646	8.578 - 8.715
	MP	7.528		7.461		7.723		8.313		8.646	
TREN (%CBL)	Bayes	66.906	65.852 - 67.899	66.848	65.79 - 67.94	66.134	64.709 - 67.596	65.788	64.089 - 67.393	65.917	64.988 - 66.834
	PIC	66.949	66.76 - 67.139	67.076	66.898 - 67.254	66.493	66.238 - 66.749	66.476	66.193 - 66.759	65.867	65.703 - 66.032
	GLS	66.934	66.857 - 67.012	66.924	66.843 - 67.006	66.474	66.364 - 66.584	66.455	66.329 - 66.581	65.963	65.894 - 66.032
	MP	66.929		66.916		66.441		66.389		65.958	
TRIN (%CBL)	Bayes	66.478	63.3 - 69.639	66.16	62.789 - 69.556	65.519	60.948 - 70.019	64.403	59.128 - 69.423	66.765	63.82 - 69.619
	PIC	67.035	66.846 - 67.225	66.388	66.21 - 66.566	66.667	66.41 - 66.923	67.023	66.739 - 67.306	66.97	66.803 - 67.137
	GLS	66.709	66.632 - 66.786	66.491	66.41 - 66.573	66.798	66.688 - 66.908	66.927	66.801 - 67.053	66.941	66.869 - 67.013
	MP	66.701		66.478		66.746		66.824		66.931	

Cranial Trait	Method	Node 1		Node 2		Node 3		Node 4		Node 5	
		Est.	95% HPD/CI	Est.	95% HPD/CI	Est.	95% HPD/CI	Est.	95% HPD/CI	Est.	95% HPD/CI
GPRW (%CBL)	<i>Bayes</i>	41.907	39.847 - 44.008	41.764	39.601 - 43.873	41.121	38.406 - 43.899	40.696	37.371 - 43.987	44.478	42.646 - 46.399
	<i>PIC</i>	42.156	41.971 - 42.342	42.476	42.299 - 42.653	41.443	41.209 - 41.676	42.114	41.837 - 42.391	45.105	44.94 - 45.269
	<i>GLS</i>	42.014	41.939 - 42.09	41.916	41.838 - 41.995	41.766	41.665 - 41.866	42.169	42.046 - 42.292	44.578	44.51 - 44.647
	<i>MP</i>	42.014		41.916		41.76		42.154		44.578	
GPOW (%CBL)	<i>Bayes</i>	46.099	42.846 - 49.268	46.319	42.977 - 49.543	45.976	41.743 - 50.19	44.965	39.804 - 50.002	50.517	47.657 - 53.464
	<i>PIC</i>	45.85	45.664 - 46.036	46.921	46.744 - 47.098	46.647	46.413 - 46.88	47.309	47.032 - 47.586	51.41	51.246 - 51.574
	<i>GLS</i>	46.246	46.17 - 46.321	46.519	46.44 - 46.597	46.921	46.821 - 47.022	47.264	47.141 - 47.386	50.702	50.634 - 50.771
	<i>MP</i>	46.246		46.52		46.931		47.284		50.704	
ZW (%CBL)	<i>Bayes</i>	46.722	44.563 - 48.802	46.816	44.64 - 48.993	46.248	43.375 - 48.989	45.457	41.916 - 49.019	50.821	48.938 - 52.717
	<i>PIC</i>	46.61	46.424 - 46.796	47.519	47.342 - 47.696	46.82	46.587 - 47.053	46.625	46.348 - 46.902	51.709	51.545 - 51.874
	<i>GLS</i>	46.783	46.708 - 46.858	46.902	46.824 - 46.981	46.788	46.687 - 46.888	46.748	46.625 - 46.87	50.934	50.865 - 51.002
	<i>MP</i>	46.782		46.901		46.786		46.744		50.933	
GWPX (%CBL)	<i>Bayes</i>	17.619	16.348 - 18.898	17.655	16.313 - 18.967	17.363	15.708 - 19.116	17.378	15.241 - 19.406	18.381	17.248 - 19.552
	<i>PIC</i>	17.574	17.388 - 17.76	17.921	17.743 - 18.098	17.309	17.075 - 17.542	18.015	17.738 - 18.292	18.565	18.401 - 18.729
	<i>GLS</i>	17.65	17.574 - 17.725	17.702	17.623 - 17.781	17.705	17.604 - 17.805	18.199	18.076 - 18.321	18.429	18.361 - 18.498
	<i>MP</i>	17.651		17.705		17.718		18.226		18.432	
GLPTF (%CBL)	<i>Bayes</i>	20.979	19.099 - 22.765	20.865	18.884 - 22.679	19.851	17.526 - 22.353	19.541	16.558 - 22.485	21.887	20.276 - 23.544
	<i>PIC</i>	21.149	20.963 - 21.335	21.645	21.467 - 21.822	20.02	19.786 - 20.253	21.222	20.944 - 21.499	22.273	22.109 - 22.437
	<i>GLS</i>	21.077	21.002 - 21.153	21.028	20.949 - 21.106	20.491	20.391 - 20.592	21.08	20.957 - 21.202	21.992	21.923 - 22.061
	<i>MP</i>	21.072		21.017		20.438		20.96		21.984	
GWPTF (%CBL)	<i>Bayes</i>	15.922	14.527 - 17.387	15.611	14.137 - 17.075	14.823	12.97 - 16.829	14.451	12.036 - 16.783	16.5	15.209 - 17.822
	<i>PIC</i>	16.395	16.205 - 16.584	16.191	16.013 - 16.369	15.118	14.884 - 15.351	15.753	15.476 - 16.03	16.852	16.688 - 17.016
	<i>GLS</i>	16.003	15.927 - 16.079	15.742	15.663 - 15.821	15.34	15.239 - 15.44	15.616	15.494 - 15.739	16.613	16.545 - 16.682
	<i>MP</i>	15.997		15.733		15.295		15.516		16.607	

Cranial Trait	Method	Node 1		Node 2		Node 3		Node 4		Node 5	
		Est.	95% HPD/CI	Est.	95% HPD/CI	Est.	95% HPD/CI	Est.	95% HPD/CI	Est.	95% HPD/CI
UTLRL (%CBL)	<i>Bayes</i>	48.542	45.663 - 51.631	48.559	45.538 - 51.627	48.606	44.751 - 52.566	46.903	42.037 - 51.497	47.674	45.113 - 50.364
	<i>PIC</i>	48.494	48.308 - 48.679	48.047	47.87 - 48.224	49.868	49.635 - 50.101	49.14	48.863 - 49.417	47.496	47.331 - 47.66
	<i>GLS</i>	48.65	48.575 - 48.726	48.758	48.68 - 48.837	49.493	49.392 - 49.593	49.024	48.901 - 49.147	47.81	47.742 - 47.879
	<i>MP</i>	48.648		48.754		49.473		48.98		47.806	
LTRL (%CBL)	<i>Bayes</i>	49.391	46.613 - 52.058	48.841	46.065 - 51.785	47.041	43.064 - 50.997	45.643	41.157 - 50.34	47.371	44.889 - 49.811
	<i>PIC</i>	50.161	49.975 - 50.347	49.378	49.201 - 49.555	48.396	48.141 - 48.652	47.907	47.624 - 48.191	47.338	47.174 - 47.503
	<i>GLS</i>	49.52	49.443 - 49.596	49.078	48.996 - 49.159	48.173	48.063 - 48.283	47.953	47.827 - 48.079	47.47	47.401 - 47.539
	<i>MP</i>	51.846		53.007		56.704		53.824		48.814	
ML (%CBL)	<i>Bayes</i>	84.76	82.489 - 86.893	84.597	82.278 - 86.526	84.636	81.717 - 87.484	83.703	80.172 - 87.185	85.03	83.082 - 86.955
	<i>PIC</i>	85.017	84.831 - 85.203	84.441	84.263 - 84.618	85.299	85.065 - 85.532	85.472	85.195 - 85.749	85.105	84.941 - 85.27
	<i>GLS</i>	84.857	84.781 - 84.932	84.746	84.668 - 84.825	85.324	85.224 - 85.425	85.356	85.234 - 85.479	85.14	85.071 - 85.209
	<i>MP</i>	80.446		77.295		69.088		74.013		82.58	
MH (%CBL)	<i>Bayes</i>	17.677	16.828 - 18.504	17.507	16.645 - 18.37	17.118	15.968 - 18.213	17.012	15.62 - 18.371	18.361	17.62 - 19.141
	<i>PIC</i>	17.926	17.737 - 18.115	17.848	17.67 - 18.026	17.212	16.979 - 17.446	17.73	17.453 - 18.007	18.622	18.457 - 18.786
	<i>GLS</i>	17.716	17.639 - 17.792	17.576	17.497 - 17.655	17.453	17.352 - 17.553	17.753	17.63 - 17.876	18.437	18.369 - 18.506
	<i>MP</i>	17.94		17.95		18.252		18.282		18.563	

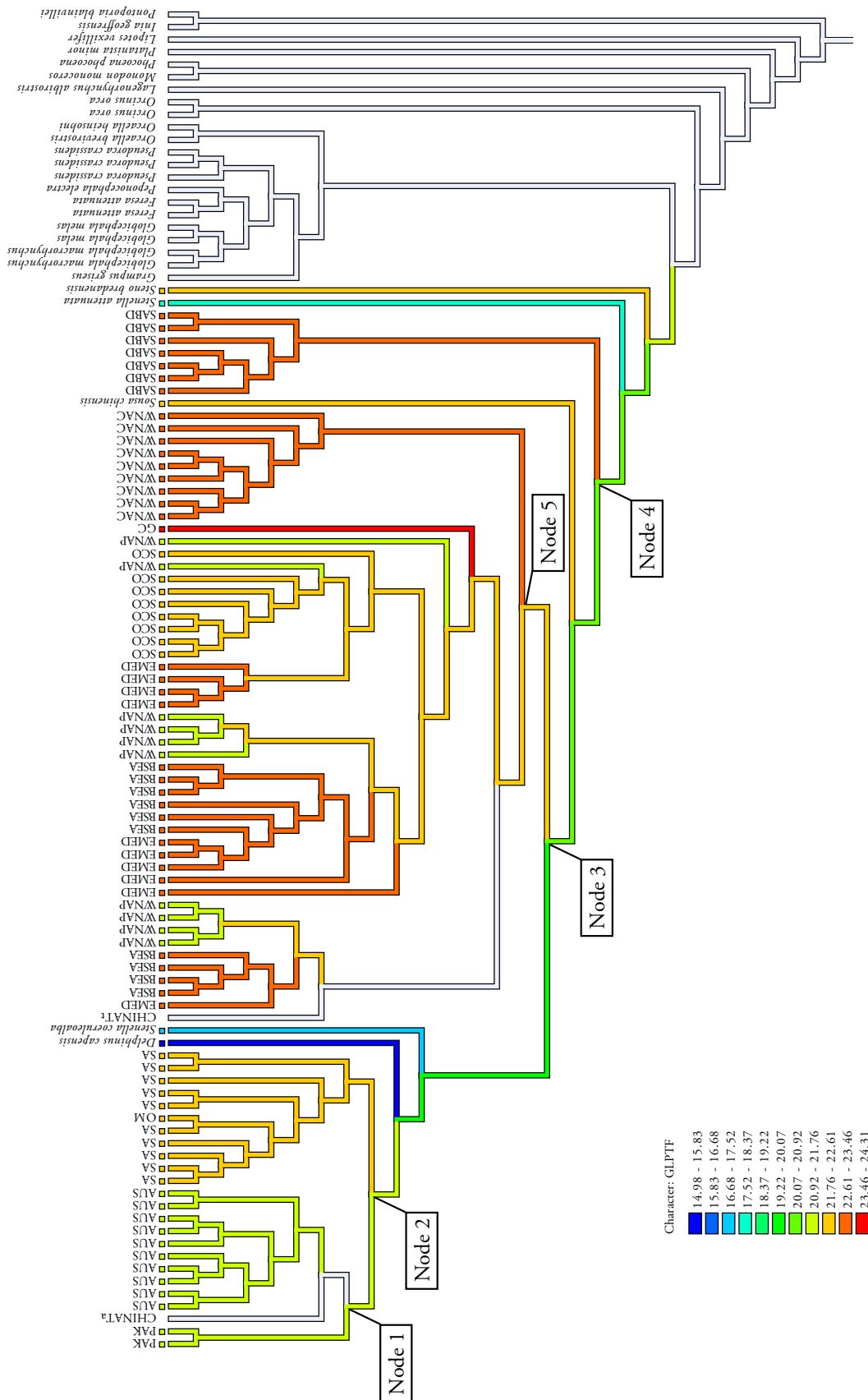


Figure 14: Maximum parsimony estimation of GLPTF relative to CBL length (%) using the mitogenome phylogeny. Node numbers correspond to those presented in Table 9. Colours represent trait values. Figure generated in MESQUITE v. 2.75 (Maddison & Maddison, 2015).

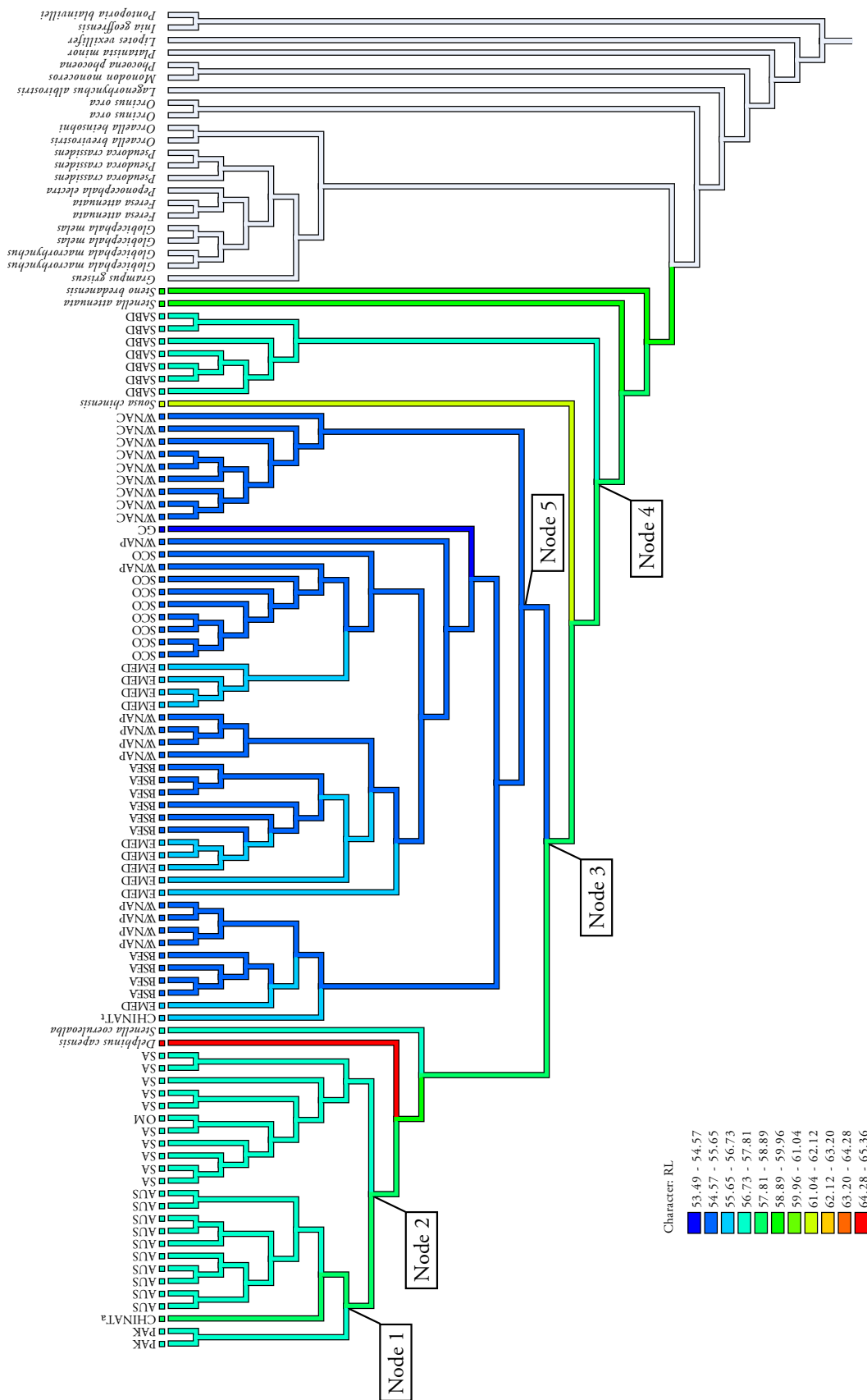


Figure 15: Maximum parsimony estimation of RL relative to CBL length (%) using the mitogenome phylogeny. Node numbers correspond to those presented in Table 9. Colours represent trait values. Figure generated in Mesquite v. 2.7.5 (Maddison & Maddison, 2015).

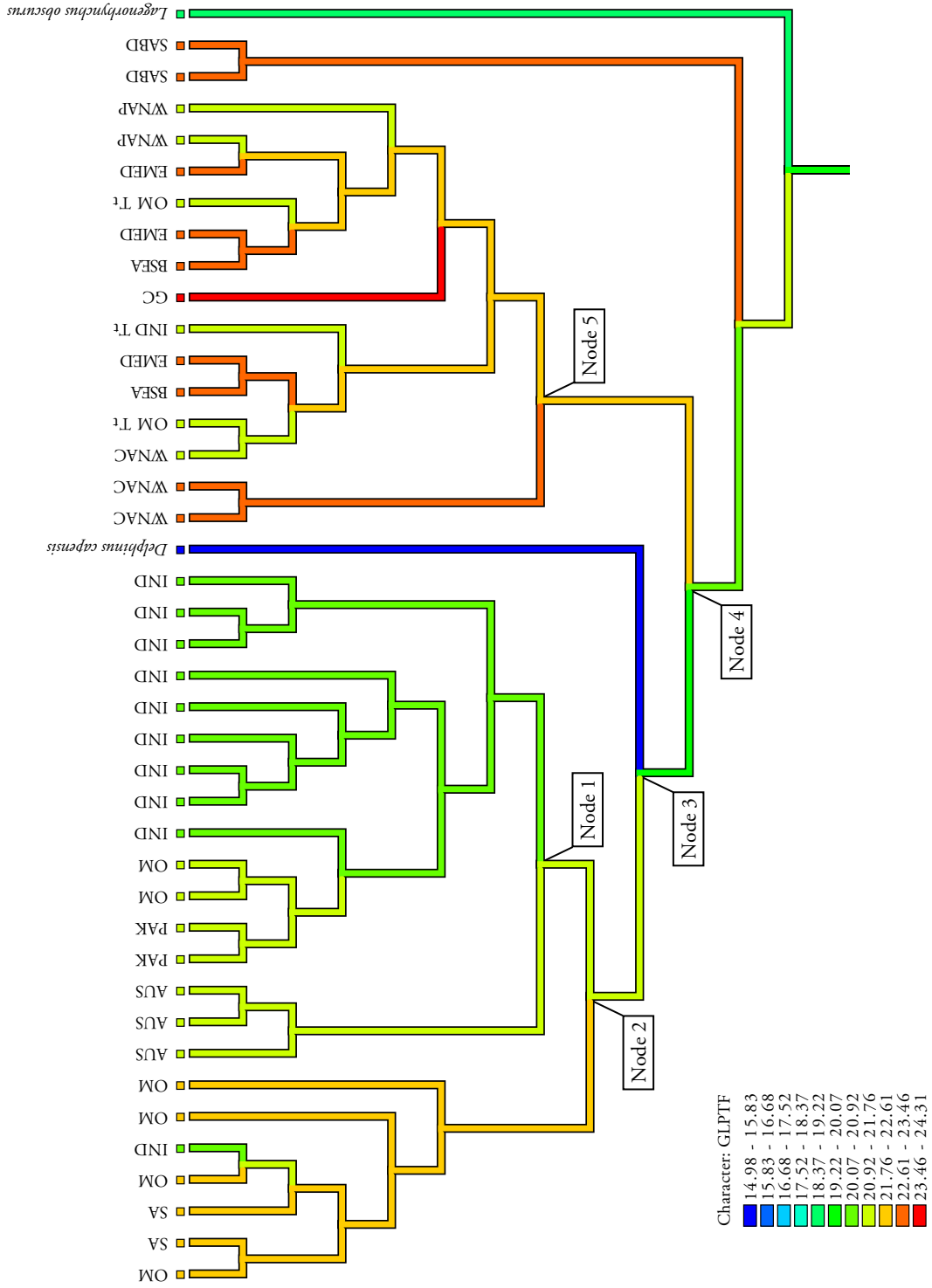


Figure 17: Maximum parsimony estimation of GLPTF relative to CBL length (%) for the concatenated mtDNA-nuDNA dataset. Node numbers correspond to those presented in Table 10. Colours represent trait values. Figure generated in MESQUITE v. 2.75 (Maddison & Maddison, 2015).

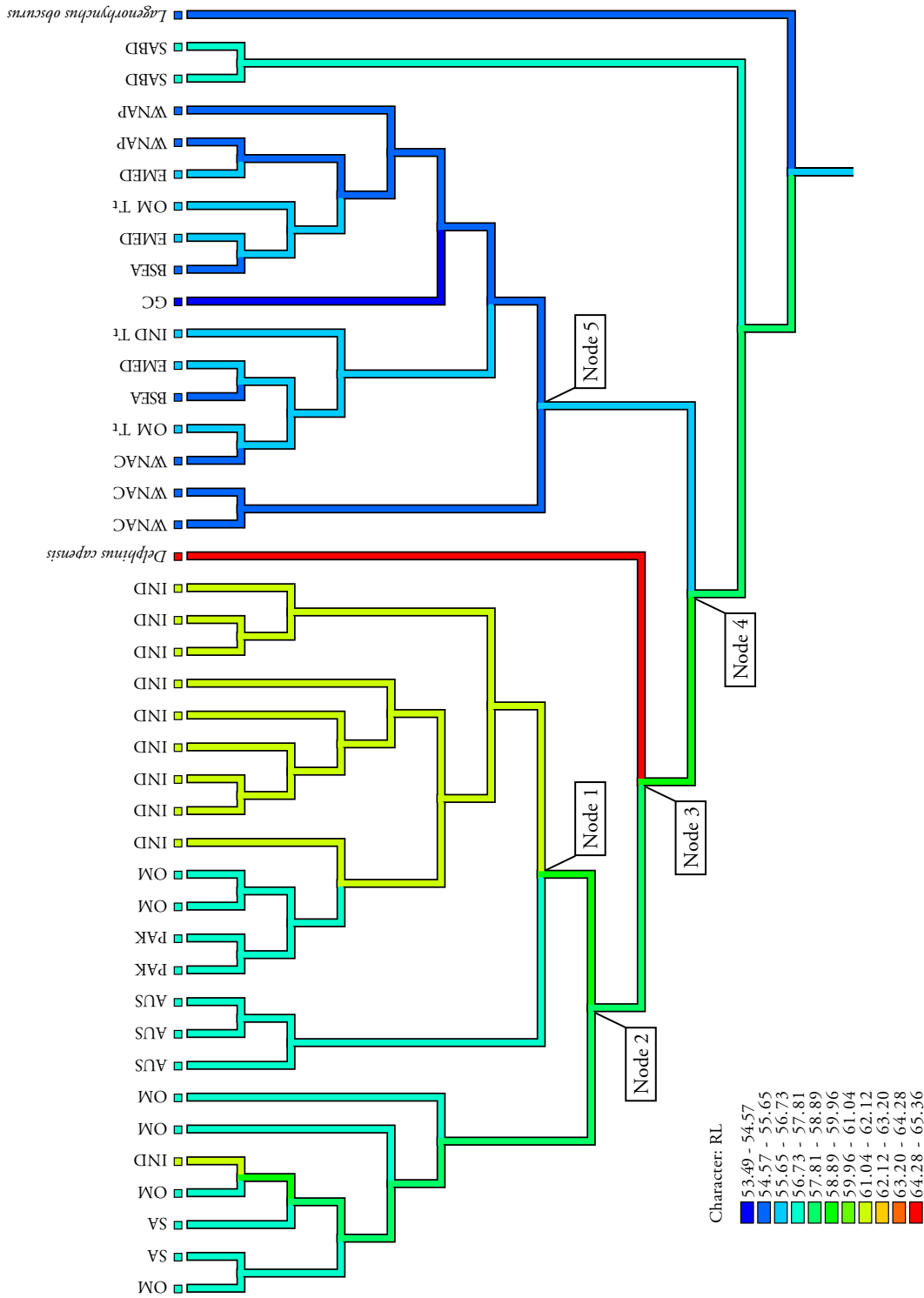


Figure 18: Maximum parsimony estimation of RL relative to CBL length (%) for the concatenated mtDNA-nuDNA dataset. Node numbers correspond to those presented in Table 10. Colours represent trait values. Figure generated in MesQUITE v. 2.7.5 (Maddison & Maddison, 2015).

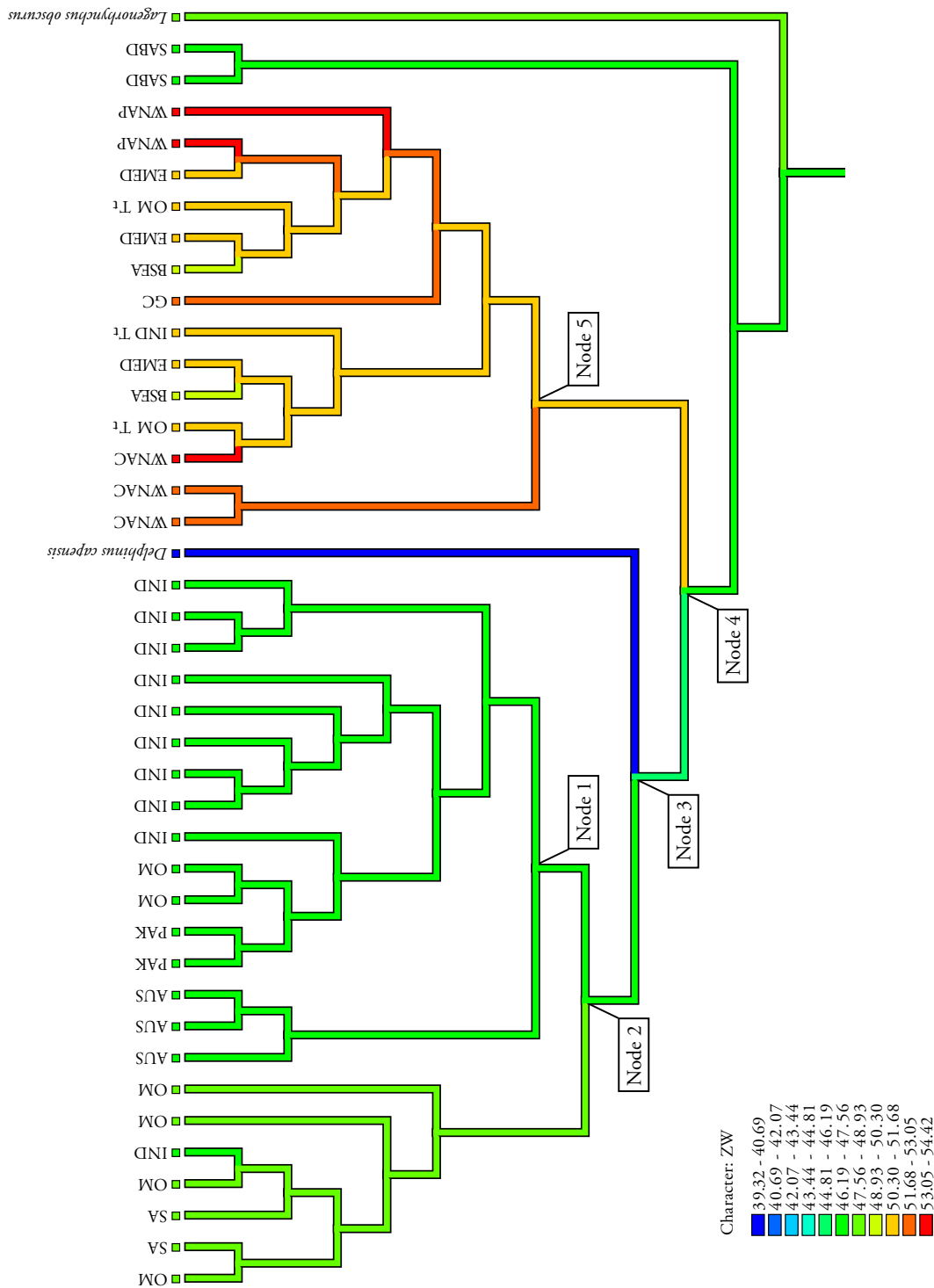


Figure 19: Maximum parsimony estimation of ZW relative to CBL length (%) for the concatenated mtDNA-nuDNA dataset. Node numbers correspond to those presented in Table 10. Colours represent trait values. Figure generated in MESQUITE v. 2.7.5 (Maddison & Maddison, 2015).

Estimated ancestral trait values were also plotted against ancestral node divergence dates generated in BEAST (see above) to visualize trait changes over time for populations represented in the Bayesian phylogeny generated from the mitogenomic dataset. These plots are presented in Figure 20 - Figure 22 showing changes in population averages for nine morphological characters relative to condylobasal length (CBL) estimated using the Phylogenetic Independent Contrasts (PIC) method. Measures are representative of rostral width (RWM), skull width (ZW), rostral length (RL), positioning of the nares relative to the rostral tip (TREN), upper and lower tooth row lengths (UTLTR, LTRL), length and width of temporal fossa (GLPTF, GWPTF) and mandibular height (MH).

2.3.4.1 Rostral and Skull Widths

Measures of skull and rostral width (ZW, RWM) relative to CBL in the *Tursiops* ancestor took on a form similar to extant *T. aduncus*-types. The zygomatic width, relative to CBL, was particularly narrow in the ancestral *Tursiops* and is very much the same as extant *T. australis* (SABD). *T. truncatus* populations exhibit wider skulls and rostra than *T. aduncus*-types, with some degree of overlap between Black Sea *T. t. ponticus* and *T. aduncus*-types in rostral width. Although *T. australis* shares a zygomatic width, relative to CBL, with the ancestral *Tursiops* and current *T. aduncus*-types, its relative rostral width is more like extant *T. truncatus* populations. The new, Arabian Sea *T. aduncus* (PAK-Ta) and Australasian *T. aduncus* have similar relative rostral widths compared to the holotype lineage of *T. aduncus* (SA-Ta). However, Arabian Sea and Australasian *T. aduncus* have comparatively narrow skulls compared to holotype *T. aduncus*, much like the ancestral *Tursiops*.

2.3.4.2 Rostral and Tooth Row Lengths and Relative Positioning of Nares

For rostral length (RL), relative to CBL, the *Tursiops* ancestor had rostra that resembled the longer rostra in extant *T. aduncus*-types. *T. truncatus* and *T. aduncus*-types are well separated based on RL and *T. australis* has an intermediate value.

The relative length of the lower tooth row is an intermediate between *T. truncatus* and *T. aduncus* for the *Tursiops* ancestor. Considerable overlap exists between *T. truncatus* and *T. aduncus* types in relative length of tooth row, particularly UTLTR. Australasian and Arabian Sea *T. aduncus* have longer average lower tooth row measures than their holotype lineage counterparts. Again, *T. australis* has taken on an intermediate form of the two.

The relative positioning of the nares to the tip of the rostrum (TREN) separates extant *T. aduncus* and *T. truncatus*-types well, whereby *T. aduncus* exhibits more telescoping than *T. truncatus*. The *Tursiops* ancestor is an intermediate of the two, with the extant *T. australis* as a close match, which slightly converges on a form similar to the eastern Mediterranean *T. truncatus* and is close to other *T. truncatus* species (China, Black Sea and northwest Atlantic-coastal).

2.3.4.3 Mandibular Height and Temporal Fossae Dimensions

The *Tursiops* ancestor exhibits a form more like extant *T. aduncus*-types on these measures relative to CBL. There is overlap between *T. truncatus* and *T. aduncus*-types for all of these measures but particularly for temporal fossae dimensions. The ancestor to *T. truncatus* and *T. aduncus*-types (Node 3) had smaller temporal fossae and a reduced mandible height compared to the *Tursiops* ancestor suggesting that these groups had different evolutionary trajectories on these traits to other dolphin species that share the same ancestor. Furthermore, the results are suggestive of homoplasy in these traits as the current form of extant *Tursiops*, particularly *T. aduncus*-types, is more like the distant ancestral form (Node 4) than the shared common ancestor (Node 3). For mandibular height and length of temporal fossa (GLPTF), *T. australis* converges on a *T. truncatus* form and is more intermediary between *T. truncatus* and *T. aduncus*-types for width of temporal fossae (GWPTF).

The same analyses were conducted using the phylogeny generated from the concatenated mtDNA-nuDNA dataset. The difference between these phylogenies is largely that of representation rather than topology, whereby the northwest Indian Ocean is better represented in the concatenated sequence tree but overall representation within the *T. truncatus* lineage is limited. Representation of other delphinids and outgroup support in the concatenated mtDNA-nuDNA phylogeny is also limited. Estimation of ancestral characters using this phylogeny revealed similar evolutionary patterns to those in the mitogenome phylogeny with small differences in degree (see Table 10 and Figure 23 - Figure 25).

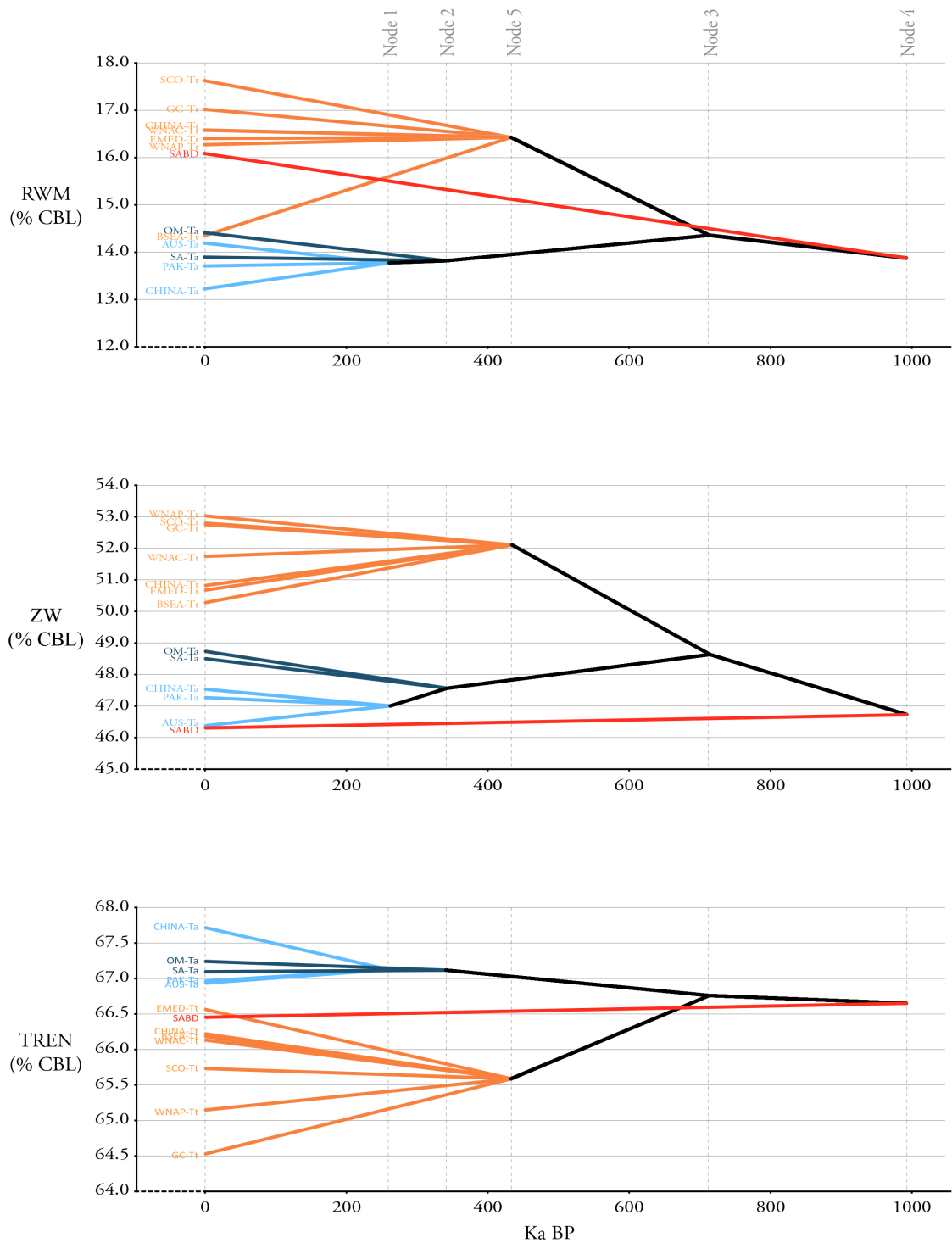


Figure 20: Trait values relative to condylobasal length (CBL); rostral width at mid-length (RWM), zygomatic width (ZW) and tip of rostrum to external nares (TREN), plotted against time as estimated from the mitogenome phylogeny. Ancestral trait values presented were estimated using the Phylogenetic Independent Contrast (PIC) method. Divergence times for nodes were estimated in BEAST v. 1.8 (Drummond & Rambaut, 2007). Trait values for extant populations are positioned at 0 Ka. Orange plots = *Tursiops truncatus* traits, blue plots = *T. aduncus*-type traits, where light blue = Arabian Sea (PAK-Ta) and Australasian-*T. aduncus* and dark blue = holotype *T. aduncus* (SA-Ta & OM-Ta). Red plot = *T. australis*. Black plots illustrate the trajectories of the ancestral traits.

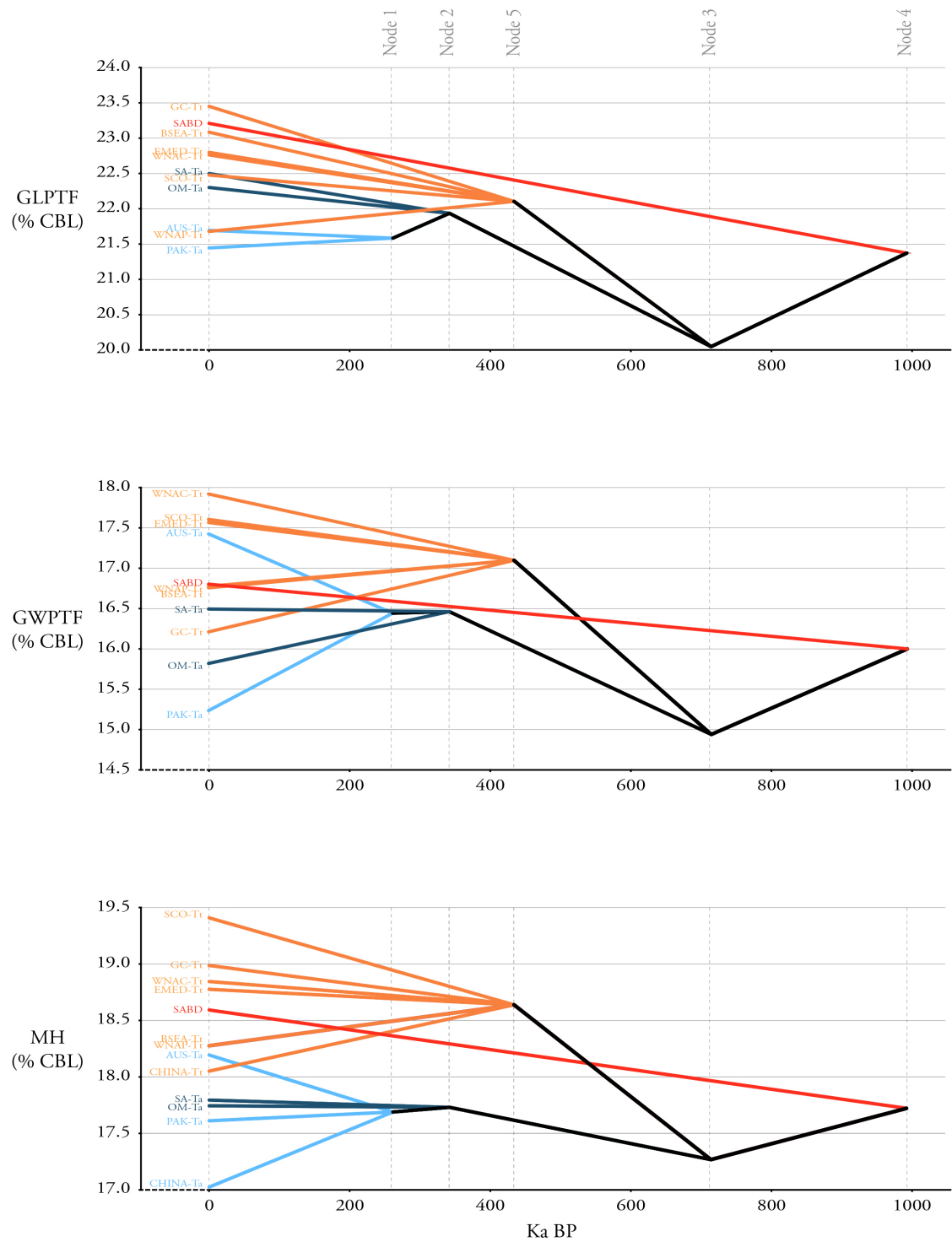


Figure 21: Trait values relative to condylobasal length (CBL); greatest length of left posttemporal fossa (GLPTF), greatest width of left posttemporal fossa (GWPTF) and mandible height (MH), plotted against time as estimated from the mitogenome phylogeny. Ancestral trait values presented were estimated using the Phylogenetic Independent Contrast (PIC) method. Divergence times for nodes were estimated in BEAST v. 1.8 (Drummond & Rambaut, 2007). Trait values for extant populations are positioned at 0 Ka. Orange plots = *Tursiops truncatus* traits, blue plots = *T. aduncus*-type traits, where light blue = Arabian Sea (PAK-Ta) and Australasian-*T. aduncus* and dark blue = holotype *T. aduncus* (SA-Ta & OM-Ta). Red plot = *T. australis*. Black plots illustrate the trajectories of the ancestral traits.

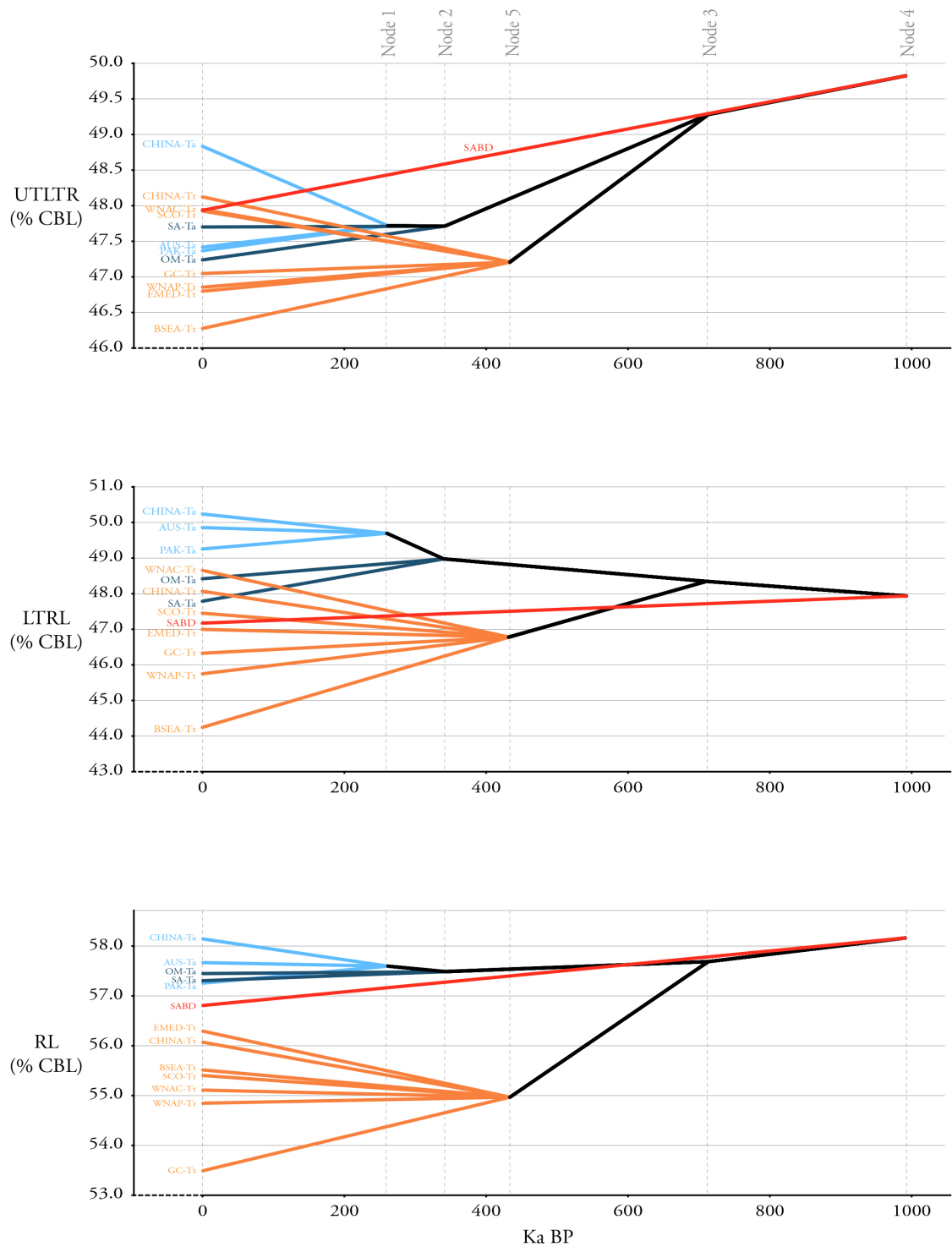


Figure 22: Trait values relative to condylobasal length (CBL); length of upper left tooth row (UTLTR), length of lower left tooth row (LTRL) and rostral length (RL), plotted against time as estimated from the mitogenome phylogeny. Ancestral trait values presented were estimated using the Phylogenetic Independent Contrast (PIC) method. Divergence times for nodes were estimated in BEAST v. 1.8 (Drummond & Rambaut, 2007). Trait values for extant populations are positioned at 0 Ka. Orange plots = *Tursiops truncatus* traits, blue plots = *T. aduncus*-type traits, where light blue = Arabian Sea (PAK-Ta) and Australasian-*T. aduncus* and dark blue = holotype *T. aduncus* (SA-Ta & OM-Ta). Red plot = *T. australis*. Black plots illustrate the trajectories of the ancestral traits.

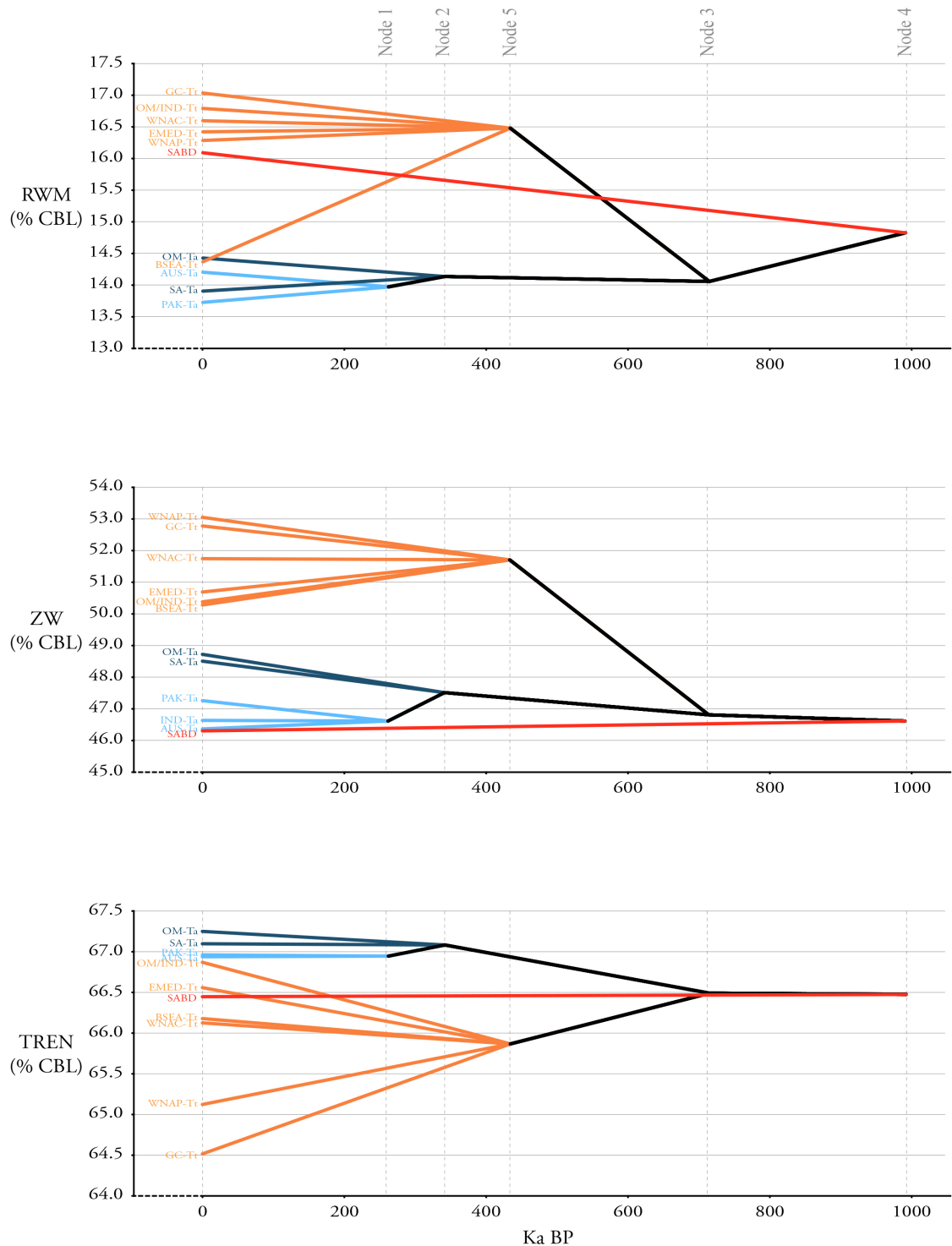


Figure 23: Trait values relative to condylobasal length (CBL); rostral width at mid-length (RWM), zygomatic width (ZW) and tip of rostrum to external nares (TREN), plotted against time as estimated from the concatenated mtDNA and nuDNA phylogeny. Ancestral trait values presented were estimated using the Phylogenetic Independent Contrast (PIC) method. Divergence times for nodes were estimated in BEAST v. 1.8 (Drummond & Rambaut, 2007). Trait values for extant populations are positioned at 0 Ka. Orange plots = *Tursiops truncatus* traits, blue plots = *T. aduncus*-type traits, where light blue = Arabian Sea (PAK-Ta) and Australasian-*T. aduncus* and dark blue = holotype *T. aduncus* (SA-Ta & OM-Ta). Red plot = *T. australis*. Black plots illustrate the trajectories of the ancestral traits.

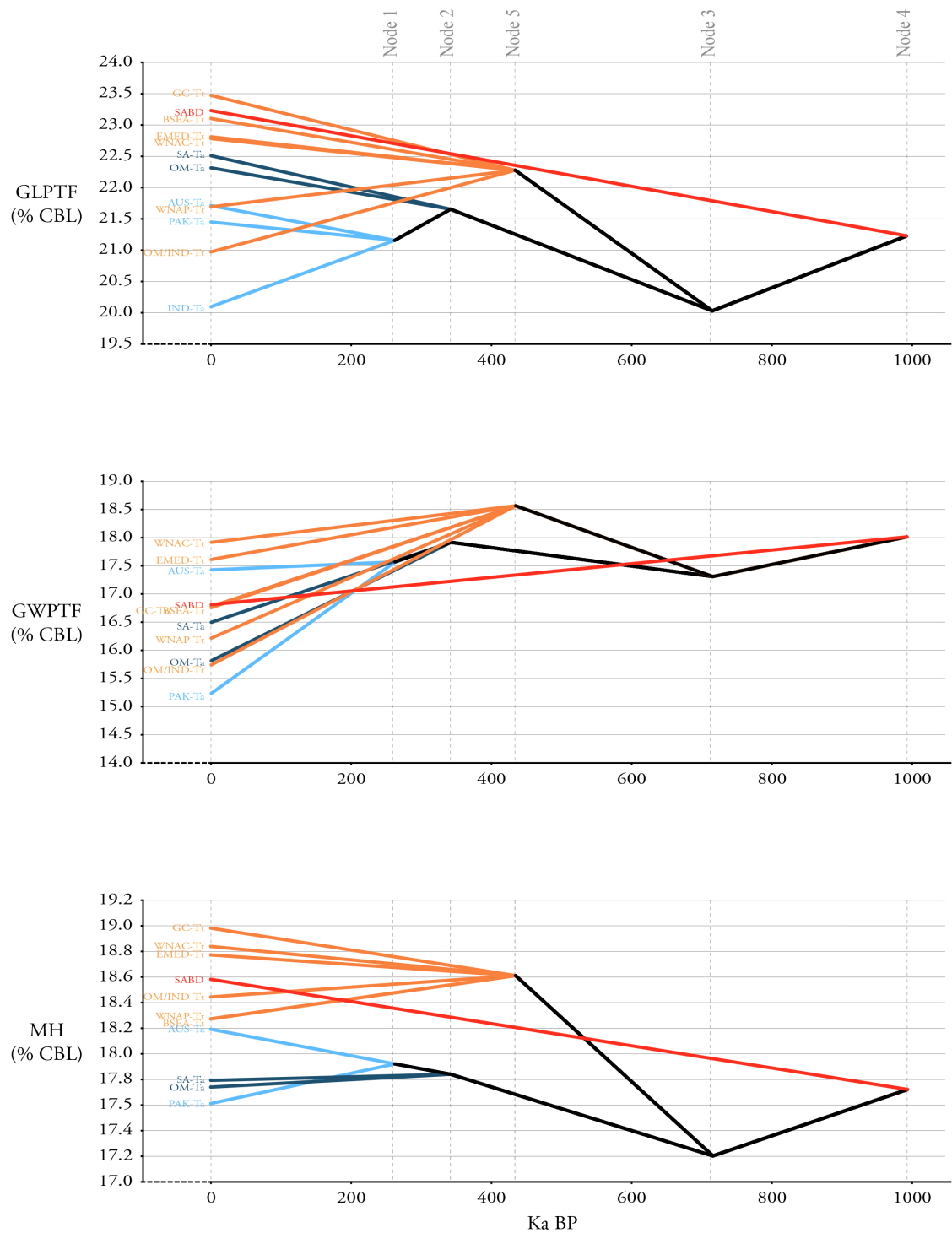


Figure 24: Trait values relative to condylobasal length (CBL); greatest length of left posttemporal fossa (GLPTF), greatest width of left posttemporal fossa (GWPTF) and mandible height (MH), plotted against time as estimated from the concatenated mtDNA and nuDNA phylogeny. Ancestral trait values presented were estimated using the Phylogenetic Independent Contrast (PIC) method. Divergence times for nodes were estimated in BEAST v. 1.8 (Drummond & Rambaut, 2007). Trait values for extant populations are positioned at 0 Ka. Orange plots = *Tursiops truncatus* traits, blue plots = *T. aduncus*-type traits, where light blue = Arabian Sea (PAK-Ta) and Australasian-*T. aduncus* and dark blue = holotype *T. aduncus* (SA-Ta & OM-Ta). Red plot = *T. australis*. Black plots illustrate the trajectories of the ancestral traits.

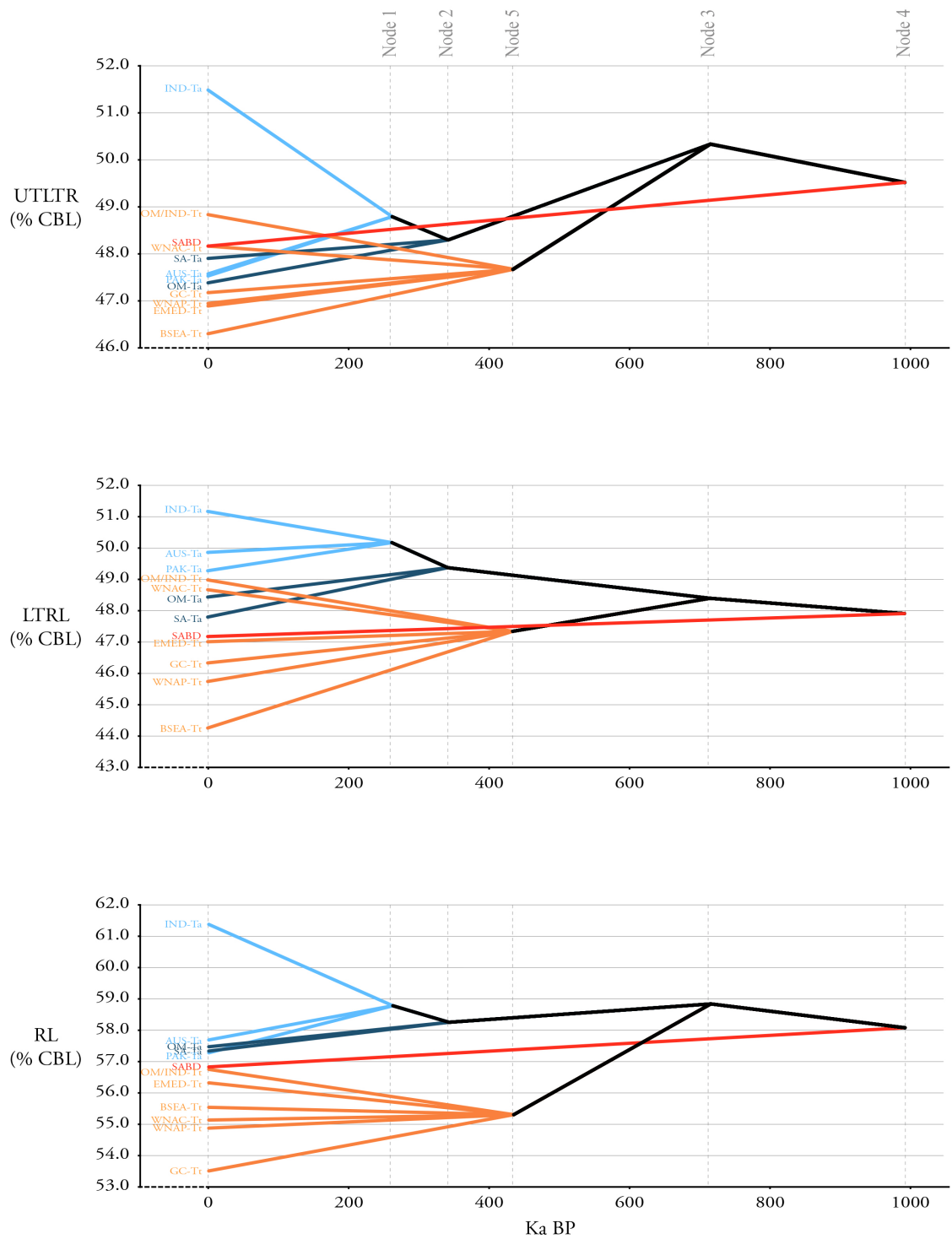


Figure 25: Trait values relative to condylobasal length (CBL); length of upper left tooth row (UTLTR), length of lower left tooth row (LTRL) and rostral length (RL), plotted against time as estimated from the concatenated mtDNA and nuDNA phylogeny. Ancestral trait values presented were estimated using the Phylogenetic Independent Contrast (PIC) method. Divergence times for nodes were estimated in BEAST v. 1.8 (Drummond & Rambaut, 2007). Trait values for extant populations are positioned at 0 Ka. Orange plots = *Tursiops truncatus* traits, blue plots = *T. aduncus*-type traits, where light blue = Arabian Sea (PAK-Ta) and Australasian-*T. aduncus* and dark blue = holotype *T. aduncus* (SA-Ta & OM-Ta). Red plot = *T. australis*. Black plots illustrate the trajectories of the ancestral traits.

2.4 Discussion

Building on the work conducted by Moura *et al.* (2013a), the present study focuses on *T. aduncus* in the northwest Indian Ocean. The propensity of this species to exhibit significant taxonomic structure (e.g. Natoli *et al.* 2004; Moura *et al.* 2013) makes their conservation management potentially complex. Investigation of bottlenose dolphin taxonomy in the region has been a recognised research priority for some time (IWC, 1999; Reeves *et al.* 2004) because knowledge of taxonomy is important for designing effective conservation strategies (see Mace, 2004). Being a coastal cetacean, *T. aduncus* is under particular threat in the region from an expanding fisheries industry (Salm *et al.* 1993; IWC, 1999; Collins *et al.* 2002; Anderson, 2014), pollution (Preen, 1991; Freije, 2015), and habitat degradation (IWC, 1999; Baldwin *et al.* 2004). Although there is national and international legislation in place across much of the region to prevent illegal hunting/trade of dolphins (e.g. IWC, CITES), there are no management strategies currently in place to address these, more indirect, impacts on dolphin populations (Ponnampalam, 2009).

Herein, phylogenetic analyses of novel sequence data of bottlenose dolphins from the northwest Indian Ocean reveal the presence of a new lineage of *T. aduncus* in the Arabian Sea. Delphinids are highly adapted to the environments they occupy and rely on healthy ecosystems for their survival (Moore, 2008), largely due to their high trophic placement (Ross, 2000). This makes them particularly sensitive to environmental change (e.g. Simmonds & Elliott, 2009). Indeed, estimations of divergence dates and reconstructions of ancestral biogeography, presented here, suggest repeated divergence events in *T. aduncus* in response to climate change over glacial periods.

The effects of climate change over the Pleistocene on sea level and oceanographic properties were substantial across the Indo-Pacific (Kassler, 1973; Fontugne & Duplessy, 1986; Shackleton, 1987; Wang *et al.* 1999a; Almogi-Labin *et al.* 2000; Voris, 2000; Sun *et al.* 2003; Bailey, 2009; Gaither & Rocha, 2013) and the contemporary oceanography in the region is also particularly heterogeneous, harbouring potential environmental breaks (discontinuities) (Mendez *et al.* 2011) and opportunities for resource polymorphisms to develop (Skúlason & Smith, 1995; Hoelzel, 1998a). These factors are likely to contribute to population and taxonomic structure across various marine taxa, e.g. reef fish (Bay *et al.* 2004; Gaither *et al.* 2011; Hubert *et al.* 2012), gastropods (Crandall *et al.* 2008), starfish (Williams & Benzie,

1998) and cetaceans (Jefferson & Van Waerebeek, 2002; 2004; Mendez *et al.* 2011; 2013; Pomilla *et al.* 2014).

2.4.1 Phylogeography

Novel mitogenome sequences were generated from Pakistan ($n = 2$) and Oman ($n = 1$) samples, comprising a total of ~50,244 bp of data. Additionally, a total of ~49,627 bp of nuDNA and ~88,920 bp of novel mtDNA data were generated from a sub-set of samples representative of the mitogenome dataset, with an increased sample representation from the northwest Indian Ocean, including samples from Pakistan, India and Oman.

Phylogenies constructed based on the mitogenomic and concatenated mtDNA-nuDNA data resulted in topologies similar to those presented in Moura *et al.* (2013a). Partitioned Bremer Support Indices suggested mtDNA and nuDNA loci were either congruent or uninformative (Figure 10). Within *T. aduncus*, three lineages were supported i) the Australasian lineage (Wang *et al.* 1999b), which includes individuals from Australia and China. ii) the holotype lineage (Natoli *et al.* 2004, Perrin *et al.* 2007) which includes individuals from South Africa, Oman and India, and iii) a new, Arabian Sea lineage which includes samples from Oman, Pakistan and India. In addition, samples from India ($n = 1$) and Oman ($n = 2$) grouped within the *T. truncatus* lineage, confirming the presence of this species in the northwest Indian Ocean. Poor resolution of these individuals within the *T. truncatus* lineage is suggestive of incomplete lineage sorting.

Reconstruction of ancestral biogeography revealed Australasia as the most likely origin for several *Tursiops* lineages and is a result shared with Moura *et al.* (2013a). The holotype lineage and other *T. aduncus* diverged ~342 Ka (95% HPD: 143, 630 Ka) while the new, Arabian Sea lineage and Australasian lineage diverged ~ 261 Ka (95% HPD: 111, 509) during the lower Pleistocene. The ~100 Kyr periodicity of these events is consistent with glacial oscillations (Gildor & Tziperman, 2000; Rohling *et al.* 2014), however due to the large credible intervals on these estimates, it cannot be confirmed whether they occurred during glacial or interglacial periods. Events in Australasia during the Pleistocene were evidently important for driving multiple divergence events in *Tursiops*, and possibly other closely related delphinids in the region, such as common dolphins, *Delphinus* spp. (see Jefferson & Van Waerebeek, 2002) and humpback dolphins (see Mendez *et al.* 2013). Australasia saw dramatic changes

in coastal topography over glacial periods (e.g. Voris, 2000; Gaither & Rocha, 2013) and in light of these, I propose a divergence mechanism (see below).

2.4.2 Pattern of Divergence

The distribution of samples of the new, Arabian Sea lineage overlaps with those of the holotype (Natoli *et al.* 2004; Perrin *et al.* 2007), as both are found in Oman and India. This suggests secondary contact is occurring between these lineages in the northwest Indian Ocean (see Chapter 3). Interactions between the Arabian Sea lineage and the Australasian lineage cannot be speculated over due to a lack of sample representation across that transitional zone. However, in order to explain the presence of three *T. aduncus* lineages across the Indo-Pacific, at least two mechanisms are considered: one driving multiple allopatric divergence events in Australasia, and the other facilitating divergence and maintaining reproductive isolation between lineages in the northwest Indian Ocean.

2.4.2.1 A Putative Divergence Mechanism

Sea level fluctuations over the Pleistocene were considerable (Shackleton, 1987), resulting in dramatic changes in coastal topography across the Indo-Pacific, such as the emptying of the Persian/Arabian Gulf (Kassler, 1973) and the near separation of the Red Sea from the Gulf of Aden (Bailey, 2009). During glacial periods, the sea level fell to 130 m below the present value, exposing the Sunda and Sahul shelves in Australasia and forming a physical barrier between the Indian and Pacific Oceans (Voris, 2000; Gaither & Rocha, 2013). I propose *T. aduncus* experienced at least two divergence events that were coincident with glacial oscillations during the Lower Pleistocene.

During glacial periods, exposure of the Sunda and Sahul shelves (Voris, 2000) caused areas of suitable habitat between the eastern Indian Ocean and the western Pacific to contract (Gaither & Rocha, 2013), thereby impeding gene flow between adjacent populations and resulting in allopatric divergence (Figure 26a). Indeed, this barrier is already thought to play a role in driving marine species diversity in that part of the world (e.g. Bay *et al.* 2004; Gaither *et al.* 2011; Hubert *et al.* 2012; Gaither & Rocha, 2013).

During interglacial periods, secondary contact between diverged *T. aduncus* lineages would have ensued. Assuming reproductive isolation was incomplete between the recently diverged

or diverging lineages, another barrier or reinforcement mechanism e.g. assortative mating or habitat specialisations, would have been required to prevent homogenization of the resultant lineages. Such a mechanism is likely still in effect where secondary contact between the new, Arabian Sea lineage and holotype lineage is apparent in the northwest Indian Ocean and presumably also between the Arabian Sea and Australasian lineages in the eastern Indian Ocean. A physical or biotic barrier in the northwest Indian Ocean is a focus of further investigation in Chapter 3.

The above mechanism implies the new lineage is more closely related to the holotype lineage than to the Australasian lineage, which is, at least superficially, incongruent with the estimated phylogeny. However, during the interglacial that followed the first divergence event ~342 Ka it is possible that more introgression may have occurred between populations experiencing secondary contact across the Indo-Pacific boundary than across the putative barrier in the northwest Indian Ocean, resulting in a phylogeny where the Arabian Sea lineage having a closer phylogenetic affinity to the Australasian lineage than the holotype lineage. Alternatively, given the recent divergence in these lineages, ambiguity in the inference drawn from the estimated phylogeny must be considered, whereby the tree topology may not reflect the true relationships of recently diverged lineages. An alternative mechanism, whereby populations in the east displaced those in the west during interglacial periods (see Figure 26b), could explain the phylogenetic pattern. However, given the tendency for this species to exhibit habitat preferences and site fidelity (e.g. Gross *et al.* 2009; Moura *et al.* 2013a) this mechanism seems less credible.

It is interesting to note that the humpback dolphin, a closely related delphinid that shares coastal habitat with *T. aduncus* (Wang & Yang 2009) shows a similar distribution pattern (Mendez *et al.* 2013). Specifically, the northwest Indian Ocean seems to be a transitional zone between *S. plumbea* and *S. chinensis*, as it appears to be for the holotype and new, Arabian Sea *T. aduncus* lineage. Jefferson & Van Waerebeek (2002) proposed a similar mechanism for the divergence of *D. capensis tropicalis*, which also occurs in waters off the northwest and northern Indian Ocean.

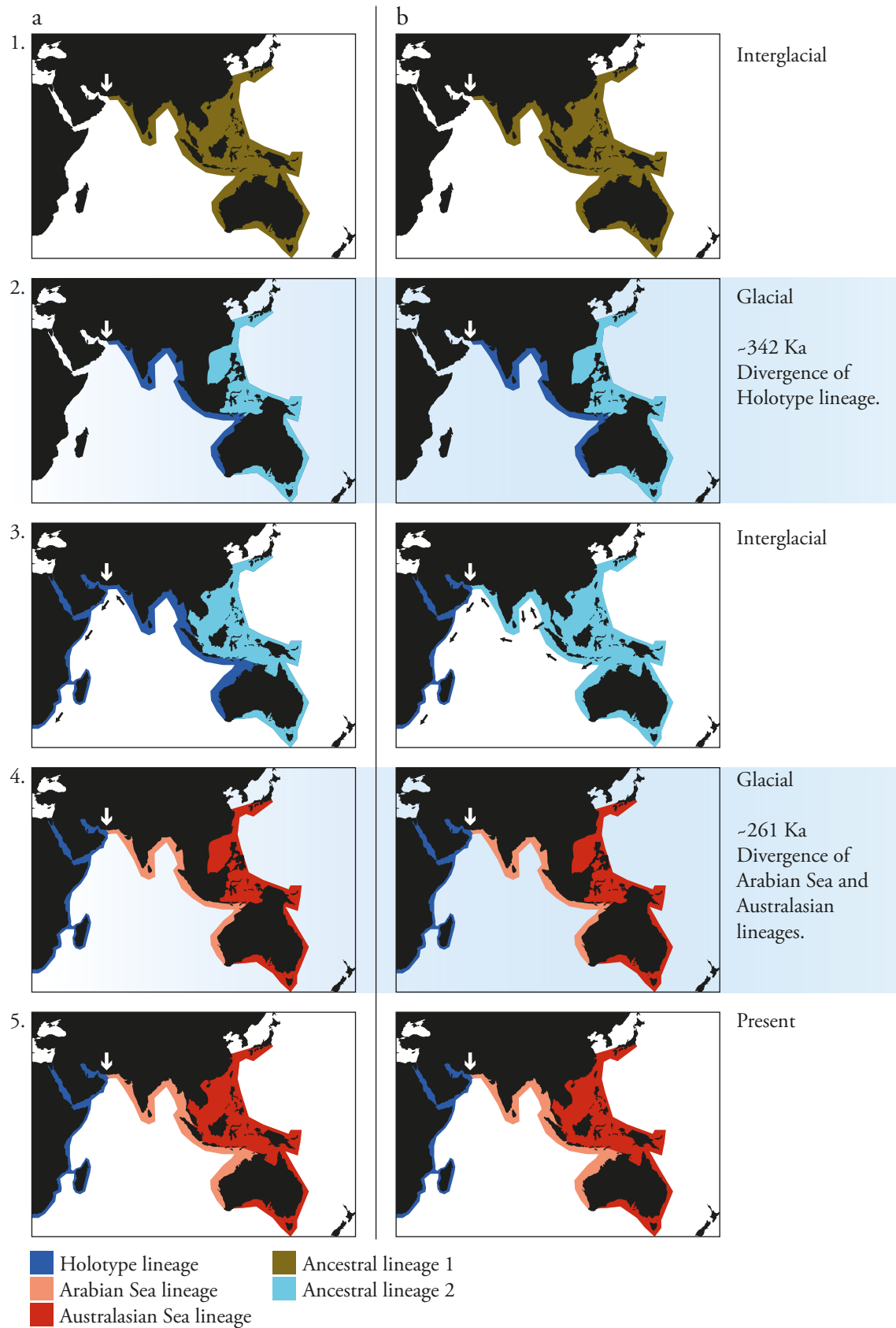


Figure 26: Two proposed mechanisms; a and b, for divergence events within *T. aduncus*. Black arrows indicate the direction of movement of dolphins. White arrow indicates the location of a putative physical or ecological barrier in the northwest Indian Ocean. The timing of movement across this barrier, illustrated during the interglacial in panels 3a and 3b, is unknown.

2.4.2.2 A Putative Barrier in the Northwest Indian Ocean

The present Asian monsoon system drives a seasonal reversal of atmospheric circulation over the northwest Indian Ocean, which influences the high primary productivity in the region (Banse & McClain, 1986; Bauer *et al.* 1991; Burkill, 1999; Kindle & Arnone, 2001; Singh *et al.* 2011). During the winter, the northeast monsoon generates coastal upwellings (Banse, 1987, Elliott & Savidge, 1990, Sheppard *et al.* 1992) driving productivity in the Gulf of Aden (Almogi-Labin *et al.* 2000), the eastern Arabian Sea and Andaman Sea (Fontugne & Duplessy, 1986; Naidu & Malmgren, 1999; Singh *et al.* 2001). The southwest monsoon is the dominant feature and prevails during the boreal summer months, generating strong upwelling along the Arabian Sea coast (Brock & McClain, 1992; Almogi-Labin *et al.* 2000). Conversely, palaeoclimate and palaeoproductivity data suggest there was great variability in the monsoon systems during the Pleistocene. The northeast and East Asian monsoons intensified and were the dominant feature during certain glacial events, while the southwest monsoons weakened (Fontugne & Duplessy, 1986; Wang *et al.* 1999a; Almogi-Labin *et al.* 2000; Sun *et al.* 2003). This shift may have changed the distributions of available prey and habitat across the Indian Ocean. For example, a population decline in killer whales, *Orcinus orca*, during the Weichselian glacial period has been attributed to changes in ocean productivity (Moura *et al.* 2014). Such changes could also result in resource polymorphisms (Skúlason & Smith, 1995; Hoelzel, 1998a), for example habitat-specific foraging specialisations (Rosel *et al.* 2009), which may continue to reinforce lineages currently experiencing secondary contact. For instance, pumpkinseed *Lepomis gibbosus*, and bluegill, *L. machrochirus*, sunfish feed on different prey when in sympatry. However, where bluegill sunfish are historically absent, pumpkinseed sunfish have differentiated into two morphotypes, one of which has taken on the planktivorous phenotype, similar to the bluegill sunfish (Robinson *et al.* 1993).

Alternatively, large-scale shifts in glacial monsoon-driven productivity in the northwest Indian Ocean (Duplessy, 1982) were inconsequential in maintaining/driving divergence in the separate *T. aduncus* lineages in the region. Instead, environmental heterogeneity across the northwest Indian Ocean (Longhurst, 2006) may be maintaining/driving sympatric differentiation through adaptation to local conditions/resources. The Arabian Sea lineage appears to dominate the eastern Arabian Sea coastline (off India and Pakistan) whereas the holotype lineage is more frequently encountered off Oman-Arabia. The coastal habitats in these regions are markedly different, as the coastal waters off India and Pakistan receive an influx of

freshwater from the Indus and Ganges deltas, carrying significant quantities of terrigenous sediments (Kolla *et al.* 1981; Longhurst, 2006). The waters off the Arabian Peninsula are characterised by comparatively high productivity. These differences in habitat could generate resource polymorphisms, manifested as differences in prey or utilization of habitat (Skúlason & Smith, 1995; Hoelzel, 1998a). Environmental heterogeneity across the western Indian Ocean has been attributed to genetic differentiation in humpback dolphins (Mendez *et al.* 2011) and could explain genetic structure in other taxa, such as mud crabs, *Scylla serrata* (Fratini & Vannini, 2002) and swordfish, *Xiphias gladius* (Lu *et al.* 2006). Indeed delineation of biogeographic provinces based on fish endemism shows that the central Indian Ocean, to the eastern limits of the Western Pacific, is a separate province from the western Indian Ocean (Briggs & Bowen, 2012). Delineated provinces may reflect broad ecosystem differences that would affect multiple taxa, including the different *T. aduncus* lineages that occupy them. Other species of dolphin show indications of taxonomic divisions or clines in the region, for example humpback dolphins, *S. plumbea*-*S. chinensis*, (Mendez *et al.* 2013) and common dolphins, longbeaked *Delphinus delphis*-*D. c. tropicalis*.

Alternatively, a physical barrier in the northwest Indian Ocean could explain the differentiation between the holotype and new, Arabian Sea *T. aduncus* lineages. Given the present overlap in the distributions of these lineages, such a barrier must either be semi-permeable or have variable intensity throughout history with a recent reduction in permeability. However, there is no indication of a physical geographic barrier in that region, suggesting an isolating mechanism driven by ecological, behavioural or oceanographical/climatic processes as a more credible explanation.

2.4.3 Ancestral Reconstruction of Morphological Traits

In order to determine the morphological affinities the *Tursiops* ancestor had to extant forms, ancestral character reconstruction analyses were performed for several morphological traits. Of the methods used, PIC, GLS and MP often yielded similar ancestral values for a trait at a given node (Table 9 and Table 10). Ancestral estimations generated from Bayesian MCMC inference were often smaller but generally followed a similar pattern. Comparisons between ancestral character estimates generated from the mitogenome phylogeny and the concatenated mtDNA-nuDNA phylogeny also revealed similar patterns in trait changes over time.

Estimated values for ancestral characters show the *Tursiops* common ancestor to resemble extant *T. aduncus*, suggestive of a coastal ancestry. Exceptions include length of lower tooth row (LTRL) and tip of rostrum to external nares (TREN), which have values intermediate of *T. truncatus* and *T. aduncus*.

The rostral length (RL), rostral width at mid-length (RWM), mandibular height (MH) and zygomatic width (ZW) of the *T. truncatus*-*T. aduncus* ancestor proportionately resembles *T. aduncus*, potentially indicative of a coastal ecology. Estimates show that the *T. truncatus*-*T. aduncus* ancestor had relatively low GWPTF and GLPTF values in proportion to CBL (see Table 10). While these low values are probably driven, in part, by the paraphyly of *Tursiops* with other species, it is possible that these findings support the theory that the common ancestor to *T. truncatus* was a coastal ecotype (Moura *et al.* 2013a). Dimensions of the temporal fossae (GLPTF, GWPTF) are associated with muscle jaw attachment, and as such potentially indicative of differences in foraging strategies and prey (Kemper, 2004; Mead & Fordyce, 2009).

Across extant *T. truncatus* and *T. aduncus* types, there is significant overlap in several cranial characters. In general, *T. aduncus* is proportionately longer, smaller and more slender than *T. truncatus*. Measurements of GLPTF from extant *T. aduncus*-types appear to suggest differences between the *T. aduncus* lineages, which may reflect local adaptation to different habitats and/or prey compositions (see Chapter 4). Zygomatic width (ZW) and rostral length (RL), relative to skull length (CBL), separate *T. aduncus* and *T. truncatus* without overlap. The Burrunan dolphin *T. australis* is a close intermediate of the two forms for most other characters.

2.4.4 Limitations

From the fossil record, there is no conclusive evidence for the origin of *Tursiops*, due to the widespread distribution of fossils from the Pliocene and Pleistocene (Barnes, 1990). The oldest occurrences of *Tursiops* sp. come from the early Pliocene: ~5 Ma in Italy, *T. cortesii* Sacco, 1891 (Barnes, 1990; Fitzgerald, 2005), ~3.5-4.5 Ma in North Carolina (in the northwest Atlantic region), *Tursiops* sp. (Barnes, 1990; Whitmore, 1994; Fitzgerald, 2005) and ~2.5-4.8 Ma off southeast Australia, *Tursiops* sp. (Fitzgerald, 2005).

In the present study, divergence times were estimated using fossil and geologic calibration points. Although these were the best supported from the different models and priors tested in the present study, and in Moura *et al.* (2013a), the divergence times within *Tursiops* are late (too recent) compared to the fossil record. Discrepancies between divergence times calibrated against fossil and biogeographic dates are recognised (Ho *et al.* 2005) and discussed in Moura *et al.* (2013a). However, one issue worthy of additional discussion is that of uncertainty over placement of the ~5 Ma fossil calibration within the *Tursiops* lineage. Following Moura *et al.* (2013a), this calibration was assigned to the earliest node in the *Tursiops* lineage (*cf.* Moura *et al.* 2013a). However, it is possible that this calibration should be applied elsewhere within the *Tursiops* phylogeny. Indeed, all of the *Tursiops* fossils reviewed in Barnes, (1990) either resemble *T. truncatus*, for example, a skull from the Jiangsu Province (Tsao, 1978), or were collected from regions where only *T. truncatus* is currently known to occur, such as fossil *Tursiops* sp. specimens collected in Italy (see Barnes, 1990), specimens from the North Sea (Kortzenboud van der Sluijs, 1983), from the northeast Pacific and northwest Atlantic (see Barnes, 1990). A specimen from southeast Australia, as represented by a right periotic described by Fitzgerald (2005), had affinities to, but was not conclusively, *Tursiops*. Fitzgerald (2005) does not refer to *T. aduncus* (only *Tursiops* sp.), however, the periotic length of the specimen falls within the range measured for *T. truncatus* (and *T. australis*) specimens from the same region and is 73 mm larger than the maximum periotic length for *T. aduncus*, reported in Charlton-Robb *et al.* (2011). In light of the distribution of recognized *Tursiops* fossil species and *T. truncatus*-type fossils, and the apparent lack of fossils that show an affinity toward *T. aduncus*, it is conceivable that all of these fossils (and fossil species) are, in fact, ancestral to *T. truncatus* only, and not *T. aduncus*. Placement of the Delphinoidea calibration point (McGowen *et al.* 2009; Steeman *et al.* 2009; Xiong *et al.* 2009) carries similar uncertainties. The recent discovery of a new dolphin fossil from northern Japan suggests that this calibration may be too recent and that further cladistic analyses utilising fossil delphinids and kentriodontids is required to resolve the correct placement of this calibration point (Murakami *et al.* 2014).

The majority of analyses presented here are based on the assumption that the mitogenome phylogeny reflects the true phylogenetic relationships between sampled individuals. These assumptions are not without merit as mtDNA has a relatively high substitution rate, thus allowing for good phylogenetic resolution between closely related individuals (May-Collado & Agnarsson, 2006). Furthermore, because mitochondrial genes are haploid, and maternally

inherited as a single linkage group, the mtDNA effective population size is a quarter that of nuclear genes, thus reducing the probability of incomplete lineage sorting (Moore, 1995). While this is the case, certain factors counteract these effects, such as male-mediated dispersal and female philopatry, which are frequently exhibited in cetacean species (e.g. Möller & Beheregaray, 2004; Escorza-Treviño & Dizon, 2000). The effects of introgression and pseudogenes can also cause discrepancy between the true phylogenetic history and that inferred from the mitogenome. These issues were tackled by incorporating nuclear markers with mtDNA markers. Partitioned Bremer support indices indicated the nuDNA markers were either congruent or uninformative with the phylogeny generated from the concatenated dataset, the nuclear markers were not very informative. Future work would benefit from incorporating further data from nuDNA markers to test for congruence between mtDNA and nuDNA.

Ancestral character reconstructions do not take intra-population variance in trait values into account. This is a limitation in the reconstruction analyses that requires further investigation. In order to overcome this problem, raw data is required for individuals within each population, in order that variation in measurements, proportional to skull length, can be incorporated into analyses. Another limitation to the analyses is that of inter-observer error. This is because measurements assigned to populations and species represented in the phylogenies were taken from published sources. As such, differences between extant taxa, and ancestral character estimates derived from them, are based on the assumption that measurement methodologies were congruent across all studies. This is probably not the case and some differences in character values are likely attributable to inter-observer bias. For example, a study on inter-observer variability in scale counts of a species of lizard, *Anolis sagrei* showed taxonomic-level distinctions based only on inter-observer differences in scoring precision of the characters (Lee, 1990). In order to overcome such bias, one observer would have to carry out all measurements, or alternatively, a team of observers would need to inter-calibrate their measuring methodologies and/or identify which characters are particularly variable between observers (e.g. Jefferson & Van Waerebeek, 2002). Finally, poor taxonomic resolution in the Delphininae, as well as incomplete sampling of taxa in the phylogeny (and associated morphological data), can make inferences about ancestral character traits difficult to make.

2.4.5 Conclusion

Herein, evidence is provided for coastal bottlenose dolphins, *T. aduncus* to exhibit signifi-

cant taxonomic structure driven by multiple divergence events in response to environmental change over the Pleistocene. Furthermore, the discovery of a new lineage of bottlenose dolphin in the northwest Indian Ocean contributes to the growing evolutionary uniqueness characteristic of cetaceans in the region (see Jefferson & Van Waerebeek, 2002; Minton *et al.* 2010; Mendez *et al.* 2013). Coastal cetaceans are under significant threat from anthropogenic activities in the Indian Ocean (IWC, 1999) and there is a growing need to develop regional conservation measures. The design of effective management strategies will need to consider this new lineage of *T. aduncus* in the Arabian Sea, particularly off Pakistan and India where the majority of samples were collected. The distribution of samples suggests secondary contact with, at least, the holotype lineage and that management of these lineages may be complex. Further research into the diet and life history of the separate lineages will further inform conservation initiatives if the lineages have adapted to different habitat characteristics or prey compositions.

More broadly, this chapter identifies divergence events in a mobile marine taxon in response to climate change over the Pleistocene. I suggest that glacial fluctuations in sea level off Australasia, and the repeated exposure of the Indo-Pacific boundary drove multiple allopatric divergence events in coastal dolphins, as has been proposed for other marine species in the region (e.g. Bay *et al.* 2004; Gaither *et al.* 2011; Hubert *et al.* 2012; Gaither & Rocha, 2013). Furthermore, I discuss the need for another mechanism, such as a physical or ecological barrier, to facilitate the divergence of lineages in the Indian Ocean. This is explored further in Chapter 3.

Chapter 3

Population Structure of Bottlenecked Dolphins (*Tursiops* spp.) in the Western Indian Ocean

3.1 Introduction

Understanding population genetic structure in the seeming absence of barriers to gene flow presents an interesting challenge to evolutionary biologists working with highly mobile marine taxa. Such taxa normally exhibit panmixia, or low levels of genetic structure, across large spatial scales (Palumbi, 1992). However, there are examples where taxa with high dispersal abilities exhibit significant degrees of population structure, for example, sea turtles (Bowen *et al.* 1993; Encalada *et al.* 1996), fish (Knutsen *et al.* 2003; Keeney *et al.* 2003; Nielsen *et al.* 2004) and marine invertebrates (Hellberg, 1996; Huang *et al.* 2000; Hoffman *et al.* 2013). Marine mammals, as a group, are exceptional as they regularly exhibit genetic differentiation across spatial scales that are outdistanced by their dispersal abilities (e.g. Tolley *et al.* 2001; Hayano *et al.* 2004; Natoli *et al.* 2004; Sellas *et al.* 2005; Fontaine *et al.* 2007; Natoli *et al.* 2008a; Andrews *et al.* 2010; Fernández *et al.* 2011; Hamner *et al.* 2012). Therefore marine mammals make interesting candidates for studying the processes that restrict gene flow and drive population structure in the marine environment.

Such processes interact on a variety of spatial and temporal scales and include: (i) behaviour, such as assortative mating and variations in resource utilisation (Skúlason & Smith, 1995; Hoelzel, 1998a), (ii) demographic history, for example male-mediated dispersal and female philopatry (Hoelzel, 1994), (iii) oceanography, including sea surface temperature, primary production and surface currents as barriers to dispersal (Fontaine *et al.* 2007; Mendez *et al.* 2011) and (iv) climatic history, for example sea level fluctuations over the Pleistocene altering habitat availability (Moura *et al.* 2013a).

Many marine mammal species are particularly sensitive to environmental change due to their high trophic placement and reliance on healthy ecosystems for survival (Moore, 2008). As a result they have been proposed as ecosystem sentinels (Ross, 2000; Wells *et al.* 2004; Moore, 2008) and are also of significant conservation concern, for example due to the effects of climate change (Simmonds & Elliott, 2009). Population genetic techniques are an important

tool in identifying populations/stocks and demographic processes to better inform and help prioritise conservation efforts (Frankham *et al.* 2002; Palumbi, 2003; Waples *et al.* 2008).

Conservation managers have recognised a specific need to identify coastal cetacean stocks in the western and northwest Indian Ocean, particularly humpback dolphins, *Sousa* spp., common dolphins, *Delphinus* spp. and bottlenose dolphins, *Tursiops* spp. (IWC, 1999). Although there is a good framework of international agreements and conventions, to which various countries in the region are member, as well as national legislation to protect marine mammals and their environments in general, the implementation of site-specific management of coastal cetaceans and their critical habitat remains limited (Ponnampalam, 2009). Arguably, the greatest threat posed to coastal cetaceans in this region is their interaction with fisheries activities (Cockcroft, 1990; IWC, 1999; Amir & Jiddawi, 2001; Collins *et al.* 2002; Peddemors *et al.* 2002; Natoli *et al.* 2008a; Amir, 2010; Anderson, 2014). In response to a recognised need to investigate dolphin stock identities in the region (IWC, 1999), morphological and genetic data have been used to assess the conservation status and taxonomy of humpback and common dolphins in the western Indian Ocean (e.g. Jefferson & Van Waerebeek, 2002; Baldwin *et al.* 2004; Jefferson & Van Waerebeek, 2004; Mendez *et al.* 2011; Amaral *et al.* 2012a; Mendez *et al.* 2013). Work on bottlenose dolphins, particularly *T. aduncus* in the western Indian Ocean, has been largely limited to South Africa (Natoli *et al.* 2004; 2008a), Zanzibar (Särnblad *et al.* 2011) and, with lower sample representation, Oman and Mayotte (Särnblad *et al. in review*). In South Africa, Natoli *et al.* (2008a) considered three *T. aduncus* populations: two resident, north and south of Ifafa, along the coast of KwaZulu-Natal and a migratory population occurring in coastal waters during the winter migration of sardines (*Sardinops ocellatus*). Natoli *et al.* (2008a) suggested the combined effect of a river estuary and reef system at Ifafa could be creating a barrier to gene flow between northern and southern populations. Off Zanzibar, Särnblad *et al.* (2011; *in review*) showed significant genetic differentiation between northern and southern Zanzibar populations based on mtDNA control region sequences (534 bp) and seven microsatellite loci. They attributed this structure to female philopatry.

The west and northwest Indian Ocean is a particularly heterogeneous environment (Banse, 1968; Swallow, 1984; Schott & McCreary Jr., 2001; Longhurst, 2006; Mendez *et al.* 2011). Contemporary oceanographic and climate conditions off the coast are strongly influenced by the Indian southwest and northwest monsoon systems, which generate significant upwellings

in the summer and winter months, respectively. It is believed that these conditions provide nutrients and food to support a variety of cetacean species throughout the year (Sheppard *et al.* 1992; Papastavrou & Van Waerebeek, 1997; Minton *et al.* 2010). Regional habitat variations across these systems may be expected to generate population structure in coastal dolphins (e.g. Natoli *et al.* 2005; 2008a; Mendez *et al.* 2010; 2011), suggesting populations in the northwest Indian Ocean might require separate management. Therefore, further work on the stock identification and demographic history of bottlenose dolphins, particularly *T. aduncus*, in the northwest Indian Ocean is pertinent.

The results in Chapter 2 indicate the presence of three lineages within the *T. aduncus* group. One lineage dominates the west and northwest Indian Ocean and was originally described off South Africa by Natoli *et al.* (2004) and has since been matched to the *T. aduncus* holotype in the Red Sea (Perrin *et al.* 2007), hereafter referred to as the holotype lineage. The waters off Australasia are occupied by a different lineage of *T. aduncus*, put forward by Wang *et al.* (1999b), hereafter referred to as the Australasian lineage. In Chapter 2 a new lineage of *T. aduncus* was discovered, which appears to dominate the northern Indian Ocean, off India and Pakistan, with some degree of overlap in range with the holotype lineage in the west/northwest Indian Ocean, along the coastline between Oman and India. Hereafter, this lineage is referred to as the Arabian Sea lineage. Unfortunately sample representation is limited to the western limits of the Arabian Sea lineage's range, making it difficult to speculate about processes happening in the eastern part of its range.

From divergence estimates in Chapter 2, it was inferred that the holotype and the other *T. aduncus* lineages diverged ~342 Ka (95% HPD: 143, 630 Ka). A second divergence event, ~261 Ka (95% HPD: 111, 509) then gave rise to the other two lineages; the Australasian lineage and the Arabian Sea lineage. Ancestral distribution reconstructions presented in Chapter 2, suggest that both divergence events occurred in Australasia over the Pleistocene. I postulate that climate change and sea level fluctuations during glacial and interglacial periods resulted in repeated exposure of the Sunda and Sahul shelves in Australasia, thus recurrently forming a geographic barrier across the Indo-Pacific. Several divergence events of allopatric populations either side of this barrier may have occurred during these periods, as has been proposed for other marine species in the region (Gaither & Rocha, 2013).

However, in order to produce these lineages, there must have been another barrier, or differ-

ent isolating mechanism, operating in the northwest Indian Ocean preventing homogenisation between populations either side of it and facilitating divergence of the holotype and Arabian Sea lineage. Furthermore, the apparent overlap in distributions of the two lineages in the northwest Indian Ocean, including biopsy samples of both lineages from the same bay in Oman (but notably at different times of the year) suggest secondary contact between them. Possible isolating mechanisms include a geographic barrier (e.g. formation of a land bridge; Dowling & Brown, 1993), oceanographic boundary (e.g. sea-surface temperatures and primary productivity; Fullard *et al.* 2000; Fontaine *et al.* 2007; Mendez *et al.* 2011), an ecological break (e.g. indirect effects of a gap in prey distribution; Bilgmann *et al.* 2007) or local adaptation in sympatry to different prey compositions (Adams & Rosel, 2006; Hoelzel, 1994; Hoelzel & Dover, 1991). Climate fluctuations over the Pleistocene, for instance monsoonal shifts during glacial/inter-glacial periods and their effects on primary production in the northern Indian Ocean (Fontugne & Duplessy, 1986; Almogi-Labin *et al.* 2000), may have changed the presence, or permeability, of such a mechanism. A similar mechanism is presumably in place between the Arabian Sea and Australasian lineages in the eastern Indian Ocean, however, due to a lack of samples from that region, it is difficult to speculate over what processes might be preventing homogenisation between those lineages.

Three general hypotheses attempt to explain the demographic history, and associated isolating mechanisms, of contemporary populations of coastal bottlenose dolphins in the western and northern Indian Ocean:

1) *The appearance of a semi-permeable 'barrier' **after** population establishment in the western Indian Ocean:*

Under this hypothesis (Figure 27a), populations in the western Indian Ocean would have been established before the appearance of a barrier in the northwest Indian Ocean. In the absence of a barrier, populations would have expanded across the region without restriction (and therefore without a reduction in N_e due to a founder event). The barrier subsequently appeared after populations were established in the western Indian Ocean and before the second *T. aduncus* divergence event ~ 261 Ka (see Chapter 2). Such a barrier may still be present.

2) *The presence of a semi-permeable 'barrier' **before** population establishment in the western Indian Ocean:*

In this case (Figure 27b), populations in the western Indian Ocean were established by a

founder event (resulting in reduced N_e) as a consequence of immigration across a barrier in the northern Indian Ocean. Such a barrier may still be present. Under this hypothesis, populations would have been established in a southerly direction (i.e. first the Oman population, followed by Zanzibar and then South Africa). Secondary contact would be explained by either recent barrier disappearance or restricted contemporary movement across it.

3) *The presence of a historic 'barrier' with refugial survival:*

In this scenario (Figure 27c), a barrier appeared in the northwest Indian Ocean after populations in the western Indian Ocean had been established (as for scenario two). This 'barrier' may have been caused by climate change over glacial periods, causing western Indian Ocean populations to contract southwards to refugia, as similarly proposed for killer whales off South Africa (Moura *et al.* 2014). Once the barrier disappeared, a northwards re-expansion out of South Africa would have resulted in the divergence of contemporary populations off Zanzibar followed by Oman (i.e. divergence pattern in a northwards direction). In this scenario, the apparent distributions of the Arabian Sea and holotype lineages of *T. aduncus* in the northwest Indian Ocean would be explained in terms of relatively recent secondary contact between expanding lineages.

In this study I have set out to investigate population structure across the northern and western Indian Ocean coastline using microsatellite DNA markers. I test the hypothesis that populations off Pakistan/India, Oman, Zanzibar and South Africa are genetically differentiated. Inclusion of mitochondrial DNA (mtDNA) control region sequence data from these populations, and those in other parts of the world, will enable phylogenetic investigation of the relationships and genetic differentiation between bottlenose dolphins across the Indo-Pacific. Additionally, I examine the degree of connectivity between populations along the East African and Arabian coastline by inferring recent migration patterns from microsatellite data. Fine-scale genetic structure reported in coastal bottlenose dolphins off South Africa (Natoli *et al.* 2008a) and Zanzibar (Särnblad *et al.* 2011; *in review*) will be investigated further, using a greater number of microsatellite loci ($n = 14$) than utilised in those previous studies. Finally, the present study aims to provide further evidence in support of the Arabian Sea lineage of *T. aduncus* in the northern Indian Ocean (see Chapter 2) and explore the various demographic and divergence hypotheses (Figure 27) that gave rise to contemporary populations of *T. aduncus* in the region.

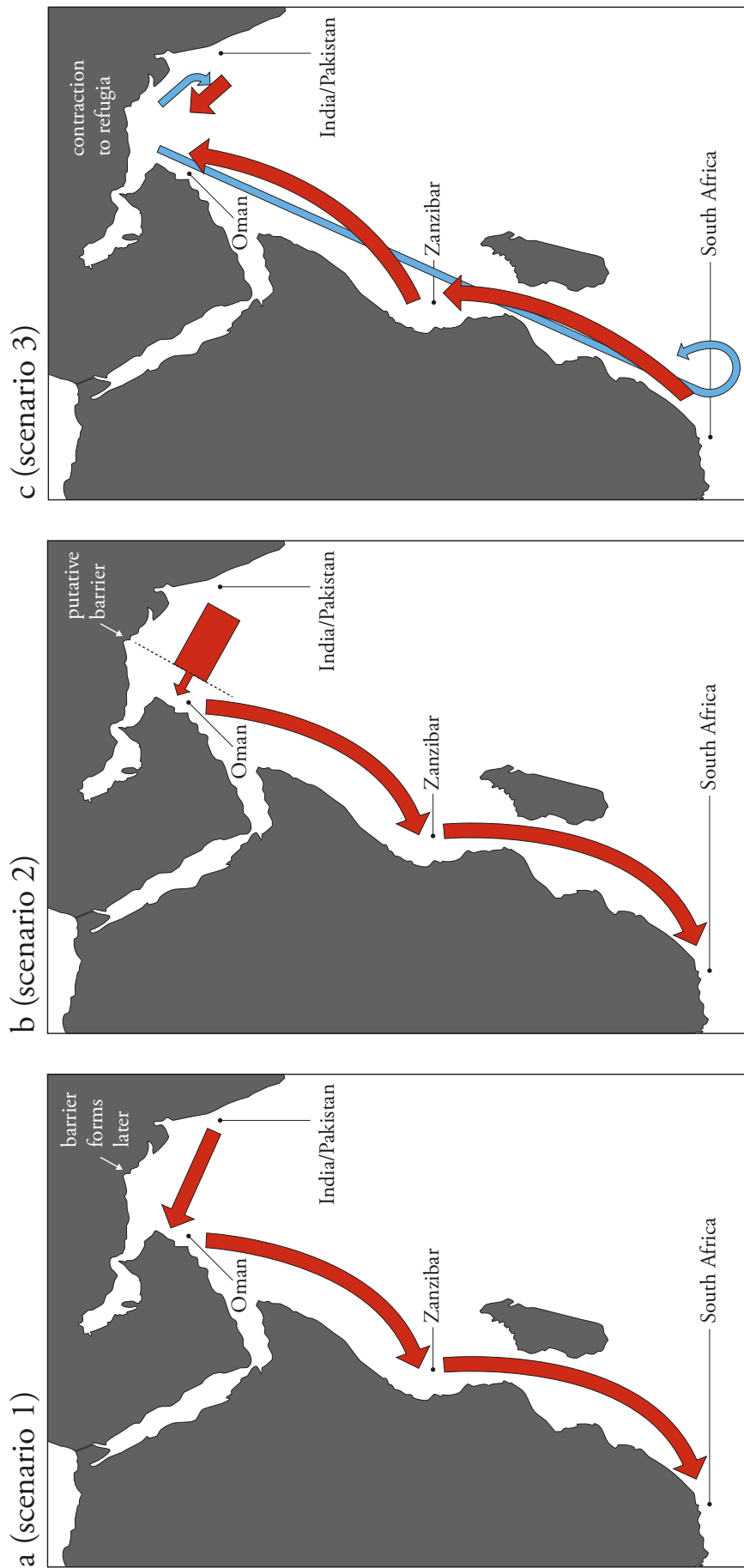


Figure 27: General hypotheses to explain the demographic history, and associated isolating mechanisms, of contemporary populations of coastal bottlenose dolphins in the western and northern Indian Ocean. a = scenario 1: a barrier in the northwest Indian Ocean is initially absent, thus no reduction in N_e as populations are established in a southward direction.. b = scenario 2: populations in Oman are founded by individuals that cross a barrier in the northwest Indian Ocean (resulting in a reduced N_e). Populations are established along the western Indian Ocean coastline in a southward direction. c = scenario 3: a historic barrier (habitat gap) causes populations to contract (reduced N_e , blue arrows) to refugia. Populations re-expand out of refugia, coming into secondary contact in the northwest Indian Ocean (where there is no longer a gap in suitable habitat).

3.2 Materials and Methods

3.2.1 Sample Acquisition

Samples of bottlenose dolphins, *Tursiops* spp. were collected in Oman, from either strandings ($n = 81$) or free-ranging ($n = 7$) individuals, by the Environment Society of Oman (ESO) and their affiliates. Skeletal remains curated at the Oman Natural History Museum (ONHM) were also sampled. Further biopsy samples ($n = 12$) were collected off Oman by the author in collaboration with ESO (see below). All samples from Zanzibar were either biopsies of free-ranging individuals ($n = 21$) or sampled from fisheries bycatch ($n = 30$) (see Särnblad *et al.* 2011). Samples from South Africa ($n = 105$) were biopsies and shark-net bycatch collected along the KwaZulu-Natal coast (see Natoli *et al.* 2008a). Samples from Pakistan ($n = 15$) were collected from beach cast individuals provided by Cetacean Conservation Pakistan (CCP) and from skeletal remains curated at the Museum am Löwentor, Staatliches Museum für Naturkunde, in Stuttgart, Germany (SMNS). One sample from Iran (Strait of Hormuz) and three from Thailand were curated at the SMNS and included in some analyses. The Environmental Specimen Bank (es-Bank), at the Center for Marine Environmental Studies, Ehime University of Japan provided Indian samples ($n = 10$). Sequences of mtDNA control region, deposited on GenBank, from Indo-Pacific bottlenose dolphins *T. aduncus* and common bottlenose dolphins *T. truncatus* were also utilised in analyses. See Figure 28 for sample locations and Table 11 for sample information. These included the *T. aduncus* holotype sequence from the Red Sea (Perrin *et al.* 2007) and a sequence from Iran (Mohsenian *et al. unpublished data*).

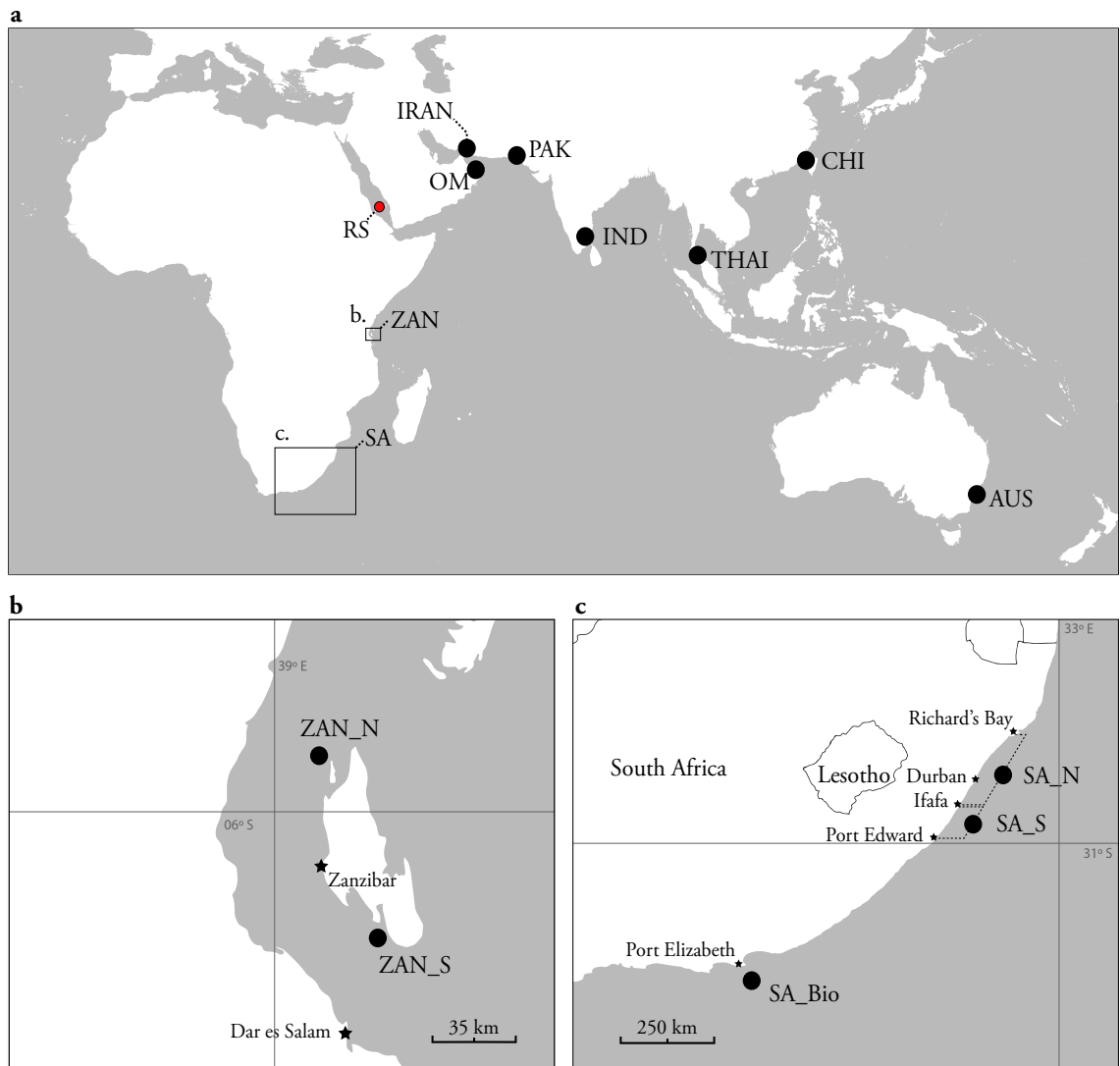


Figure 28: Locations of bottlenose dolphin (*Tursiops* spp.) samples utilised in this study. Box a) shows the distribution of sample locations (black circles) across the Indo-Pacific. The red circle indicates the location of the *T. aduncus* holotype specimen (Perrin *et al.* 2007). Boxes b) and c) show further details of sampling sites as adapted from Särnblad *et al.* (2011) and Natoli *et al.* (2008), respectively. Refer to Table 11 for definitions of sample location codes.

Table 11: Summary of sample locations and numbers, *N*, used for a) microsatellite and b) mitochondrial DNA markers. ‘Code’ correspond to regions in the map presented in Figure 28; ‘Population’ refers to the population designation used in mitochondrial DNA analyses where some samples are pooled; ‘Reference’ refers to the sample sources; ‘Sequence Source’ refers to the sample sources and published sequences. *Pakistan and India samples are compared using seven microsatellite markers.

a**Microsatellites**

Code	Location	<i>N</i>	Reference
<i>Tursiops aduncus</i>			
OM	Oman	19	This study
ZAN_N	North Zanzibar	25	Särnblad <i>et al.</i> 2011
ZAN_S	South Zanzibar	25	Särnblad <i>et al.</i> 2011
SA_(Bio)	South Africa (Migratory)	54	Natoli <i>et al.</i> 2008a
SA_N	South Africa (North KwaZulu-Natal Coast)	24	Natoli <i>et al.</i> 2008a
SA_S	South Africa (South KwaZulu-Natal Coast)	27	Natoli <i>et al.</i> 2008a
IND_PAK*	Pakistan & India	15	This study

b**Mitochondrial DNA**

Code	Location	<i>N</i>	Population	Sequence Source
<i>Tursiops aduncus</i>				
OM	Oman	100	ARABIA	This study
ZAN_N	North Zanzibar	21	ZAN_N	Särnblad <i>et al.</i> 2011
ZAN_S	South Zanzibar	22	ZAN_S	Särnblad <i>et al.</i> 2011
SA_(Bio)	South Africa (Migratory)	17	SA_(Bio)	Natoli <i>et al.</i> 2008a
SA_N	South Africa (North KwaZulu-Natal Coast)	18	SA_N	Natoli <i>et al.</i> 2008a
SA_S	South Africa (South KwaZulu-Natal Coast)	15	SA_S	Natoli <i>et al.</i> 2008a
PAK	Pakistan	15	IND_PAK	This study
IND	India	10	IND_PAK	This study
IRAN	Iran	2	ARABIA	This study; Mohsenian <i>et al.</i> unpublished data
RS	Red Sea (<i>T. aduncus</i> holotype specimen)	1	ARABIA	Perrin <i>et al.</i> 2007
THAI	Thailand	3	CHI_THAI	This study
CHI	China	17	CHI_THAI	Wang <i>et al.</i> 1999
AUS	Southeast Australia	58	AUS	Möller & Beheregaray, 2001; Wiszniewski <i>et al.</i> 2010
<i>Tursiops truncatus</i>				
OM	Oman	35	NWIO_Tt	This study
IND	India	2	NWIO_Tt	This study
CHI	China	16	CHI_Tt	Wang <i>et al.</i> 1999b

3.2.2 Biopsy Sampling, Oman

Biopsy sampling was conducted off the Musundam Peninsula in the north of Oman between May and July, 2012, and off the town of Hasik, in Oman's Dhofar region in February and October, 2013. Dolphins were approached in a 5.9m Rigid-hulled Inflatable Boat (RIB) with a single 60hp YAMAHA 4-stroke engine off Musundam and from a 6.5 m RIB with twin 75hp HONDA 4-stroke engines off Hasik. On occasion, biopsy sampling was successfully conducted onboard a fishing skiff off Hasik. Biopsy sampling protocols were as outlined in Chapter 2.

3.2.3 Bone Sampling

Bone samples were collected from specimens curated at the ONHM and the SMNS. Teeth and small bone fragments were collected where available and were homogenized in the lab (see below). Where teeth and bone fragments were not available, bone powder was collected from skulls by drilling into the occipital condyle where the bone is dense and the DNA concentration is relatively high. Drill sites were sterilised with ethanol and drill-bits were regularly cleaned with ethanol and flame to prevent contamination between samples. The drilling was also conducted in a room separate to the specimen collection to limit aerosol contamination.

3.2.4 DNA Extraction from Tissue

Standard phenol-chloroform DNA extraction protocols, as adapted from Hoelzel (1998b), were carried out on tissue samples. Approximately 100 mg of tissue was finely chopped and added to 500 μ l of extraction buffer (50 mM Tris pH 7.5, 1 mM EDTA, 100 mM NaCl, 1% (w/v) SDS). A further 45 μ l of proteinase-K (10 mg/ml) was added to the solution and the tissue was left to digest overnight in a water-bath at 37°C with occasional agitation. 500 μ l of phenol was added to the digestions, mixed thoroughly, and then centrifuged for 5 min at 7000 x g to separate the phases. The surface aqueous phase was pipetted off and transferred to a new tube while the organic layer took no further part in the extraction process and was appropriately discarded. This process was repeated a second time with phenol and then with a mixture of phenol:chloroform:isoamyl-alcohol (25:24:1 by vol.). Using chloroform:isoamyl alcohol (24:1 by vol.) the process was repeated once more and the final separated aqueous phase was transferred to a new tube. Subsequently, 0.1 vol. (~45 μ l) of 3M sodium acetate was added and mixed 1 ml of chilled 100% ethanol was then added to precipitate the DNA and put in a freezer to incubate at -20°C for approximately 1 hr. Once precipitated, the DNA

was centrifuged at 7000 x *g* for 15 min to pellet the DNA. The supernatant was removed and replaced with chilled 70% ethanol and centrifuged again to clean the DNA pellet. The supernatant was removed and the DNA pellets were dried in a centrifugal evaporator. DNA was re-suspended in an appropriate volume (~200 µl) of TE buffer (10 mM Tris pH 8.0, 1 mM EDTA pH 8.0).

3.2.5 DNA Extraction from Bone

Where the sample was not already powdered (see bone sampling above), sand paper was used to clean contaminants off the surface of the tooth or bone fragment. A variable speed DREMEL® drill was used to drill into the pulp cavity of each tooth or bone fragment until approximately 1 g of displaced powder was collected for DNA extraction. Where teeth were too small to use the DREMEL® drill, a Mikro-Dismembrator (Sartorius Group) homogenised whole teeth for DNA extraction. Powder was digested overnight in 0.5 ml of buffer (50 mM Tris pH 7.5; 500 mM EDTA; 100 mM NaCl and 1% w/v SDS) with 50 µl of proteinase-K (20 mg/ml). Digestions were constantly agitated and incubated at 50°C. QIAquick PCR purification columns (Qiagen, BmbH, Germany) were used to perform DNA extractions. To prevent aerosol contamination, the procedure was conducted in a dedicated laboratory under a laminar-flow hood, separate from laboratories performing PCR reactions and working with modern DNA. All equipment and reagents were regularly sterilised and decontaminated. Disposable gloves and protective clothing were also worn throughout the procedure. Extractions without tissue were included as negative controls to test for reagent contamination and cross contamination during the extraction procedure.

3.2.6 Microsatellite Analysis

Samples, as listed in Table 11a, were screened for 18 published microsatellite loci following Moura (2011) (see Table 12). A sub-set of seven microsatellite loci (Dde84, Dde66, Dde69, Dde59, Dde70, Dde72, KWM12a) were amplified and screened for the Indian and Pakistan samples. Indian and Pakistan data were considered as one population (IND_PAK) representing individuals off the northern Sea of Oman and Arabian Sea coastline. These data were included in some analyses. Further analyses included the genotype data for two additional microsatellite loci, KWM9b and TexVet7, taken from Natoli *et al.* (2008a), and added to the South Africa dataset for further analyses between South African populations.

Two multiplex mixes consisting of 6 and 12 loci (see Table 12) were amplified using Multiplex PCR kits (Qiagen). The PCR profiles were as follows: initial denaturation at 95°C for 15 min, followed by 40 cycles of 95°C for 30 sec, annealing temperature of 50°C (Mix A) or 57°C (Mix B) for 40 sec and an extension step at 72°C for 1 min. A final extension of 6°C for 30 min completed the reaction.

The presence of duplicate samples was examined using pairwise relatedness coefficients, r (Queller & Goodnight, 1989) as calculated in KINGROUP v. 2 (Konovalov *et al.* 2004). Duplicate samples were removed from the dataset.

The presence of null alleles, large allele dropout, and scoring errors were detected using MICROCHECKER (Van Oosterhout *et al.* 2004). Deviations from Hardy-Weinberg equilibrium were assessed for each locus within each population using a test analogous to Fisher's exact test (Guo & Thompson, 1992) as implemented in ARLEQUIN v. 3.5 (Excoffier & Lischer, 2010) using a Markov chain method (chain length = 1,000,000, dememorisation steps = 10,000, Bonferroni correction applied). Pairwise linkage disequilibrium between loci was assessed for each population through a likelihood ratio test utilizing the Expectation-Maximisation (EM) algorithm (1000 permutations, Bonferroni correction applied) (Slatkin & Excoffier, 1996). Loci under selection were identified using the LOSITAN workbench (see Antao *et al.* 2008). Runs were conducted using the Infinite Alleles mutation model for 50,000 simulations, applying the 'neutral mean F_{ST} ', which removes potential non-neutral markers from initial mean F_{ST} calculations, and the 'force mean F_{ST} ' options. A 95% confidence limit and False Discovery Rate of 0.05 were applied.

In order to assess whether null alleles, where they were identified, were influencing F_{ST} values, the software package FREENA (Chapuis & Estoup, 2007) was used to apply a null allele correction (ENA) as described in Chapuis & Estoup (2007). F -statistics from datasets with and without loci exhibiting null alleles were also compared. If F_{ST} values were similar, between the corrected and uncorrected datasets, and if the differentiation pattern between datasets with and without loci exhibiting null alleles was the same, then uncorrected loci were retained.

Differentiation between putative populations was assessed by estimating F -statistics in ARLEQUIN v. 3.5 (Excoffier & Lischer, 2010). Significance levels were determined through 100

permutations and Bonferroni correction was applied to account for Type-I error. Microsatellite allelic richness was calculated using FSTAT v. 2.9.3.2 (Goudet, 2001) and Welch's t -test was used to investigate differences in richness between putative populations. A Factorial Correspondence Analysis (FCA) was performed on the microsatellite genotypes in GENETIX (Belkhir *et al.* 2004) in order to visualize the relationships between the putative populations.

BAYESASS v. 1.3 (Wilson & Rannala, 2003) was used to investigate recent dispersal between populations and hence recent gene-flow patterns. The burn-in length was set to 10^6 followed by 10^7 MCMC iterations with a sampling interval of 1000 iterations. All mixing parameters, ΔA , ΔF and ΔM were set to 1 to improve chain mixing. Trace files were viewed in TRACER v. 1.6 (Rambaut *et al.* 2014) and the log-probability was examined for convergence and good chain mixing. Analyses were also run multiple times to check runs had converged on similar posterior mean parameter estimates. A Circos plot of migration dynamics was generated in R v. 3.0 (R Core Team, 2013) from the BAYESASS output using the package *circulize* (Gu *et al.* 2014), following Sander *et al.* (2014).

The number of populations (K) was determined through Bayesian clustering analysis as performed in STRUCTURE v. 2.3 (Pritchard, *et al.* 2000). The program was run with and without a sampling location prior, LOCPRIOR (Hubisz *et al.* 2009) while using both the admixture ancestry and correlated allele frequency models. The burn-in length was set to 10^5 followed by 10^6 iterations. The parameter ALPHAPROPSD was set to 0.5 to improve mixing. Five independent runs were assessed for each value of K ranging from 1 to 8. The most likely value for K was determined using the web server CLUMPAK (Kopelman *et al.* 2015; <http://clumpak.tau.ac.il/index.html>), whereby both the rate of change in the log probability between successive values of K (ΔK) (Evanno *et al.* 2005) and the log likelihoods for each value of K were examined. Graphical representation of the clustering analyses was generated using the main pipeline on CLUMPAK. Once optimal values of K were inferred, a similar run was performed to investigate gene flow, or hybridisation/introgression, between populations using the USE-POPINFO option (Pritchard *et al.* 2000). This assumes pure ancestry for the majority of individuals sampled from a population with a small proportion of individuals with mixed ancestry. In order to identify migrants, and mixed ancestry in individuals with a single parent or grandparent from an alternative population, GENSBACK was set to 2. The prior probability that an individual had pure ancestry from its sampled population was set to 0.95, i.e. MIGRPRIOR = 0.05.

In order to infer population decline or expansion from the microsatellite dataset, a hierarchical Bayesian model was implemented, which makes use of the coalescent process, in *MSVAR* v. 1.3 (Beaumont, 1999; Storz & Beaumont 2002). The model assumes that a stable population of size N_1 changes exponentially to a size of N_0 over a time period, ta to the present time. An MCMC iteration process was used to find posterior probabilities for the parameters N_1 , N_0 and ta . Microsatellite loci were assumed to evolve under a single-step mutation model (SMM). Four different analyses were run for the Oman, Zanzibar, South Africa (all 14 loci) and Pakistan/Indian (seven loci) populations, respectively. Two independent runs of each analysis were performed with different random seed numbers to confirm parameter posterior probabilities were converging on similar values. Adequate chain mixing was checked using the program *TRACER* v. 1.6 (Rambaut *et al.* 2014). The maximum number of thinned update steps was set to 2×10^4 and with 10^6 lines of output, resulting in a total of 2×10^{10} steps. A 10% burn-in was also applied. For each run a generation time of 21 years was assumed (Taylor *et al.* 2007). The prior and hyperprior values used are shown in Table 13.

Table 12: Overview of microsatellite markers amplified in this study. Size ranges displayed are those available for *Tursiops truncatus* as outlined in Bourret *et al.* (2008). The sources given below are where the markers were first described.

Locus	Oligonucleotide	Dye	Repeat Motif	Annealing Temp. (°C)	Size/Size Range for <i>T. truncatus</i> (bp)	Source
Multiplex A						
D08	F GATCCATCATAATTGTCAAGTT R TCCTGGGTGATGAGTCTTC	FAM	(TG) _n	54.3	103	Shinohara <i>et al.</i> 1997
KWM2a	F GCTGTGAAAATTAATGT R CACTGTGGACAAAATGTAA	FAM	(CA) _n	47.3	-	Hoelzel <i>et al.</i> 1998
KWM2b	F AGGGTATAAGTGTAAAGG R CAACCTTAATTTGGATTTC	HEX	-	50.4	166-182	Hoelzel <i>et al.</i> 2002
KWM12a	F CCATACAATCCAGCAGTC R CACTGCAGAAATGATGACC	NED	(CA) _n	56	161-185	Hoelzel <i>et al.</i> 1998
TexVet5	F GATTGTGCAAATGGAGACA R TTGAGATGACTCCTGTGGG	FAM	(CA) _n	49	236-260	Rooney <i>et al.</i> 1999
KWM1b	F TAAGAACCTAAAATTTGGC R TGTGGGTCTGATAAATG	HEX	-	47.3	180-196	Hoelzel <i>et al.</i> 2002
Multiplex B						
TexVet9	F TTTTCTTAGTACCAGAACTTGTGTCAG R TCCAGTTGCCCTTCAAGTCTAG	FAM	(CA) _n	5.5	124	Rooney <i>et al.</i> 1999
EV37Mn	F AGCTTGA TTTGGAAAGTCA TGA R TAGTAGAGCCGTGA TAAAGTGC	NED	(AC) _n	51.7	192-252	Valsecchi & Amos, 1996
Ttru AAT44	F CCTGCTCTTCATCCCTCACTAA R CGAAGCACCAAAACAAGTCATAGA	HEX	(AAT) _n	55	161	Caldwell <i>et al.</i> 2002
Dde09	F GAAAGATTTTACCCTGCCCTGTC	FAM	(CTAT) _n	55	224	Coughlan <i>et al.</i> 2006

Locus	Oligonucleotide	Dye	Repeat Motif	Annealing Temp. (°C)	Size/Size Range for <i>T. truncatus</i> (bp)	Source
Dde70	R GATCTGTGCTCCTTAGGGAAA F ACACCAGCACCTACA TTCACA	HEX	(CA) _n	56	125-145	Coughlan <i>et al.</i> 2006
Dde84	R TCAGCAGCA TTCATAACCAAAC F AATAATCCTTTGTGGTTTCTGTT	FAM	(CA) _n	56	148-154	Coughlan <i>et al.</i> 2006
Dde65	R CATTCCAGGTACAGCTTTTCA F GGTAGTCGTAGGAAAGGTA	FAM	(CTAT) _n	56	188-204	Coughlan <i>et al.</i> 2006
Dde69	R AGCAGCCCTAGCAACCTTA TA F TTTTCAGTAGTGTGCATGTGTAT	HEX	(GATA) _n and (CA) _n	56	-	Coughlan <i>et al.</i> 2006
Dde72	R GAATACCCAGAGGGCAAGG F TGCTCAACAGATTTACACACTT	HEX	(CTAT) _n	56	227-262	Coughlan <i>et al.</i> 2006
Dde66	R AAGGAAACAAAAGTA TCTGAGCA F AACATTGCCAGTGCCCTTAGAA	FAM	(GT) _n	56	336-362	Coughlan <i>et al.</i> 2006
Dde59	R GTGGAACAGACGGCGCATAT F TACACAGCTTACTTACCTTACCAA	HEX	(GATA) _n	56	236-400	Coughlan <i>et al.</i> 2006
EV14Pm	R GTCCCTTTGAGCAGAGTTCTA F TAAACATCAAAAGCAGACCC	NED	(GT) _n	52	-	Valsecchi & Amos, 1996
	R CCAGAGCCAAAGGTCAAGAG					

Table 13: Prior and hyperprior values for analyses conducted in M_{SVAR}.

Prior values for all loci														
	Dde84	Dde65	Dde09	Dde66	AAT44	Dde70	Dde69	Dde72	Dde59	EV14	EV37	TexVet5	KWM2b	KWM12a
N_0	1.0E+04	5.0E+04	1.0E+04	1.0E+04	1.0E+04	1.0E+04	1.0E+04	1.0E+04	1.0E+04	1.0E+04	1.0E+04	1.0E+04	1.0E+04	1.0E+04
N_1	1.0E+04	1.0E+04	1.0E+04	1.0E+04	5.0E+04	1.0E+04	1.0E+04	1.0E+04	1.0E+04	1.0E+04	1.0E+04	1.0E+04	1.0E+04	1.0E+04
θ	1.0E-04	2.0E-04	1.0E-05	1.0E-04	2.0E-04	3.0E-04	5.0E-05	5.0E-05	3.0E-04	1.0E-04	5.0E-05	5.0E-05	3.0E-04	1.0E-04
ta	1.0E+05	5.0E+04	2.0E+05	3.0E+05	4.0E+05	1.0E+05	1.0E+03	1.0E+05	1.0E+05	2.0E+05	1.0E+03	1.0E+05	1.0E+05	2.0E+05

Prior mean and variance	Hyperprior values for means and variances			
	mean	var	mean	var
$\text{Log}(N_0)$	4	1	6	2
$\text{Log}(N_1)$	4	1	5	2
$\text{Log}(\theta)$	-3.5	1	-3.5	0.25
$\text{Log}(ta)$	5	1	5	2

3.2.7 Mitochondrial DNA Analysis

A 404 bp fragment of the mtDNA control region hypervariable region 1 (HVR1) was sequenced for *T. aduncus* and *T. truncatus* throughout the Indo-Pacific (see Table 11). Further sequences were obtained from GenBank (see Table 11). In total, 299 sequences of *T. aduncus* and 53 sequences of *T. truncatus* were utilised in this study. Sequences were pooled into populations as shown in Table 11.

Amplifications were performed in 20 µl final reaction volumes containing approximately 1.0 µl of template DNA, 1.25U of GoTaq Flexi DNA polymerase, 10x buffer (Promega), 0.2 mM dNTP, 3 mM MgCl₂ and 0.2 µM of each primer; TRO (L15812) 5' CCT CCC TAA GAC TCA AGG AAG 3' (developed at the Southwest Fisheries Science Centre, see Zerbini *et al.* 2007) and D (H16498) 5' CCT GAA GTA AGA ACC AGA TG 3' (Rosel *et al.* 1994). The PCR profile included initial heating at 95°C for 2 min, followed by 40 cycles of 95°C for 40 sec, annealing temperature of 60°C for 40 sec and 72°C for 1 min, and a final 72°C extension for 10 min. PCR products were purified with QIAgen PCR purification columns (Qiagen, GmbH, Germany) and sequenced using an ABI automated sequencer.

Initial alignment of novel sequences (i.e. those unique to this study) was performed using the MUSCLE algorithm (Edgar, 2004) as implemented in GENEIOUS v. 7.1.2 (<http://www.geneious.com>, Kearse *et al.* 2012) also included were 10 sequences of *T. aduncus* from Australasia, available on GenBank (Accession No.s: AF049100, AF056233-36, 39-43). Three sequences of *Sousa chinensis* (Accession No.s: DQ665785, 87-88) were included as an out-group. A 50% majority-rule consensus neighbor-joining phylogeny was generated over 1,000 bootstrap replicates in GENEIOUS v. 7.1.2 (<http://www.geneious.com>, Kearse *et al.* 2012) using a Tamura-Nei genetic distance model, as identified using jMODELTEST v. 2.1.6 (Darriba *et al.* 2012). This was performed to visualize the phylogenetic relationships between novel sequences. For all further mtDNA analyses, novel sequences were truncated down to 267 bp so that they were homologous with those obtained from GenBank (see Table 11).

ARLEQUIN v. 3.5 (Excoffier & Lischer, 2010) was used to calculate pairwise F_{ST} and Φ_{ST} between putative populations. To calculate Φ_{ST} a Tamura-Nei genetic distance model was applied with a gamma-correction shape parameter value of $\alpha = 0.191$ identified as the best model using BIC in jMODELTEST v. 2.1.6 (Darriba *et al.* 2012). Haplotype (h) and nucleo-

tide (π) diversities were estimated and pairwise comparisons were made between populations using Welch's t -test. Tajima's D and Fu's F_s neutrality test statistics were estimated (Tajima, 1989; Fu, 1997) and a mismatch distribution analysis (Rogers & Harpending, 1992) was implemented in ARLEQUIN (Excoffier & Lischer, 2010). Expected distributions were simulated for a demographic expansion model from 100 parametric bootstrap replicates. The Sum-of-Squared-Deviations (SSD) and Harpending's Raggedness Index (HRI) were calculated along with their respective P values (proportion of simulated SSD/HRI \geq observed SSD/HRI). Significant SSD values (i.e. where $P < 0.05$) reject the sudden expansion model and the HRI values quantify the 'smoothness' of the observed mismatch distribution. Low HRI values are characteristic of an expanding population while high HRI values are characteristic of a stationary or contracting population (Harpending *et al.* 1993). The parameters $\theta_0 = (2N_0\mu)$, $\theta_1 = (2N_1\mu)$ and $\tau = (2\mu t)$ were estimated for each population, where N_0 = initial effective population size before expansion event, N_1 = current effective population size, μ = substitutions per locus per generation and t = number of generations since expansion. When the expansion model was not rejected (i.e. SSD $P > 0.05$), τ was converted into years. Two published substitution rates for the cetacean mtDNA control region were used: 7.0×10^{-8} substitutions per site per year (Harlin *et al.* 2003) and 5.0×10^{-7} substitutions per site per year (Ho *et al.* 2007). A generation time of 21 yrs was assumed (Taylor *et al.* 2007).

A median-joining haplotype network (Bandelt *et al.* 1999) was generated from 267 bp mtDNA control region sequences using POPART (<http://popart.otago.ac.nz>, Leigh & Bryant, 2015), $\epsilon = 0$, to visualize the phylogenetic relationships between haplotypes across the region.

3.2.8 Estimates of Population Divergence Times

The software MDIV (Nielsen & Wakeley, 2001) uses the coalescence process to simultaneously estimate the parameter theta ($\theta = 4N_e\mu$), the migration rate (m) per locus per generation scaled to effective population size ($M = 2N_e m$), and the divergence time (t) per generation per locus scaled to effective population size ($T = t/2N_e$). Sequences of the mtDNA control region (283 bp) were used and therefore these parameters were scaled to the effective population size of females, N_{ef} ($\theta = 2N_{ef}\mu$, $M = N_{ef} m$, $T = t/N_{ef}$). Where μ = the mutation rate per locus per generation. Under the model, population sizes are assumed to be equal and migration rates symmetric between two populations. Pairwise analyses were conducted for Oman, South Africa (pooled SA_Bio, SA_S and SA_N) and Zanzibar (pooled ZAN_N

and ZAN_S). Utilising the HKY model of sequence evolution (Hasegawa *et al.* 1985), two independent MCMC runs of 5,000,000 cycles with 10% burn-in were performed for each analysis, using different random seeds. Priors for the parameters T and M were set to 10 and the default value (as defined by the software) was set for θ (OM-SA = 6; OM-ZAN = 6.54; ZAN-SA = 4.80). Posterior probabilities were examined for convergence. Divergence times were calculated based on mutation rates of 7.0×10^{-8} substitutions per site per year (Harlin *et al.* 2003) and 5.0×10^{-7} substitutions per site per year (Ho *et al.* 2007). A generation time of 21 years was used (Taylor *et al.* 2007).

3.2.9 Inference of Demographic History in the Western Indian Ocean

To investigate hypotheses for the demographic history of populations in the western Indian Ocean (and associated barrier mechanisms), three scenarios were tested (summarised in Figure 29) using Approximate Bayesian Computation (ABC) as implemented in DIYABC v. 2.0.4 (Cornuet *et al.* 2014). A dataset representing four populations (Oman, Zanzibar, South Africa and Pakistan-India) was used, consisting of seven microsatellite loci, and 267 bp of mtDNA control-region sequences. The sample sizes for South Africa and Zanzibar were reduced to 20 in order to avoid oversampling alleles compared to the less well-sampled populations (Leberg, 2002). For the mtDNA locus, a HKY substitution model (Hasegawa *et al.* 1985) was applied with a gamma-correction shape parameter value of $\alpha = 0.67$ with 55% invariant sites, as identified using Bayesian Information Criteria (BIC) in jMODELTEST v. 2.1.6 (Darriba *et al.* 2012). A Generalised Stepwise Mutation model was applied to the microsatellite loci (Estoup *et al.* 2002). Three million datasets were simulated across the three scenarios i.e. 1 million simulations each. Summary statistics used for microsatellite loci were (i) one-sample statistics: mean number of alleles across loci, mean genic diversity across loci (Nei, 1987), mean allele size variance across loci and mean M index across loci, which is the mean ratio of allele number to the range in allele size (Garza & Williamson, 2001; Excoffier *et al.* 2005); (ii) two-sample statistics: mean number of alleles, mean genic diversity across loci, mean allele size variance across loci, F_{ST} (Weir & Cockerham, 1984), and $(d\mu)^2$ distance (Goldstein *et al.* 1995). For mtDNA loci, summary statistics were (i) one sample statistics: number of distinct haplotypes, number of segregating sites, mean number of pairwise differences and variance of pairwise differences; (ii) two-sample statistics: number of distinct haplotypes, number of segregating sites and F_{ST} (Hudson *et al.* 1992). A Principal Component Analysis (PCA) was carried out to see how well the simulated data fitted the observed data.

Posterior probabilities of parameters were estimated based on the closest 1% of simulated data to the observed data. Assessment of which scenario was performing the best was carried out using the logistic regression method (Fagundes *et al.* 2007; Beaumont, 2008).

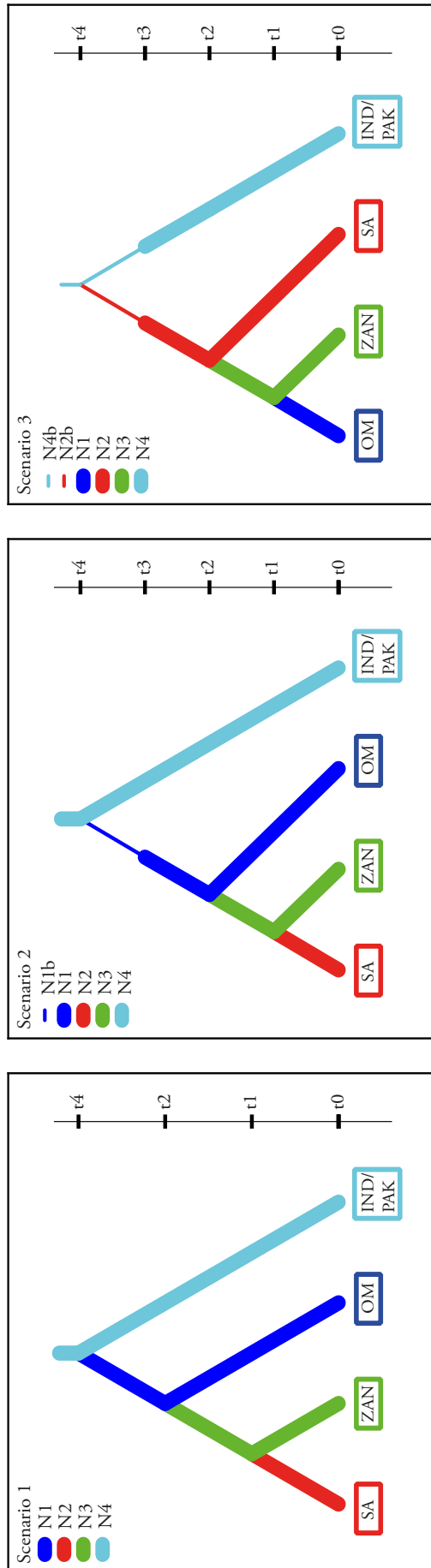


Figure 29: Demographic scenarios tested in DIYabc. OM = Oman, ZAN = Zanzibar, SA = South Africa, IND/PAK = India/Pakistan, t = time, N_e = effective population size (N_e). Times are not shown to scale. Scenario 1: OM and IND/PAK diverge at t_1 and other populations are established in a southwards direction without a founding event. Scenario 2: OM and IND/PAK diverge at t_1 and OM experiences a reduced N_e as founders immigrate across a barrier into the western Indian Ocean. Populations founded in Oman recover at t_2 and southward expansion established populations of ZAN and SA. Scenario 3: IND/PAK and SA ancestors diverge and experience a historic reduction in N_e at t_2 due to a contraction to glacial refugia. Populations recover at t_3 and populations expand out of South African refugia in a northwards direction, establishing populations off Zanzibar and Oman.

3.3 Results

3.3.1 Microsatellites

3.3.1.1 Fourteen Loci Dataset

Pairwise relatedness coefficients, r (Queller & Goodnight, 1989) revealed the presence of three duplicate samples (where $r = 1$) which were removed from the dataset. Two of the removed duplicates were from the migratory population off South Africa (SA_Bio) and the other duplicate came from the northern Zanzibar population, (ZAN_N). Because the SA_Bio samples were biopsies, sample duplication was credible, however the ZAN_N samples were from by-caught individuals collected in different areas at different times and could therefore not be duplicates. The samples exhibited identical genotypes across all loci. An error during sample labelling or genotyping in the lab is the most likely cause.

One microsatellite locus, TexVet9, was monomorphic and therefore omitted from analyses. The presence of null alleles was detected in five loci across four populations in MICROCHECKER (Van Oosterhout *et al.* 2004), Dde09 (for ZAN_N), EV14 (for SA_N), EV37Mn (for SA_N and SA_S), D08 (for ZAN_S) and KWM2a (for SA_N). Significant Hardy-Weinberg deviation was detected in D08 and KWM2a but only for South African (SA) populations ($P < 0.05$, with Bonferroni correction) (see Table 14). Linkage disequilibrium was also detected between these loci in SA_(Bio) and SA_S ($P < 0.05$, with Bonferroni correction). At the 95% confidence interval, strong directional selection was detected in D08 and KWM1b and weak balancing selection was detected in Dde72. The majority of population genetic models assume loci evolve neutrally, that allele frequencies are in Hardy-Weinberg equilibrium and that there is no linkage disequilibrium between loci. Therefore, a further three loci were removed from the dataset as they did not fulfil these requirements; D08, KWM2a and KWM1b. F -statistics between populations with and without adjustment for null alleles were compared in FREENA (Chapuis & Estoup, 2007) to test whether inclusion of loci with null alleles would produce different results. F_{ST} values with and without the loci exhibiting null alleles were also compared. Similar F_{ST} values were estimated between adjusted and unadjusted loci and the reduced dataset revealed a similar differentiation pattern. Therefore, loci were retained without null allele adjustment. Overall, 14 loci remained for all subsequent analyses. The average missing data across all remaining loci was 0.4%.

Pairwise comparisons of allelic richness (Table 15) between populations were not significant-

ly different ($P > 0.05$). Pairwise F -statistics between most putative populations were highly significant ($P < 0.001$, Bonferroni correction applied) with the exception of those within South Africa (SA), which were not significant at $P = 0.05$ (see Table 16).

3.3.1.2 Seven Loci Dataset (Including Indian and Pakistan Samples)

Similar checks for scoring error, the presence of null alleles and deviations from neutral theory were carried out for the seven loci dataset (as above). Only one locus (Dde70) deviated significantly from Hardy-Weinberg equilibrium for the IND_PAK population ($P < 0.05$ after Bonferroni correction). Linkage disequilibrium was not detected between any loci. Null alleles were detected in Dde66 and Dde70 in the SA_S and IND_PAK populations respectively using MICROCHECKER. Adjustment for the presence of null alleles in FREENA did not reveal significant changes in F_{ST} values and removal of loci with null alleles did not alter the pattern of genetic differentiation. Similarly, removal of Dde70 from the dataset did not significantly alter F_{ST} values calculated in ARLEQUIN. Directional selection was not identified for any loci but weak balancing selection was detected in locus Dde72. As a result, all loci were retained for further analyses, without null allele adjustment, because there was little indication that the data were consistently violating the assumptions of neutral theory.

Pairwise comparisons of allelic richness for seven loci between populations were not significantly different ($P > 0.05$, Welch's t -test). Pairwise F -statistics between most putative populations were highly significant ($P < 0.001$, Bonferroni correction applied) for most comparisons with the exception of those within South Africa (SA) and for some comparisons involving ZAN_N, ZAN_S and Oman (See Table 16). Relatively high F_{ST} values (range 0.117-0.170, $P < 0.001$) were characteristic of pairwise comparisons with the IND_PAK population.

3.3.1.3 Sixteen Loci Dataset (Comparison of South African Populations)

A further two microsatellite loci (KWM9b and TexVet7, from Natoli *et al.* 2008a) were added to the South African dataset. As reported for other datasets (above) checks were carried out for the presence of scoring error and null alleles as well as deviations from neutrality. Loci D08 and KWM2a deviated significantly from Hardy-Weinberg for all populations (SA_Bio, SA_N, SA_S) and exhibited linkage disequilibrium for SA_S and SA_Bio. Null alleles were present in single populations for Dde09, EV14, and KWM2a and two populations for EV37. Directional selection was revealed in TexVet7 but, as it was weak, this locus was retained in

further analyses. Data for three loci were removed from the dataset. These loci were D08 and KWM2a due to significant deviations from Hardy-Weinberg and linkage equilibrium. Locus EV37 was also removed because null alleles were present for two of the three South African populations. Allele frequencies adjusted for null alleles revealed similar F_{ST} values to unadjusted allele frequencies and the same differentiation pattern was exhibited when loci with null alleles were removed. Therefore those loci were retained in further analyses without null allele adjustment. Overall, 16 loci remained for analyses of the three putative South African populations.

Using 16 loci revealed the F_{ST} value between SA_Bio and SA_N ($F_{ST} = 0.0098$) to be significant at $P < 0.05$ (after Bonferonni correction). However, further comparisons between South African populations remained insignificant.

3.3.1.4 Factorial Correspondence Analyses

The results of the Factorial Correspondence Analysis (FCA) using the 14-microsatellite loci dataset are shown in Figure 30. Factors 1, 2 and 3 accounted for 84.45% of the total variance, contributing 47.3%, 25.48% and 11.66%, respectively. The Zanzibar populations (ZAN_S and ZAN_N) were clearly differentiated from the South African populations (SA_N, SA_S and SA_Bio) along Factor 1 and Factor 2. There was also clear differentiation between the Oman population (OM) and all other populations (see Figure 30a). Factor 3 differentiated between ZAN_N and ZAN_S populations (see Figure 30b).

An FCA was conducted using the seven-microsatellite loci dataset (see Figure 31). Factors 1, 2 and 3 accounted for 85.23% of the total variance, contributing 48.46%, 26.26% and 10.52% respectively. The IND_PAK population was well differentiated from the other populations along Factor 1 (Figure 31a). Along Factor 2 there was differentiation between the Zanzibar and South African populations (Figure 31b). There was also discrimination between OM and ZAN_N along Factor 3 (Figure 31b).

An FCA conducted between the three putative South African populations utilising the 16-microsatellite loci dataset showed that all three could be distinguished, though there was a degree of overlap (Figure 32).

3.3.1.5 Inference of Recent Migration

Dispersal estimates were inferred for the 14 loci dataset in BAYESAss v. 1.3 (Wilson & Rannala, 2003). The estimates are displayed in Table 17 and visualized as a Circos plot in Figure 33. These results suggest a general trend of asymmetrical migration northwards from the South African migrating population, (SA_Bio) to the other South African populations (SA_S = 26.6%, SA_N = 28.3% from SA_Bio) and Oman (OM = 9.5% from SA_Bio). However, migration from South Africa to Zanzibar appears to be minimal (1.4-2.3%). Southern Zanzibar (ZAN_S) is also an important source for dispersal to northern Zanzibar (ZAN_N = 26.6% from ZAN_S) and Oman (OM= 15.5% from ZAN_S). Southwards migration and migration between other populations appears to be minimal.

3.3.1.6 Bayesian Clustering Analysis

Clustering implemented in STRUCTURE v. 2.3 (Pritchard, *et al.* 2000) using the 14-microsatellite loci dataset was run with and without prior information about sampling locality, LOCPRIOR. When run with LOCPRIOR, the value for ΔK using the Evanno method (Evanno *et al.* 2005), and the highest posterior probability [$\ln P(D)$], were both $K = 3$. When run without LOCPRIOR, $\Delta K = 3$ but the highest [$\ln P(D)$] was $K = 4$. From examining the individual assignment probabilities, as plotted in Figure 34, it is apparent that the most likely number of populations is three. These correspond to 1) the Oman population (OM), 2) all South African populations (SA_Bio, SA_N, SA_S) and 3) all Zanzibar populations (ZAN_N, ZAN_S). Although significant differentiation was detected between the Zanzibar populations using 14 microsatellite loci ($F_{ST} = 0.015$, $P < 0.001$), this was not detected in the STRUCTURE analysis.

STRUCTURE was also run using the seven loci dataset (see Figure 35). When run with LOCPRIOR, $\Delta K = 2$ and the highest posterior probability [$\ln P(D)$] was for $K = 4$. When run without LOCPRIOR, $\Delta K = 3$ and the highest [$\ln P(D)$] remained at $K = 4$. Individual assignment probability plots reveal a similar pattern to the 14 loci dataset, with the addition of Pakistan and India as a fourth population.

3.3.1.7 Estimations of Ancestry and Identification of Migrants

Estimates of individual ancestry in STRUCTURE using the 14-microsatellite loci dataset revealed high assignment posterior probabilities for the majority of individuals to the popu-

lations they were sampled from (see Figure 36). All but two individuals from the Oman population had assignment probabilities to Oman of 90% or higher. Of the remaining two individuals, one showed a possible parent (12%) or grandparent (8%) ancestry to South Africa while the other showed a possible origin (14%) to Zanzibar or had a parent (20%) or grandparent (9%) from Zanzibar. The majority (90.5%) of individuals sampled off South Africa had assignment probabilities of 90% or higher. With the exception of one migrant from Oman (100% assignment), the remaining individuals (6%) largely showed potential parent (0-13%) or grandparent (11-19%) ancestry to Zanzibar. Within the Zanzibar population, the majority of individuals (82%) had assignment probabilities to Zanzibar of 90% or higher. Two migrants from Oman were detected (100%). The remaining individuals sampled in Zanzibar (14%) showed indications of mixed ancestry with either a parent or grandparent from South Africa or Oman.

Similar estimates were drawn from the seven loci dataset, which included individuals from Pakistan and India (see Figure 37). The results were largely congruent with those presented for the 14 loci dataset for the Oman, Zanzibar and South Africa populations. For individuals sampled off Pakistan and India, the majority (73%) showed posterior probability assignments of 90% or higher to Pakistan/India. Three individuals showed reduced assignment probabilities to Pakistan/India (76-89%) with low probabilities of mixed ancestry in Oman and South Africa. One individual from Pakistan showed a relatively low assignment probability to Pakistan/India (49%) and was either a migrant from Oman (22%) or had a single parent (17%) or grandparent (8%) from Oman.

3.3.1.8 Signals of Expansion and Decline in Microsatellite Loci

For each population, India/Pakistan, Oman, Zanzibar and South Africa, visual inspection of posterior probabilities generated from independent runs in MSVAR confirmed convergence had been reached. For each population, median posterior probabilities and respective 95% highest posterior densities for each parameter (N_0 , N_1 and ta) are presented in Table 18. All populations showed signals of gradual decline with decline occurring more recently in the Zanzibar and Oman populations than the Pakistan/India and South Africa populations. Credible intervals are large and overlap considerably for all parameters. As a result, inference of the demographic changes occurring within populations based on microsatellite loci remains unresolved.

Table 14: Number of alleles and expected (exp.) and observed (obs.) heterozygosities (Het) for each locus within each population. OM = Oman; SA_Bio = South Africa migratory; SA_N = South Africa northern; SA_S = South Africa; ZAN_N = Zanzibar northern; ZAN_S = Zanzibar southern; IND_PAK = India and Pakistan (only 7 loci are considered for this population); * = loci deviating significantly from Hardy-Weinberg equilibrium ($P < 0.05$ after Bonferroni correction).

Locus	OM	SA_Bio	SA_N	SA_S	ZAN_N	ZAN_S	IND_PAK
Dde84							
No. of Alleles	5	4	5	3	4	6	6
Het (exp.)	0.586	0.360	0.449	0.352	0.366	0.607	0.782
Het (obs.)	0.579	0.315	0.417	0.370	0.320	0.640	0.867
Dde65							
No. of Alleles	6	5	5	4	4	4	
Het (exp.)	0.700	0.550	0.551	0.489	0.718	0.737	
Het (obs.)	0.737	0.630	0.500	0.444	0.720	0.840	
Dde09							
No. of Alleles	6	6	6	5	5	5	
Het (exp.)	0.750	0.611	0.711	0.605	0.766	0.762	
Het (obs.)	0.579	0.500	0.708	0.704	0.480	0.720	
Dde66							
No. of Alleles	4	4	5	3	5	4	4
Het (exp.)	0.518	0.238	0.235	0.297	0.491	0.432	0.193
Het (obs.)	0.526	0.259	0.208	0.185	0.520	0.440	0.200
Ttru AAT44							
No. of Alleles	5	6	7	4	4	3	
Het (exp.)	0.407	0.518	0.461	0.433	0.566	0.456	
Het (obs.)	0.368	0.556	0.458	0.370	0.600	0.400	
Dde70							
No. of Alleles	4	2	4	2	4	3	8
Het (exp.)	0.450	0.228	0.378	0.283	0.497	0.313	0.816
Het (obs.)	0.316	0.185	0.333	0.333	0.360	0.280	0.400
Dde69							
No. of Alleles	5	6	5	5	6	5	6
Het (exp.)	0.745	0.768	0.756	0.807	0.581	0.698	0.793
Het (obs.)	0.632	0.755	0.875	0.889	0.640	0.640	0.667
Dde72							
No. of alleles	6	6	6	6	5	6	6
Het (exp.)	0.797	0.805	0.826	0.806	0.730	0.706	0.791
Het (obs.)	0.790	0.815	0.667	0.815	0.800	0.667	0.667
Dde59							
No. of alleles	6	2	4	2	6	7	5
Het (exp.)	0.647	0.480	0.432	0.475	0.694	0.592	0.501
Het (obs.)	0.526	0.482	0.375	0.593	0.600	0.625	0.400

Locus	OM	SA_Bio	SA_N	SA_S	ZAN_N	ZAN_S	IND_PAK
EV14Pm							
No. of Alleles	10	9	10	9	10	11	
Het (exp.)	0.862	0.785	0.828	0.768	0.803	0.829	
Het (obs.)	0.737	0.759	0.625	0.741	0.680	0.920	
EV37Mn							
No. of Alleles	15	8	10	12	8	7	
Het (exp.)	0.937	0.821	0.861	0.835	0.595	0.502	
Het (obs.)	0.842	0.722	0.667	0.667	0.520	0.560	
D08							
No. of Alleles	6	5	2	3	7	7	
Het (exp.)	0.584	0.097	0.383	0.046	0.758	0.755	
Het (obs.)	0.444	0.1000*	0.0000*	0.0455*	0.680	0.542	
KWM2a							
No. of Alleles	6	5	5	5	6	6	
Het (exp.)	0.704	0.411	0.485	0.426	0.535	0.716	
Het (obs.)	0.526	0.4600*	0.2105*	0.2857*	0.480	0.800	
TexVet5							
No. of Alleles	6	8	9	7	7	6	
Het (exp.)	0.725	0.724	0.747	0.649	0.710	0.715	
Het (obs.)	0.722	0.679	0.826	0.731	0.600	0.560	
KWM2b							
No. of Alleles	2	3	3	2	2	2	
Het (exp.)	0.102	0.203	0.159	0.230	0.115	0.040	
Het (obs.)	0.105	0.226	0.167	0.259	0.120	0.040	
KWM1b							
No. of Alleles	2	2	3	3	4	3	
Het (exp.)	0.149	0.496	0.502	0.491	0.366	0.280	
Het (obs.)	0.053	0.426	0.522	0.500	0.240	0.200	
KWM12a							
No. of Alleles	6	9	7	9	8	8	8
Het (exp.)	0.809	0.775	0.764	0.624	0.785	0.807	0.853
Het (obs.)	0.895	0.811	0.625	0.577	0.840	0.680	0.867

Table 15: mtDNA (control region) and microsatellite diversity statistics for each putative population, considering 14 loci and 7 loci (in parentheses). Pop = population, π = nucleotide diversity, b = haplotype diversity, k = average number of alleles, H_o = observed heterozygosity, H_e = expected heterozygosity. * = IND_PAK population (which was only considered in the 7 microsatellite loci analyses).

Mitochondrial DNA		Microsatellites, 14 loci (7 loci)										
Pop	No. of haplotypes	π	b	Pop	k	Allele richness	H_o	H_e	H_o	H_e		
ARABIA	14	0.012	0.665	OM	6.143	(5.143)	5.995	(4.826)	0.594	(0.609)	0.647	(0.650)
SA_N	3	0.004	0.451	SA_N	6.143	(5.143)	5.613	(4.492)	0.530	(0.500)	0.584	(0.549)
SA_S	2	0.001	0.133	SA_S	5.214	(4.286)	4.662	(3.869)	0.545	(0.534)	0.550	(0.524)
SA_Bio	3	0.002	0.228	SA_Bio	5.571	(4.714)	4.513	(3.876)	0.546	(0.518)	0.566	(0.526)
ZAN_N	5	0.006	0.681	ZAN_N	5.571	(5.429)	5.103	(4.512)	0.557	(0.577)	0.601	(0.583)
ZAN_S	4	0.006	0.567	ZAN_S	5.500	(5.571)	5.001	(4.631)	0.569	(0.560)	0.589	(0.601)
AUS	4	0.007	0.555	IND_PAK*	-	(6.143)	-	(5.875)	-	(0.581)	-	(0.676)
CHI_THAI	11	0.022	0.895									
IND_PAK	13	0.020	0.907									
NWIO_Tt	24	0.031	0.961									
CHI_Tt	10	0.022	0.867									

Table 16: Pairwise F_{ST} values for all populations considering 14 microsatellite loci (below diagonal) and 7 microsatellite loci (above diagonal). * = significant ($P < 0.001$). Cell colour corresponds to F_{ST} value whereby darker shades represent larger values and lighter shades represent lower values.

	OM	SA_(Bio)	SA_N	SA_S	ZAN_N	ZAN_S	IND_PAK
OM	-	0.048*	0.043*	0.044*	0.028*	0.014	0.117*
SA_(Bio)	0.049*	-	0.008	0.002	0.084*	0.058*	0.160*
SA_N	0.040*	0.001	-	0.012	0.087*	0.050*	0.164*
SA_S	0.054*	-0.001	0.006	-	0.096*	0.065*	0.170*
ZAN_N	0.046*	0.081*	0.069*	0.089*	-	0.017	0.139*
ZAN_S	0.047*	0.081*	0.065*	0.088*	0.015*	-	0.140*

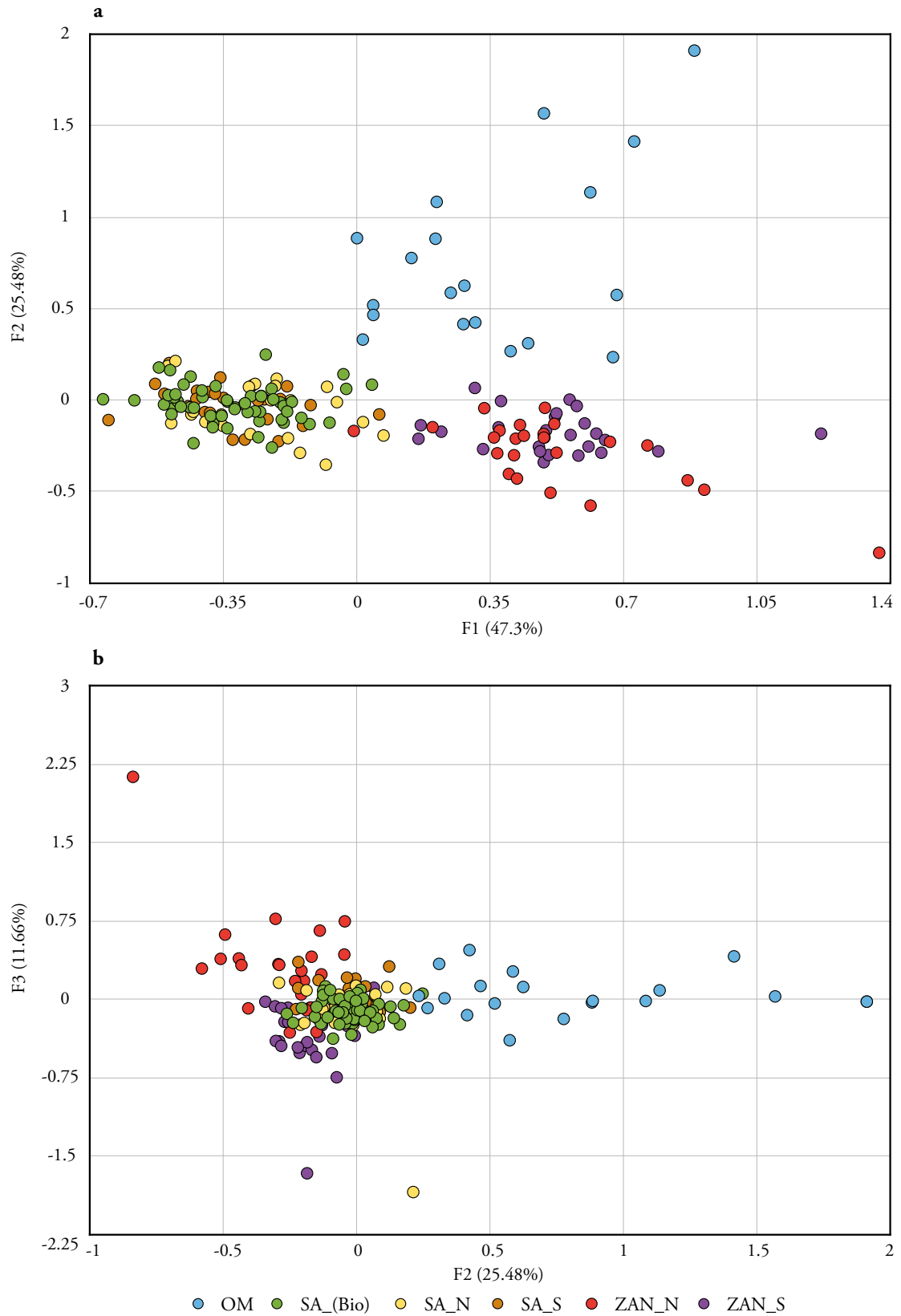


Figure 30: FCA plots for 14 microsatellites. Implemented in GENETIX (Belkhir *et al.* 2004). a) F1 vs F2 and b) F2 vs F3. Percentage of variance explained by each factor is shown in parentheses.

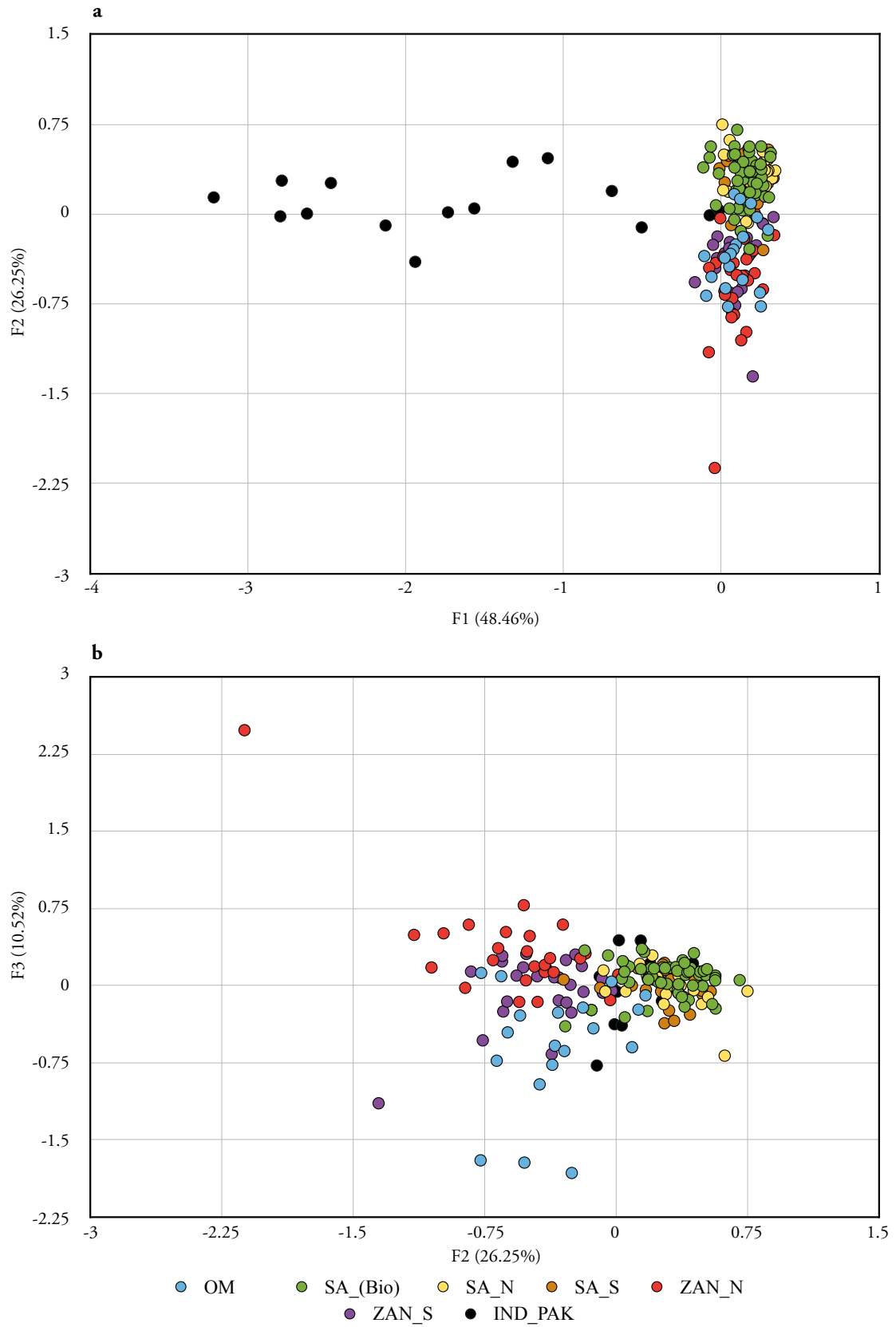


Figure 31: FCA plots for seven microsatellites. Implemented in GENETIX (Belkhir *et al.* 2004). a) F1 vs F2 and b) F2 vs F3. Percentage of variance explained by each factor is shown in parentheses.

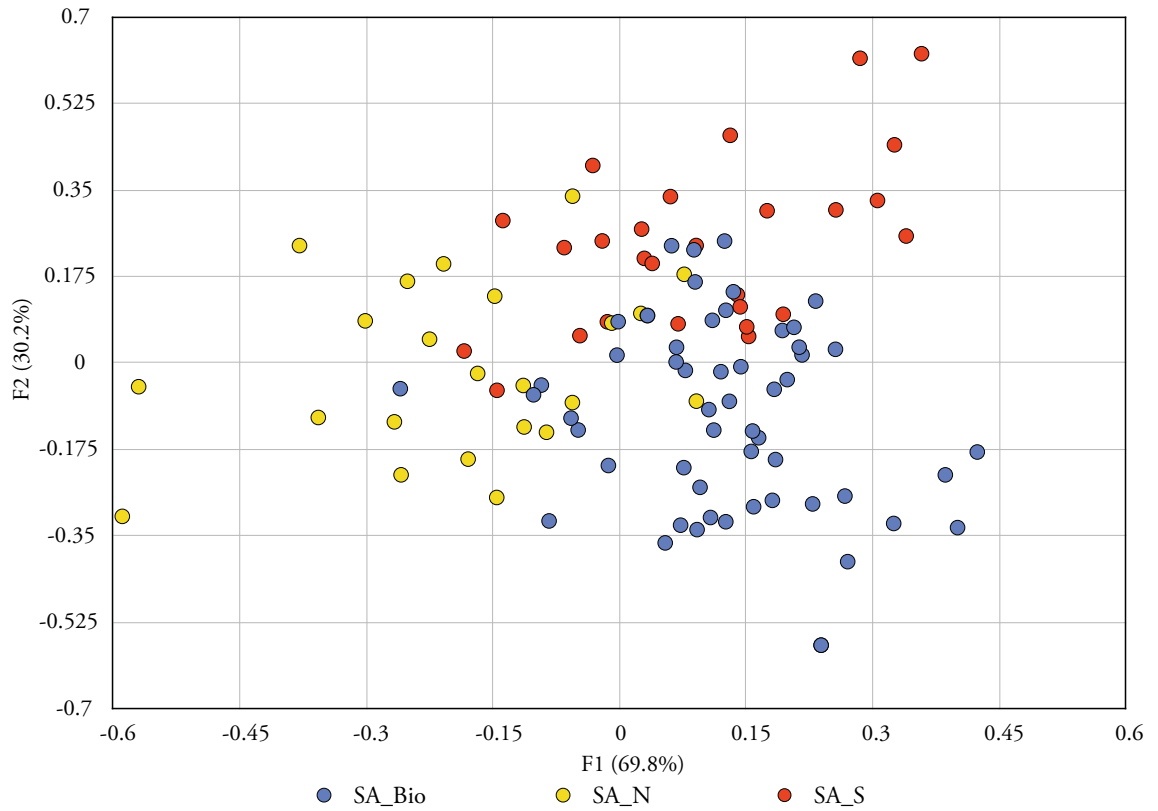


Figure 32: FCA plots utilising genotype data from 16 microsatellite loci from the South African populations (F1 vs F2). Implemented in GENETIX (Belkhir *et al.* 2004). Percentage of variance explained by each factor is shown in parentheses.

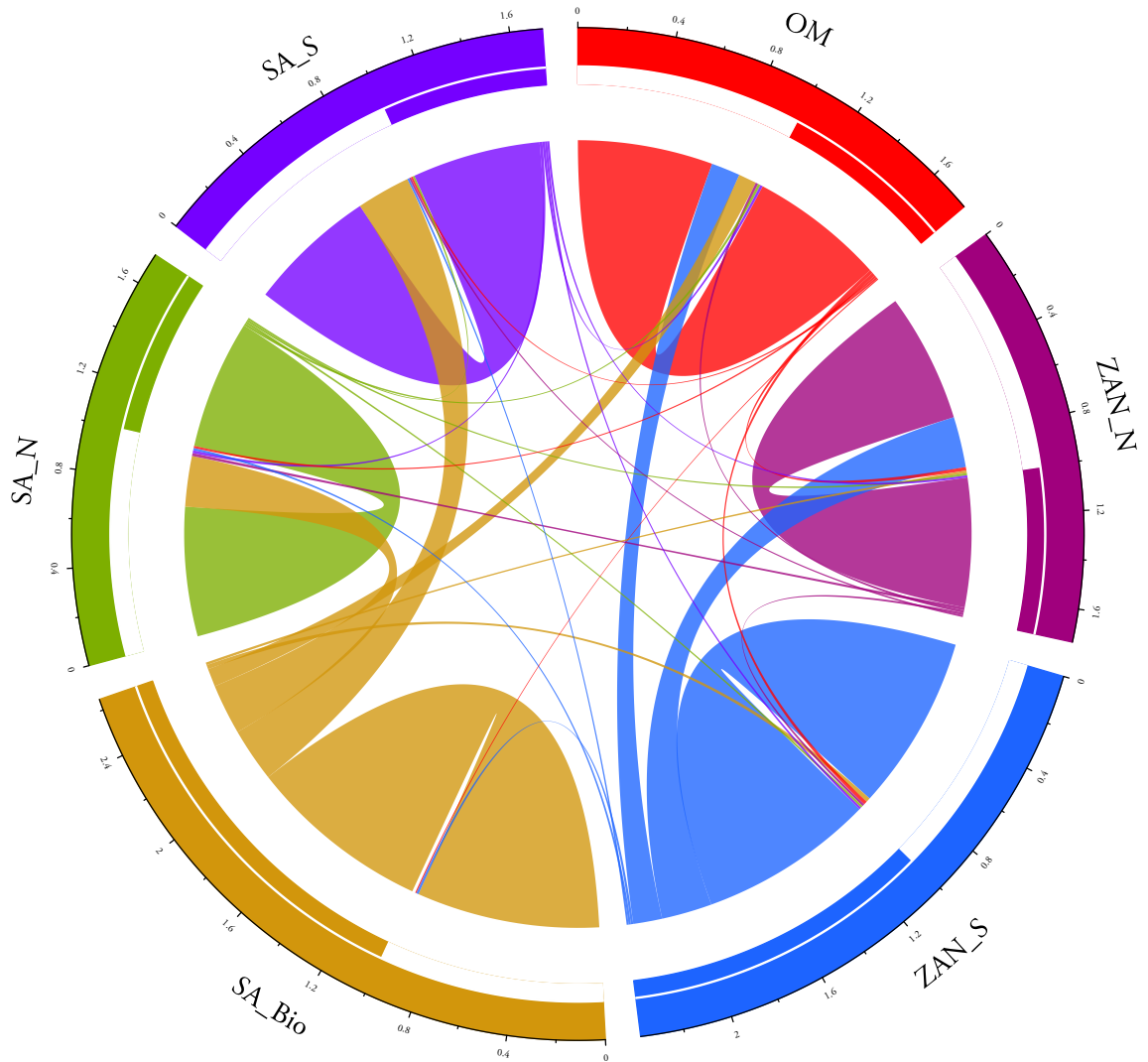


Figure 33: Patterns of migration between populations in the Western Indian Ocean. Circos plot generated from BAYESASS v. 1.3 (Wilson & Rannala, 2003) output for fourteen microsatellites in R v. 3.0 (R Core Team, 2013) using the package *circize* (Gu *et al.* 2014) following Sander *et al.* (2014). Migration out of a population (source) is illustrated by a double bar in the respective segment. A single bar is indicative of movement into the population (current). Migration curve widths are proportional to the number of migrants.

Table 17: Posterior mean estimates for migration rates. Rates defined as the proportion of individuals in a ‘Current’ population that are migrants derived from a ‘Source’ population, per generation. Values inferred in BAYESAss v. 1.3 (Wilson & Rannala, 2003). Standard deviations given in parentheses.

		Source Population					
		OM	SA_(Bio)	SA_N	SA_S	ZAN_N	ZAN_S
Current Population	OM	0.712 (0.029)	0.095 (0.044)	0.013 (0.013)	0.013 (0.013)	0.013 (0.013)	0.153 (0.047)
	SA_Bio	0.006 (0.006)	0.965 (0.015)	0.006 (0.006)	0.006 (0.006)	0.006 (0.006)	0.013 (0.010)
	SA_N	0.011 (0.011)	0.266 (0.025)	0.681 (0.013)	0.015 (0.014)	0.015 (0.014)	0.012 (0.012)
	SA_S	0.010 (0.010)	0.283 (0.021)	0.010 (0.010)	0.677 (0.010)	0.010 (0.010)	0.010 (0.010)
	ZAN_N	0.018 (0.014)	0.014 (0.013)	0.012 (0.011)	0.012 (0.011)	0.679 (0.012)	0.266 (0.025)
	ZAN_S	0.019 (0.015)	0.023 (0.018)	0.012 (0.011)	0.012 (0.011)	0.012 (0.012)	0.923 (0.027)

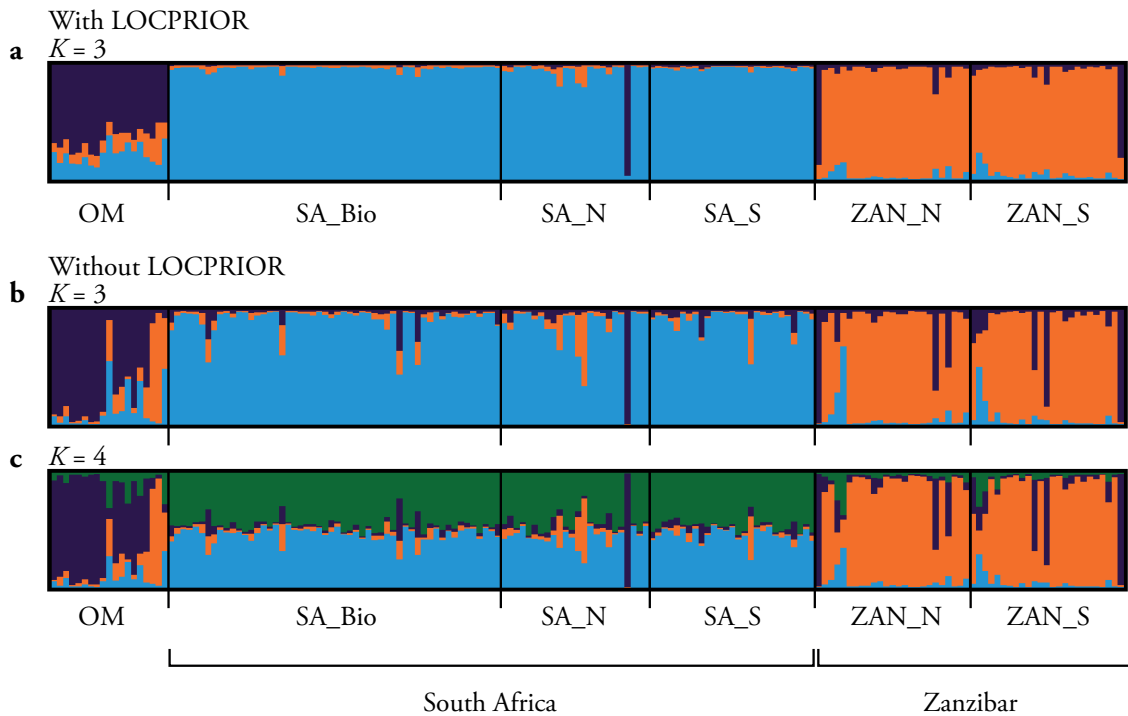


Figure 34: Probability assignment of individuals based on 14 microsatellite loci. Assignments carried out in STRUCTURE v. 2.3 (Pritchard *et al.* 2000) and generated using CLMUMPAK (Kopelman *et al.* 2015). a) $K = 3$ where LOCPRIOR information was used. Plots b) $K = 3$ and c) $K = 4$ were generated without locprior information. Vertical coloured bars represent individuals and black lines delineate the respective putative populations sampled.

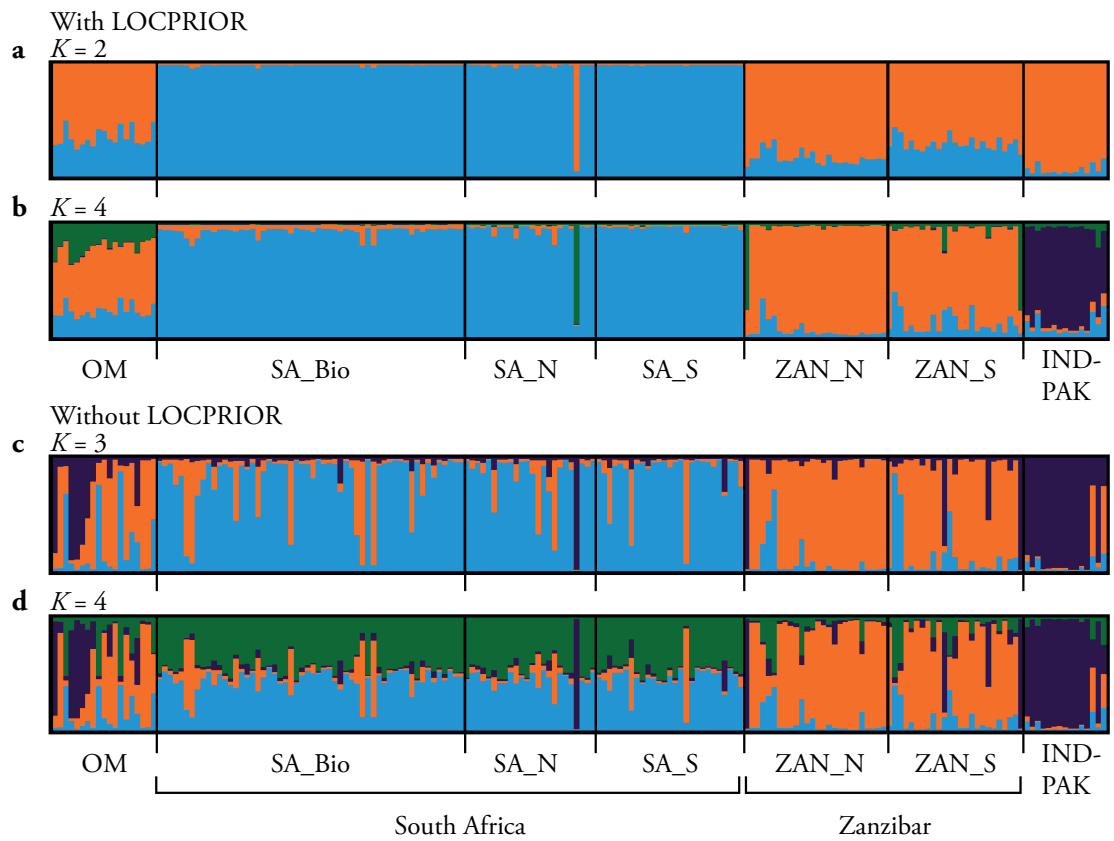


Figure 35: Probability assignment of individuals based on 7 microsatellite loci. Assignments carried out in STRUCTURE v. 2.3 (Pritchard *et al.* 2000) and generated using CLUMPAK (Kopelman *et al.* 2015). a) $K = 2$ and b) $K = 4$ where LOCPRIOR information was used. Plots c) $K = 3$ and d) $K = 4$ were generated without LOCPRIOR information. Vertical coloured bars represent individuals and black lines delineate the respective putative populations sampled.

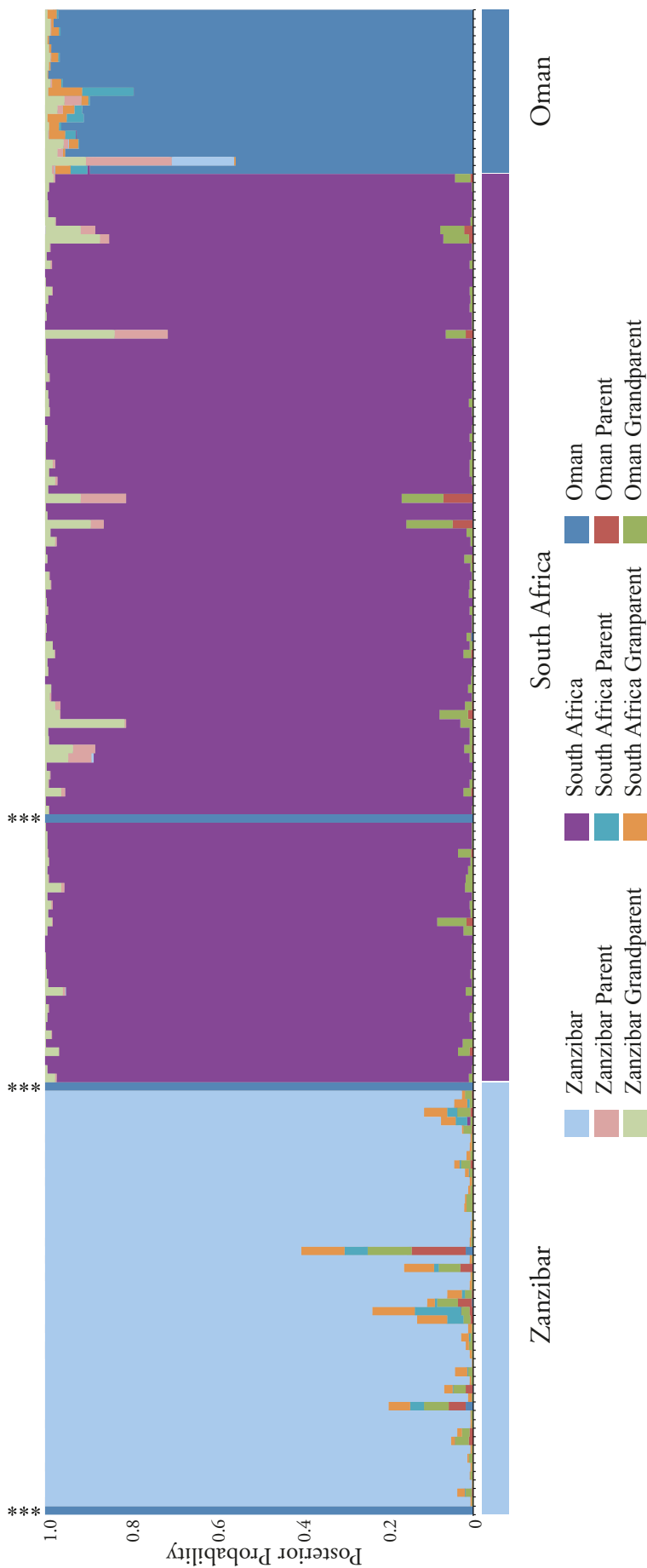


Figure 36: Ancestry posterior probabilities for each individual in the Oman, South Africa and Zanzibar populations using the 14 loci dataset. Probabilities, generated in STRUCTURE v. 2.3 (Pritchard *et al.* 2000), are given for populations assignment (pure ancestry) and whether an individual had a parent or grandparent from an alternative population. *** = putative migrant individuals i.e. individuals in a population with a high assignment probability to a different population.

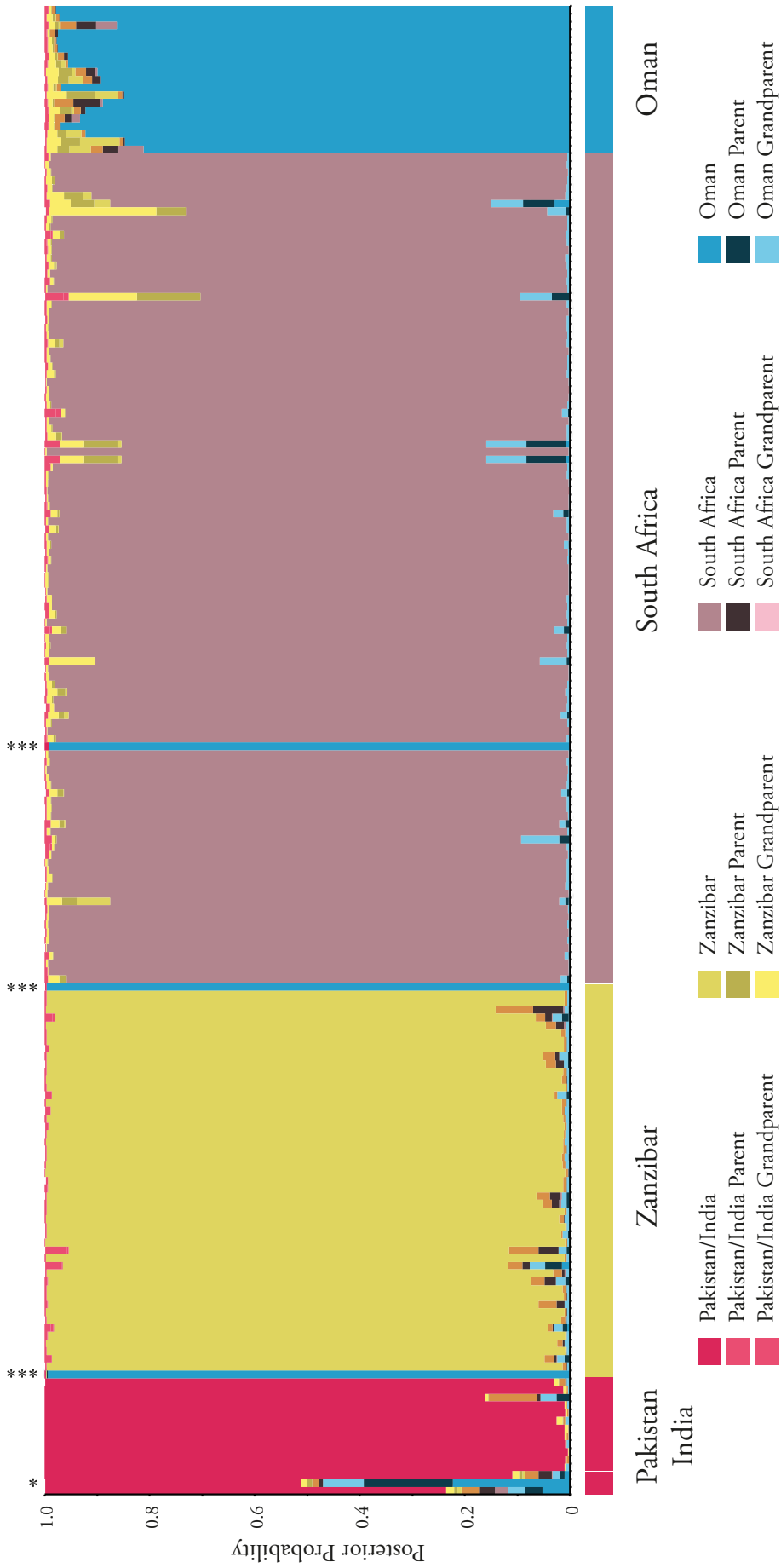


Figure 37: Ancestry posterior probabilities for each individual in the Oman, South Africa, Zanzibar and Indian/Pakistan populations using the seven loci dataset. Probabilities, generated in STRUCTURE v. 2.3 (Pritchard *et al.* 2000), are given for populations assignment (pure ancestry) and whether an individual had a parent or grandparent from an alternative population. *** = putative migrant individuals i.e. individuals in a population with a high assignment probability to a different population. * = individual with strong indication of mixed ancestry. A white line delineates between Pakistan ($n = 3$) and India ($n = 12$) individuals.

Table 18: Posterior probabilities for N_0 , N_1 and ta . Values estimated in Msvar v. 1.3 (Beaumont, 1999; Storz & Beaumont, 2002). 95% HPD = 95% highest posterior densities; * = analysis performed using the seven loci dataset.

	N_0	95% HPD	N_1	95% HPD	ta	95% HPD
India*	2,777	67 - 29,154	23,137	2,723 - 397,558	59,772	312 - 6,953,445
Oman	1,840	37 - 26,254	12,286	2,413 - 62,878	18,928	57 - 1,828,100
Zanzibar	786	53 - 5,280	13,791	2,864 - 68,754	17,997	392 - 287,806
South Africa	1,621	411 - 6,552	22,055	5,030 - 107,078	74,216	10,797 - 481,837

3.3.2 Mitochondrial DNA

3.3.2.1 Phylogeography

From the majority consensus neighbour-joining phylogenetic tree based on 404 bp of control region sequences, four different lineages were evident in the dataset (see Figure 38). These correspond to *T. truncatus*, the holotype lineage of *T. aduncus* (Natoli *et al.* 2004, Perrin *et al.* 2007), the Australasian lineage of *T. aduncus* (Wang *et al.* 1999b) and the Arabian Sea *T. aduncus*, a novel lineage off the northern Indian Ocean (see Chapter 2). The majority of samples collected along Oman's Arabian Sea coast ($n = 85/104$, 81.7%) were representative of the holotype *T. aduncus* lineage. Of the remaining samples collected along that coastline, seven (6.7%) were representative of the Arabian Sea *T. aduncus* lineage and 12 (11.5%) of *T. truncatus*. The Arabian Sea *T. aduncus* lineage was sampled at its southernmost-recorded point near Hasik and Ras Nus in Oman's Dhofar region. It was also sampled further north near Ras Madrasah, Barr al Hikmann and Masirah Island.

T. truncatus was sampled around Hasik, Ras Madrasah, Barr al Hikman, Masirah Island and near Khuwaymah. Off Oman's Sea of Oman coast, all samples collected were *T. truncatus*. Of the samples collected off the Musundam Peninsula and the Strait of Hormuz ($n = 8$), all were representative of the holotype *T. aduncus* lineage. Moving eastwards, of the samples collected in Pakistan ($n = 15$) between Gwadar and Keti Bandar in the Indus River Delta, the majority ($n = 14/15$, 93.3%) represent the Arabian Sea *T. aduncus* lineage with only one sample representing the holotype lineage collected on the eastern side of Sonmiani Bay. For samples collected along India's coastline ($n = 12$), the locations of eight are unknown. Of these, six (75%) belong to the Arabian Sea lineage, one to the holotype *T. aduncus* lineage and one to the *T. truncatus* lineage. Although the precise sample collection location of the holotype individual is unknown, this sample represents the eastern-most record of this lineage. Four samples were collected near Parangipettai on India's eastern coastline. Of these, one was *T. truncatus*

and the rest belonged to the Arabian Sea *T. aduncus* lineage. These samples represent the eastern-most records of the Arabian Sea *T. aduncus* lineage. Three samples were collected near Songkhla on the eastern coast of Thailand. These were also included in some analyses and all grouped with the Australasian *T. aduncus* lineage in the phylogeny (see Figure 38).

3.3.2.2 Genetic Diversity and Structure

Across the 352 individuals at 267 bp of mtDNA control region sequence, a total of 82 haplotypes and 24 polymorphic sites were identified (see Table 19). Only four haplotypes were shared between combinations of the South African, Zanzibar and Arabian populations. Within the IND_PAK population, one haplotype was shared between India and Pakistan (see Table 19). Relatively low values of nucleotide (π) and haplotype (h) diversities were observed in the South African, Zanzibar and Australian populations, whereas relatively high values for π and h were seen in the CHI_THAI, IND_PAK, NWIO_Tt, and CHI_Tt populations (See Table 15). Pairwise comparisons between populations for π and h using Welch's t -test (see Table 20) generally show that the ARABIA, CHI_THAI, IND_PAK, NWIO_Tt and CHI_Tt populations have significantly higher π and h than other populations.

Pairwise F_{ST} and Φ_{ST} values were highly significant ($P < 0.001$, after Bonferroni correction) for the majority of comparisons (see Table 21). No significant differences in F_{ST} or Φ_{ST} were observed among the South African populations.

3.3.2.3 Demography

Values for Tajima's D and Fu's F_S were not statistically significant after Bonferroni correction ($P > 0.05$, $P > 0.02$ for Fu's F_S) (Table 22). Mismatch distribution analyses failed to reject the expansion model for a number of populations (see SSD and HRI values in Table 22). Expansion times are estimated based on two published mutation rates for the cetacean mtDNA control region presented in Table 22.

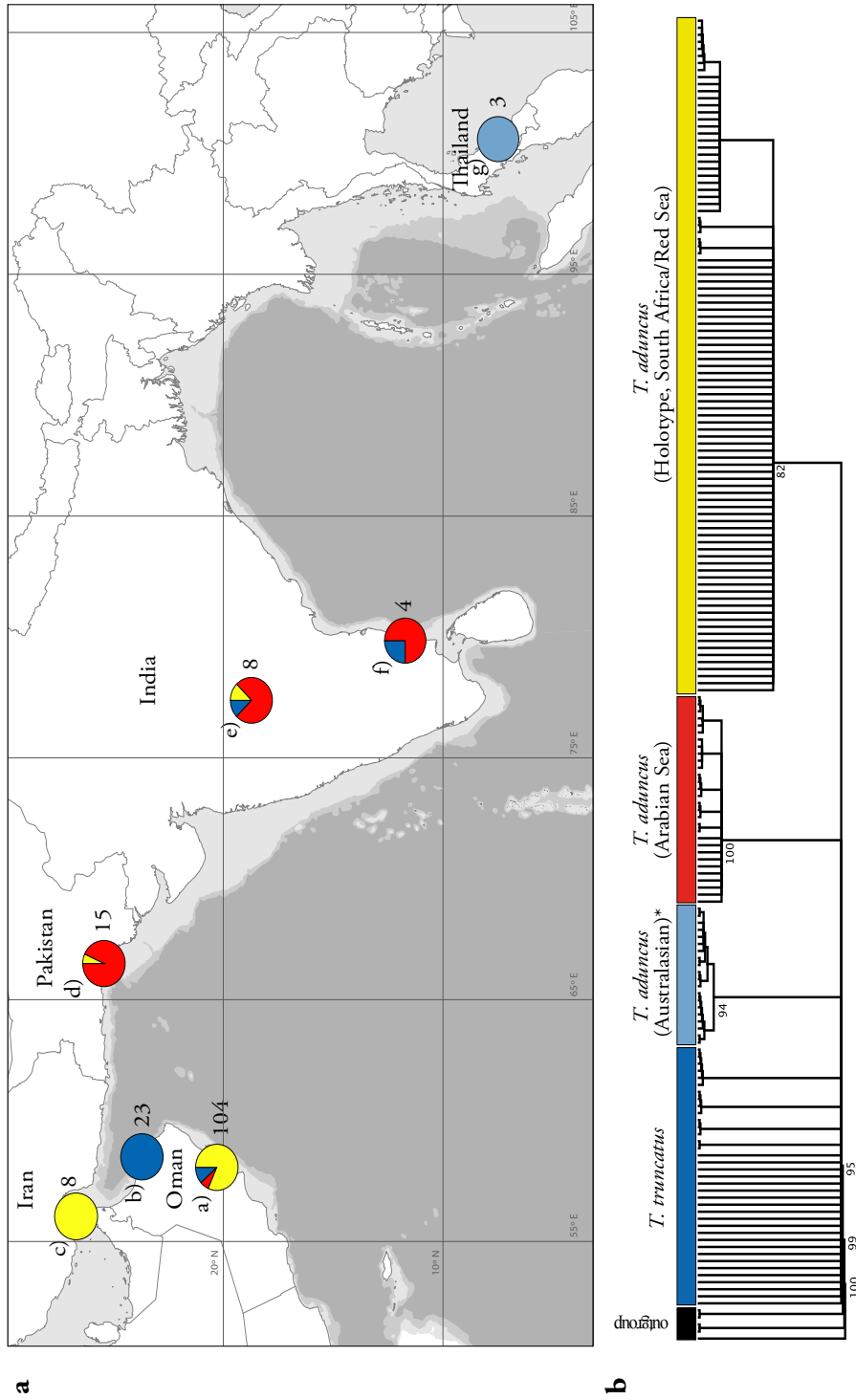


Figure 38: Distributions and frequencies of sampled bottlenose dolphin lineages. a): Pie charts showing the proportional representation of different lineages across the study area. Regions considered include a) the Oman Arabian Sea coastline, b) the Oman Sea of Oman coastline, c) the Musundam Peninsula and Straits of Hormuz, d) Pakistan, e) India (unknown sampling locations), f) East India, g) East Thailand. Numbers next to charts indicate sample size; b): Majority consensus neighbour-joining phylogenetic tree generated in GENEIOUS v. 7.1.2. All sequences presented in this tree are new to this study with the exception of 10 sequences from the Australasian lineage(*), which were obtained from GenBank (Accession No.s: AF049100, AF056233-36, 39-43) and outgroup sequences from humpback dolphins, *Sousa chinensis* (Accession No.s: DQ665785, 87-88). Bootstrap support values are indicated.

Table 19: Haplotype frequencies for each bottlenose dolphin population. *The Arabian population consists of samples collected in Oman but also includes 2 samples from the Straits of Hormuz (Iran); one sample is JQ9344964 (Mohsenian *et al. unpublished data*) and the other sequence was generated in this study (museum specimen SMNS_45_711). The Arabian population also includes the sequence DQ517442 collected from the *Tursiops aduncus* holotype specimen from the Red Sea (see Perrin *et al.* 2007).

Haplotype	ARABIA*	SA_N	SA_S	SA_Bio	ZAN_N	ZAN_S	AUS	CHI		IND		NWIO		CHI_Tt
								THAI	THAI	PAK	PAK	OM	IND	
XXXXXX	1	-	-	-	-	-	-	-	-	-	-	-	-	-
AY962628, EF636207, EF636208, JQ934964, DQ517442*	54	13	14	15	4	14	-	-	-	-	1	-	-	-
AF056233, AF049100	-	-	-	-	-	-	-	2	-	-	-	-	-	-
AF056242	-	-	-	-	-	-	-	1	-	-	-	-	-	-
AF056243	-	-	-	-	-	-	-	1	-	-	-	-	-	-
AF056234, AF056239	-	-	-	-	-	-	-	6	-	-	-	-	-	-
AF056235	-	-	-	-	-	-	-	1	-	-	-	-	-	-
AF056236	-	-	-	-	-	-	-	1	-	-	-	-	-	-
AF056240	-	-	-	-	-	-	-	3	-	-	-	-	-	-
AF056241	-	-	-	-	-	-	-	2	-	-	-	-	-	-
AF056227	-	-	-	-	-	-	-	-	-	-	-	-	-	1
AF056228	-	-	-	-	-	-	-	-	-	-	-	-	-	1
AF056229, AF056221	-	-	-	-	-	-	-	-	-	-	-	-	-	2
AF056230	-	-	-	-	-	-	-	-	-	-	-	-	-	1
AF056231, AF056220	-	-	-	-	-	-	-	-	-	-	-	-	-	6
AF056223	-	-	-	-	-	-	-	-	-	-	-	-	-	1
AF056232	-	-	-	-	-	-	-	-	-	-	-	-	-	1
AF056224	-	-	-	-	-	-	-	-	-	-	-	-	-	1
AF056225	-	-	-	-	-	-	-	-	-	-	-	-	-	1
AF056226	-	-	-	-	-	-	-	-	-	-	-	-	-	1
XXXXXX	-	-	-	-	-	-	-	-	-	1	-	-	-	-
XXXXXX	-	-	-	-	-	-	-	-	-	1	-	-	-	-
XXXXXX	-	-	-	-	-	-	-	-	-	2	-	-	-	-
XXXXXX	-	-	-	-	-	-	-	-	-	1	-	-	-	-
XXXXXX	-	-	-	-	-	-	-	-	-	1	-	-	-	-
XXXXXX	-	-	-	-	-	-	-	-	-	1	-	-	-	-
XXXXXX	-	-	-	-	-	-	-	-	-	1	-	-	-	-
XXXXXX	-	-	-	-	-	-	-	-	-	1	5	-	-	-
XXXXXX	-	-	-	-	-	-	-	-	-	-	-	-	1	-
XXXXXX	-	-	-	-	-	-	-	-	-	-	-	-	1	-
HM104228	25	-	-	-	1	-	-	-	-	-	-	-	-	-

Haplotype	ARABIA*	SA_N	SA_S	SA_Bio	ZAN_N	ZAN_S	AUS	CHI		IND		NWIO		CHI_Tt
								THAI	THAI	IND	PAK	OM	IND	
XXXXXX	2	-	-	-	-	-	-	-	-	-	-	-	-	-
XXXXXX	5	-	-	-	-	-	-	-	-	-	-	-	-	-
XXXXXX	1	-	-	-	-	-	-	-	-	-	-	-	-	-
XXXXXX	5	-	-	-	-	-	-	-	-	-	-	-	-	-
XXXXXX	1	-	-	-	-	-	-	-	-	-	-	-	-	-
XXXXXX	4	-	-	-	-	-	-	-	-	-	-	-	-	-
XXXXXX	1	-	-	-	-	-	-	-	-	-	-	-	-	-
XXXXXX	1	-	-	-	-	-	-	-	-	-	-	-	-	-
XXXXXX	1	-	-	-	-	-	-	-	-	-	-	-	-	-
XXXXXX	1	-	-	-	-	-	-	-	-	-	-	-	-	-
XXXXXX	1	-	-	-	-	-	-	-	-	-	-	-	-	-
XXXXXX	1	-	-	-	-	-	-	-	-	-	-	-	-	-
XXXXXX	-	-	-	-	-	-	-	-	-	-	-	1	-	-
XXXXXX	-	-	-	-	-	-	-	-	-	-	-	1	-	-
XXXXXX	-	-	-	-	-	-	-	-	-	-	-	1	-	-
XXXXXX	-	-	-	-	-	-	-	-	-	-	-	2	-	-
XXXXXX	-	-	-	-	-	-	-	-	-	-	-	2	-	-
XXXXXX	-	-	-	-	-	-	-	-	-	-	-	1	-	-
XXXXXX	-	-	-	-	-	-	-	-	-	-	-	3	-	-
XXXXXX	-	-	-	-	-	-	-	-	-	-	-	6	-	-
XXXXXX	-	-	-	-	-	-	-	-	-	-	-	1	-	-
XXXXXX	-	-	-	-	-	-	-	-	-	-	-	1	-	-
XXXXXX	-	-	-	-	-	-	-	-	-	-	-	1	-	-
XXXXXX	-	-	-	-	-	-	-	-	-	-	-	3	-	-
XXXXXX	-	-	-	-	-	-	-	-	-	-	-	1	-	-
XXXXXX	-	-	-	-	-	-	-	-	-	-	-	1	-	-
XXXXXX	-	-	-	-	-	-	-	-	-	-	-	1	-	-
XXXXXX	-	-	-	-	-	-	-	-	-	-	-	3	-	-
XXXXXX	-	-	-	-	-	-	-	-	-	-	-	1	-	-
XXXXXX	-	-	-	-	-	-	-	-	-	-	-	1	-	-
XXXXXX	-	-	-	-	-	-	-	-	-	-	-	1	-	-
XXXXXX	-	-	-	-	-	-	-	-	-	-	-	1	-	-
XXXXXX	-	-	-	-	-	-	-	-	-	-	-	4	-	-
XXXXXX	-	-	-	-	-	-	-	-	-	-	-	4	-	-
XXXXXX	-	-	-	-	-	-	-	-	-	-	-	1	-	-
EF636209, AY962626	-	4	1	1	4	-	-	-	-	-	-	-	-	-
EF636210	-	-	-	1	-	-	-	-	-	-	-	-	-	-
EF636212	-	1	-	-	-	-	-	-	-	-	-	-	-	-
EF581128, AF287953	-	-	-	-	-	-	2	-	-	-	-	-	-	-

Haplotype	ARABIA*	SA_N	SA_S	SA_Bio	ZAN_N	ZAN_S	AUS	CHI		IND		NWIO		CHI_Tt
								THAI	THAI	PAK	PAK	OM	IND	
AF287952	-	-	-	-	-	-	30	-	-	-	-	-	-	-
AF287951	-	-	-	-	-	-	25	-	-	-	-	-	-	-
AF287954	-	-	-	-	-	-	1	-	-	-	-	-	-	-
XXXXXX	-	-	-	-	-	-	-	-	1	-	-	-	-	-
XXXXXX	-	-	-	-	-	-	-	-	1	-	-	-	-	-
XXXXXX	-	-	-	-	-	-	-	-	1	-	-	-	-	-
HM104224	-	-	-	-	11	4	-	-	-	-	-	-	-	-
HM104225	-	-	-	-	-	3	-	-	-	-	-	-	-	-
HM104226	-	-	-	-	-	1	-	-	-	-	-	-	-	-
HM104227	-	-	-	-	1	-	-	-	-	-	-	-	-	-
XXXXXX	-	-	-	-	-	-	-	-	-	1	-	-	-	-

Table 20: P -values in pairwise comparisons of π (below diagonal) and h (above diagonal) using Welch's t -test. Shaded values indicate significant differences at $P = 0.05$, after Bonferroni correction.

	ARABIA	SA_N	SA_S	SA_Bio	ZAN_N	ZAN_S	AUS	CHI_THAI	IND_PAK	NWIO_Tt	CHI_Tt
ARABIA	-	<0.0001	<0.0001	<0.0001	0.4103	0.0003	<0.0001	<0.0001	<0.0001	<0.0001	<0.0001
SA_N	<0.0001	-	<0.0001	<0.0001	<0.0001	0.0024	0.0017	<0.0001	<0.0001	<0.0001	<0.0001
SA_S	<0.0001	0.001	-	0.0342	<0.0001	<0.0001	<0.0001	<0.0001	<0.0001	<0.0001	<0.0001
SA_Bio	<0.0001	0.0315	0.1225	-	<0.0001	<0.0001	<0.0001	<0.0001	<0.0001	<0.0001	<0.0001
ZAN_N	<0.0001	0.0941	<0.0001	0.0007	-	0.0003	<0.0001	<0.0001	<0.0001	<0.0001	<0.0001
ZAN_S	<0.0001	0.0936	<0.0001	0.0006	1	-	0.5991	<0.0001	<0.0001	<0.0001	<0.0001
AUS	<0.0001	0.0028	<0.0001	<0.0001	0.3708	0.3708	-	<0.0001	<0.0001	<0.0001	<0.0001
CHI_THAI	0.0022	<0.0001	<0.0001	<0.0001	<0.0001	<0.0001	<0.0001	-	0.389	<0.0001	0.235
IND_PAK	0.0022	<0.0001	<0.0001	<0.0001	<0.0001	<0.0001	<0.0001	0.5781	-	<0.0001	0.0737
NWIO_Tt	<0.0001	<0.0001	<0.0001	<0.0001	<0.0001	<0.0001	<0.0001	0.0242	0.0026	-	0.0003
CHI_Tt	0.0067	<0.0001	<0.0001	<0.0001	0.0001	0.0001	0.0002	1	0.6075	0.0361	-

Table 21: Mitochondrial DNA F_{ST} values below diagonal and Φ_{ST} above the diagonal. Colours are indicative of the cell value whereby darker shades correspond to higher values and lighter shades to lower values. * = $P < 0.001$ after Bonferroni correction.

	ARABIA	SA_N	SA_S	SA_Bio	ZAN_N	ZAN_S	AUS	CHI_THAI	IND_PAK	NWIO_Tt	CHI_Tt
ARABIA	-	0.025	0.009	0.015	0.303*	0.065	0.888*	0.808*	0.780*	0.742*	0.800*
SA_N	0.084	-	0.019	-0.019	0.385*	-0.006	0.924*	0.802*	0.789*	0.693*	0.817*
SA_S	0.138*	0.053	-	-0.044	0.534*	0.041	0.931*	0.815*	0.802*	0.693*	0.827*
SA_Bio	0.117	0.028	-0.048	-	0.482*	0.023	0.930*	0.815*	0.801*	0.698*	0.828*
ZAN_N	0.244*	0.306*	0.466*	0.431*	-	0.309*	0.910*	0.771*	0.774*	0.720*	0.824*
ZAN_S	0.069	0.056	0.115	0.084	0.204*	-	0.917*	0.798*	0.795*	0.703*	0.817*
AUS	0.384*	0.483*	0.578*	0.555*	0.395*	0.440*	-	0.311*	0.908*	0.871*	0.921*
CHI_THAI	0.243*	0.322*	0.456*	0.425*	0.213*	0.272*	0.305*	-	0.785*	0.751*	0.808*
IND_PAK	0.217*	0.287*	0.410*	0.381*	0.197*	0.240*	0.293*	0.099*	-	0.668*	0.719*
NWIO_Tt	0.203*	0.264*	0.374*	0.349*	0.170*	0.222*	0.255*	0.071*	0.066*	-	0.036
CHI_Tt	0.257*	0.347*	0.493*	0.458*	0.230*	0.292*	0.324*	0.119*	0.112*	0.083*	-

Table 22: Neutrality tests and mismatch distribution analysis. Expansion times (YrsBP) calculated using substitutions/locus/generation $\mu = 2.80 \times 10^{-3}$ and $\mu = 3.92 \times 10^{-4}$ (5×10^{-7} substitutions/site/yr and 7×10^{-8} substitutions/site/yr, respectively for a sequence length = 267 bp and generation time = 21 yrs). Tajima's D and Fu's F_s values were not statistically significant at $P = 0.05$ ($P = 0.02$ for Fu's F_s), Bonferroni correction applied. Sum-of-Squared-Deviations (SSD) and Harpending's Raggedness Index (HRI) are shaded where $P > 0.05$. $\tau = (2\mu t)$; $\theta_0 = (2N_0\mu)$; $\theta_1 = (2N_1\mu)$, where N_0 = initial effective population size before expansion event, N_1 = current effective population size, μ = substitutions per locus per generation and t = number of generations since expansion.

Pop	Neutrality Tests				Mismatch Analysis							
	Tajima's D	Fu's F_s	SSD	HRI	τ	(95% CI)	Yrs BP $\mu=2.80 \times 10^{-3}$	Yrs BP $\mu=3.92 \times 10^{-4}$	θ_0	(95% CI)	θ_1	(95% CI)
ARABIA	-1.299	-2.433	0.018	0.109	0.938	(0.441 - 1.291)	-	-	0.000	(0.000 - 0.074)	99999	(6.783 - 99999)
SA_N	-0.538	1.011	0.158	0.664	2.996	(0.000 - 4.863)	-	-	0.002	(0.000 - 0.023)	1.055	(0.000 - 99999)
SA_S	-1.491	0.235	0.025	0.787	3.215	(0.439 - 3.215)	12,041	86,004	0.056	(0.000 - 0.000)	0.113	(0.000 - 99999)
SA_Bio	-1.049	-0.126	0.025	0.608	3.000	(0.498 - 3.500)	11,236	80,257	0.000	(0.000 - 0.217)	0.203	(0.000 - 99999)
ZAN_N	0.91	-0.068	0.018	0.072	2.971	(0.000 - 5.559)	11,126	79,473	0.000	(0.000 - 1.290)	2.469	(0.751 - 99999)
ZAN_S	0.245	1.079	0.433	0.232	0.000	(0.000 - 0.287)	-	-	0.000	(0.000 - 0.009)	99999	(99869 - 99999)
AUS	0.744	2.761	0.239	0.645	3.885	(0.000 - 6.992)	14,550	103,926	0.000	(0.000 - 0.925)	2.228	(0.443 - 99999)
CHI_THAI	0.407	-1.957	0.019	0.048	6.867	(1.697 - 10.508)	25,720	183,713	0.000	(0.000 - 2.858)	11.607	(5.128 - 99999)
IND_PAK	-0.595	-3.596	0.007	0.015	1.023	(0.000 - 6.938)	3,833	27,379	2.665	(0.000 - 7.546)	40.313	(3.987 - 99999)
NWIO_Tt	-0.687	-10.191	0.005	0.014	7.660	(3.922 - 9.883)	28,690	204,927	0.005	(0.000 - 3.793)	28.047	(20.527 - 99999)
CHI_Tt	-0.476	-2.16	0.016	0.035	6.490	(0.861 - 11.783)	24,308	173,628	0.207	(0.000 - 2.310)	8.622	(4.654 - 99999)

3.3.2.4 Haplotype Network

From the median-joining network (Figure 39) generated in POPART (<http://popart.otago.ac.nz>, Leigh & Bryant, 2015) using the full mtDNA dataset of 267 bp sequences, there is clear separation between the four lineages. Individuals from Australia, China and Thailand represent the Australasian *T. aduncus* lineage. The holotype *T. aduncus* lineage is well represented in this network, particularly haplotype-1 (H1) which has a broad distribution, including individuals from South Africa, Zanzibar, Arabia (Oman, Iran, Red Sea), Pakistan and India. The Arabian Sea lineage of *T. aduncus* includes individuals from India, Pakistan and Oman. The *T. truncatus* lineage is represented by individuals from China, India and Oman and is separated from the *T. aduncus* groups by three or four mutation steps (see Figure 39). Within this group there is also inference of multiple un-sampled haplotypes. The Arabian Sea *T. aduncus* lineage is separated from the holotype lineage by six mutation steps and the Australasian *T. aduncus* is separated from the holotype *T. aduncus* lineage by eight mutational steps.

3.3.2.5 Estimates of population divergence times

Posterior probability distributions were checked for convergence on similar parameter estimates. The values of parameters θ , M and T , as inferred in M_{DIV} (Nielsen & Wakeley, 2001), are presented in Table 23. Divergence times were also calculated. The oldest divergence time is between Oman and Zanzibar and the most recent between Zanzibar and South Africa.

Table 23: Values for θ , M and T , estimated for Oman, Zanzibar and South Africa. Parameters were estimated in M_{DIV} (Nielsen & Wakeley, 2001). $\theta = 2N_{ef}\mu$, $M = N_{ef}m$, $T = t/N_{ef}$. N_{ef} = effective population size of females; μ = mutation rate per locus per generation; m = migration rate per locus per generation; t = divergence times per locus per generation. Divergence times (YrsBP) were calculated using a mutation rate, μ of 2.97×10^{-3} and 4.16×10^{-4} mutations per locus per generation (see methods).

Population	θ	M	T	Yrs BP $\mu=2.97 \times 10^{-3}$	Yrs BP $\mu=3.92 \times 10^{-4}$
Oman-Zanzibar	1.91	0.24	0.82	5,534	39,531
Oman-South Africa	1.38	0.28	0.66	3,218	22,988
Zanzibar-South Africa	1.24	1.08	0.26	1,139	8,137

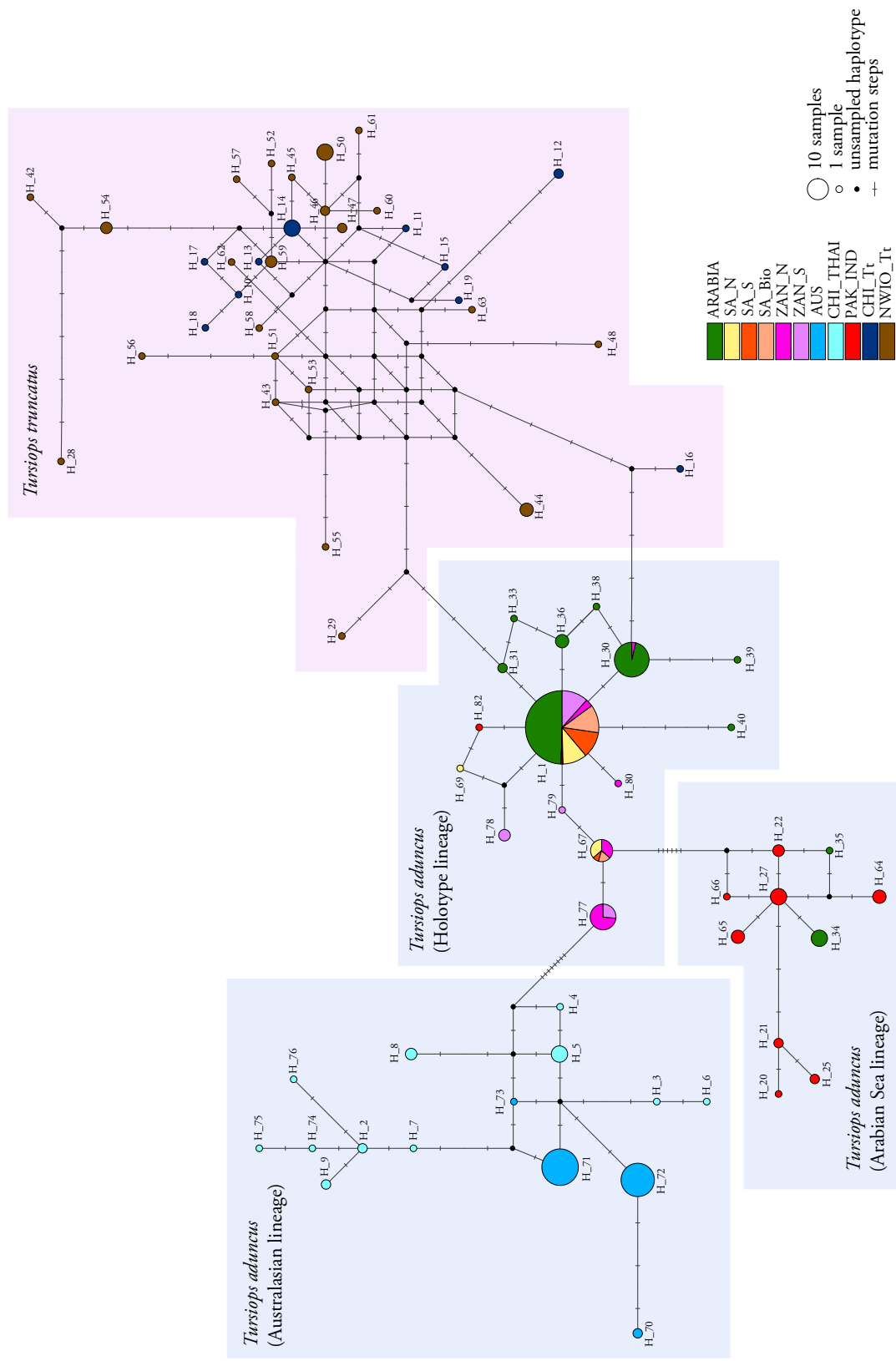


Figure 39: Bottlenecked dolphin median-joining haplotype network. Generated in PopART (Leigh & Bryant, 2015) from mtDNA control region sequences.

3.3.3 Inference of Demographic History in the Western Indian Ocean

In the ABC analysis, logistic regression of the posterior probabilities of each evolutionary scenario (see methods) revealed the scenario associated with refugial re-expansion out of South Africa (scenario 3) to be the most favoured (see Figure 40). The next most favoured scenario (scenario 2), was associated with a southbound establishment of populations preceded by a founding event off Arabia across a barrier. Confidence intervals for scenario 3 did not overlap with scenario 1. However, confidence intervals for scenarios 2 and 3 overlapped substantially (see Figure 40). Therefore, both scenarios are considered below. Posterior estimates of parameters were inferred for all scenarios using the closest 1% of the simulated datasets to the observed data (see Table 24).

Under scenario 3, populations representing the holotype and Arabian Sea lineages diverged (t_4) ~ 132 Ka (HPD: 39-294 Ka). During this time, populations contracted, and effective population sizes were reduced to $\sim 4,200$ individuals in the South African (HPD: 488-7,810) and Indian/Pakistan (HPD: 374-17,200) populations. Populations recovered and expanded out of South Africa (t_3) ~ 88 Ka (HPD: 6-200 Ka), establishing the Zanzibar population (t_2) ~ 13 Ka (HPD: 4-53 Ka) and the Oman population (t_1) ~ 11 Ka (HPD: 2-31 Ka). Population sizes recovered in all populations except those off South Africa which remained low at $\sim 4,400$ (HPD: 1580-9100) individuals (see Table 24).

Under scenario 2, the holotype and Arabian Sea lineages diverged due to the presence of a barrier in the northwest Indian Ocean, which was crossed ~ 133 Ka (HPD: 38-296 Ka), resulting in a founding event off Oman. Populations recovered ~ 56 Ka (HPD: 3-188 Ka) and expanded southwards, establishing populations off Zanzibar ~ 16 Ka (HPD: 5-62 Ka) and South Africa ~ 5 Ka (HPD: 0.7-24 Ka). Effective population sizes for Oman, Zanzibar and India/Pakistan were $\sim 13,300$ (HPD: 6,040-19,600), $\sim 11,600$ (HPD: 4,670-19,000) and $\sim 15,800$ (7,190-27,200) individuals, respectively. The population off South Africa remained low at $\sim 4,390$ (HPD: 1,050-9,430) individuals.

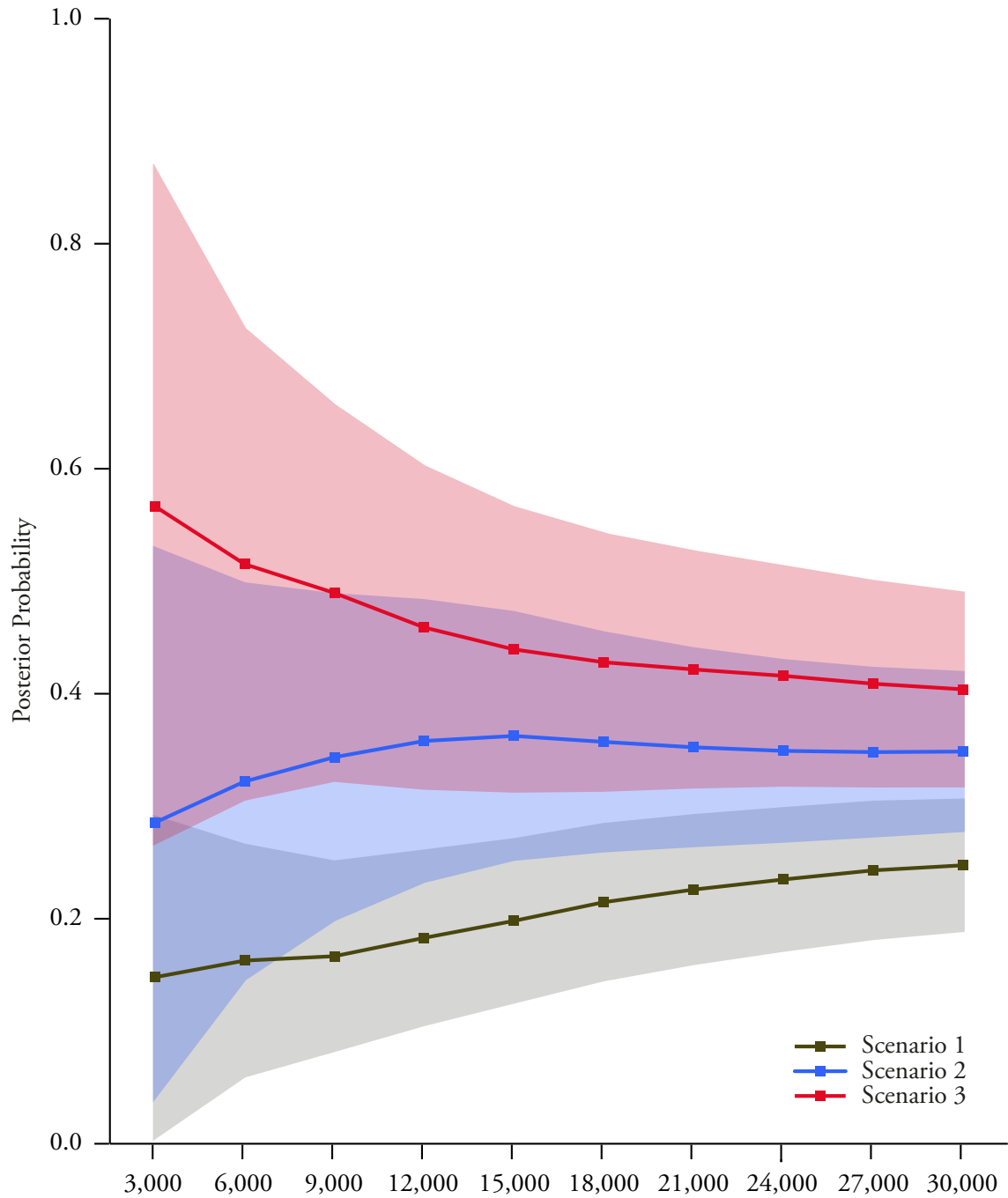


Figure 40: Logistic regression of posterior probabilities for each demographic scenario (1-3) against the number of simulated datasets. 1% of total simulated datasets for each scenario = 30,000. Scenarios tested in DIYABC v. 2.0.4 (Cornuet *et al.* 2014) from 7 microsatellite loci and mtDNA control region sequences. The posterior probability 95% confidence-intervals for each subset of simulated data are presented as a colour band.

Table 24: Prior and posterior distributions of parameters across all scenarios. Values generated in DIYABC v. 2.0.4 (Cornuet *et al.* 2014). $N1$ = Oman effective population size (N_e); $N2$ = South Africa N_e ; $N3$ = Zanzibar N_e ; $N4$ = India/Pakistan N_e ; $N1b$, $N2b$, $N4b$ = variations in N_e for respective populations due to a bottleneck or founding event; $t4$ = divergence time of Zanzibar, South Africa and Oman from ancestral population; $t3$ = time of founding event (scenario 2) or bottleneck (scenario 3) in ancestral populations; $t2$, $t1$ = sequential population divergence times; μ_{mic} = mean mutation rate for microsatellite loci; μ_{mtc} = mean P coefficient for microsatellite loci; μ_{smic} = mean SNI rate for microsatellite loci; μ_{seq} = mutation rate for mitochondrial sequences; k_{seq} = mean coefficient kC/T; Time parameter estimates ($t1$ - $t4$) are converted to YrsBP using median posterior distribution values and a generation time of 21 years.

Parameter	Distribution	Min	Max	Posterior					
				Scenario 1		Scenario 2		Scenario 3	
				Median	95% HPD	Median	95% HPD	Median	95% HPD
N1	Uniform	10	20,000	9,350	4,400 - 16,300	13,300	6,040 - 19,600	12,200	3,530 - 19,500
N2	Uniform	10	10,000	4,630	1,130 - 9,470	4,390	1,050 - 9,430	4,400	1,580 - 9,100
N3	Uniform	10	20,000	11,300	4,400 - 19,000	11,600	4,670 - 19,000	12,300	5,020 - 19,300
N4	Uniform	10	30,000	16,800	7,880 - 27,400	15,800	7,190 - 27,200	20,700	8,950 - 29,400
N1b	Uniform	10	10,000	na	na - na	4,550	523 - 9,580	na	na - na
N2b	Uniform	10	8,000	na	na - na	na	na - na	4,220	488 - 7,810
N4b	Uniform	10	20,000	na	na - na	na	na - na	4,260	374 - 17,200
t1	Uniform	10	2,000	4,935	819 - 22,050	5,019	777 - 23,730	10,500	1,806 - 31,080
t2	Uniform	10	4,000	13,503	3,738 - 55,440	16,275	4,515 - 62,160	13,167	3,885 - 52,920
t3	Uniform	10	10,000	na	na - na	56,490	3,318 - 188,370	87,570	6,216 - 199,500
t4	Uniform	10	15,000	102,060	27,510 - 283,500	132,720	38,010 - 296,100	131,880	38,640 - 294,000
μ_{mic}	Uniform	1.00E-04	4.00E-04	1.21E-04	1.00E-04 - 2.65E-04	1.26E-04	1.00E-04 - 2.73E-04	1.53E-04	1.02E-04 - 3.29E-04
pmic	Uniform	1.00E-01	1	4.24E-01	1.51E-01 - 9.00E-01	4.25E-01	1.51E-01	4.55E-01	1.64E-01
smimic	Uniform	1.00E-08	1.00E-05	4.56E-08	1.00E-08 - 1.40E-06	2.53E-08	1.00E-08	3.39E-08	1.00E-08
μ_{seq}	Uniform	2.00E-09	2.50E-06	1.30E-06	6.59E-07 - 2.26E-06	1.19E-06	6.30E-07	1.66E-06	1.00E-06
kseq	Uniform	0.05	1,000,000	462,000	21,900 - 967,000	520,000	23,300	469,000	23,500

3.4 Discussion

In the present study, multiple analyses, based on mtDNA and microsatellite loci, uncover significant population structure between *T. aduncus* populations in the western Indian Ocean with evidence for further substructure off Zanzibar and South Africa, as has been reported elsewhere (Natoli *et al.* 2008; Särnblad *et al.* 2011; *in review*). A general pattern of north-bound asymmetric migration between populations is identified. These results will influence the delineation of management units for regional conservation initiatives (see Palsbøll *et al.* 2007). The distributions of samples analysed is suggestive of secondary contact between lineages in the northwest Indian Ocean and population ancestry assignments provide limited evidence for introgression/hybridisation between individuals in this region. Tests for population expansion/contraction based on microsatellite data were inconclusive and neutrality tests based on mtDNA were not significant. However, mismatch distribution analyses failed to reject the expansion model for a number of populations (see Table 22).

Divergence date estimates between adjacent populations in the western Indian Ocean suggest populations established in a southbound direction and had an Arabian Sea ancestry. Comparable results have been reported in humpback dolphin populations from similar localities (Mendez *et al.* 2011). One of two demographic scenarios identified as plausible in ABC analyses supports this Arabian Sea ancestry (scenario 2), however the other scenario (scenario 3) suggests a South African ancestry. Both scenarios suggest a reduced effective population size in the holotype ancestor. Whether this reduction in effective population size was due to a bottleneck or founding event remains unknown.

3.4.1 Phylogeography

Work conducted by Natoli *et al.* (2004) on worldwide genetic differentiation across bottlenose dolphin populations suggested that *T. aduncus* populations off South Africa were a distinct lineage from those described in China (Wang *et al.* 1999b). The lineage off South Africa was later identified as a match for the *T. aduncus* holotype specimen collected from the Red Sea (Perrin *et al.* 2007) and further support for the lineage was provided by a phylogeny of the genus based on mitochondrial genomes (Moura *et al.* 2013a; Chapter 2). The results presented here build on the work conducted by Natoli *et al.* (2004) and support the presence of a new, Arabian Sea lineage of *T. aduncus* (Chapter 2) in the northwest/northern Indian Ocean based on mtDNA and microsatellite loci; distinct from the lineages described

off South Africa (Natoli *et al.* 2004) and Australasia (Wang *et al.* 1999b). Results presented here also confirm that *T. truncatus* are present in the Indian Ocean.

The distributions of samples that match the Arabian Sea *T. aduncus* lineage (represented by individuals from India, Pakistan and Oman) appear to overlap with those of the holotype lineage (represented by individuals off Oman, Zanzibar and South Africa) suggestive of secondary contact between them. This apparent overlap occurs from at least as far south as the Dhofar region of Oman and along the northern Indian Ocean coastline off Pakistan and into India. The percentage of samples that match the *T. aduncus* holotype lineage diminish to rarity as one moves from Arabia (92%) towards India (8%) while the frequency of the Arabian Sea lineage increases in the same direction (from 8% to 92%). It should be noted that the majority of samples were collected from stranded specimens and therefore may not represent the distribution of free-ranging individuals due to the potential for carcasses to drift prior to stranding (e.g. Peltier *et al.* 2012). However, one biopsy sample was collected from an Arabian Sea lineage animal in the same bay as a biopsied holotype lineage animal in Dhofar, Oman (at the southernmost extreme of the Arabian Sea lineage's perceived range). Although this supports a range overlap, and potential secondary contact, these samples were collected at different times of the year, therefore it is still possible that temporal differences in distribution, or indeed differences in habitat use, are maintaining some level of isolation between the two groups. Evidence for introgression between the lineages (discussed below) is particularly indicative of secondary contact between the *T. aduncus* lineages in the northwest Indian Ocean.

Only *T. truncatus* samples were collected along Oman's Sea of Oman coast. This is not surprising given the narrow continental shelf and offshore habitat along this stretch of coastline (Minton *et al.* 2011). Indeed, *T. truncatus* appears to have been sampled along Oman's Arabian Sea coastline in areas where the continental shelf is narrow, for example near Hasik and on Masirah Island. Although *T. aduncus*-type dolphins are not represented off Oman's Sea of Oman coast in this study, they have been previously reported from this region (Baldwin *pers. comm.*). Since the majority of *T. aduncus* samples from the northern (Strait of Hormuz) and southern (Ras al Hadd, Arabian Sea) extremities of Oman's Sea of Oman coastline were a match for the holotype lineage, it seems likely that *T. aduncus* sighted off Oman's Sea of Oman coast would also be a match for this lineage.

Of the three samples collected in eastern Thailand, all were a match for the Australasian *T. aduncus* lineage (Wang *et al.* 1999b). This would suggest that the transition from the Arabian Sea lineage to the Australasian lineage may occur somewhere between east India and east Thailand, perhaps in the Bay of Bengal.

3.4.2 Demographic History in the Western Indian Ocean

A mechanism would have been necessary in the northwest Indian Ocean to facilitate divergence events within *T. aduncus* to form three lineages and prevent homogenisation between established lineages currently coming into secondary contact. The present study considered three hypotheses to explain the distribution and demographic history of populations in the northwest Indian Ocean in the context of such a mechanism. These were: (scenario 2) the presence of a persistent (Figure 27b) or (scenario 1) more recent (Figure 27a) barrier in the northern Indian Ocean or (scenario 3) a range contraction/re-expansion from the southern Indian Ocean (Figure 27c). These hypotheses were tested using ABC analysis (Figure 28).

Scenario 3 outperformed scenarios 1 and 2. However, while confidence intervals did not overlap between scenarios 1 and 3 the overlap was substantial for scenarios 2 and 3. Therefore, these scenarios (2 and 3) are both considered plausible demographic histories for populations in the western Indian Ocean. Scenario 3 differs from scenario 2 by allowing for a reduction in N_e in both ancestral populations (South Africa and India/Pakistan) and by reversing the order of demographic events such that populations are established in a northward direction. Due to the similar performance of scenarios 2 and 3, it is possible that the true demographic history of populations in the western Indian Ocean includes elements of both scenarios. Indeed, both scenarios include a reduced effective population size in the ancestor of the holotype lineage.

ABC has a number of limitations, for instance only a limited number of potential scenarios can be explored within the full hypothesis space, amongst others (see Templeton, 2009, but also see Beaumont *et al.* 2010). One key restriction with DIYabc is that it does not take migration into account (Cornuet *et al.* 2008). Therefore, contemporary asymmetric migration out of South Africa and Zanzibar (see below) could create a false impression that, for example, populations were established in a northern direction from southern Africa (*cf.* scenario 3, Figure 29).

As *T. aduncus* is a coastal species, it seems likely that individuals originally expanded into the western Indian Ocean from the Arabian Sea. Estimates of population divergence times in MDIV suggest the Arabian population diverged basally, followed by Zanzibar and then South Africa, suggesting the populations were established in a southerly direction (Table 23). Divergence estimates of humpback dolphin populations off South Africa, Mozambique, Tanzania and Oman display a similar divergence pattern (Mendez *et al.* 2011). Specifically, the most basal divergence was between Oman-Tanzania, followed by Tanzania-Mozambique and Mozambique-South Africa (Mendez *et al.* 2011).

Although positive and negative values were obtained for Tajima's D and Fu's F_s for different populations, no values were statistically significant and therefore provide no support for population expansion or contraction. However, mismatch analyses indicated significant expansion signals in various populations. I discuss the results here using expansion times estimated from a slow mutation rate, $\mu = 7 \times 10^{-8}$ substitutions per site per year (Harlin *et al.* 2003) and a fast mutation rate, $\mu = 5.0 \times 10^{-7}$ substitutions per site per year (Ho *et al.* 2007). South Africa (SA_S, SA_Bio) and northern Zanzibar populations showed expansion signals during an inter-glacial period ~ 79 -86 Ka or ~ 11 -12 Ka based on the lower and upper mutation rates, respectively. During these times the southwest monsoon was strong and associated productivity was relatively high (Anderson & Prell, 1993). The Indian-Pakistan population has the most recent expansion signal ~ 27 Ka (based on the Harlin *et al.* 2003 mutation rate) which roughly coincides with the last glacial maximum and associated reduction in strength of the southwest monsoon and intensification of the winter monsoon, increasing productivity in the northern Indian Ocean (Duplessy, 1982). The expansion signal based on the faster mutation rate Ho *et al.* (2007) suggests a more recent expansion in this population. The Australian population had an expansion signal ~ 100 Ka or ~ 14.5 Ka for the lower and upper mutation rates, respectively. The China-Thailand (CHI_THAI) and the *T. truncatus* populations (CHI_Tt and NWIO_Tt) showed expansion signals ~ 174 -205 Ka or ~ 24 -29 Ka for the lower and upper mutation rates, respectively. For the lower mutation rate (Harlin *et al.* 2003), these dates seem to coincide with high sea levels during inter-glacials (Rohling *et al.* 2014), perhaps suggestive of expansion into new areas. Dates estimated from the faster mutation rate (Ho *et al.* 2007) suggest expansion in these populations was occurring during a time that approximately coincides with the LGM. During this time, productivity was high in the Bay of Bengal and Andaman Sea due to an intensification of the northeast monsoon (Fon-

tugne & Duplessy, 1986; Almogi-Labin *et al.* 2000). Although the credible intervals for these dates remain high (see Table 22), it is interesting to compare them with lineage divergence dates inferred in Chapter 2 and Moura *et al.* (2013a). Dates estimated using fossil and biogeographic calibration times in Chapter 2 resulted in divergence estimates for the holotype lineage and other *T. aduncus* lineages ~342 Ka (95% HPD: 143, 630 Ka) and ~261 Ka (95% HPD: 111, 509) between the Australasian lineage and the new, Arabian Sea lineage. However due to inconsistencies between dates inferred utilising fossil and biogeographic calibration points (e.g. Ho *et al.* 2005) these recent divergence times are probably more accurate when based on the biogeographic calibration point alone, where the divergence between the Australasian and holotype lineages was estimated at 192 Ka (Moura *et al.* 2013a). All expansion times fall within 30 Ka, using the faster mutation rate (Ho *et al.* 2007), however expansion times are more consistent with lineage divergence times as inferred in Moura *et al.* (2013a) when the slower mutation rate is used (Harlin *et al.* 2003).

Results from microsatellite data using MsvAR appear to suggest that all *T. aduncus* populations in the region have been experiencing a long-term decline (see Table 18). However, because the credible intervals estimated for the parameters are large and overlapping, such interpretations remain inconclusive.

3.4.3 Population Structure

Analyses using inbreeding coefficients did not resolve the population differentiation within South Africa reported by Natoli *et al.* (2008a). F_{ST} values based on 14 microsatellite loci (*cf.* nine in Natoli *et al.* 2008a) were low and not statistically significant at $P = 0.05$ (after Bonferroni correction). The F_{ST} and Φ_{ST} values based on mtDNA were similar to those obtained for the same sequences in Natoli *et al.* (2008a) and were not significant between South African populations. Only a sub-set of samples from the Natoli *et al.* (2008a) dataset is considered here and it is possible that inclusion of further samples and/or loci would better resolve the distinction between these populations. Indeed, inclusion of a further two loci revealed significant differentiation between SA_Bio and SA_N ($P < 0.05$, after Bonferroni correction). However, further F -statistic comparisons amongst South African populations remained insignificant. On the other hand, an FCA plot did show a degree of separation between all three South African populations. The range of the migratory population (SA_Bio) is believed to seasonally overlap with that of the 'resident' population south of Ifafa (SA_S) as they follow

the annual sardine run, however they are not observed north of Ifafa where the northern population (SA_N) resides (Peddemors, 1999; Natoli *et al.* 2008a). Therefore, it is possible that SA_Bio individuals were being sampled as part of the SA_S population during the annual sardine run. This would reduce the differentiation signal observed between them. However, Natoli *et al.* (2008a) investigated this and found no indication of SA_Bio individuals amongst the SA_S samples, although they suggest that this could be due to a lack of resolving power (e.g. Latch *et al.* 2006). Additional samples and loci would be required to assess this fine-scale population subdivision off South Africa further.

Särnblad *et al.* (2011; *in review*) showed significant structure between the northern and southern populations off Zanzibar based on mtDNA (Särnblad *et al.* 2011) and small but significant structure based on seven microsatellite loci (Särnblad *et al.* *in review*). Similar results are reported for those populations here. Bayesian clustering analysis using more loci than Särnblad *et al.* (*in review*) did not detect this population structure (Figure 34). However, this is consistent with the expected limits of power for this method (e.g. see Latch *et al.* 2006). Support for differentiation between north and south Zanzibar is given by an FCA analysis (Figure 30b). It is worth noting that different sampling regimes were adopted in the north and south of Zanzibar whereby all samples in the north were from fisheries by-catch and the majority of those in the south were biopsy samples (see Särnblad *et al.* 2011). This bias seems unlikely to have influenced results presented here and those presented in Särnblad *et al.* (2011; *in review*).

While significant structure is observed between northern and southern Zanzibar based on mtDNA and autosomal DNA, the mtDNA differentiation is more evident. Särnblad *et al.* (*in review*), suggest that this incongruence is likely due to male mediated dispersal and female philopatry off Zanzibar. However, the effects of genetic drift on mtDNA are stronger compared to nuDNA because the mtDNA $N_e = \frac{1}{4}$ nuDNA N_e , and therefore one would expect mtDNA to exhibit an elevated differentiation signal. Results reported here generally accord with those in Särnblad *et al.* (*in review*), however no correction was made for the difference in N_e between the markers. Following Hedrick *et al.* (2013), the estimated ratio of male to female gene flow, m/mf between these populations = 7.41, suggestive of substantially more male-mediated gene-flow. Northern Zanzibar is also significantly differentiated from the Arabian and South African populations based on mtDNA, whereas southern Zanzibar is

not. This would suggest that southern Zanzibar is either more connected with these populations than it is to northern Zanzibar or that the southern Zanzibar population was more recently established. Alternatively, sampling effects may have led to a stochastic difference in the strength of the signal of differentiation.

Analyses conducted with the seven-microsatellite dataset and mtDNA revealed highly significant differentiation for all comparisons with the Indian/Pakistan population. This is further indicative of the phylogenetic placement of bottlenose dolphins in Pakistan/India as a separate lineage.

All pairwise mtDNA F_{ST} and Φ_{ST} comparisons outside the holotype *T. aduncus* lineage showed high significance ($P < 0.001$, Bonferroni correction applied) with the exception of the comparison between the *T. truncatus* populations in the northwest Indian Ocean and China, which did not have a significant Φ_{ST} value. These two populations are pelagic and as such reduced genetic structure might be expected given the higher dispersal and/or larger home ranges (gene flow) exhibited in pelagic forms of this species (Hoelzel *et al.* 1998; Quérouil *et al.* 2007).

Mendez *et al.* (2011) found similar patterns of population structure in humpback dolphins, *Sousa plumbea* in the western Indian Ocean. Dolphins often exhibit fine-scale population genetic structure in conjunction with habitat differentiation, which may be driven by resource polymorphisms and local adaptation in sympatry (Skúlason & Smith, 1995; Hoelzel, 1998a). Examples of this include, spinner dolphins, *Stenella longirostris*, in the Hawaiian Archipelago (Andrews *et al.* 2010), inshore bottlenose dolphins in eastern Australia (Ansmann *et al.* 2012) and common dolphins, *Delphinus delphis* in southeast Australia (Möller *et al.* 2011). Therefore, Mendez *et al.* (2011) set out to quantitatively investigate the relationship between humpback dolphin genetic structure and environmental heterogeneity across the western Indian Ocean. Using mtDNA control region sequences and remote sensing data, such as chlorophyll concentrations and sea surface temperatures, Mendez *et al.* (2011) tested for correlations between genetic and environmental differentiation in a similar fashion to testing for isolation by distance (Wright, 1943), although in this case; 'isolation by environmental distance' (IBED). Despite finding no evidence for IBED among humpback dolphin populations, Mendez *et al.* (2011) found a significant overlap in genetic and environmental structure.

Amongst other hypotheses, Mendez *et al.* (2011) suggest that the magnitude of environmental structure may not be as important as its presence in driving local adaptation and population differentiation. In particular, they identify a putative environmental break at $\sim 10^\circ$ S, where the South Equatorial Current meets the east African coastline and splits into the northbound East African Coastal Current and the southbound current into the Mozambique Channel. This environmental break is present throughout the year and may explain the population structure observed between South African/Mozambique and Tanzanian humpback dolphins (Mendez *et al.* 2011). The comparison of the humpback dolphin study (Mendez *et al.* 2011) with the present bottlenose dolphin study is particularly relevant as the populations sampled are from very similar locations and the patterns of genetic structure are much the same. Because bottlenose and humpback dolphin habitat overlaps (Wang & Yang, 2009), and mixed assemblages between these species are documented (e.g Saayman & Tayler, 1973, 1979; Corkeron, 1990; Stensland *et al.* 1998; *pers. obs.*), it is possible that bottlenose dolphin structure is similarly influenced by such environmental breaks and that the environmental heterogeneity in the region may be driving local adaptation in a similar way. At the same time, there are ecological differences between these species, for instance in Oman, humpback and bottlenose dolphin stomach contents overlap for only one prey species; the tigertooth croaker, *Otolithes ruber*, an important prey species for humpback dolphins but not for bottlenose dolphins (Ponnampalam *et al.* 2012). Such differences in targeted prey between the two dolphin species could drive local adaptation and population structure in alternative ways.

3.4.4 Migration Patterns, Identification of Migrants and Introgression

Estimates of contemporary migration patterns indicate asymmetric gene flow northwards between populations in the western Indian Ocean. This suggests that individuals moving out of South Africa and Zanzibar are migrating to populations further north. This bias has been similarly reported in humpback dolphins, where no southbound migration was detected between Oman and Tanzania or Tanzania and Mozambique (Mendez *et al.* 2011). This asymmetry is coincident with the northbound movement of the East African Coastal Current, which originates south of Tanzania (*cf.* Zanzibar) where the South Equatorial Current bisects as it meets the African coast. This current is seasonally intensified by the southwest monsoon to speeds exceeding 0.5 ms^{-1} (1.8 kmh^{-1}) when it becomes continuous with the Arabian coastline (Longhurst, 2006). Mendez *et al.* (2011) suggest this seasonal intensification of the East African Current may be enhancing the bias in northbound migration in humpback dolphins.

Indeed, from the results presented here, this could also be the case for bottlenose dolphins in the region. However, bottlenose dolphins move routinely against prevailing currents (e.g. Photopoulou *et al.* 2011) and move against the daily ebb and flood tides (Shane, 1980). However, there is some evidence to suggest large groups are more likely to move with the tidal currents (Irvine *et al.* 1981). Satellite telemetry of a rehabilitated bottlenose dolphin showed the individual to move both against and with the prevailing currents during long-distance movements (Wells *et al.* 1999).

Dolphin distributions are often associated with the distribution of foraging habitat and prey (Hastie *et al.* 2004; Torres *et al.* 2008), for example the *T. aduncus* population (SA_Bio) that follows the seasonal migration of sardines off South Africa (Peddemors, 1999) against the prevailing current (Darbyshire, 1964). A more credible explanation for the northward migration bias in bottlenose dolphin could be the adaptation of habitat-specific resource polymorphisms, such as foraging specialisations (Rosel *et al.* 2009), in northern populations. For example, distributions of groups of coastal bottlenose dolphins, *T. truncatus*, off Florida are restricted to habitats that provide the highest success given the foraging specializations adopted exclusively by the different groups (Torres & Read, 2009).

Contemporary migration patterns, however, may not reflect historic migration patterns. If currents are influencing the dispersal of dolphins in the region, as suggested by Mendez *et al.* (2011), then it is possible that migration may have been more symmetrical, or perhaps more favourable southwards, during glacial periods when the northbound currents were weaker due to a reduced southwest monsoon (Prell *et al.* 1980; Duplessy, 1982; Fontugne & Duplessy, 1986; Anderson & Prell, 1993; Almogi-Labin *et al.* 2000).

Estimation of individual ancestry and identification of migrants in STRUCTURE v. 2.3 (Pritchard, *et al.* 2000) revealed an absence of migrants between the holotype and Arabian Sea lineage (Chapter 2). However, based on mixed ancestry inference, there is evidence for a degree of admixture between populations in Oman and Pakistan/India, indicative of introgression between the holotype and Arabian Sea lineages, respectively. Furthermore, cross-referencing lineage assignment based on microsatellite loci with that based on mtDNA-haplotypes revealed that one Indian sample belonged to the Arabian Sea lineage according to microsatellite loci ($P = 98.9\%$) but was a match for the holotype lineage based on mtDNA control region sequence. Additional sampling and use of more genetic markers will help

elucidate the extent of hybridisation/introgression between these lineages. Migrants from Oman were also identified in the South Africa and Zanzibar populations, suggesting that even though migration is biased northwards, southbound migration does occur between populations in the western Indian Ocean.

3.4.5 Consideration for an Isolating Mechanism in the Northwest Indian Ocean

As explained above, the *T. aduncus* holotype lineage likely expanded into the western Indian Ocean from the north, following the Indian Ocean coastline. Indeed, population divergence estimates in MDIV, suggest the Arabian population diverged with Zanzibar first, and then Zanzibar with South Africa. However, from the DIYabc analyses there is support for this and for a South African ancestry in the contemporary populations off east Africa and Arabia. Upon establishment of the holotype lineage, currently represented by populations in the western Indian Ocean, there must have been a mechanism preventing homogenisation with the lineage that is ancestral to the Arabian Sea and Australasian lineages that diverged ~261 Ka (see Chapter 2). The present distribution of lineages in the northwest Indian Ocean suggests the isolating mechanism may still be present east of the Strait of Hormuz because the transition between the lineages occurs over a relatively short distance, even though there is an overlap in range. DIYabc analyses provide some support for recent secondary contact (~10.5 Ka) between these lineages after a historic separation (~132 Ka) (scenario 3).

During glacial periods, the intensity of the southwest monsoon would have been reduced, causing a decrease in upwelling and productivity in the northern Indian Ocean. At the same time, however, productivity would have increased in the Bay of Bengal and Andaman Sea due to the intensification of the northeast monsoon (Fontugne & Duplessy, 1986; Almogi-Labin *et al.* 2000). It is conceivable that this disruption of the southwest monsoon and the reduction in productivity was enough to reduce the genetic exchange between the holotype and Arabian Sea lineages due to a contraction in habitat (scenario 3). It is also conceivable that the isolating mechanism that now exists between these lineages is an ecological one, whereby dolphins in the western and northern Indian Ocean have adapted to a particular locality. Indeed, significant differences in cranial morphology are present between the lineages, which may be suggestive of adaptation to different prey compositions (see Chapter 2 and 4).

Other cetaceans in the northwest/northern Indian Ocean show similar patterns in their population structure and biogeography. Arabian Sea humpback whales, *Megaptera novaeangliae*,

are a genetically isolated, non-migratory population restricted to the region (Minton *et al.* 2011, Pomilla *et al.* 2014). Based on historic records of illegal whaling, this population has also been recorded off Oman and Pakistan (Mikhalev, 1997). Although the arrival of humpback whales to the northwest Indian Ocean from the southern hemisphere is relatively recent, ~70 Ka (Pomilla *et al.* 2014), their presence is an interesting example of how the environmental conditions in the northwest Indian Ocean, likely associated with the high productivity of the region, provide opportunities for a variety of cetacean species to adapt to local conditions. In common dolphins there is an overlap in the western Indian Ocean between long beaked, *D. delphis*, and Indo-Pacific common dolphins, *D. capensis tropicalis* (Jefferson & Van Waerebeek, 2002; Amaral *et al.* 2012a). Based on morphometric analyses, there appears to be clinal variation in morphology between the two taxonomic units, with the *D. c. tropicalis* long beaked morphology being the most prominent off India and less so east towards Japan or west towards the Arabian Peninsula (Jefferson & Van Waerebeek, 2002).

In a comprehensive assessment on the taxonomy of humpback dolphins using morphological and genetic data, there was an indication of a similar transitional zone from *S. plumbea* to *S. chinensis* in the northern Indian Ocean where they are sympatric from the central eastern Indian Ocean to at least Myanmar (Mendez *et al.* 2013). Interestingly, Mendez *et al.* (2013) suggest the potential presence of a further assemblage of humpback dolphins off Thailand-Bangladesh based on preliminary molecular analyses. Speculatively, if bottlenose dolphin divergence dates are indeed coinciding with reductions in sea level during glacial periods (see Chapter 2), then a further lineage may exist in this locality; the result of a glacial period as yet unaccounted for in the phylogeographic analyses e.g. the LGM or Eemian. The region appears to be a convergence zone for several intra-genus taxonomic units of dolphin, such as *S. plumbea* and *S. chinensis*, as well as harbouring unique lineages adapted to local environmental conditions, such as the non-migratory humpback whale and *D. c. tropicalis*. Therefore, conditions in the northern/northwest Indian Ocean appear to be important for a variety of cetacean species.

3.4.6 Implications for Management, Taxonomy and Future Research

The results presented here indicate significant population structure exists in *T. aduncus* along the western Indian Ocean coastline. Recognition of this will be important in establishing units for conservation management in the region (see Punt & Donovan, 2007). Considera-

tion must be given for three populations in the western Indian Ocean (i) a South African population (for which there is evidence for three sub-populations, *cf.* Natoli *et al.* 2008a), (ii) a Zanzibar population (which likely consists of two sub-populations; *cf.* Särnblad *et al.* 2011; *in review*) and (iii) an Arabian population. Furthermore the results support the presence of a fourth population, and new Arabian Sea lineage, in the northern Indian Ocean. According to the ABC analysis, the effective population size off South Africa is relatively low, ~4,400 individuals (95% HPD: 1580, 9100), compared to populations off Arabia, Zanzibar and India/Pakistan (see Table 24). A low population size will have management implications, particularly as the South African population has evidence for sub-structure and is at risk from by-catch from shark nets (see Natoli *et al.* 2008).

Further work should include samples from areas across the Indian Ocean that are underrepresented, or not represented, in this study. Specifically, populations along the east African coast and off the Arabian Peninsula could exhibit further population structure. Further sampling in the northern and northeast Arabian Sea, Bay of Bengal and Andaman Sea would also be valuable for discovering the transitional zone between the Arabian Sea lineage and the Australasian lineage and establish the mechanism of reproductive isolation between them. A good understanding of population identity and structure in the region will be important for regional conservation initiatives. Indeed current initiatives are lacking (Ponnampalam, 2009) and there is a need to conserve these populations currently under threat from anthropogenic activities, particularly habitat degradation and fisheries activities (IWC, 1999).

Future work should endeavour to investigate the mechanisms that drive or maintain reproductive isolation between lineages of *T. aduncus* after divergence. Assessment of local adaptation through utilisation of next generation sequencing techniques in conjunction with continued field-based work on aspects of ecology, behaviour, morphology and life-history will further our understanding of the evolutionary processes driving local adaptation and maintaining differentiation between closely related sympatric lineages.

Chapter 4

Comparative Cranial Morphology of Three Bottlenose Dolphin Lineages (*Tursiops* spp.) in the Northwest Indian Ocean Utilising Traditional and Geometric Morphometric Techniques

4.1 Introduction

The conservation status of many cetacean species remains unresolved (Reeves *et al.* 2004). This is particularly the case in the northwest Indian Ocean where taxonomic studies have been limited. Within the Delphinidae, the taxonomy of bottlenose dolphins, *Tursiops* spp. is particularly confused, despite extensive research over the last few decades (Mead & Potter 1990; Ross & Cockcroft, 1990; Hoelzel *et al.* 1998; Wang *et al.* 1999b; Möller & Beheregaray, 2001, Natoli *et al.* 2004, Charlton-Robb *et al.* 2011; Moura *et al.* 2013a). Due to the high levels of morphological variation observed within the genus, previous literature describes over 20 putative species (Hershkovitz, 1966). However, most of these descriptions were based on limited data and many species were later considered synonymous with the common bottlenose dolphin, *T. truncatus* (Rice, 1998). One species that retained its nominal species status was the, now recognised, Indo-Pacific bottlenose dolphin *T. aduncus*, which was shown, in South Africa, to be morphologically distinct from *T. truncatus* based on rostrum length, body size and ventral spotting (Ross, 1977).

Evidence for the case of a separate species based on pelagic and coastal morphological variations remained controversial (Ross & Cockcroft, 1990) and many authors only recognised the single species *T. truncatus*, with only the coastal *T. aduncus*-type as a potential subspecies (Walker, 1981; Ross & Cockcroft, 1990; Mead & Potter, 1995). A study on the phylogenetic relationships within the family Delphinidae, conducted by LeDuc *et al.* (1999) using entire sequences of the mitochondrial DNA (mtDNA) gene, cytochrome-*b*, indicated a need to revise the species classification system within the family. The study suggests that *Tursiops* is an unresolved, polyphyletic, assemblage, whereby the nominal *T. aduncus* is more closely related to *Stenella* and *Delphinus* species, than to *T. truncatus*. This is in accordance with Curry

(1997) who found a similar distinction between *T. truncatus* and *T. aduncus* haplotypes using sequences from the mtDNA control region (LeDuc *et al.* 1999). Furthermore, morphological similarities between the genus *Tursiops*, particularly what was then referred to as the *T. aduncus* 'morphotype' (i.e. contemporary *T. aduncus*), and *Stenella* spp. had been noted previously elsewhere (see, Perrin *et al.* 1987). Genetic studies conducted by Wang *et al.* (1999b), on *T. truncatus* and *T. aduncus* morphotypes living in sympatry off China, revealed the two to be reciprocally monophyletic at the mtDNA control region, thus providing further evidence for two distinct species.

The species *T. aduncus* has been documented from inshore/coastal waters throughout the Indo-Pacific. While the distribution of this species is still not wholly understood (Wang & Yang, 2009), it has been reported off the east coast of Africa, the Red Sea and the Persian/Arabian Gulf, the Gulf of Aden, off the Arabian peninsula, and eastwards off the coasts of Iran, Pakistan, India, as far as Taiwan, and south off the coast of Australia (Pilleri & Gahr, 1972, Lal Mohan, 1982; Baldwin *et al.* 1999; Kemper, 2004; Preen, 2004; Jayasankar *et al.* 2008; Wang & Yang, 2009; Braulik *et al.* 2010; Minton *et al.* 2010). All coastal/inshore populations outside of the Indo-Pacific are classified as *T. truncatus*, as are all offshore variants, including those in the Indo-Pacific (Wells & Scott, 2009). In the northern Atlantic Ocean *T. truncatus* has been recorded as far north as Nova Scotia in the west, and off the coast of Norway and Iceland in the east (Wells & Scott, 1999). Its range also extends into the Mediterranean Sea and Black Sea, where the subspecies *T. truncatus ponticus* is recognised (Viaud-Martinez *et al.* 2008). In the North Pacific, *T. truncatus* are seen off California in the east and the Okhotsk Sea in the west. The southern limit of their range extends as far south as Tierra del Fuego, South Africa, Australia and New Zealand (Wells & Scott, 2009).

In a worldwide comparison of *Tursiops* populations, based on mtDNA control region sequences and microsatellite markers, Natoli *et al.* (2004) found considerable genetic diversity and differentiation among all populations studied. Results supported the designation of *T. aduncus*, as put forward by Wang *et al.* (1999b), as a species distinct from *T. truncatus*. Furthermore, results revealed the presence of another distinct lineage of *T. aduncus* from South Africa, thus suggesting a third putative species within the *Tursiops* genus. The species *T. aduncus* was originally described from a stranded individual seen during the Hemprich and Ehrenberg expedition in 1825 on 'Insel Belhossa', currently an un-named island off Eritrea

in the Red Sea at 15°20' N, 40° 40' E. This holotype specimen was believed to have been lost until it was rediscovered in the collections at the Zoologisches Museum Berlin, Humboldt Universität zu Berlin Museum für Naturkunde by Peter van Bree in 1978 (Perrin *et al.* 2007). Perrin *et al.* (2007) sequenced 399 bp of the mtDNA control region from the specimen and found it to be identical to those off South Africa. Therefore, the South African *aduncus*-form, as put forward by Natoli *et al.* (2004), should retain the name *T. aduncus* and it is the Chinese form, put forward by Wang *et al.* (1999b), which should be reclassified. A recent genetic and morphological study on southeast Australian bottlenose dolphins has put forwards the case for another species within the *Tursiops* genus, the Burrunan dolphin, *T. australis* (Charlton-Robb *et al.* 2011).

Observations of *Tursiops* populations in the northwest Indian Ocean suggest they are common in Arabian waters (Baldwin *et al.* 1999; Minton *et al.* 2010). Both *T. truncatus* and *T. aduncus* are thought to occur in parapatry or sympatry (Minton *et al.* 2010). Observations of cetaceans seen during live-capture operations for the Tel Aviv Dolphinarium in the Gulf of Suez and Gulf of Aquaba in the early 1980s revealed two types of bottlenose dolphin to inhabit the waters off the Sinai Peninsula (Beadon, 1991)

“Two types of bottlenose dolphin, [recognised then as] *Tursiops truncatus*, were seen and caught. One was small (to no more than about 2.2 m) and relatively slender, with a gentle slope from the melon onto a relatively elongated snout. They were pale grey on the back and sides, lighter on the ventrum, and frequently had spotting, particularly on the throat.... The second type of bottlenose dolphin was large (4 m or more) and robust with a comparatively steeper melon, shorter, broader snout, and apparent lack of ventral spotting.”

[Beadon, 1991]

These descriptions of bottlenose dolphins from the Red Sea suggest that both *T. truncatus* and *T. aduncus* occur in sympatry or parapatry in these waters. However, the sizes of *T. truncatus* reported in Beadon, (1991) are exceptionally large (> 4 m). Lengths of *T. truncatus* are more generally reported between 2.5 - 3.8 m (Wells & Scott, 2009). Further investigation of *Tursiops* in the Red Sea is evidently needed. Dolphins resembling larger *T. truncatus* (in excess

of 3 m) have occasionally been reported in deep waters off Oman (Minton *et al.* 2010; *pers. obs.*). However, sightings of *T. truncatus*-types that resemble pelagic variants in other parts of the world are more the norm from Oman (Minton *et al.* 2010; *pers. obs.*) and elsewhere in the region, such as Pakistan (Gore *et al.* 2012) and India (Jayasankar *et al.* 2008). Bottlenose dolphins biopsied in the western Indian Ocean by Ballance & Pitman (1998) were genetically identified as *T. truncatus* (Curry, 1997; Ballance & Pitman, 1998).

Dolphins resembling *T. aduncus* have been observed in shallow, coastal regions of the Arabian Sea (Salm *et al.* 1993; Baldwin *et al.* 1999; Minton *et al.* 2010), the Arabian Gulf (Al-Robbae, 1974; Gallagher, 1991; Preen, 2004) and the northern coastline of the Sea of Oman, off Oman's Musundam enclave (*unpublished data; pers. obs.*), Iran (Braulik *et al.* 2010), Pakistan (Gore *et al.* 2012) and India (Jayasankar *et al.* 2008). Along the southern coastline of the Sea of Oman, off Oman's Al-Batinah region and Muscat Capital area, individuals resembling *T. aduncus* appear to be absent (Minton *et al.* 2010). However, before ~2000, small groups of *T. aduncus* were regularly reported near sheltered bays around Bandar al-Khayran and Qurum off Muscat and off the Daymaniyat Islands off the Al Batinah coastline (Baldwin *pers. comm.*). Occasionally, there are still reports of bottlenose dolphins resembling *T. aduncus* from these areas but sightings have certainly diminished. It is conceivable that this disappearance, or decrease in sightings, coincides with the increase in anthropogenic activities seen around the capital over the last 30 - 40 yrs, including coastal development, shipping, recreational boat traffic, dolphin watching, and fisheries activities. Interestingly, the humpback dolphin, *Sousa plumbea*, another dolphin species reportedly widespread across the nearshore/coastal areas of the region, also appears to be absent from the Al-Batinah and Muscat capital area (Salm *et al.* 1993; Baldwin & Salm, 1994; Baldwin *et al.* 1999).

In a genetic study on the population structure of *T. aduncus* in the western Indian Ocean; samples from Zanzibar, Mayotte and Oman were a match for the *T. aduncus* holotype based on partial sequences of the mtDNA control region (Särnblad *et al. in review*). One partial sequence of the mtDNA control region belonging to an individual from Iran, deposited on GenBank by Mohsenian *et al. (unpublished sequence)* Ascension No. JQ934964, was also a match for the holotype *T. aduncus* (see Chapter 3). In India, Jayasankar *et al.* (2008) identified bottlenose dolphin individuals to be *T. aduncus* based on partial mtDNA cytochrome-*b* sequences. Across four individuals, two haplotypes were identified, one of which was a match

for a Japanese individual published by Shirakihara *et al.* (2003). These genetic studies suggest that the range of the *T. aduncus* holotype extends northwards from South Africa to at least Iran (but see Chapter 2). The Indian *aduncus*-type individual that was a match for a Japanese individual suggests the Indian peninsula might be a transitional zone between, the *T. aduncus* holotype lineage (Natoli *et al.* 2004) and the Chinese/Australasian *T. aduncus* (Wang *et al.* 1999b).

However, phylogeographic analysis of *Tursiops* spp. in the northwest Indian Ocean, presented in Chapter 2, reveals the presence of a new *T. aduncus* lineage off Oman, Pakistan and India. Concordance between morphology and the phylogenetic conclusions reported in Chapter 2 would provide strong support for the new *T. aduncus* lineage (see Reeves *et al.* 2004). Hereafter, this lineage is referred to as the Arabian Sea *T. aduncus*.

Several studies and reviews have incorporated the use of morphometric data from small cetacean skeletal remains from the region, predominantly the Sultanate of Oman. Cetaceans examined have included humpback dolphins (Baldwin *et al.* 2004; Jefferson & Van Waerebeek, 2004) spinner dolphins, *Stenella longirostris*, rough toothed dolphins, *Steno bredanensis*, melon-headed whales, *Peponocephala electra* (Van Waerebeek *et al.* 1999) and common dolphins, *Delphinus* spp. (Jefferson & Van Waerebeek, 2002). Reviews of small cetaceans in the region can be found in Leatherwood, (1986), de Silva, (1987) and Baldwin *et al.* (1999).

As the coastlines develop in the northwest Indian Ocean, fisheries activities, areas of construction, shipping and oil exploration continue to overlap with identified habitat for many small cetacean species (IWC, 1999; Collins *et al.* 2002; Anderson, 2014). The effective conservation and management of impacted populations will depend on an understanding of species taxonomy, as well as their distributions and conservation status. Here, I utilise traditional and geometric morphometric techniques to explore the morphological relationships between three putative bottlenose dolphin species in the region: i) *T. aduncus* holotype, ii) *T. aduncus*, Arabian Sea lineage iii) *T. truncatus*. Furthermore, congruence, between conclusions drawn from the morphological data and the available phylogenetic data (presented in Chapter 2), is examined. Such information will be important in taxonomic level classification (Reeves *et al.* 2004), which will be important for effective conservation and management (Mace, 2004) of coastal cetaceans in the region.

4.2 Materials and Methods

4.2.1 Specimen Acquisition

Bottlenose dolphin (*Tursiops* spp.) specimens, collected along Oman's coast, were curated at the Oman Natural History Museum (ONHM) and specimens collected in Pakistan and Iran were curated at the Museum am Löwentor, Staatliches Museum für Naturkunde, in Stuttgart, Germany (SMNS). All of the ONHM specimens were beach-cast individuals, the skeletal remains of which were collected on various survey expeditions across Oman, predominantly led by the Oman Whale and Dolphin Research Group (OWDRG) from 2000 to present. Before the millennium, M. Gallagher pioneered the collection of whale and dolphin skeletal material in Oman. Field biologists R. Salm and V. Papastavrou also made further contributions in the late 1980s. A small amount of the skeletal material was collected opportunistically by members of the public who either deposited the material directly to ONHM or indirectly, through OWDRG. Specimens curated at the SMNS were collected in Pakistan around the Indus River Delta and the Strait of Hormuz, Iran on expeditions by G. Pilleri & M. Gühr (1973-1974), (Pilleri, 1974) (see Figure 41).

4.2.2 Lineage Assignment

Specimens were assigned *a priori* to one of three groups based on their position within a neighbour-joining phylogenetic tree; these were (i) holotype *T. aduncus* (Hol-Ta), (ii) new, Arabian Sea *T. aduncus* (AS-Ta), and (iii) *Tursiops truncatus* (Tt).

DNA was extracted from bone (refer to Chapter 3 for protocol). Specimens were included in the phylogenetic analysis if a 404 bp fragment of the mtDNA control region was amplifiable in a PCR reaction. Amplifications were performed in a 20 µl final reaction volume containing ~1.0 µl of template DNA, 1.25U of GoTaq Flexi DNA polymerase, 10x buffer (Promega), 0.2 mM dNTP, 3 mM MgCl₂ and 0.2 µM of each primer; TRO (L15812) 5' CCT CCC TAA GAC TCA AGG AAG 3' (developed at the Southwest Fisheries Science Centre, see Zerbini *et al.* 2007) and D (H16498) 5' CCT GAA GTA AGA ACC AGA TG 3' (Rosel *et al.* 1994). The PCR profile included initial heating at 95°C for 2 min, followed by 40 cycles of 95°C for 40 sec, annealing temperature of 60°C for 40 sec and 72°C for 1 min, and a final 72°C extension for 10 min. PCR products were purified with QIAGEN PCR purification columns (Qiagen, GmbH, Germany) and sequenced using an ABI automated sequencer.

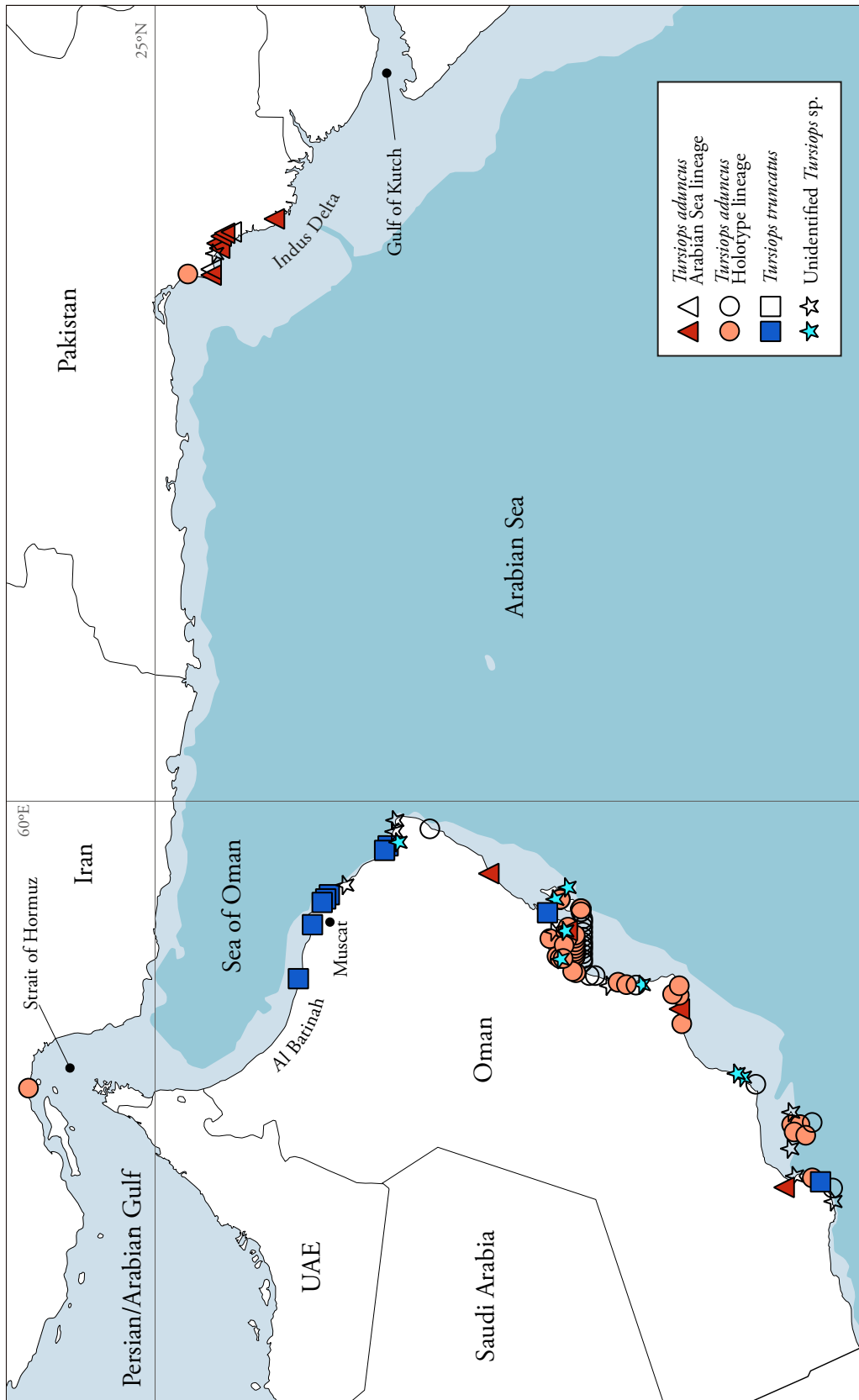


Figure 41: Map showing locations of bottlenose dolphin specimens. Shaded shapes are those specimens that were used in exploratory analyses. All other shapes (not-shaded) represent specimens omitted from analyses. Specimens were omitted where they did not meet the criteria required for analyses e.g. were cranially immature or too damaged. The 200m isobath is shown.

In total, sequences from 73 specimens were utilised in the phylogenetic analysis. Alignment was performed using the MUSCLE algorithm (Edgar, 2004) as implemented in GENEIOUS v. 7.1.2 (<http://www.geneious.com>, Kearse *et al.* 2012). Also included were 10 sequences of *T. aduncus* from Australasia, available on GenBank (Accession No.s: AF049100, AF056233-36, 39-43) and three sequences of *T. aduncus* from Thailand (see Chapter 3). One sequence of *S. chinensis* (Accession No.: DQ665785) was included as an outgroup. A 50% majority-rule consensus neighbour-joining phylogeny was generated over 1,000 bootstrap replicates in GENEIOUS v. 7.1.2 (<http://www.geneious.com>, Kearse *et al.* 2012) using a Tamura-Nei genetic distance model, as identified using JMODELTEST v. 2.1.6 (Darriba *et al.* 2012).

4.2.3 Assessment of Maturity

To eliminate variability associated with development, only specimens that were considered adult were included in morphometric analyses, (Perrin & Heyning, 1993). Where present, the degree of ankylosis of thoracic vertebrae was used to determine the physical maturity of a specimen to infer age (Ross & Cockcroft, 1990; Perrin & Heyning, 1993; Galatius & Kinze, 2003). Another valuable criteria for assessing age is sexual maturity (Ross & Cockcroft, 1990). Unfortunately, this information was not available for any of the museum specimens. Where post-cranial bones were absent, cranial maturity was used to infer age. Specimens were considered cranially mature if the maxillary plates were fused to the cranium (Ross & Cockcroft, 1990; Kemper 2005).

4.2.4 Traditional (Linear) Morphometric Analyses

A total of 91 skulls, identified as bottlenose dolphins (*Tursiops* spp.), were measured, including 80 from the ONHM collection and 11 from the SMNS collection. A list of specimens examined is given in Appendix VIII. Vernier and dial calipers were used to measure 40 cranial characters for the ONHM specimens and 36 characters for the SMNS specimens (see Table 25). Four meristic characters (tooth counts) were also quantified in each case but were later reduced to two (see below). The majority of characters measured are illustrated in Figure 42.

Table 25: Descriptions of measured cranial characters and whether they were measured for ONHM and SMNS specimens.

Character	Description	Source	ONHM	SMNS
BL	Greatest length of bulla of left tympanoperiotic	Perrin (1975)	Y	Y
BW	Greatest width of bulla of left tympanoperiotic	Perrin (1975)	Y	Y
POL	Greatest length of periotic of left tympanoperiotic	Perrin (1975)	Y	Y
TPC	Tip of rostrum to the apex of the premaxillary convexity	Wang <i>et al.</i> (2000)	Y	Y
CBL	Condylbasal length, from tip of rostrum to hindmost margin of occipital condyles	Perrin (1975)	Y	Y
RL	Rostrum length, from tip to line across hindmost limits of antorbital notches	Perrin (1975)	Y	Y
TREN	Tip of rostrum to external nares, to mesial end of anterior transverse margin of right naris	Perrin (1975)	Y	Y
DFWN	Dorsal frontal width at nasals	Kemper (2004)	Y	Y
DFWM	Dorsal frontal width at maxilla	Kemper (2004)	Y	Y
GWEN	Greatest width of external nares	Perrin (1975)	Y	Y
GWPX	Greatest width of premaxillaries	Perrin (1975)	Y	Y
PRW	Width of premaxillaries at mid-rostral length	Perrin (1975)	Y	Y
LWPTF	Least width between posterior borders of temporal fossa	Kemper (2004)	Y	Y
GLPT	Greatest length of left pterygoid	Perrin (1975)	Y	Y
PL	Palatine length, from anteriormost apex of left pterygoid to base of palate	This Study	Y	Y
PWPT	Palate width at apices of pterygoids	Van Waerebeek <i>et al.</i> (1990)	Y	N
WAS	Width of alisphenoid at suture with basisphenoid	Wang <i>et al.</i> (2000)	Y	Y
GPOW	Greatest postorbital width	Perrin (1975)	Y	Y
GPRW	Greatest preorbital width	Perrin (1975)	Y	Y
ZW	Greatest width across zygomatic process of squamosal	Perrin (1975)	Y	Y
GWIN	Greatest width of internal nares	Perrin (1975)	Y	Y
VW	Vomer width (as illustrated in Kemper, 2004)	Kemper (2004)	Y	Y
RWB _{perrin}	Rostrum width of rostrum at base, along line across hindmost limits of antorbital notches	Perrin (1975)	Y	N
RWB _{min}	Minimal width of rostrum at base, points either side of the maxillaries	This Study	Y	Y
RWM	Rostrum width at mid-length	Perrin (1975)	Y	Y

Character	Description	Source	ONHM	SMNS
RW75%	Rostrum width at 3/4 length as measured from posterior end (base)	Perrin (1975)	Y	Y
RW60	Rostrum width at 60mm anterior to line across hindmost limits of antorbital notches	Perrin (1975)	Y	Y
TRIN	Tip of rostrum to internal nares (to mesial end of posterior margin of right pterygoid)	Perrin (1975)	Y	Y
UTLTR	Length of upper left tooth row, from hindmost margin of hindmost alveolus to tip of rostrum	Perrin (1975)	Y	Y
GLPTF	Greatest length of left posttemporal fossa, measured to external margin of raised suture	Perrin (1975)	Y	Y
GWPTF	Greatest width of left posttemporal fossa, at right angles to greatest width	Perrin (1975)	Y	Y
LO	Length of left orbit - from apex of preorbital process of frontal apex of orbital process	Perrin (1975)	Y	Y
LAL	Length of antorbital process of left lacrimal	Perrin (1975)	Y	Y
GPARW	Greatest parietal width, within posttemporal fossae	Perrin (1975)	Y	Y
MXOC	Maximum span of occipital condyles	Baldwin <i>et al.</i> (2004)	Y	N
BCH	Vertical external height of braincase from midline of basisphenoid to summit of supraoccipital crest, but not including supraoccipital crest	Perrin (1975)	Y	N
LTRL	Length of lower left tooth row - from hindmost margin of hindmost alveolus to tip of mandible	Perrin (1975)	Y	Y
ML	Greatest length of left ramus	Perrin (1975)	Y	Y
MFL	Length of mandibular fossa, measured to mesial rim of internal surface of condyle	Perrin (1975)	Y	Y
MH	Greatest height of left ramus at right angles to greatest length	Perrin (1975)	Y	Y
MSL	Mandibular symphysis length	Kemper (2004)	Y	Y
TTL	Greatest lower tooth/alveolar count	Perrin (1975)	Y	Y
TTU	Greatest upper tooth/alveolar count	Perrin (1975)	Y	Y
TWTMJ	Transversal width of teeth at mid-jaw (1mm below gum-line)	Baldwin <i>et al.</i> (2004)	Y	Y
MAJDTF	Major diameter of anterior left temporal fossa	Kemper (2004)	N	Y

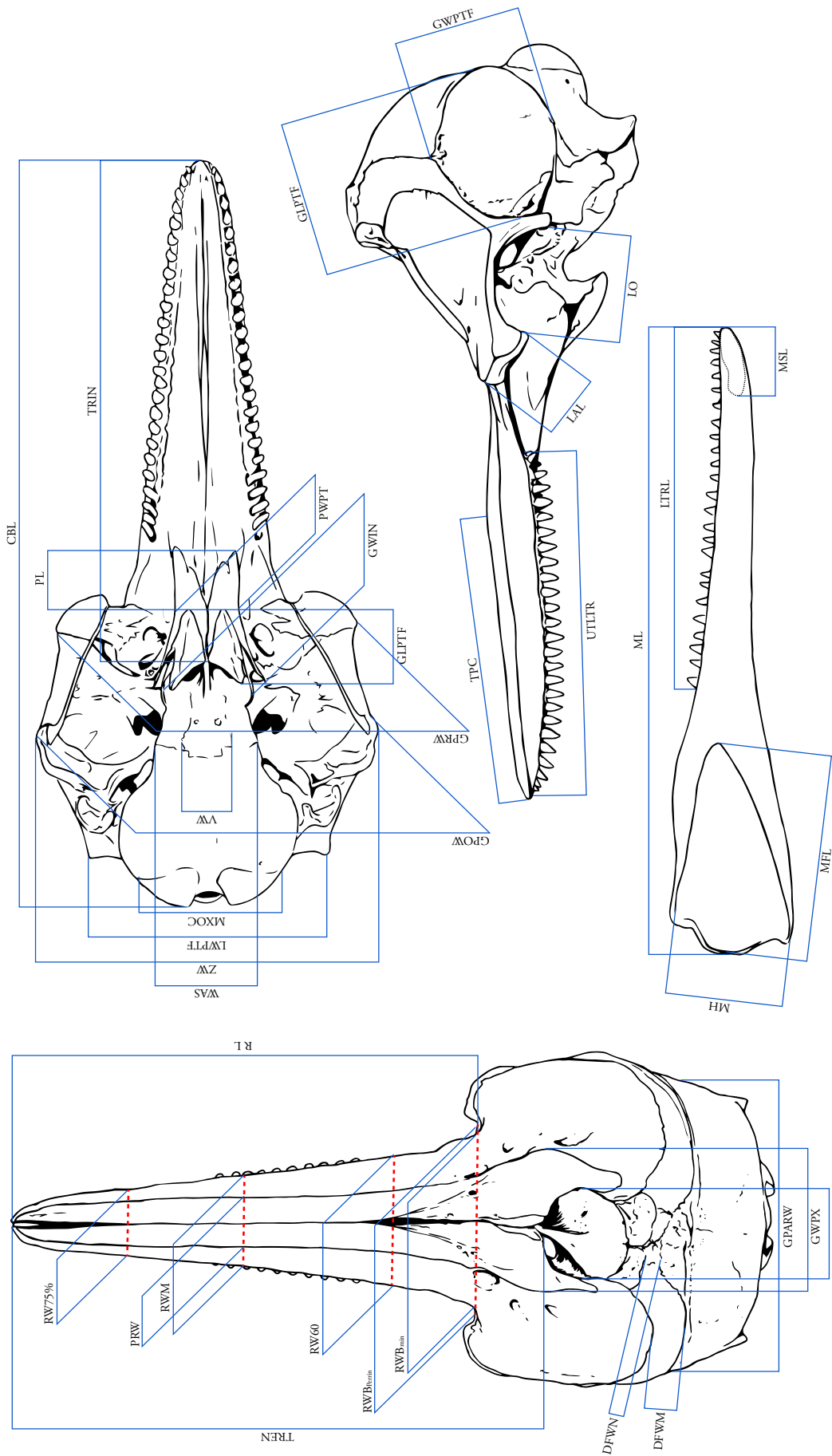


Figure 42: Morphological measurements taken. As adapted from Perrin (1975). BL, BW, POL, TTL, TTUTWTMJ, MAJDTF and BCH not illustrated.

Measurements up to 150 mm were taken to the nearest 0.02 mm. Measurements from 150 mm to 300 mm were taken to the nearest 0.05 mm. All measurements greater than 300 mm were taken to the nearest millimeter. Measurements were not attempted where characters were damaged, thus resulting in missing data. Measurements from the tip of the rostrum to the apex of premaxillary convexity (TPC), as described in Wang *et al.* (2000), were performed in retrospect from photographs, taken in lateral-left aspect, imported into TpsDIG v. 2.05 (Rohlf, 2005). Photos were scaled using CBL measurements for each individual. Where CBL measurements were not available (due to damage) an alternative measurement was used, such as LO. A *t*-test was performed in EXCEL (Microsoft Inc.) to compare photograph measurements with caliper measurements that were available for a sub-set of specimens ($n = 12$). No significant difference ($P = 0.34$) was detected between the methodologies, thus allowing measurements of TPC from photographs to be incorporated into analyses. Specimens were assigned single upper (TTU) and lower (TTL) tooth counts using the highest counts for each side (Amaha, 1994; Jefferson & Van Waerebeek, 2002).

To investigate intra-observer error, all measurements were taken in triplicate for both SMNS and ONHM Datasets. Repeat measurements were taken 'blindly', i.e. without prior knowledge of previous measurements taken. Several days often elapsed between successive rounds of measuring to limit bias. It was assumed that cranial characters measured with a percentage error of $> 1\%$ across repeats were measured unreliably, and therefore omitted from analyses.

Although the author measured all of the specimens, SMNS measurements were taken prior to a measuring calibration exercise with another marine mammal taxonomist (Dr. K. Van Waerebeek), thus effectively introducing inter-observer bias between the SMNS and ONHM Datasets. Therefore, differences between prior- and post-calibration measurements were explored before pooling cranial character measurements shared by the ONHM and SMNS Datasets ($n = 27$) in a combined analysis. Twelve specimens curated at the ONHM were measured prior- and post-calibration so that such comparisons could be made. The means of cranial measurements prior- and post-calibration were compared using *t*-tests in EXCEL (Microsoft Inc.).

Several studies have documented sexual dimorphism in bottlenose dolphins. Tolley *et al.* (1995) found that *T. truncatus* males off Florida were significantly larger than females in

20 out of 29 external measurements. However, only one of eight head measurements (rostral girth) exhibited sexual dimorphism. Hersh *et al.* (1990) found similar dimorphism in body measurements of dolphins from the same region, however, only two cranial characters (GPRW and LO) out of 28 exhibited minor dimorphism across 69 skulls. Kemper (2004), found no significant sexual dimorphism using 30 cranial characters across 65 *Tursiops* spp. skulls off South Australia. Wang *et al.* (2000) also found no evidence of sexual dimorphism using cranial measurements in *Tursiops* spp. in Chinese waters. Similarly, Ross (1977) found no evidence for sexual dimorphism in osteological characters in both *T. aduncus* and *T. truncatus*-type dolphins off South Africa. From these studies it would appear that the majority of dimorphism in bottlenose dolphins is exhibited in the external morphology and only minor dimorphism, at most, is observed in the cranium. Therefore, given the limited information available for museum specimens on gender, and the difficulties associated with DNA-based sexing (Bérubè & Palsbøll, 1996) of museum specimens due to DNA degradation (Pääbo, 1989), sexual dimorphism was not considered here. Sex bias is also not considered.

4.2.4.1 Data Analysis

Tooth counts were analysed separately because they are categorical and independent of size and maturity. Lower tooth counts (TTL) were omitted from analyses as the majority of specimens were missing this data due to missing mandibles. A *k*-means cluster analysis (see below) was applied to upper tooth counts (TTU).

Because multivariate analyses are sensitive to missing data (Kim & Curry, 1977), characters missing measurements for more than 20% of the cranially mature specimens were removed. Any specimens with more than 30% missing data for the remaining characters were also removed from analyses. This was done in order to minimise the number of specimens with missing data, thereby limiting error introduced through value substitution (see Brown *et al.* 2012), while maximising statistical power. The mean value of available data was substituted for remaining missing data (e.g. Jefferson & Van Waerebeek, 2002). Data were scaled and centred using the *scale* function in the *base* package implemented in R v. 3 (R Core Team, 2013).

The AS-Ta lineage was better represented in the Combined Dataset than in the ONHM Dataset. Truncation of character variables was required from the ONHM specimens (and to

a lesser degree the SMNS specimens) when pooling data into the Combined Dataset in order to eliminate bias associated with measurements taken prior and post-calibration. Similar analyses were performed on the ONHM and Combined-Datasets.

4.2.4.2 Principal Component Analyses

Principal Component Analyses (PCAs) were carried out using the *prcomp* function in the *stats* package in R (R Core Team, 2013).

4.2.4.3 Cluster Analyses

Cluster analysis was performed in R using the *k*-means algorithm (Hartigan & Wong, 1979) as implemented with the *kmeans* function in the *stats* package (R Core Team, 2013). The *k*-means algorithm uses an *a priori* number of clusters (*k*) and partitions specimens into these clusters through minimising the total within-cluster sum of squares (WCSS), based on Euclidean distances, of data points to assigned centres. Initially, a *k* number of cluster centres are randomly placed within the dataset. Once data points are assigned, the means of each cluster become the new cluster centres and data-points are assigned once again. This process is continued in an iterative fashion until convergence is reached and the cluster centres become stable. Several values for *k* were considered, ranging from 1 to 10.

The ‘elbow’ in a plot of the within-cluster sum of squares (WCSS) for a *k* number of clusters, for which the *k*-means algorithm had been applied, was used to determine the optimal number of clusters to consider (Hothorn & Everitt, 2014).

A *k*-medoids cluster analysis (Kaufman & Rousseeuw, 1987) was also performed on the data by implementing the *pam* function in the *cluster* R package (Maechler *et al.* 2015). The *k*-medoids algorithm works on a similar principal to the *k*-means algorithm however, under *k*-medoids a cluster is represented by an actual data point (medoid) rather than the mean of its constituents. Data points are assigned to a cluster depending on which medoid they are nearest to. The algorithm aims to minimise the average dissimilarity (average distance) between the representative medoid and its nearest neighbour data points. As a result, the algorithm is more robust to outliers and “noisy” data.

Silhouette clustering was carried out to determine the optimal number of clusters for the *k*-

medoids clustering analysis using the *silhouette* function in the R *cluster* package (Maechler *et al.* 2015). This method considers how close data points are to neighbouring clusters. Silhouette values for each data point (specimen) provide an indication of how well the clusters are separated (see Kaufman & Rousseeuw, 2009). The highest average silhouette width for different values of k is indicative of the most optimal number of clusters to consider. The function *clusplot* in the *cluster* package (Maechler *et al.* 2015) was used to plot ellipses around respective clusters on the PCA plots.

Agglomerative hierarchical clustering analysis was performed in R using the *pvclust* function in the *fpc* package (see Suzuki & Shimodaira, 2006). Agglomerative hierarchical clustering partitions the data through a series of successive fusions whereby each specimen is considered as its own cluster to begin with and are ultimately reduced to a single cluster containing all specimens. Ward's-minimum-variance-criterion (ward.D) was the agglomerative method used, whereby clusters are merged to keep within-cluster variance to a minimum (Murtagh, 1985; Murtagh & Legendre, 2014). Bootstrap replications were set to 10,000. The *pvclust* function calculates two cluster support values, the bootstrap probability (BP), which is the frequency at which a particular cluster appears in the bootstrap replicates, and the P -values, which are the approximately unbiased (AU) probability values and are calculated from multi-scale bootstrap resampling (see Shimodaira, 2002; 2004). Cluster assignments were compared to lineage assignments based on mtDNA sequences (from Chapter 3).

4.2.4.4 Discriminant Function Analyses

A Discriminant Function Analysis (DFA) was carried out on both datasets using the *lda* function in the R *MASS* package (Venables & Ripley, 2002). Individuals that could not be genetically assigned *a priori* to a lineage (Hol-Ta, AS-Ta or Tt) were omitted from the DFA analysis (see Results). A MANOVA was carried out in R using the *manova* function as implemented in the *stats* package (R Core Team, 2013) to test whether character measurements were statistically significant between groups.

In order to ascertain which characters were the most important for discriminating between groups, a stepwise selection of characters was carried out using the *greedy.wilks* function in the R *klaR* package (Weihs *et al.* 2005). The Wilks' lambda criterion is used to retain characters with relatively high importance and omit those with low explanatory power. The procedure

begins with the character that explains the most separation between groups. New characters are then added in a stepwise fashion by selecting ones that minimise the Wilks' lambda of the model, including it if the P -value still shows statistical significance (using a default $P < 0.2$ threshold).

Leave-one-out cross-validation analysis was performed on the most important characters in R using the *lda* function under the *MASS* package (Venables & Ripley, 2002). During this process, a single individual is removed from the dataset and different DFs are calculated from the remaining data. The new DF model is then used to assign the individual to one of the three groups. This is carried out for each individual and cross-validation scores are generated.

Because lineages (groups) were better represented in the Combined Dataset, a pairwise, stepwise, DFA was carried out to elucidate which characters discriminated the best between each pair of groups.

4.2.5 Geometric Morphometric Analyses

A total of 52 cranially mature (see above) and intact bottlenose dolphin (*Tursiops* spp.) skulls from the ONHM collection and eight skulls from the SMNS collection were photographed for geometric morphometric (GM) analysis.

4.2.5.1 Photography

Photographs were taken at right angles to each other in dorsal, ventral and lateral (left) aspect. For dorsal and ventral photographs, skulls were positioned with the rostrum parallel to the horizontal plane using a target spirit level and plasticine to position the skull. The spirit level was placed between the premaxillary foramen, just anterior of the premaxillary rostral surface, in dorsal aspect, and placed mid-way and centrally along the palatine process in ventral aspect. Images were taken with a CANON IXUS 115 HS digital camera at 4000 x 3000 pixels, ISO 300-400, 1/40 shutter speed, f/3.2, focal length 7.0 mm, no flash. The same camera was used throughout the study to avoid equipment error. The camera was positioned on a tripod directly above the skull. The camera was also leveled parallel to the horizontal plane using a target spirit level. In lateral aspect, skulls were placed ventral-side down and positioned similarly to the dorsal photographs. The camera was positioned perpendicular to the horizontal plane. In this case, it was not necessary for the rostrum to be parallel to the horizontal plane,

as rotation through it would be corrected in a Generalised Procrustes Analysis (GPA) (see below). Only correction for ‘lob-sidedness’ was made so that the lateral plane of the skull was perpendicular to the horizontal plane and facing the camera. To assess intra-observer error introduced by orientation, photographs were taken in triplicate, with the skull being repositioned for each repeat.

4.2.5.2 Landmark Digitization and Repeatability Tests

Landmarks (LMs) were digitised on the left side of the skull for each aspect using TpsDIG 2.05 (Rohlf, 2005). See Figure 43 and Table 26 for LM descriptions and positioning. Only unilateral data were used because the focus here was to determine variation in cranial shape and not bilateral asymmetry. Furthermore, to use bilateral LMs would be treating each side as independent from the other and would inflate our degrees of freedom during analyses (Zelditch *et al.* 2012). The majority of LMs used were Type II, characterised by maximum or minimum curvatures or endpoints of structures. The remainder of LMs used were Type I, characterised by the juxtaposition of tissues, such as the intersection between three sutures (see Table 26) (Bookstein, 1997).

To investigate error associated with LM digitisation, a repeatability test was carried out on a subset of specimens ($n = 13$) where a single photo of each specimen was digitised three times. In total, 10 LMs were tested in dorsal aspect, 13 in ventral and 16 in lateral aspect. Generalised Procrustes Analyses (GPAs) were carried out on the LMs in MORPHEUS ET AL. (Slice, 1998), where the sum of squared distances between homologous LMs is minimised through reflecting, translating, scaling and rotating configurations to best fit the mean shape for the entire dataset. Doing so removes all information that does not pertain to shape (Kendall, 1977; Mitteroecker & Gunz, 2009; Klingenberg, 2011). Each LM configuration is thus projected as a single point in Kendall’s non-Euclidean shape space, with dimensions:

$$k m - m - m(m - 1/2) - 1$$

Where k = number of LMs and m = dimensionality of those LMs (Kendall, 1984). In this case, $m = 2$, given the two-dimensionality of the LMs, and $k = 10$ in dorsal aspect, $k = 13$ in ventral aspect and $k = 14$ in lateral aspect, thus giving 14, 20 and 22 dimensions in Kendall’s shape space for the dorsal, ventral and lateral aspect respectively.

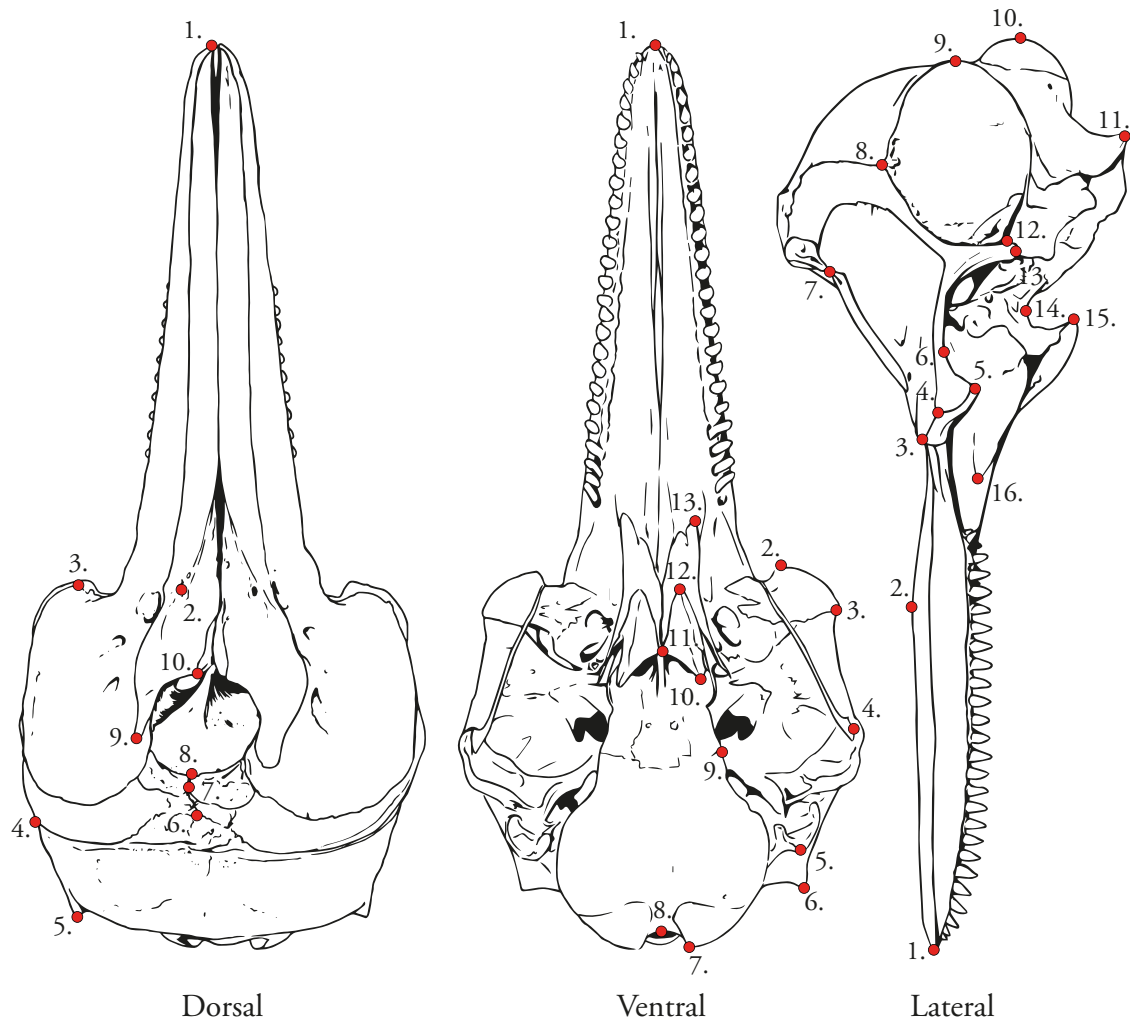


Figure 43: Positioning of landmarks on a bottlenose dolphin (*Tursiops aduncus*) skull.

Given the curved, non-linear nature of Kendall's shape space, standard multivariate analyses, which generally assume a Euclidean space, cannot be carried out (Viarsdóttir *et al.* 2002; Webster & Sheets, 2010). Therefore, points are projected into a linear space, tangent to Kendall's shape space, where the tangent point is the mean configuration of LMs for the entire dataset, to which all configurations are superimposed during GPA.

To check LM digitization repeatability, a Principal Component Analysis (PCA) was performed in MORPHOJ v. 1.05f (Klingenberg, 2011) (O'Higgins & Jones, 1998; Viarsdóttir *et al.* 2002). Tight clustering of repeats would suggest that precision errors in landmark digitization were minimal compared to inter-specimen variation. To test the repeatability of the LMs further, Euclidean distances of LMs to their respective configuration centroids were calculated and used to calculate percentage errors across repeats for each specimen (Singleton, 2002). Landmarks that showed < 1% digitization error were included in further analyses.

Table 26: Landmark descriptions and summary of associated statistics.

Dorsal		Digitization repeatability test		Intra-specimen digitization error across repeats	
LM	Description	type	Source	Average % Error	Average % Error
1	Rostral tip	II	Amaral <i>et al.</i> (2009)	0.02	0.14
2	Anterionmost point of premaxillary foramen	II	Loy <i>et al.</i> (2011)	0.17	0.5
3	Anterionmost point on antorbital notch on maxilla	II	Amaral <i>et al.</i> (2009)	0.19	0.5
4	Intersection between the parietal bone and frontal-interparietal suture	I	Amaral <i>et al.</i> (2009)	0.1	0.55
5	Posteriormost point on temporal crest	II	Amaral <i>et al.</i> (2009)	0.06	0.66
6	Intersection between the frontal-interparietal suture	I	Amaral <i>et al.</i> (2009)	0.16	0.6
7	Mid-point of the nasal bone suture	I	Amaral <i>et al.</i> (2009)	0.3	0.67
8	Suture between the nasals and ethmoid	I	Loy <i>et al.</i> (2011)	0.19	0.71
9	Posteriormost point on ascending premaxillary process	II	Loy <i>et al.</i> (2011)	0.48	1.17
10	Posteriormost point on premaxilla bone at nares	II	Amaral <i>et al.</i> (2009)	0.6	0.91
Ventral		Digitization repeatability test		Intra-specimen digitization error across repeats	
LM	Description	type	Source	Average % Error	Average % Error
1	Rostral tip	II	Amaral <i>et al.</i> (2009)	0.04	0.12
2	Anteriormost point on antorbital notch on the lacrimal bone	II	This study	0.18	0.37
3	Externalmost point along lacrimal suture below the supraorbital process	II	Amaral <i>et al.</i> (2009)	0.19	0.41
4	Externalmost point of jugal-squamosal suture	II	This study	0.37	0.4
5	Posteriormost point of paraoccipital process	II	This study	0.17	0.33
6	Posteriormost point on temporal crest	II	Amaral <i>et al.</i> (2009)	0.08	0.33
7	Posteriormost point on occipital condyle	II	Amaral <i>et al.</i> (2009)	0.07	0.19
8	Centremost point on intercondyloid notch	II	This study	0.08	0.15
9	Intersection between basoccipital-pterygoid suture along basoccipital crest	I	Amaral <i>et al.</i> (2009)	0.27	0.78
10	Posteriormost point of pterygoid	II	Amaral <i>et al.</i> (2009)	0.56	0.83
11	Interiormost point of pterygoid	II	This study	0.22	0.44

Ventral		Digitization repeatability test	Intra-specimen digitization error across repeats
LM	Description	Average % Error	Average % Error
12	Anteriormost point of pterygoid at suture with palatine	0.27	0.4
13	Anteriormost point on the palatine	0.11	0.35
	type Source		
	II This study		
	II Amaral <i>et al.</i> (2009)		
Lateral		Digitization repeatability test	Intra-specimen digitization error across repeats
LM	Description	Average % Error	Average % Error
1	Rostral tip	0.03	0.17
2	Tip of premaxillary convexity	0.12	0.53
3	Anteriormost point on antorbital notch on maxilla	0.19	0.55
4	Intersection between lacrimal-frontal-maxilla suture	0.27	0.61
5	Posteriormost point on lacrimal	0.82	1.85
6	Flexion point in the antero-lateral region of frontal	0.71	2.81
7	Posteriormost point on ascending premaxillary process	0.16	0.36
8	Intersection between the parietal bone and frontal-interparietal suture	0.1	0.21
9	Posteriormost point on temporal crest	0.08	0.18
10	Posteriormost point on occipital condyle	0.05	0.33
11	Anteriormost point of paraoccipital process	0.07	0.15
12	Anterior-superior tip of zygomatic process	0.2	0.47
13	Inferior tip of frontal, at the zygomatic process	0.16	0.5
14	Flexion point of pterygoid	0.59	0.71
15	Posteriormost point of pterygoid	0.15	0.33
16	Anteriormost point along palatine-maxilla suture	0.25	0.41
	type Source		
	II Loy <i>et al.</i> (2011)		
	II This study		
	II Loy <i>et al.</i> (2011)		
	I Loy <i>et al.</i> (2011)		
	II Loy <i>et al.</i> (2011)		
	II Loy <i>et al.</i> (2011)		
	I Loy <i>et al.</i> (2011)		
	II This study		
	II This study		
	II This study		
	II Loy <i>et al.</i> (2011)		
	II Loy <i>et al.</i> (2011)		
	II Loy <i>et al.</i> (2011)		
	II Loy <i>et al.</i> (2011)		
	II Loy <i>et al.</i> (2011)		

4.2.5.3 Landmark Digitization Error due to Orientation

All LMs that showed good repeatability (see Results and Table 26) were digitised for each triplicate of photos for every specimen. A GPA was conducted on all triplicates for all specimens, including those with missing LMs, in MORPHEUS ET AL. (Slice, 1998). Procrustes-fit coordinates were then used to calculate percentage error for each LM between pairs of photos within each triplicate, using the Euclidean distance method described above. Configurations that showed the least error across LMs in the pairwise photo comparison for each triplicate were retained for further analyses and the third configuration was omitted. This was done to minimise the error introduced by specimen orientation at the photography stage. LMs were removed from a specimen, and treated as missing data alongside LMs that were absent due to specimen damage, when the intra-specimen error was high between duplicate photos ($> 1.5\%$ error). Landmarks were omitted from analyses when the average percentage error across all specimens was $> 1.5\%$ (see Results and Table 26). Further to this, specimens missing more than four LMs were also omitted from analyses. This was because, in general, missing LMs could not be reliably estimated (see below) from configurations that had more than four missing.

4.2.5.4 Estimation of Missing Landmark Coordinates

Coordinates for missing LMs were estimated using the thin-plate spline interpolating method as implemented using the *estimate.missing* function in the R package *geomorph* (Adams & Otárola-Castillo, 2013). The Procrustes group average for all available data was used as the reference configuration for estimating missing LMs in target configurations. Thin-plate spline interpolations were computed based on available LMs shared between the target and reference configurations. Interpolations for each target-reference pair were then used to map missing LMs from the reference to the target configuration, keeping the deformation, ‘bending energy’, to a minimum (Mitteroecker & Gunz, 2009). Coordinates for missing LMs were then returned for the target configuration of interest.

Once data were truncated (see Results) and missing LMs estimated, configurations for each duplicate of photos were Procrustes averaged so that each specimen was represented by one configuration of LMs in each aspect.

4.2.5.5 *Principal Component Analysis and Visualisation of Shape Differences*

Data were first submitted to a GPA in MORPHOJ v. 1.05f (Klingenberg, 2011) and a covariance matrix was then generated from the Procrustes-fit coordinates, thus allowing for PCA exploratory analysis of shape relationships between the specimens. A MANOVA was performed in R using the *manova* function in the *stats* package (R Core Team, 2013) to test whether the PCs showed significant differences between genetically allocated groups. To visualise shape changes associated with the extreme values of principal components and to compare average group shapes, thin-plate spline transformation grids and wireframe graphs were generated in MORPHOJ v. 1.05f (Klingenberg, 2011).

4.2.5.6 *Allometric Effects on Shape*

Size is represented by centroid size, which is the square root of the summed squared distances from the configuration centroid to each LM. To investigate the effects of allometry on the shape differences within groups, a pooled, within-group, multivariate regression analysis was performed on log centroid size, as the independent variable, and the Procrustes coordinates as the multidimensional dependent variables of shape in MORPHOJ v. 1.05f (Klingenberg, 2011). A permutation test was performed (10,000 rounds) to investigate whether shape was significantly independent of size. To correct for the effects of allometry, a PCA was performed on the regression residuals and a MANOVA on the retained PCs (those which explained up to 80% of the total variance) was used to test for group differences in allometry-corrected shape. An ANOVA and Procrustes ANOVA were also performed in MORPHOJ v. 1.05f (Klingenberg, 2011) to test for differences between groups in size and shape, respectively.

4.2.5.7 *Canonical Variates Analysis and Discriminant Function Analysis*

A canonical variates analysis (CVA) and a discriminant function analysis (DFA), with leave-one-out cross-validation, were also carried out on groups to which specimens were assigned *a priori* based on mtDNA sequences (see Results). For both the CVA and DFA analyses, differences in shape between groups were quantified as Mahalanobis distances, which is a measure of group differences relative to the variation within groups (Klingenberg & Monteiro, 2005), and Procrustes distances, which is a measure of group deviation from the population average (Klingenberg & Monteiro, 2005). Associated *P*-values for each distance were generated from permutation tests (1000 rounds). All analyses were performed for each aspect and implemented in MORPHOJ v. 1.05f (Klingenberg, 2011).

4.2.5.8 *Congruence Between Cranial Geometry and Phylogenetic Data*

Specimen shapes, as represented by PC and CV scores, were mapped to the available phylogeny (see Results) for all aspects in MORPHOJ v. 1.05f (Klingenberg, 2011). A permutation test for a phylogenetic signal (10,000 rounds) was implemented to generate a *P*-value to determine whether the signal was significant. The phylogenetic tree was then plotted against the CVA plot for visualization.

4.3 Results

4.3.1 *Lineage Assignment*

Three lineages of *T. aduncus* (Ta) (Australasian Ta, Hol-Ta and AS-Ta) and one lineage of *T. trunactus* (Tt) were clearly defined in the neighbour-joining phylogenetic tree (Figure 44). A total of 73 specimens were genetically assigned to one of three lineages relevant to this study based on their position in the phylogeny.

4.3.2 *Assessment of Maturity*

Post-cranial skeletal material was available for a total of 15 specimens ($n = 9$ ONHM, $n = 6$ SMNS). Post-cranials were absent for the majority of specimens, (ONHM $n = 71$, SMNS $n = 12$). Maturity was identified in 54 of the 80 ONHM specimens and eight of the 11 SMNS specimens. Those specimens that were not considered mature were omitted from further analyses with the exception of analyses considering meristic characters, which are independent of age.

4.3.3 *Cranial Morphometrics*

4.3.3.1 *Data Truncation*

Examination of observer measurement error across repeated measurements revealed that four characters (DFWN, DFWM, WAS and VW) were being measured unreliably (see Table 27). Therefore these were omitted from analyses.

A total of 14 characters from the ONHM Dataset and 13 from the Combined Dataset had more than 20% missing data across specimens (see Table 27) and so were removed from respective analyses. Nine of these characters were measurements associated with the mandibles, bullae and petrotic bones, which were frequently missing from the museum specimens.

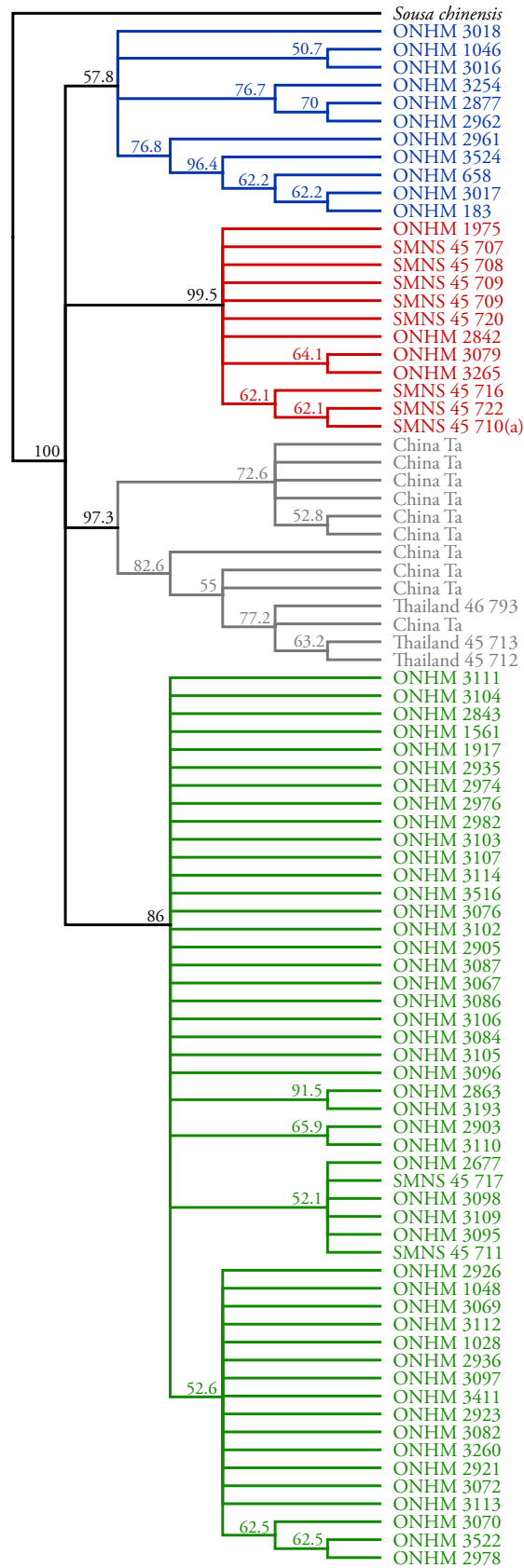


Figure 44: Neighbour-joining phylogenetic tree. Constructed using sequence data generated in GENEIOUS v. 7.1.2 (<http://www.geneious.com>, Kearse *et al.* 2012). The dark blue clade represents *Tursiops truncatus* individuals, red represents the new, Arabian Sea lineage of *T. aduncus* and green represents the holotype *T. aduncus*. The grey clade represents Chinese/Australasian *T. aduncus*. Bootstrap support values > 50% are indicated.

A total of four and nine specimens were missing data for more than 30% of the remaining characters in the ONHM and Combined Datasets, respectively. Therefore these were also removed from further analyses.

Morphological characters not measured in both museum collections were also removed from the Combined Dataset (see Table 27). Only one character was unique to the SMNS collection and four characters were unique to the ONHM collection. Post and prior-calibration measurements were significantly different ($P < 0.05$) for five characters (TREN, RWB_{min}, TRIN, GWPTF, GPARW) and were therefore also omitted from further analyses using the Combined Dataset (see Table 27).

Data from the different museum collections were pooled into a Combined Dataset, predominantly because the AS-Ta lineage (assigned to specimens based on mtDNA) had better representation in the Combined Dataset ($n = 9$) than the ONHM Dataset ($n = 4$). However, the ONHM Dataset was also analysed because a loss of data was required from this dataset in order to pool the datasets together and eliminate bias associated with measurements taken prior- and post-calibration. Therefore, although the Combined Dataset had a greater representation across lineages, the ONHM Dataset had more statistical power because it included more characters (Nakagawa & Freckleton, 2008). After data truncation, the ONHM Dataset included measurements for 26 cranial characters across 50 individuals (Hol-Ta: $n = 29$, AS-Ta: $n = 4$, Tt: $n = 9$, unknown: $n = 8$), whereas the Combined Dataset (SMNS $n = 11$, ONHM $n = 46$) included 18 characters across a total of 57 individuals (Hol-Ta: $n = 29$, AS-Ta: $n = 9$, Tt: $n = 8$, unknown: $n = 8$).

Eight individuals could not be genetically assigned *a priori* to a lineage (see above). These specimens were omitted from the DFA analyses. All measurements for the specimens considered mature are summarised in Table 27.

Table 27: Summary of measurements (mm) and associated statistics for *Tursiops truncatus*, *T. aduncus* (holotype lineage) and *T. aduncus* (Arabian Sea lineage). Unidentified specimen numbers given. Overall measurement error for each character also given. † = unreliable character due to measurement error; ‡ = significant difference between prior- and post-calibration measurements using *t*-tests ($P < 0.05$); § = characters unique to ONHM dataset; ¶ = characters unique to SMNS dataset; ¶ = more than 20% of specimens missing data for the ONHM dataset; # = More than 20% of specimens missing data for the Combined dataset; For Wilks' λ , * = $P < 0.05$; ** = $P < 0.001$; ns = not significant ($P > 0.05$)

Character	<i>T. truncatus</i>			<i>T. aduncus</i> (holotype lineage)			<i>T. aduncus</i> (Arabian Sea lineage)			Total		Measurement Error (%)	Truncation	ONHM	Combined	Wilks' λ	
	Mean	n	±SD	Range	Mean	n	±SD	Range	Mean	n	±SD						Range
BL	35.81	1	-	35.82 - 35.82	36.37	4	1.09	34.97 - 37.41	37.01	3	0.82	36.08 - 37.58	1	9	0.14	¶, #	
BW	21.46	1	-	21.46 - 21.46	20.68	4	0.23	20.34 - 20.82	20.7	3	0.44	20.22 - 21.09	1	9	0.38	¶, #	
POL	31.4	1	-	31.4 - 31.4	31.85	4	1.21	30.56 - 33.46	33.47	3	1.68	31.85 - 35.21	1	9	0.12	¶, #	
TPC	167.35	9	17.74	137.14 - 200.61	169.82	32	11.28	150.91 - 196.2	174.39	10	15.85	151.76 - 204.31	8	59	0.47	ns	ns
CBL	515.24	9	19.68	483.34 - 539	464.87	33	11.71	447.67 - 494.34	468.4	10	19.68	441.34 - 507	8	60	0.03	**	**
RL	292.23	9	14.12	267.79 - 309	267.04	31	10.77	248.74 - 293.34	268.17	10	15.46	240.49 - 293.77	8	58	0.03	**	**
TREN	344.53	9	16.66	315.34 - 364.34	312.61	29	12.19	289 - 345	313.66	10	16.1	283.97 - 344.6	7	55	0.06	‡	**
DFWN	10.87	9	3.04	6.38 - 14.6	10.28	33	2.87	4.07 - 16.16	13.72	11	5.16	6.22 - 22.42	9	62	3.16	†	
DFWM	16.94	9	7.23	7.74 - 32.74	15.06	33	3.94	7.04 - 23.14	16.03	11	4.53	7.77 - 21.15	10	63	3.38	†	
GWEN	55.29	9	3.52	49.18 - 59.09	56.04	33	2.44	50.1 - 60.62	55.17	11	2.25	50.81 - 58.7	10	63	0.17	ns	ns
GWTPX	91.64	9	6.8	81.85 - 99.79	86.24	30	4.64	75.42 - 95.4	85.59	11	3.16	81.53 - 92.03	9	59	0.09	*	*
PRW	47.35	9	3.59	42.26 - 53.34	35.53	31	2.46	29.39 - 40.12	36.16	10	3.8	30.34 - 42.49	8	58	0.28	**	**
LWPTF	151.7	9	6	139.3 - 158.72	148.27	33	8.41	123.2 - 164.47	148.13	10	7.84	137.47 - 162.02	9	61	0.08	ns	ns
GLPT	76.27	4	3.99	72.78 - 81.24	59.54	22	3.78	53.16 - 67.14	61.2	8	4.03	56.57 - 65.64	7	41	0.2	¶, #	
PL	44.64	9	6.35	35.22 - 52.37	46.66	33	4.14	37.46 - 56.37	45.73	11	6.48	36.84 - 57.56	9	62	0.31	ns	ns
PWPT	52.98	9	4.3	48.78 - 58.92	42.09	31	2.36	36.77 - 45.8	44.27	4	2.43	40.94 - 46.73	9	53	0.34	§	**

Character	<i>T. truncatus</i>			<i>T. aduncus</i> (holotype lineage)			<i>T. aduncus</i> (Arabian Sea lineage)			Total	Measurement Error (%)	Truncation	Wilks' λ				
	Mean	n	±SD	Range	Mean	n	±SD	Range	Mean					n	±SD	Range	n
WAS	76.69	8	8.09	64.34 - 87.31	57.9	31	5.93	45.83 - 68.31	55.08	11	6.83	43.52 - 67.37	10	60	2.25	†	
GPOW	255.76	9	12.4	235.54 - 272.5	225.13	31	8.72	198.35 - 237.3	206.78	9	15.74	186.55 - 227.94	9	58	0.03	**	**
GPRW	232.76	9	11.87	216.07 - 248.87	199.95	27	6.99	185.97 - 210.72	186.96	9	28.53	118.72 - 212.5	7	52	0.03	**	**
ZW	259.54	9	12.26	237.84 - 278.7	226.51	32	7.02	209.54 - 238.82	221.38	10	13.22	202.25 - 240.75	9	60	0.02	**	**
GWIN	75.47	9	6.07	68.02 - 84.55	60.56	32	2.58	55.68 - 66.19	59.42	10	2.89	53.08 - 61.96	10	61	0.16	**	**
VW	48.73	9	9.67	39.88 - 67.56	29.2	30	3.72	20.96 - 34.98	27.02	11	5.69	16.43 - 35.34	9	59	0.64	†	
RWB _{Berrin}	145.05	9	10.65	132.48 - 162.94	129.27	25	5.29	118.22 - 138.27	130.42	4	4.67	125.46 - 136.08	7	45	0.15	§	**
RWB _{min}	137.35	9	8.52	123.42 - 149.05	118.11	31	5.4	104.29 - 125.74	113.07	11	8.98	99.06 - 125.24	8	59	0.16	‡	**
RWM	86.52	8	4.65	82.6 - 96.96	67.03	27	3.2	60.94 - 73.21	64.25	9	5.99	55.18 - 72.06	7	51	0.17	**	**
RW75%	65.48	7	4.19	58.85 - 71.2	53.56	24	4	44.79 - 62.32	52.13	8	7.28	41.43 - 58.99	7	46	0.24	¶	**
RW60	104.19	8	4.72	99.4 - 110.34	81.78	28	3.19	72.83 - 86.32	79.36	11	5.83	70 - 88.34	6	53	0.14	**	**
TRIN	361.56	3	14.37	346 - 374.34	304.07	22	11.38	282.34 - 330.34	312.16	9	16.03	292 - 41.77	6	40	0.06	‡,§,#	**
UTLTR	250.07	9	12.47	229.27 - 266.67	219.59	31	9.29	200.79 - 237.84	221.86	10	12.75	199.6 - 243.24	8	58	0.06	**	**
GLPTF	107.99	8	6.17	99.92 - 115.96	103.69	32	5.69	87.4 - 114.98	100.44	9	7.6	90.32 - 111.36	9	58	0.11	ns	ns
GWPTF	81.13	9	4.8	73.78 - 89.08	73.56	33	3.1	68.31 - 79.25	71.39	11	5.04	63.42 - 81.15	10	63	0.24	‡	**
LO	71.16	9	5.83	61.48 - 80.36	64.31	29	2.74	57.41 - 68.3	62.58	10	3.88	58.37 - 67.65	10	58	0.22	**	**
LAL	58.55	9	4.55	50.78 - 64.08	41.89	26	2.89	35.02 - 45.88	42.4	10	2.83	39.12 - 48.52	7	52	0.21	¶	**
GPARW	183.55	9	7.72	172.94 - 197.52	170.2	33	4.24	161.39 - 177.27	173.55	11	6.42	162.77 - 186.65	10	63	0.05	‡	**
MXOC	112.49	9	7.97	104.89 - 129.28	103.62	31	4.42	90.13 - 116.58	105.2	4	2.51	103.38 - 108.9	10	54	0.11	§	**

Character	<i>T. truncatus</i>			<i>T. aduncus</i> (holotype lineage)			<i>T. aduncus</i> (Arabian Sea lineage)			Total	Measurement Error (%)	Truncation	ONHM	Wilks' λ			
	Mean	n	±SD	Range	Mean	n	±SD	Range	Mean						n	±SD	Range
LTRL	252.39	3	6.52	245.94 - 258.97	225.13	8	7.16	213.64 - 234.67	230.79	6	10.13	218.22 - 244.72	3	20	0.04	§,#	Combined
ML	453	3	15.38	438.34 - 469	387.57	7	3.9	381 - 393.67	398.06	6	17.96	375 - 428	3	19	0.03	§,#	
MFL	137.31	3	10.87	126.52 - 148.25	125.73	7	4.13	118.86 - 129.76	127.13	6	9.22	115.06 - 140.92	3	19	0.09	§,#	
MH	95.07	3	6.53	89.72 - 102.35	82.51	7	5.21	71.92 - 87.52	82.51	6	4.73	76.62 - 89.71	3	19	0.16	§,#	
MSL	80.84	3	3.77	77.21 - 84.74	62.17	6	4.07	59.06 - 69.86	59.03	4	9.23	45.62 - 66.18	3	16	0.28	§,#	
TTL	22.67	3	0.58	22 - 23	25.67	9	1	24 - 27	26.67	6	0.82	26 - 28	3	19	0.07	§,#	
TTU	24.29	7	1.11	23 - 26	25.23	30	1.28	23 - 28	26.13	8	0.83	25 - 27	8	50	0.15	**	
TWTMJ	8.29	1	-	8.3 - 8.3	7.29	8	0.48	6.37 - 7.86	6.98	4	1.01	5.73 - 8.17	2	15	0.96	§,#	
MAJDTF	-	-	-	-	62.03	2	0.74	61.51 - 62.56	62.75	7	3.55	57.98 - 66.86	0	9	0.23	§,#	

4.3.3.2 Meristic Characters

A within-cluster sum of squares (WCSS) plot using the k -means algorithm identified $k=2$ as optimal (Figure 45). A two-means cluster analysis supported two distinct clusters based on upper tooth counts for 72 specimens ($F_{1,70} = 125.81$, $P < 0.001$). Where the phylogenetic assignment of specimens based on mtDNA was known, all of the AS-Ta ($n = 8$) and the majority of of the Hol-Ta ($n = 34/45$, 76%) specimens were correctly assigned to Cluster 1. The majority of the Tt specimens ($n = 4/7$, 57%) were correctly assigned to Cluster 2. The overall misclassification rate was high (23%), which is due to the substantial overlap between tooth counts within groups (see Figure 46).

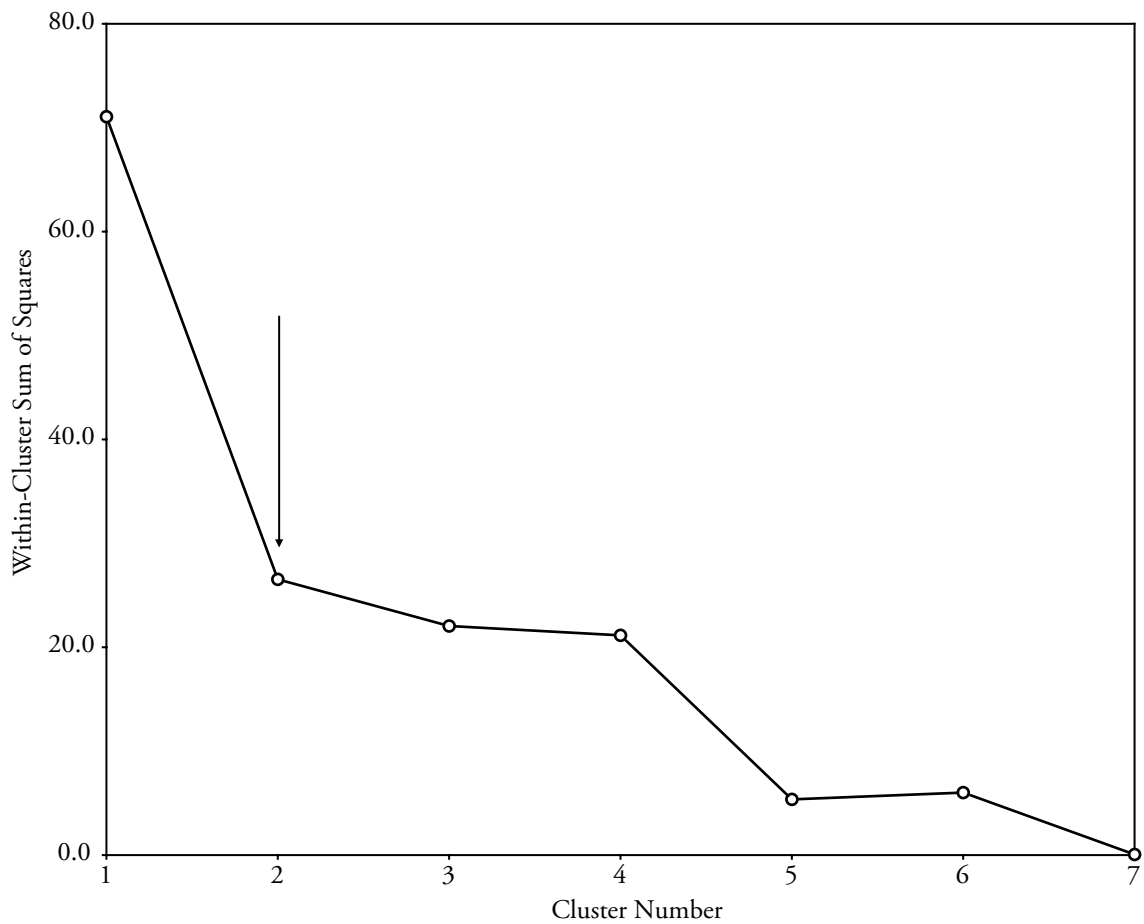


Figure 45: Within-cluster sum of squares for different numbers of clusters (k) using meristic characters. Arrow indicates 'elbow' point where the change in within-cluster sum of squares decreases.

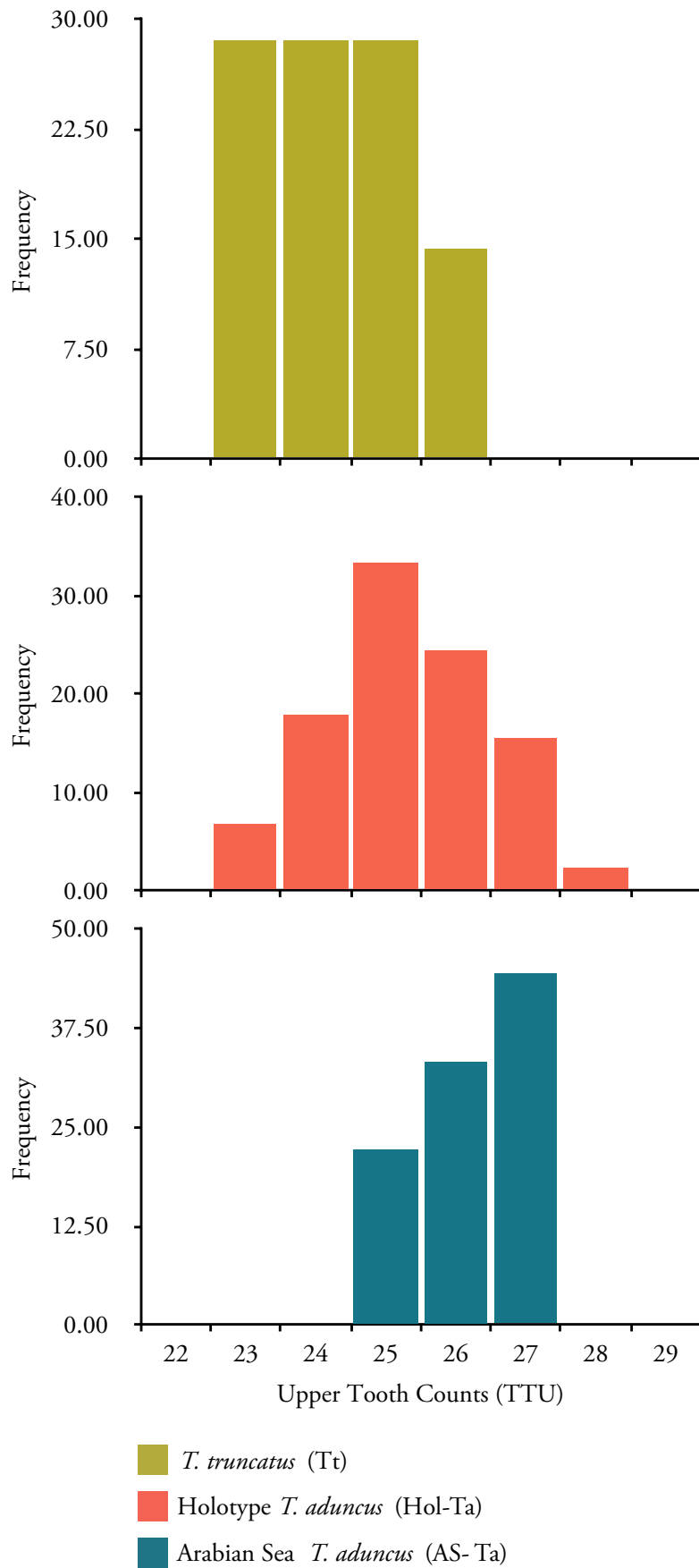


Figure 46: Group-wise plots of TTU frequencies (%) illustrating the overlap of tooth counts.

4.3.3.3 Principal Component Analysis: ONHM Dataset

Four principal components (PCs) were regarded as informative based on a screeplot (Figure 47) and Kaiser's criterion, where the variance for the first four PCs is greater than 1.0 (Guttman, 1954; Kaiser, 1960). These PCs explained 79.78% of the total variance in the data, with PCs 1-4 explaining 56.69%, 11.35%, 7.30% and 4.41% of the variance, respectively. The loadings for each PC are shown in Table 28. The loadings indicate that the characters contributing the most to PC1 are those associated with size (e.g. condylobasal length, CBL and zygomatic width, ZW) whereas the character contributing the most to PC2 is the length from the tip of rostrum to the apex of the premaxillary convexity (TPC). The first PC differentiates well between individuals identified as *T. truncatus* and those identified as *T. aduncus* (Figure 48).

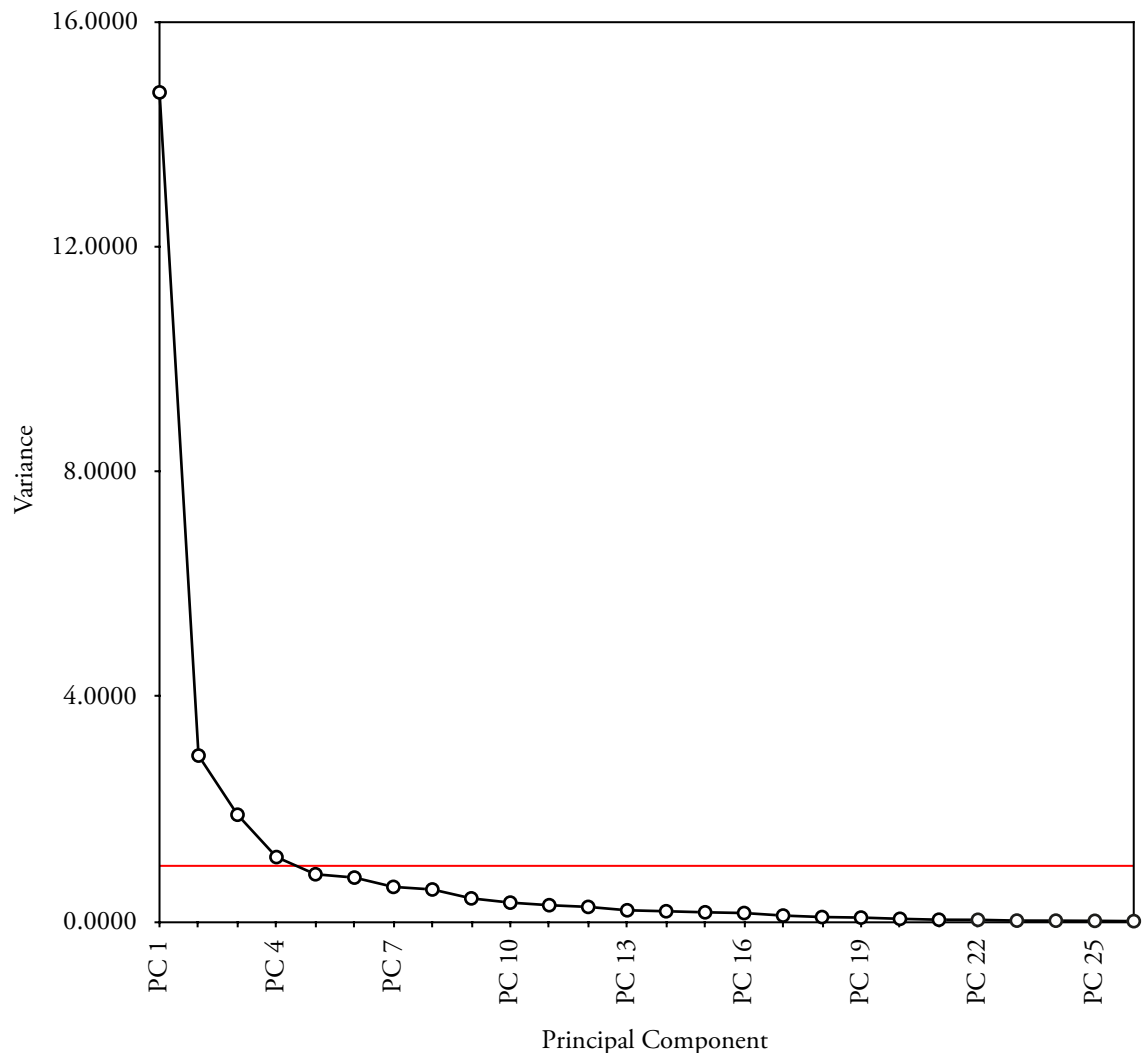


Figure 47: Screeplot showing the variance explained by each PC from a PCA on the ONHM Dataset. The red line highlights the 'elbow' in the plot. All variance explained by the components after this point is considered small.

Table 28: Principal Component loadings for PCA on the ONHM Dataset.

Character	PC 1	PC 2	PC 3	PC 4
TPC	0.052	-0.471	0.13	-0.148
CBL	0.224	-0.206	0.218	-0.046
RL	0.188	-0.293	0.295	-0.092
TREN	0.202	-0.258	0.282	-0.102
GWEN	0.009	-0.284	-0.462	-0.301
GWPX	0.161	-0.181	-0.238	-0.368
PRW	0.22	0.147	0.004	0.207
LWPTF	0.056	0.375	0.09	-0.563
PL	-0.028	-0.167	-0.445	0.155
PWPT	0.216	0.115	0.024	0.058
GPOW	0.251	0.067	-0.109	0.004
GPRW	0.246	0.047	-0.091	0.027
ZW	0.25	0.071	-0.115	0.047
GWIN	0.231	0.117	0.001	0.079
RWB _{Perrin}	0.224	-0.022	-0.212	0.029
RWBmin	0.238	0.028	-0.137	0.029
RWM	0.215	0.181	0.007	0.212
RW60	0.228	0.009	0.135	0.123
UTLTR	0.206	-0.228	0.268	-0.02
GLPTF	0.131	-0.269	-0.164	0.241
GWPTF	0.179	0.088	0.057	0.195
LO	0.178	-0.067	-0.162	0.217
LAL	0.239	0.063	0.037	-0.029
GPARG	0.208	0.192	0.027	-0.181
MXOC	0.198	0.003	-0.21	-0.172
BCH	0.199	0.172	-0.057	-0.259

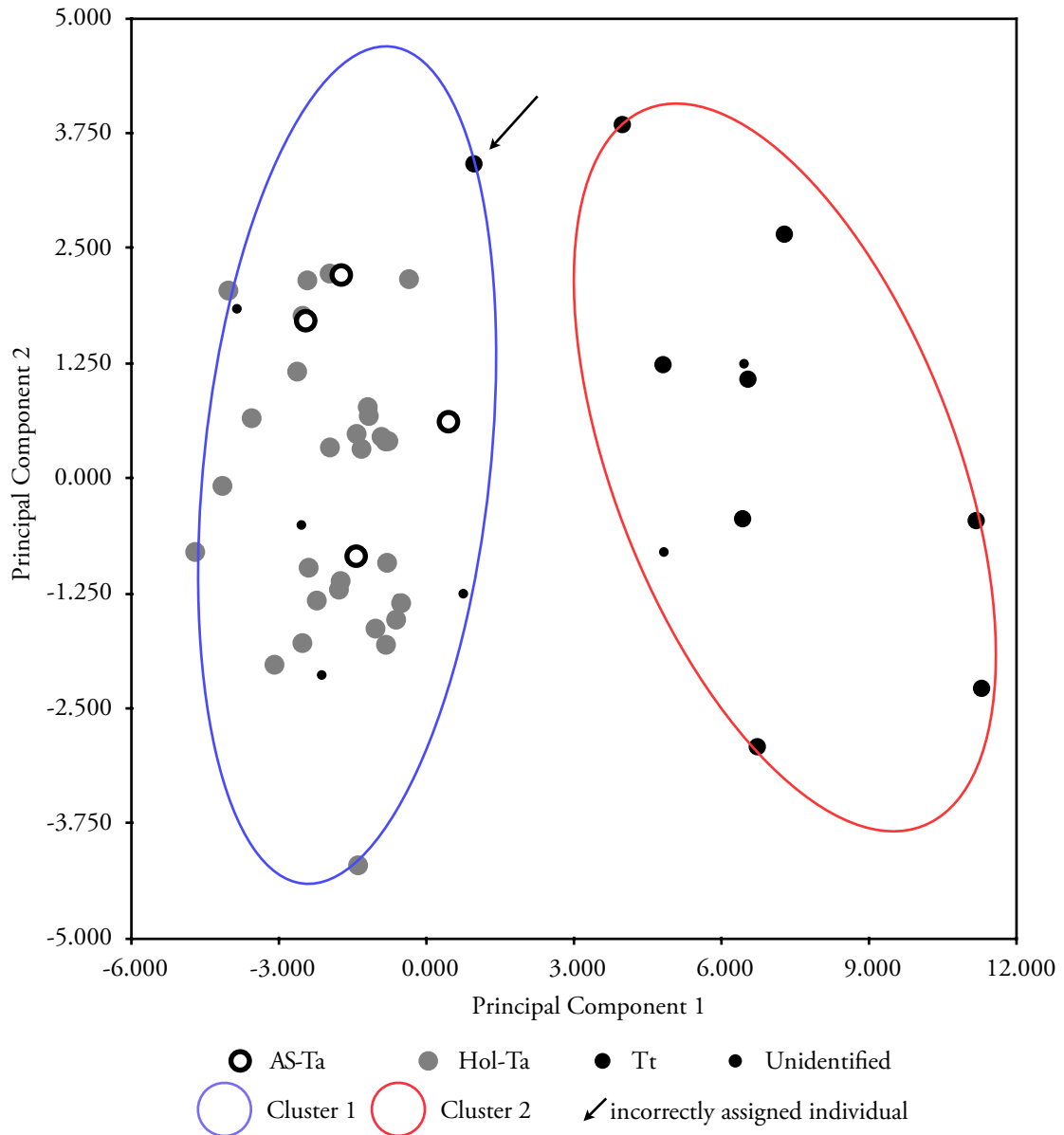


Figure 48: PCA on ONHM Dataset. Plot of PC1 against PC2 explaining 56.69% and 11.35% of the variance, respectively. Specimens assigned to clusters based on the k -medoids algorithm and drawn using the *clusplot* function in the *cluster* R package (Maechler *et al.* 2015).

4.3.3.4 Cluster Analysis: ONHM Dataset

A two-means clustering analysis revealed statistical support for two distinct clusters in the data ($F_{1,48} = 43.60$, $P < 0.001$). From the ‘elbow’ in the within-cluster sum of squares (WCSS) plot (Figure 49), it is evident that the optimal value for $k = 2$. The clusters likely reflect the distinction between *T. truncatus* and *T. aduncus*-type specimens. Of the specimens where phylogenetic placement was known, all of the Hol-Ta specimens ($n = 29$) and AS-Ta specimens ($n = 4$) were assigned to Cluster 1. All of Tt specimens were assigned to Cluster 2 with the exception of one individual, which was incorrectly assigned to Cluster 1 with the *T. aduncus*-type specimens. Where phylogenetic placement was unknown ($n = 8$), six were assigned to

Cluster 1 (Ta-type) and two were assigned to Cluster 2 (Tt-type). As the misclassification rate was low (2.38%), it is likely that these cluster assignments are indicative of the phylogenetic placement of these specimens.

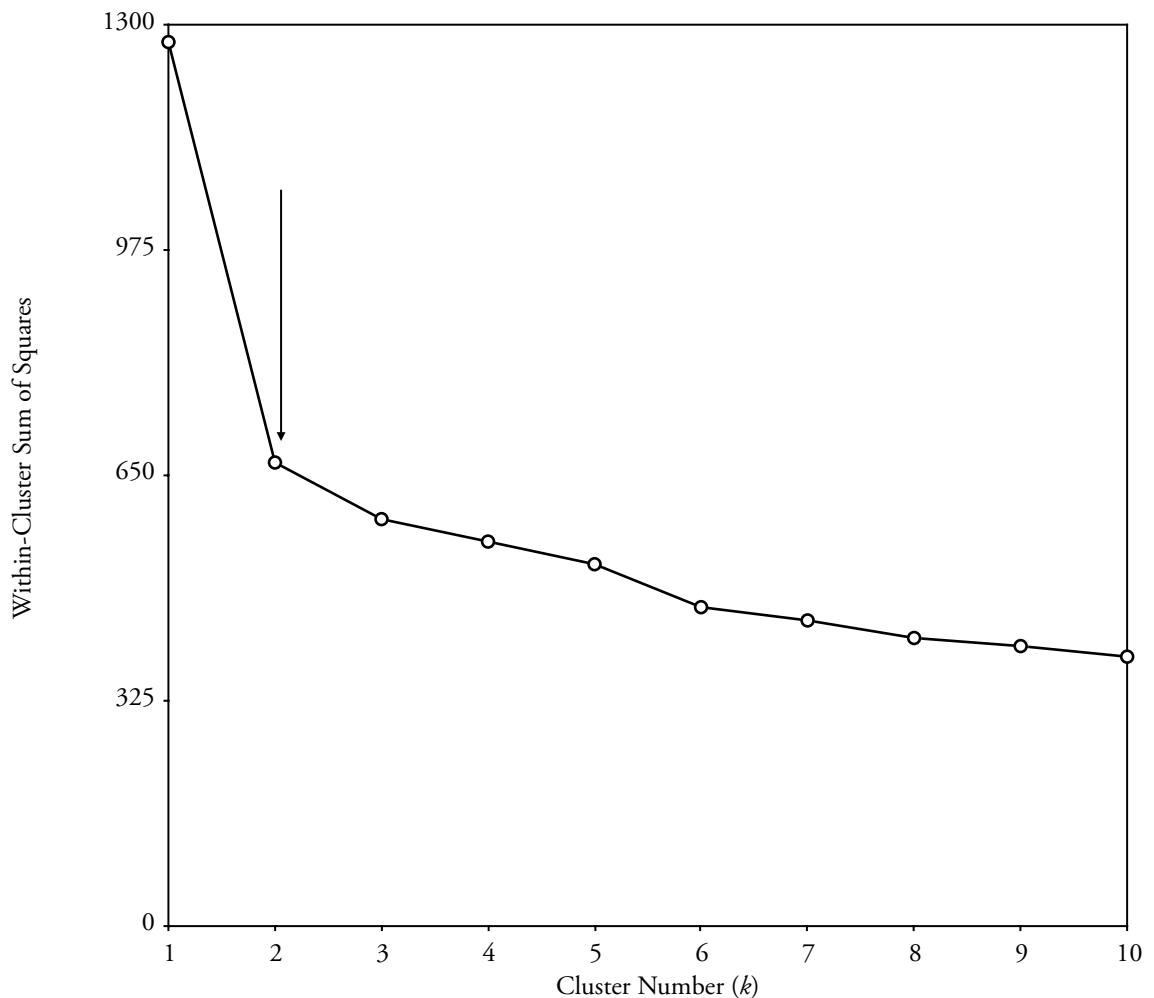


Figure 49: Within-cluster sum of squares for different numbers of clusters under the k -means cluster algorithm for the ONHM Dataset. The arrow highlights the ‘elbow’ point in the plot, where the change in within-cluster sum of squares decreases.

A two-medoids cluster analysis was also performed on the ONHM Dataset. Silhouette clustering for $k = 1$ to $k = 10$ confirmed the optimal number of clusters as two, average silhouette width = 0.49 (see Figure 50). The silhouette plot for $k = 2$ is shown in Figure 51. The two-medoids and two-means cluster analysis both resulted in identical cluster assignments for all specimens. The function *clusplot* in the *cluster* package was implemented in R to plot ellipses around the assigned clusters on the PCA plot (Figure 48).

The dendrogram, generated in an agglomerative hierarchical cluster analysis, shows two well supported clusters ($P = 74$), distinguishing between *T. truncatus* and *T. aduncus*-type

specimens (Figure 52). No misclassification between known *T. truncatus* and *T. aduncus*-type specimens was observed and there is no apparent morphological differentiation between the *T. aduncus*-types.

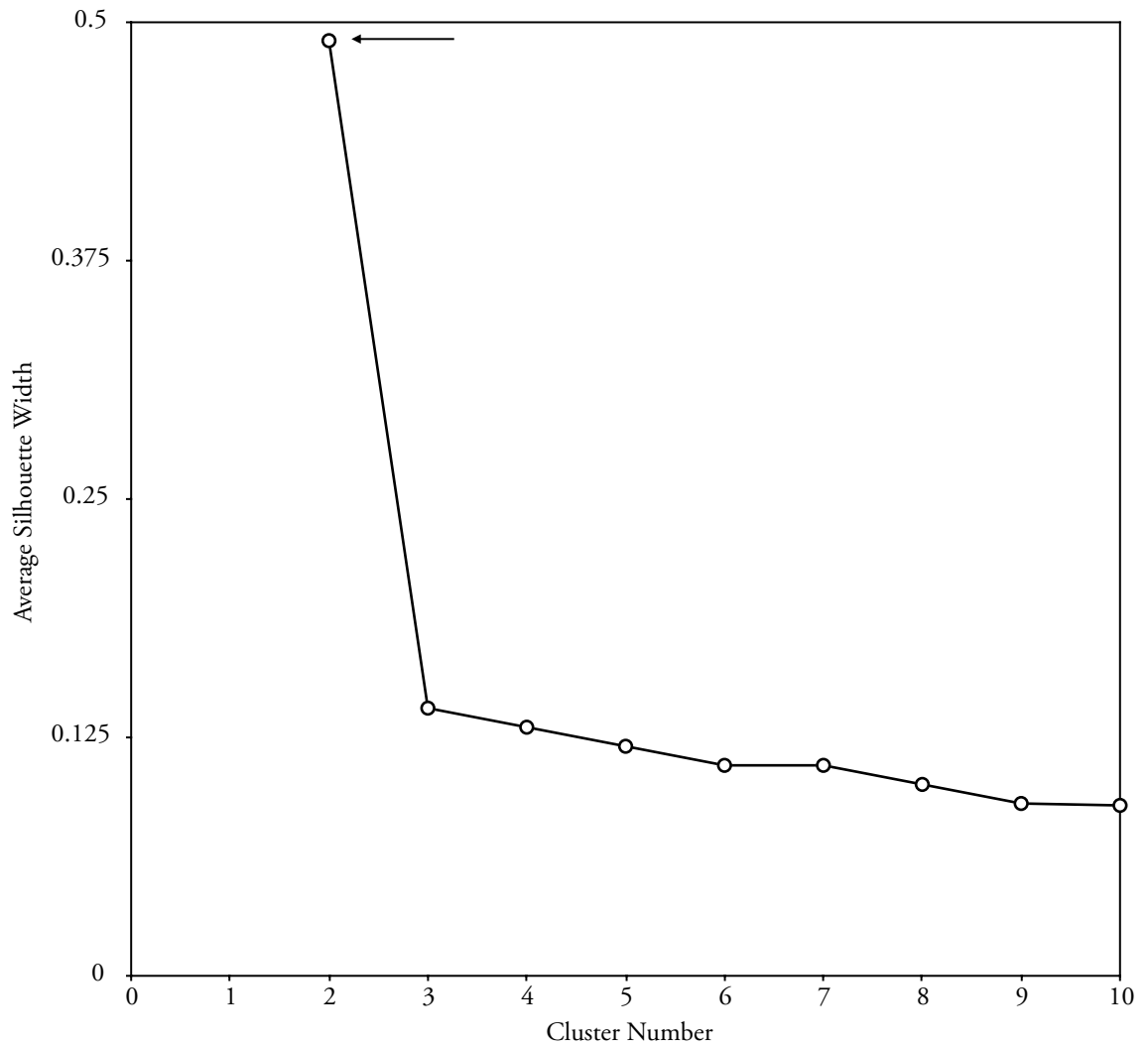


Figure 50: Average silhouette widths, considering different numbers of clusters, using the k -medoids algorithm on the ONHM Dataset. Arrow shows the highest average silhouette width (0.49), indicative of the most optimal number of clusters ($k = 2$).

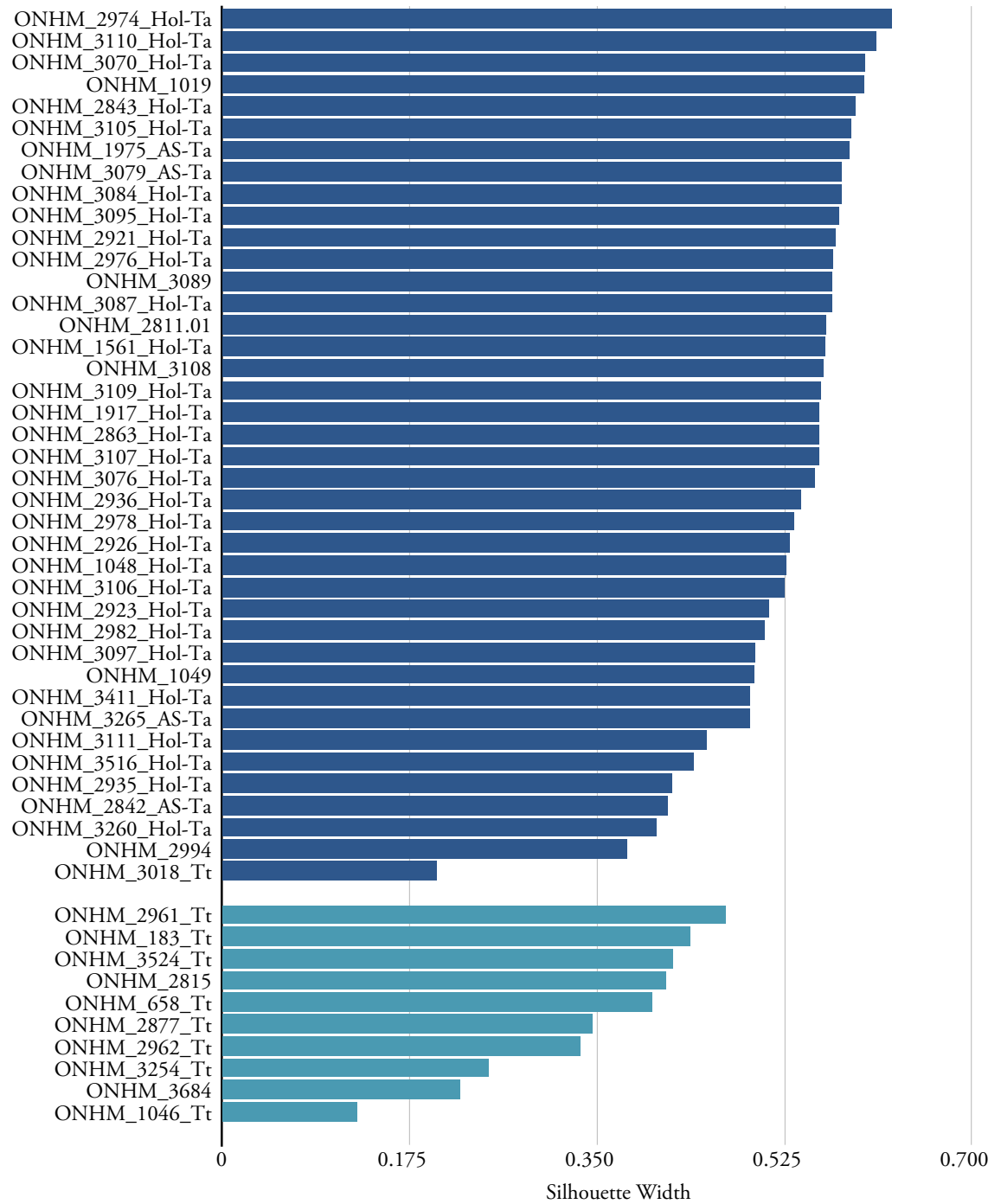


Figure 51: Silhouette plot for most optimal number of clusters ($k = 2$) for ONHM Dataset using the k -medoids clustering algorithm. Average silhouette width = 0.49; Dark blue bars = Cluster 1 (*T. aduncus*-type) and Light blue bars = Cluster 2 (*T. truncatus*-type).

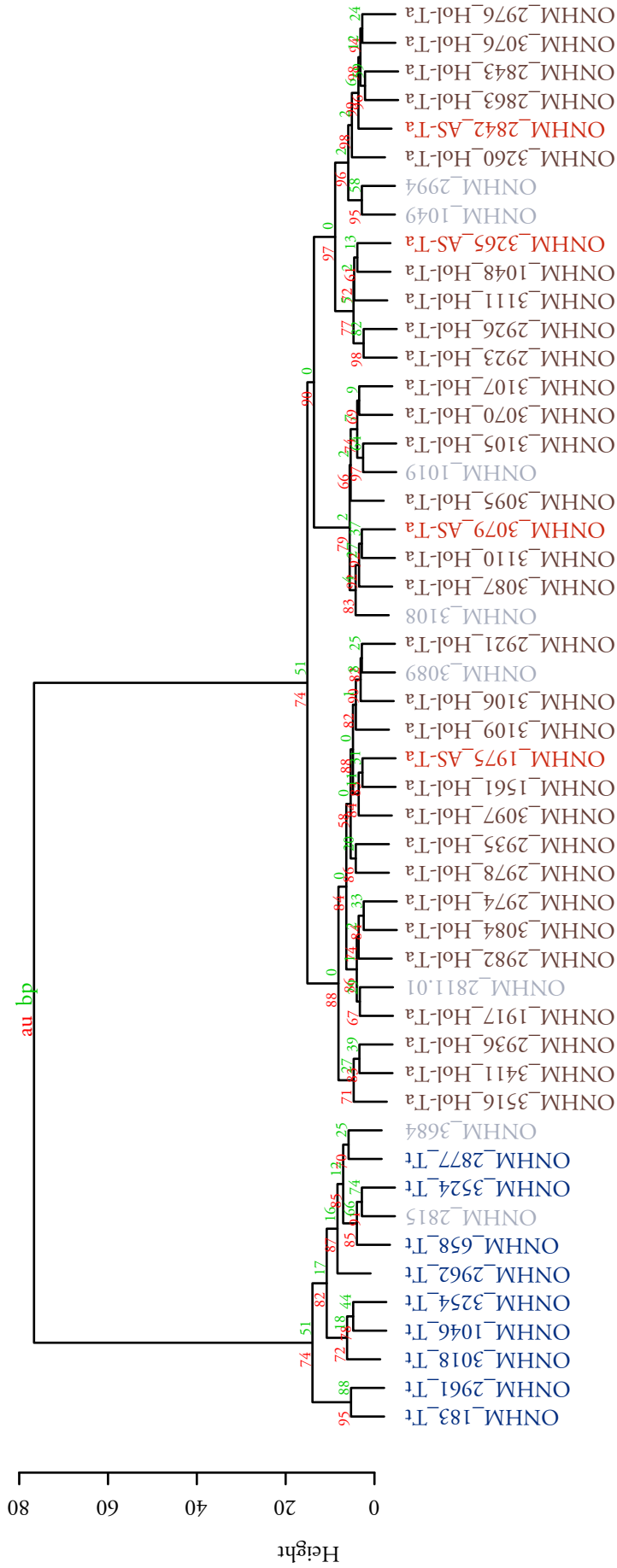


Figure 52: Hierarchical cluster analysis using ONHM Dataset.

4.3.3.5 Discriminant Function Analysis: ONHM Dataset

The DFA scatterplot of canonical scores clearly separates the groups, Hol-Ta, AS-Ta and Tt, into three clusters (Figure 53). The group-standardised coefficients of linear discriminants are listed in Table 29. For DF1, the characters contributing the most are CBL, RL, TREN, GPRW, ZW, RWB_{Perrin}, RWM, RW60 and GPARW. For DF2, the characters contributing the most are CBL, TREN, PRW, GPOW, GPRW, GWIN, RWM, UTLTR and GPARW. The percentage separations achieved by DF1 and DF2 are 96.22% and 3.78%, respectively and both DF1 (Wilks' lambda = 0.02, $F_{2,39} = 935, P < 0.001$) and DF2 (Wilks' lambda = 0.35, $F_{2,39} = 36.71, P < 0.001$) discriminate between the groups significantly. Twenty-one of the 26 measured characters differed significantly between groups (Wilks' lambda MANOVA = 0.01, $F_{52,28} = 5.86 P < 0.001$) (see Table 27).

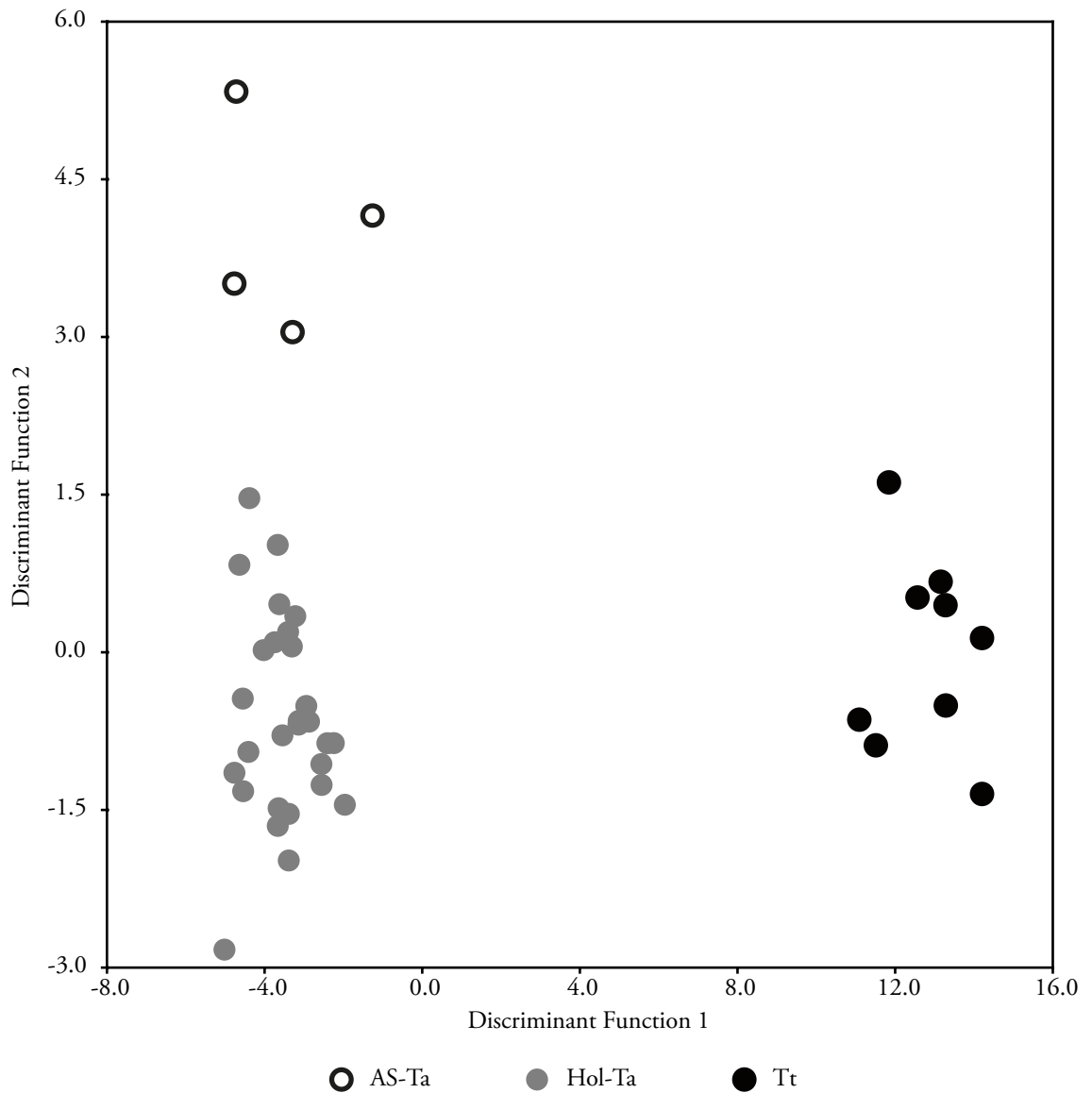


Figure 53: DFA for the ONHM Dataset.

Table 29: Group standardised coefficients of linear discriminants for all characters in the ONHM Dataset.

Character	DF1	DF2
TPC	-0.623	0.721
CBL	1.873	-1.367
RL	2.964	-0.753
TREN	-3.786	-0.817
GWEN	0.037	-0.315
GWPX	0.575	-1.022
PRW	-0.089	1.367
LWPTF	-0.872	0.031
PL	-0.21	-0.217
PWPT	0.385	0.267
GPOW	-0.085	1.686
GPRW	1.777	-1.535
ZW	-1.713	0.935
GWIN	0.535	-1.196
RWB _{Perrin}	-1.941	-0.082
RWB _{min}	0.646	0.25
RWM	1.434	-1.535
RW60	1.046	0.708
UTLTR	-0.469	1.581
GLPTF	-0.597	-0.114
GWPTF	0.096	-0.452
LO	0.127	0.822
LAL	0.712	-0.394
GPARG	-1.2	1.278
MXOC	-0.016	0.397
BCH	0.968	-0.884

Nine characters were retained in the stepwise DFA, where width characters, particularly rostral widths, were the most informative (Table 30). See Table 30 for group-standardised coefficients of linear discriminants and Figure 54 for the scatterplot of DF1 against DF2 for each specimen. The percentage separation achieved by DF1 and DF2 were 95.95% and 4.05%, respectively and both DF1 (Wilks' lambda = 0.06, $F_{2,39} = 305.44$, $P < 0.001$) and DF2 (Wilks' lambda = 0.60, $F_{2,39} = 12.90$, $P < 0.001$) discriminated between the groups significantly.

Cross-validation analysis scores were generated and are displayed in Table 30. Tt and Hol-Ta individuals were correctly assigned 100% of the time. However, the AS-Ta individuals had a high misclassification rate of 50%. While this could reflect a poor discrimination between the groups, the small sample size for AS-Ta ($n = 4$), in this analysis, should be noted.

Table 30: Stepwise-selection of characters for the ONHM Dataset. Characters were retained if the *P*-value (*P* difference) for the model that included the character remained below the significance threshold ($P < 0.2$). Group standardised coefficients of linear discriminants (DF1 & DF2) for the most important characters in ONHM Dataset are also shown.

Character	Wilks' λ	F Overall	<i>P</i>	F Difference	<i>P</i> Difference	DF1	DF2
RW60	0.2	77.888	2.40E-14	77.888	2.40E-14	0.853	-0.01
PRW	0.104	39.923	5.61E-18	17.588	3.59E-06	0.318	1.185
PWPT	0.077	31.986	1.10E-18	6.339	4.21E-03	0.526	0.304
RWB Perrin	0.07	25.015	6.11E-18	1.911	1.62E-01	-0.921	0.734
GPRW	0.058	22.114	6.13E-18	3.694	3.47E-02	0.737	-0.522
RWM	0.052	19.274	2.18E-17	2.036	1.46E-01	0.396	-1.058
GPARW	0.045	17.483	5.09E-17	2.385	1.07E-01	-0.347	0.869
GWPX	0.04	15.887	1.74E-16	1.839	1.75E-01	0.039	-0.828
GWIN	0.036	14.679	5.35E-16	1.859	1.72E-01	0.096	-0.677

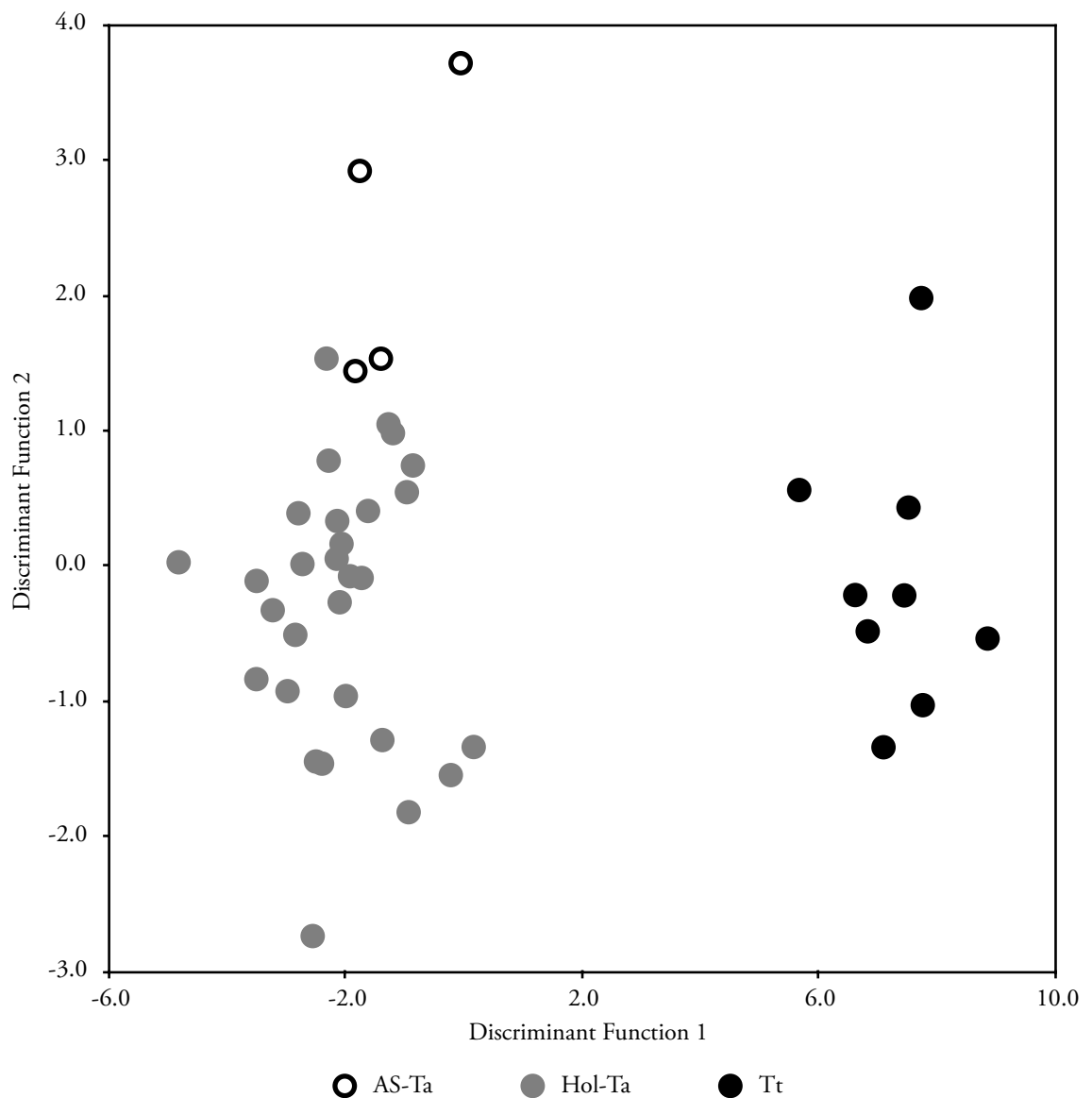


Figure 54: DFA considering only the most important characters for the ONHM Dataset.

Table 31: Cross-validation scores for ONHM Dataset.

True Group	Classified as AS-Ta	Classified as Hol-Ta	Classified as Tt	Misclassification n	Misclassification Rate (%)	Total n	Overall Misclassification Rate (%)
AS-Ta	2	2	0	4	50	42	5
Hol-Ta	0	29	0	29	0		
Tt	0	0	9	9	0		

4.3.3.6 Principal Component Analysis: Combined Dataset

Three PCs were identified based on a screeplot (see Figure 55) and account for 79.39% of the total variance, with PCs 1-3 explaining 57.31%, 13.89% and 8.19% of the variance, respectively. The loadings for each PC are shown in Table 32. Similar to the ONHM Dataset, PC1 is represented by length and width measurements pertaining to size e.g. CBL and ZW. Variation in the second PC seems to be predominantly explained by TPC, GWEN, GWPX, LWPTF, RWM, RW75% and GLPTF (see Table 25 for descriptions). The first PC differentiates well between individuals identified as *T. truncatus* from those identified as *T. aduncus* (Figure 56).

Table 32: Principal Component loadings for the Combined Dataset.

Character	PC 1	PC 2	PC 3
TPC	0.062	0.477	0.329
CBL	0.273	0.181	0.268
RL	0.235	0.271	0.362
GWEN	0.038	0.366	-0.481
GWPX	0.202	0.272	-0.137
PRW	0.272	-0.181	0.046
LWPTF	0.031	-0.368	0.207
GPOW	0.285	-0.074	-0.24
GPRW	0.252	-0.073	-0.22
ZW	0.297	-0.068	-0.117
GWIN	0.272	-0.139	-0.007
RWM	0.261	-0.26	-0.02
RW75%	0.237	-0.241	0.003
RW60	0.293	-0.095	0.02
UTLTR	0.252	0.192	0.332
GLPTF	0.192	0.254	-0.321
LO	0.231	0.109	-0.212
LAL	0.28	-0.082	0.124

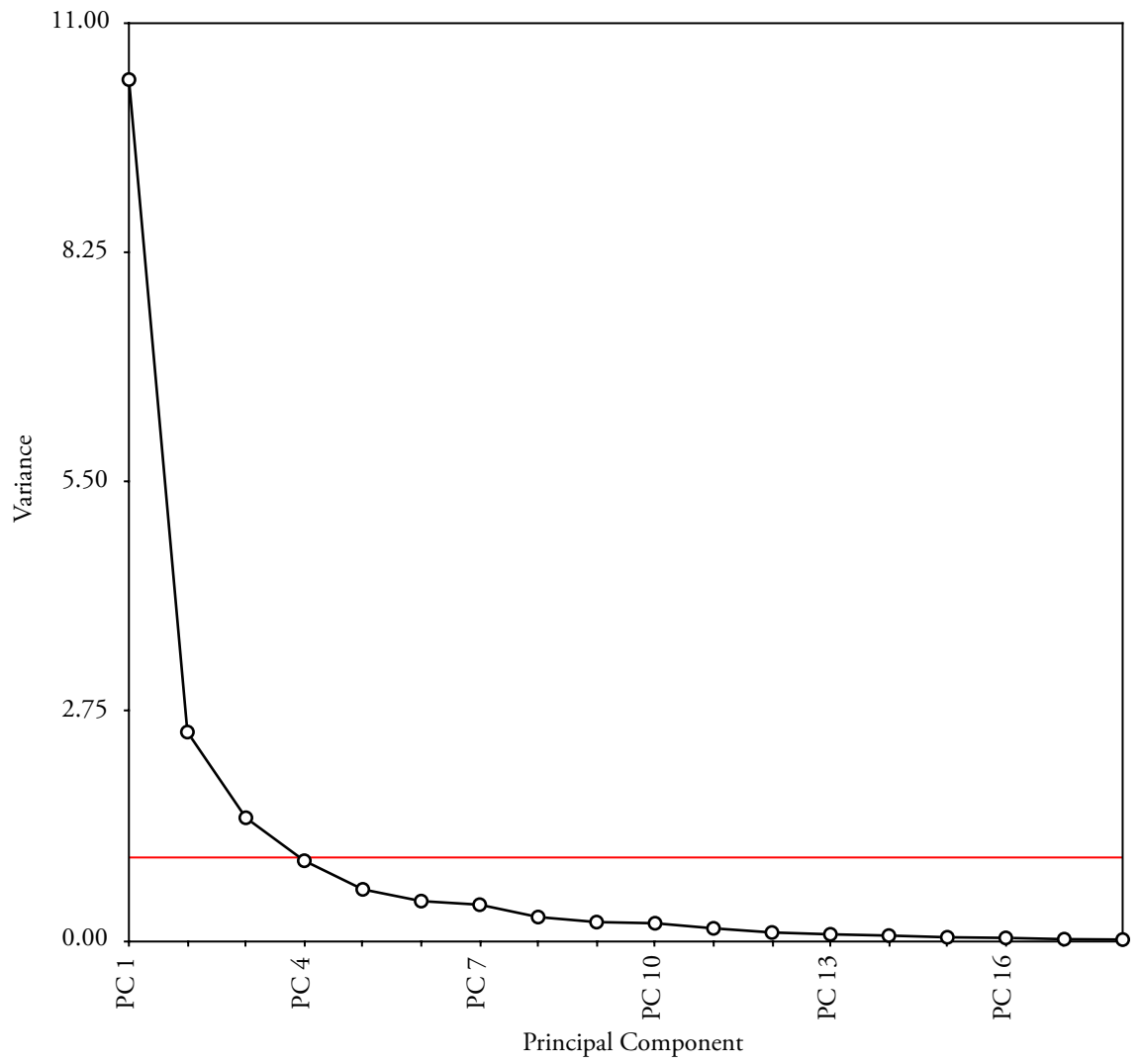


Figure 55: PCA screeplot illustrating the contribution of each PC to the total variance for the Combined Dataset. The red line illustrates the ‘elbow’ point, taken to be the number of PCs to consider describing the majority of the variation.

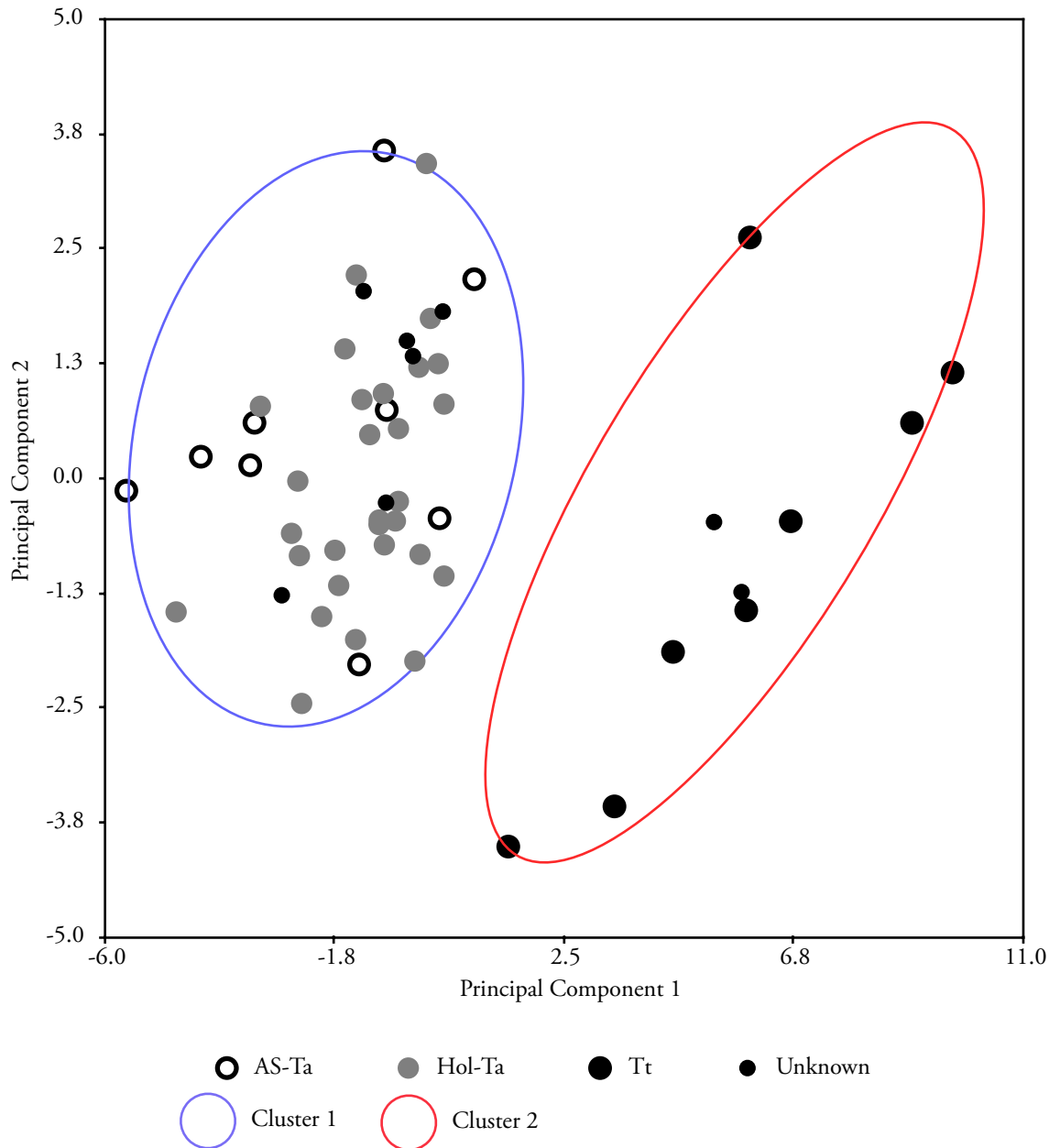


Figure 56: PCA on the Combined Dataset. Plot of PC1 against PC2. Specimens assigned to clusters based on the *k*-medoids algorithm.

4.3.3.7 Cluster Analyses: Combined Dataset

Examination of the within-cluster sum of squares plot (Figure 57), generated using the *k*-means algorithm, indicated the optimal value for *k* = 2. However due to a steady decrease in the within-cluster sum of squares values it is difficult to identify the correct number of clusters to consider. A two-means cluster analysis was performed generating two significantly different clusters ($F_{1,52} = 40.50, P < 0.001$).

Where specimens were genetically assigned to a lineage, all of the Hol-Ta (*n* = 29) and AS-

Ta ($n = 9$) specimens were assigned to Cluster 1 and the majority of Tt specimens ($n = 7/8$, 88.9%) were assigned to Cluster 2 with one Tt individual being incorrectly assigned to Cluster 1. Of the specimens where phylogenetic assignment was unknown ($n = 8$), six were assigned to Cluster 1 (*T. aduncus*-type) and two to Cluster 2 (*T. truncatus*-type). Again, the misclassification rate was low (2.38%) allowing for tentative assignment of specimens to either *T. truncatus* or *T. aduncus* based on their cluster assignments.

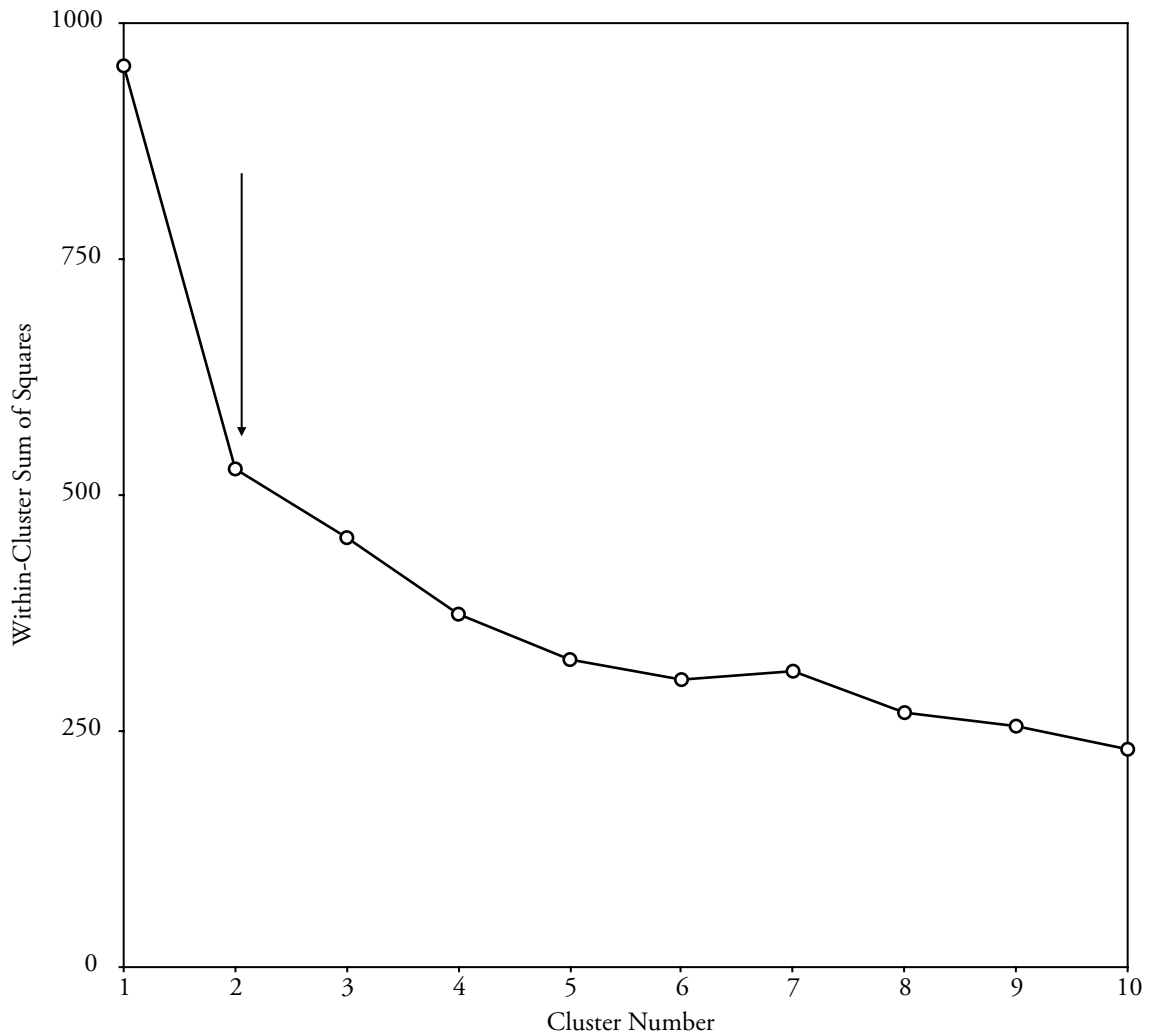


Figure 57: Within-cluster sum of squares for different numbers of clusters under the k -means cluster algorithm using the Combined Dataset. The arrow highlights the 'elbow' point in the plot, where the change in within-cluster sum of squares decreases

Silhouette clustering using the k -medoids clustering algorithm confirmed the optimal number of $k = 2$ (average silhouette width = 0.48) (Figure 58). The silhouette plot for $k = 2$ is shown in Figure 59. All *T. aduncus*-type specimens were assigned to Cluster 1 (Hol-Ta, $n = 29$; AS-Ta, $n = 9$) and, in contrast to the two-means clustering, all, known Tt individuals were assigned to Cluster 2 ($n = 8$). For the specimens where phylogenetic assignment was not available ($n = 8$), six were assigned to Cluster 1 and two to Cluster 2. When considering

only specimens with known lineage assignments based on mtDNA ($n = 46$), the k -medoids misclassification rate for the Combined Dataset was 0%. This result supports the classification of unidentified individuals as either *T. truncatus* or *T. aduncus*-type based on their cluster assignments. Ellipses were plotted around the assigned clusters on the PCA plot (Figure 56).

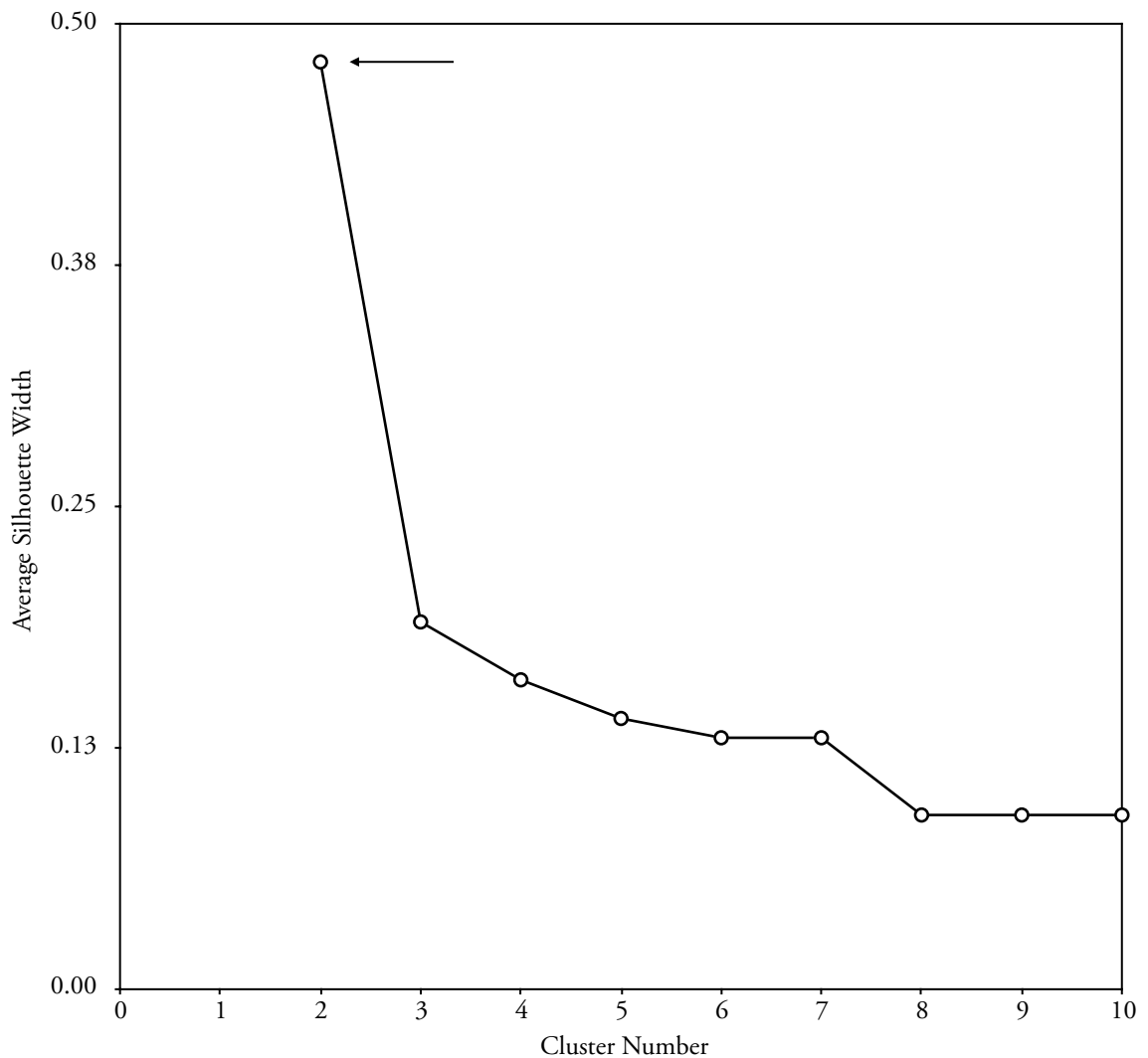


Figure 58: Average silhouette widths, considering different numbers of clusters (k), using the k -medoids algorithm on the Combined Dataset. Arrow shows the highest average silhouette width (0.49), indicative of the most optimal number of clusters ($k = 2$)

The dendrogram generated from the agglomerative hierarchical cluster analysis supported two major clusters, representing *T. truncatus* and *T. aduncus*-type specimens ($P = 89$) (Figure 60). Of the specimens where phylogenetic classification was known (based on mtDNA), no misclassifications were made between these two clusters. Within the *T. aduncus*-type cluster there is appears to be further partitioning into sub-clusters. However, there is no indication that these reflect geographic location or phylogenetic classification.

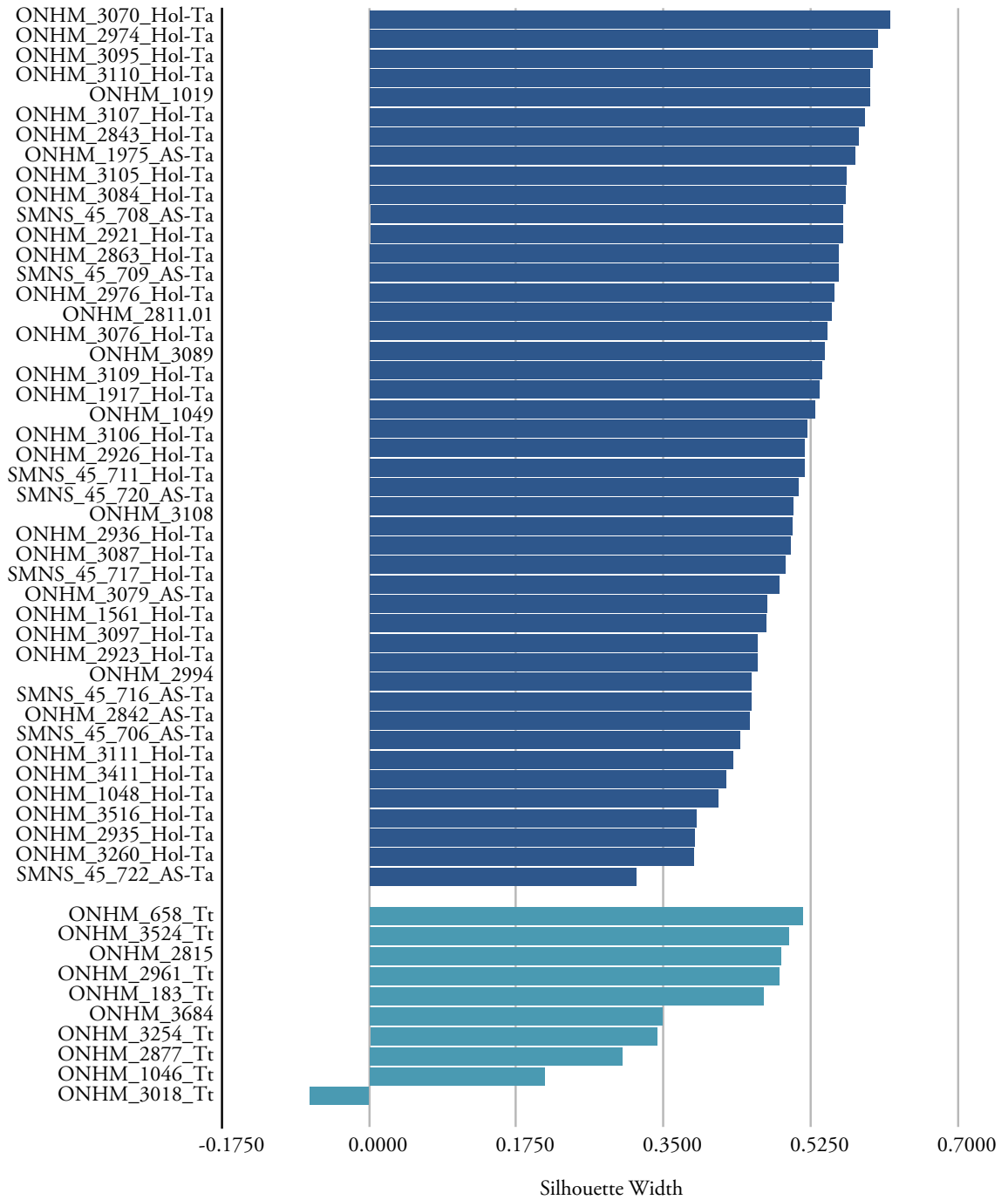


Figure 59: Silhouette plot for most optimal number of clusters ($k = 2$) for the Combined Dataset using the k -medioids clustering algorithm. Average silhouette width = 0.49; Dark blue bars = Cluster 1 (*T. aduncus*-type) and light blue bars = Cluster 2 (*T. truncatus*-type).

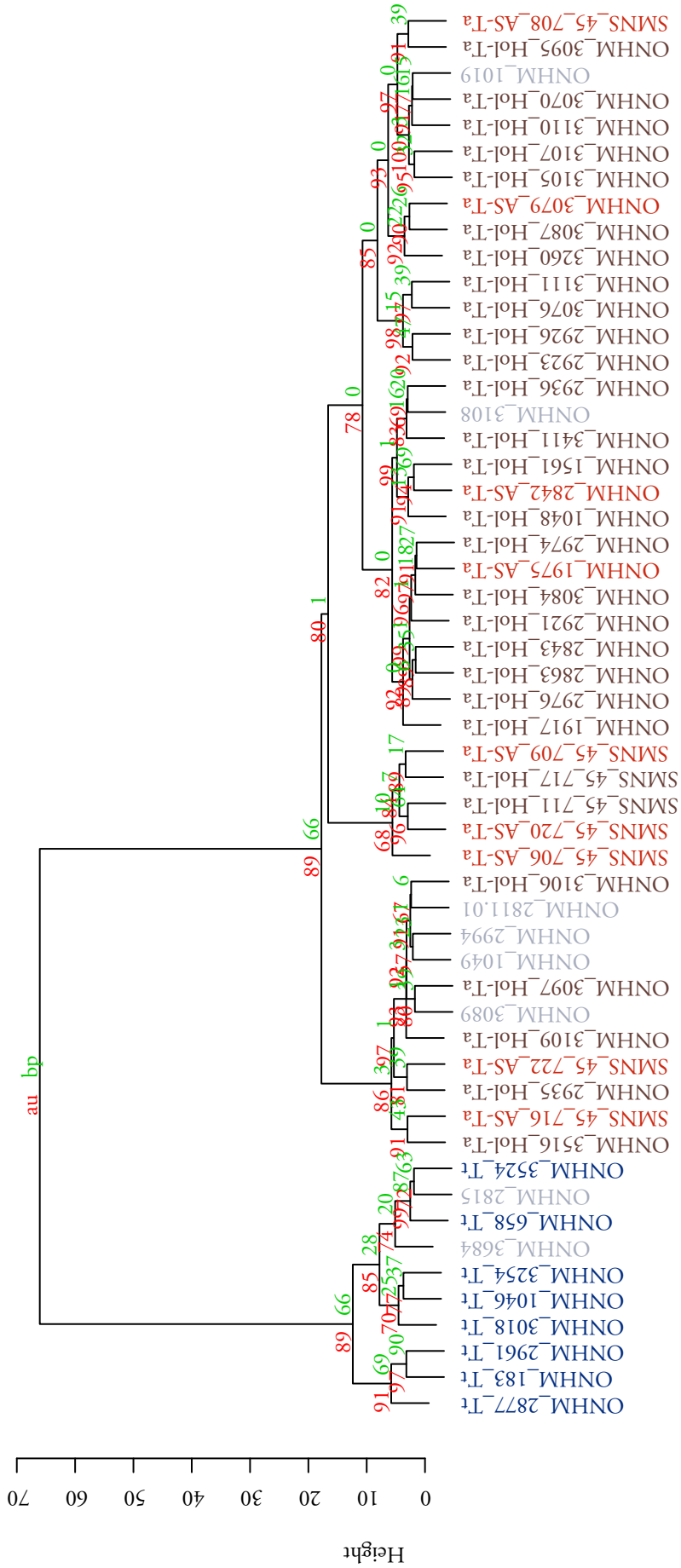


Figure 60: Hierarchical cluster analysis using Combined Dataset.

4.3.3.8 Discriminant Function Analysis: Combined Dataset

The DFA scatterplot of canonical scores separates the groups (Hol-Ta, AS-Ta and Tt) into three clusters, with some overlap between the Hol-Ta and AS-Ta groups (Figure 61). The group-standardised coefficients of linear discriminants are listed in Table 33. For DF1, the characters contributing the most to separation between groups are length measurements, CBL and RL. Characters contributing the most to DF2 are width measurements, ZW and GPOW. The percentage separation achieved by DF1 and DF2 are 87.53% and 12.47% respectively and both DF1 (Wilks' lambda = 0.07, $F_{2,43} = 270.75$, $P < 0.001$) and DF2 (Wilks' lambda = 0.35, $F_{2,43} = 38.586$, $P < 0.001$) discriminate between the groups significantly. Fourteen of the 18 measured characters differed significantly between groups (Wilks' lambda MANOVA = 0.02, $F_{36,52} = 8.00$ $P < 0.001$) (see Table 27).

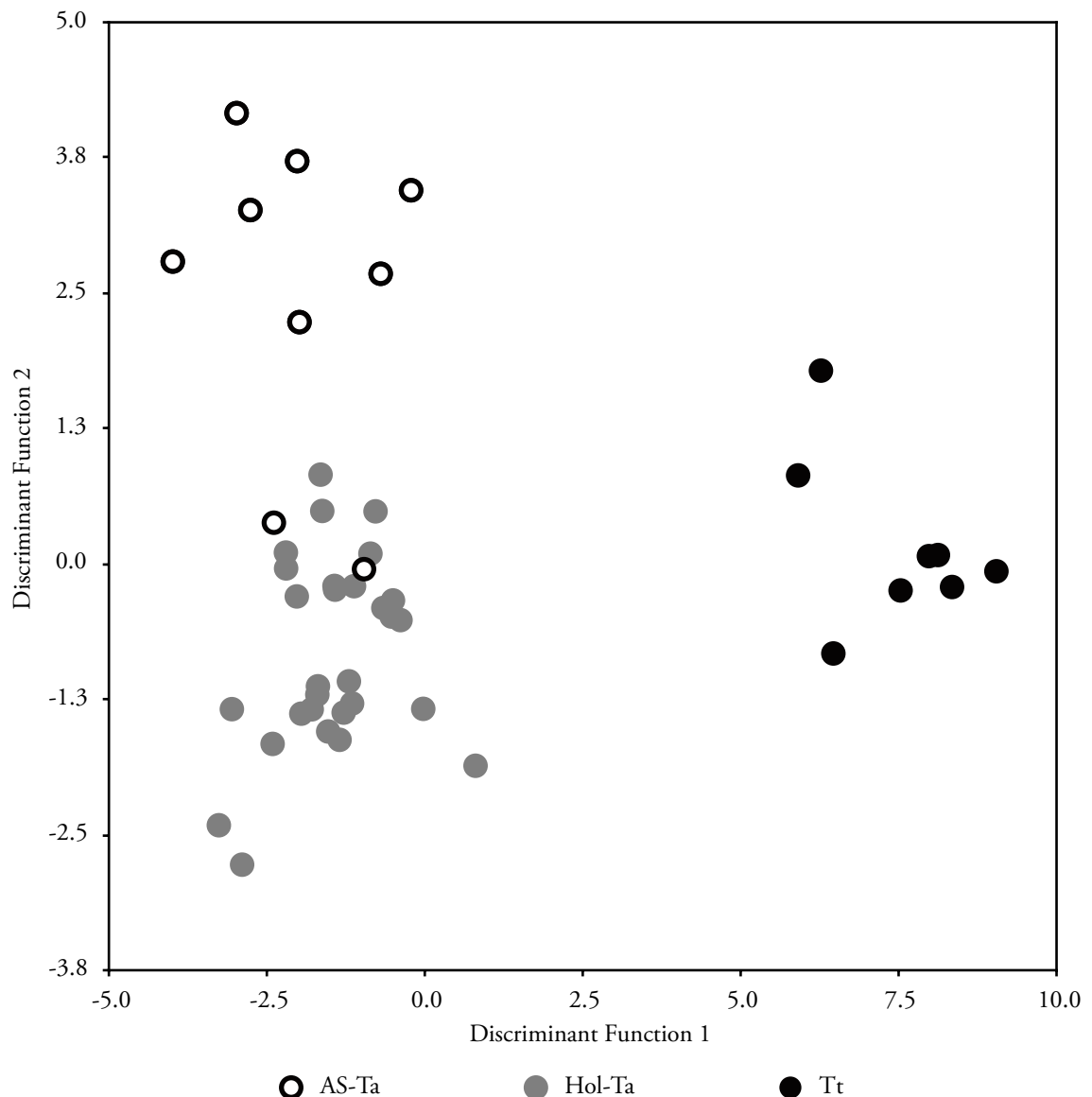


Figure 61: DFA considering the Combined Dataset.

Table 33: Group standardised coefficients of linear discriminants for the Combined Dataset.

Character	DF1	DF2
TPC	-0.395	-0.21
CBL	1.045	-0.921
RL	-1.152	0.608
GWEN	-0.461	-0.487
GWPX	0.23	-0.186
PRW	0.083	0.487
LWPTF	-0.723	0.158
GPOW	0.794	-2.526
GPRW	-0.205	-0.504
ZW	-0.331	3.146
GWIN	0.047	-0.242
RWM	0.757	-0.026
RW75%	-0.46	-0.774
RW60	0.427	-0.662
UTLTR	0.782	0.352
GLPTF	-0.961	0.581
LO	-0.138	0.502
LAL	0.432	0.191

For the Combined Dataset, eight characters were retained in a stepwise DFA. These were LAL and width measurements RWM, GPOW, ZW, RW60, LWPTF and GWEN. GLPTF was also an important measurement (see Table 34). A DFA using the most discriminative characters between groups was performed. For group-standardised coefficients of linear discriminants see Table 34 and for the scatterplot of DF1 against DF2 for each individual see Figure 62. Percentage separation achieved by DF1 was 88.04% and was significant (Wilks' lambda = 0.10, $F_{2,43} = 187.59$, $P < 0.001$). Separation was also significant for DF2 (11.96%), (Wilks' lambda = 0.46, $F_{2,43} = 25.489$, $P < 0.001$).

Table 34: Stepwise-selection of characters for the Combined Dataset. Characters were retained if the P -value (P difference) for the model that included the character remained below the significance threshold ($P < 0.2$). Group standardised coefficients of linear discriminants (DF1 & DF2) also shown.

Character	Wilks' λ	F Overall	P	F	P	DF1	DF2
				Difference	Difference		
LAL	0.211	80.322	3.01E-15	80.322	3.01E-15	0.777	0.195
RWM	0.139	35.304	2.80E-17	10.875	1.51E-04	0.515	-0.176
GPOW	0.118	26.121	3.74E-17	3.671	3.39E-02	0.489	-2.453
ZW	0.082	25.02	7.82E-19	8.94	6.00E-04	-0.311	2.476
RW60	0.072	21.239	1.99E-18	2.538	9.17E-02	0.501	-0.403
GLPTF	0.064	18.616	5.50E-18	2.273	1.16E-01	-0.737	0.435
LWPTF	0.053	17.717	3.12E-18	4.077	2.49E-02	-0.643	-0.093
GWEN	0.047	16.246	7.83E-18	2.2	1.25E-01	-0.26	-0.45

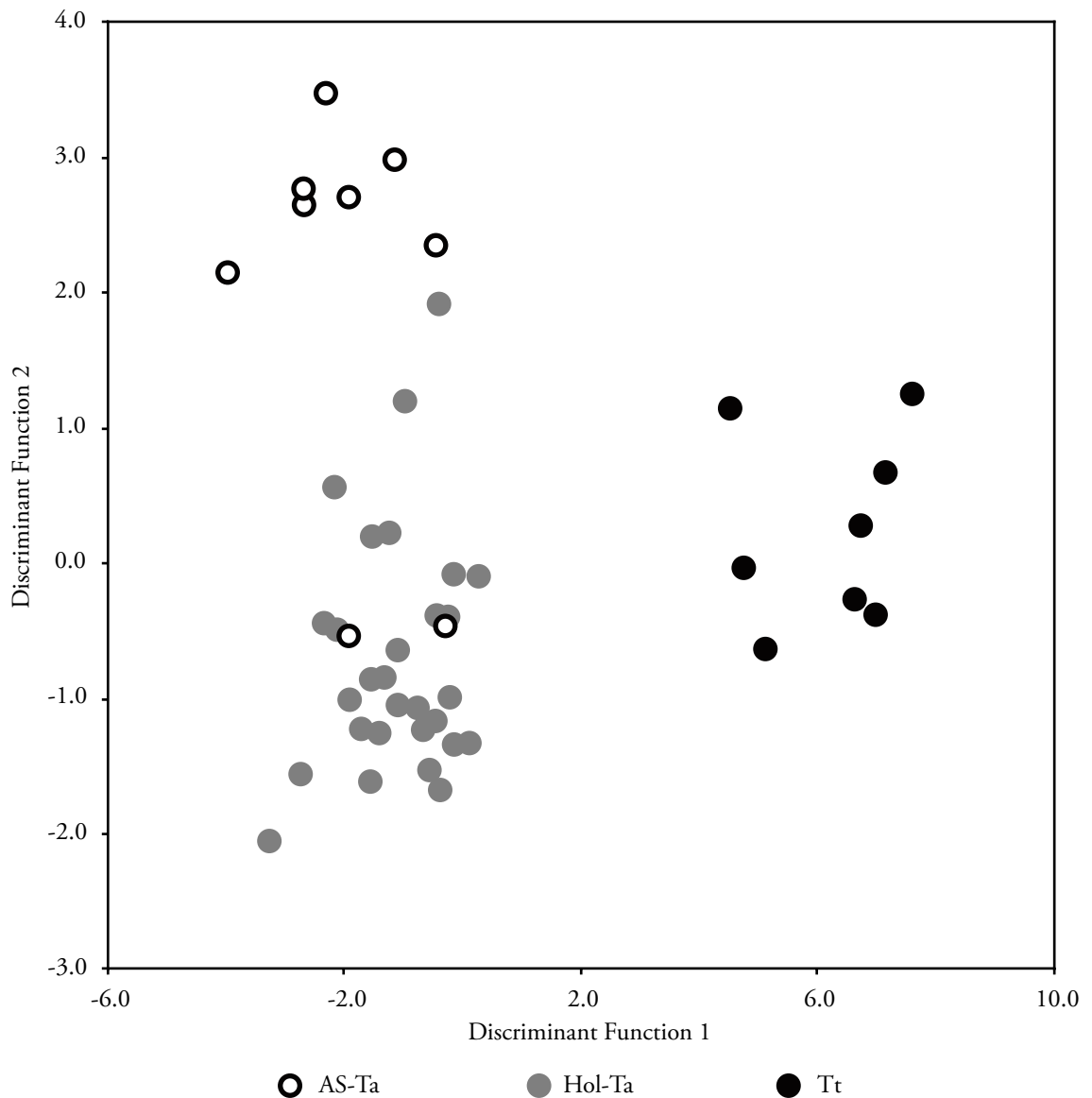


Figure 62: DFA considering only the most important characters for the Combined Dataset.

To identify which characters discriminated the best between each pair of groups (Hol-Ta, AS-Ta and Tt), a pairwise, stepwise, DFA was carried out. Significant differences between the *T. aduncus*-types (Hol-Ta and AS-Ta) were revealed (Wilks' lambda = 0.42, $F_{1,36} = 49.21$, $P < 0.001$). The characters which discriminated the best between *T. aduncus*-types were, in order of importance, GPOW, ZW, RW60, LO and RWM. However, there was overlap in the lengths of all characters examined. Significant differences were also determined between *T. truncatus* and *T. aduncus*-types (AS-Ta/Tt, Wilks' lambda = 0.087, $F_{1,15} = 156.6$, $P < 0.001$; Hol-Ta/Tt, Wilks' lambda = 0.037, $F_{1,35} = 911.8$, $P < 0.001$). Refer to Table 35 for the group-standardised coefficients of linear discriminants for the pairwise comparisons to see which characters discriminated the most between the different groups. The ratio of the rostral

width at 60 mm from the base (RW60) to zygomatic width (ZW) was particularly useful at discriminating between *T. truncatus* and *T. aduncus*-types without overlap (Figure 63).

Table 35: Pairwise DFA group standardised coefficients of linear discriminants for most important characters.

Hol-Ta/AS-Ta		Hol-Ta/Tt		AS-Ta/Tt	
Character	DF1	Character	DF1	Character	DF1
GPOW	2.679	RW60	1.361	LAL	0.853
ZW	-2.713	GLPTF	-0.827	TPC	-0.61
RW60	0.445	PRW	0.841	PRW	0.397
LO	-0.768	UTLTR	1.012		
RWM	0.473	TPC	-1.234		
		LWPTF	-0.485		
		GPRW	1.751		
		GPOW	-0.898		

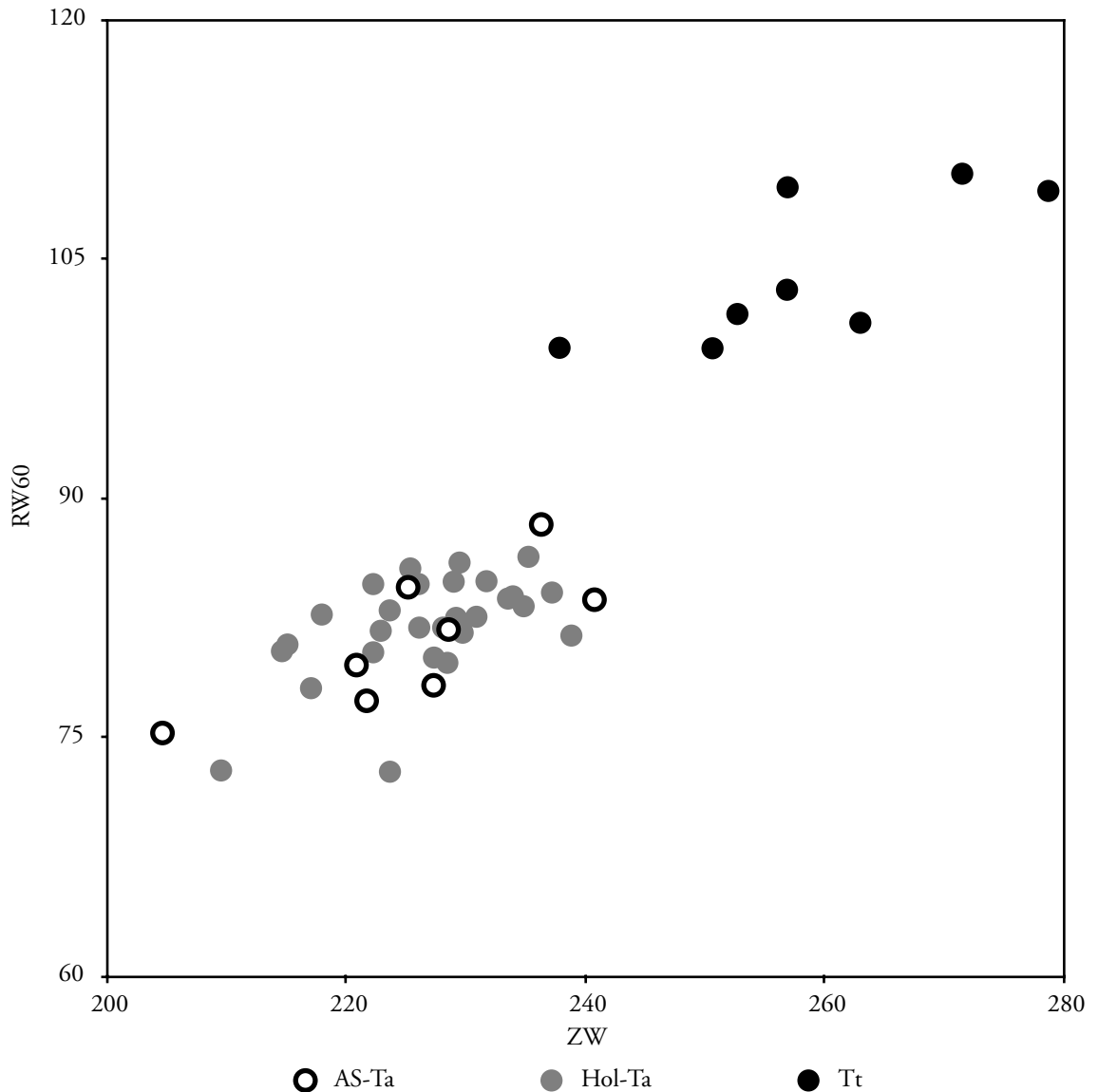


Figure 63: Plot of RW60 against ZW. Discrimination, without overlap, between *T. truncatus* and *T. aduncus*-types illustrated.

Leave-one-out cross validation results for the Combined Dataset revealed a 33% misclassification rate for AS-Ta individuals and 10% for Hol-Ta individuals. All Tt individuals were correctly assigned (Table 36). Overall misclassification rate was 13%. Misclassification rates within the *T. aduncus*-type individuals suggest that the morphologies of Hol-Ta and AS-Ta overlap.

Table 36: Cross-validation scores for the Combined Dataset.

True Group	Classified as AS-Ta	Classified as Hol-Ta	Classified as Tt	<i>n</i>	Misclassification Rate (%)	Total <i>n</i>	Overall Misclassification Rate (%)
AS-Ta	6	3	0	9	33	46	13
Hol-Ta	3	26	0	29	10		
Tt	0	0	8	8	0		

4.3.4 Geometric Morphometrics

4.3.4.1 Data Truncation

Investigation of LM digitization repeatability showed that all LMs across all aspects (ventral, dorsal and lateral) could be reliably digitized based on a PCA plot showing repeats clustered tightly per specimen, thus indicating that precision errors in landmark digitization were minimal compared to inter-specimen variation. Further to this, average percentage errors for all LMs (Singleton, 2002) were < 1% and so all were considered repeatable.

Two landmarks had an average percentage error > 1.5% across all specimens (LM4, 1.85% and LM5, 2.81% in lateral aspect) and were therefore omitted from analyses (see Table 26). One individual was removed from the dorsal aspect dataset because it was missing too many LMs.

Landmark and specimen numbers for the final datasets were as follows: (i) 10 LMs in dorsal aspect (Hol-Ta, $n = 32$; AS-Ta, $n = 10$; Tt, $n = 9$; unknown, $n = 8$), (ii) 13 LMs in ventral aspect (Hol-Ta, $n = 33$; AS-Ta, $n = 10$; Tt, $n = 9$; unknown, $n = 8$), and (iii) 14 LMs in lateral aspect (Hol-Ta, $n = 33$; AS-Ta, $n = 10$; Tt, $n = 9$; unknown, $n = 8$).

4.3.4.2 Principal Component Analysis

Morphological relationships were explored using PCA in dorsal, ventral and lateral aspect. Principal components (PCs) were considered important when the total explained variance was > 80% and when they were supported by an elbow in a screeplot (see Figure 64).

In dorsal aspect, PCs 1-5 accounted for 81.00% of the total variance, explaining 31.49%, 20.80%, 14.26%, 9.07% and 5.37%, respectively. These five PCs showed significant dorsal shape differences between genetically assigned groups (Wilks' lambda MANOVA = 0.40, $F_{10,88} = 5.49$, $P < 0.001$). In ventral aspect, PCs 1-7 accounted for 83.06% of the total variance, explaining 25.25%, 23.08%, 10.98%, 7.85%, 6.63%, 6.61% and 3.71%, respectively. A MANOVA on these PCs revealed significant differences between genetically assigned groups in ventral shape (Wilks' lambda MANOVA = 0.18, $F_{14,86} = 8.49$, $P < 0.001$). For the lateral aspect, PCs 1-8 accounted for 81.88% of the total variation, explaining 20.63%, 15.18%, 14.84%, 9.00%, 6.82%, 6.81%, 5.39% and 3.95%, respectively. Significant differences in lateral shape between groups were supported by a MANOVA using these PCs

(Wilks' lambda MANOVA = 0.21, $F_{16, 84} = 6.15$, $P < 0.001$). PC coefficients are listed for each aspect in Table 37, Table 38 and Table 39.

Scatterplots of the first two principal components were plotted for each aspect and accounted for 52.29%, 48.33% and 35.81% of the total variation in dorsal, ventral and lateral aspect, respectively. For the dorsal aspect (Figure 65), separation between *T. truncatus* and *T. aduncus*-type specimens was achieved at the extremes of PC1. The same holds true for PC2 in ventral aspect (Figure 66) and PC1 in lateral aspect (Figure 67). The *T. aduncus*-types (Hol-Ta and AS-Ta) were less well separated with almost no separation in dorsal and ventral aspect on PC1 and PC2 respectively. In contrast, separation was achieved between *T. aduncus*-types in lateral aspect along PC2. Exploration of all other PCs did not reveal further morphological separation between the groups.

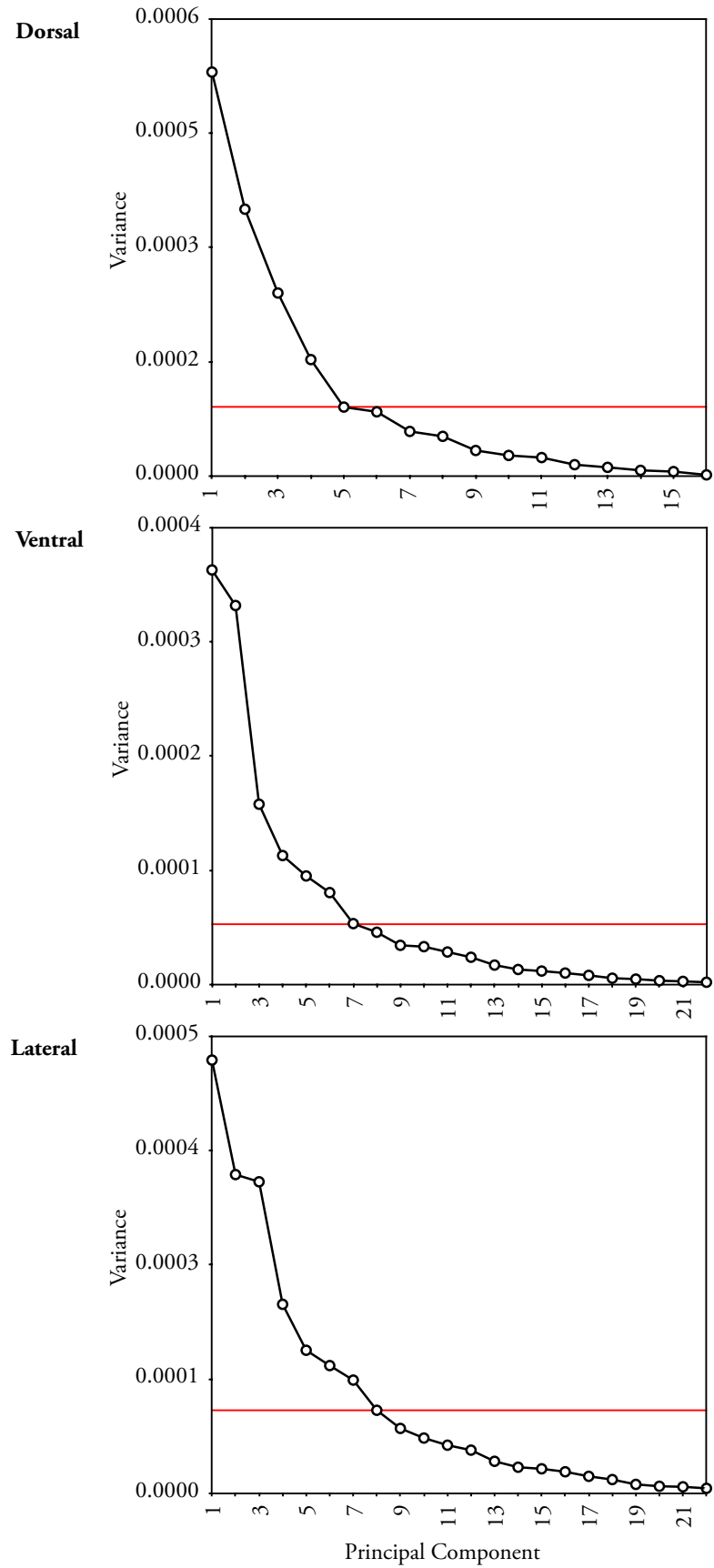


Figure 64: PCA screeplots for dorsal, ventral and lateral aspect. PCA scree-plots for dorsal, ventral and lateral aspect. The red line highlights the ‘elbow’ in the plot where components explain >80% of the variance in the data. All variance explained by components beyond this point is considered small.

Table 37: Dorsal Principal Component (PC) Coefficients for each Landmark (LM).

LM	PC 1	PC 2	PC 3	PC 4	PC 5
x1	0.129	-0.409	-0.156	-0.021	0.047
y1	0.118	-0.045	0.101	-0.15	-0.171
x2	0.056	0.354	0.148	0.335	0.121
y2	0.101	0.055	-0.025	0.02	0.014
x3	0.049	0.39	0.059	0.121	-0.573
y3	-0.002	0.264	-0.005	0.015	0.417
x4	0.362	0.102	-0.418	-0.4	-0.121
y4	-0.011	0.268	-0.187	-0.493	0.12
x5	0.647	-0.308	0.246	0.115	0.14
y5	-0.083	-0.191	0.69	-0.377	-0.055
x6	-0.373	-0.321	-0.178	-0.005	0.269
y6	-0.043	-0.157	-0.176	0.308	0.029
x7	-0.355	-0.131	0.031	-0.08	-0.159
y7	-0.04	-0.09	-0.095	0.258	-0.135
x8	-0.313	-0.101	-0.05	-0.148	-0.233
y8	-0.023	-0.098	-0.1	0.221	-0.09
x9	-0.08	0.23	0.026	-0.07	0.449
y9	-0.069	0.035	-0.093	0.149	-0.002
x10	-0.123	0.194	0.293	0.152	0.06
y10	0.052	-0.042	-0.11	0.048	-0.126

Table 38: Ventral Principal Component (PC) Coefficients for each Landmark (LM).

LM	PC 1	PC 2	PC 3	PC 4	PC 5	PC 6	PC 7
x1	-0.463	0.295	-0.017	-0.302	-0.042	0.03	0.086
y1	0.018	-0.23	-0.347	-0.304	0.143	0.116	-0.211
x2	-0.157	-0.348	0.212	0.324	-0.04	0.026	-0.162
y2	-0.102	0.092	-0.035	0.221	-0.178	-0.084	0.246
x3	0.016	0.057	0.261	0.221	-0.115	0.211	-0.383
y3	-0.147	0.269	-0.115	0.186	-0.149	-0.042	0.024
x4	0.017	0.161	0.211	0.193	0.077	0.275	0.125
y4	-0.212	0.326	-0.228	0.164	0.002	-0.152	0.005
x5	0.055	0.314	0.091	0.074	0.397	0.272	0.309
y5	0.003	0.202	-0.165	-0.037	0.234	-0.025	-0.312
x6	-0.246	-0.093	0.225	0.023	-0.17	-0.446	-0.268
y6	-0.235	-0.259	-0.275	0.209	-0.09	0.56	-0.163
x7	-0.257	-0.158	-0.042	-0.239	0.013	-0.08	0.092
y7	0.098	-0.228	0.084	-0.109	0.016	0.013	0.075
x8	-0.234	-0.192	-0.058	-0.386	0.002	0.021	0.204
y8	0.143	-0.165	0.17	-0.106	0.119	0.016	0.072
x9	0.3	0.138	0.048	-0.266	0.145	0.131	-0.192
y9	0.068	0.15	0.128	-0.11	0.075	-0.201	-0.298
x10	0.342	0.112	-0.068	-0.083	-0.163	0.035	-0.117
y10	0.081	0.081	0.16	-0.038	-0.035	-0.074	-0.044
x11	0.365	0.099	-0.332	-0.036	-0.501	-0.07	0.036

LM	PC 1	PC 2	PC 3	PC 4	PC 5	PC 6	PC 7
y11	0.085	-0.113	0.304	-0.082	0.072	0.016	0.11
x12	0.149	-0.203	-0.219	0.138	-0.139	-0.007	0.222
y12	0.119	-0.083	0.214	-0.021	-0.083	-0.06	0.157
x13	0.111	-0.182	-0.311	0.339	0.535	-0.399	0.048
y13	0.079	-0.042	0.106	0.028	-0.124	-0.081	0.339

Table 39: Lateral Principal Component (PC) Coefficients for each Landmark (LM).

LM	PC 1	PC 2	PC 3	PC 4	PC 5	PC 6	PC 7	PC 8
x1	0.333	-0.022	0.486	0.046	0.123	0.116	-0.25	0.163
y1	0.203	-0.099	-0.358	0.256	0.02	0.176	-0.144	0.212
x2	-0.485	-0.04	-0.21	0.127	0.266	-0.442	-0.315	-0.249
y2	0.095	0.099	0.042	0.111	0.092	-0.154	0.035	-0.216
x3	-0.289	0.285	-0.084	-0.047	-0.396	0.115	0.093	0.186
y3	0.068	-0.097	0.165	-0.33	-0.224	-0.165	-0.086	0.005
x4	-0.048	0.306	-0.162	-0.121	-0.252	0.123	-0.053	0.07
y4	0.011	-0.138	0.148	-0.37	-0.211	-0.185	-0.108	0.105
x5	-0.28	-0.127	0.112	-0.021	0.407	-0.008	0.487	0.414
y5	0.075	0.002	0.284	0.105	0.253	-0.141	0.174	0.141
x6	-0.145	0.175	0.287	-0.042	0.001	0.064	0.042	-0.182
y6	-0.084	-0.026	0.097	0.284	-0.176	-0.355	-0.088	0.027
x7	-0.051	0.099	0.305	0.261	-0.079	0.026	-0.099	-0.14
y7	-0.084	0.053	-0.098	0.287	-0.13	-0.078	-0.104	0.55
x8	-0.135	-0.337	0.13	0.09	-0.016	0.427	-0.258	-0.113
y8	0.172	0.125	-0.096	0.302	0.037	0.142	0.009	-0.143
x9	0.301	-0.06	-0.155	-0.082	0.169	-0.033	-0.27	0.05
y9	0.037	0.041	-0.178	-0.02	0.193	0.168	0.265	-0.252
x10	0.274	0.295	-0.118	-0.19	0.118	-0.145	0.058	0.022
y10	-0.101	-0.211	-0.036	-0.309	0.101	0.149	0.031	-0.065
x11	0.22	0.291	-0.15	-0.183	0.095	-0.17	0.05	0.001
y11	-0.178	-0.167	-0.044	-0.246	-0.036	0.009	-0.106	0.012
x12	0.021	-0.186	-0.191	0.04	-0.058	0.089	-0.033	-0.039
y12	-0.117	0.115	-0.01	-0.13	0.039	0.23	0.007	-0.001
x13	0.115	-0.351	-0.239	-0.076	0.058	-0.042	0.048	0.013
y13	-0.163	0.229	0.022	0.038	0.062	0.311	0.037	-0.126
x14	0.169	-0.329	-0.011	0.198	-0.438	-0.121	0.499	-0.196
y14	0.066	0.074	0.062	0.022	-0.019	-0.106	0.079	-0.248

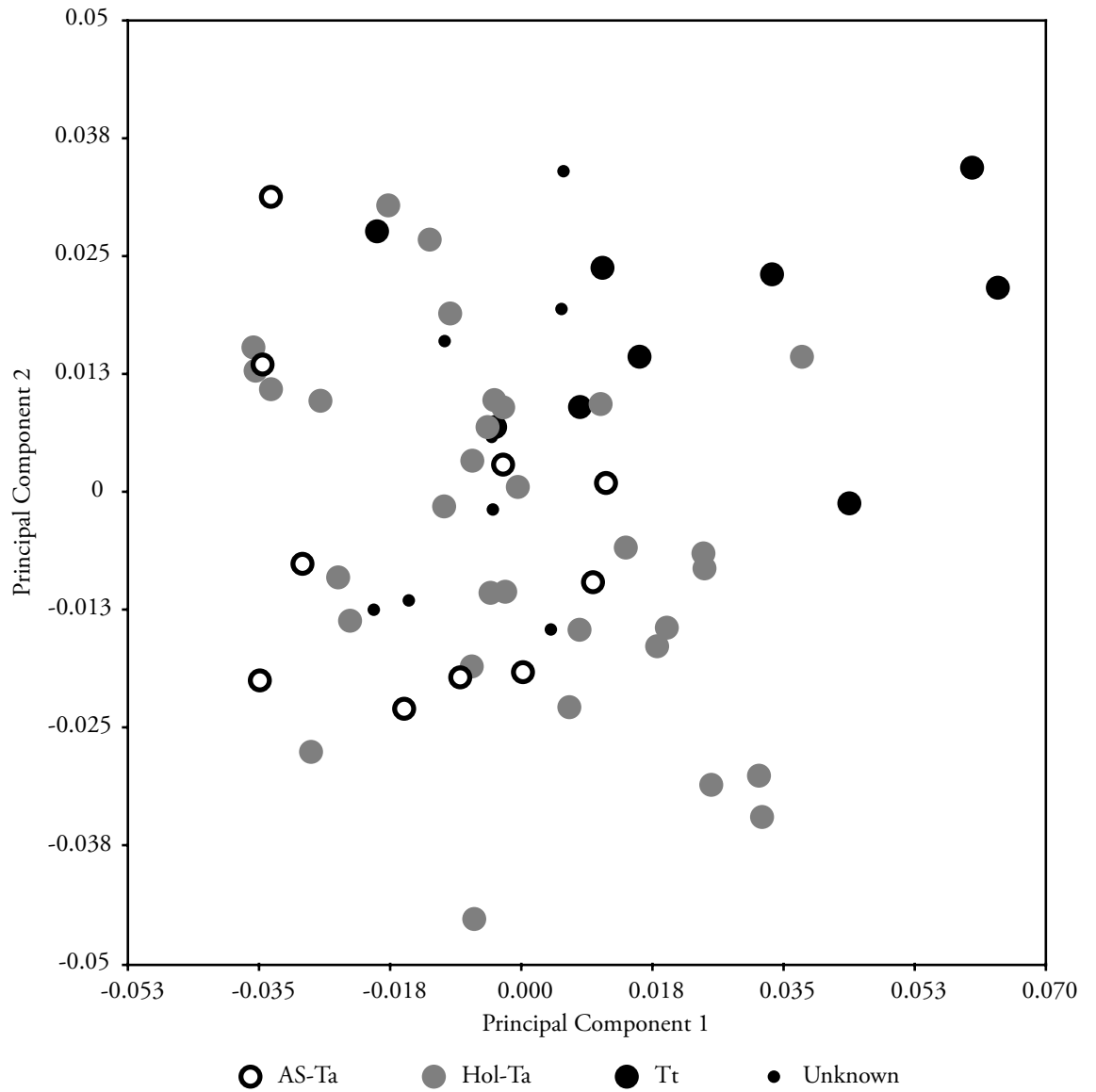


Figure 65: PCA in Dorsal aspect. Plot of PC1 against PC2.

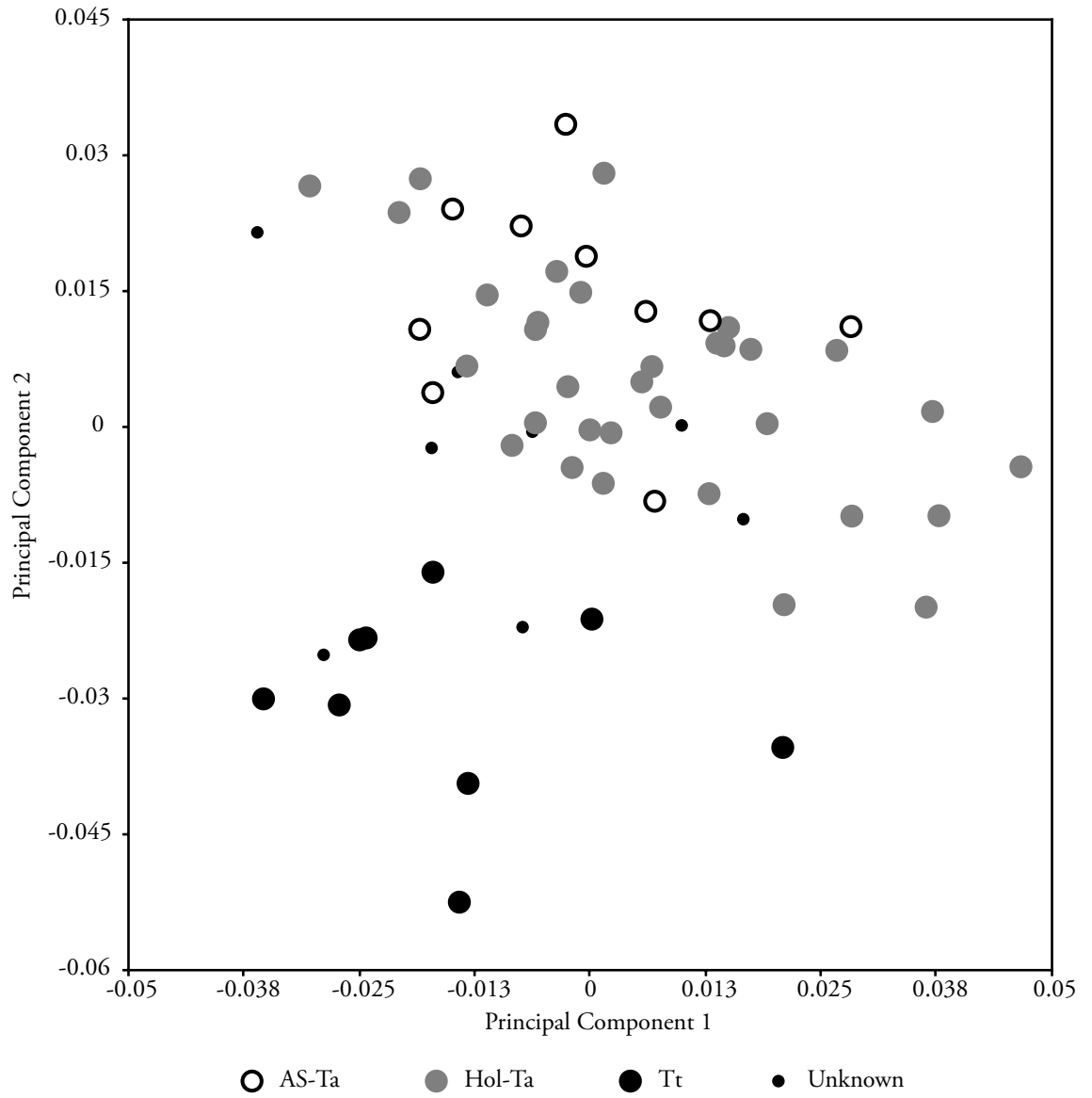


Figure 66: PCA in Ventral aspect. Plot of PC1 against PC2.

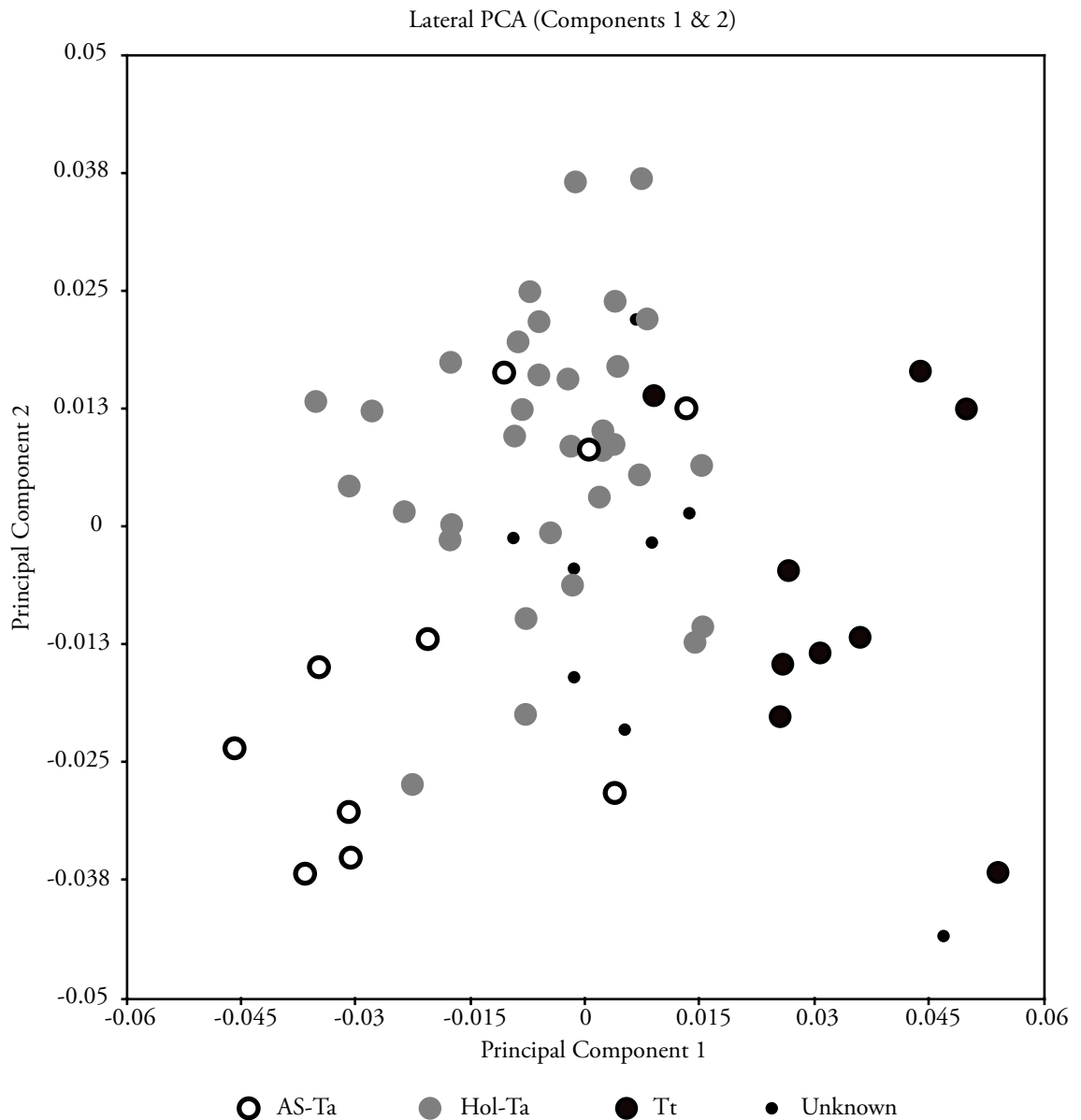


Figure 67: PCA in Lateral aspect. Plot of PC1 against PC2.

4.3.4.3 Visualisation of Shape Differences

Thin-plate spline transformation grids and wireframe graphs were generated to visualise the shape changes at the extremes of PCs 1 and 2 for each aspect (Figure 68). From these, the main shape changes involve the relative position of the posteriormost point of the temporal crest to the posterior features of the skull and are happening along PC1 in dorsal aspect, PC2 in ventral and PC1 in lateral aspect. Other features that change along these PCs include the relative position of the suture between the nasals and the ethmoid bone in dorsal aspect, the anteriormost point of the antorbital notch in ventral aspect and the relative positioning of the premaxillary convexity, in lateral aspect. Along PC2 in lateral aspect, where the two *T. aduncus*-type groups appear to have separated the most, the shape differences involve the

relative positioning of the premaxillary convexity, lacrimal bone, antorbital notch, zygomatic process and posteriormost point of the temporal crest.

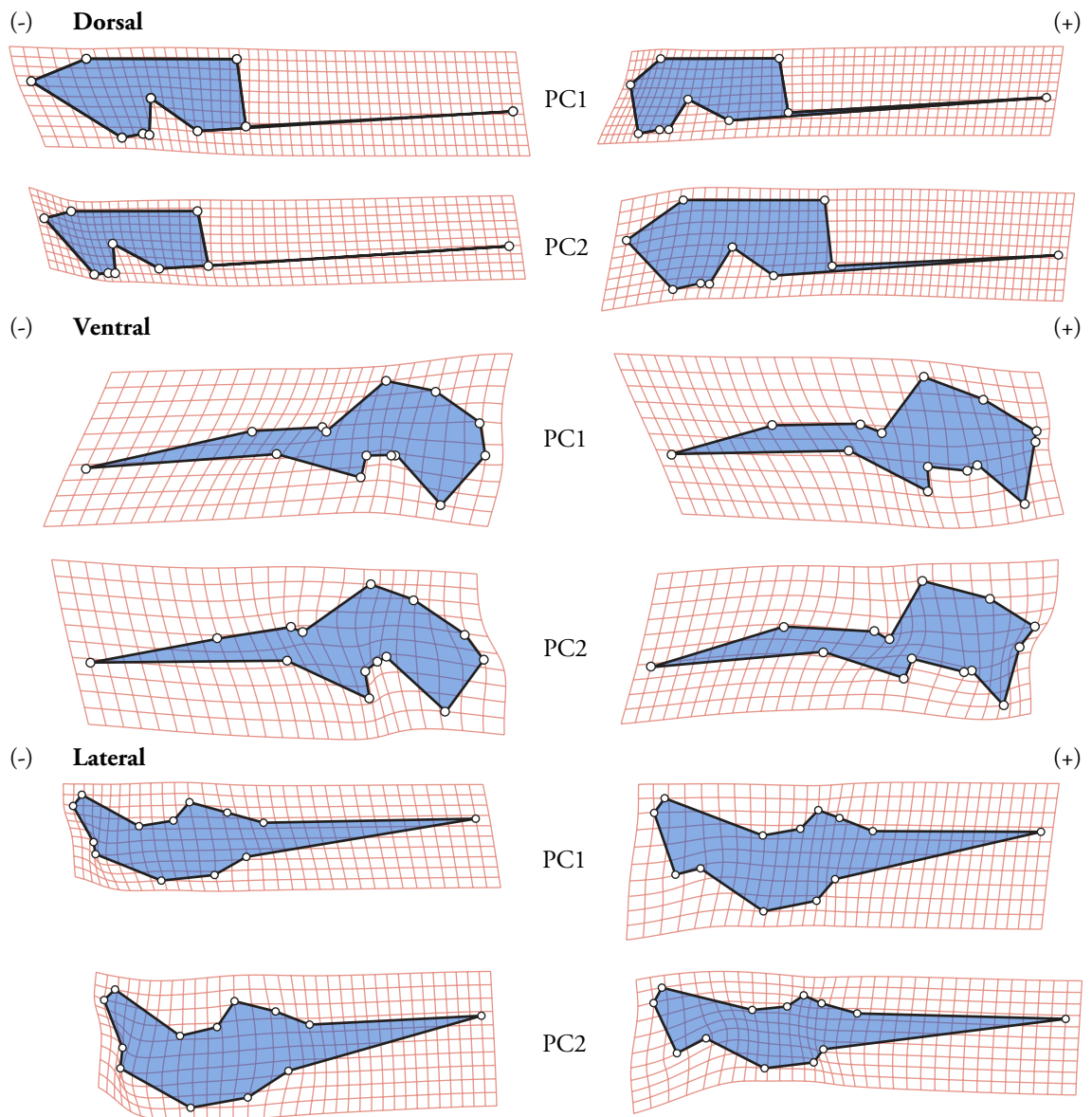


Figure 68: Visualisation of shape changes along extreme values (-0.1 and +0.1) of principal components 1 and 2 in dorsal ventral and lateral aspect. Thin-plate spline transformation grids (showing warping from the total average configuration) with overlaid wireframe graphs are illustrated.

4.3.4.4 Visualisation of Average Group Shapes

Thin-plate spline transformation grids illustrating shape changes from the total average configuration with superimposed wireframe graphs were generated for the average shapes of each group (AS-Ta, Hol-Ta and Tt) in dorsal, ventral and lateral aspect (Figure 69). In dorsal aspect there are few differences in shape between the *T. aduncus*-type specimens. The relative positioning of the premaxillary foramen to the rostral midline is closer in AS-Ta and the placement of the posteriormost point of the temporal crest relative to the rest of the

skull is also closer to the midline in AS-Ta. This is either suggestive of a slight slendering or elongating in shape for AS-Ta relative to Hol-Ta or of changes in the positioning of the temporal crest. Dorsal comparisons of *T. aduncus*-type specimens with *T. truncatus* show more pronounced shape differences with the relative position of the temporal crest to the rest of the skull suggesting a wider cranium and/or changes to the temporal crest. Shape changes at the nasals and ethmoid bone, where these are more posteriorly positioned in *T. truncatus*, are suggestive of proportionately larger external nares. Placement of the premaxillary foramen relative to nasal landmarks in *T. truncatus* is more anteriorly positioned than for the *T. aduncus*-types, suggestive of a shorter rostrum.

In ventral aspect, comparisons between the *T. aduncus*-types reveal very similar shapes, with the AS-Ta specimens being fractionally more slender or elongated than their Hol-Ta counterparts. Comparisons between *T. aduncus*-types and *T. truncatus* reveal significant shape differences in the positioning of the posteriormost point of the temporal crest relative to the ventral features of the skull. In *T. truncatus*, the temporal crest is positioned towards the midline from the paraoccipital process whereas in *T. aduncus*-types, the temporal crest is positioned exteriorly of the paraoccipital process. Furthermore, the temporal crest extends further posteriorly, relative to the rest of the skull, in *T. aduncus*-types than *T. truncatus*. These changes are likely suggestive of a wider skull in *T. truncatus*, but might also suggest more exaggerated temporal crests in *T. aduncus* specimens. The pterygoids are proportionately larger in *T. truncatus* in comparison to the *T. aduncus*-types.

In lateral aspect, there were notable shape differences between *T. aduncus*-types. In Hol-Ta, the premaxillary convexity is marginally more pronounced than in AS-Ta and the position of the posteriormost point of the temporal crest relative to the posteriormost point of the occipital condyle is more anterior in AS-Ta than it is in Hol-Ta. Again, this is possibly suggestive of a more slender or elongated skull in AS-Ta or due to changes in the shape of the temporal crest. The relative position of the zygomatic process and the postorbital process to the pterygoid flexion point and lacrimal landmarks are more anteriorly placed in AS-Ta than in Hol-Ta suggestive of a narrower, or tighter, curvature to the orbit in AS-Ta and/or anterior shape differences in the temporal fossa. In lateral comparisons between *T. aduncus*-types and *T. truncatus*, the pterygoids are proportionately larger in *T. truncatus* and the rostrum is stockier with a reduced premaxillary convexity. The preorbital lacrimal process is larger in

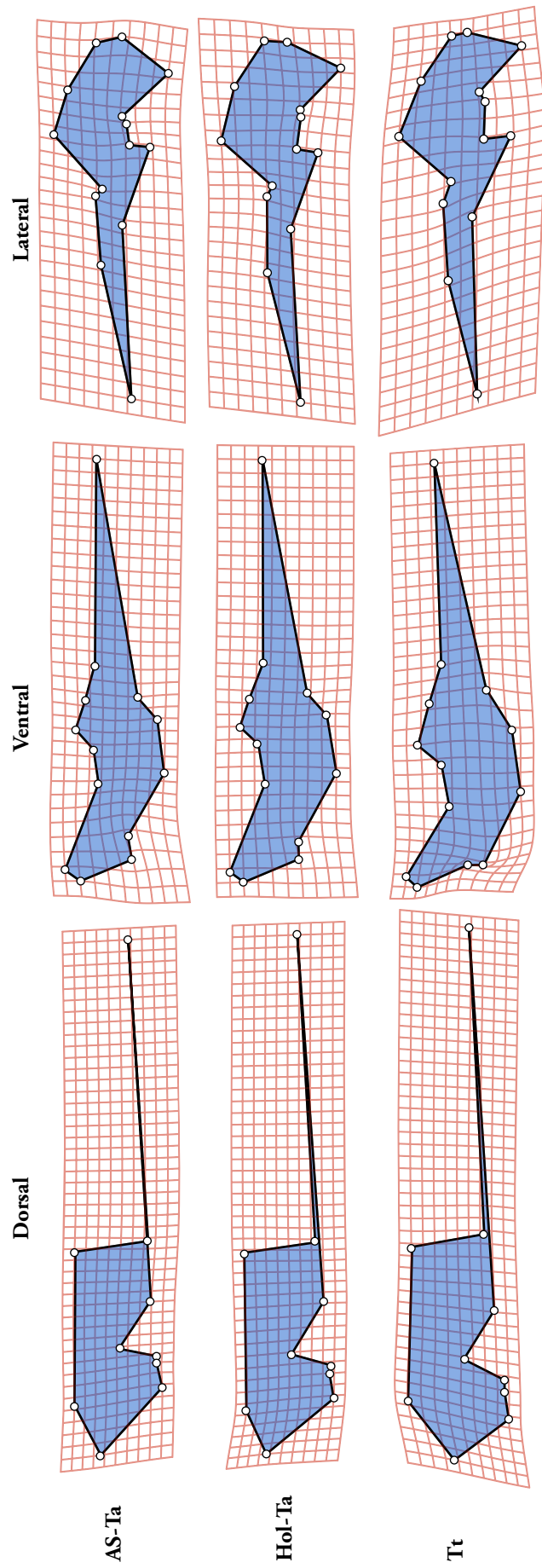


Figure 69: Visual comparisons of average group shapes, AS-Ta, Hol-Ta and Tt, for all aspects. Thin-plate spline transformation grids, showing warping from the total average configuration, with overlaid wireframe graphs are illustrated.

T. truncatus and the positioning of the postorbital and zygomatic process is more posteriorally placed, suggestive of differences in temporal fossa shape. The position of the posteriormost point of the temporal crest in *T. truncatus* is slightly anterior of the occipital condyle, similar to that of AS-Ta, but is more ventrally positioned.

4.3.4.5 Allometric Effects on Shape

For dorsal aspect, size predicted 11.26 % of the variance in shape. Permutation tests showed that shape was significantly dependent on size ($P < 0.001$). Size corrected shape differences between groups were still significant across five PCs (Wilks' lambda MANOVA = 0.24, $F_{10,88} = 9.25$, $P < 0.001$). In ventral aspect, size predicted 4.18% of the total shape variance. Shape was significantly dependent on size ($P = 0.032$) and size corrected shape differences between groups remained significant across seven PCs (Wilks' lambda MANOVA = 0.25, $F_{14,86} = 6.2478$, $P < 0.001$). In lateral aspect, size only predicted 2.98% of the variance in shape. Shape and size were significantly independent ($P > 0.05$) and shape differences between groups remained significant across nine PCs (Wilks' lambda MANOVA = 0.21, $F_{18,82} = 5.36$, $P < 0.001$).

For each aspect, an Analysis of Variance (ANOVA) and Procrustes ANOVA were performed to explore the group-wise differences in size and shape, respectively. In dorsal aspect, a significant difference was detected between groups in size ($F_{2,48} = 30.18$, $P < 0.001$) and shape ($F_{32,768} = 4.27$, $P < 0.001$, Pillai's trace = 1.03, $P = 0.0027$). When only considering *T. aduncus*-type specimens (AS-Ta and Hol-Ta) no significant difference was observed between groups for size ($F_{1,40} = 0.31$, $P = 0.58$) or shape ($F_{16,640} = 1.37$, $P = 0.15$, Pillai's trace = 0.35, $P = 0.63$). This would suggest that the significant differences observed in dorsal shape between the groups reflect differences between *T. aduncus* and *T. truncatus*-type specimens. Pairwise Procrustes ANOVAs between all groups confirmed this (AS-Ta – Tt: $F_{16,272} = 5.68$, $P < 0.001$, Pillai's trace = 0.99, $P = 0.0748$; Hol-Ta – Tt: $F_{16,624} = 6.25$, $P < 0.001$, Pillai's trace = 0.75, $P < 0.001$).

In ventral aspect, considering the dataset as a whole, there was a significant difference between groups in size ($F_{2,49} = 61.38$, $P < 0.001$) and shape ($F_{44,1078} = 6.67$, $P < 0.001$, Pillai's trace = 1.34, $P < 0.001$). As for dorsal aspect, pairwise Procrustes ANOVAs between groups in ventral aspect showed that these differences were between *T. aduncus* and *T. truncatus* specimens

(AS-Ta – Tt: $F_{22, 374} = 8.85$, $P < 0.001$; Hol-Ta – Tt: $F_{22, 880} = 10.35$, $P < 0.001$, Pillai's trace = 0.93, $P < 0.001$). No significant difference was observed between the *T. aduncus* groups in size ($F_{1, 41} = 0.01$, $P = 0.92$). However, a difference in ventral shape was inferred, although Pillai's trace statistic was not significant ($F_{22, 902} = 1.74$, $P = 0.02$, Pillai's trace = 0.57, $P = 0.34$).

Significant differences between all groups were observed in lateral aspect for size ($F_{2, 49} = 60.62$, $P < 0.001$) and shape ($F_{48, 1176} = 5.48$, $P < 0.001$, Pillai's trace = 1.42, $P = 0.001$). As for the other aspects, pairwise Procrustes ANOVAs were performed and revealed significant differences in shape between *T. aduncus* and *T. truncatus*-type groups (AS-Ta – Tt: $F_{24, 408} = 6.87$, $P < 0.001$; Hol-Ta – Tt: $F_{24, 960} = 6.93$, $P < 0.001$, Pillai's trace = 0.86, $P < 0.01$). No significant difference was observed in size between AS-Ta and Hol-Ta groups in lateral aspect ($F_{1, 41} = 0.65$, $P = 0.424$) however, in contrast to the dorsal and ventral aspects, a significant difference was observed in shape ($F_{24, 984} = 3.28$, $P < 0.001$, Pillai's trace = 0.77, $P < 0.05$).

4.3.4.6 Canonical Variates Analysis

To further explore shape differences between groups, a CVA was performed for each aspect. In dorsal (Figure 70), ventral (Figure 71) and lateral (Figure 72) aspect, there is separation of *T. truncatus* specimens from *T. aduncus*-type specimens along CV1. Along CV2 there is some indication of separation between the *T. aduncus* groups, with the separation being most prominent in lateral aspect (Figure 72).

Mahalanobis distances and Procrustes distances between pairs of groups and associated P -values are presented in Table 40. Results indicate a highly significant difference in shape between *T. truncatus* and *T. aduncus*-type specimens in all aspects. The shape differences between the *T. aduncus* groups are less pronounced, but significant for all aspects when considering Mahalanobis distances between groups. When considering Procrustes distances, the shape differences between the *T. aduncus* groups are not significant in dorsal or ventral aspects, but remain significant in lateral aspect ($P < 0.01$).

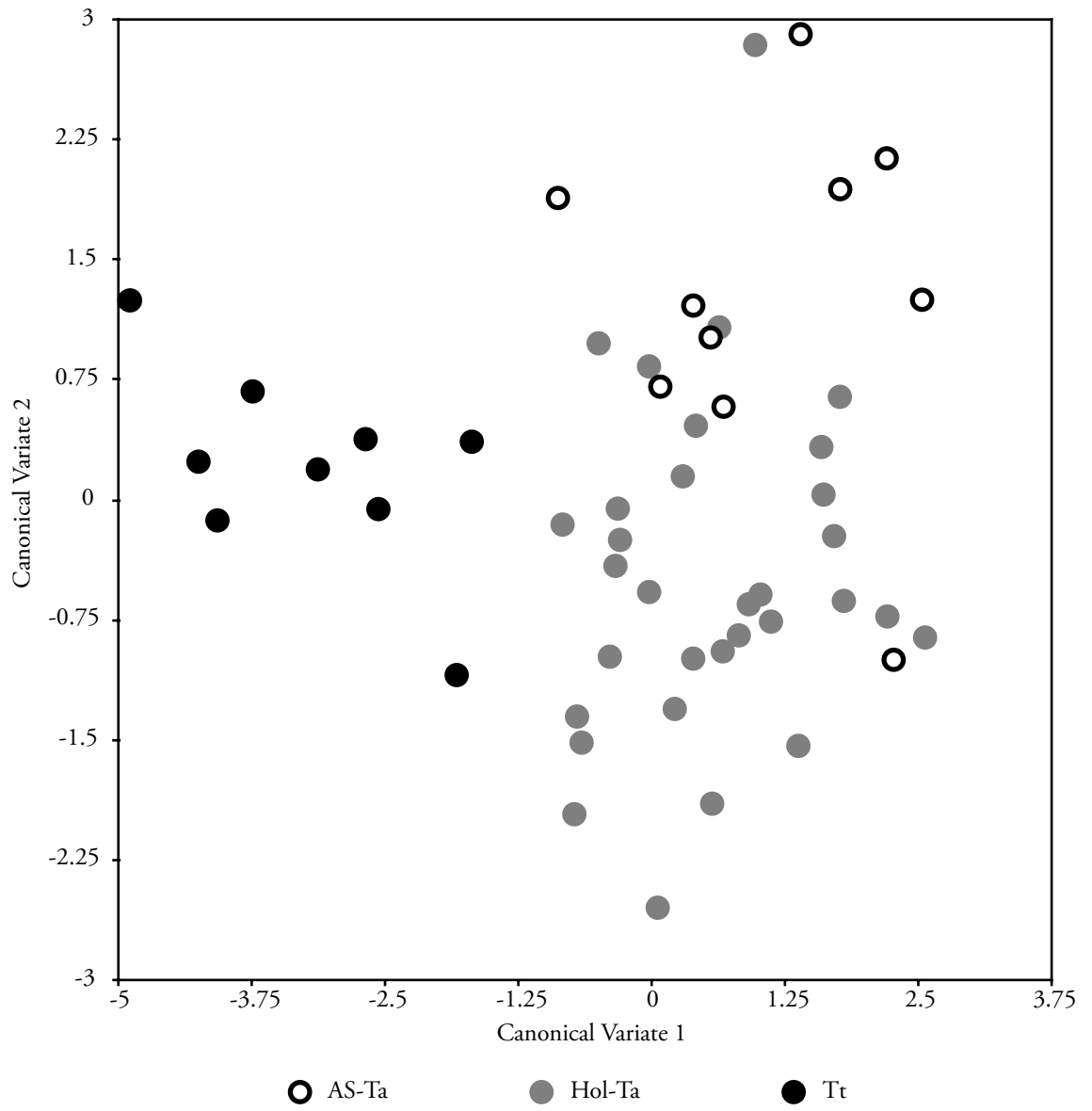


Figure 70: CVA for Dorsal aspect. Scatterplot for CV1 and CV2.

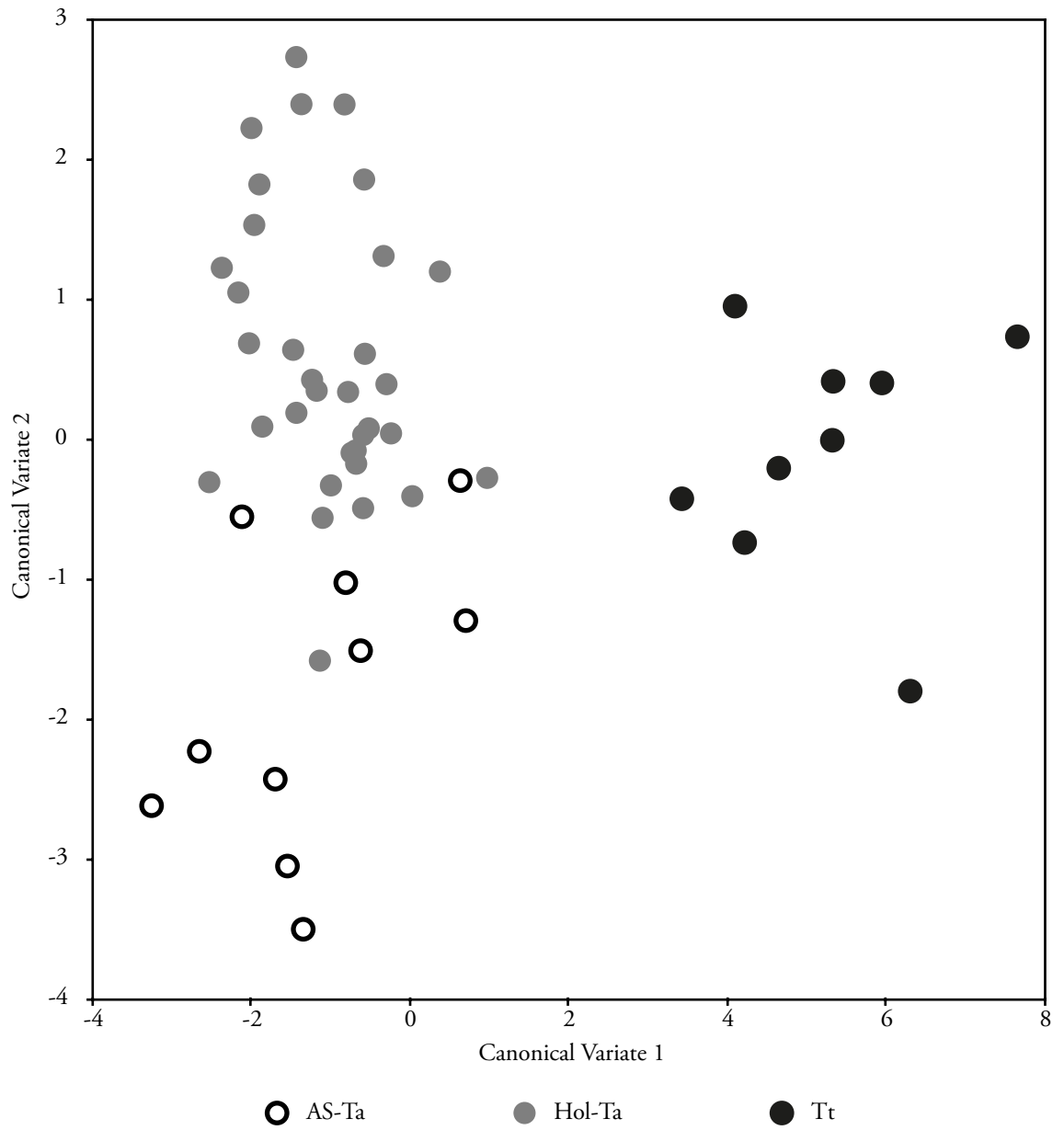


Figure 71: CVA for Ventral aspect. Scatterplot for CV1 and CV2.

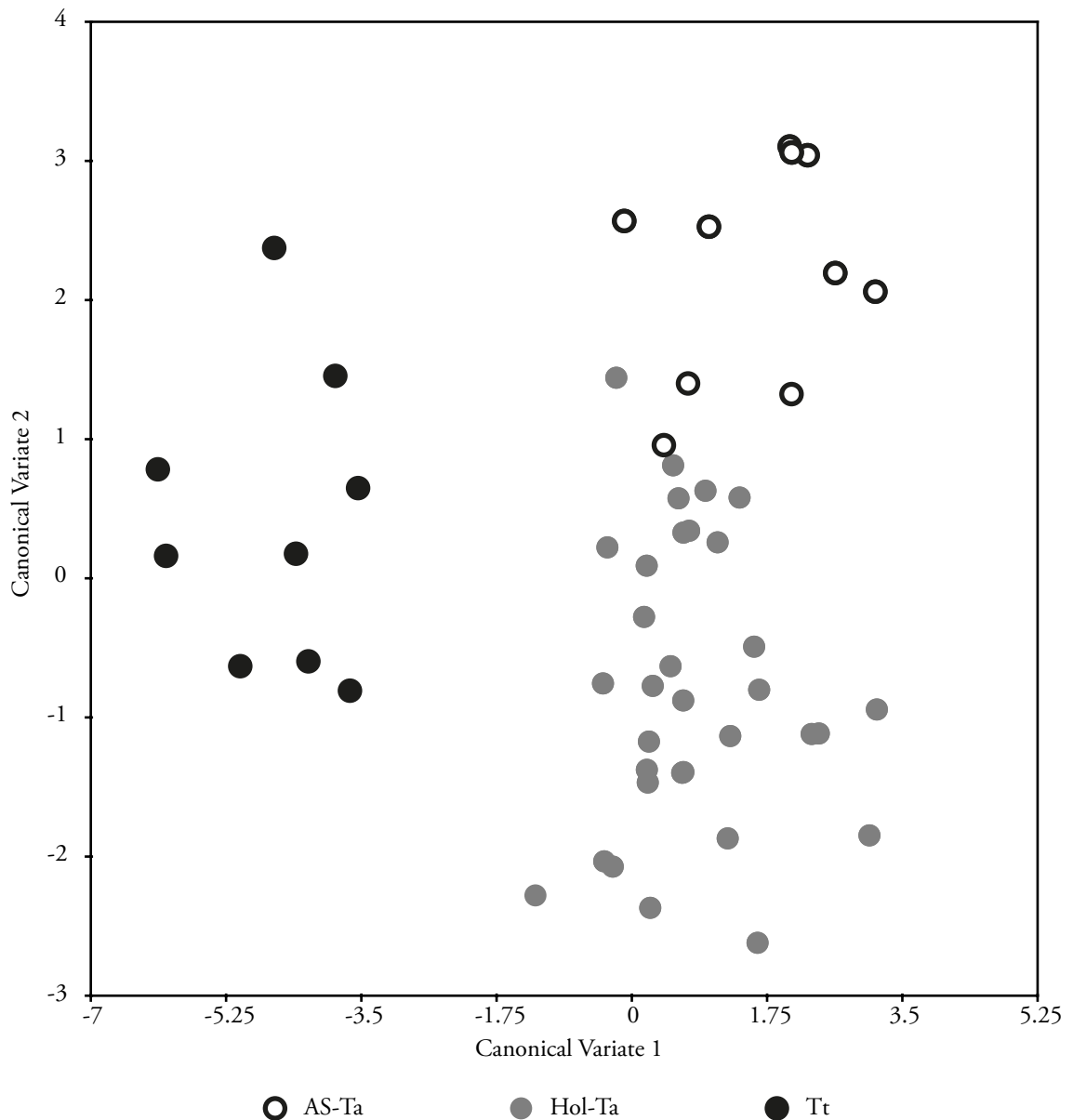


Figure 72: CVA for Lateral aspect. Scatterplot for CV1 and CV2.

4.3.4.7 Discriminant Function Analysis

Results of the pairwise DFAs are displayed in Table 41. DFAs between *T. aduncus* and *T. truncatus* correctly assigned specimens to groups for all aspects. Results between *T. aduncus* groups also showed good discrimination. The reliability of the discrimination between groups was tested using leave-one-out cross-validation, the results of which are in Table 42. The best discrimination in shape was between Hol-Ta and Tt with high percentages of specimens being correctly assigned to their respective groups (> 75%). There was poor discrimination between AS-Ta and Tt individuals for all aspects, however, it should be noted that the sample sizes were small for this comparison (AS-Ta, $n = 10$; Tt, $n = 9$). Discrimination between Hol-Ta and AS-Ta was poor in dorsal and ventral aspect but was prominent in lateral aspect.

Table 40: CVA pair-wise Mahalanobis and Procrustes distances between groups. Associated *P* values generated from permutation tests (1000 permutations).

Groups	Dorsal			Ventral			Lateral		
	Mahalanobis Distance	<i>P</i>	Procrustes Distance	Mahalanobis Distance	<i>P</i>	Procrustes Distance	Mahalanobis Distance	<i>P</i>	Procrustes Distance
	Hol-Ta/ AS-Ta	1.7978	0.0425	0.0162	0.2087	0.0002	0.016	3.1164	<0.0001
Hol-Ta/ Tt	3.8218	<0.0001	0.0381	0.0001	<0.0001	0.0423	5.5021	<0.0001	0.0443
AS-Ta/Tt	4.4346	<0.0001	0.0451	0.0003	<0.0001	0.0474	6.4914	<0.0001	0.0552

Table 41: Discriminant Function Analysis pairwise Mahalanobis and Procrustes distances between groups for dorsal, ventral and lateral aspect. Associated *P* values generated from permutation tests (1000 permutations).

Groups	Dorsal			Ventral			Lateral		
	Mahalanobis Distance	<i>P</i>	Procrustes Distance	Mahalanobis Distance	<i>P</i>	Procrustes Distance	Mahalanobis Distance	<i>P</i>	Procrustes Distance
	Hol-Ta/ AS-Ta	1.6897	0.639	0.016203	0.205	0.348	0.015959	4.1761	0.034
Hol-Ta/ Tt	4.0965	<0.0001	0.038059	<0.0001	<0.0001	0.042264	5.9092	0.001	0.044307
AS-Ta/Tt	19.1588	0.078	0.045052	<0.0001	0.007	0.047444	11.1106	<0.0001	0.055188

Table 42: DFA pairwise group allocation table and cross-validation scores for dorsal, ventral and lateral aspect.

		Dorsal				Ventral				Lateral			
Hol-Ta/AS-Ta	True Group	Group Assigned		% Correct	Group Assigned		% Correct	Group Assigned		% Correct	Group Assigned		% Correct
		Hol-Ta	AS-Ta		Hol-Ta	AS-Ta		Hol-Ta	AS-Ta		Hol-Ta	AS-Ta	
Discriminant Function	Hol-Ta	25	7	32	78	30	3	33	91	32	1	33	97
	AS-Ta	1	9	10	90	1	9	10	90	0	10	10	100
Cross-Validation	Hol-Ta	21	11	32	66	20	13	33	61	27	6	33	82
	AS-Ta	6	4	10	40	6	4	10	40	3	7	10	70
<hr/>													
Hol-Ta - Tt	True Group	Group Assigned		% Correct	Group Assigned		% Correct	Group Assigned		% Correct	Group Assigned		% Correct
		Hol-Ta	Tt		Hol-Ta	Tt		Hol-Ta	Tt		Hol-Ta	Tt	
Discriminant Function	Hol-Ta	32	0	32	100	33	0	33	100	33	0	33	100
	Tt	0	9	9	100	0	9	9	100	0	9	9	100
Cross-Validation	Hol-Ta	29	3	32	91	32	1	33	97	29	4	33	88
	Tt	2	7	9	78	2	7	9	78	2	7	9	78
<hr/>													
AS-Ta - Tt	True Group	Group Assigned		% Correct	Group Assigned		% Correct	Group Assigned		% Correct	Group Assigned		% Correct
		AS-Ta	Tt		AS-Ta	Tt		AS-Ta	Tt		AS-Ta	Tt	
Discriminant Function	AS-Ta	10	0	10	100	10	0	10	100	10	0	10	100
	Tt	0	9	9	100	0	9	9	100	0	9	9	100
Cross-Validation	AS-Ta	7	3	10	70	7	3	10	70	9	1	10	90
	Tt	3	6	9	67	3	6	9	67	4	5	9	56

4.3.4.8 Congruence Between Cranial Geometry and Phylogenetic Data

Shapes (represented by PC and CV scores) were mapped to the neighbour-joining phylogeny (Figure 44) for all aspects. A permutation test showed a strong phylogenetic signal in all aspects for PC scores ($P < 0.001$) (plots not shown). CV scores also showed highly significant phylogenetic signals for all aspects ($P < 0.001$). Phylogenies were superimposed onto CVA plots for all aspects (Figure 73, Figure 74, Figure 75).

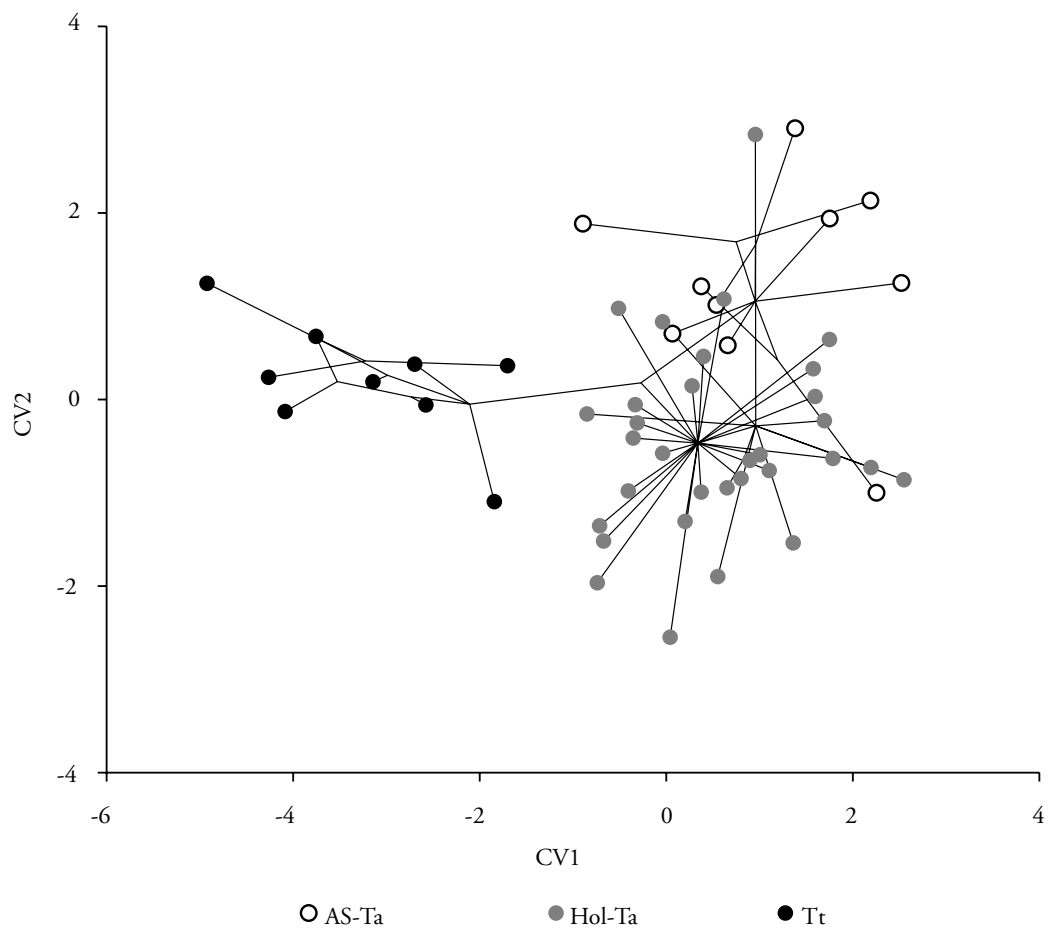


Figure 73: Dorsal aspect CVA Plot with superimposed phylogeny.

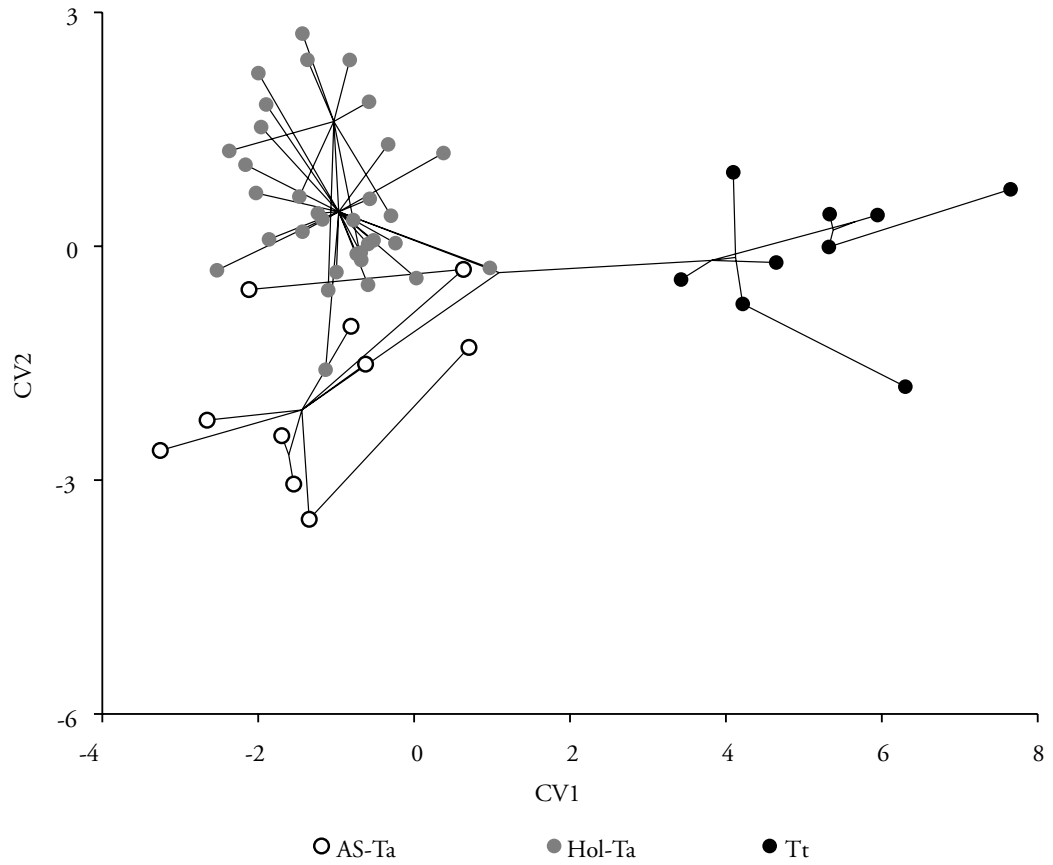


Figure 74: Ventral aspect CVA Plot with superimposed phylogeny.

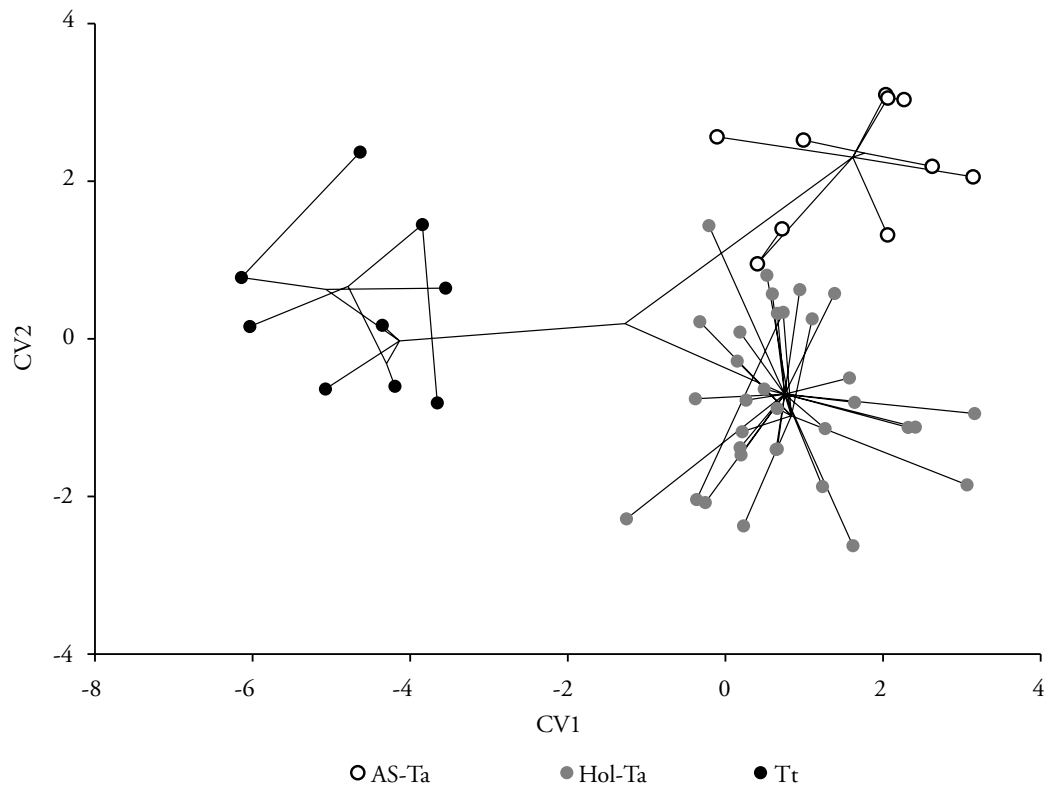


Figure 75: Lateral aspect CVA Plot with superimposed phylogeny.

4.4 Discussion

In this study I explore the morphological differences in skull geometry and size between three lineages of bottlenose dolphins in the northwest Indian Ocean. These were *T. truncatus* (Tt), the holotype lineage of *T. aduncus* (Hol-Ta) and a new, Arabian Sea, lineage of *T. aduncus* (AS-Ta) (see Chapter 2). Exploratory analyses were conducted on both linear measurements of morphological traits (traditional morphometrics) and on two-dimensional coordinates that capture the geometry of morphological traits (geometric morphometrics). The methods yielded similar results, although geometric morphometric techniques appeared to identify morphological variation more readily than the traditional method. Strong morphological differentiation was identified between *T. truncatus* and *T. aduncus* species utilising both linear and geometric morphometric methods. In general, morphological differentiation between the two putative lineages of *T. aduncus* was less pronounced. However, using linear measurements, differentiation was detected in DFA analyses where several measures of cranial/rostral width, as well as orbit length, were identified as important characters for discriminating between the two lineages (see below). Similarly, using the geometric morphometric toolkit, DFA and CVA analyses showed significant differentiation in cranial geometry between *T. aduncus* lineages in all aspects (dorsal, ventral and lateral), particularly in lateral view. Lateral shape was also independent of allometric effects. Visualisations of the shape differences suggest a more slender or elongated skull in the Arabian Sea *T. aduncus* lineage than the holotype lineage, with shape differences in either the temporal fossae or orbits.

Strong support for a phylogenetic signal in cranial geometry was also detected suggesting congruence between genetic and morphological inference. Multiple lines of evidence (from genetic and morphological data) continue to support the presence of a new lineage of *T. aduncus* in the Arabian Sea. This information will be important in the design of regional conservation initiatives, which are duly needed (see Chapter 1).

Morphological differences between *T. truncatus* and *T. aduncus* have been reported elsewhere (e.g. Ross, 1977; Wang *et al.* 2000; Kemper, 2004). Comparison of the *T. aduncus* morphologies suggests the lineages have adapted to local environmental conditions or exhibit phenotypic plasticity. Different foraging strategies (perhaps associated with highly turbid conditions off Pakistan and India) or different prey compositions could be driving adaptation in these morphological traits. Interestingly, variants of other dolphin species in the region,

such as common dolphins (Jefferson & Van Waerebeek, 2002), spinner dolphins (Van Waerebeek *et al.* 1999) and humpback dolphins (Jefferson & Van Waerebeek, 2004), appear to be converging on a similar ‘long-beaked’ morphotype, suggesting species are adapting to local environmental conditions in similar ways.

More broadly, local adaptation in highly mobile marine taxa currently experiencing secondary contact, or sympatric speciation, in response to current environmental heterogeneity or historic climate change (see Chapter 2 & Chapter 3), in the northwest Indian Ocean is of interest to the study of evolutionary processes.

4.4.1 Morphological differences between T. truncatus and T. aduncus

Cluster analysis using tooth counts (meristic data) revealed two groups that were dominated by Ta-types and Tt respectively. However, misclassification rates were high (23%), due to the substantial overlap in tooth counts between Ta-types and Tt, as seen elsewhere (e.g. Ross, 1977; Wang *et al.* 2000; Kemper, 2004; Charlton-Robb *et al.* 2011).

PCA, *k*-means, *k*-medoids and agglomerative hierarchical cluster analysis of linear character measurements divided specimens into two groups representing Tt and Ta-types for both the ONHM and Combined Datasets. Only one individual (ONHM 3018), genetically classified as Tt, was incorrectly assigned to the Ta-type group in some analyses. Although this individual was classified as cranially mature based on fusion of the maxillary plates to the cranium (Ross & Cockcroft, 1990; Kemper 2005), it was still a young individual with recent fusion (Van Waerebeek, 1993; Chen *et al.* 2011) for the majority of other cranial sutures. Therefore, it is possible that allometric affects were causing this Tt specimen to occasionally cluster with Ta-type individuals. Indeed, when considering the geometric data, where measures of size are lost, this individual consistently clustered with other Tt specimens.

Although Tt was larger than the Ta-types on average, significant overlap in measurements for condylobasal length (CBL) was observed for all groups (Tt: 483.34 – 539 mm; Hol-Ta: 447.67 - 494.34 mm; AS-Ta: 441.34 - 507.00 mm). CBL has not been able to distinguish between Tt and Ta-types in other morphological studies on bottlenose dolphins. For example, off South Australia, Kemper (2004) found overlap in CBL measurements for Tt and Ta-type groups. This is in contrast to Charlton-Robb *et al.* (2011) who found no overlap in CBL

measurements between Tt and Ta-type specimens from very similar geographic locations, but their sample size was small for the Ta group, $n = 5$. Hale *et al.* (2000) looked at *Tursiops* spp. CBL measurements across a large geographic scale, including eastern, northern and southern Australia, southeast Africa (data from Ross, 1977; 1984), and East and South China Seas (data from Gao *et al.* 1995). They found only a small overlap in CBL measurements between Tt and Ta-types but separated them without overlap when plotted against total body length.

DFA of linear measurements revealed significant differences between Tt and Ta-types and cross-validation supported the distinction. Pairwise comparisons revealed that the most important characters for discriminating between Tt and Ta-types were RW60, GLPTF, PRW, UTLTR, TPC, LWPTF, GPRW, GPOW and LAL (see Table 25 for descriptions). A large number of characters overlapped between Ta-types and Tt, with the exception of GPRW, GWIN, RW60, and LAL (see Table 25). The ratio of RW60 to ZW was particularly useful at discriminating Ta-types from Tt (Figure 63).

Kemper (2004) noted differences in the shape and size of the temporal fossa between Tt and Ta-types off South Australia and found LWPTF to be an important character for distinguishing between the two species. Charlton-Robb *et al.* (2011) did not find measurements associated with the temporal fossa to be important, however, Ta-types were under represented in their morphological study and so important characters may have been biased towards differences detected between *T. australis* and Tt. Cranial variation in offshore and inshore ecotypes of Tt in Californian waters observed inshore forms to have larger temporal fossae than offshore forms (Perrin *et al.* 2011). Kemper (2004) also noted that, from photos representing Tt and Ta-types in Wang *et al.* (2000), the temporal fossae are smaller and more elliptical in the former and larger and more circular in the latter. The specimens analysed in my study exhibit significant variation in temporal fossa shape and this description appears to hold true. Specifically, the anterior limit of the temporal fossa (as defined by the postorbital process of the frontal bone) is significantly angular to produce a rounded shape in the temporal fossa in Ta-type specimens and relatively straight in Tt forming a 'D' shape when viewed in lateral left aspect (see Figure 76). Unfortunately Wang *et al.* (2000) did not take measurements associated with the temporal fossae. Ross & Cockcroft (1990) also found LWPTF and MAJDTF to be important characters in PCA analysis. In the current study, two measurements associated with the temporal fossa (LWPTF, GLPTF) were identified as important characters for discriminating between Tt and Ta-types.

Wang *et al.* (2000) developed an identification key for distinguishing between Tt and Ta-type specimens based on the cranial morphology of bottlenose dolphins in Chinese waters. They proposed ratios of GWEN to GPRW and of TPC to CBL, UTLTR and RL (see Table 25), as useful for distinguishing between Tt and Ta-types. In the present study, these ratios performed reasonably well with a Tt misclassification of 12.5% and a Hol-Ta misclassification rate of 13.2%. All AS-Ta specimens were correctly identified as *T. aduncus* based on the key, which is interesting given the closer phylogenetic relationship of the AS-Ta to the Chinese *T. aduncus* (see Chapter 2).

From the geometric morphometric data, visualisation of the average Procrustes configurations for each group (Tt, Hol-Ta and AS-Ta) revealed shape differences generally indicative of proportionately stockier and wider skulls in Tt compared with Ta-types (see Figure 69). As for the linear measurements, results suggested shape differences associated with the temporal fossae between Tt and Ta-types. PCAs revealed good separation between Tt and Ta-types in the dorsal, ventral and lateral aspects. Pairwise ANOVAs compared sizes (centroid size) between groups and revealed significant size differences between Tt and Ta-types and pairwise Procrustes ANOVAs revealed significant differences in skull geometry between Tt and Ta-type specimens. CVA and DFA, with cross-validation, supported a clear distinction between Tt and Ta-type specimens.

The temporal fossa is particularly interesting as it is the location for jaw muscle attachment (Mead & Fordyce, 2009) and so differences in shape and size may suggest differences in feeding ecology. Indeed, investigations into stomach contents of dolphins in the region (Ponnampalam *et al.* 2012) reveal bottlenose dolphins to be feeding in either inshore/coastal habitats or offshore. Furthermore, those dolphins feeding inshore have a diet that includes species such as the croaker, *Otolithes ruber*, that occur on sandy and muddy substrates (Ponnampalam *et al.* 2012), which is indicative of different foraging strategies between the Tt and Ta-types in the region.

4.4.2 Morphological differences between *T. aduncus* (Hol-Ta) and *T. aduncus* (AS-Ta)

Cluster analyses of linear measurements were unable to detect differences between the two Ta-types (Hol-Ta and AS-Ta). DFA provided some support for a distinction between the Ta-type groups, with high misclassification rates for the AS-Ta specimens in cross-validation analyses.

Discrimination between Hol-Ta and AS-Ta specimens were largely based on GPOW, ZW, RW60, LO and RWM (see Table 25). However, there was some degree of overlap between all characters examined.

The shape differences between the Ta-types based on geometric morphometric data were most pronounced in the lateral view, suggesting a more slender or elongated skull for AS-Ta, or differences in temporal fossa shape. Another shape difference of note is the relative position of the zygomatic process and the postorbital process, which appear to be more anteriorly placed in AS-Ta. This could be suggestive of a narrower, or tighter curvature in the orbit of the AS-Ta, or a more ovoid temporal fossa. Interestingly, comparisons between Ta-types in the DFA using linear measurements in the Combined Dataset revealed GPOW, ZW and LO as important characters, which might reflect these shape changes and suggest congruence between the results from the linear and geometric morphometric datasets.

PCAs only revealed limited separation of the two Ta-type lineages in lateral aspect (Figure 67). Pairwise ANOVA revealed no significant differences in size between Ta-type specimens. Procrustes ANOVAs revealed no significant differences in dorsal shape between Ta-type specimens. Ventral geometric differences between Ta-types were evident, although these were not significant when Pillai's trace statistic (which is more conservative) was considered. Lateral shape differences between Ta-types were consistently significant. CVA and DFA, with cross-validation, revealed consistently significant differences between the Ta-types when considering the skulls in lateral aspect.

As discussed above, differences in temporal fossa geometry could be suggestive of different foraging strategies or prey. Further to this, more slender/elongated skulls in AS-Ta might be expected if the lineage were adapted to foraging in an environment with high turbidity, for example river dolphins (Cassens *et al.* 2000; Smith & Reeves, 2012). Changes to the orbit of the AS-Ta lineage might also be a result of living in a more turbid environment, again, the extreme being found in river dolphins, which have small eyes (Herald *et al.* 1969). Indeed, AS-Ta specimens dominate the Pakistan (and Indian, see Chapter 2) coastline, where river influx (e.g. the Indus river delta) discharges freshwater and organic material, resulting in a brackish and turbid coastal environment (Longhurst, 2006).

4.4.3 Comparison of Methodologies

Analyses of linear measurements and of geometric morphometric data generally yielded similar results. Both methodologies detected morphological differences between *T. truncatus* and *T. aduncus* and were able to identify morphological differences between the two *T. aduncus* lineages when discriminatory analyses (e.g. DFA and CVA) were performed on groups assigned, *a priori*, based on mtDNA genetic sequences. However, geometric morphometric techniques appeared to detect variations in morphology more readily than the traditional method. Increasingly, morphology studies have utilised geometric morphometric techniques due to the advantages they have over traditional methods (Adams *et al.* 2004). In cetaceans, geometric morphometrics have been used to investigate taxonomic relationships (e.g. Amaral *et al.* 2009), intragenus differentiation on a global scale (e.g. Nicolosi & Loy, 2010), intragenus differentiation on a regional scale (Monteiro-Filho *et al.* 2002), intraspecific differentiation on a regional scale (e.g. Loy *et al.* 2011), and allometric effects on cranial shape (e.g. Parés-Casanova & Fabre, 2013). The present study has also revealed geometric morphometric methods to be useful at resolving relationships in cranial morphology between closely related species.



SMNS 45-720 *Tursiops aduncus* (Arabian Sea type), Pakistan



ONHM 3524 *Tursiops truncatus*, Oman

Figure 76: Example specimens of Ta-type (SMNS 45-720) from Pakistan and a Tt (ONHM 3524) from Oman in lateral (left) aspect.

4.4.4 Distribution of Samples and Evidence for Hybridization/Introgression

Ta-type specimens were collected from as far south as the Dhofar region in Oman, through to the waters off the Indus Delta in Pakistan. Off Oman, along the Sea of Oman coastline, specimens only represented Tt. This is consistent with the majority of sightings, and the pelagic habitat, off that stretch of coastline (Minton, *et al.* 2010). In contrast, no Tt specimens were represented from Pakistan although they are likely to occur there (Gore *et al.* 2012). Both Hol-Ta and AS-Ta were represented by specimens collected in Oman (Hol-Ta, $n = 29$; AS-Ta, $n = 4$) and Pakistan (Hol-Ta, $n = 2$; AS-Ta, $n = 6$). According to the phylogeny of these lineages, the two Ta-types form monophyletic groups (see Chapter 2). However, with the extensive overlap in range between both types it is conceivable that hybridization and

introgression are responsible for the overlap in cranial morphology observed between the Ta-type lineages. For example, two specimens from Oman (ONHM 1975 and 3079) that were identified as AS-Ta, from mtDNA control region sequences, consistently clustered with the Hol-Ta specimens in the DFA analyses conducted on linear measurements (see Figure 61 and Figure 62). However, from CVA analyses, conducted on the geometric data, although these specimens were geometrically close to Hol-Ta specimens, they were not the outliers they appear to be in the DFA analyses conducted on linear measurements. Although this could suggest allometric effects were influencing the DFA, which were absent from the geometric CVA, there was no evidence that these specimens were cranially immature. Further evidence for hybridization and introgression between these lineages comes from microsatellite data, which is discussed in Chapter 3. Future morphological analyses should endeavor to include more specimens from the region, and further afield, to include specimens from the Australasian *T. aduncus* lineage (Wang *et al.* 2000).

4.4.4.1 Conclusions

In the present study morphological separation is identified between three lineages of bottlenose dolphin in the Indian Ocean based on both linear and geometric morphometric techniques. The techniques yielded similar results, but the geometric morphometrics technique was apparently more sensitive to detecting morphological differentiation. The morphological distinction between the two *T. aduncus* lineages is suggestive of adaptation to local habitats in the northwest Indian Ocean and provides strong support for a separate conservation unit in the region (see Reeves *et al.* 2004). Morphological differences could be due to the high-turbidity waters off Pakistan and India (Longhurst, 2006), particularly as similar morphological differences are exhibited in other dolphin species in the region (e.g. Jefferson & Van Waerebeek, 2002). Such findings will be of broad interest to the study of evolutionary processes in highly mobile marine taxa, particularly as these *T. aduncus* lineages are either experiencing secondary contact (after divergence in allopatry) or are diverging in sympatry. The morphological differences between the lineages reflect differences in the ecology of these populations that will require further investigation, e.g. through dietary and life-history studies. The outcomes of such analyses will be of interest to conservation initiatives in the region.

Chapter 5

Population Structure of Common Dolphins (*Delphinus* spp.): Novel Insights from the Northwest Indian Ocean

5.1 Introduction

Delimiting taxonomic units, and measuring their evolutionary relationships in a geographic context, is the focus of phylogeographic studies (Bermingham & Moritz, 1998). Such analyses can be employed to study evolutionary patterns and processes over time and space (e.g. Rissler & Apodaca, 2007), as well as highlight regions of taxonomic/evolutionary endemism to better inform conservation initiatives (Moritz & Faith, 1998). Phylogeographic analysis of closely related species, or incipient species, is particularly interesting for studying the mechanisms responsible for speciation and poses unique challenges to overcome, such as incomplete lineage sorting and introgression (Funk & Omland, 2003). These are particularly compounded when the taxa under investigation express a similar phenotype (*cf.* morphological convergence) or exhibit a high degree of phenotypic variation and/or plasticity (Bermingham & Moritz, 1998). For example, pocket gophers *Cratogeomys* spp. and *Pappogeomys* spp. are morphologically plastic mammals (Patton & Brylzki, 1987) resulting in the description of several species based on morphological analyses (Russell, 1968), some of which could not be delimited based on genetic analyses (Demastes *et al.* 2002). This resultant paraphyly was attributed to intra-specific morphological variation and plasticity within pocket gophers (Demastes *et al.* 2002); however, in other taxa, similar patterns can arise due to incomplete lineage sorting and/or introgression. In another example, the taxonomic resolution of eight cryptic species of mouse lemur, *Microcebus* spp., described from morphological and genetic studies (Rasoloarison *et al.* 2000; Yoder *et al.* 2000; Heckman *et al.* 2007), was limited to three lineages at nuclear loci due to incomplete lineage sorting (Heckman *et al.* 2007).

In the marine environment, where barriers to dispersal are difficult to identify and are often not physical, taxa normally exhibit genetic homogeneity across large spatial scales (Palumbi, 1992). However, marine mammals are extraordinary as they regularly exhibit genetic differentiation within their cruising range (e.g. Tolley *et al.* 2001; Natoli *et al.* 2004; Natoli *et al.* 2008a; Hayano *et al.* 2004; Fontaine *et al.* 2007; Sellas *et al.* 2005; Andrews *et al.* 2010;

Fernández *et al.* 2011; Hamner *et al.* 2012). Recent radiation in Delphinidae (McGowen *et al.* 2009; McGowen, 2011) has resulted in several closely related species that remain taxonomically unresolved, despite extensive phylogenetic analyses (e.g. LeDuc *et al.* 1999, May-Collado & Agnarsson, 2006; Agnarsson & May-Collado, 2008; Caballero *et al.*, 2008; Kingston *et al.* 2009; McGowen *et al.* 2009; McGowen, 2011; Amaral *et al.* 2012b). The still more recent diversification of the sub-family Delphininae (McGowen *et al.* 2009; McGowen, 2011; Amaral *et al.* 2012b) makes these taxa particularly interesting candidates for studying incipient speciation in the presence of confounding phenomena such as incomplete lineage sorting and introgression.

Within Delphininae, the taxonomy of common dolphins, *Delphinus* spp., is still not fully resolved and the genus is characterised by a high degree of morphological variation across its range (e.g. Bell *et al.* 2002; Jefferson & Van Waerebeek, 2002; Stockin & Visser, 2005; Murphy *et al.* 2006; Westgate, 2007; Tavares *et al.* 2010). Although such variation likely resulted in the description of over 30 putative species (Hershkovitz, 1966), only two are currently recognised; the long-beaked common dolphin, *D. capensis* and the short-beaked common dolphin, *D. delphis* (Heyning & Perrin, 1994; Rosel *et al.* 1994). The distinction between these species was identified in the northeast Pacific, where they occur in sympatry, based on morphological characteristics (particularly the ratio of rostral length to the greatest width across zygomatic processes) (Heyning & Perrin, 1994). This distinction was corroborated by genetic analyses in a parallel study where long- and short-beaked morphotypes in the northeast Pacific were shown to be reciprocally monophyletic based on mitochondrial DNA (mtDNA) control region sequences (Rosel *et al.* 1994). However, AFLP analyses revealed incomplete lineage sorting at nuclear loci (Kingston & Rosel, 2004) suggesting recent divergence of these lineages. Faster lineage sorting is expected from mtDNA, as the effective population size is a quarter that of nuDNA and the mutation rate is higher (Moore, 1995; May-Collado & Agnarsson, 2006). Overall, the results suggested long- and short-beaked variants in other parts of the world might also be *D. capensis* and *D. delphis*, respectively (Heyning & Perrin, 1994).

However, although long- and short-beaked populations have been described in other parts of the world (Amaha, 1994), the distinction has not always been clear, with clines and intermediate forms also commonplace (Amaha, 1994, Bell *et al.* 2002, Jefferson & Van Waerebeek, 2002; Murphy *et al.* 2006, Pinela *et al.* 2008). Furthermore, where the morphological dis-

inction could be made, genetic analyses of populations outside the northeast Pacific consistently showed long- and short-beaked dolphins to be polyphyletic (Natoli *et al.* 2006, Amaral *et al.* 2012a). The fact that long- and short-beaked morphotypes do not form reciprocally monophyletic lineages worldwide suggests regional lineage sorting is incomplete and that multiple coastal populations have converged independently on a *D. capensis* morphotype (Natoli *et al.* 2006; Amaral *et al.* 2012c).

One species that maintained its nominal status was *D. tropicalis* (van Bree, 1971), which was later described as a subspecies, *D. capensis tropicalis* based on morphological analyses (Jefferson & Van Waerebeek, 2002). Although *D. c. tropicalis* was morphologically distinct, Jefferson & Van Waerebeek (2002) showed a clinal variation in *Delphinus* morphology across the Indo-Pacific, where conspecifics exhibited an extreme (*D. c. tropicalis*) morphotype (narrow skull, extremely long rostrum and high tooth counts) off India. Jefferson & Van Waerebeek (2002) suggested hybridisation and introgression were occurring between overlapping populations of *D. c. tropicalis* and adjacent populations of long-beaked *D. delphis*.

In a broad-scale phylogeographic study, Natoli *et al.* (2006) found long-beaked *Delphinus* populations in South Africa to be highly differentiated from those in the Atlantic based on nine microsatellite loci and mtDNA control region sequences. In a larger phylogeographic study (using mtDNA and nuclear DNA (nuDNA) loci), Amaral *et al.* (2012a) showed *D. c. tropicalis* in the northwest Indian Ocean to form a distinct lineage, diverging basally with populations outside the northeast Pacific. Interestingly, Amaral *et al.* (2007) found evidence for a highly diverged group of *Delphinus* in the northeast Atlantic ('Clade X') with a genetic (but probably not morphological) affinity for *D. c. tropicalis*, including individuals off Portugal and Scotland. However, they cautiously discuss hypotheses that may have resulted in such a divergent group, including sampling effects, introgressive hybridization and the independent evolution of cryptic taxa.

Amaral *et al.* (2012a) utilised a number of samples from the northwest Indian Ocean for their analyses, mtDNA ($n = 25$) and nuDNA ($n = 5$), while Natoli *et al.* (2006) did not include any from the region. In the present study, I build on analyses conducted by Amaral *et al.* (2012a) and Natoli *et al.* (2006) by assessing genetic differentiation between *D. c. tropicalis* in the northwest Indian Ocean, long-beaked *D. delphis* off South Africa and short-beaked

D. delphis in the northeast Atlantic utilising 14 microsatellite loci. In addition, I investigate contemporary dispersal (gene flow), and hybridization/introgression using the same dataset. Novel mtDNA control region sequences of *D. c. tropicalis* from Oman/Pakistan were used as part of a broader comparative analysis using published sequences from *Delphinus* populations worldwide. The available evidence suggests that these populations will be significantly differentiated from one another. Such differentiation would result from reduced connectivity between populations, possibly through local adaptation to particular habitats and/or prey compositions, as has been suggested elsewhere (e.g. Amaral *et al.* 2012a, Jefferson & Van Waerebeek, 2002).

Asymmetrical migration patterns in coastal dolphins in the region, such as humpback dolphins, *Sousa plumbea*, and bottlenose dolphins, *Tursiops aduncus*, reveal a northward migration bias (Mendez *et al.* 2011; Chapter 3). While there are significant ecological differences between *Delphinus* and these species, it is conceivable that general oceanographic processes are influencing them in a similar way. Given the morphological cline and range overlap between dolphins described as long-beaked *D. delphis* and *D. c. tropicalis* in the Indian Ocean (Jefferson & Van Waerebeek, 2002), as well as the divergent *D. c. tropicalis*-like group in the northeast Atlantic (Amaral *et al.* 2007), evidence for migration and/or hybridization/introgression between these populations is explored. Results from the present study will inform conservation initiatives on broad-scale population structure of *Delphinus* between the Atlantic and Indian Ocean as well as provide an example of the challenges associated with delimiting incipient species.

5.2 Materials and Methods

5.2.1 Sample Acquisition and DNA extraction

Bone ($n = 24$) and tissue ($n = 23$) samples of common dolphins, *Delphinus* sp. were collected from stranded ($n = 42$) and free-ranging ($n = 5$) individuals in Oman. Samples from Pakistan ($n = 6$) were collected from strandings. From South Africa, samples ($n = 26$) were collected from bycaught or stranded individuals (see Natoli *et al.* 2006) and samples collected in Portugal ($n = 30$) were from free-ranging individuals (see Moura *et al.* 2013b). DNA extraction protocols for tissue and bone are as outlined in Chapter 3. Sequences of mitochondrial DNA (mtDNA) deposited on GenBank, from various locations around the world were also utili-

sedin some analyses (See Figure 77 for sample locations and Table 43 for sample information).

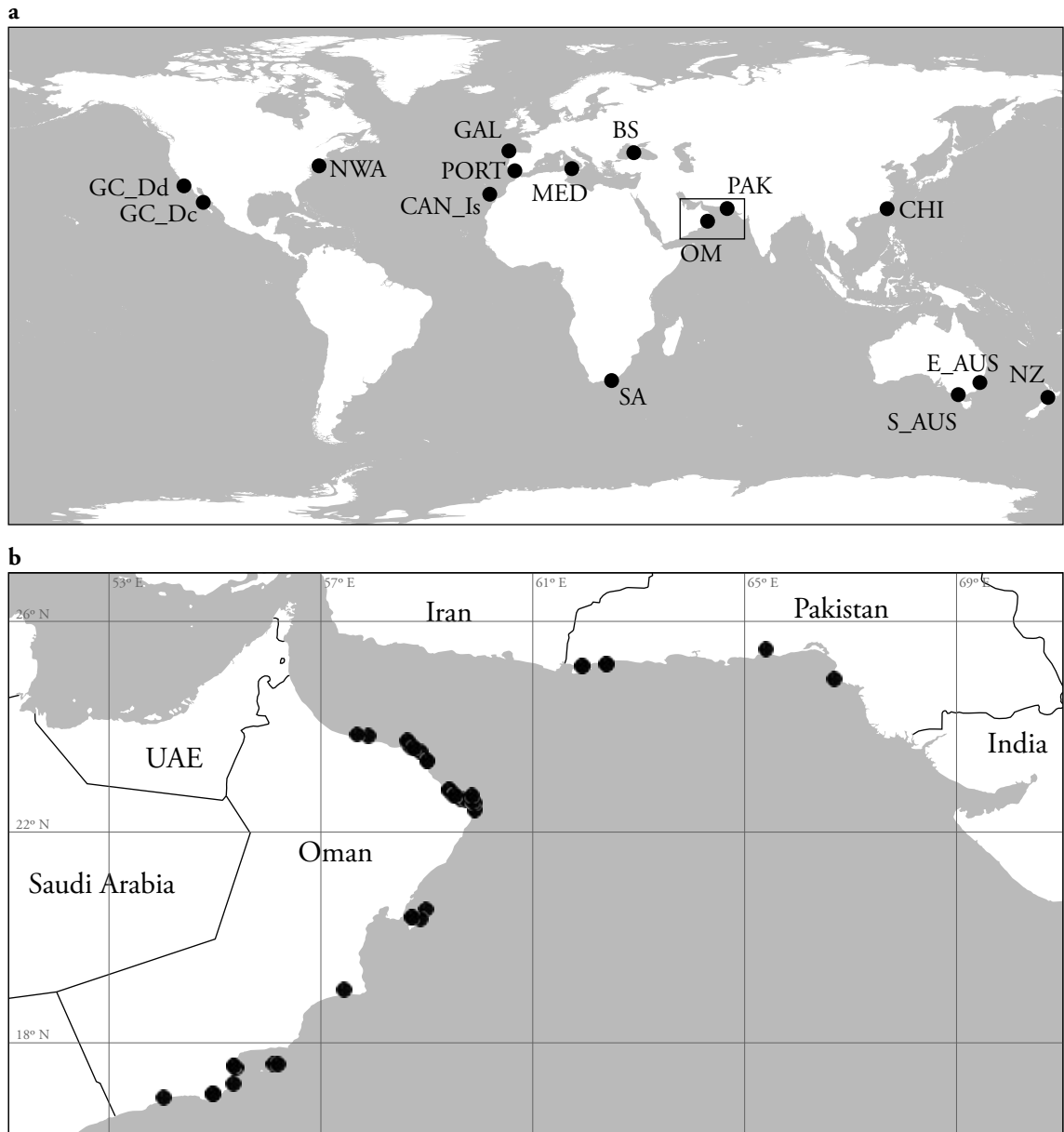


Figure 77: Locations of common dolphin (*Delphinus* spp.) samples utilised. a) Locations of sampled populations. GC_Dd = Gulf of California *Delphinus delphis*; GC_Dc = Gulf of California *Delphinus capensis*; NWA = Northwest Atlantic; CAN_Is = Canary Islands; PORT = Portugal; GAL = Galicia; MED = Mediterranean; BS = Black Sea; PAK = Pakistan; OM = Oman; SA = South Africa; E_AUS = Eastern Australia; S_AUS = Southern Australia; NZ = New Zealand. b) Locations of novel samples (black circles) collected in Oman and Pakistan from free-ranging and stranded individuals. Refer to Table 43 for information on which samples were included in microsatellite and mitochondrial DNA analyses.

Table 43: Numbers of samples used for each population in analyses using (a) microsatellites and (b) mitochondrial DNA respectively. Sources of samples are also shown.**a****Microsatellites**

Code	Location	<i>N</i>	Reference
OM	Oman	20	This study
SA	South Africa	25	Natoli <i>et al.</i> 2006
PORT	Portugal	30	Moura <i>et al.</i> 2013b

b**Mitochondrial DNA**

Code	Location	<i>N</i>	Sequence Source
BS	Black Sea	9	Rosel <i>et al.</i> (1994); Natoli <i>et al.</i> (2008b)
CAN_Is	Canary Islands (Spain)	21	Hildebrandt <i>et al.</i> (<i>unpublished sequences</i>)
CHI	China	8	Wang <i>et al.</i> (<i>unpublished sequences</i>)
E_AUS	Eastern Australia	113	Möller <i>et al.</i> (2011)
GAL	Galicia (Spain)	28	Natoli <i>et al.</i> (2008b)
GC_Dc	Gulf of California, <i>Delphinus capensis</i>	108	Segura-Garcia (<i>unpublished sequences</i>)
GC_Dd	Gulf of California, <i>Delphinus delphis</i>	33	Segura-Garcia (<i>unpublished sequences</i>)
MED	Mediterranean	58	Natoli <i>et al.</i> (2008b)
NWA	Northwest Atlantic	55	Mirimin <i>et al.</i> (2009)
NZ	New Zealand	90	Stockin <i>et al.</i> (2013)
OM	Oman	47	This study
PAK	Pakistan	6	This study
S_AUS	Southern Australia	64	Bilgmann <i>et al.</i> 2014
SA	South Africa	31	Natoli <i>et al.</i> 2006

5.2.2 Microsatellite Loci

Eighteen microsatellite loci were amplified as described in Chapter 3. Because a number of samples were collected from free-ranging individuals, the dataset was checked for duplicate samples using pairwise relatedness coefficients, r (Queller & Goodnight, 1989) as calculated in KINGROUP v. 2 (Konovalov *et al.* 2004).

Null alleles, large allele dropout, and scoring errors were identified using MICROCHECKER (Van Oosterhout *et al.* 2004). Deviations from Hardy-Weinberg equilibrium were assessed for each locus within each population using a test analogous to Fisher's exact test (Guo & Thompson, 1992) as implemented in ARLEQUIN v. 3.5 (Excoffier & Lischer, 2010) using a Markov Chain method (chain length = 1,000,000, dememorisation steps = 10,000, Bonferroni correction applied). Pairwise linkage disequilibrium between loci was assessed for each

population through a likelihood ratio test utilizing the Expectation-Maximisation (EM) algorithm (1000 permutations, Bonferroni correction applied) (Slatkin & Excoffier, 1996). Loci under positive selection were identified using the LOSITAN workbench (Antao *et al.* 2008). Runs were conducted using the Infinite Alleles mutation model for 50,000 simulations, applying the ‘neutral mean F_{ST} ’, which removes potential non-neutral markers from initial mean F_{ST} calculations, and the ‘force mean F_{ST} ’ options. A 95% confidence limit and False Discovery Rate of 0.05 were applied.

In order to assess whether null alleles were influencing F_{ST} values, where they were present, the software package FREENA (Chapuis & Estoup, 2007) was used to apply a null allele correction (ENA) as described in Chapuis & Estoup (2007). F -statistics from datasets with and without loci exhibiting null alleles were also compared. If F_{ST} values were similar, between the corrected and uncorrected datasets, and if the differentiation pattern between datasets with and without loci exhibiting null alleles was the same, then uncorrected loci were retained.

F -statistics were calculated in ARLEQUIN v. 3.5 (Excoffier & Lischer, 2010) to explore differentiation between putative populations. Significance levels were determined through 100 permutations and Bonferroni correction was applied to account for Type-I error. Allelic richness was calculated using FSTAT v. 2.9.3.2 (Goudet, 2001) and Welch’s t -test was used test for differences in richness between putative populations. Relationships between putative populations were visualised through a Factorial Correspondence Analysis (FCA) performed in GENETIX (Belkhir *et al.* 2004).

Contemporary gene flow was assessed through investigation of dispersal patterns between populations in BAYESAss v. 1.3 (Wilson & Rannala, 2003). The burn-in length was set to 10^6 followed by 10^7 MCMC iterations with a sampling interval of 1000 iterations. All mixing parameters were altered to improve mixing: $\Delta A = 0.5$, $\Delta F = 0.5$ and $\Delta M = 0.2$. Trace files were viewed in Tracer v. 1.6 (Rambaut *et al.* 2014) and the log-probability was examined for convergence and good chain mixing. Analyses were also run multiple times to check runs had converged on similar posterior mean parameter estimates.

The number of populations (K) was determined through Bayesian clustering analysis as performed in STRUCTURE v. 2.3 (Pritchard, *et al.* 2000). The program was run with and without

a sampling location prior, LOCPRIOR (Hubisz *et al.* 2009) using the admixture ancestry and correlated allele frequency models. Burn-in length was set to 10^5 followed by 10^6 iterations and ALPHAPROPSD was set to 0.5 to improve admixture. Five independent runs were assessed for each value of K ranging from 1 to 5. Values for K were estimated using the web server CLUMPAK (Kopelman *et al.* 2015; <http://clumpak.tau.ac.il/index.html>), whereby both the rate of change in the log probability between successive values of K (ΔK) (Evanno *et al.* 2005) and the log likelihoods for each value of K were examined. Graphical representation of the clustering analyses was generated using the main pipeline on CLUMPAK. Once optimal values of K were inferred, a similar run was performed to investigate gene flow, or hybridisation/introgression, between populations using the USEPOPINFO option (Pritchard *et al.* 2000). This assumes pure ancestry for the majority of individuals sampled from a population with a small proportion of individuals with mixed ancestry. In order to identify migrants, and mixed ancestry in individuals with a single parent or grandparent from an alternative population, GENSBACK was set to 2. The prior probability that an individual had pure ancestry from its sampled population was set to 0.95, i.e. MIGRPRIOR = 0.05.

5.2.3 Mitochondrial DNA

A 308 bp fragment of the mtDNA control region was sequenced for all collected samples. Further sequences from worldwide populations were obtained from GenBank (see Table 43). In total, 671 sequences of *Delphinus* sp. were utilised in various analyses. Amplifications and sequencing were performed as described in Chapter 3.

Alignment of all sequences was performed using the MUSCLE algorithm (Edgar, 2004) as implemented in GENEIOUS v. 7.1.2 (<http://www.geneious.com>, Kearse *et al.* 2012). ARLEQUIN v. 3.5 (Excoffier & Lischer, 2010) was used to calculate pairwise F_{ST} and Φ_{ST} between putative populations. To calculate Φ_{ST} a Tamura-Nei genetic distance model was applied with a gamma-correction shape parameter $\alpha = 0.187$ as identified in jMODELTEST v. 2.1.6 (Darriba *et al.* 2012). Haplotype (h) and nucleotide (π) diversities were estimated and pairwise comparisons were made between populations using Welch's t -test. Tajima's D and Fu's F_s neutrality test statistics were also estimated (Tajima, 1989; Fu, 1997).

A median-joining haplotype network (Bandelt *et al.* 1999) was generated using POPART (<http://popart.otago.ac.nz>, Leigh & Bryant, 2015), $\epsilon = 0$, to visualize the phylogenetic rela-

tionships between haplotypes. A large number of ambiguous loops were exhibited in this network, making interpretation and visualisation difficult. Therefore, a minimum-spanning tree was computed in ARLEQUIN v. 3.5 (Excoffier & Lischer, 2010) based on pairwise distances between haplotypes and was visualised using HAPSTAR v. 0.7 (Teacher & Griffiths, 2011). The caveat to using the simplified minimum-spanning tree is that it is arbitrarily selected from several, equally optimal, trees.

The software M_{DI}V (Nielsen & Wakeley, 2001) uses the coalescence process to simultaneously estimate the parameter theta ($\theta = 4N_e\mu$), the migration rate (m) per locus per generation scaled to effective population size ($M = 2N_e m$), and the divergence time (t) per generation per locus scaled to effective population size ($T = t/2N_e$). Sequences of the mtDNA control region (283 bp) were used and therefore these parameters were scaled to the effective population size of females, N_{ef} ($\theta = 2N_{ef}\mu$, $M = N_{ef}m$, $T = t/N_{ef}$). Where μ = the mutation rate per locus per generation. Under the model, population sizes are assumed to be equal and constant, and migration rates symmetric, for each pairwise analysis. South African and South Australian populations were run with the Oman population in order to establish the chronological order of divergence events across the Indo-Pacific. Two MCMC runs of 5,000,000 cycles with 10% burn-in were performed using different random seeds. Priors used in the South Africa-Oman analysis for the parameters T and M were set to 10 and the default value (as defined by the software) was set for θ . For the Oman-South Australia analysis, T , M and θ were set to 2, 4 and 70 respectively. Posterior probabilities of the different runs were examined for convergence. Divergence times were calculated based on mutation rates of 7.0×10^{-8} substitutions per site per year (Harlin *et al.* 2003) and a faster rate of 5.0×10^{-7} substitutions per site per year (Ho *et al.* 2007). A generation time of 21 years was applied (Taylor *et al.* 2007). A mitogenome mutation rate of 9.86×10^{-9} (Vilstrup *et al.* 2011) and a generation time of 7 years (Murphy *et al.* 2009; Perrin, 2009) were also used, as conducted in Amaral *et al.* (2012a).

5.3 Results

5.3.1 Microsatellite Loci

Pairwise relatedness coefficients, r (Queller & Goodnight, 1989) revealed the presence of two duplicate samples (where $r = 1$). Duplicates exhibited identical genotypes across all loci, and were removed from further analyses. One duplicate was collected from strandings in Oman and the other from bycatch in South Africa. An error during labelling in the field or laboratory is deemed the most likely cause.

The presence of null alleles was detected in six loci across all three populations (OM, SA, PORT) in MICROCHECKER (Van Oosterhout *et al.* 2004), Dde65 (SA), Dde69 (OM), EV37Mn (PORT and SA), KWM2a (PORT), TexVet5 (PORT) and KWM1b (OM). Significant Hardy-Weinberg deviation was detected in Dde69 (OM), EV37 (PORT), DO8 (SA), KWM2a (SA) and TexVet5 (PORT) where $P < 0.05$, with Bonferroni correction applied (see Table 44). No linkage disequilibrium was detected between any loci for any population ($P < 0.05$, with Bonferroni correction). Positive selection was detected in Dde66, AAT44 and D08 and balancing selection was detected in Dde72. In light of these tests, four loci, D08, Dde66, AAT44 and EV37, were removed.

F -statistics between populations with and without adjustment for null alleles were compared in FREENA (Chapuis & Estoup, 2007) to test whether inclusion of loci with null alleles would produce different results. F_{ST} values with and without the loci exhibiting null alleles were also compared. Similar F_{ST} values were estimated between adjusted and unadjusted loci and the reduced dataset revealed a similar differentiation pattern. Therefore, 14 loci remained for all subsequent analyses. The average missing data across all remaining loci was 0.02%.

Pairwise comparisons of allelic richness (Table 45) between populations were not significantly different ($P > 0.05$). Pairwise F -statistics (Table 46) between putative populations were all highly significant ($P < 0.001$, Bonferroni correction applied).

The results of the Factorial Correspondence Analysis (FCA) are shown in Figure 78. Factors 1, and 2 accounted for 100% of the total variance, contributing 55.86%, and 44.18%, respectively. All three populations were clearly differentiated from each other, whereby Factor 1 differentiated between Oman and the other two populations, and Factor 2 separated South Africa from Portugal.

Dispersal estimates, as inferred in BAYESASS v. 1.3 (Wilson & Rannala, 2003), are shown in Table 47. The results suggest that contemporary migration between Portugal, South African and Oman is limited with $< 5\%$ of each population consisting of migrants (per generation) from other populations. The population receiving the most migrants per generation appears to be Oman with 2.0 and 2.5% of migrants per generation from Portugal and South Africa, respectively. Portugal received migrants from South Africa (1.9%) and Oman (1.2%) and

South Africa received migrants from Portugal (1.4%) and Oman (1.3%).

Bayesian clustering analysis, as implemented in STRUCTURE v. 2.3 (Pritchard, *et al.* 2000), was carried out to determine the numbers of populations present in our dataset. These analyses were run with and without prior information about sampling locality (LOCPRIOR). The highest hierarchical level for K , as estimated by the Evanno method (Evanno *et al.* 2005), and the highest posterior probability [$\ln P(D)$], were $K=3$, both with and without LOCPRIOR information (Figure 79). These correspond to i) the Oman population (OM), ii) the South African population (SA) and iii) the Portugal population (PORT). Estimates of individual ancestry revealed high assignment posterior probabilities (90% or higher), for the majority of individuals, to the populations they were sampled from (see Figure 80). Only one individual from Portugal has a reduced assignment probability of 79%, with a 17% probability of having a grandparent from the Oman population, suggestive of introgression.

Table 44: Number of alleles and expected and observed heterozygosities for each locus within each population. *=loci which deviated significantly from Hardy-Weinberg equilibrium ($P < 0.05$ after Bonferroni correction).

Locus	OM	SA	PORT
TexVet9			
No. of Alleles	2	2	2
Het (exp.)	0.0476	0.0385	0.1554
Het (obs.)	0.0476	0.0385	0.1667
Dde84			
No. of Alleles	10	10	9
Het (exp.)	0.8734	0.8929	0.778
Het (obs.)	0.7619	0.8846	0.8
Dde65			
No. of Alleles	6	7	7
Het (exp.)	0.7642	0.8085	0.6887
Het (obs.)	0.8095	0.6154	0.7333
Dde09			
No. of Alleles	5	4	7
Het (exp.)	0.7666	0.6418	0.7627
Het (obs.)	0.6191	0.6154	0.6667
Dde66			
No. of Alleles	4	6	11
Het (exp.)	0.338	0.8009	0.8791
Het (obs.)	0.2381	0.7692	0.9
Ttru AAT44			
No. of Alleles	6	5	8
Het (exp.)	0.8084	0.5769	0.7972
Het (obs.)	0.9524	0.7692	0.7667
Dde70			
No. of Alleles	11	7	13
Het (exp.)	0.8862	0.8311	0.9068
Het (obs.)	0.7619	0.8462	0.8
Dde69			
No. of Alleles	5	6	5
Het (exp.)	0.7306	0.6991	0.7328
Het (obs.)	0.3810*	0.5385	0.6333
Dde72			
No. of Alleles	6	9	8
Het (exp.)	0.7828	0.8484	0.8441
Het (obs.)	0.8095	0.7692	0.8
Dde59			

Locus	OM	SA	PORT
No. of Alleles	8	6	8
Het (exp.)	0.7933	0.7692	0.7944
Het (obs.)	0.8095	0.8462	0.7
EV14Pm			
No. of Alleles	11	9	15
Het (exp.)	0.8223	0.8303	0.926
Het (obs.)	0.7619	0.8846	0.7667
EV37Mn			
No. of Alleles	14	9	17
Het (exp.)	0.8513	0.7768	0.8825
Het (obs.)	0.8571	0.5769*	0.4667
D08			
No. of Alleles	13	9	10
Het (exp.)	0.8815	0.7534	0.8209
Het (obs.)	0.7143	0.4231	0.8667*
KWM2a			
No. of Alleles	10	8	12
Het (exp.)	0.849	0.6305	0.8689
Het (obs.)	0.7143	0.3462	0.7333*
TexVet5			
No. of Alleles	8	8	11
Het (exp.)	0.8165	0.7888	0.8622
Het (obs.)	0.8571	0.7308	0.5333
KWM2b			
No. of Alleles	4	4	6
Het (exp.)	0.7236	0.5784	0.8277
Het (obs.)	0.6191	0.6154*	0.9333
KWM1b			
No. of Alleles	3	-	4
Het (exp.)	0.417	-	0.2181
Het (obs.)	0.1429	-	0.2
KWM12a			
No. of Alleles	8	6	8
Het (exp.)	0.8386	0.8175	0.804
Het (obs.)	0.7619	0.6923	0.8

Table 45: Mitochondrial DNA (control region) and microsatellite diversity statistics for each putative population, considering 14 loci. Pop = population, π = nucleotide diversity, h = haplotype diversity, k = average number of alleles, H_o = observed heterozygosity, H_e = expected heterozygosity.

Mitochondrial DNA		Microsatellites, 14 loci						
Pop	No. of haplotypes	π	h	Pop	k	Allele richness	H_o	H_e
BS	7	0.011	0.917	OM	6.929	5.803	0.621	0.722
CAN_Is	19	0.022	0.991	SA	6.214	5.264	0.606	0.657
CHI	7	0.013	0.964	PORT	8.214	6.476	0.662	0.726
E_AUS	25	0.015	0.869					
GAL	20	0.022	0.966					
GC_Dc	26	0.013	0.902					
GC_Dd	30	0.028	0.994					
MED	23	0.021	0.907					
NWA	50	0.025	0.996					
NZ	63	0.027	0.990					
OM	14	0.007	0.775					
PAK	5	0.036	0.933					
S_AUS	60	0.029	0.998					
SA	8	0.021	0.789					

Table 46: Pairwise F_{ST} values for all populations considering 14 microsatellite loci. *=significant ($P < 0.001$).

	OM	SA	PORT
OM	-		
SA	0.096*	-	
PORT	0.073*	0.065*	-

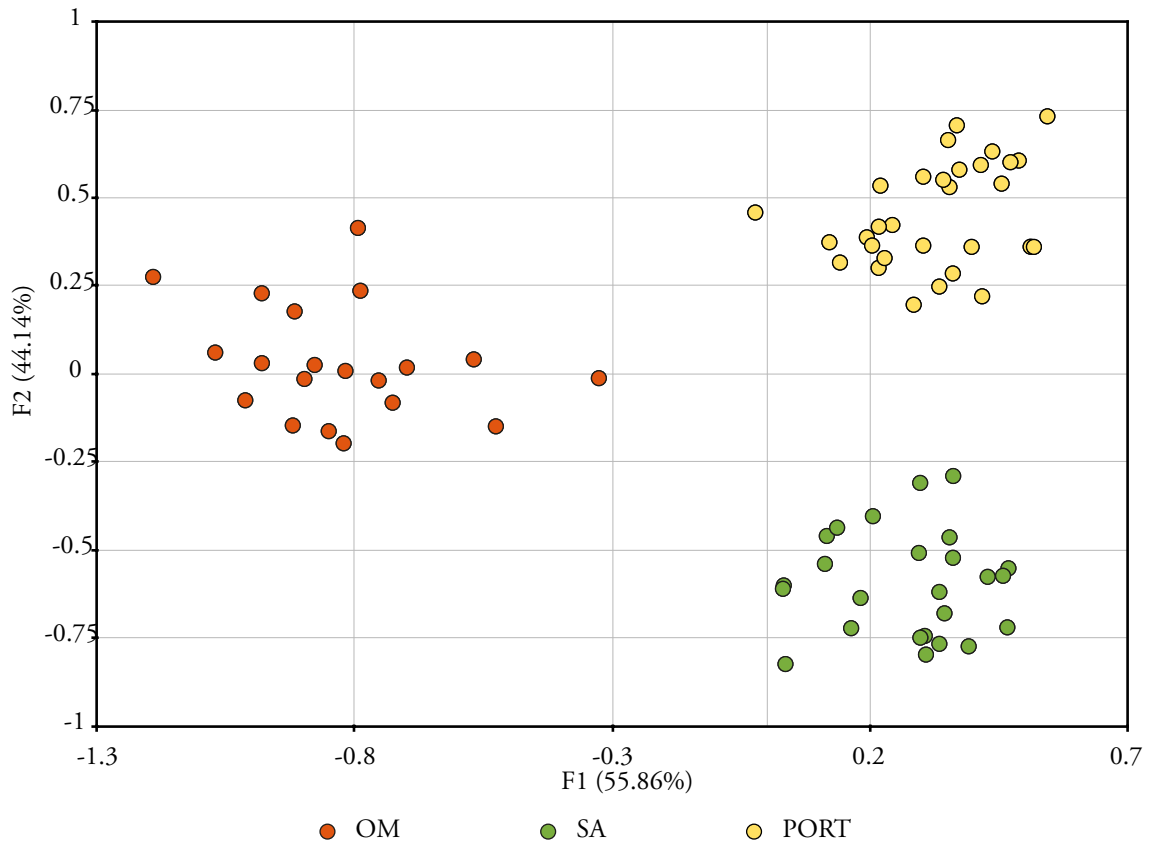


Figure 78: FCA plots for 14 microsatellites. Implemented in GENETIX (Belkhir *et al.* 2004). F1 vs F2. OM = Oman, SA = South Africa, PORT = Portugal. Percentage of variance explained by each factor is shown in parentheses.

Table 47: Posterior mean estimates for migration rates. Rates defined as the proportion of individuals in a ‘Current’ population that are migrants derived from a ‘Source’ population, per generation. Values inferred in BAYESASS v. 1.3 (Wilson & Rannala, 2003). Standard deviations given in parentheses.

	Source population		
	OM	PORT	SA
Current population			
OM	0.955 (0.026)	0.02 (0.018)	0.025 (0.021)
PORT	0.012 (0.011)	0.969 (0.019)	0.019 (0.016)
SA	0.013 (0.012)	0.014 (0.014)	0.973 (0.018)

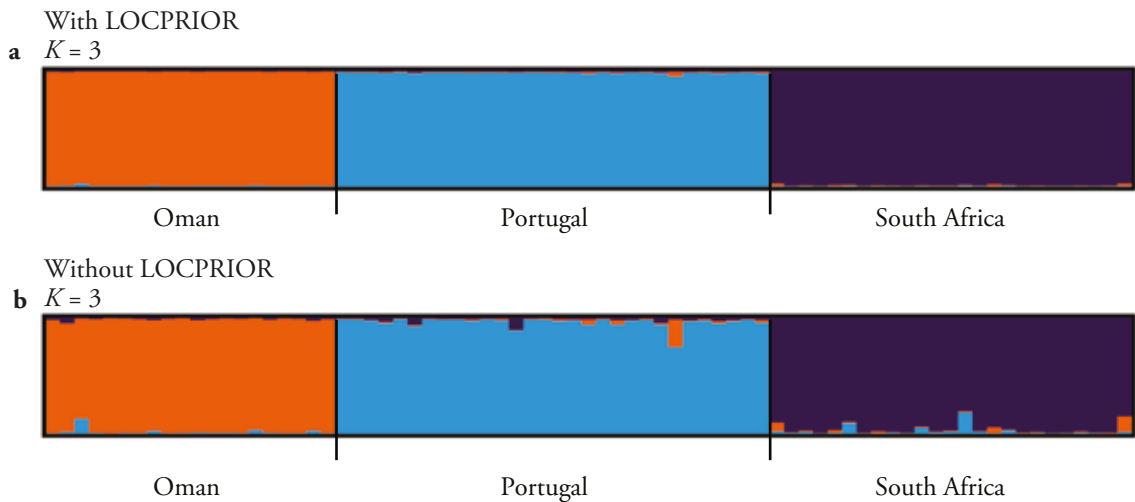


Figure 79: Probability assignment of individuals based on 14 microsatellite loci. Assignments carried out in STRUCTURE v. 2.3 (Pritchard *et al.* 2000) and generated using CLMUMPAK (Kopelman *et al.* 2015). a) $K = 3$ where LOCPRIOR information was used. b) $K = 3$ without LOCPRIOR information. Vertical coloured bars represent individuals and black lines delineate the respective putative populations sampled.

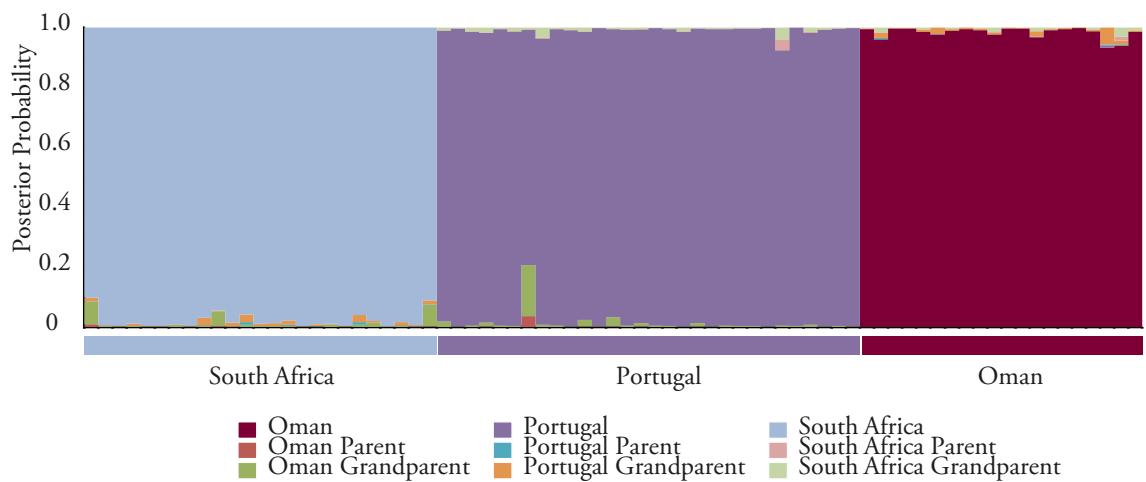


Figure 80: Ancestry posterior probabilities for each individual in the Oman, South Africa and Portugal populations using 14 microsatellite loci. Probabilities, generated in STRUCTURE v. 2.3 (Pritchard *et al.* 2000), are given for population assignment (pure ancestry) and whether an individual had a parent or grandparent from an alternative population.

5.3.2 Mitochondrial DNA

Across the 671 individuals at 308 bp of mtDNA control region sequence, a total of 294 haplotypes and 96 polymorphic sites were identified (see Appendix IX). Of the shared haplotypes ($n = 45$), the majority were shared exclusively between populations in the Atlantic, Mediterranean and Black Sea ($n = 21$). This group shared one haplotype with the South African population. Haplotypes were also shared within a group including populations from southern Australia, eastern Australia and New Zealand ($n = 19$). One haplotype was shared between South Africa and New Zealand. Two haplotypes were shared between Australian-New Zea-

land populations and *D. delphis* in the Gulf of California. The *D. capensis* population in the Gulf of California shared one haplotype with the population off Pakistan and another with New Zealand. No haplotypes were shared with the populations off Oman or China.

Measures of nucleotide (π) diversity ranged between 0.007 and 0.036 (see Table 45). Pairwise Welch's *t*-tests (Table 48) revealed the Oman populations to have significantly reduced nucleotide diversity ($\pi = 0.007$) compared to most populations ($P < 0.05$ after Bonferroni correction) except the Black Sea, Pakistan and China. However, these populations had relatively low sample sizes, reducing the statistical power in determining whether differences in π were significant. Populations of *D. capensis* off the Gulf of California also showed significantly low measures of nucleotide diversity compared to some populations, including *D. delphis* in the Gulf of California. The eastern Australian population and Black Sea population also showed significantly reduced π in some pairwise comparisons (see Table 48). Measures of haplotypic diversity (h) ranged between 0.775 and 0.998 (see Table 45). The Oman population showed significantly reduced h compared to most populations, except the Black Sea, Pakistan and South Africa. South Africa also had significantly lowered h compared to most other populations. Various populations showed significantly different haplotypic diversities (see Table 48).

Pairwise F_{ST} values were highly significant ($P < 0.001$, after Bonferroni correction) for all pairwise comparisons with Oman and South African populations (see Table 49). The majority of comparisons with *D. capensis* in the Gulf of California and New Zealand also yielded statistically significant F_{ST} values. Limited differentiation was exhibited between populations in the Atlantic, Mediterranean and Black Sea. Significant differentiation was exhibited between populations in Australia and New Zealand.

Patterns for Φ_{ST} were similar to F_{ST} . Comparisons between all populations outside the Atlantic, Mediterranean and Black Sea yielded highly significant Φ_{ST} values ($P < 0.001$, after Bonferroni correction), with the exception of New Zealand-Gulf of California *D. capensis* and Oman-Pakistan comparisons (see Table 49).

Table 48: P-values in pairwise comparisons of π (below diagonal) and h (above diagonal) using Welch's t -test. Shaded values indicate significant differences at $P = 0.05$, after Bonferroni correction. BS = Black Sea; CAN_Is = Canary Islands; CHI = China; E_AUS = Eastern Australia; GAL = Galicia (Spain); GC_Dc = Gulf of California *D. capensis*; GC_Dd = Gulf of California *D. delphis*; MED = Mediterranean; NWA = Northwest Atlantic; NZ = New Zealand; OM = Oman; PAK = Pakistan; S_AUS = Southern Australia; SA = South Africa.

	BS	CAN_Is	CHI	E_AUS	GAL	GC_Dc	GC_Dd	MED	NWA	NZ	OM	PAK	S_AUS	SA
N	9	21	8	113	28	108	33	58	55	90	47	6	64	31
BS	-	0.044	0.2657	0.1553	0.1522	0.6493	0.0354	0.7705	0.0323	0.0439	0.002	0.7834	0.0292	0.0028
CAN_Is	0.0045	-	0.3736	<0.0001	<0.0001	<0.0001	0.3726	<0.0001	0.1766	0.8993	<0.0001	0.303	0.0691	<0.0001
CHI	0.6385	0.0291	-	0.01	0.9637	0.0573	0.3088	0.077	0.2837	0.3778	0.0002	0.6015	0.2568	0.0002
E_AUS	0.1441	0.0166	0.4888	-	<0.0001	<0.0001	<0.0001	<0.0001	<0.0001	<0.0001	<0.0001	0.2492	<0.0001	<0.0001
GAL	0.0023	0.9677	0.0208	0.0048	-	<0.0001	<0.0001	<0.0001	<0.0001	<0.0001	<0.0001	0.5454	<0.0001	<0.0001
GC_Dc	0.519	0.0022	0.9616	0.0255	0.0003	-	<0.0001	0.1268	<0.0001	<0.0001	<0.0001	0.559	<0.0001	<0.0001
GC_Dd	<0.0001	0.1141	0.0009	<0.0001	0.0968	<0.0001	-	<0.0001	0.3188	0.0114	<0.0001	0.2744	0.0281	<0.0001
MED	0.0033	0.6723	0.0331	0.0007	0.5985	<0.0001	0.018	-	<0.0001	<0.0001	<0.0001	0.6251	<0.0001	<0.0001
NWA	0.0002	0.4306	0.0044	<0.0001	0.4094	<0.0001	0.2769	0.0967	-	<0.0001	<0.0001	0.2627	0.008	<0.0001
NZ	<0.0001	0.1239	0.0012	<0.0001	0.093	<0.0001	0.6964	0.004	0.326	-	<0.0001	0.3055	<0.0001	<0.0001
OM	0.1333	<0.0001	0.0901	<0.0001	<0.0001	<0.0001	<0.0001	<0.0001	<0.0001	<0.0001	-	0.0255	<0.0001	0.2866
PAK	0.0447	0.2078	0.0513	0.0698	0.2077	0.0505	0.4559	0.1636	0.2832	0.3817	0.024	-	0.2496	0.0364
S_AUS	<0.0001	0.0426	0.0004	<0.0001	0.0277	<0.0001	0.7932	0.0009	0.0994	0.4018	<0.0001	0.4977	-	<0.0001
SA	0.0056	0.6617	0.0433	0.0123	0.5986	0.0006	0.0271	0.944	0.1386	0.0147	<0.0001	0.1636	0.0036	-

Table 49: Mitochondrial DNA F_{ST} values below diagonal and Φ_{ST} above the diagonal. Colours are indicative of the cell value whereby darker shades correspond to higher values and lighter shades to lower values. * = $P < 0.001$ after Bonferroni correction.

	N	BS	CAN_Is	CHI	E_AUS	GAL	GC_Dc	GC_Dd	MED	NWA	NZ	OM	PAK	S_AUS	SA
BS	9	-	0.159	0.532*	0.377*	0.171*	0.648*	0.146*	0.104	0.107	0.177*	0.854*	0.516*	0.167*	0.133
CAN_Is	21	0.012	-	0.317*	0.178*	-0.008	0.557*	0.03	0.012	-0.018	0.066*	0.722*	0.301*	0.035	0.161*
CHI	8	0.06	0.021	-	0.347*	0.361*	0.725*	0.208*	0.275*	0.284*	0.188*	0.783*	0.402*	0.180*	0.392*
E_AUS	113	0.112*	0.076	0.093	-	0.241*	0.603*	0.143*	0.209*	0.167*	0.048*	0.724*	0.476*	0.051*	0.280*
GAL	28	0.03	-0.011	0.035	0.087*	-	0.566*	0.058*	0.076*	0.003	0.107*	0.709*	0.319*	0.088*	0.198*
GC_Dc	108	0.092*	0.057*	0.072	0.115*	0.068*	-	0.539*	0.547*	0.526*	0.512*	0.817*	0.593*	0.494*	0.629*
GC_Dd	33	0.04*	0.008	0.019	0.072*	0.020*	0.054*	-	0.066*	0.040*	0.021	0.679*	0.307*	0.029	0.154*
MED	58	0.019	0.027	0.069	0.113*	0.038*	0.095*	0.050*	-	0.024	0.089*	0.674*	0.350*	0.073*	0.137*
NWA	55	0.02	-0.008	0.018	0.070*	0.002	0.052*	0.005	0.025*	-	0.061*	0.652*	0.312*	0.055*	0.120*
NZ	90	0.042*	0.01	0.021	0.069*	0.022*	0.052*	0.007*	0.051*	0.007*	-	0.605*	0.302*	0.016*	0.116*
OM	47	0.168*	0.125*	0.149*	0.174*	0.134*	0.157*	0.118*	0.157*	0.113*	0.113*	-	0.415	0.612*	0.765*
PAK	6	0.076	0.034	0.05	0.107	0.048	0.022	0.031	0.082	0.03	0.033	0.166*	-	0.274*	0.462*
S_AUS	64	0.038*	0.006	0.017	0.059*	0.018*	0.051*	0.004*	0.047*	0.003	0.004*	0.111*	0.029	-	0.131*
SA	31	0.157*	0.108*	0.138*	0.167*	0.117*	0.148*	0.108*	0.145*	0.101*	0.101*	0.218*	0.155*	0.101*	-

Values for Tajima's D were not statistically significant after Bonferroni correction ($P = 0.05$). The Fu's F_S test is more powerful than Tajima's D at detecting deviations from neutrality/stationarity (Fu, 1997). Statistically significant values of Fu's F_S ($P < 0.02$, Bonferroni correction applied) were large and negative for *Delphinus* populations off the Canary Islands, Galicia (Spain), Gulf of California *D. delphis*, northwest Atlantic, New Zealand, and southern Australia, indicative of expansions in these populations (Table 50).

Table 50: Tajima's D and Fu's F_S values. No Tajima's D values were statistically significant at $P < 0.05$, after Bonferroni correction. * = Fu's F_S values that are statistically significant ($P < 0.02$), Bonferroni correction applied.

Pop	Tajima's D	Fu's F_S
BS	0.543	-2.444
CAN_Is	-0.384	-12.854*
CHI	-0.161	-2.928
E_AUS	-0.955	-7.46
GAL	-0.495	-9.244*
GC_Dc	-0.55	-10.332
GC_Dd	-1.109	-24.437*
MED	-0.396	-6.349
NWA	-0.503	-25.201*
NZ	-1.356	-25.02*
OM	-1.261	-6.308
PAK	1.092	0.606
S_AUS	-1.244	-25.03*
SA	0.074	2.723

The median-joining network (Appendix X) consisted of a large number of loops making visualisation difficult. Although this was the case, the haplotypes appear to form three haplotype clusters corresponding to a highly diverse *D. delphis* group (largely distributed worldwide), *D. capensis* (Gulf of California) and *D. c. tropicalis* in the northwest Indian Ocean (Oman and Pakistan). The minimum-spanning tree (Figure 81) is a simplification of the minimum-spanning network (not shown) but reveals a clustering pattern similar to the median-joining network (Appendix X).

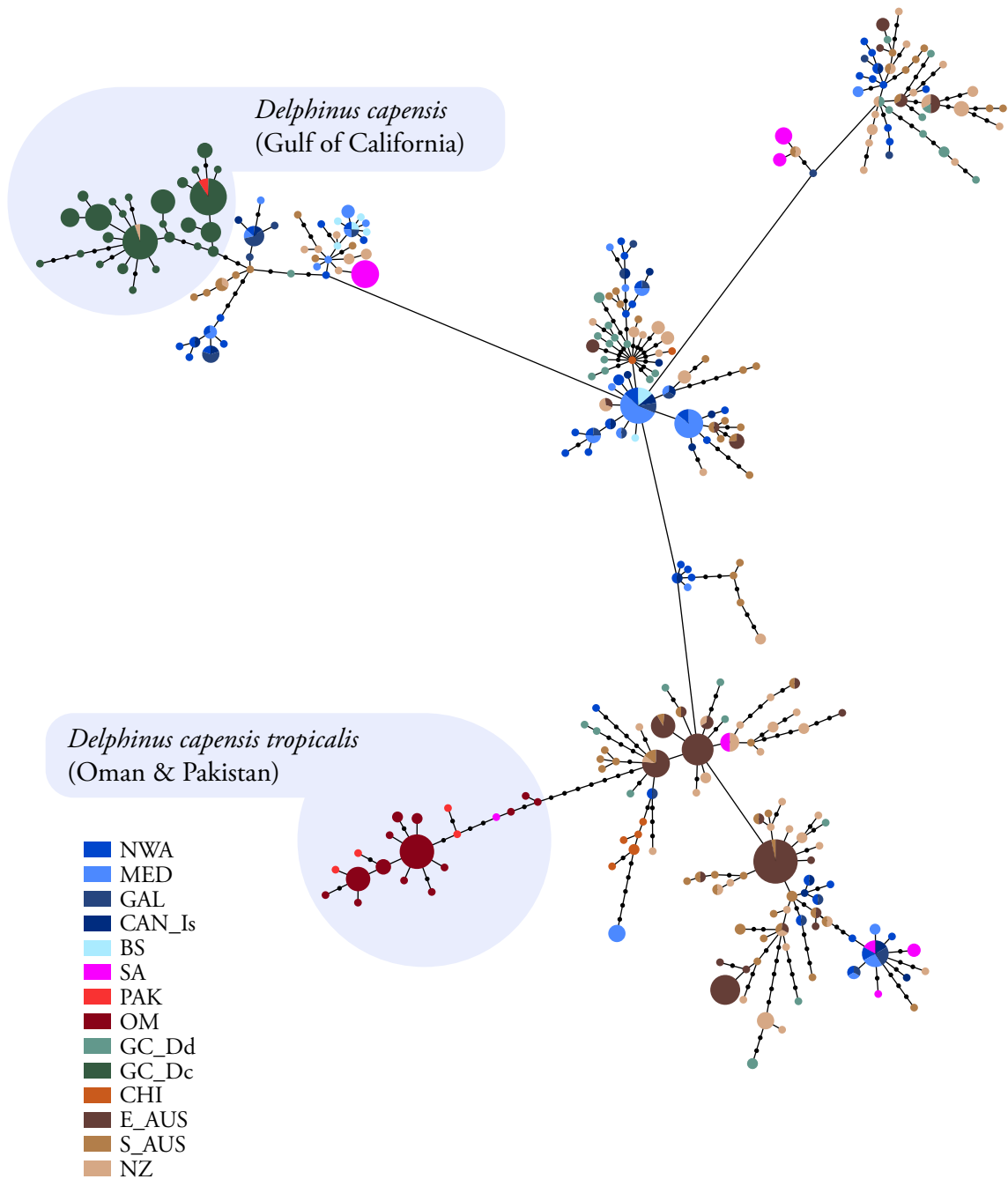


Figure 81: Common dolphin minimum spanning tree. Generated in HAPSTAR v. 0.7 (Teacher & Griffiths, 2011) from ARLEQUIN v. 3.5 (Excoffier & Lischer, 2010) output for all mtDNA sequences. Branch edge length corresponds to pairwise distance between haplotypes. Size of circle corresponds to number of individuals. Colours correspond to geographic location/population. Pale blue circles designate *D. capensis* from the Gulf of California and *D. capensis tropicalis* from the Indian Ocean.

The values of parameters θ , M and T , as inferred in MDiv (Nielsen & Wakeley, 2001), are presented in Table 51. The oldest population divergence is between Oman and South Australia (slow mutation rate = ~ 358 Ka; fast mutation rate = ~ 50 Ka) followed by Oman and South Africa (slow mutation rate = ~ 214 Ka; fast mutation rate = ~ 30 Ka). Using the same

generation time and mutation rate as Amaral *et al.* (2012a) these dates were estimated as \sim 2.54 Ma and \sim 1.52 Ma respectively.

Table 51: Values for θ , M and T . Parameters were estimated in M_{DIV} (Nielsen & Wakeley, 2001). Divergence times (YrsBP) were calculated using a mutation rate, μ of 3.23×10^{-4} , 2.31×10^{-3} and 2.13×10^{-5} mutations per locus per generation (see methods).

Analysis	θ	M	T	YrsBP $\mu = 3.23 \times 10^{-4}$	YrsBP $\mu = 2.31 \times 10^{-3}$	YrsBP $\mu = 2.13 \times 10^{-5}$
Oman/South Australia	59.36	0.04	0.26	357,922	50,109	2,541,029
Oman/South Africa	4.27	0.12	2.16	213,896	29,945	1,518,532

5.4 Discussion

The present study demonstrates the difficulties associated with delimiting taxonomic units in closely related, or incipient, species. Novel comparisons are made between common dolphins in the northwest Indian Ocean and other populations around the world based on microsatellite loci and mtDNA control region sequences. Additional evidence is provided for the taxonomic distinction of *D. c. tropicalis* from *D. delphis* and *D. capensis*, as reported elsewhere (Jefferson & Van Waerebeek, 2002; Amaral *et al.* 2012a). Consequently, further attention is brought to the northwest Indian Ocean as an area of evolutionary uniqueness for cetaceans. No signals for population expansion or decline were detected in *D. c. tropicalis* based on mtDNA control region sequences. However, this may be due to a lack of resolving power in the data as previous work, using a multi-locus dataset, identified a more complex demographic history for *D. c. tropicalis* (see Amaral *et al.* 2012a and below). Contemporary gene flow between the northwest Indian Ocean (Oman), southwest Indian Ocean (South Africa) and the Atlantic (Iberia) appears to be limited, with little evidence for mixed ancestries for individuals. These results will inform the delimitation of management units and design of conservation strategies, which are duly needed in the region given the anthropogenic threats faced by coastal cetaceans (see IWC, 1999; Anderson, 2014). The mechanisms that continue to give rise to taxonomic structure across cetacean genera in the region will be of broader interest to the study of speciation and evolutionary processes in highly mobile marine taxa.

The apparently independent convergence of multiple coastal populations of *Delphinus* on a long-beaked morphotype (Natoli *et al.* 2006) has arguably resulted in the incorrect assignment of these populations to *D. capensis*, such as long-beaked morphotypes off South Africa (Jefferson & Van Waerebeek, 2002). Alternatively, it is conceivable that what appears to be convergent evolution in unresolved lineages (due to incomplete lineage sorting and/or intro-

gression) is in fact phenotypic plasticity. For example, De Luna *et al.* (2012) suggest a plastic response to habitat/prey compositions as responsible for differences in beak-length exhibited between populations of harbor porpoise, *Phocoena phocoena*. In another example, trophic polymorphisms in pumpkinseed sunfish, *Lepomis gibbosus* are largely the result of phenotypic plasticity, rather than genetic differences (Robinson & Wilson, 1996).

5.4.1 Population Structure

Microsatellite data confirm that putative populations off Oman, South Africa and Portugal (already recognized by some at the species or subspecies level) were highly differentiated. The Oman-South Africa and Oman-Portugal comparisons, using microsatellite loci, are novel (this study). However significant differentiation between populations in the eastern Atlantic (Portugal) and off South Africa has been documented earlier using fewer loci ($n = 9$) (Natoli *et al.* 2006).

Analyses using mtDNA control region sequences permitted a broader range of comparisons, incorporating published data (Table 43). South Africa and Oman were significantly differentiated from most other populations, except Oman was not significantly differentiated from Pakistan based on Φ_{ST} . Differentiation between Oman and South Africa is consistent with the microsatellite data (this study) and earlier studies investigating *D. c. tropicalis* morphology (Jefferson & Van Waerebeek, 2002) and phylogeography (Amaral *et al.* 2012a).

Previous work suggests that populations occupying different ocean basins, or different sides of the same basin, exhibit significant genetic differentiation (Natoli *et al.* 2006; Mirimin *et al.* 2009; Amaral *et al.* 2012a; 2012b). However, comparison of sequences from the northwest Atlantic (obtained from Mirimin *et al.* 2009) with sequences in the eastern Atlantic, including sequences from the Canary Islands (Hildebrandt *et al. unpublished data*), Black Sea (Rosel *et al.* 1994; Natoli *et al.* 2008b), Galicia (Spain) (Natoli *et al.* 2008b) and Mediterranean Sea (Natoli *et al.* 2008b), revealed a general lack of differentiation between opposite sides of the Atlantic basin, with only populations in the northwest Atlantic and Mediterranean Sea exhibiting significant differentiation. This dissimilarity is likely the result of comparatively fewer base pairs of sequence data per individual in the present study (308 bp), thus reducing the power to resolve between closely related populations. Amongst the east Atlantic populations (Black Sea, Mediterranean Sea, Canary Islands and Galicia), there was significant

structure between populations in the Mediterranean Sea and Galicia (Spain), which has been documented before (see Natoli *et al.* 2008b). Galicia was also significantly differentiated from the Black Sea population based on Φ_{ST} .

In the Pacific, populations off New Zealand (from Stockin *et al.* 2013) were not significantly differentiated from populations of *D. delphis* in the northeast Pacific (from Segura-Garcia *et al. unpublished data*). A phylogeny based on cytochrome-*b* sequences showed that New Zealand individuals clustered with *D. delphis* from the northeast Pacific (Stockin *et al.* 2013), thereby supporting a lack of differentiation between these populations based on control region sequences (this study). All populations compared in the western Pacific, off China (Wang *et al. unpublished data*), southern Australia (Bilgmann *et al.* 2014), eastern Australia (Möller *et al.* 2011) and New Zealand (Stockin *et al.* 2013), were significantly differentiated from one another based on Φ_{ST} . Evidently there is greater regional-scale differentiation between populations in the Pacific than in the northern Atlantic, particularly around Oceania. The comparative lack of differentiation in the northern Atlantic may be explained by a relatively recent re-colonisation of the region after the last glacial maximum (LGM), whereby not enough time has elapsed for separate populations to accumulate genetic differences (Mirimin *et al.* 2009).

Amaral *et al.* (2012a) found *D. c. tropicalis* in the Arabian Sea (Oman) to form a distinct lineage, diverging basally to other lineages outside of the northeast Pacific, in a species tree generated from combined mitochondrial (one locus) and nuclear DNA (five loci) sequences. However, Amaral *et al.* (2012a) did not detect reciprocal monophyly for species and morphotypes, finding *D. c. tropicalis* cytochrome-*b* haplotypes clustered with haplotypes from the Atlantic, southwest Pacific and southeast Indian Ocean in a median-joining network. Furthermore, two *D. capensis* cytochrome-*b* haplotypes, from the northeast Pacific, clustered with *D. c. tropicalis* haplotypes (Amaral *et al.* 2012a). Long- and short-beaked morphotypes within *D. delphis* showed little regional genetic sub-division (Natoli *et al.* 2006; Amaral *et al.* 2012a).

A northeast Pacific origin for *Delphinus* has been posited by Amaral *et al.* (2012a), based largely on the distribution of cytochrome-*b* haplotypes within their median-joining network and the basal divergence of northeast Pacific *D. capensis* populations in their species phylog-

eny. Although this lineage diverged basally, it would be incorrect to assume that the northeast Pacific lineage was ‘basal/ancestral’ and the other lineages were derived because they include more extant (or sampled) taxa (see Krell & Cranston, 2004; Crisp & Cook, 2005). However, Amaral *et al.* (2012a) suggest that northeast Pacific cytochrome-*b* haplotypes nested within Atlantic haplotypes, and a lack of southeast Indian Ocean (*cf.* southern Australian) haplotypes amongst the Pacific haplotypes, support a northeast Pacific origin. Older lineages in the northeast Pacific, and more recent ones in the Atlantic, could partially explain the relative lack of differentiation in the Atlantic (incomplete lineage sorting), the sub-species status of *D. c. tropicalis* in the Indian Ocean and the species status of *D. capensis* in the northeast Pacific (complete lineage sorting at mtDNA control region) (Rosel *et al.* 1994).

Taxonomic resolution in Amaral *et al.* (2012a) is better than the present study because their inferences are based on sequences of mtDNA and multiple nuDNA markers, comprising a total of 271 segregating sites, whereas my study utilizes a single mtDNA locus of only 90 segregating sites. In addition, even though tests for congruence between loci were not implemented in Amaral *et al.* (2012a), for example, calculation of partitioned Bremer Support Indices (Baker & DeSalle, 1997) or implementation of hierarchical clustering methods (Leigh *et al.* 2008), haplotype networks generated from the different markers showed similar haplotype distribution patterns, suggesting congruence between markers.

Nevertheless, the control region haplotype network (Appendix X) and minimum-spanning tree (Figure 81) showed haplotypes from *D. c. tropicalis* and *D. capensis* to form lineages that were better resolved geographically compared to the cytochrome-*b* network presented in Amaral *et al.* (2012a). In the *D. c. tropicalis* cluster (this study), one haplotype included individuals sampled off South Africa while the rest were represented by *D. c. tropicalis* sampled off Oman and Pakistan. Within the *D. capensis* haplotype cluster, one haplotype was shared with *D. c. tropicalis* individuals sampled off Pakistan and another shared with a *D. delphis* individual from New Zealand. Within the diverse cluster of worldwide *D. delphis* haplotypes, none were shared with samples of *D. capensis* from the northeast Pacific or *D. c. tropicalis* from the northwest Indian Ocean. *D. delphis* haplotypes from the northeast Pacific generally formed clusters with haplotypes from Oceania. Associations between the Atlantic and northeast Pacific *D. delphis* haplotypes were in support of the westward dispersal of common dolphins from the Indo-Pacific, as posited by Amaral *et al.* (2012a).

5.4.2 Demographic Expansion, Population Divergence and Genetic Diversity

Neutrality tests using mtDNA sequences revealed significant demographic expansion signals in several populations around the world, including the Canary Islands, Galicia (Spain), Gulf of California *D. delphis*, northwest Atlantic, New Zealand, and southern Australia. These expansions have been documented in other studies (particularly Amaral *et al.* 2012a), either utilising the same sequences or using samples from similar areas. These were: the Canary Islands, Galicia (*cf.* ECA and GAL in Natoli *et al.* 2006), northwest Atlantic (Mirimin *et al.* 2009), New Zealand (Stockin *et al.* 2013; *cf.* Sb_SWPAC_NZ in Amaral *et al.* 2012a) Gulf of California *D. delphis* (Segura-Garcia, 2011; *cf.* Sb_NEPAC) and southern Australia (*cf.* Sb_SEIND in Amaral *et al.* 2012a). No signals of significant decline were detected in any population. Several populations did not show expansion signals based on neutrality tests (this study) even though expansions have been documented elsewhere based on other markers and analyses (e.g. Natoli *et al.* 2006; Amaral *et al.* 2012a). These include populations off South Africa (*cf.* Lb_SEATL in Amaral *et al.* 2012a), Oman/Pakistan (*cf.* Tro_WIND in Amaral *et al.* 2012a), *D. capensis* in the northeast Pacific (Natoli *et al.* 2006; Segura-Garcia, 2011; *cf.* Lb_NEPAC in Amaral *et al.* 2012a) and eastern Australia (*cf.* Sb_SWPAC_AUS in Amaral *et al.* 2012a). Again, this is likely due to the dataset (this study) encompassing comparatively fewer base pairs of sequence per individual. More data would be expected to provide more power to detect population expansions if they were present.

Haplotypic diversities (h) for South Africa and Oman were significantly reduced in comparison to other populations. Nucleotide diversities (π) were also significantly low for Oman but not South Africa. The reduced diversity in the South African population has been reported before (Natoli *et al.* 2006; Amaral *et al.* 2012a). The reduced diversity in coastal populations, and expansion in some long-beaked populations, is the result of founding events from oceanic populations followed by local adaptation to coastal environments (Natoli *et al.* 2006; Amaral *et al.* 2012a). Although Natoli *et al.* (2006) did not find a signal for expansion in the South African population, based on control region sequences, Amaral *et al.* (2012a) did find expansion in this population based on mismatch distribution analyses and extended Bayesian skyline plots (Drummond *et al.* 2005) using a multi-locus dataset. Although not detected in the present study, historic expansion signals, and signals for recent population decline, were detected in the Oman population of *D. c. tropicalis* by Amaral *et al.* (2012a) suggesting that this population may also have resulted from an independent founding event, followed by

expansion and adaptation to a coastal environment. This expansion coincides with a high productivity event in the Arabian Sea ~ 0.5 Ma (Amaral *et al.* 2012a). It has been suggested that recent re-colonisation of the northwest Atlantic after the LGM may have resulted in expansion signals in these populations (Mirimin *et al.* 2009).

Divergence dates inferred in M_{DIV} generally support a westward direction of population divergence events, as proposed elsewhere (e.g. Amaral *et al.* 2012a), whereby the *D. c. tropicalis* (Oman) population in the northwest Indian Ocean diverged from Australia *D. delphis* (slow mutation rate = ~ 358 Ka; fast mutation rate = ~ 50 Ka) before the divergence with South African long-beaked dolphins *D. delphis* (slow rate = ~ 214 Ka; fast rate = ~ 30 Ka). Divergence dates are determined by an estimated mutation rate for the locus, which is generally not precisely known. Here, I consider several mutation rates from the literature (see methods). Furthermore, M_{DIV} assumes symmetrical migration, constant and equal population sizes, and population sub-division is assumed to be absent (Nielsen & Wakeley, 2001). Many of these assumptions are likely to be violated. For example, demographic fluctuations over time are likely to have occurred, and Bilgmann *et al.* (2014) found population sub-division off southern Australia. The calculated divergence dates are generally more recent than those presented by Amaral *et al.* (2012a) based on cytochrome-*b* sequences. However, when applying the slower mitogenome mutation rate used by Amaral *et al.* (2012a), the divergence dates were considerably older. The divergence between *D. c. tropicalis* (Oman) and *D. delphis* from South Africa (estimated in the present study as 1.52 Ma) fell within the credible interval estimated in Amaral *et al.* (2012a) in a similar analysis (*cf.* LbATL-TroIND, ~ 0.744 Ma, 95% HPD: 0.702-1.968 Ma). The mutation rates presented in Harlin *et al.* (2003) and Ho *et al.* (2007) are more appropriate for the control region sequences used in the present study, and the divergence dates estimated are more consistent with the divergence between *Delphinus* sp. and *T. aduncus* (~ 490 Ka), as inferred from a mitogenome phylogeny (Moura *et al.* 2013a).

5.4.3 Contemporary Gene Flow

From the microsatellite data, inference of contemporary migration rates between the eastern Atlantic, South Africa and Oman, revealed limited genetic exchange between these locations with more than 95% of individuals per generation composed of non-migrants for each population. A signal for migration along the East and West African coastline suggests a South African emigration bias towards the eastern Atlantic, as previously reported in Natoli *et al.* (2006), and Oman (this study). The population off Oman exhibited the most immigration

but contributed the fewest immigrants to other populations. A bias in northward migration has been reported for other coastal dolphin species in the region, such as bottlenose dolphins, *Tursiops aduncus* (Chapter 3) and humpback dolphins, *Sousa plumbea* (Mendez *et al.* 2011). Mendez *et al.* (2011) suggest, based on observed correlations between population genetic structure and environmental heterogeneity, that northbound currents off east Africa and the Arabian Peninsula (during the southwest monsoon) influence humpback dolphin dispersal patterns in the region. Conversely, there is little evidence to suggest that ocean currents influence dolphin dispersal (*cf.* discussion in Chapter 3). Alternatively, it is conceivable that *D. c. tropicalis* express a higher degree of site fidelity, for example due to foraging specialisations (Rosel *et al.* 2009), than other common dolphin populations. If so, migration out of Oman could be more restricted. For example, distributions of groups of coastal bottlenose dolphins, *T. truncatus*, off Florida are restricted to habitats that provide the highest success given the foraging specializations adopted exclusively by the different groups (Torres & Read, 2009). Foraging specialization has been reported in common dolphin populations off Portugal (Moura *et al.* 2012) and South Africa (Young & Cockcroft, 1994) where they target pelagic shoaling fish.

The exceptionally long rostrum, characteristic of *D. c. tropicalis* (Jefferson & Van Waerebeek, 2002), suggests adaptation to local prey compositions, environmental conditions, or foraging strategies that may be habitat-specific. Stable isotope analysis of common dolphin skulls off Mauritania showed $\delta^{15}\text{N}$ to be significantly positively correlated with rostral length, indicating that dolphins with longer rostra are feeding at higher trophic levels (Pinela *et al.* 2011). Although this study was conducted on common dolphins elsewhere, this finding could imply that *D. c. tropicalis* are targeting prey at higher trophic levels. The limited documentation of *D. c. tropicalis* stomach contents from India and Pakistan (Pilleri & Gühr, 1972; James *et al.* 1987; Krishnan *et al.* 2008) suggests they feed on a variety of demersal and pelagic prey species, predominantly at high trophic levels, such as daggertooth conger pike (4.4 ± 0.67 se) and (Indian) mackerel (-3.2 ± 0.38 se) (FishBase, <http://www.fishbase.org>). However, these prey species do not appear to be particularly unusual for common dolphins (e.g. Pusineri *et al.* 2007; Meynier *et al.* 2008a; Meynier *et al.* 2008b)

There is clinal variation in common dolphin rostral length as one moves along the Indian Ocean coastline, reaching an extreme off India (Jefferson & Van Waerebeek, 2002), conse-

quent with waters that are characterised by high turbidity, due to river influx (Longhurst, 2006), and coastal mudbanks (Vivekanandan *et al.* 2003). Therefore, it is conceivable that the longer rostra exhibited in *D. c. tropicalis* are either adapted to targeting prey in low-visibility environments or are advantageous in foraging over habitats that are specific to the Indian coastline (Vivekanandan *et al.* 2003). For example, ‘rooting’ behaviour is a foraging strategy where the rostrum is used to flush out hidden prey, as seen in bottlenose dolphins, *Tursiops truncatus* (Rosbach & Herzing, 1997; Nowacek, 2002) and Ganges river dolphins, *Platanista gangetica* (Smith, 1993). However, given the observed cline in rostral length (Jefferson & Van Waerebeek, 2002), it seems more likely that the longer rostra exhibited in *D. c. tropicalis* are adaptive to foraging in a highly turbid/low-visibility environment rather than being adaptive to a specialised foraging strategy like ‘rooting’. Nevertheless, common dolphin habitat-specific foraging strategies may still be in place in the region, which could restrict the distribution and migration pattern of *D. c. tropicalis* (e.g. Rosel *et al.* 2009; Torres & Read, 2009) relative to more opportunistic foragers, such as populations off South Africa (Young & Cockcroft, 1994).

A longer rostrum is a characteristic shared with other dolphins in the region, for example spinner dolphins, *Stenella longirostris* (Van Waerebeek *et al.* 1999), humpback dolphins, *Sousa plumbea* (Jefferson & Van Waerebeek, 2004) and bottlenose dolphins, *Tursiops aduncus* (Chapter 4), suggesting convergence on a long-beaked phenotype (or phenotypic plasticity) in response to shared environmental gradients (e.g. turbidity). Adaptive and/or plastic responses to environmental gradients have been documented in other species, such as adaptation to altitude in common frogs, *Rana temporaria* (Bonin *et al.* 2006) and clinal variation in coat pigmentation of oldfield mice, *Peromyscus polionotus*, in response to soil type (Mullen & Hoekstra, 2008).

Alternatively, a cline in rostral-length could be the result of hybridization and introgression between *D. c. tropicalis* and adjacent populations producing intermediate forms (Jefferson & Van Waerebeek, 2002). For example, recent secondary contact between the Caspian gull, *Larus cachinnans*, and herring gull, *Larus argentatus* resulted in intermediate phenotypes within a hybridization/introgression zone (Gay *et al.* 2007). Investigation of hybridization and introgression based on microsatellite loci (this study) revealed little indication of introgression or hybridisation between populations off South Africa and *D. c. tropicalis* (off

Oman). However, in order to establish whether hybridisation/introgression was occurring between *D. c. tropicalis* and adjacent populations, more extensive sampling within the region is required. Evidence for introgression between *D. c. tropicalis* (off Oman) and *D. delphis* (Portugal) comes from one Portuguese individual that exhibited a 17% posterior probability of having a grandparent from Oman. This finding is interesting given the *D. c. tropicalis*-like 'Clade X' off the northeast Atlantic presented in Amaral *et al.* (2007).

5.4.4 Conclusions

Novel insights presented in this study remain restricted to comparisons with *D. c. tropicalis* in the northwest Indian Ocean based on novel mtDNA control region sequences (Oman and Pakistan) and microsatellite loci (Oman, Portugal and South Africa). There is strong differentiation between *D. c. tropicalis* off Oman and long-beaked *D. delphis* off South Africa, which supports findings based on other mtDNA and nuDNA loci (Amaral *et al.* 2012a). As reported elsewhere, there is generally little lineage sorting to establish regional lineages. However, based on a median-joining network (Appendix X) and minimum-spanning tree (Figure 81), *D. c. tropicalis* individuals off Oman/Pakistan and *D. capensis* individuals from the northeast Pacific largely group with their respective haplotype clusters. Expansion signals in various populations in the north Atlantic, and a comparative lack of differentiation, suggests recent re-colonisation of areas that were inaccessible during the LGM (Mirimin *et al.* 2009). Correspondingly, strong differentiation between various populations in the Indo-Pacific supports the perception that these populations are older (Amaral *et al.* 2012a). The strong differentiation of individuals in the northwest Indian Ocean (Oman/Pakistan), as well as the apparent limited emigration out of the region, leads me to speculate that their distribution is either physically determined by the regional environment, for example strong northbound currents (e.g. Mendez *et al.* 2011), or that their distribution is restricted to habitats unique to the region, to which they are particularly adapted (e.g. foraging specialisations) compared to conspecifics elsewhere, such as common dolphins off South Africa, which may be more opportunistic foragers (Young & Cockcroft, 1994). There is little indication of introgression/hybridisation between populations in my dataset, but such inference is limited by the distribution of samples. This study provides detail to the current understanding of common dolphin population structure, particularly as it pertains to populations in the northwest Indian Ocean. In addition, the present study further highlights the northwest/northern Indian Ocean as a region of taxonomic/evolutionary endemism, which will be informative to region-

al conservation initiatives. Finally, this study presents an example from the marine environment of the difficulties associated with delimiting taxonomic units in closely related species.

Chapter 6

General Discussion

6.1 Summary of Key Findings

Identifying evolutionarily significant units and delineating management units is important for the recognition and protection of evolutionary heritage (Moritz, 1994). The current study reveals the presence of a new *T. aduncus* lineage (Arabian Sea lineage), predominantly found off Pakistan and India, based on novel genetic and morphological data from the northwest Indian Ocean. Based on genetic criteria (Moritz, 1994), the Arabian Sea *T. aduncus* lineage can be considered an evolutionarily significant unit as it is reciprocally monophyletic for mtDNA (mitogenomes and mtDNA loci) and shows significant divergence of allele frequencies at nuclear loci (seven microsatellites). The estimated divergence date of the new lineage coincides with glacial climate change and exposure of the Indo-Pacific barrier off Australasia ~261 Ka. The distribution of *T. aduncus* holotype lineage and the Arabian Sea lineage samples suggests they occur in sympatry in the region. Furthermore, there is some evidence of hybridisation/introgression between these lineages. Whether divergence occurred in sympatry (coincidental with regional environmental heterogeneity) or allopatry (due to a historic ecological barrier) remains unknown. Further confirmation for the presence of *T. truncatus* and *Delphinus capensis tropicalis* in the northwest Indian Ocean is also provided.

This thesis identifies two management units of *T. aduncus* in the northwest Indian Ocean not previously documented, specifically off Oman/Arabia and Pakistan/India. Additional evidence is also presented for two management units off Zanzibar and three off South Africa, as documented elsewhere (Natoli *et al.* 2008; Särnblad *et al.* 2011; *in review*). Management units can be distinguished from evolutionarily significant units, as reciprocal monophyly at mtDNA loci is not a prerequisite. However, significant divergence of allele frequencies at nuclear or mitochondrial loci should be observed (Moritz, 1994). Such units are of particular use to short-term conservation initiatives for monitoring population trends and demographic study as, given the low levels of gene flow between them, they are functionally independent (Moritz, 1994).

Below, I outline a case for the conservation of cetaceans in the northwest Indian Ocean and follow this with discussion on the implications for the taxonomy and management of *T.*

aduncus and *Delphinus* spp. in the region. I then make a case for the study of evolutionary processes using marine mammal taxa and go on to summarise the evolutionary history inferred for bottlenose dolphins based on this thesis and discuss putative processes that underlie the evolution of bottlenose dolphins across the Indo-Pacific. Next, I discuss the findings in this thesis under the broader context of cetacean evolution and taxonomy in the region and follow this with a discussion on the comparative population structure and taxonomy of the species investigated here. I then briefly highlight recommendations for further research and finish my discussion with a concluding statement of the key findings.

6.2 A Case for the Conservation of Coastal Cetaceans in the Northwest Indian Ocean

The results presented in this thesis will inform much needed conservation efforts for dolphins in the northwest Indian Ocean. Although there is a good framework of international agreements, treaties and, in some cases, national legislation in place to protect cetaceans and their environment in general (see Chapter 1), enforcement is often weak (Anderson, 2014) and specific conservation initiatives for cetaceans are largely absent (Ponnampalam, 2009).

One exception is the regional initiative, which is building momentum (IWC, 2015; Minton *et al.* 2015), to conserve the isolated, non-migratory, population of Arabian Sea humpback whales, *Megaptera novaeangliae* (Minton *et al.* 2008). This population was exploited by illegal soviet whaling in the 1960s (Mikhalev, 1997) and current population size estimates off Oman, based on mark-recapture analyses, suggest ‘numbers in the low hundreds or fewer’ (Minton *et al.* 2011). This estimate was more recently corroborated by genetic analyses, suggesting an effective population size of ~100 individuals, and declining (Pomilla *et al.* 2014). In the wake of over a decade of research, the population has been listed as ‘Endangered’ on the IUCN Red List of Threatened Species (Minton *et al.* 2008), but may warrant ‘Critically Endangered’ status (see Pomilla *et al.* 2014), and is recognised by the IWC as a unique, isolated, sub-population which is of significant conservation concern given its small, and declining, population size (including associated threats, such as inbreeding depression and disease) as well as substantial anthropogenic threats in the region, such as incidental fisheries net entanglements and coastal development (IWC, 2010; IWC, 2015). From these developments, further research and monitoring of this population is being carried out (e.g. Willson *et al.* 2014) and important mitigation measures for oil exploration (e.g. seismic surveys) and port operations have been put in place to limit anthropogenic impacts in areas identified as critical

habitat (IWC, 2015). Work on humpback whales continues to pioneer cetacean research and conservation in the region and will provide a ('flagship' or 'umbrella') platform from which further initiatives can build from or work within (Baldwin *et al.* 2010).

Coastal cetaceans in the region, including humpback whales and a number of dolphin species, are under particular threat from incidental takes, and in some cases illegal directed takes, from fisheries activities (IWC, 1999; Collins *et al.* 2002; Anderson, 2014). *T. aduncus*, largely the focus of this thesis, and *D. c. tropicalis*, rely heavily on shallow, coastal and continental shelf habitats in the region, respectively (Minton *et al.* 2011). In certain locations, the impact on coastal dolphin populations (or indeed other marine life, e.g. marine turtles) of habitat fragmentation/degradation caused by construction of coastal hotels/resorts, motorways and ports remains largely unknown. Oil exploration (e.g. seismic surveys), pollution, shipping traffic and unregulated dolphin tourism contribute to the anthropogenic threats to these species in the region.

T. aduncus is a long-lived species that feeds at high trophic levels (Wells *et al.* 2004; Wang & Yang, 2009). Some populations exhibit strong site fidelity (Wang & Yang, 2009), possibly a result of the fitness advantages associated with familiarity of habitats/resources and conspecifics to form alliances with (e.g. Tsai & Mann, 2013). These factors render *T. aduncus* particularly susceptible to local environmental change, making them (and other cetacean species) potentially valuable sentinels, or 'indicator species', for monitoring ecosystem health (Katona & Whitehead, 1988; Ross, 2000; Wells *et al.* 2004; Simmonds & Isaac, 2007; Moore, 2008; Bossart, 2011). The concept of dolphins (particularly common dolphins, *Delphinus* sp. and spinner dolphins, *Stenella longirostris*) as 'indicator species' is somewhat reflected in the way their association with yellowfin tuna, *Thunnus albacares*, (Hall, 1998) is used by fishermen in the region, and other parts of the world, e.g. in the eastern Pacific (Lennert-Cody & Scott, 2005), as a visual cue for locating tuna (Baldwin *et al.* 1999; Ponnampalam, 2009; Anderson, 2014). Dolphins are also increasingly becoming an important commodity for the growing eco-tourism industry in the region. Off Muscat, the industry was worth an estimated US\$ 390,000 in 2009 and has continued to grow (Ponnampalam, 2009). Therefore, as well as a need to conserve the biological diversity and evolutionary potential of cetaceans in the region, there is also some important economic value in the conservation of coastal dolphins like *T. aduncus* and *D. c. tropicalis*.

6.3 Implications for Bottlenose Dolphin Taxonomy and Management

6.3.1 Contributions to the Resolution of Bottlenose Dolphin Taxonomy

The phylogenetic species concept (PSC) and biological species concept (BSC) are recognised for delineating species in cetacean taxonomy (Reeves *et al.* 2004). While the PSC has been applied extensively in cetaceans (e.g. Dalebout *et al.* 2002; Beasley *et al.* 2005), application of the BSC is more difficult given the readiness of cetaceans to hybridise (e.g. Bérubé & Aguilar, 1998; Silva Jr *et al.* 2005). More recent delineations have attempted to combine these concepts into a Genealogical Concordance Concept (GCC) (e.g. Charlton-Robb *et al.* 2011; Mendez *et al.* 2013), which utilises multiple lines of evidence such as morphology, or independent genetic loci, to delineate species (Reeves *et al.* 2004). Assessment of bottlenose dolphin taxonomy in the northwest Indian Ocean has been a conservation priority for some time (see IWC, 1999; Reeves *et al.* 2004). This thesis, in part, has set out to investigate whether the northwest Indian Ocean harbours any novel taxonomic units and to confirm the presence of taxonomic units already believed to occur in those waters.

For *Tursiops*, there is strong evidence for the presence of *T. aduncus*-type dolphins and *T. truncatus* in the northwest/northern Indian Ocean. This comes from multiple lines of evidence, including cranial morphology (utilising traditional and geometric morphometric techniques) and multiple mitochondrial loci. Two independent nuclear loci showed low phylogenetic resolving power when considered separately, however when included in a combined phylogenetic analysis, with mtDNA loci, they were congruent with the mtDNA phylogeny based on Partitioned Bremer Support Indices (Baker & DeSalle, 1997). *T. aduncus* and *T. truncatus* occur in parapatry throughout the region in coastal and pelagic habitats respectively, potentially coming into contact in areas where the continental shelf is particularly narrow, such as the Sea of Oman coastline off Oman or Oman's Dhofar region (see Minton *et al.* 2010).

There is also evidence for a new, *T. aduncus* lineage (herein referred to as the Arabian Sea lineage) in the northwest/northern Indian Ocean. This is based on phylogenies generated from mitogenome sequences and combined mtDNA-nuDNA loci (as above). Furthermore, there is high differentiation based on seven microsatellite loci with *T. aduncus* populations belonging to the holotype lineage. There is also evidence for significant delineation between the Arabian Sea and holotype lineage cranial morphologies (utilising both traditional and geometric morphometric techniques), although the distinctions are subtle compared to those

drawn from the genetic data. Taken together, these results fulfil the genetic criteria (Moritz, 1994) and the Genealogical Concordance Concept (Reeves *et al.* 2004) for the Arabian Sea *T. aduncus* to be considered an evolutionarily significant unit from the holotype *T. aduncus*. Therefore, the Arabian Sea lineage may be a candidate for species assignment, along with other lineages within the *T. aduncus* complex in Australasia (Wang *et al.* 1999b; 2000) and the holotype lineage (Natoli *et al.* 2004; Perrin *et al.* 2007). Although the PSC applies in this case it is more difficult to determine whether the lineages are reproductively isolated; a requisite for the BSC. Although one cannot speculate over what is happening in the eastern part of the Arabian Sea lineage's range (e.g. the Bay of Bengal and Andaman Sea) due to a lack of sample representation from this area, the sample locations in the western part of its range show a considerable overlap with the holotype lineage (Perrin *et al.* 2007) along the coast between Oman and India (see Figure 82). Indeed the majority of samples utilised herein have come from beach-cast specimens, calling into question whether they reflect the true distribution of free-ranging individuals, however one biopsy sample of the Arabian Sea lineage was collected in Oman's Dhofar region in a bay where the holotype lineage was also biopsied. Although these samples were obtained at different times of the year, it seems likely that these lineages are occurring in sympatry in at least some locations along the coastline between Oman and India. From analyses utilising morphological data (Chapter 4) and microsatellite/mtDNA data (Chapter 3) there is some indication of introgression/hybridisation (see below) suggesting that the BSC may not hold for these lineages. The taxonomic implications of this are uncertain; further work should attempt to identify whether a mechanism is in place preventing homogenisation of these lineages, such as assortative mating, or whether these lineages are coming into secondary contact after divergence in allopatry.

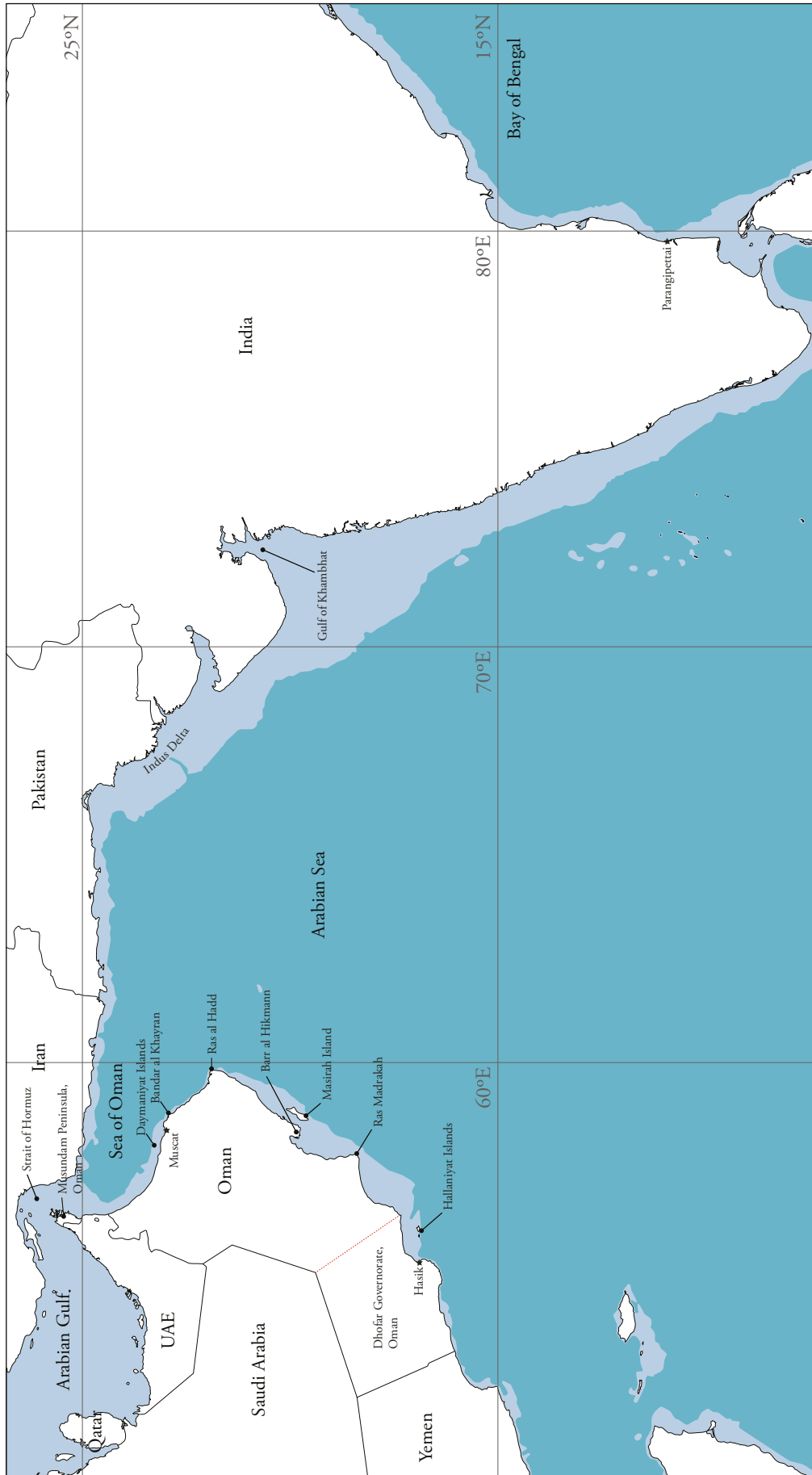


Figure 82: The coastlines of the Arabian Peninsula, Iran, Pakistan and India. Colour change = 200m isobath.

6.3.2 Evidence for Hybridisation and Introgression Between T. aduncus Lineages

In this thesis preliminary insights are made into natural hybridisation and introgression between two *T. aduncus* lineages. There are instances within the morphological analyses (Chapter 4) where taxonomic assignment of individuals based on morphology are incongruent with those based on mtDNA sequences. This could be explained in terms of hybridisation and introgression where individuals that are morphologically one type are carrying the mtDNA of the other. No microsatellite (nuDNA) data were available for the morphological specimens. The distribution of mtDNA control region haplotypes (Chapter 3) suggests an overlap between the lineages along the Arabian Sea coastline between Oman and India. Therefore, although there may be seasonal or habitat differences in the distribution of these separate lineages, it seems likely that there are opportunities for the lineages to hybridise. Cross-referencing lineage assignments based on nuDNA with those based on mtDNA suggested the lineages were admixing. One Indian sample belonged to the Arabian Sea lineage according to nuDNA ($P = 98.9\%$) but was a match for the holotype lineage based on mtDNA. Another individual from India was assigned to the Arabian Sea lineage based on nuDNA ($P = 83.9\%$), but may have had a grandparent from the holotype lineage ($P = 9.2\%$). An individual from Pakistan was assigned to the Arabian Sea lineage with a low probability based on nuDNA ($P = 48.6\%$), even though it was match for this lineage based on mitogenome sequence (Chapter 2). Another Pakistan sample was a match for the Arabian Sea lineage based on mtDNA, but showed some indication of ancestry or origin from the holotype lineage from its nuDNA. No samples genotyped for microsatellites within populations of the holotype lineage (Oman, Zanzibar and South Africa) were a match for the Arabian Sea lineage based on mtDNA, therefore no similar comparisons could be made within the holotype lineage. However, there was no indication of alternative origin/ancestry in the Oman samples based on nuDNA with high assignment probabilities to Oman ($P = 81.2 - 97.9\%$).

A degree of hybridisation/introgression between populations in Oman and Pakistan/India is indicative of admixture between the Arabian Sea and holotype lineages. Further sampling, and use of more genetic markers, is clearly necessary to fully measure the extent of this and determine what the conservation implications are.

6.3.3 Identification of Management Units

This thesis presents significant population genetic differentiation in *T. aduncus* in the western Indian Ocean using seven and 14-microsatellite loci datasets. Herein, I identify at least four management units in the region, encompassing two lineages, represented by individuals off 1) Pakistan/India, 2) Arabia, 3) Zanzibar, and 4) South Africa. Evidence for further structure, as documented elsewhere, off Zanzibar (Särnblad *et al.* 2011) and South Africa (Natoli *et al.* 2008b) was also observed.

Given the small sample sizes and coarse geographic scale, it is possible that complex and important sub-structure has been missed here. Further work should be carried out at a finer scale, and include regions not sampled here, in order to identify complex structure that might be significant towards resolution of management units (e.g. Bowen *et al.* 2005).

6.3.4 Estimates of Effective Population Size and Genetic Diversity

In the ABC analyses, two demographic scenarios (Sc. 2 and Sc. 3) performed similarly, with overlapping confidence intervals. Estimates for effective population sizes for the different management units based on the scenario with the highest posterior probability (Sc. 3) are as follows; Pakistan/India = \sim 20,700 (HPD: 8,950 – 29,400), 2) Arabia = \sim 12,200 (HPD: 3,530 – 19,500), 3) Zanzibar = \sim 12,300 (HPD: 5,020 – 19,300), 4) South Africa = \sim 4,400 (1,580 – 9,100). Estimates for the other scenario (Sc. 2) are similar (but see Chapter 3). The relatively low population size off South Africa has been reported previously (Natoli *et al.* 2008a).

Values of allelic richness (k) based on microsatellite loci were similar for all populations ($k = 5.214 - 6.143$), however haplotypic (h) and nucleotide (π) diversities in mtDNA were relatively low for the populations off South Africa ($h = 0.133 - 0.451$, $\pi = 0.001 - 0.004$) and Zanzibar ($h = 0.567 - 0.681$, $\pi = 0.006$). Natoli *et al.* (2008a) report similar results and suggest a founder-expansion model to explain the reduced genetic diversity in the South African populations, however expansion signals were not detected in their data (but see below). The populations off Zanzibar may similarly have experienced a founder or bottleneck event (Särnblad *et al.* 2011). Effective conservation management should take the reduced genetic diversities off South Africa and Zanzibar into consideration. The haplotypic and nucleotide diversities for the Arabian population ($h = 0.665$, $\pi = 0.012$) were lower than those reported

for Australasian *T. aduncus* off China ($h = 0.93$, $\pi = 0.016$) (Wang *et al.* 1999). The Pakistan/Indian population haplotypic and nucleotide diversities ($h = 0.907$, $\pi = 0.020$) were approximately equivalent to those reported for *T. aduncus* by Wang *et al.* (1999). The diversities observed in *T. truncatus* in the region were high ($h = 0.961$, $\pi = 0.031$) and comparable to *T. truncatus* populations in the Mediterranean and north Atlantic (Natoli *et al.* 2004; Qu erouil *et al.* 2010). The novel values of genetic diversity reported here are important baselines from which to monitor trends in genetic diversity (e.g. Pichler & Baker, 2000).

6.3.5 Population Dynamics

From the mtDNA, no significant deviations from population stationarity were detected based on neutrality tests (Tajima's D and Fu's F_s). However, expansion signals were detected using mismatch distribution analyses in the Pakistan/India population and sub-populations off South Africa (SA_S and SA_Bio) and Zanzibar (ZAN_N). In contrast, there is some evidence for population decline from the microsatellite data for South Africa, Zanzibar, Oman and Pakistan/India. However, the timing of these declines is not well resolved with large and overlapping credible intervals for posterior estimates (see Chapter 3). Signals of expansion in mtDNA and decline in nuDNA may be suggestive of recent expansions not yet detected in the nuDNA but detected in the mtDNA due to lower effective population size and elevated effects of drift in that locus. These mixed results suggest we need increased power (more samples and data) to unequivocally measure a population decline or expansion based on genetic data. Furthermore, it should be noted that much of the coastal development and growth of fisheries in the region has only come in recent decades and at an unprecedented pace (Baldwin *et al.* 2010). With a modernisation in fishing technology (e.g. off Oman), including the use of outboard engines and fibreglass fishing boats, fishing activities in the region have expanded rapidly (Ponnampalam, 2009). As dolphins are long-lived, it is possible that genetic signals of population decline, in response to these recent anthropogenic stressors, remain undetected at present (e.g. Pittman *et al.* 2011).

6.3.6 Identification of Migrants and Gene Flow

Movement of *T. aduncus* along the east African coastline and Arabia is asymmetrically northbound, with the majority of immigrants coming from the southern Zanzibar and (migratory) South Africa populations. This is similarly reported in *S. plumbea* in the region (Mendez *et al.* 2011). Mendez *et al.* (2011) suggest the northbound East African Coastal Current, which

intensifies during the southwest monsoon (Longhurst, 2006), as a putative reason for this. However, dolphins regularly travel against prevailing ocean currents (e.g. Wells *et al.* 1999; Photopoulou *et al.* 2011) and routinely move against the daily ebb and flood tides (Shane, 1980; Irvine *et al.* 1981). Therefore, a more credible explanation for the perceived northward migration bias in *T. aduncus* (and possibly *S. plumbea*) could be restricted movement of northern populations due to the adaptation of habitat-specific resource polymorphisms, such as foraging specialisations (Rosel *et al.* 2009). For example, distributions of groups of coastal bottlenose dolphins, *T. truncatus*, off Florida are restricted to habitats that provide the highest success given the foraging specializations adopted exclusively by the different groups (Torres & Read, 2009). If *T. aduncus* populations in the northwest Indian Ocean were uniquely adapted to the habitats they occupied, such that their dispersal was restricted compared to adjacent populations, this would be informative to regional conservation initiatives. Identification of critical habitat for *T. aduncus*, and observational study of their behaviour within those habitats, alongside dietary analyses, would elucidate this.

6.4 Implications for Common Dolphin Taxonomy and Management

6.4.1 Management Units, Genetic Diversity, Population Dynamics and Gene Flow

This thesis presents further support, based on novel microsatellite data and mtDNA sequences, for *D. c. tropicalis* as an evolutionarily significant unit; distinct from *D. delphis* and true *D. capensis*. Further support is given for the two management units in the Indian Ocean, one off South Africa (long beaked *D. delphis*) and the other off Oman/Pakistan (*D. c. tropicalis*). These are also distinct from units in the northeast Atlantic (short beaked *D. delphis*).

Relative measures of k for microsatellite data among populations off Oman, South Africa and Portugal were not significantly different. The population off Portugal was the most diverse ($k = 8.214$) while Oman and South Africa had similar measures of diversity ($k = 6.929$ and 6.214 , respectively). Haplotypic and nucleotide diversities for the Oman population were relatively low ($h = 0.775$, $\pi = 0.007$) compared to other populations ($h = 0.869 - 0.998$, $\pi = 0.011 - 0.036$). Amaral *et al.* (2012a) found evidence of decline in this population even though this was not detected here. This is likely due to comparatively less statistical power in this study. The design of management strategies in the region should consider the reduced genetic diversity in *D. c. tropicalis* off Oman.

Migration (gene flow) between populations off Oman, Portugal and South Africa was limited. With the exception of one *D. delphis* individual from Portugal, which showed evidence for having a *D. c. tropicalis* grandparent from Oman ($P = 17\%$), there was little evidence for introgression/hybridisation. These data confirm that these three populations should be managed separately.

6.5 Towards the Study of Evolutionary Processes

Because of the attributes that make dolphins particularly sensitive to ecological changes, as described above, they are exceptional candidates for the study of evolutionary processes in the marine environment in response to environmental change or heterogeneity. The study of such processes can provide a unique insight into how marine species and ecosystems may respond to future climate change or other anthropogenic stressors (Hoelzel *et al.* 2010). Furthermore, because dolphins feed at high trophic levels and their evolutionary histories often produce signatures coincident with environmental change (e.g. Mendez *et al.* 2011; Amaral *et al.* 2012a; Moura *et al.* 2013a), it is possible that phylogeographic analyses may uncover changes to marine ecosystems in response to cryptic environmental change or discontinuities. For example, phylogeographic analyses have provided insights into cryptic refugia and the extent of environmental change during glacial periods (Provan & Bennett, 2008; Fraser *et al.* 2009). Environmental heterogeneity (Longhurst, 2006) and a complex climatic history (Fontugne & Duplessy, 1986; Wang *et al.* 1999a; Almogi-Labin *et al.* 2000, Sun *et al.* 2003) are characteristic of the northwest Indian Ocean. Therefore, one might expect to see significant genetic differentiation in dolphin populations across the region. Indeed, this thesis provides insights into the effects of climate change and environmental heterogeneity on creating barriers to dolphin movement across the Indo-Pacific boundary and in the northwest Indian Ocean. The barrier across the Indo-Pacific has been proposed as a mechanism for divergence in other marine taxa (see Gaither & Rocha, 2013). However, insights into a putative barrier in the northwest Indian are novel.

6.6 Evolutionary History of Bottlenose Dolphins in the Northwest/Western Indian Ocean

6.6.1 Phylogeography and Evolutionary History

Novel phylogeographic analyses, based on multiple loci, reveal the Arabian Sea *T. aduncus* lineage as most closely related to the Australasian *T. aduncus* (Wang *et al.* 1999b; 2000) and

is represented off Pakistan, India and Oman. Novel divergence date estimates and reconstructions of ancestral biogeography, suggest the Arabian Sea *T. aduncus* lineage diverged from the Australasian lineage ~261 Ka (95% HPD: 111, 509) in a vicariance event, possibly associated with dispersal. Similarly, the divergence of the western Indian Ocean lineage (holotype) from other *T. aduncus* took place ~100 Ka earlier, ~342 Ka (95% HPD: 143, 630 Ka) in a vicariance event, possibly associated with dispersal. Ancestral biogeographic reconstructions suggest Australasia as the origin for several nodes within the *Tursiops* lineage, including ancestors within *T. aduncus*, the ancestor to *T. aduncus* and *T. truncatus* and the ancestor common to all *Tursiops* (see Chapter 2). These results are suggestive of an Australasian origin for the *Tursiops* genus, as suggested by Moura *et al.* (2013a).

Moura *et al.* (2013a) suggested the ancestor to the *Tursiops* genus was a coastal ecotype, based on reconstructions of ancestral biogeography (*cf.* Chapter 2). In the present study reconstructions of ancestral morphological states were performed to determine which morphological traits were ancestral and which were derived. Estimated values suggested a common ancestor to *Tursiops* that resembled extant *T. aduncus*-type dolphins for the majority of measured characters. This was also true for the *T. aduncus* - *T. truncatus* ancestor, supporting the hypothesis of a coastal origin for the *Tursiops* lineages.

Within the *T. aduncus* holotype lineage, divergence dates of adjacent populations in the western Indian Ocean suggest populations were established in a southerly direction whereby the oldest divergence events occurred off Arabia, then Zanzibar and finally South Africa. A similar pattern was recorded in *S. plumbea* populations from similar locations (Mendez *et al.* 2011), suggesting they have a similar evolutionary history to *T. aduncus* in the region. Although various demographic scenarios were explored to determine the direction and timing of population divergence events along the western Indian Ocean coastline (see ABC analyses above), the results remained largely inconclusive (see Chapter 3).

Off Oman, individuals representing the Arabian Sea lineage are rare, while the majority represent the *T. aduncus* holotype lineage (Natoli *et al.* 2004; Perrin *et al.* 2007). In an earlier study, Särnblad *et al.* (*in review*) identified four samples from Oman to be a genetic match for the *T. aduncus* holotype. This lineage has been reported off South Africa (Natoli *et al.* 2004), Mayotte (Särnblad *et al.* *in review*), Zanzibar (Särnblad *et al.* 2011; *in review*), the

Red Sea (holotype) (Perrin *et al.* 2007), Iran (Mohsenian *et al. unpublished data*; this study) and India (this study). Samples collected near Songkhla, along the east coast of Thailand (see Chapter 3) were a match for the Australasian *T. aduncus* lineage (Wang *et al.* 1999b; 2000). This suggests that the transition from the Arabian Sea lineage to the Australasian lineage may occur in the Andaman Sea or Bay of Bengal. Further samples from these regions would help elucidate this.

The range overlap between the Arabian Sea and holotype lineages in the northwest Indian Ocean suggests there is currently no barrier, impermeable to dispersal, between them (see Chapter 3). However, in order for three lineages of *T. aduncus*, to exist across the Indo-Pacific, at least two divergence events must have occurred; one in the waters around Australasia and the other in the northwest Indian Ocean.

6.6.2 A Putative Barrier to Dolphin Dispersal in the Northwest Indian Ocean

To facilitate divergence and prevent homogenisation between lineages (or populations experiencing incipient divergence) during inter-glacial secondary contact, a divergence mechanism would have been required in the northwest Indian Ocean. In the absence of any obvious contemporary or historic geological/physical barrier, such a mechanism may be ecological, for example adaptation to local habitats after establishment of resource polymorphisms (Hoelzel, 1998a). Indeed, there are distinct habitat differences between the east and west Arabian Sea coastlines. The coastlines off India and Pakistan are characterised by brackish waters with high organic discharges from river systems (Longhurst, 2006), for example, the Indus river delta. The waters off Oman are characterised by very high productivity through seasonal reversal of the monsoon system (Banse & McClain, 1986; Bauer *et al.* 1991; Burkill, 1999; Kindle & Arnone, 2001; Singh *et al.* 2011). Based on fish endemism, Briggs & Bowen (2012) suggest the western Indian Ocean be considered a separate marine biogeographic province from the central Indian Ocean and western Pacific. Differences in fish species compositions in these provinces may result in local adaptation of dolphin lineages to different prey. Such differences in habitat and resources could be drivers in the divergence of these lineages in sympatry (Hoelzel, 1998a). Differentiation in skull geometry, associated with the temporal fossa, was found between the holotype and Arabian Sea *T. aduncus* lineages (Chapter 4), suggesting shape differences in the location for jaw muscle attachment (Mead & Fordyce, 2009). This could be indicative of different foraging strategies or target prey between these lineages. Work on stomach contents and stable isotopes would be required to explore this further.

Humpback dolphins, *S. plumbea*, in Oman appear to be absent along the Sea of Oman coast (Baldwin *et al.* 2004), which could be indicative of a barrier or environmental break for *T. aduncus*. However, this stretch of coastline as a barrier seems unlikely because bottlenose dolphins sampled off Musundam (the Strait of Hormuz) are a match for the holotype lineage, and are therefore continuous with the western Arabian Sea populations. Furthermore, coastal bottlenose dolphins are occasionally (and historically) reported along the Sea of Oman coast (Baldwin *pers. comm.*). The more recent absence of *T. aduncus* sightings along this stretch of coastline is a concern, and likely the result of increased coastal development, and fisheries activities. It is also possible that humpback dolphins suffered an earlier disappearance from this stretch of coastline before their presence could be recorded (Baldwin *et al.* 2004).

Alternatively, a historic barrier, now absent, could have caused populations to diverge in allopatry in the region. Palaeoproductivity data from the northern Indian Ocean suggests great variability in the Asian Monsoon system over the Pleistocene (Fontugne & Duplessy, 1986; Wang *et al.* 1999a Almogi-Labin *et al.* 2000, Sun *et al.* 2003). Furthermore, off Pakistan and India, turbidite deposits from the Indus delta were higher during glacial periods, suggesting the environment may have been particularly turbid (von Rad & Tahir, 1997). Such changes in monsoon associated productivity, or turbidity along the India-Pakistan coastline, may have formed a break in habitat or resources, resulting in divergence in allopatry. Under this scenario, the apparent overlap between the holotype and Arabian Sea lineages would be explained in terms of relatively recent secondary contact.

6.6.3 A Putative Barrier to Dolphin Dispersal Across the Indo-Pacific Boundary

Although the credible intervals of estimates are large, the two divergence dates that gave rise to three *T. aduncus* lineages coincide approximately with low sea level stands during the Pleistocene at ~261 Ka and ~342 Ka (see Rohling *et al.* 2014 and Chapter 2). Furthermore, ancestral reconstructions of biogeography suggest these divergence events were vicariant, perhaps associated with dispersal out of Australasia. Due to the geographic placement and timing of these events, it seems credible that repeated exposure of the Indo-Pacific boundary in Australasia (Voris, 2000) created a barrier between populations either side of it and thereby facilitating divergence in allopatry (see Chapter 2). A similar divergence mechanism has been proposed for tropical reef fish species in that region, see (Gaither & Rocha, 2013).

Interestingly, Mendez *et al.* (2013) suggest the potential presence of a further assemblage of humpback dolphins off Thailand-Bangladesh based on preliminary molecular analyses. If bottlenose dolphin divergence dates do coincide with low sea level stands during glacial periods, then it is conceivable that a further lineage of *T. aduncus* exists in this locality; the result of a glacial period as yet unaccounted for in the present phylogeographic analyses e.g. the last glacial maximum or the Eemian. Further investigations should include samples from this region.

6.7 The Regional Context

Productivity in the northwest Indian Ocean, particularly the Arabian Sea, is governed by the seasonal reversal of the Asian monsoon system (Banse & McClain, 1986; Bauer *et al.* 1991; Burkill, 1999; Kindle & Arnone, 2001; Singh *et al.* 2011). The coastal waters off India/Pakistan are characterised by river outflows, such as the Indus and Ganges river deltas, discharging organic material, creating a turbid, brackish environment for coastal species (Longhurst, 2006).

Overall, the observed pattern of *T. aduncus* population structure and taxonomy generally reflects that of *Sousa* spp. in the region (Mendez *et al.* 2011; 2013). In this species, genetic differentiation in sympatry appears to coincide with local differences in habitat and the presence of environmental discontinuities 'breaks' (Mendez *et al.* 2011), suggesting adaptation to local habitat as a driving force. Mendez *et al.* (2011) identify an important 'break' where the South Equatorial Current bisects as it encounters the African continent and suggest this could provide a barrier to gene flow between *S. plumbea* populations off South Africa and Zanzibar. Habitats preferences for *T. aduncus* and *Sousa* spp. are known to overlap (Wang & Yang, 2009), therefore it is possible both species experience similar evolutionary pressures, resulting in similar patterns of genetic structure. However, it should be noted that Ponnampalam *et al.* (2012) found Oman *Tursiops* spp. and *S. plumbea* prey compositions in stomach contents to overlap for only one prey species; the tigertooth croaker, *Otolithes ruber*. This prey species was of low importance to *Tursiops* (modified Index of Relative Importance (IRI) = 166.5) but was the most important prey species for *S. plumbea* (IRI=1384.8). Therefore, if the evolutionary pressures for local adaptation are similar between the dolphin species they are more likely to do with behavioural or environmental conditions for foraging in general, or specialising on a particular ecological guild, rather than adaptation to targeting the same prey

species. However, given low sample sizes, the study by Ponnampalam *et al.* (2012) should be regarded as preliminary. Additionally, little distinction is made between *T. truncatus* and *T. aduncus* making it is possible that the IRI values for certain prey species may be incorrect for *T. aduncus*. Furthermore, investigating stomach contents of stranded animals is not without its caveats due to an uncertainty over whether they represent the diet of healthy, free-ranging individuals (see Sekiguchi *et al.* 1992; Krishnan *et al.* 2007), although there is some indication that they do (see Dunshea *et al.* 2013).

The taxonomy of *Sousa* spp. (Mendez *et al.* 2013) also broadly corresponds with that of *T. aduncus*, with a distinct lineage in the northern Indian Ocean, namely *S. chinensis*. Being a coastal dolphin, it is conceivable that *Sousa* lineages diverged as described here for *T. aduncus*. Common dolphins in the region form a distinct evolutionarily significant unit, *D. c. tropicalis* (Jefferson & Van Waerebeek, 2002; Amaral *et al.* 2012a). There is also some preliminary evidence to suggest spinner dolphins, *Stenella longirostris*, are morphologically distinct in the northern Indian Ocean (Van Waerebeek *et al.* 1999). In mysticetes, humpback whales, *Megaptera novaeangliae* in the Arabian Sea are a genetically distinct and isolated population of non-migratory humpback whales in the northwest Indian Ocean (Mikhalev, 1997; Minton *et al.* 2011; Pomilla *et al.* 2014). It is unlikely that the divergence of this population from southern hemisphere stocks ~70 Ka (Pomilla *et al.* 2014) is linked to the putative mechanisms proposed above for coastal dolphins, however it is an interesting example of how the environmental conditions in the northern Indian Ocean, likely associated with the high productivity of the region, are unique, and provide opportunities for a variety of cetacean species to adapt to local conditions. Other mysticete species, such as Bryde's whales, *Balaenoptera brydeiledeni* (see Kershaw *et al.* 2013) and blue whales, *B. musculus* (Branch *et al.* 2007) also show indications of population-level endemism to the northern Indian Ocean.

6.8 Differentiation in Bottlenose and Common Dolphins: A Comparison

The general pattern of taxonomic structure exhibited within the *Delphinus* genus, to some extent, mirrors that of the *Tursiops* genus, in that the northwest Indian Ocean harbours a distinct taxonomic unit of *Delphinus* (*D. c. tropicalis*) and *Tursiops* (Arabian Sea *T. aduncus*). Furthermore, both *Delphinus* and *Tursiops* have coastal and pelagic variants/species across the Indo-Pacific region.

Tursiops apparently exhibits higher genetic differentiation and complexity than *Delphinus* on a taxonomic level. For instance, within *Tursiops*, at least three species are considered; *T. australis*, *T. truncatus* and *T. aduncus* (LeDuc *et al.* 1999; Wang *et al.* 1999b; Charlton-Robb *et al.* 2011). Furthermore, there is increasing support for further species-level division within the *T. aduncus* group into three lineages (Natoli *et al.* 2004; Moura *et al.* 2013a; this study). Conversely, within *Delphinus* only two species, *D. capensis* and *D. delphis* (Heyning & Perrin, 1994; Rosel *et al.* 1994; Amaral *et al.* 2012a) and one subspecies, *D. c. tropicalis* (Jefferson & Van Waerebeek, 2002; Amaral *et al.* 2012a), are recognised. Coastal lineages are more sensitive to environmental change and differentiation, particularly where changes in coastal topography restrict movement between regions, for example, exposure of the Sunda/Sahul shelves separating *T. aduncus* populations in the eastern Indian Ocean and western Pacific. As a result, coastal populations often exhibit higher levels of genetic differentiation than pelagic populations (e.g. Quérouil *et al.* 2007; 2010). Indeed the ancestor to *T. truncatus* and *T. aduncus* appears to have exhibited a morphology resembling extant *T. aduncus*, a coastal species.

The pelagic ancestry of *Delphinus* (Amaral *et al.* 2012a) would suggest that the relative number of opportunities for taxonomic divergence and fine-scale population differentiation, particularly in response to coastal environmental change or differentiation, are fewer than for *Tursiops*. Because of this, parallels may be drawn, in terms of divergence mechanisms giving rise to coastal forms within *T. truncatus* rather than the *Tursiops* genus in its entirety. For instance, we may draw a parallel between the divergences of *D. capensis*-types from pelagic *D. delphis*-types with the divergence of coastal ecotypes of *T. truncatus* from pelagic variants in the northwest Atlantic. The *D. c. tropicalis* in the northwest Indian Ocean and *D. capensis* in the northeast Pacific may have been early, independent, transitions to a coastal ecotype within *Delphinus* (see Amaral *et al.* 2012a). Estimations of ancestral biogeography and divergence dates, as presented for *Tursiops* (Moura *et al.* 2013a; Chapter 2), would be required in order to compare the divergence patterns within *Delphinus* and *Tursiops* in the context of the divergence mechanisms presented for *T. aduncus* above. However, given the pelagic nature of *Delphinus* in comparison to *Tursiops*, the genus may have been less affected by exposure of the Sunda/Sahul shelves in Australasia than *T. aduncus* ancestors.

Results from microsatellite data compare *D. c. tropicalis* with *Delphinus* sp. off the southwest Indian Ocean and northeast Atlantic, whereas similar data from *T. aduncus*, compare populations in the western Indian Ocean. The results presented on fine-scale population structure within the genera, using microsatellite data, are not truly comparable because these comparisons are largely intra-lineage for *Tursiops*, whereas they are inter-lineage for *Delphinus*. However, it is interesting to note that *D. c. tropicalis* and the new, Arabian Sea *T. aduncus* occur in similar locations in the northwest Indian Ocean. Although investigations using mitochondrial DNA control region sequence data cover a larger area for both *Delphinus* and *Tursiops*, few areas overlap such that useful comparisons, pertaining to geography, can be drawn. Nonetheless, both genera exhibit significant genetic differentiation across relatively small spatial scales, suggesting local adaptation to habitat characteristics, prey compositions or differential use of resources, may be driving fine-scale population structure in both genera.

From the morphological analyses it is interesting to note that both *D. c. tropicalis* (see Jefferson & Van Waerebeek, 2002) and the new, Arabian Sea lineage of *T. aduncus* (see Chapter 4) exhibit slender skulls with long rostra when compared to their conspecifics in other parts of the world. This would suggest that the environmental conditions in the northwest Indian Ocean are driving convergent evolution in these different species towards a morphotype that is presumably suited to foraging in this region. Indeed, other cetaceans in the region appear to exhibit comparatively longer rostra, for example spinner dolphins, *Stenella longirostris* (see Van Waerebeek *et al.* 1999) and humpback dolphins, *Sousa plumbea* (Jefferson & Van Waerebeek, 2004). Longer rostra may be associated with foraging in low visibility environments, for example river dolphins (Smith & Reeves, 2012), as observed in the Arabian Sea, reaching an extreme off India due to river influx (Longhurst, 2006).

6.9 Recommendations for Further Research

Further research should endeavour to include samples from regions not included here, particularly along the east African coastline, in the eastern Arabian Sea and Bay of Bengal (see Figure 82) where there is a paucity of samples. Investigations of taxonomic and population structure in these regions will provide further insight into the evolutionary processes governing divergence and speciation in bottlenose and common dolphins in the region. Such information will be of interest to the study of evolution in highly mobile marine taxa as well as be informative to regional conservation initiatives. The use of further markers will help us

to further resolve the genetic differences and isolating mechanisms between lineages within bottlenose and common dolphins in the region and investigate their demographic histories. Such work would benefit from parallel morphological studies, using both external and skeletal morphometrics. Utilisation of next generation sequencing technologies in future research would provide an opportunity to investigate loci under selection, which may offer insight into local adaptation and the evolutionary mechanisms which result in population differentiation in coastal dolphins.

In this thesis, morphological differences between *T. aduncus* lineages suggest differences in foraging behaviour or target prey species. Investigation of diet through stable isotopes analysis and further stomach contents analysis will shed light on the differences in prey/habitat use between populations/lineages. Photo-identification studies (e.g. Wilson *et al.* 1997; Stensland *et al.* 2006), behavioural studies (e.g. Neumann, 2001; Connor *et al.* 2006) and characterisation of vocalisations (e.g. Nowacek, 2005; Gridley *et al.* 2015) would provide further valuable information on how and when populations/lineages are utilising habitat. This information would be of paramount importance for effective conservation of the species discussed here. Additionally, such investigations could work in tandem with analysis of social structure, demographics, relatedness and further population genetic analyses to further our understanding of how dolphin populations adapt to local environments and become reproductively isolated from one another. Further investigation and monitoring of the threats faced by coastal dolphins is also encouraged, particularly those posed by local fisheries.

6.10 Conclusions

In this thesis, evidence suggests the presence of a previously undocumented evolutionarily significant unit of *T. aduncus* in the Arabian Sea, particularly off India and Pakistan. These inferences are based on multiple genetic loci as well as morphological data. These findings will have conservation implications. The identification of further management units in the region will also inform conservation initiatives in the region. Further to this, the evolutionary history of *Tursiops* is investigated, particularly as it pertains to *T. aduncus* in the northwest Indian Ocean. It is likely that climate change over the Pleistocene provided opportunities for at least two divergence events within *T. aduncus* in Australasia and the northwest Indian Ocean. More broadly, this thesis provides insights into the evolutionary processes that drive speciation and the development of population structure in the marine environment. Specifically,

even though taxa may exhibit high dispersal ability, behavioural processes, such as site fidelity or the tendency to develop resource polymorphisms, such as site-specific foraging strategies, may be key drivers in shaping population structure and facilitating speciation. Evidently, taxa that are particularly vulnerable to local environmental change, for example due to their high trophic placement and dependency on specific habitats, have a propensity to exhibit population structure and genetic differentiation in response to environmental differentiation on multiple spatiotemporal scales.

Appendices

Appendix VI: GenBank accession numbers for bottlenose dolphin sequences used. Tt= *Tursiops truncatus*; Ta= *Tursiops aduncus*; GC=Gulf of California; WNAC=northwest Atlantic (coastal ecotype); WNAP=northwest Atlantic (pelagic ecotype); SCO=Scotland; EMED=eastern Mediterranean; BSEA=Black Sea; OM=Oman; PAK=Pakistan; IND=India; SA=South Africa; SABD=Burren dolphin, *T. australis*; AUS=Australasian Indo-Pacific bottlenose dolphin; CHINA=Australasia (China).

Sample Code	Species/Ecotype	GenBank Accession Number				Source
		Mtgenome	mtDNA (partial)	α -Lactalbumin	Actin	
-	<i>Inia geoffrensis</i>	AJ554059				Arnason <i>et al.</i> (2004)
-	<i>Pontoporia blainvillei</i>	NC_005277				Arnason <i>et al.</i> (2004)
-	<i>Platanista minor</i>	AJ554058				Arnason <i>et al.</i> (2004)
-	<i>Lipotes vexillifer</i>	AY89529				Yan <i>et al.</i> (2005)
-	<i>Phocoena phocoena</i>	AJ554063	AJ554063	AJ007811	EF092971	Arnason <i>et al.</i> (2004); Milinkovitch <i>et al.</i> (1998); Harlin-Cognato & Honeycutt (2006)
-	<i>Monodon monoceros</i>	AJ554062				Arnason <i>et al.</i> (2004)
-	<i>Lagenorhynchus albirostris</i>	AJ554061				Arnason <i>et al.</i> (2004)
-	<i>Orcinus orca</i>	GU187173				Morin <i>et al.</i> (2010)
-	<i>Orcinus orca</i>	GU187192				Morin <i>et al.</i> (2010)
-	<i>Orcaella brevirostris</i>	JF289177				Vilstrup <i>et al.</i> (2011)
-	<i>Orcaella heinsobni</i>	JF339977				Vilstrup <i>et al.</i> (2011)
-	<i>Grampus griseus</i>	EU557095				Xiong <i>et al.</i> (2009)
-	<i>Pseudorca crassidens</i>	JF289173				Vilstrup <i>et al.</i> (2011)
-	<i>Pseudorca crassidens</i>	JF289174				Vilstrup <i>et al.</i> (2011)
-	<i>Peponocephala electra</i>	JF289176				Vilstrup <i>et al.</i> (2011)
-	<i>Feresa attenuata</i>	JF289171				Vilstrup <i>et al.</i> (2011)
-	<i>Feresa attenuata</i>	JF289172				Vilstrup <i>et al.</i> (2011)

Sample Code	Species/Ecotype	GenBank Accession Number				Source
		Mtgenome	mtDNA (partial)	α -Lactalbumin	Actin	
-	<i>Globicephala macrorhynchus</i>	HM060333				Morin <i>et al.</i> (2010)
-	<i>Globicephala macrorhynchus</i>	JF339976				Vilstrup <i>et al.</i> (2011)
-	<i>Globicephala melas</i>	HM060334				Morin <i>et al.</i> (2010)
-	<i>Globicephala melas</i>	JF339972				Vilstrup <i>et al.</i> (2011)
-	<i>Steno bredanensis</i>	JF339982				Vilstrup <i>et al.</i> (2011)
-	<i>Stenella attenuata</i>	EU557096				Xiong <i>et al.</i> (2009)
SABD 2	<i>Tursiops australis</i> (coastal)	KF570365		XXXX	XXXX	Moura <i>et al.</i> (2013a)
SABD 5	<i>Tursiops australis</i> (coastal)	KF570367				Moura <i>et al.</i> (2013a)
SABD 7	<i>Tursiops australis</i> (coastal)	KF570363				Moura <i>et al.</i> (2013a)
SABD 6	<i>Tursiops australis</i> (coastal)	KF570368				Moura <i>et al.</i> (2013a)
SABD 4	<i>Tursiops australis</i> (coastal)	KF570369				Moura <i>et al.</i> (2013a)
SABD 3	<i>Tursiops australis</i> (coastal)	KF570366		XXXX	XXXX	Moura <i>et al.</i> (2013a)
SABD 1	<i>Tursiops australis</i> (coastal)	KF570364				Moura <i>et al.</i> (2013a)
-	<i>Sousa chinensis</i>	EU557091				Xiong <i>et al.</i> (2009)
-	<i>Stenella coeruleoalba</i>	EU557097				Xiong <i>et al.</i> (2009)
-	<i>Delphinus capensis</i>	EU557094				Xiong <i>et al.</i> (2009)
SA-Ta 120	<i>Tursiops aduncus</i> (coastal)	KF570357				Moura <i>et al.</i> (2013a)
SA-Ta 99	<i>Tursiops aduncus</i> (coastal)	KF570362		XXXX	XXXX	Moura <i>et al.</i> (2013a); This Study
OM-Ta 64	<i>Tursiops aduncus</i> (coastal)	XXXX		XXXX	XXXX	This Study
SA-Ta 95	<i>Tursiops aduncus</i> (coastal)	KF70360				Moura <i>et al.</i> (2013a)
SA-Ta 102	<i>Tursiops aduncus</i> (coastal)	KF570354				Moura <i>et al.</i> (2013a)
SA-Ta 26	<i>Tursiops aduncus</i> (coastal)	KF570339				Moura <i>et al.</i> (2013a)
SA-Ta 133	<i>Tursiops aduncus</i> (coastal)	KF570358		XXXX	XXXX	Moura <i>et al.</i> (2013a); This Study

Sample Code	Species/Ecotype	GenBank Accession Number				Source
		Mtgenome	mtDNA (partial)	α -Lactalbumin	Actin	
SA-Ta 115	<i>Tursiops aduncus</i> (coastal)	KF570355				Moura <i>et al.</i> (2013a)
SA-Ta 98	<i>Tursiops aduncus</i> (coastal)	KF570361				Moura <i>et al.</i> (2013a)
SA-Ta 101	<i>Tursiops aduncus</i> (coastal)	KF570353				Moura <i>et al.</i> (2013a)
SA-Ta 116	<i>Tursiops aduncus</i> (coastal)	KF570356				Moura <i>et al.</i> (2013a)
PAK-Ta 5	<i>Tursiops aduncus</i> (coastal)	XXXX		XXXX	XXXX	This Study
PAK-Ta 6	<i>Tursiops aduncus</i> (coastal)	XXXX		XXXX	XXXX	This Study
CHINA-Ta	<i>Tursiops aduncus</i> (coastal)	EU557092				Xiong <i>et al.</i> (2009)
AUS-Ta 1	<i>Tursiops aduncus</i> (coastal)	KF570335				Moura <i>et al.</i> (2013a)
AUS-Ta 2	<i>Tursiops aduncus</i> (coastal)	KF570336				Moura <i>et al.</i> (2013a)
AUS-Ta 3	<i>Tursiops aduncus</i> (coastal)	KF570337				Moura <i>et al.</i> (2013a)
AUS-Ta 4	<i>Tursiops aduncus</i> (coastal)	KF570338		XXXX	XXXX	Moura <i>et al.</i> (2013a)
AUS-Ta 7	<i>Tursiops aduncus</i> (coastal)	KF570341				Moura <i>et al.</i> (2013a)
AUS-Ta 9	<i>Tursiops aduncus</i> (coastal)	KF570343				Moura <i>et al.</i> (2013a)
AUS-Ta 8	<i>Tursiops aduncus</i> (coastal)	KF570344		XXXX	XXXX	Moura <i>et al.</i> (2013a)
AUS-Ta 5	<i>Tursiops aduncus</i> (coastal)	KF570339				Moura <i>et al.</i> (2013a)
AUS-Ta 6	<i>Tursiops aduncus</i> (coastal)	KF570340				Moura <i>et al.</i> (2013a)
AUS-Ta 10	<i>Tursiops aduncus</i> (coastal)	KF570342		XXXX	XXXX	Moura <i>et al.</i> (2013a)
WNAC-Tt 8	<i>Tursiops truncatus</i> (coastal)	KF570378				Moura <i>et al.</i> (2013a)
WNAC-Tt 14	<i>Tursiops truncatus</i> (coastal)	KF570372		XXXX	XXXX	Moura <i>et al.</i> (2013a); This Study
WNAC-Tt 16	<i>Tursiops truncatus</i> (coastal)	KF570373				Moura <i>et al.</i> (2013a)
WNAC-Tt 22	<i>Tursiops truncatus</i> (coastal)	KF570375				Moura <i>et al.</i> (2013a)
WNAC-Tt 11	<i>Tursiops truncatus</i> (coastal)	KF570370				Moura <i>et al.</i> (2013a)
WNAC-Tt 19	<i>Tursiops truncatus</i> (coastal)	KF570374				Moura <i>et al.</i> (2013a)

Sample Code	Species/Ecotype	GenBank Accession Number				Source
		Mtgenome	mtDNA (partial)	α -Lactalbumin	Actin	
WNAC-Tt 13	<i>Tursiops truncatus</i> (coastal)	KF570371				Moura <i>et al.</i> (2013a)
WNAC-Tt 25	<i>Tursiops truncatus</i> (coastal)	KF570377				Moura <i>et al.</i> (2013a)
WNAC-Tt 23	<i>Tursiops truncatus</i> (coastal)	KF570376		XXXX	XXXX	Moura <i>et al.</i> (2013a); This Study
CHINA-Tt	<i>Tursiops truncatus</i>	EU557093				Xiong <i>et al.</i> (2009)
WNAP-Tt 26	<i>Tursiops truncatus</i> (pelagic)	KF570385		XXXX	XXXX	Moura <i>et al.</i> (2013a); This Study
WNAP-Tt 7	<i>Tursiops truncatus</i> (pelagic)	KF570386				Moura <i>et al.</i> (2013a)
WNAP-Tt 11	<i>Tursiops truncatus</i> (pelagic)	KF570379				Moura <i>et al.</i> (2013a)
WNAP-Tt 12	<i>Tursiops truncatus</i> (pelagic)	KF570380				Moura <i>et al.</i> (2013a)
EMED-Tt 9	<i>Tursiops truncatus</i> (coastal)	KF570322		XXXX	XXXX	Moura <i>et al.</i> (2013a)
BSEA-Tt 3	<i>Tursiops truncatus ponticus</i> (coastal)	KF570326				Moura <i>et al.</i> (2013a)
BSEA-Tt 8	<i>Tursiops truncatus ponticus</i> (coastal)	KF570332		XXXX	XXXX	Moura <i>et al.</i> (2013a)
BSEA-Tt 1	<i>Tursiops truncatus ponticus</i> (coastal)	KF570327				Moura <i>et al.</i> (2013a)
BSEA-Tt 4	<i>Tursiops truncatus ponticus</i> (coastal)	KF570331				Moura <i>et al.</i> (2013a)
GC-Tt 1	<i>Tursiops truncatus</i> (coastal)	KF570389		XXXX	XXXX	Moura <i>et al.</i> (2013a); This Study
WNAP-Tt 8	<i>Tursiops truncatus</i> (pelagic)	KF570387		XXXX	XXXX	Moura <i>et al.</i> (2013a); This Study
SCO-Tt 5	<i>Tursiops truncatus</i> (coastal)	KF570352				Moura <i>et al.</i> (2013a)
EMED-Tt 2	<i>Tursiops truncatus</i> (coastal)	KF570319		XXXX	XXXX	Moura <i>et al.</i> (2013a)
EMED-Tt 5	<i>Tursiops truncatus</i> (coastal)	KF570398				Moura <i>et al.</i> (2013a)
EMED-Tt 4	<i>Tursiops truncatus</i> (coastal)	KF570399				Moura <i>et al.</i> (2013a)
EMED-Tt 1	<i>Tursiops truncatus</i> (coastal)	KF570400				Moura <i>et al.</i> (2013a)
WNAP-Tt 21	<i>Tursiops truncatus</i> (pelagic)	KF570401		XXXX	XXXX	Moura <i>et al.</i> (2013a); This Study

Sample Code	Species/Ecotype	GenBank Accession Number				Source
		Mtgenome	mtDNA (partial)	α -Lactalbumin	Actin	
SCO-Tt 3	<i>Tursiops truncatus</i> (coastal)	KF570402				Moura <i>et al.</i> (2013a)
SCO-Tt 6	<i>Tursiops truncatus</i> (coastal)	KF570403				Moura <i>et al.</i> (2013a)
SCO-Tt 8	<i>Tursiops truncatus</i> (coastal)	KF570404				Moura <i>et al.</i> (2013a)
SCO-Tt 1	<i>Tursiops truncatus</i> (coastal)	KF570405				Moura <i>et al.</i> (2013a)
SCO-Tt 2	<i>Tursiops truncatus</i> (coastal)	KF570406				Moura <i>et al.</i> (2013a)
SCO-Tt 7	<i>Tursiops truncatus</i> (coastal)	KF570407				Moura <i>et al.</i> (2013a)
SCO-Tt 4	<i>Tursiops truncatus</i> (coastal)	KF570408				Moura <i>et al.</i> (2013a)
EMED-Tt 3	<i>Tursiops truncatus</i> (coastal)	KF570409				Moura <i>et al.</i> (2013a)
WNAP-Tt 17	<i>Tursiops truncatus</i> (pelagic)	KF570410				Moura <i>et al.</i> (2013a)
WNAP-Tt 19	<i>Tursiops truncatus</i> (pelagic)	KF570411				Moura <i>et al.</i> (2013a)
WNAP-Tt 22	<i>Tursiops truncatus</i> (pelagic)	KF570412				Moura <i>et al.</i> (2013a)
WNAP-Tt 9	<i>Tursiops truncatus</i> (pelagic)	KF570413				Moura <i>et al.</i> (2013a)
EMED-Tt 10	<i>Tursiops truncatus</i> (coastal)	KF570414				Moura <i>et al.</i> (2013a)
BSEA-Tt 7	<i>Tursiops truncatus ponticus</i> (coastal)	KF570415				Moura <i>et al.</i> (2013a)
BSEA-Tt 10	<i>Tursiops truncatus ponticus</i> (coastal)	KF570416				Moura <i>et al.</i> (2013a)
BSEA-Tt 6	<i>Tursiops truncatus ponticus</i> (coastal)	KF570417				Moura <i>et al.</i> (2013a)
BSEA-Tt 9	<i>Tursiops truncatus ponticus</i> (coastal)	KF570418				Moura <i>et al.</i> (2013a)
BSEA-Tt 2	<i>Tursiops truncatus ponticus</i> (coastal)	KF570419				Moura <i>et al.</i> (2013a)
BSEA-Tt 5	<i>Tursiops truncatus ponticus</i> (coastal)	KF570420		XXXX	XXXX	Moura <i>et al.</i> (2013a)
EMED-Tt 8	<i>Tursiops truncatus</i> (coastal)	KF570421				Moura <i>et al.</i> (2013a)
EMED-Tt 7	<i>Tursiops truncatus</i> (coastal)	KF570422				Moura <i>et al.</i> (2013a)
EMED-Tt 6	<i>Tursiops truncatus</i> (coastal)	KF570423		XXXX	XXXX	Moura <i>et al.</i> (2013a)

Sample Code	Species/Ecotype	GenBank Accession Number			Source	
		Mtgenome	mtDNA (partial)	α -Lactalbumin		
-	<i>Lagenorhynchus obscurus</i>		KC312621	AF228410	EF093008	Alexander <i>et al.</i> (2013a); Waddell <i>et al.</i> (2000); Harlin-Cognato & Honeycutt (2006)
IND-Tt EW01306	<i>Tursiops truncatus</i>		XXXX	XXXX	XXXX	This Study
OM-Tt 108	<i>Tursiops truncatus</i> (pelagic)		XXXX	XXXX	XXXX	This Study
OM-Tt 109	<i>Tursiops truncatus</i> (pelagic)		XXXX	XXXX	XXXX	This Study
OM-Ta 119	<i>Tursiops aduncus</i> (coastal)		XXXX	XXXX	XXXX	This Study
OM-Ta 61	<i>Tursiops aduncus</i> (coastal)		XXXX	XXXX	XXXX	This Study
OM-Ta 65	<i>Tursiops aduncus</i> (coastal)		XXXX	XXXX	XXXX	This Study
IND-Ta EW01317	<i>Tursiops aduncus</i> (coastal)		XXXX	XXXX		This Study
IND-Ta EW01309	<i>Tursiops aduncus</i> (coastal)		XXXX	XXXX	XXXX	This Study
IND-Ta EW01307	<i>Tursiops aduncus</i> (coastal)		XXXX	XXXX	XXXX	This Study
IND-Ta EW01315	<i>Tursiops aduncus</i> (coastal)		XXXX	XXXX	XXXX	This Study
IND-Ta EW01314	<i>Tursiops aduncus</i> (coastal)		XXXX	XXXX	XXXX	This Study
OM-Ta 75	<i>Tursiops aduncus</i> (coastal)		XXXX	XXXX	XXXX	This Study
OM-Ta 111	<i>Tursiops aduncus</i> (coastal)		XXXX	XXXX	XXXX	This Study
IND-Ta EW01312	<i>Tursiops aduncus</i> (coastal)		XXXX	XXXX	XXXX	This Study
IND-Ta EW01303	<i>Tursiops aduncus</i> (coastal)		XXXX	XXXX	XXXX	This Study
IND-Ta EW01310	<i>Tursiops aduncus</i> (coastal)		XXXX	XXXX	XXXX	This Study
IND-Ta EW01304	<i>Tursiops aduncus</i> (coastal)		XXXX	XXXX	XXXX	This Study
IND-Ta EW01311	<i>Tursiops aduncus</i> (coastal)		XXXX	XXXX	XXXX	This Study

Appendix VIII: List of bottlenose dolphin specimens. T = *Tursiops* sp.; Tt = *T. truncatus*; Ta = *T. aduncus*; Uk = Unknown; Hol-Ta = holotype Ta lineage; AS-Ta = Arabian Sea, new Ta lineage; AUS-Ta = Australasian Ta lineage; M = Male; F = Female. For mtDNA identification cf. Chapter 3. Where omitted from Linear and Geometric Morphometric (GM) analyses the reason is given.

Individual ID	Other No.	Species ID (Museum)	mtDNA ID	Location	Date Collected	Collected by	Sex	Linear Analyses	GM Analyses	Reason for Omission
ONHM 1018		T	Uk	Ras Shiya, GK 728969	16/04/1987	R Salm & V Papastavrou, IUCN Coastal Management Project	Uk			immature
ONHM 1019		Tt	Uk	Sawqirah, DF524075	13/01/1987	R Salm & V Papastavrou, IUCN Coastal Management Project	Uk	Y	Y	
ONHM 1028		Ta	Hol-Ta	Ras al Junayz, GK 920823	16/04/1987	R Salm & V Papastavrou, IUCN Coastal Management Project	Uk			immature
ONHM 1046	V Papastavrou 27	T	Tt	Ras Nus, 1715, 5515	14/04/1988	V Papastavrou & Salm	Uk	Y	Y	
ONHM 1048	V Papastavrou 29	Ta	Hol-Ta	Wadi Ismoor, 1718, 5516	14/04/1988	V Papastavrou	Uk	Y	Y	
ONHM 1049		Ta	Uk	Barr al Hikmann, 2023, 5823	04/05/1987	R Salm & V Papastavrou	Uk	Y	Y	
ONHM 1106		Ta	Uk	Ras al Hadd	28/09/1988	JP Ross	Uk			immature
ONHM 1516		T	Hol-Ta	Qaysad, near Lakbi, Jasn coast	17/03/1986	RP Whitecombe	Uk			immature
ONHM 1561	MD Gallagher 8250	Ta?	Hol-Ta	Ras Bintawt, 2021, 5757	27/04/1990	S Henry	Uk	Y	Y	
ONHM 183	MD Gallagher 7432	Tt	Tt	Suwadi al Batha	28/12/1984	M Gallagher	Uk	Y	Y	
ONHM 1917	MD Gallagher 8427	T	Hol-Ta	Barr al Hikmann, 2022, 5820	27/11/1991	M Gallagher	Uk	Y	Y	
ONHM 1975	MD Gallagher 8445A	Ta	AS-Ta	Near Quhayd, 2117, 5905	23/01/1992	M Gallagher	Uk	Y	Y	
ONHM 2677		T	Hol-Ta	6km S. of Ras al Ghubbah, 2006, 5750	20/04/1997	Ian Harrison	Uk			immature

Individual ID	Other No.	Species ID (Museum)	mDNA ID	Location	Date Collected	Collected by	Sex	Linear Analyses	GM Analyses	Reason for Omission
ONHM 2811.01		Tt	Uk	Near (Kahal) Lakbi, near Rima	1998	Nasser Al-Harthy, PDO	Uk	Y	Y	
ONHM 2815		T	Uk	Sur Lagoon, 2234.5 5934.0	12/05/1998	S Reilly & M Donohue (IWC)	Uk	Y	Y	
ONHM 2842		Tt	AS-Ta	Near Khor Dirif, 1856, 5726	10/02/1999	Ian Harrison	Uk	Y	Y	
ONHM 2843		Tt	Hol-Ta	Khor Dirif, 1856, 5726	10/02/1999	Ian Harrison	Uk	Y	Y	
ONHM 2862		Tt	Hol-Ta	Khaluf (long beach)	Sep-99	T Collins	Uk			immature
ONHM 2863		Tt	Hol-Ta	3 Palm Lagoon	Sep-99	T Collins	Uk	Y	Y	
ONHM 2877		T	Tt	Barr al Hikmann, 2038, 5835	03/12/1999	Ian Harrison	Uk	Y	Y	
ONHM 2903		T	Hol-Ta	SW tip of Masirah, UTM: 0670266, 2233000	16/03/2000	G Minton	Uk			immature
ONHM 2917	HAL002	T	Hol-Ta	Hallaniyah, 17.52779, 56.00152		G Minton	Uk			immature
ONHM 2921	HAL010	Tt	Hol-Ta	Hallaniyah, 17.52532, 55.99346	08/02/2000	G Minton & T Collins	Uk	Y	Y	
ONHM 2923	HAL012	T	Hol-Ta	Hallaniyah, 17.52532, 55.99346	08/02/2000	T Collins & G Minton	Uk	Y	Y	
ONHM 2926	HAL015	Tt	Hol-Ta	Hallaniyah, 17.51763, 55.97264	Feb-01	Steve Dover	Uk	Y	Y	
ONHM 2928	HAL018	T	Uk	Hallaniyah, 17.51085, 56.08301		G Minton & T Collins	Uk			damaged
ONHM 2935		T	Hol-Ta	Ras Madrakah, 3 Palm Lagoon,	Sep-99	T Collins	Uk	Y	Y	

Individual ID	Other No.	Species ID (Museum)	mDNA ID	Location	Date Collected	Collected by	Sex	Linear Analyses	GM Analyses	Reason for Omission
ONHM 2936		T	Hol-Ta	Ras Madrakah, 3 Palm Lagoon	Sep-99	T Collins	Uk	Y	Y	
ONHM 2957	?-Nov-98-01	Tt	Hol-Ta	Khaluf village	Nov-98	T Collins	Uk			immature
ONHM 2961		Tt	Tt	Between Sifah & Ras Abu Daud, 23.35411, 58.961	06/09/2000	T Collins	Uk	Y	Y	
ONHM 2962		Tt	Tt	Between Sifah & Ras Abu Daud, 23.36041, 58.85247	06/09/2000	T Collins	Uk	Y	Y	
ONHM 2963	06-09-00-3	Tt	Uk	Between Sifah & Ras Abu Daud 23.35613, 58.85680	06/09/2000	T Collins	Uk			immature
ONHM 2974	14-10-00-01	T	Hol-Ta	Barr al Hikmann, 20.35135, 58.41820	14/10/2000	G Minton & T Collins	Uk	Y	Y	
ONHM 2976	11-10-00-01	T	Hol-Ta	Khaluf, 20.44881, 58.03930	11/10/2000	T Collins & G Minton	Uk	Y	Y	
ONHM 2978	14-10-00-02	T	Hol-Ta	Barr al Hikmann, 20.36206, 58.38725	14/10/2000	T Collins & G Minton	Uk	Y	Y	
ONHM 2982		T	Hol-Ta	Khaluf, 20.48292, 58.06717	11/10/2000	G Minton & T Collins	Uk	Y	Y	
ONHM 2992	11-10-00-03	T	Uk	S. Khaluf, 20.44637, 58.03064	11/10/2000	G Minton & T Collins	Uk			damaged
ONHM 2994		T	Uk	Khaluf, 20.44637, 58.03064	11/10/2000	T Collins & G Minton	Uk	Y	Y	
ONHM 3018	05-11-00-03	T	Tt	South of Sifah, 23.36811, 58.84659	05/11/2000	G Minton & T Collins	Uk	Y	Y	
ONHM 3056	20-02-01-01	T	Uk	Hasik, 17.45256, 55.24987	20/02/2001	T Collins & G Minton	Uk			immature
ONHM 3057	22-02-01-01	T	Uk	Ras Jinjali	22/02/2001	T Collins	Uk			immature

Individual ID	Other No.	Species ID (Museum)	mDNA ID	Location	Date Collected	Collected by	Sex	Linear Analyses	GM Analyses	Reason for Omission
ONHM 3067	25-05-01-14	T	Hol-Ta	Barr al Hikmann, 20.37990, 58.33583	25/05/2001	G Minton, K Van Waerebeek, T Collins, R Baldwin	Uk			immature
ONHM 3070		T	Hol-Ta	Barr al Hikmann, 20.37106, 58.27190	25/05/2001	G Minton, K Van Waerebeek, T Collins, R Baldwin	Uk	Y	Y	
ONHM 3074	14-10-00-03	T	Hol-Ta	Barr al Hikmann, 20.53627, 58.40246	14/10/2000	G Minton & T Collins	Uk			immature
ONHM 3076	12-06-01-02	Ta?	Hol-Ta	Duqm	12/06/2001	B Woodward & T Collins	Uk	Y	Y	
ONHM 3078	26-05-01-03	T	Hol-Ta	Barr al Hikmann, 20.37674, 58.36161	26/05/2001	G Minton, K Van Waerebeek, T Collins, R Baldwin	Uk			immature
ONHM 3079	14-03-01-05	T	AS-Ta	Barr al Hikmann, 20.36166, 58.38899	14/03/2001	T Collins	Uk	Y	Y	
ONHM 3082	26-05-01-04	T	Hol-Ta	Barr al Hikmann, 20.36760, 58.38478	26/05/2001	G Minton, K Van Waerebeek, T Collins, R Baldwin	Uk			immature
ONHM 3084	26-05-01-07	T	Hol-Ta	Barr al Hikmann, 20.36120, 58.39639	26/05/2001	G Minton, K Van Waerebeek, T Collins, R Baldwin	Uk	Y	Y	
ONHM 3085	12-06-01-03	T	Uk	Duqm	12/06/2001	B Woodward	Uk			immature
ONHM 3087	25-05-01-12	T	Hol-Ta	Barr al Hikmann, 20.37031, 58.29010	25/02/2001	G Minton, K Van Waerebeek, T Collins, R Baldwin	Uk	Y	Y	
ONHM 3089	12-06-01-04	T	Uk	Duqm, 19.54, 57.70	12/06/2001	T Collins	Uk	Y	Y	
ONHM 3095	16-02-01-03	T	Hol-Ta	Hallaniyah, 17.52523, 55.98829	16/02/2001	G Minton & T Collins	Uk	Y	Y	
ONHM 3096	26-09-01-05	T	Hol-Ta	Duqm, 19deg, 32.9079', 57deg, 41.8643'	26/09/2001	OWDRG	Uk			immature
ONHM 3097	27-09-01-04	T	Hol-Ta	Sirab, 20.250067, 57.857550	27/09/2001	OWDRG	Uk	Y	Y	

Individual ID	Other No.	Species ID (Museum)	mDNA ID	Location	Date Collected	Collected by	Sex	Linear Analyses	GM Analyses	Reason for Omission
ONHM 3098	27-09-01-01	T	Hol-Ta	Ras Halmit, 20o, 09', 975", 57o, 49', 826"	27/09/2001	OWDRG	Uk			immature
ONHM 3102	29-09-01-07	T	Hol-Ta	Barr al Hikmann, 2023, 5823	29/09/2001	OWDRG	Uk		Y	
ONHM 3103	28-09-01-08	T	Hol-Ta	Khaluf, 20.450020, 20.378807	28/09/2001	OWDRG	Uk			immature
ONHM 3104	29-09-01-08	T	Hol-Ta	Barr al Hikmann, 20.351497, 58.425218	29/09/2001	OWDRG	Uk		Y	
ONHM 3105	30-09-01-03	T	Hol-Ta	Barr al Hikmann, 20.38013217, 58.3433217	30/09/2001	OWDRG	Uk	Y	Y	
ONHM 3106	30-09-01-01	T	Hol-Ta	Barr al Himann, 20.3677, 58.3846	30/09/2001	OWDRG	Uk	Y	Y	
ONHM 3107	06-10-01-03	T	Hol-Ta	Masirah, 20187449, 58670130	06/10/2001	OWDRG	Uk	Y	Y	
ONHM 3108	11-10-01-02	T	Uk	Masirah, 5847562, 2019170	11/10/2001	OWDRG	Uk	Y	Y	
ONHM 3109	11-10-01-01	T	Hol-Ta	Masirah, 2018549, 5847020	11/10/2001	OWDRG	Uk	Y	Y	
ONHM 3110	01-11-01-06	T	Hol-Ta	Barr al Hikmann, 20.40004, 58.20698	01/11/2001	T Collins, G Minton, V Cockcroft	Uk	Y	Y	
ONHM 3111	01-11-01-04	T	Hol-Ta	Barr al Hikmann, 20.40004, 58.20698	01/11/2001	T Collins, G Minton, V Cockcroft	Uk	Y	Y	
ONHM 3112		T	Hol-Ta	Masirah, 20.189449, 58.670130	06/10/2001	AHD, AW(?)	Uk			immature
ONHM 3183	28-09-01-07	T	Uk	Khaluf, 20.447724, 58.035010	28/09/2001	OWDRG	Uk			immature
ONHM 3193		T	Hol-Ta	Ras Bintawt, 2021, 5758	22/02/2002	Ian Harrison	Uk			immature

Individual ID	Other No.	Species ID (Museum)	mDNA ID	Location	Date Collected	Collected by	Sex	Linear Analyses	GM Analyses	Reason for Omission
ONHM 3254		T	Tt	Sur	02/04/2002	Ian Harrison	Uk	Y	Y	
ONHM 3259	29-09-01-05	T	Hol-Ta	Barr al Hikmann, 20.350564, 58.434262	29/09/2001	OWDRG	Uk			immature
ONHM 3260	02-11-01-03	T	Hol-Ta	Barr al Hikmann, 20.57909, 58.28236	02/11/2001		Uk	Y	Y	
ONHM 3262	26-02-02-04	T	Uk	Hasik, 17.501530, 55.225870	26/02/2002	T Collins, G Minton, K Findlay	Uk			immature
ONHM 3265	26-02-02-07	T	AS-Ta	Hasik, 17.491370, 55.22990	26/02/2002	T Collins, G Minton, K Findlay	Uk	Y	Y	
ONHM 3411	23-11-02-02	T	Hol-Ta	Ash Shuwayr, 19.522110, 57.698660	23/11/2002	T Collins	Uk	Y	Y	
ONHM 3516	26-09-03-01	T	Hol-Ta	Barr al Hikmann, 5827, 2037	26/09/2003	G Minton	Uk	Y	Y	
ONHM 3522	29-09-01-04	T	Hol-Ta	Barr al Hikmann, 2038, 5826	29/09/2001	OWDRG	Uk			immature
ONHM 3524	11-01-02-05	T	Tt	Ijab, 2257, 5956	11/01/2002	OWDRG	Uk	Y	Y	
ONHM 3684		T	Uk	Masirah	May-09	H Gray	Uk	Y	Y	
ONHM 658	MD Gallagher 7936	Tt	Tt	Azaiba, 2336, 5828	02/02/1987	M Gallagher	Uk	Y	Y	
SMNS 45 706	494	Ta	AS-Ta	Point Monze, W. Pakistan	1971	G Pilleri	F	Y	Y	
SMNS 45 707	495	Ta	AS-Ta	Karachi, W. Pakistan	1971	G Pilleri	Uk			immature
SMNS 45 708	496	Ta	AS-Ta	Karachi, Clifton, W. Paki- stan	1971	G Pilleri	Uk	Y	Y	
SMNS 45 709	551	Ta	AS-Ta	Clifton coast, Karachi. W. Pakistan	1972	G. Pilleri, Natha legit	Uk	Y	Y	
SMNS 45 710	552 (a)	Ta	AS-Ta	Birkhori, Hub river, W. Pakistan	1972	G. Pilleri, Natha legit	Uk			immature

Individual ID	Other No.	Species ID (Museum)	mtDNA ID	Location	Date Collected	Collected by	Sex	Linear Analyses	GM Analyses	Reason for Omission
SMNS 45 710 (b)	552 (b)	Ta	Uk	Bitkhorri, Hub river, W. Pakistan	1972	G. Pilleri, Natha legit	Uk			partial
SMNS 45 711	559	Ta	Hol-Ta	Persian Gulf, Strait of Hormuz	1973	G Pilleri	Uk	Y	Y	
SMNS 45 712	560/20	Ta	AUS-Ta	Songkhla, Thailand	1973	G Pilleri	M			from Thailand
SMNS 45 713	561/21	Ta	AUS-Ta	Songkhla, Thailand	1973	G Pilleri	M			from Thailand
SMNS 45 714	572	Ta	Uk	Kurangi Creek, Indus Delta, W. Pakistan	1974	G Pilleri	Uk			immature
SMNS 45 715	573	Ta	<i>S. chinensis</i>	Kurangi Creek, Indus Delta, W. Pakistan	1974	G Pilleri	Uk			mis-ID
SMNS 45 716	575	Ta	AS-Ta	Khardo Duo, Indus Delta, W. Pakistan	1974	G Pilleri	Uk	Y	Y	
SMNS 45 717	574	Ta	Hol-Ta	Dam, Sonmiani Bay, W. Pakistan	1974	G Pilleri	Uk	Y	Y	
SMNS 45 718	578	Ta	Uk	Kurangi Creek, Indus Delta, W. Pakistan	1974	G Pilleri	Uk			immature
SMNS 45 719	579	Ta	<i>S. chinensis</i>	Piti Creek, Indus Delta, W. Pakistan	1974	G Pilleri	Uk			immature
SMNS 45 720	615	Ta	AS-Ta	Korangi Creek, Indus Delta, W. Pakistan	1975	G Pilleri	Uk	Y	Y	
SMNS 45 722	751	Ta	AS-Ta	Gizri Creek, Clifton (Kachhi)	1979	G Pilleri	Uk	Y	Y	
SMNS 45 750	506	Ta	<i>S. chinensis</i>	Sonmiani Bay, W. Pakistan	1971	G Pilleri	Uk			damaged
SMNS 46 793	562	Ta	AUS-Ta	Songkhla, Thailand	1973	G Pilleri	F			from Thailand

Appendix IX: Haplotype frequencies for each common dolphin population.

Haplotype	BS	CAN_Is	CHI	E_AUS	GAL	GC_Dc	GC_Dd	MED	NWA	NZ	OM	PAK	S_AUS	SA
DDU02640, FM211527, EU365150	1	-	-	-	1	-	-	1	1	-	-	-	-	-
DDU02641	1	-	-	-	-	-	-	-	-	-	-	-	-	-
DQ520106, DQ520122, EU365129, EU365135, EU365154, FM211489, FM211496, FM211498	3	2	-	-	2	-	-	12	3	-	-	-	-	-
EU365130	1	-	-	-	-	-	-	-	-	-	-	-	-	-
EU365131	1	-	-	-	-	-	-	-	-	-	-	-	-	-
EU365132	1	-	-	-	-	-	-	-	-	-	-	-	-	-
EU365133	1	-	-	-	-	-	-	-	-	-	-	-	-	-
DQ520104	-	1	-	-	-	-	-	-	-	-	-	-	-	-
DQ520105, FM211539	-	1	-	-	-	-	-	-	1	-	-	-	-	-
DQ520107, EU365158-59, FM211506	-	1	-	-	3	-	-	-	1	-	-	-	-	-
DQ520108	-	1	-	-	-	-	-	-	-	-	-	-	-	-
DQ520109, FM211533	-	1	-	-	-	-	-	-	1	-	-	-	-	-
DQ520110, FM211525	-	1	-	-	-	-	-	-	1	-	-	-	-	-
ASN79, DQ520111, DQ520115, EU365137, EU365162, FM211501, FM211517, UMH168	-	2	-	-	3	-	-	3	2	-	-	-	-	2
DQ520112, FM211491	-	1	-	-	-	-	-	-	1	-	-	-	-	-
DQ520113	-	1	-	-	-	-	-	-	-	-	-	-	-	-
DQ520114	-	1	-	-	-	-	-	-	-	-	-	-	-	-
DQ520116	-	1	-	-	-	-	-	-	-	-	-	-	-	-
DQ520117, EU365155, FM211513	-	1	-	-	4	-	-	1	1	-	-	-	-	-
DQ520118	-	1	-	-	-	-	-	-	-	-	-	-	-	-
DQ520119, FM211509	-	1	-	-	-	-	-	-	1	-	-	-	-	-
DQ520120, EU365149	-	1	-	-	1	-	-	1	-	-	-	-	-	-

Haplotype	BS	CAN_Is	CHI	E_AUS	GAL	GC_Dc	GC_Dd	MED	NWA	NZ	OM	PAK	S_AUS	SA
DQ520121	-	1	-	-	-	-	-	-	-	-	-	-	-	-
DQ520123, EU365165	-	1	-	-	1	-	-	-	-	-	-	-	-	-
DQ520124	-	1	-	-	-	-	-	-	-	-	-	-	-	-
AY185137	-	-	1	-	-	-	-	-	-	-	-	-	-	-
AY185138	-	-	1	-	-	-	-	-	-	-	-	-	-	-
AY185139, AY185141	-	-	2	-	-	-	-	-	-	-	-	-	-	-
AY185140	-	-	1	-	-	-	-	-	-	-	-	-	-	-
AY185142	-	-	1	-	-	-	-	-	-	-	-	-	-	-
AY185143	-	-	1	-	-	-	-	-	-	-	-	-	-	-
AY185144	-	-	1	-	-	-	-	-	-	-	-	-	-	-
HQ223451, HQ2234510- 19, HQ223460, KJ493733,	-	-	-	32	-	-	-	-	-	-	-	-	1	-
HQ223452, HQ223455	-	-	-	17	-	-	-	-	-	-	-	-	-	-
HQ223453, KJ493761	-	-	-	2	-	-	-	-	-	-	-	-	1	-
HQ223454	-	-	-	3	-	-	-	-	-	-	-	-	-	-
HQ223456-57, KJ493754	-	-	-	9	-	-	-	-	-	-	-	-	1	-
HQ223458, KJ493748	-	-	-	3	-	-	-	-	-	-	-	-	1	-
HQ223459, KC295617	-	-	-	2	-	-	-	-	-	1	-	-	-	-
HQ223461, HQ223475, KC295619, KJ493710-11	-	-	-	10	-	-	-	-	-	1	-	-	2	-
HQ223462, KJ493714	-	-	-	1	-	-	-	-	-	-	-	-	1	-
HQ223463, KJ493735	-	-	-	1	-	-	-	-	-	-	-	-	1	-
HQ223464, KC295625	-	-	-	1	-	-	-	-	-	2	-	-	-	-
HQ223465, KJ493746	-	-	-	1	-	-	-	-	-	-	-	-	1	-
HQ223466, KJ493736	-	-	-	1	-	-	-	-	-	-	-	-	1	-
HQ223467, KJ493707	-	-	-	1	-	-	-	-	-	-	-	-	1	-
HQ223468, KC295626, KJ493721	-	-	-	1	-	-	-	-	-	1	-	-	1	-
HQ223469	-	-	-	1	-	-	-	-	-	-	-	-	-	-
HQ223470	-	-	-	1	-	-	-	-	-	-	-	-	-	-

Haplotype	BS	CAN_Is	CHI	E_AUS	GAL	GC_Dc	GC_Dd	MED	NWA	NZ	OM	PAK	S_AUS	SA
HE680129, HQ223471, KC295629, KC295655	-	-	-	3	-	-	1	-	-	2	-	-	-	-
HQ223472	-	-	-	3	-	-	-	-	-	-	-	-	-	-
HQ223473	-	-	-	1	-	-	-	-	-	-	-	-	-	-
HQ223474	-	-	-	1	-	-	-	-	-	-	-	-	-	-
HQ223476, KJ493717	-	-	-	1	-	-	-	-	-	-	-	-	1	-
HQ223477	-	-	-	1	-	-	-	-	-	-	-	-	-	-
HQ223478	-	-	-	15	-	-	-	-	-	-	-	-	-	-
HQ223479	-	-	-	1	-	-	-	-	-	-	-	-	-	-
EU365142, FM211524	-	-	-	-	1	-	-	2	1	-	-	-	-	-
EU365148, FM211507	-	-	-	-	1	-	-	2	1	-	-	-	-	-
EU365151	-	-	-	-	1	-	-	1	-	-	-	-	-	-
EU365160	-	-	-	-	1	-	-	-	-	-	-	-	-	-
EU365161	-	-	-	-	1	-	-	-	-	-	-	-	-	-
EU365163, FM211522	-	-	-	-	1	-	-	-	1	-	-	-	-	-
EU365164, FM211504	-	-	-	-	1	-	-	-	1	-	-	-	-	-
EU365166	-	-	-	-	1	-	-	-	-	-	-	-	-	-
EU365167	-	-	-	-	1	-	-	-	-	-	-	-	-	-
EU365168, FM211519	-	-	-	-	1	-	-	-	1	-	-	-	-	-
EU365144, EU365169, FM211516	-	-	-	-	1	-	-	1	1	-	-	-	-	-
EU365170	-	-	-	-	1	-	-	-	-	-	-	-	-	-
EU365171	-	-	-	-	1	-	-	-	-	-	-	-	-	-
HE680152	-	-	-	-	-	1	-	-	-	-	-	-	-	-
HE680153	-	-	-	-	-	1	-	-	-	-	-	-	-	-
HE680154	-	-	-	-	-	2	-	-	-	-	-	-	-	-
HE680155-56	-	-	-	-	-	2	-	-	-	-	-	-	-	-
HE680157-59, HE680201	-	-	-	-	-	12	-	-	-	-	-	-	-	-
HE680160-61	-	-	-	-	-	6	-	-	-	-	-	-	-	-
HE680162, HE680163	-	-	-	-	-	2	-	-	-	-	-	-	-	-
HE680164	-	-	-	-	-	1	-	-	-	-	-	-	-	-

Haplotype	BS	CAN_Is	CHI	E_AUS	GAL	GC_Dc	GC_Dd	MED	NWA	NZ	OM	PAK	S_AUS	SA
HE680165-69, HE680172, HE680175-76, HE680181-84, HE680202, KC295661	-	-	-	-	-	20	-	-	-	1	-	-	-	-
HE680170	-	-	-	-	-	1	-	-	-	-	-	-	-	-
HE680171	-	-	-	-	-	1	-	-	-	-	-	-	-	-
HE680173	-	-	-	-	-	1	-	-	-	-	-	-	-	-
HE680174	-	-	-	-	-	1	-	-	-	-	-	-	-	-
HE680177	-	-	-	-	-	10	-	-	-	-	-	-	-	-
HE680178	-	-	-	-	-	1	-	-	-	-	-	-	-	-
HE680179, HE680180	-	-	-	-	-	2	-	-	-	-	-	-	-	-
HE680185	-	-	-	-	-	4	-	-	-	-	-	-	-	-
HE680186	-	-	-	-	-	2	-	-	-	-	-	-	-	-
PAK_7, PAK_8, HE680187-88, HE680190-91, HE680195, HE680197	-	-	-	-	-	21	-	-	-	-	-	2	-	-
HE680189	-	-	-	-	-	1	-	-	-	-	-	-	-	-
HE680192	-	-	-	-	-	7	-	-	-	-	-	-	-	-
HE680193	-	-	-	-	-	4	-	-	-	-	-	-	-	-
HE680194, HE680199	-	-	-	-	-	2	-	-	-	-	-	-	-	-
HE680196	-	-	-	-	-	1	-	-	-	-	-	-	-	-
HE680198	-	-	-	-	-	1	-	-	-	-	-	-	-	-
HE680200	-	-	-	-	-	1	-	-	-	-	-	-	-	-
HE680104	-	-	-	-	-	-	1	-	-	-	-	-	-	-
HE680110-11	-	-	-	-	-	-	2	-	-	-	-	-	-	-
HE680112	-	-	-	-	-	-	1	-	-	-	-	-	-	-
HE680113	-	-	-	-	-	-	1	-	-	-	-	-	-	-
HE680114	-	-	-	-	-	-	1	-	-	-	-	-	-	-
HE680115	-	-	-	-	-	-	1	-	-	-	-	-	-	-
HE680116	-	-	-	-	-	-	1	-	-	-	-	-	-	-
HE680117	-	-	-	-	-	-	1	-	-	-	-	-	-	-
HE680118	-	-	-	-	-	-	1	-	-	-	-	-	-	-
HE680119	-	-	-	-	-	-	1	-	-	-	-	-	-	-
HE680120	-	-	-	-	-	-	1	-	-	-	-	-	-	-
HE680121	-	-	-	-	-	-	1	-	-	-	-	-	-	-
HE680122	-	-	-	-	-	-	1	-	-	-	-	-	-	-
HE680123	-	-	-	-	-	-	1	-	-	-	-	-	-	-
HE680124-25	-	-	-	-	-	-	2	-	-	-	-	-	-	-
HE680126	-	-	-	-	-	-	1	-	-	-	-	-	-	-
HE680127	-	-	-	-	-	-	1	-	-	-	-	-	-	-

Haplotype	BS	CAN_Is	CHI	E_AUS	GAL	GC_Dc	GC_Dd	MED	NWA	NZ	OM	PAK	S_AUS	SA
HE680128, KC295611	-	-	-	-	-	-	1	-	-	1	-	-	-	-
HE680130	-	-	-	-	-	-	1	-	-	-	-	-	-	-
HE680131	-	-	-	-	-	-	1	-	-	-	-	-	-	-
HE680132	-	-	-	-	-	-	1	-	-	-	-	-	-	-
HE680133	-	-	-	-	-	-	1	-	-	-	-	-	-	-
HE680134-35	-	-	-	-	-	-	2	-	-	-	-	-	-	-
HE680136	-	-	-	-	-	-	1	-	-	-	-	-	-	-
HE680137	-	-	-	-	-	-	1	-	-	-	-	-	-	-
HE680138	-	-	-	-	-	-	1	-	-	-	-	-	-	-
HE680139	-	-	-	-	-	-	1	-	-	-	-	-	-	-
HE680140	-	-	-	-	-	-	1	-	-	-	-	-	-	-
HE680141	-	-	-	-	-	-	1	-	-	-	-	-	-	-
EU365134	-	-	-	-	-	-	-	5	-	-	-	-	-	-
EU365136	-	-	-	-	-	-	-	3	-	-	-	-	-	-
EU365138	-	-	-	-	-	-	-	1	-	-	-	-	-	-
EU365139, FM211512, FM211536	-	-	-	-	-	-	-	12	2	-	-	-	-	-
EU365140	-	-	-	-	-	-	-	2	-	-	-	-	-	-
EU365141, FM211494	-	-	-	-	-	-	-	2	1	-	-	-	-	-
EU365143	-	-	-	-	-	-	-	1	-	-	-	-	-	-
EU365145	-	-	-	-	-	-	-	1	-	-	-	-	-	-
EU365146	-	-	-	-	-	-	-	1	-	-	-	-	-	-
EU365147	-	-	-	-	-	-	-	1	-	-	-	-	-	-
EU365152	-	-	-	-	-	-	-	1	-	-	-	-	-	-
EU365153	-	-	-	-	-	-	-	2	-	-	-	-	-	-
EU365156	-	-	-	-	-	-	-	1	-	-	-	-	-	-
EU365157	-	-	-	-	-	-	-	1	-	-	-	-	-	-
FM211490	-	-	-	-	-	-	-	-	1	-	-	-	-	-
FM211492	-	-	-	-	-	-	-	-	1	-	-	-	-	-
FM211493	-	-	-	-	-	-	-	-	1	-	-	-	-	-
FM211495	-	-	-	-	-	-	-	-	1	-	-	-	-	-
FM211497	-	-	-	-	-	-	-	-	1	-	-	-	-	-
FM211499	-	-	-	-	-	-	-	-	1	-	-	-	-	-
FM211500	-	-	-	-	-	-	-	-	1	-	-	-	-	-
FM211502, FM211541	-	-	-	-	-	-	-	-	2	-	-	-	-	-
FM211503	-	-	-	-	-	-	-	-	1	-	-	-	-	-
FM211505	-	-	-	-	-	-	-	-	1	-	-	-	-	-
FM211508	-	-	-	-	-	-	-	-	1	-	-	-	-	-
FM211510	-	-	-	-	-	-	-	-	1	-	-	-	-	-
FM211511	-	-	-	-	-	-	-	-	1	-	-	-	-	-
FM211514	-	-	-	-	-	-	-	-	1	-	-	-	-	-

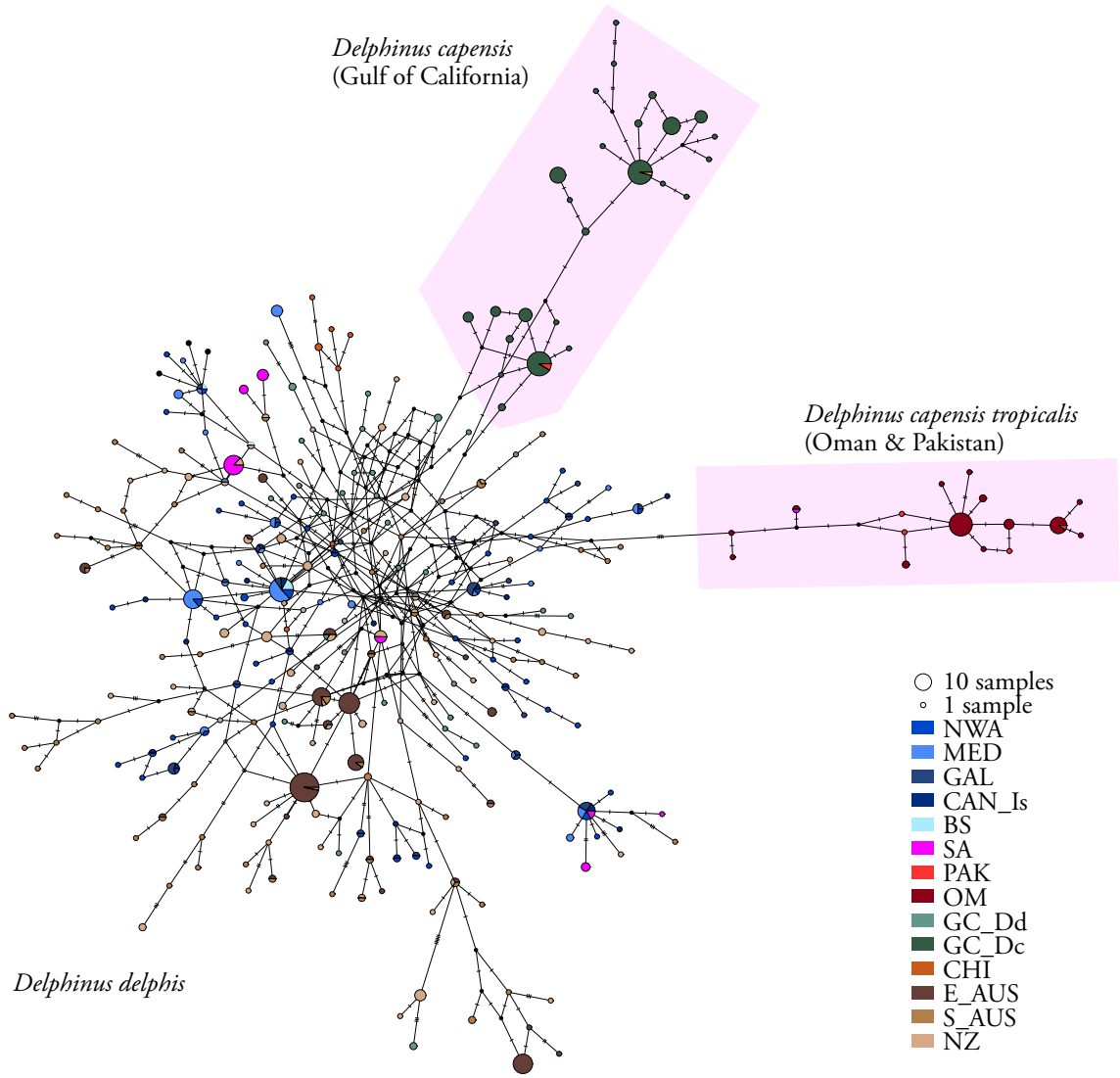
Haplotype	BS	CAN_Is	CHI	E_AUS	GAL	GC_Dc	GC_Dd	MED	NWA	NZ	OM	PAK	S_AUS	SA
FM211515	-	-	-	-	-	-	-	-	1	-	-	-	-	-
FM211518	-	-	-	-	-	-	-	-	1	-	-	-	-	-
FM211520	-	-	-	-	-	-	-	-	1	-	-	-	-	-
FM211521	-	-	-	-	-	-	-	-	1	-	-	-	-	-
FM211523	-	-	-	-	-	-	-	-	1	-	-	-	-	-
FM211526	-	-	-	-	-	-	-	-	1	-	-	-	-	-
FM211528	-	-	-	-	-	-	-	-	1	-	-	-	-	-
FM211529	-	-	-	-	-	-	-	-	1	-	-	-	-	-
FM211530	-	-	-	-	-	-	-	-	1	-	-	-	-	-
FM211531	-	-	-	-	-	-	-	-	1	-	-	-	-	-
FM211532	-	-	-	-	-	-	-	-	1	-	-	-	-	-
FM211534	-	-	-	-	-	-	-	-	1	-	-	-	-	-
FM211535	-	-	-	-	-	-	-	-	1	-	-	-	-	-
FM211537	-	-	-	-	-	-	-	-	1	-	-	-	-	-
FM211538	-	-	-	-	-	-	-	-	1	-	-	-	-	-
FM211540	-	-	-	-	-	-	-	-	1	-	-	-	-	-
FM211542	-	-	-	-	-	-	-	-	1	-	-	-	-	-
FM211543	-	-	-	-	-	-	-	-	1	-	-	-	-	-
KC295601	-	-	-	-	-	-	-	-	-	2	-	-	-	-
KC295602	-	-	-	-	-	-	-	-	-	1	-	-	-	-
KC295603	-	-	-	-	-	-	-	-	-	2	-	-	-	-
KC295604	-	-	-	-	-	-	-	-	-	1	-	-	-	-
KC295605	-	-	-	-	-	-	-	-	-	1	-	-	-	-
KC295606	-	-	-	-	-	-	-	-	-	1	-	-	-	-
KC295607	-	-	-	-	-	-	-	-	-	1	-	-	-	-
KC295608	-	-	-	-	-	-	-	-	-	1	-	-	-	-
KC295609	-	-	-	-	-	-	-	-	-	4	-	-	-	-
KC295610	-	-	-	-	-	-	-	-	-	1	-	-	-	-
KC295612	-	-	-	-	-	-	-	-	-	1	-	-	-	-
KC295613	-	-	-	-	-	-	-	-	-	3	-	-	-	-
KC295614	-	-	-	-	-	-	-	-	-	1	-	-	-	-
KC295615, KJ493731	-	-	-	-	-	-	-	-	-	1	-	-	1	-
KC295616	-	-	-	-	-	-	-	-	-	1	-	-	-	-
KC295618, KJ493762	-	-	-	-	-	-	-	-	-	1	-	-	1	-
KC295620	-	-	-	-	-	-	-	-	-	1	-	-	-	-
KC295621, KJ493741	-	-	-	-	-	-	-	-	-	1	-	-	1	-
KC295622	-	-	-	-	-	-	-	-	-	1	-	-	-	-
KC295623	-	-	-	-	-	-	-	-	-	3	-	-	-	-
KC295624	-	-	-	-	-	-	-	-	-	1	-	-	-	-
KC295627	-	-	-	-	-	-	-	-	-	1	-	-	-	-
KC295628	-	-	-	-	-	-	-	-	-	1	-	-	-	-

Haplotype	BS	CAN_Is	CHI	E_AUS	GAL	GC_Dc	GC_Dd	MED	NWA	NZ	OM	PAK	S_AUS	SA
KC295630	-	-	-	-	-	-	-	-	-	1	-	-	-	-
KC295631, KJ493713	-	-	-	-	-	-	-	-	-	1	-	-	1	-
KC295632	-	-	-	-	-	-	-	-	-	1	-	-	-	-
KC295633	-	-	-	-	-	-	-	-	-	2	-	-	-	-
KC295634	-	-	-	-	-	-	-	-	-	2	-	-	-	-
KC295635	-	-	-	-	-	-	-	-	-	2	-	-	-	-
KC295636	-	-	-	-	-	-	-	-	-	3	-	-	-	-
KC295637, SA_NA62, SA_UMD36	-	-	-	-	-	-	-	-	-	3	-	-	-	3
KC295638	-	-	-	-	-	-	-	-	-	1	-	-	-	-
KC295639	-	-	-	-	-	-	-	-	-	2	-	-	-	-
KC295640	-	-	-	-	-	-	-	-	-	1	-	-	-	-
KC295641	-	-	-	-	-	-	-	-	-	1	-	-	-	-
KC295642	-	-	-	-	-	-	-	-	-	1	-	-	-	-
KC295643	-	-	-	-	-	-	-	-	-	1	-	-	-	-
KC295644	-	-	-	-	-	-	-	-	-	1	-	-	-	-
KC295645	-	-	-	-	-	-	-	-	-	2	-	-	-	-
KC295646, KC295656	-	-	-	-	-	-	-	-	-	2	-	-	-	-
KC295647	-	-	-	-	-	-	-	-	-	1	-	-	-	-
KC295648	-	-	-	-	-	-	-	-	-	1	-	-	-	-
KC295649	-	-	-	-	-	-	-	-	-	1	-	-	-	-
KC295650, KJ493756-57	-	-	-	-	-	-	-	-	-	1	-	-	2	-
KC295651	-	-	-	-	-	-	-	-	-	1	-	-	-	-
KC295652	-	-	-	-	-	-	-	-	-	1	-	-	-	-
KC295653	-	-	-	-	-	-	-	-	-	1	-	-	-	-
KC295654	-	-	-	-	-	-	-	-	-	1	-	-	-	-
KC295657	-	-	-	-	-	-	-	-	-	2	-	-	-	-
KC295658	-	-	-	-	-	-	-	-	-	1	-	-	-	-
KC295659	-	-	-	-	-	-	-	-	-	5	-	-	-	-
KC295660	-	-	-	-	-	-	-	-	-	1	-	-	-	-
KC295662	-	-	-	-	-	-	-	-	-	1	-	-	-	-
KC295663	-	-	-	-	-	-	-	-	-	2	-	-	-	-
KC295664	-	-	-	-	-	-	-	-	-	1	-	-	-	-
KC295665	-	-	-	-	-	-	-	-	-	1	-	-	-	-
OM_100-101	-	-	-	-	-	-	-	-	-	-	2	-	-	-

Haplotype	BS	CAN_Is	CHI	E_AUS	GAL	GC_Dc	GC_Dd	MED	NWA	NZ	OM	PAK	S_AUS	SA
OM_79, OM_90-91, OM_93, OM_97-99, OM_103, OM_105-106, OM_142, OM_1140, OM_1386, OM_2925, OM_2929, OM_3030, OM_3038, OM_3269, OM_3405, OM_KA_25	-	-	-	-	-	-	-	-	-	-	20	-	-	-
OM_104	-	-	-	-	-	-	-	-	-	-	1	-	-	-
OM_80, OM_133, OM_1395, OM_1499, OM_2808, OM_2966, OM_2984, OM_2996, OM_3037, OM_3088	-	-	-	-	-	-	-	-	-	-	10	-	-	-
OM_82, OM_1490, OM_3407, OM_KA_02	-	-	-	-	-	-	-	-	-	-	4	-	-	-
OM_2801	-	-	-	-	-	-	-	-	-	-	1	-	-	-
OM_2919	-	-	-	-	-	-	-	-	-	-	1	-	-	-
OM_3055	-	-	-	-	-	-	-	-	-	-	1	-	-	-
OM_96, OM_3268	-	-	-	-	-	-	-	-	-	-	2	-	-	-
OM_3270	-	-	-	-	-	-	-	-	-	-	1	-	-	-
OM_3278	-	-	-	-	-	-	-	-	-	-	1	-	-	-
OM_89	-	-	-	-	-	-	-	-	-	-	1	-	-	-
OM_92	-	-	-	-	-	-	-	-	-	-	1	-	-	-
OM_KA_24	-	-	-	-	-	-	-	-	-	-	1	-	-	-
PAK_10	-	-	-	-	-	-	-	-	-	-	-	1	-	-
PAK_32	-	-	-	-	-	-	-	-	-	-	-	1	-	-
PAK_34	-	-	-	-	-	-	-	-	-	-	-	1	-	-
PAK_36	-	-	-	-	-	-	-	-	-	-	-	1	-	-
KJ493702	-	-	-	-	-	-	-	-	-	-	-	-	1	-
KJ493703	-	-	-	-	-	-	-	-	-	-	-	-	1	-
KJ493704	-	-	-	-	-	-	-	-	-	-	-	-	1	-
KJ493705	-	-	-	-	-	-	-	-	-	-	-	-	1	-

Haplotype	BS	CAN_Is	CHI	E_AUS	GAL	GC_Dc	GC_Dd	MED	NWA	NZ	OM	PAK	S_AUS	SA
KJ493706	-	-	-	-	-	-	-	-	-	-	-	-	1	-
KJ493708	-	-	-	-	-	-	-	-	-	-	-	-	1	-
KJ493709	-	-	-	-	-	-	-	-	-	-	-	-	1	-
KJ493712	-	-	-	-	-	-	-	-	-	-	-	-	1	-
KJ493715	-	-	-	-	-	-	-	-	-	-	-	-	1	-
KJ493716, KJ493718	-	-	-	-	-	-	-	-	-	-	-	-	2	-
KJ493719, KJ493764	-	-	-	-	-	-	-	-	-	-	-	-	2	-
KJ493720	-	-	-	-	-	-	-	-	-	-	-	-	1	-
KJ493722	-	-	-	-	-	-	-	-	-	-	-	-	1	-
KJ493723	-	-	-	-	-	-	-	-	-	-	-	-	1	-
KJ493724	-	-	-	-	-	-	-	-	-	-	-	-	1	-
KJ493725	-	-	-	-	-	-	-	-	-	-	-	-	1	-
KJ493726	-	-	-	-	-	-	-	-	-	-	-	-	1	-
KJ493727	-	-	-	-	-	-	-	-	-	-	-	-	1	-
KJ493728	-	-	-	-	-	-	-	-	-	-	-	-	1	-
KJ493729	-	-	-	-	-	-	-	-	-	-	-	-	1	-
KJ493730	-	-	-	-	-	-	-	-	-	-	-	-	1	-
KJ493732	-	-	-	-	-	-	-	-	-	-	-	-	1	-
KJ493734	-	-	-	-	-	-	-	-	-	-	-	-	1	-
KJ493737	-	-	-	-	-	-	-	-	-	-	-	-	1	-
KJ493738	-	-	-	-	-	-	-	-	-	-	-	-	1	-
KJ493739	-	-	-	-	-	-	-	-	-	-	-	-	1	-
KJ493740	-	-	-	-	-	-	-	-	-	-	-	-	1	-
KJ493742	-	-	-	-	-	-	-	-	-	-	-	-	1	-
KJ493743	-	-	-	-	-	-	-	-	-	-	-	-	1	-
KJ493744	-	-	-	-	-	-	-	-	-	-	-	-	1	-
KJ493745	-	-	-	-	-	-	-	-	-	-	-	-	1	-
KJ493747	-	-	-	-	-	-	-	-	-	-	-	-	1	-
KJ493749	-	-	-	-	-	-	-	-	-	-	-	-	1	-
KJ493750	-	-	-	-	-	-	-	-	-	-	-	-	1	-
KJ493751	-	-	-	-	-	-	-	-	-	-	-	-	1	-
KJ493752	-	-	-	-	-	-	-	-	-	-	-	-	1	-
KJ493753	-	-	-	-	-	-	-	-	-	-	-	-	1	-
KJ493755	-	-	-	-	-	-	-	-	-	-	-	-	1	-
KJ493758	-	-	-	-	-	-	-	-	-	-	-	-	1	-
KJ493759	-	-	-	-	-	-	-	-	-	-	-	-	1	-
KJ493760	-	-	-	-	-	-	-	-	-	-	-	-	1	-
KJ493763	-	-	-	-	-	-	-	-	-	-	-	-	1	-
KJ493765	-	-	-	-	-	-	-	-	-	-	-	-	1	-

Haplotype	BS	CAN_Is	CHI	E_AUS	GAL	GC_Dc	GC_Dd	MED	NWA	NZ	OM	PAK	S_AUS	SA
SA_ASN82, SA_BAL37, SA_BRI81, SA_SAL20, SA_SAL23, SA_UMH102, SA_UMH99	-	-	-	-	-	-	-	-	-	-	-	-	-	13
SA_BAL15, SA_DUR328	-	-	-	-	-	-	-	-	-	-	-	-	-	3
SA_BRI77, SA_SCO60	-	-	-	-	-	-	-	-	-	-	-	-	-	3
SA_BRI78	-	-	-	-	-	-	-	-	-	-	-	-	-	1
SA_MG76, SA_SP20	-	-	-	-	-	-	-	-	-	-	-	-	-	5
SA_ST26	-	-	-	-	-	-	-	-	-	-	-	-	-	1



Appendix X: Common dolphin median-joining network. Generated in POPART (<http://popart.otago.ac.nz>, Leigh & Bryant, 2015).

References

- Adams D.C., Rohlf F.J. and Slice D.E.** (2004) Geometric Morphometrics: Ten Years of Progress Following the Revolution?. *Italian Journal of Zoology*. **71:1**, pp.5-16
- Adams L.D. and Rosel P.E.** (2006) Population Differentiation of the Atlantic Spotted Dolphin (*Stenella frontalis*) in the Western North Atlantic, Including the Gulf of Mexico. *Marine Biology*. **148:3**, pp.671-681
- Adams D.C. and Otárola-Castillo E.** (2013) Geomorph: An R Package for the Collection and Analysis of Geometric Morphometric Shape Data. *Methods in Ecology and Evolution*. **4:4**, pp.393-399
- Agnarsson I. and May-Collado L.J.** (2008) The Phylogeny of Cetartiodactyla: the Importance of Dense Taxon Sampling, Missing Data, and the Remarkable Promise of Cytochrome B to Provide Reliable Species-Level Phylogenies. *Molecular Phylogenetics and Evolution*. **48:3**, pp.964-985
- Al-Robbae K.** (1974) *Tursiops aduncus* Bottlenosed Dolphin: a New Record for Arab Gulf, with Notes on Cetacea of the Region. *Bulletin of the Basrah Natural History Museum*. **1:1**, pp.7-15
- Alexander A., Steel D., Slikas B., Hoekzema K., Carraher C., Parks M., Cronn R. and Baker C.S.** (2013) Low Diversity in the Mitogenome of Sperm Whales Revealed by Next-Generation Sequencing. *Genome Biology and Evolution*. **5:1**, pp.113-29
- Almogi-Labin A., Schmiedl G., Hemleben C., Siman-Tov R., Segl M. and Meischner D.** (2000) The Influence of the NE Winter Monsoon on Productivity Changes in the Gulf of Aden, NW Arabian Sea, During the Last 530Ka as Recorded by Foraminifera. *Marine Micropaleontology*. **40:3**, pp.295-319
- Amaha A.** (1994) Geographic Variation of the Common Dolphin, *Delphinus delphis* (Odontoceti: Delphinidae). Ph.D. thesis, Graduate School of Fisheries Tokyo University of Fisheries, Tokyo. pp.211
- Amaral A.R., Sequeira M., Martínez-Cedeira J. and Coelho M.M.** (2007) New Insights on Population Genetic Structure of *Delphinus delphis* from the Northeast Atlantic and Phylogenetic Relationships Within the Genus Inferred from Two Mitochondrial Markers. *Marine Biology*. **151:5**, pp.1967-1976
- Amaral A.R., Coelho M.M., Marugan-Lobon J. and Rohlf F.J.** (2009) Cranial Shape Differentiation in Three Closely Related Delphinid Cetacean Species: Insights Into Evolutionary History. *Zoology*. **112:1**, pp.38-47
- Amaral A.R., Beheregaray L.B., Bilgmann K., Freitas L., Robertson K.M., Sequeira M., Stockin K.A., Coelho M.M. and Möller L.M.** (2012a) Influences of Past Climatic Changes on Historical Population Structure and Demography of a Cosmopolitan Marine Predator, the Common Dolphin (Genus *Delphinus*). *Molecular Ecology*. **21:19**, pp.4854-71

- Amaral A.R., Jackson J.A., Möller L.M., Beheregaray L.B. and Coelho M.M.** (2012b) Species Tree of a Recent Radiation: the Subfamily Delphininae (Cetacea, Mammalia). *Molecular Phylogenetics and Evolution*. **64:1**, pp.243-53
- Amaral A.R., Lovewell G., Coelho M.M., Amato G. and Rosenbaum H.C.** (2014) Hybrid Speciation in a Marine Mammal: the Clymene Dolphin (*Stenella clymene*). *Plos One*. **9:1**, e83645
- Amir O. and Jiddawi N.** (2001) Dolphin Tourism and Community Participation in Kizimkazi Village, Zanzibar. Marine Science Development in Tanzania and Eastern Africa. WIOMSA Book Series. pp.551-560
- Amir O.A.** (2010) Biology, Ecology and Anthropogenic Threats of Indo-Pacific Bottlenose Dolphins in East Africa. PhD thesis, Stockholm University, Faculty of Science, Department of Zoology. pp. 31
- Anderson D.M. and Prell W.L.** (1993) A 300 Kyr Record of Upwelling off Oman During the Late Quaternary: Evidence of the Asian Southwest Monsoon. *Paleoceanography*. **8:2**, pp.193-208
- Anderson R.C.** (2014) Cetaceans and Tuna Fisheries in the Western and Central Indian Ocean. *International Pole and Line Federation Technical Report*. **2**, pp.133
- Andrews K.R., Karczmarski L., Au W.W.L., Rickards S.H., Vanderlip C.A., Bowen B.W., Gordon Grau E. and Toonen R.J.** (2010) Rolling Stones and Stable Homes: Social Structure, Habitat Diversity and Population Genetics of the Hawaiian Spinner Dolphin (*Stenella longirostris*). *Molecular Ecology*. **19:4**, pp.732-48
- Ansmann I.C., Parra G.J., Lanyon J.M. and Seddon J.M.** (2012) Fine-Scale Genetic Population Structure in a Mobile Marine Mammal: Inshore Bottlenose Dolphins in Moreton Bay, Australia. *Molecular Ecology*. **21:18**, pp.4472-85
- Antao T., Lopes A., Lopes R.J., Beja-Pereira A. and Luikart G.** (2008) LOSITAN: a Workbench to Detect Molecular Adaptation Based on a F_{ST} -Outlier Method. *BMC Bioinformatics*. **9:1**, pp.323
- Arnason U., Gullberg A. and Janke A.** (2004) Mitogenomic Analyses Provide New Insights into Cetacean Origin and Evolution. *Gene*. **333**, pp.27-34
- Baele G., Lemey P., Bedford T., Rambaut A., Suchard M.A. and Alekseyenko A.V.** (2012) Improving the Accuracy of Demographic and Molecular Clock Model Comparison While Accommodating Phylogenetic Uncertainty. *Molecular Biology and Evolution*. **29:9**, pp.2157-67
- Baele G., Lemey P. and Vansteelandt S.** (2013) Make the Most of Your Samples: Bayes Factor Estimators for High-Dimensional Models of Sequence Evolution. *BMC Bioinformatics*. **14**, pp.85
- Bailey G.** (2009) The Red Sea, Coastal Landscapes, and Hominin Dispersals. In: Petraglia, M.D. and Rose J.I. (Eds). *The Evolution of Human Populations in Arabia. Vertebrate Paleobiology and Paleoanthropology*. Springer Netherlands. pp.15-37

- Baker R.H. and Desalle R.** (1997) Multiple Sources of Character Information and the Phylogeny of Hawaiian Drosophilids. *Systematic Biology*. **46:4**, pp.654-673
- Baker R.H., Yu X. and Desalle R.** (1998) Assessing the Relative Contribution of Molecular and Morphological Characters in Simultaneous Analysis Trees. *Molecular Phylogenetics and Evolution*. **9:3**, pp.427-436
- Baldwin R. and Salm R.** (1994) Whales and Dolphins Along the Coast of Oman. Muscat Printing Press, Muscat, Oman. pp.65
- Baldwin R.M., Gallagher M. and Van Waerebeek K.** (1999) A Review of Cetaceans from Waters off the Arabian Peninsula. In: Fisher, M., Ghazanfar S. and Spalton A. (Eds). *The Natural History of Oman: A Festschrift for Michael Gallagher*. Backhuys Publishers, Leiden. pp.161-189
- Baldwin R.M., Collins M., Van Waerebeek K. and Minton G.** (2004) The Indo-Pacific Humpback Dolphin of the Arabian Region: A Status Review. *Aquatic Mammals*. **30:1**, pp.111-124
- Ballance L.T., Pitman R.L., Reilly S.B. and Force M.P.** (1996) Report of a Cetacean, Seabird, Marine Turtle, and Flying Fish Survey of the Western Tropical Indian Ocean Aboard the Research Vessel *Malcolm Baldrige*, March 21-July 26, 1995. US Department of Commerce, National Oceanic and Atmospheric Administration, National Marine Fisheries Service, Southwest Fisheries Science Center. pp.133
- Ballance L.T. and Pitman R.L.** (1998) Cetaceans of the Western Tropical Indian Ocean: Distribution, Relative Abundance, and Comparisons with Cetacean Communities of Two Other Tropical Ecosystems. *Marine Mammal Science*. **14:3**, pp.429-459
- Bandelt H.-J., Forster P. and Röhl A.** (1999) Median-Joining Networks for Inferring Intraspecific Phylogenies. *Molecular Biology and Evolution*. **16:1**, pp.37-48
- Banguera-Hinestroza E.** (2008) Phylogeography of *Lagenorhynchus acutus* and *Lagenorhynchus albirostris* and Phylogeny of the Genus *Lagenorhynchus*. Phd thesis, Durham theses, Durham University. Available at Durham E-Theses Online: <http://etheses.dur.ac.uk/2509/>. pp.194
- Banguera-Hinestroza E., Hayano A., Crespo E. and Hoelzel A.R.** (2014) Delphinid Systematics and Biogeography with a Focus on the Current Genus *Lagenorhynchus*: Multiple Pathways for Antitropical and Trans-Oceanic Radiation. *Molecular Phylogenetics and Evolution*. **80**, pp.217-30
- Banse K.** (1968) Hydrography of the Arabian Sea Shelf of India and Pakistan and Effects on Demersal Fishes. *Deep Sea Research and Oceanographic Abstracts*. **15:1**, pp.45-79
- Banse K. and McClain C.R.** (1986) Winter Blooms of Phytoplankton in the Arabian Sea As Observed by the Coastal Zone Color Scanner. *Marine Ecology Progress Series*. **34**, pp.201-211

- Banse K.** (1987) Seasonality of Phytoplankton Chlorophyll in the Central and Northern Arabian Sea. *Deep Sea Research Part A. Oceanographic Research Papers*. **34:5**, pp.713-723
- Barluenga M., Stölting K.N., Salzburger W., Muschick M. and Meyer A.** (2006) Sympatric Speciation in Nicaraguan Crater Lake Cichlid Fish. *Nature*. **439:7077**, pp.719-23
- Barnes L.G.** (1990) The Fossil Record and Evolutionary Relationships of the Genus *Tursiops*. In: Leatherwood S. and Reeves R.R. (Eds). *The Bottlenose Dolphin*. Academic Press Limited 24-48 Oval Road, London NW1 7DX. pp.3-26
- Bauer S., Hitchcock G.L. and Olson D.B.** (1991) Influence of Monsoonally-Forced Ekman Dynamics Upon Surface Layer Depth and Plankton Biomass Distribution in the Arabian Sea. *Deep Sea Research Part A. Oceanographic Research Papers*. **38:5**, pp.531-553
- Bay L., Choat J.H., Van Herwerden L. and Robertson D.R.** (2004) High Genetic Diversities and Complex Genetic Structure in An Indo-Pacific Tropical Reef Fish (*Chlorurus sordidus*): Evidence of An Unstable Evolutionary Past? *Marine Biology*. **144:4**, pp.757--767
- Beadon J.** (1991) Cetaceans Seen and Caught in the Gulf of Aquaba and the Gulf of Suez 13 September 1980 Through 1 September 1981. In: Donovan S. and Leatherwood G. (Eds). *Cetaceans and Cetacean Research in the Indian Ocean Sanctuary*. United Nations Environmental Programme, Nairobi, Kenya. pp.111-114
- Beasley I., Robertson K.M. and Arnold P.** (2005) Description of a New Dolphin, the Australian Snubfin Dolphin *Orcaella heinsohni* sp. n. (Cetacea, Delphinidae). *Marine Mammal Science*. **21:3**, pp.365-400
- Beaumont M.A.** (1999) Detecting Population Expansion and Decline Using Microsatellites. *Genetics*. **153:4**, pp.2013-2029
- Beaumont M.A.** (2008) Joint Determination of Topology, Divergence Time, and Immigration in Population Trees. In: Renfrew C., Matsumura S. and Forster P. (Eds). *Simulation, Genetics and Human Prehistory*. McDonald Institute for Archaeological Research, Cambridge. pp.134-1541
- Beaumont M.A., Nielsen R., Robert C., Hey J., Gaggiotti O., Knowles L., Estoup A., Panchal M., Corander J. and Hickerson M.** (2010) In Defence of Model-Based Inference in Phylogeography. *Molecular Ecology*. **19:3**, pp.436-446
- Belkhir K., Borsa P., Chikhi L., Raufaste N. and Bonhomme F.** (2004) GENETIX 4.05, Population Genetics Software for Windows TM. Université De Montpellier Ii. Montpellier.
- Bell C.H., Kemper C.M. and Conran J.G.** (2002) Common Dolphins (*Delphinus delphis*) in Southern Australia: A Morphometric Study. *Australian Mammalogy*. **24:1**, pp.1-10

- Berlocher S.H.** (1998) Can Sympatric Speciation Via Host or Habitat Shift be Proven from Phylogenetic and Biogeographic Evidence. *In*: Howard D.J. and Berlocher S.H. (Eds). *Endless Forms: Species and Speciation*. Oxford University Press. pp.99--113
- Bermingham E. and Moritz C.** (1998) Comparative Phylogeography: Concepts and Applications. *Molecular Ecology*. **7:4**, pp.367-369
- Bernal R., Olavarria C. and Moraga R.** (2003). Occurrence and Long-Term Residency of Two Long-Beaked Common Dolphins, *Delphinus capensis* (Gray 1828), in Adjacent Small Bays on the Chilean Central Coast. *Aquatic Mammals*. **29:3**, pp.396-399
- Bérubé M. and Palsbøll P.** (1996) Identification of Sex in Cetaceans by Multiplexing with Three ZFX and ZFY Specific Primers. *Molecular Ecology*. **5:2**, pp.283-287
- Bérubé M. and Aguilar A.** (1998) A New Hybrid Between a Blue Whale, *Balaenoptera musculus*, and a Fin Whale, *B. physalus*: Frequency and Implications of Hybridization. *Marine Mammal Science*. **14:1**, pp.82-98
- Bickford D., Lohman D.J., Sodhi N.S., Ng P.K.L., Meier R., Winker K., Ingram K.K. and Das I.** (2007) Cryptic Species As a Window on Diversity and Conservation. *Trends in Ecology and Evolution*. **22:3**, pp.148-55
- Bilgmann K., Möller L.M., Harcourt R.G., Gibbs S.E. and Beheregaray L.B.** (2007) Genetic Differentiation in Bottlenose Dolphins from South Australia: Association with Local Oceanography and Coastal Geography. *Marine Ecology Progress Series*. **341**, pp.265
- Bilgmann K., Möller L.M., Harcourt R.G., Gales R. and Beheregaray L.B.** (2008) Common Dolphins Subject to Fisheries Impacts in Southern Australia Are Genetically Differentiated: Implications for Conservation. *Animal Conservation*. **11:6**, pp.518-528
- Bilgmann K., Parra G., Zanardo N., Beheregaray L. and Möller L.** (2014) Multiple Management Units of Short-Beaked Common Dolphins Subject to Fisheries Bycatch off Southern and Southeastern Australia. *Marine Ecology Progress Series*. **500**, pp.265-279
- Bolnick D.I. and Fitzpatrick B.M.** (2007) Sympatric Speciation: Models and Empirical Evidence. *Annual Review of Ecology, Evolution, and Systematics*. **38**, pp.459-487
- Bonin A., Taberlet P., Miaud C. and Pompanon F.** (2006) Explorative Genome Scan to Detect Candidate Loci for Adaptation Along a Gradient of Altitude in the Common Frog (*Rana temporaria*). *Molecular Biology and Evolution*. **23:4**, pp.773-783
- Bonjean F. and Lagerloef G.S.E.** (2002) Diagnostic Model and Analysis of the Surface Currents in the Tropical Pacific Ocean. *Journal of Physical Oceanography*. **32:10**, pp.2938-2954
- Bookstein F.L.** (1989) Principal Warps: Thin-Plate Splines and the Decomposition of Deformations. *IEEE Transactions on Pattern Analysis and Machine Intelligence*. **2:6**, pp.567--585

- Bookstein F.L.** (1997) *Morphometric Tools for Landmark Data: Geometry and Biology*. Cambridge University Press. pp.456
- Bookstein F.L.** (1998) A Hundred Years of Morphometrics. *Acta Zoologica Academiae Scientiarum Hungaricae*. **44:1-2**, pp.7-59
- Bossart G.D.** (2011) Marine Mammals As Sentinel Species for Oceans and Human Health. *Veterinary Pathology*. **48:3**, pp.676-90
- Bowen B.W., Nelson W.S. and Avise J.C.** (1993) A Molecular Phylogeny for Marine Turtles: Trait Mapping, Rate Assessment, and Conservation Relevance. *Proceedings of the National Academy of Sciences*. **90:12**, pp.5574-5577
- Branch T.A., Stafford K.M., Palacios D.M., Allison C., Bannister J.L., Burton C.L.K., Cabrera E., Carlson C.A., Galletti Vernazzani B., Gill P.C., Hucke-Gaete R., Jenner K.C.S., Jenner M.-N.M., Matsuoka K., Mikhalev Y.A., Miyashita T., Morrice M.G., Nishiwaki S., Sturrock V.J., Tormosov D., Anderson R.C., Baker A.N., Best P.B., Borsa P., Brownell Jr R.L., Childerhouse S., Findlay K.P., Gerrodette T., Ilangakoon A.D., Joergensen M., Kahn B., Ljungblad D.K., Maughan B., McCauley R.D., Mckay S., Norris T.F., Oman Whale and Dolphin Research Group, Warneke R.M., Rankin S., Samaran F., Thiele D., and Van Waerebeek K.** (2007) Past and Present Distribution, Densities and Movements of Blue Whales *Balaenoptera musculus* in the Southern Hemisphere and Northern Indian Ocean. *Mammal Review*. **37:2**, pp.116-175
- Braulik G.T., Ranjbar S., Owfi F., Aminrad T., Dakhteh S.M.H., Kamrani E. and Mohsenizadeh F.** (2010) Marine Mammal Records from Iran. *Journal of Cetacean Research and Management*. **11:1**, pp.49--64
- Briggs J.C. and Bowen B.W.** (2012) A Realignment of Marine Biogeographic Provinces with Particular Reference to Fish Distributions. *Journal of Biogeography*. **39:1**, pp.12-30
- Brock J.C. and McClain C.R.** (1992) Interannual Variability in Phytoplankton Blooms Observed in the Northwestern Arabian Sea During the Southwest Monsoon. *Journal of Geophysical Research*. **97:1**, pp.733-750
- Brown C.M., Arbour J.H. and Jackson D.A.** (2012) Testing of the Effect of Missing Data Estimation and Distribution in Morphometric Multivariate Data Analyses. *Systematic Biology*. **61:6**, pp.941-54
- Bruno S., Politi E. and Bearzi G.** (2004) Social Organisation of a Common Dolphin Community in the Eastern Ionian Sea: Evidence of a Fluid Fission-Fusion Society. *European Research on Cetaceans*. **15**, pp.49-51
- Burkill P.H.** (1999) Arabesque: An Overview. *Deep Sea Research Part II: Topical Studies in Oceanography*. **46:3**, pp.529-547

- Caballero S., Jackson J., Mignucci-Giannoni A.A., Barrios-Garrido H., Beltrán-Pedrerros S., Montiel-Villalobos M.A.G., Robertson K.M. and Baker C.S.** (2008) Molecular Systematics of South American Dolphins *Sotalia*: Sister Taxa Determination and Phylogenetic Relationships, with Insights into a Multi-Locus Phylogeny of the Delphinidae. *Molecular Phylogenetics and Evolution*. **46:1**, pp.252-68
- Caldwell M., Gaines M.S. and Hughes C.R.** (2002) Eight Polymorphic Microsatellite Loci for Bottlenose Dolphin and Other Cetacean Species. *Molecular Ecology Notes*. **2:4**, pp.393-395
- Cassens I., Vicario S., Waddell V.G., Balchowsky H., Van Belle D., Ding W., Fan C., Lal Mohan R., Simões-Lopes P.C., Bastida R., Meyer A., Stanhope M.J., Milinkovitch M.C.** (2000) Independent Adaptation to Riverine Habitats Allowed Survival of Ancient Cetacean Lineages. *Proceedings of the National Academy of Sciences*. **97:21**, pp.11343-11347
- Chapuis M.P. and Estoup A.** (2007) Microsatellite Null Alleles and Estimation of Population Differentiation. *Molecular Biology and Evolution*. **24:3**, pp.621-31
- Charlton K., Taylor A.C. and Mckechnie S.W.** (2006) A Note on Divergent mtDNA Lineages of Bottlenose Dolphins from Coastal Waters of Southern Australia. *Journal of Cetacean Research and Management*. **8:2**, pp.173
- Charlton-Robb K., Gershwin L.A., Thompson R., Austin J., Owen K. and Mckechnie S.** (2011) A New Dolphin Species, the Burrunan Dolphin *Tursiops australis* sp. nov., Endemic to Southern Australian Coastal Waters. *Plos One*. **6:9**, e24047
- Chen I., Chou L.-S., Chen Y.-J. and Watson A.** (2011) The Maturation of Skulls in Postnatal Risso's Dolphins (*Grampus griseus*) from Taiwanese Waters. *Taiwania*. **56:3**, pp.177-185
- Cockcroft V.** (1990) Dolphin Catches in the Natal Shark Nets, 1980 to 1988. *South African Journal of Wildlife Research/Suid-Afrikaanse Tydskrif vir Natuurnavorsing*. **20:2**, pp.44-51
- Cockcroft V.G. and Peddemors V.M.** (1990) Seasonal Distribution and Density of Common Dolphins *Delphinus delphis* off the South-East Coast of Southern Africa. *South African Journal of Marine Science*. **9:1**, pp.371-377
- Collins T., Minton G., Baldwin R., Van Waerebeek K., Hywel-Davies A. and Cockcroft V.** (2002) A Preliminary Assessment of the Frequency, Distribution and Causes of Mortality of Beach Cast Cetaceans in the Sultanate of Oman, January 1999 to February 2002. IWC Scientific Committee Document. SC/54/O4. pp.13
- Connor R.C., Smolker R.A., and Richards A. F.** (1992) Two Levels of Alliance Formation Among Male Bottlenose Dolphins (*Tursiops* sp.). *Proceedings of the National Academy of Sciences*. **89:3**, pp.987-990

- Connor R.C., Heithaus M.R., Berggren P. and Miksis J.L.** (2000) “Kerplunking”: Surface Fluke-Splashes During Shallow-Water Bottom Foraging by Bottlenose Dolphins. *Marine Mammal Science*. **16:3**, pp. 646-653
- Connor R.C.** (2000) Group Living in Whales and Dolphins. *In: Mann, J. (Eds) Cetacean Societies: Field Studies of Dolphins and Whales*. University of Chicago Press. pp.199-218
- Connor R.C., Smolker R. and Bejder L.** (2006) Synchrony, Social Behaviour and Alliance Affiliation in Indian Ocean Bottlenose Dolphins, *Tursiops aduncus*. *Animal Behaviour*. **72:6**, pp.1371-1378
- Corkeron P.J.** (1990) Aspects of the Behavioral Ecology of Inshore Dolphins *Tursiops truncatus* and *Sousa chinensis* in Moreton Bay, Australia. *In: Leatherwood S. and Reeves R.R. (Eds). The Bottlenose Dolphin*. Academic Press Limited 24-48 Oval Road, London NW1 7DX. pp.285-293
- Cornuet J.M., Santos F., Beaumont M.A., Robert C.P., Marin J.M., Balding D.J., Guillemaud T. and Estoup A.** (2008) Inferring Population History with DIY ABC: a User-Friendly Approach to Approximate Bayesian Computation. *Bioinformatics*. **24:23**, pp.2713-9
- Cornuet J.M., Pudlo P., Veyssier J., Dehne-Garcia A., Gautier M., Leblois R., Marin J.M. and Estoup A.** (2014) DIYabc v2. 0: A Software to Make Approximate Bayesian Computation Inferences About Population History Using Single Nucleotide Polymorphism, DNA Sequence and Microsatellite Data. *Bioinformatics*. **30:8**, pp.1187-1189
- Coughlan J., Mirimin L., Dillane E., Rogan E. and Cross T.F.** (2006) Isolation and Characterization of Novel Microsatellite Loci for the Short-Beaked Common Dolphin (*Delphinus delphis*) and Cross-Amplification in Other Cetacean Species. *Molecular Ecology Notes*. **6**, pp.490-492
- Coyne J. and Orr H.** (2004) Speciation. Sinauer Associates Sunderland, MA
- Crandall E.D., Frey M.A., Grosberg R.K. and Barber P.H.** (2008) Contrasting Demographic History and Phylogeographical Patterns in Two Indo-Pacific Gastropods. *Molecular Ecology*. **17:2**, pp.611-26
- Crisp M.D. and Cook L.G.** (2005) Do Early Branching Lineages Signify Ancestral Traits? *Trends in Ecology and Evolution*. **20:3**, pp.122-8
- Cunha H.A., de Castro R.L., Secchi E.R., Crespo E.A., Lailson-Brito J., Azevedo A.F., Lazoski C. and Solé-Cava A.M.** (2015) Molecular and Morphological Differentiation of Common Dolphins (*Delphinus* sp.) in the Southwestern Atlantic: Testing the Two Species Hypothesis in Sympatry. *PloS one*. **10:11**
- Cunningham C.W., Omland K.E. and Oakley T.H.** (1998) Reconstructing Ancestral Character States: a Critical Reappraisal. *Trends in Ecology and Evolution*. **13:9**, pp.361-366

- Curry B.E.** (1997) Phylogenetic Relationships Among Bottlenose Dolphins (Genus *Tursiops*) in a Worldwide Context. PhD thesis, Texas A & M University.
- Dalebout M.L., Mead J.G., Baker C.S., Baker A.N. and Helden A.L.** (2002) A New Species of Beaked Whale *Mesoplodon perrini* sp. n. (Cetacea: Ziphiidae) Discovered Through Phylogenetic Analyses of Mitochondrial DNA Sequences. *Marine Mammal Science*. **18:3**, pp.577-608
- Darbyshire J.** (1964) A Hydrological Investigation of the Agulhas Current Area. *Deep Sea Research and Oceanographic Abstracts*. **2:5**, pp.781-815
- Darriba D., Taboada G.L., Doallo R. and Posada D.** (2012) Jmodeltest 2: More Models, New Heuristics and Parallel Computing. *Nature Methods*. **9:8**, pp.772-772
- De Luna C.J., Goodman S.J., Thatcher O., Jepson P., Andersen L., Tolley K. and Holzner A.** (2012) Phenotypic and Genetic Divergence Among Harbour Porpoise Populations Associated with Habitat Regions in the North Sea and Adjacent Seas. *Journal of Evolutionary Biology*. **25:4**, pp.674-681
- de Silva P.** (1987) Cetaceans (Whales, Dolphins and Porpoises) Recorded off Sri Lanka, India, from the Arabian Sea and Gulf, Gulf of Aden and from the Red Sea. *Journal of the Bombay Natural History Society*. **84:3**, pp.505-525
- Demastes J.W., Spradling T.A., Hafner M.S., Hafner D.J. and Reed D.L.** (2002) Systematics and Phylogeography of Pocket Gophers in the Genera *Cratogeomys* and *Pappogeomys*. *Molecular Phylogenetics and Evolution*. **22:1**, pp.144-54
- Dizon A.E., Lockyer C., Perrin W.F., Demaster D.P. and Sisson J.** (1992). Rethinking the Stock Concept: A Phylogeographic Approach. *Conservation Biology*. **6:1**, pp.24-36.
- Dobzhansky T.** (1937) Genetic Nature of Species Differences. *American Naturalist*. **71:735**, pp.404-420
- Donovon G.P.** (2009) The International Whaling Commission. In: Perrin W.F., Würsig B. and Thewissen, J.G.M. (Eds). *Encyclopedia of Marine Mammals*. pp.624-628
- Dowling T.E. and Brown W.M.** (1993) Population Structure of the Bottlenose Dolphin (*Tursiops truncatus*) As Determined by Restriction Endonuclease Analysis of Mitochondrial DNA. *Marine Mammal Science*. **9:2**, pp.138-155
- Drummond A.J., Rambaut A., Shapiro B. and Pybus O.G.** (2005) Bayesian Coalescent Inference of Past Population Dynamics from Molecular Sequences. *Molecular Biology and Evolution*. **22:5**, pp.1185-1192
- Drummond A.J. and Rambaut A.** (2007) BEAST: Bayesian Evolutionary Analysis by Sampling Trees. *BMC Evolutionary Biology*. **7**, pp.214
- Dunsha G., Barros N.B., Berens McCabe E.J., Gales N.J., Hindell M.A., Jarman S.N. and Wells R.S.** (2013) Stranded Dolphin Stomach Contents Represent the Free-Ranging Population's Diet. *Biology Letters*. **9:3**, pp.5

- Duplessy J.C.** (1982) Glacial to Interglacial Contrasts in the Northern Indian Ocean. *Nature*. **295**, 494 - 498
- Edgar R.C.** (2004) MUSCLE: Multiple Sequence Alignment with Improved Accuracy and Speed. Computational Systems Bioinformatics Conference, 2004. CSB 2004. Proceedings. 2004 IEEE. pp.728-729
- Elliott A.J. and Savidge G.** (1990) Some Features of the Upwelling off Oman. *Journal of Marine Research*. **48:2**, pp.319-333
- Encalada S., Lahanas P., Bjorndal K., Bolten A., Miyamoto M. and Bowen B.** (1996) Phylogeography and Population Structure of the Atlantic and Mediterranean Green Turtle *Chelonia mydas*: a Mitochondrial DNA Control Region Sequence Assessment. *Molecular Ecology*. **5:4**, pp.473-483
- Escorza-Treviño S. and Dizon A.** (2000) Phylogeography, Intraspecific Structure and Sex-Biased Dispersal of Dall's Porpoise, *Phocoenoides dalli*, Revealed by Mitochondrial and Microsatellite DNA Analyses. *Molecular Ecology*. **9:8**, pp.1049-1060
- Estoup A., Jarne P. and Cornuet J.** (2002) Homoplasy and Mutation Model at Microsatellite Loci and Their Consequences for Population Genetics Analysis. *Molecular Ecology*. **11:9**, pp.1591-1604
- Evanno G., Regnaut S. and Goudet J.** (2005) Detecting the Number of Clusters of Individuals Using the Software STRUCTURE: a Simulation Study. *Molecular Ecology*. **14:8**, pp.2611-2620
- Excoffier L., Laval G. and Schneider S.** (2005) ARLEQUIN (Version 3.0): An Integrated Software Package for Population Genetics Data Analysis. *Evolutionary Bioinformatics Online*. **1**, pp.47
- Excoffier L. and Lischer H.E.** (2010) ARLEQUIN Suite Ver 3.5: a New Series of Programs to Perform Population Genetics Analyses Under Linux and Windows. *Molecular Ecology Resources*. **10:3**, pp.564-567
- Fagundes N.J., Ray N., Beaumont M., Neuenschwander S., Salzano F.M., Bonatto S.L. and Excoffier L.** (2007) Statistical Evaluation of Alternative Models of Human Evolution. *Proceedings of the National Academy of Sciences*. **104:45**, pp.17614-17619
- Feder J.L., Chilcote C.A. and Bush G.L.** (1988) Genetic Differentiation Between Sympatric Host Races of the Apple Maggot Fly *Rhagoletis pomonella*. *Nature*. **336:6194**, pp.61-64
- Felsenstein J.** (1985) Phylogenies and the Comparative Method. *American Naturalist*. **125:1**, pp.1-15
- Fernandez R., Santos M.B., Pierce G.J., Llavona A., Lopez A., Silva M.A., Ferreira M., Carrillo M., Cermeno P., Lens S. and Piertney S.B.** (2011) Fine-Scale Genetic Structure of Bottlenose Dolphins, *Tursiops truncatus*, in Atlantic Coastal Waters of the Iberian Peninsula. *Hydrobiologia*. **670:1**, pp.111-125

- Fitzgerald E.M.** (2005) Pliocene Marine Mammals from the Whalers Bluff Formation of Portland, Victoria, Australia. *Memoirs of Museum Victoria*. **62:1**, pp.67-89
- Fitzpatrick B.M., Fordyce J. and Gavrillets S.** (2008) What, if Anything, is Sympatric Speciation? *Journal of Evolutionary Biology*. **21:6**, pp.1452-1459
- Fontaine M.C., Baird S.J.E., Piry S., Ray N., Tolley K.A., Duke S., Birkun A., Ferreira M., Jauniaux T., Llavona A., Ozturk B., Ozturk A.A., Ridoux V., Rogan E., Sequeira M., Siebert U., Vikingsson G.A., Bouquegneau J.M. and Michaux J.R.** (2007) Rise of Oceanographic Barriers in Continuous Populations of a Cetacean: the Genetic Structure of Harbour Porpoises in Old World Waters. *BMC Biology*. **5:30**, pp.16
- Fontugne M.R. and Duplessy J.-C.** (1986) Variations of the Monsoon Regime During the Upper Quaternary: Evidence from Carbon Isotopic Record of Organic Matter in North Indian Ocean Sediment Cores. *Palaeogeography, Palaeoclimatology, Palaeoecology*. **56:1**, pp.69-88
- Frankham R., Briscoe D.A. and Ballou J.D.** (2002) Introduction to Conservation Genetics. Cambridge University Press
- Fraser D.J. and Bernatchez L.** (2001) Adaptive Evolutionary Conservation: Towards a Unified Concept for Defining Conservation Units. *Molecular Ecology*. **10:12**, pp.2741-2752
- Fratini S. and Vannini M.** (2002) Genetic Differentiation in the Mud Crab *Scylla serrata* (Decapoda: Portunidae) Within the Indian Ocean. *Journal of Experimental Marine Biology and Ecology*. **272:1**, pp.103-116
- Freije A.M.** (2015) Heavy Metal, Trace Element and Petroleum Hydrocarbon Pollution in the Arabian Gulf: Review. *Journal of the Association of Arab Universities for Basic and Applied Sciences*. **17**, pp.90-100
- Fu Y.X.** (1997) Statistical Tests of Neutrality of Mutations Against Population Growth, Hitchhiking and Background Selection. *Genetics*. **147:2**, pp.915-25
- Fullard K.J., Early G., Heide-J M. P., Bloch D., Rosing-Asvid A. and Amos W.** (2000) Population Structure of Long-Finned Pilot Whales in the North Atlantic: a Correlation with Sea Surface Temperature? *Molecular Ecology*. **9:7**, pp.949-958
- Funk D.J. and Omland K.E.** (2003) Species-Level Paraphyly and Polyphyly: Frequency, Causes, and Consequences, with Insights from Animal Mitochondrial DNA. *Annual Review of Ecology and Systematics*. **34:1**, pp.397-423
- Futuyma D.J. and Mayer G.C.** (1980) Non-Allopatric Speciation in Animals. *Systematic Biology*. **29:3**, pp.254-271

- Gaither M.R., Bowen B.W., Bordenave T.R., Rocha L.A., Newman S.J., Gomez J.A., Van Herwerden L. and Craig M.T.** (2011) Phylogeography of the Reef Fish *Cephalopholis argus* (Epinephelidae) Indicates Pleistocene Isolation Across the Indo-Pacific Barrier with Contemporary Overlap in the Coral Triangle. *BMC Evolutionary Biology*. **11**, pp.189
- Gaither M.R. and Rocha L.A.** (2013) Origins of Species Richness in the Indo-Malay-Philippine Biodiversity Hotspot: Evidence for the Centre of Overlap Hypothesis. *Journal of Biogeography*. **40:9**, pp.1638-1648
- Galatius A. and Kinze C.C.** (2003) Ankylosis Patterns in the Postcranial Skeleton and Hyoid Bones of the Harbour Porpoise (*Phocoena phocoena*) in the Baltic and North Sea. *Canadian Journal of Zoology*. **81:11**, pp.1851-1861
- Gallagher M.** (1991) Collection of Skulls of Cetacea: Odontoceti from Bahrain, United Arab Emirates and Oman, 1969-1990. UNEP Marine Mammal Technical Report. 3, pp.89-97
- Gao A., Zhou K. and Wang Y.** (1995) Geographical Variation in Morphology of Bottlenose Dolphins (*Tursiops* Sp.) in Chinese Waters. *Aquatic Mammals*. **21:2**, pp.121-135
- Garza J.C. and Williamson E.G.** (2001) Detection of Reduction in Population Size Using Data from Microsatellite Loci. *Molecular Ecology*. **10:2**, pp.305-318
- Gaspari S., Azzellino A., Airoidi S. and Hoelzel A.R.** (2007) Social Kin Associations and Genetic Structuring of Striped Dolphin Populations (*Stenella coeruleoalba*) in the Mediterranean Sea. *Molecular Ecology*. **16:14**, pp.2922-2933
- Gay L., Neubauer G., Zagalska-Neubauer M., Debain C., Pons J.M., David P. and Crochet P.A.** (2007) Molecular and Morphological Patterns of Introgression Between Two Large White-Headed Gull Species in a Zone of Recent Secondary Contact. *Molecular Ecology*. **16:15**, pp.3215-3227
- Gazda S.K., Connor R.C., Edgar R.K. and Cox F.** (2005) A Division of Labour with Role Specialization in Group-Hunting Bottlenose Dolphins (*Tursiops truncatus*) off Cedar Key, Florida. *Proceedings of the Royal Society of London B: Biological Sciences*. **272:1559**, pp.135-140
- Gildor H. and Tziperman E.** (2000) Sea Ice As the Glacial Cycles' Climate Switch: Role of Seasonal and Orbital Forcing. *Paleoceanography*. **15:6**, pp.605-615
- Glennie K.** (1996) Geology of Abu Dhabi. In: Osborne P.E. (Ed). *Desert Ecology of Abu Dhabi: A Review and Recent Studies*. Pisces, Newbury. pp.16--35
- Goldstein D.B., Linares A.R., Cavalli-Sforza L.L. and Feldman M.W.** (1995) An Evaluation of Genetic Distances for Use with Microsatellite Loci. *Genetics*. **139:1**, pp.463-471

- Gore M.A., Kiani M.S., Ahmad E., Hussain B., Ormond R.F., Siddiqui J., Waqas U. and Culloch R.** (2012) Occurrence of Whales and Dolphins in Pakistan with Reference to Fishers' Knowledge and Impacts. *Journal of Cetacean Research and Management*. **12**, pp.235-247
- Goudet J.** (2001) FSTAT, a Program to Estimate and Test Gene Diversities and Fixation Indices (Version 2.9. 3). Updated from Goudet (1995). Available from <http://www.unil.ch/izea/software/fstat.html>.
- Gridley T., Nastasi A., Kriesell H. and Elwen S.** (2015) The Acoustic Repertoire of Wild Common Bottlenose Dolphins (*Tursiops truncatus*) in Walvis Bay, Namibia. *Bioacoustics*. **24:2**, pp.153--174
- Gross A., Kiszka J., Van Canneyt O., Richard P. and Ridoux V.** (2009) A Preliminary Study of Habitat and Resource Partitioning Among Co-Occurring Tropical Dolphins Around Mayotte, Southwest Indian Ocean. *Estuarine, Coastal and Shelf Science*. **84:3**, pp.367-374
- Gu Z., Gu L., Eils R., Schlesner M. and Brors B.** (2014) *Circlize* Implements and Enhances Circular Visualization in R. *Bioinformatics*. **30:19**, pp.2811-2812
- Guo S.W. and Thompson E.A.** (1992) Performing the Exact Test of Hardy-Weinberg Proportion for Multiple Alleles. *Biometrics*. **48**, pp.361-372
- Guttman L.** (1954) Some Necessary Conditions for Common-Factor Analysis. *Psychometrika*. **19:2**, pp.149-161
- Hale P.T., Barreto A.S. and Ross G.J.B.** (2000) Comparative Morphology and Distribution of the *aduncus* and *truncatus* Forms of Bottlenose Dolphin *Tursiops* in the Indian and Western Pacific Oceans. *Aquatic Mammals*. **26:2**, pp.101-110
- Hammond P.S., Bearzi G., Bjørge A., Forney K., Karczmarski L., Kasuya T., Perrin W.F., Scott M.D., Wang J.Y., Wells R.S. and Wilson B.** (2008a) *Delphinus delphis*. The IUCN Red List of Threatened Species 2008: e.T6336A12649851. <http://dx.doi.org/10.2305/IUCN.UK.2008.RLTS.T6336A12649851.en>
- Hammond P.S., Bearzi G., Bjørge A., Forney K., Karczmarski L., Kasuya T., Perrin W.F., Scott M.D., Wang J.Y., Wells R.S. and Wilson B.** (2008b) *Delphinus capensis*. The IUCN Red List of Threatened Species 2008: e.T6337A12663800. <http://dx.doi.org/10.2305/IUCN.UK.2008.RLTS.T6337A12663800.en>
- Hammond P.S., Bearzi G., Bjørge A., Forney K., Karczmarski L., Kasuya T., Perrin W.F., Scott M.D., Wang J.Y., Wells R.S. and Wilson B.** (2012a) *Tursiops aduncus*. The IUCN Red List of Threatened Species 2012: e.T41714A17600466. <http://dx.doi.org/10.2305/IUCN.UK.2012.RLTS.T41714A17600466.en>
- Hammond P.S., Bearzi G., Bjørge A., Forney K., Karczmarski L., Kasuya T., Perrin W.F., Scott M.D., Wang J.Y., Wells R.S. and Wilson B.** (2012b) *Tursiops truncatus*. The IUCN Red List of Threatened Species 2012: e.T22563A17347397. <http://dx.doi.org/10.2305/IUCN.UK.2012.RLTS.T22563A17347397.en>

- Hamner R.M., Pichler F.B., Heimeier D., Constantine R. and Baker C.S.** (2012) Genetic Differentiation and Limited Gene Flow Among Fragmented Populations of New Zealand Endemic Hector's and Maui's Dolphins. *Conservation Genetics*. **13:4**, pp.987-1002
- Harlin A.D., Markowitz T., Baker C.S., Wursig B. and Honeycutt R.L.** (2003) Genetic Structure, Diversity, and Historical Demography of New Zealand's Dusky Dolphin (*Lagenorhynchus obscurus*). *Journal of Mammalogy*. **84:2**, pp.702-717
- Harlin-Cognato A.D. and Honeycutt R.L.** (2006) Multi-Locus Phylogeny of Dolphins in the Subfamily Lissodelphininae: Character Synergy Improves Phylogenetic Resolution. *BMC Evolutionary Biology*. **6**, pp.87
- Harpending H.C., Sherry S.T., Rogers A.R. and Stoneking M.** (1993) The Genetic Structure of Ancient Human Populations. *Current Anthropology*. **34:4**, pp.483-496
- Hartigan J.A. and Wong M.A.** (1979) Algorithm AS 136: A K-Means Clustering Algorithm. *Applied Statistics*. **28:1**, pp.100-108
- Hasegawa M., Kishino H. and Yano T.** (1985) Dating of the Human-Ape Splitting by a Molecular Clock of Mitochondrial DNA. *Journal of Molecular Evolution*. **22:2**, pp.160-174
- Hastie G.D., Wilson B., Wilson L.J., Parsons K.M. and Thompson P.M.** (2004) 'unctional Mechanisms Underlying Cetacean Distribution Patterns: Hotspots for Bottlenose Dolphins Are Linked to Foraging. *Marine Biology*. **144:2**, pp.397-403
- Hayano A., Yoshioka M., Tanaka M. and Amano M.** (2004) Population Differentiation in the Pacific White-Sided Dolphin *Lagenorhynchus obliquidens* Inferred from Mitochondrial DNA and Microsatellite Analyses. *Zoological Science*. **21:9**, pp.989-999
- Heckman K.L., Mariani C.L., Rasoloarison R. and Yoder A.D.** (2007) Multiple Nuclear Loci Reveal Patterns of Incomplete Lineage Sorting and Complex Species History Within Western Mouse Lemurs (*Microcebus*). *Molecular Phylogenetics and Evolution*. **43:2**, pp.353-67
- Hedrick P.W., Allendorf F.W. and Baker C.S.** (2013) Estimation of Male Gene Flow from Measures of Nuclear and Female Genetic Differentiation. *Journal of Heredity*. **104:5**, pp.713-7
- Hellberg M.E.** (1996) Dependence of Gene Flow on Geographic Distance in Two Solitary Corals with Different Larval Dispersal Capabilities. *Evolution*. **50:3**, pp.1167-1175
- Herald E.S., Brownell R.L., Frye F.L., Morris E.J., Evans W.E. and Scott A.B.** (1969) Blind River Dolphin: First Side-Swimming Cetacean. *Science*. **166:3911**, pp.1408-1410
- Hersh S.L. and Duffield D.A.** (1990) Distinction Between Northwest Atlantic Offshore and Coastal Bottlenose Dolphins Based on Hemoglobin Profile and Morphometry. *In: Leatherwood S. and Reeves R.R. (Eds). The Bottlenose Dolphin*. Academic Press Limited 24-48 Oval Road, London NW1 7DX. pp.129-139

- Hersh S.L., Odell D.K. and Asper E.D.** (1990) Sexual Dimorphism in Bottlenose Dolphins from the East Coast of Florida. *Marine Mammal Science*. **6:4**, pp.305-315
- Hershkovitz P.** (1966) Catalog of Living Whales. Smithsonian Institution Bulletin 246. pp.256
- Heyning J.E. and Perrin W.F.** (1994) Evidence for Two Species of Common Dolphins (Genus *Delphinus*) from the Eastern North Pacific. *Contributions in Science*. **442**, pp.1-35
- Hillis D.M.** (1987) Molecular Versus Morphological Approaches to Systematics. *Annual Review of Ecology and Systematics*. **18**, pp.23-42
- Ho S.Y.W., Phillips M.J., Cooper A. and Drummond A.J.** (2005) Time Dependency of Molecular Rate Estimates and Systematic Overestimation of Recent Divergence Times. *Molecular Biology and Evolution*. **22:7**, pp.1561-1568
- Ho S.Y.W., Kolokotronis S.O. and Allaby R.G.** (2007) Elevated Substitution Rates Estimated from Ancient DNA Sequences. *Biology Letters*. **3:6**, pp.702-705
- Hoelzel A.R. and Dover G.A.** (1991) Genetic Differentiation Between Sympatric Killer Whale Populations. *Heredity*. **66:2**, pp.191-195
- Hoelzel A.R., Hancock J.M. and Dover G.A.** (1991) Evolution of the Cetacean Mitochondrial D-Loop Region. *Molecular Biology and Evolution*. **8:4**, pp.475-493
- Hoelzel A.R.** (1994) Genetics and Ecology of Whales and Dolphins. *Annual Review of Ecology and Systematics*. **25**, pp.377-399
- Hoelzel A.R.** (1998a) Genetic Structure of Cetacean Populations in Sympatry, Parapatry, and Mixed Assemblages: Implications for Conservation Policy. *Journal of Heredity*. **89:5**, pp.451-458
- Hoelzel A.R.** (1998b) Molecular Genetic Analysis of Populations: A Practical Approach. Oxford University Press.
- Hoelzel A.R., Potter C.W. and Best P. B.** (1998). Genetic Differentiation Between Parapatric 'Nearshore' and 'Offshore' Populations of the Bottlenose Dolphin. *Proceedings of the Royal Society of London B: Biological Sciences*. **265:1402**, pp.1177-1183
- Hoelzel A.R., Natoli A., Dahlheim M.E., Olavarria C., Baird R.W. and Black N.A.** (2002) Low Worldwide Genetic Diversity in the Killer Whale (*Orcinus orca*): Implications for Demographic History. *Proceedings of the Royal Society of London. Series B, Biological Sciences*. **269:1499**, pp.1467-14673
- Hoelzel A.R.** (2010) Looking Backwards to Look Forwards: Conservation Genetics in a Changing World. *Conservation Genetics*. **11:2**, pp.655-660
- Hoffman J.I., Clarke A., Clark M.S. and Peck L.S.** (2013) Hierarchical Population Genetic Structure in a Direct Developing Antarctic Marine Invertebrate. *Plos One*. **8:5**, pp.8

- Hofreiter M. and Stewart J.** (2009) Ecological Change, Range Fluctuations and Population Dynamics During the Pleistocene. *Current Biology*. **19:14**, pp.584-594
- Hoskin C.J., Higgie M., McDonald K.R. and Moritz C.** (2005) Reinforcement Drives Rapid Allopatric Speciation. *Nature*. **437:7063**, pp.1353-6
- Hothorn T. and Everitt B.S.** (2014) A Handbook of Statistical Analyses Using R. CRC Press.
- Huang B., Peakall R. and Hanna P.** (2000) Analysis of Genetic Structure of Blacklip Abalone (*Haliotis rubra*) Populations Using RAPD, Minisatellite and Microsatellite Markers. *Marine Biology*. **136:2**, pp.207-216
- Hubert N., Meyer C.P., Bruggemann H.J., Guérin F., Komeno R.J.L., Espiau B., Causse R., Williams J.T. and Planes S.** (2012) Cryptic Diversity in Indo-Pacific Coral-Reef Fishes Revealed by DNA-Barcoding Provides New Support to the Centre-Of-Overlap Hypothesis. *Plos One*. **7:3**, pp.8
- Hubisz M.J., Falush D., Stephens M. and Pritchard J.K.** (2009) Inferring Weak Population Structure with the Assistance of Sample Group Information. *Molecular Ecology Resources*. **9:5**, pp.1322-1332
- Hudson R., Boos D.D. and Kaplan N.** (1992) A Statistical Test for Detecting Geographic Subdivision. *Molecular Biology and Evolution*. **9:1**, pp.138-151
- Huelsenbeck J.P. and Ronquist F.** (2001) MrBayes: Bayesian Inference of Phylogenetic Trees. *Bioinformatics*. **17:8**, pp.754-755
- Ingram T.** (2011) Speciation Along a Depth Gradient in a Marine Adaptive Radiation. *Proceedings of the Royal Society of London. Series B, Biological Sciences*. **278:1705**, pp.613-8
- Irvine A., Scott M., Wells R. and Kaufmann J.** (1981) Movements and Activities of the Atlantic Bottlenose Dolphin, *Tursiops truncatus*, Near Sarasota, Florida. *Fishery Bulletin*. **79:4**, pp.671-688
- IWC** (1999) Annex I Report of the Standing Sub-Committee on Small Cetaceans. *Journal of Cetacean Research and Management* (Suppl.). pp.211-225
- IWC** (2010) Annex H Report of the Sub-Committee on Other Southern Hemisphere Whale Stocks. *Journal of Cetacean Research and Management* (Suppl.). pp.1-24
- James P., Lipton A., Karbari J., Mohan M., Mohan R.L., Rajagopalan M., Gopakumar G., Rajapandian M., Pillai S.K., Sivadas M., Nammalwar P. and Radhakrishnan G.** (1987) Investigations on Whales, Dolphins and Dugongs (FB/PR/14). Central Marine Fisheries Research Institute, Cochin. Annual Report. pp.29-30
- Jayasankar P., Anoop B., Reynold P., Krishnakumar P.K., Kumaran P.L., Afsal V.V. and Anoop A.K.** (2008) Molecular Identification of Delphinids and Finless Porpoise (Cetacea) from the Arabian Sea and Bay of Bengal. *Zootaxa*. **1853**, pp.57-67

- Jefferson T.A. and Van Waerebeek K.** (2002) The Taxonomic Status of the Nominal Dolphin Species *Delphinus tropicalis* van Bree, 1971. *Marine Mammal Science*. **18:4**, pp.787-818
- Jefferson T.A. and Van Waerebeek K.** (2004) Geographic Variation in Skull Morphology of Humpback Dolphins (*Sousa* spp.). *Aquatic Mammals*. **30**, pp.3-17
- Jones G. and Van Parijs S.M.** (1993) Bimodal Echolocation in Pipistrelle Bats: Are Cryptic Species Present? *Proceedings of the Royal Society of London. Series B, Biological Sciences*. **251:1331**, pp.119-125
- Kaiser H.F.** (1960) The Application of Electronic Computers to Factor Analysis. *Educational and Psychological Measurement*. **20:1**, pp.141-151
- Kassler P.** (1973) The Structural and Geomorphic Evolution of the Persian Gulf. In: Purser, B.H. (Ed). *The Persian Gulf*. Springer Berlin Heidelberg. pp.11-32
- Kaufman L. and Rousseeuw** (1987) Clustering by Means of Medoids. *Statistical Data Analysis Based on the L1-Norm and Related Methods*.
- Kaufman L. and Rousseeuw P.J.** (2009) Finding Groups in Data: An Introduction to Cluster Analysis. John Wiley & Sons.
- Kearse M., Moir R., Wilson A., Stones-Havas S., Cheung M., Sturrock S., Buxton S., Cooper A., Markowitz S., Duran C., Thierer T., Ashton B., Meintjes P. and Drummond A.** (2012) Geneious Basic: An Integrated and Extendable Desktop Software Platform for the Organization and Analysis of Sequence Data. *Bioinformatics*. **28:12**, pp.1647-9
- Keeney D., Heupel M., Hueter R. and Heist E.** (2003) Genetic Heterogeneity Among Blacktip Shark, *Carcharhinus limbatus*, Continental Nurseries Along the US Atlantic and Gulf of Mexico. *Marine Biology*. **143:6**, pp.1039-1046
- Kemper C.M.** (2004) Osteological Variation and Taxonomic Affinities of Bottlenose Dolphins, *Tursiops* spp., from South Australia. *Australian Journal of Zoology*. **52:1**, pp.29-48
- Kendall D.G.** (1977) The Diffusion of Shape. *Advances in Applied Probability*. **9:3**, pp.428-430
- Kendall D.G.** (1984) Shape Manifolds, Procrustean Metrics, and Complex Projective Spaces. *Bulletin of the London Mathematical Society*. **16:2**, pp.81-121
- Kershaw F., Leslie M.S., Collins T., Mansur R.M., Smith B.D., Minton G., Baldwin R., Leduc R.G., Anderson R.C. and Brownell R.L.** (2013) Population Differentiation of 2 Forms of Bryde'S Whales in the Indian and Pacific Oceans. *Journal of Heredity*. **104:6**, pp.755-764
- Kim J.O. and Curry J.** (1977) The Treatment of Missing Data in Multivariate Analysis. *Sociological Methods and Research*. **6:2**, pp.215-240

- Kindle J.C. and Arnone R.A.** (2001) A Review of the Surface Circulation of the Northern Arabian Sea. Report of the Indian Ocean Synthesis Group on the Arabian Sea Process Study. pp.3-8
- Kingston S.E. and Rosel P.E.** (2004) Genetic Differentiation Among Recently Diverged Delphinid Taxa Determined Using AFLP Markers. *Journal of Heredity*. **95:1**, pp.1-10
- Kingston S.E., Adams L.D. and Rosel P.E.** (2009) Testing Mitochondrial Sequences and Anonymous Nuclear Markers for Phylogeny Reconstruction in a Rapidly Radiating Group: Molecular Systematics of the Delphininae (Cetacea: Odontoceti: Delphinidae). *BMC Evolutionary Biology*. **9:245**, pp.19
- Klingenberg C.P. and Monteiro L.R.** (2005) Distances and Directions in Multidimensional Shape Spaces: Implications for Morphometric Applications. *Systematic Biology*. **54:4**, pp.678-88
- Klingenberg C.P.** (2011) Morphoj: An Integrated Software Package for Geometric Morphometrics. *Molecular Ecology Resources*. **11:2**, pp.353-357
- Knutsen H., Jorde P.E., André C. and Stenseth N.** (2003) Fine-Scaled Geographical Population Structuring in a Highly Mobile Marine Species: the Atlantic Cod. *Molecular Ecology*. **12:2**, pp.385-394
- Kolla V., Ray P.K. and KostECKI J.A.** (1981) Surficial Sediments of the Arabian Sea. *Marine Geology*. **41:3**, pp.183-204
- Konovalov D.A., Manning C. and Henshaw M.T.** (2004) Kingroup: a Program for Pedigree Relationship Reconstruction and Kin Group Assignments Using Genetic Markers. *Molecular Ecology Notes*. **4:4**, pp.779-782
- Kopelman N.M., Mayzel J., Jakobsson M., Rosenberg N.A. and Mayrose I.** (2015) CLUMPAK: A Program for Identifying Clustering Modes and Packaging Population Structure Inferences Across K. *Molecular Ecology Resources*. **15:5**, pp.1179-1191.
- Kortebout Van Der Sluijs G.** (1983) De Resten Van Zoogdieren Uit De Noordzee. *Grondboor En Hamer*. **37**, pp.4-7
- Krell F.-T. and Cranston P.S.** (2004) Which Side of the Tree Is More Basal? *Systematic Entomology*. **29:3**, pp.279-281
- Krishnan A.A., Yousuf K.S.S., Kumaran P.L.L., Harish N., Anoop B., Afsal V.V.V., Rajagopalan M., Vivekanandan E., Krishnakumar P.K.K. and Jayasankar P.** (2008) Stomach Contents of Cetaceans Incidentally Caught Along Mangalore and Chennai Coasts of India. *Estuarine, Coastal and Shelf Science*. **76:4**, pp.909-913
- Krützen M., Sherwin W.B., Connor R.C., Barré L.M., Van de Castele T., Mann J. and Brooks R.** (2003) Contrasting Relatedness Patterns in Bottlenose Dolphins (*Tursiops* sp.) with Different Alliance Strategies. *Proceedings of the Royal Society of London B: Biological Sciences*. **270:1514**, pp.497-502

- Krützen M., Sherwin W.B., Berggren P. and Gales N.** (2004) Population Structure in An Inshore Cetacean Revealed by Microsatellite and mtDNA Analysis: Bottlenecked Dolphins (*Tursiops* sp.) in Shark Bay, Western Australia. *Marine Mammal Science*. **20:1**, pp.28-47
- Lal Mohan R.** (1982) A Note on the Fetuses of the Dolphins *Tursiops aduncus* and *Sousa plumbea* from the South West Coast of India. *Indian Journal of Fisheries*. **29:1&2**, pp.249-252
- Lanfear R., Calcott B., Ho S.Y.W. and Guindon S.** (2012) Partitionfinder: Combined Selection of Partitioning Schemes and Substitution Models for Phylogenetic Analyses. *Molecular Biology and Evolution*. **29:6**, pp.1695-701
- Lanfear R., Calcott B., Kainer D., Mayer C. and Stamatakis A.** (2014) Selecting Optimal Partitioning Schemes for Phylogenomic Datasets. *BMC Evolutionary Biology*. **14:1**, pp.82
- Latch E.K., Dharmarajan G., Glaubitz J.C. and Rhodes Jr O.E.** (2006) Relative Performance of Bayesian Clustering Software for Inferring Population Substructure and Individual Assignment At Low Levels of Population Differentiation. *Conservation Genetics*. **7:2**, pp.295-302
- Leatherwood S.** (1986) Whales, Dolphins, and Porpoises of the Indian Ocean Cetacean Sanctuary: A Catalogue of Available Information. United Nations Environment Programme. pp.206
- Leberg P.L.** (2002) Estimating Allelic Richness: Effects of Sample Size and Bottlenecks. *Molecular Ecology*. **11:11**, pp.2445-2449
- LeDuc R.G., Perrin W.F. and Dizon A.E.** (1999) Phylogenetic Relationships Among the Delphinid Cetaceans Based on Full Cytochrome B Sequences. *Marine Mammal Science*. **15:3**, pp.619-648
- Lee J.C.** (1990) Sources of Extraneous Variation in the Study of Meristic Characters: The Effect of Size and of Inter-Observer Variability. *Systematic Biology*. **39:1**, pp.31-39
- Leigh J.W., Susko E., Baumgartner M. and Roger A.J.** (2008) Testing Congruence in Phylogenomic Analysis. *Systematic Biology*. **57:1**, pp.104-115
- Leigh J.W. and Bryant D.** (2015) POPART: Full-Feature Software for Haplotype Network Construction. *Methods in Ecology and Evolution*. **6:9**, pp.1110-1116
- Lewontin R.C. and Hubby J.L.** (1966) A Molecular Approach to the Study of Genic Heterozygosity in Natural Populations. II. Amount of Variation and Degree of Heterozygosity in Natural Populations of *Drosophila pseudoobscura*. *Genetics*. **54:2**, pp.595-609
- Li Y.C., Korol A.B., Fahima T., Beiles A. and Nevo E.** (2002) Microsatellites: Genomic Distribution, Putative Functions and Mutational Mechanisms: A Review. *Molecular Ecology*. **11:12**, pp.2453-2465

- Librado P. and Rozas J.** (2009) DNASP v5: A Software for Comprehensive Analysis of DNA Polymorphism Data. *Bioinformatics*. **25:11**, pp.1451-1452
- Longhurst A.** (2006) Ecological Geography of the Sea. Academic Press, Amsterdam, Boston, MA.
- Louis M., Fontaine M.C., Spitz J., Schlund E., Dabin W., Deaville R., Caurant F., Cherel Y., Guinet C. and Simon-Bouhet B.** (2014) Ecological Opportunities and Specializations Shaped Genetic Divergence in a Highly Mobile Marine Top Predator. *Proceedings of the Royal Society of London. Series B, Biological Sciences*. **281:1795**, pp.9
- Loy A., Tamburelli A., Carlini R. and Slice D.E.** (2011) Craniometric Variation of Some Mediterranean and Atlantic Populations of *Stenella coeruleoalba* (Mammalia, Delphinidae): A Three-Dimensional Geometric Morphometric Analysis. *Marine Mammal Science*. **27:2**, pp.65-78
- Lu C.P., Chen C.A., Hui C.F., Tzeng T.D. and Yeh S.Y.** (2006) Population Genetic Structure of the Swordfish, *Xiphias gladius* (Linnaeus, 1758), in the Indian Ocean and West Pacific Inferred from the Complete DNA Sequence of the Mitochondrial Control Region. *Zoological Studies*. **45:2**, pp.269-279
- Lutjeharms J., Catzel R. and Valentine H.** (1989) Eddies and Other Boundary Phenomena of the Agulhas Current. *Continental Shelf Research*. **9:7**, pp.597-616
- Lyrholm T., Leimar O., Johanneson B. and Gyllensten U.** (1999) Sex-Biased Dispersal in Sperm Whales: Contrasting Mitochondrial and Nuclear Genetic Structure of Global Populations. *Proceedings of the Royal Society of London B: Biological Sciences*. **266:1417**, pp.347--354
- Mace G.M.** (2004) The Role of Taxonomy in Species Conservation. *Philosophical Transactions of the Royal Society of London. Series B, Biological Sciences*. **359:1444**, pp.711-719
- Maddison W. and Maddison D.** (2015) Mesquite: a Modular System for Evolutionary Analysis. Version 2.75. 2011. Available from <http://mesquiteproject.org>.
- Maechler M., Rousseeuw P., Struyf A., Hubert M., Hornik K., Studer M. and Roudier P.** (2015) Cluster: Cluster Analysis Basics and Extensions. R Package Version 2.0.3.
- Mallet J., Meyer A., Nosil P. and Feder J.L.** (2009) Space, Sympatry and Speciation. *Journal of Evolutionary Biology*. **22:11**, pp.2332-2341
- Mardis E.R.** (2008) The Impact of Next-Generation Sequencing Technology on Genetics. *Trends in Genetics*. **24:3**, pp.133-41
- Martien K.K., Baird R.W., Hedrick N.M., Gorgone A.M., Thieleking J.L., McSweeney D.J., Robertson K.M. and Webster D.L.** (2012) Population Structure of Island-Associated Dolphins: Evidence from Mitochondrial and Microsatellite Markers for Common Bottlenose Dolphins (*Tursiops truncatus*) Around the Main Hawaiian Islands. *Marine Mammal Science*. **28:3**, pp.208-232.

- Martins E.P. and Hansen T.F.** (1997) Phylogenies and the Comparative Method: A General Approach to Incorporating Phylogenetic Information Into the Analysis of Inter-specific Data. **149:4**, *American Naturalist*. pp.646-667
- May-Collado L. and Agnarsson I.** (2006) Cytochrome B and Bayesian Inference of Whale Phylogeny. *Molecular Phylogenetics and Evolution*. **38:2**, pp.344-54
- Maynard Smith J.** (1966) Sympatric Speciation. *American Naturalist*. **100:916**, pp.637-650
- Mayr E.** (1942) Systematics and the Origin of Species, from the Viewpoint of a Zoologist. Harvard University Press.
- Mayr E.** (1947) Ecological Factors in Speciation. *Evolution*. **1:4**, pp.263-288
- Mayr E.** (1963) Animal Species and Evolution. Belknap Press of Harvard University Press Cambridge, Massachusetts.
- Mayr E.** (1970) Populations, Species, and Evolution: An Abridgment of Animal Species and Evolution. Harvard University Press.
- McGowen M.R., Spaulding M. and Gatesy J.** (2009) Divergence Date Estimation and a Comprehensive Molecular Tree of Extant Cetaceans. *Molecular Phylogenetics and Evolution*. **53:3**, pp.891-906
- McGowen M.R.** (2011) Toward the Resolution of an Explosive Radiation: A Multilocus Phylogeny of Oceanic Dolphins (Delphinidae). *Molecular Phylogenetics and Evolution*. **60:3**, pp.345-57
- McGowen M.R., Grossman L.I. and Wildman D.E.** (2012) Dolphin Genome Provides Evidence for Adaptive Evolution of Nervous System Genes and a Molecular Rate Slowdown. *Proceedings of the Royal Society of London. Series B, Biological Sciences*. **279:1743**, pp.3643-3651
- Mead J.G. and Potter C.W.** (1990) Natural History of Bottlenose Dolphins Along the Central Atlantic Coast of the United States. In: Leatherwood S. and Reeves R.R. (Eds). *The Bottlenose Dolphin*. Academic Press Limited 24-48 Oval Road, London NW1 7DX. pp.165-195
- Mead J.G. and Potter C.W.** (1995) Recognising Two Populations of the Bottlenose Dolphin *Tursiops truncatus* off the Atlantic Coast of North America: Morphological and Ecological Considerations. Ibi Reports No. 5, National Museum of Natural History. USA: Smithsonian Institution.
- Mead J.G. and Fordyce R.E.** (2009) The Therian Skull: A Lexicon with Emphasis on the Odontocetes. Smithsonian Contributions to Zoology. pp.1-248
- Mendez M., Rosenbaum H.C., Subramaniam A., Yackulic C. and Bordino P.** (2010) Isolation by Environmental Distance in Mobile Marine Species: Molecular Ecology of Franciscana Dolphins At Their Southern Range. *Molecular Ecology*. **19:11**, pp.2212-2228

- Mendez M., Subramaniam A., Collins T., Minton G., Baldwin R., Berggren P., Särnblad A., Amir O.A., Peddemors V.M., Karczmarski L., Guissamulo A. and Rosenbaum H.C.** (2011) Molecular Ecology Meets Remote Sensing: Environmental Drivers to Population Structure of Humpback Dolphins in the Western Indian Ocean. *Heredity*. **107:4**, pp.349-61
- Mendez M., Jefferson T.A., Kolokotronis S.O., Krützen M., Parra G.J., Collins T., Minton G., Baldwin R., Berggren P., Särnblad A., Amir O.A., Peddemors V.M., Karczmarski L., Guissamulo A., Smith B., Sutaria D., Amato G. and Rosenbaum H.C.** (2013) Integrating Multiple Lines of Evidence to Better Understand the Evolutionary Divergence of Humpback Dolphins Along Their Entire Distribution Range: A New Dolphin Species in Australian Waters? *Molecular Ecology*. **22:23**, pp.5936-5948
- Meyer M. and Kircher M.** (2010) Illumina Sequencing Library Preparation for Highly Multiplexed Target Capture and Sequencing. *Cold Spring Harbor Protocols*. **2010:6**, pdb.prot5448
- Meynier L., Pusineri C., Spitz J., Santos M., Pierce G. and Ridoux V.** (2008a) Intraspecific Dietary Variation in the Short-Beaked Common Dolphin *Delphinus delphis* in the Bay of Biscay: Importance of Fat Fish. *Marine Ecology Progress Series*. **354**, pp.277-287
- Meynier L., Stockin K.A.A., Bando M.K.H. and Duignan P.J.** (2008b) Stomach Contents of Common Dolphin (*Delphinus* sp.) from New Zealand Waters. *New Zealand Journal of Marine and Freshwater Research*. **42:2**, pp.257-268
- Mikhalev Y.A.** (1997) Humpback Whales *Megaptera novaeangliae* in the Arabian Sea. *Marine Ecology Progress Series*. **149**, pp.13-21
- Milinkovitch M.C., Bérubé M. and Palsbøll Per J.** (1998) Cetaceans Are Highly Derived Artiodactyls. In: Thewissen J.G.M. (Ed). *The Emergence of Whales: Evolutionary Patterns in the Origin of Cetacea*. Plenum Press, New York. pp. 133-131
- Miller M., Pfeiffer W. and Schwartz T.** (2010) Creating the CIPRES Science Gateway for Inference of Large Phylogenetic Trees. Proceedings of the Gateway Computing Environments Workshop (GCE), 14 Nov. 2010, New Orleans, LA. pp.1-8
- Millicent E. and Thoday J.** (1960) Gene Flow and Divergence Under Disruptive Selection. *Science*. **131:3409**, pp.1311-1312
- Minton G., Collins T., Pomilla C., Findlay K., Rosenbaum H., Baldwin R. and Brownell Jr R.** (2008) *Megaptera novaeangliae* (Arabian Sea Subpopulation): IUCN Red List of Threatened Species.<http://www.iucnredlist.org/details/132835>
- Minton G., Collins T., Findlay K. and Baldwin R.** (2010) Cetacean Distribution in the Coastal Waters of the Sultanate of Oman. *Journal of Cetacean Research and Management*. **11(3)**, pp.301-313

- Minton G., Collins T., Findlay K., Ersts P., Rosenbaum H. and Baldwin R.** (2011) Seasonal Distribution, Abundance, Habitat Use and Population Identity of Humpback Whales in Oman. *Journal of Cetacean Research and Management (Special Issue)*. **3**, pp.185-198
- Mirimin L., Westgate A., Rogan E., Rosel P.R., Read A.R., Coughlan J. and Cross T.** (2009) Population Structure of Short-Beaked Common Dolphins (*Delphinus delphis*) in the North Atlantic Ocean as Revealed by Mitochondrial and Nuclear Genetic Markers. *Marine Biology*. **156**, pp.821-834
- Mitteroecker P. and Gunz P.** (2009) Advances in Geometric Morphometrics. *Evolutionary Biology*. **36:2**, pp.235-247
- Mladenov P.V., Allibone R.M. and Wallis G.P.** (1997) Genetic Differentiation in the New Zealand Sea Urchin *Evechinus chloroticus* (Echinodermata: Echinoidea). *New Zealand Journal of Marine and Freshwater Research*. **31:2**, pp.261-269
- Möller L.M., Beheregaray L.B., Harcourt R.G. and Krützen M.** (2001). Alliance Membership and Kinship in Wild Male Bottlenose Dolphins (*Tursiops aduncus*) of Southeastern Australia. *Proceedings of the Royal Society of London B: Biological Sciences*. **268:1479**, pp.1941-1947.
- Möller L.M. and Beheregaray L.B.** (2001) Coastal Bottlenose Dolphins from Southeastern Australia are *Tursiops aduncus* According to Sequences of the Mitochondrial DNA Control Region. *Marine Mammal Science*. **17:2**, pp.249-263
- Möller L.M. and Beheregaray L.B.** (2004) Genetic Evidence for Sex-Biased Dispersal in Resident Bottlenose Dolphins (*Tursiops aduncus*). *Molecular Ecology*. **13:6**, pp.1607-1612
- Möller L.M., Beheregaray L.B., Allen S.J. and Harcourt R. G.** (2006). Association Patterns and Kinship in Female Indo-Pacific Bottlenose Dolphins (*Tursiops aduncus*) of Southeastern Australia. *Behavioral Ecology and Sociobiology*. **61:1**, pp.109-117
- Möller L.M., Bilgmann K., Charlton-Robb K. and Beheregaray L.** (2008) Multi-Gene Evidence for a New Bottlenose Dolphin Species in Southern Australia. *Molecular Phylogenetics and Evolution*. **49:2**, pp.674-681
- Möller L., Valdez F.P., Allen S., Bilgmann K., Corrigan S. and Beheregaray L.B.** (2011) Fine-Scale Genetic Structure in Short-Beaked Common Dolphins (*Delphinus delphis*) Along the East Australian Current. *Marine Biology*. **158:1**, pp.113-126
- Möller L.M.** (2012). Sociogenetic Structure, Kin Associations and Bonding in Delphinids. *Molecular Ecology*. **21:3**, pp.745-764.
- Monteiro-Filho E.L.D.A., Monteiro L.R. and Reis S.F.D.** (2002) Skull Shape and Size Divergence in Dolphins of the Genus *Sotalia*: a Tridimensional Morphometric Analysis. *Journal of Mammalogy*. **83:1**, pp.125-134
- Moore W.S.** (1995) Inferring Phylogenies from mtDNA Variation: Mitochondrial-Gene Trees Versus Nuclear-Gene Trees. *Evolution*. **49:4**, pp.718-726

- Moore S.E.** (2008) Marine Mammals As Ecosystem Sentinels. *Journal of Mammalogy*. **89:3**, pp.534-540
- Morin P.A. and Dizon, A.E.** (2009) Genetics for Management. *In: Perrin W.F., Würsig B. and Thewissen, J.G.M. (Eds). Encyclopedia of Marine Mammals*. pp.477-483
- Morin P.A., Archer F.I., Foote A.D., Vilstrup J., Allen E.E., Wade P., Durban J., Parsons K., Pitman R., Li L., Bouffard P., Abel Nielsen S.C., Rasmussen M., Willerslev E., Gilbert M.T.P. and Harkins T.** (2010) Complete Mitochondrial Genome Phylogeographic Analysis of Killer Whales (*Orcinus orca*) Indicates Multiple Species. *Genome Research*. **20:7**, pp.908-916
- Moritz, C.** (1994). Defining 'Evolutionarily Significant Units' for Conservation. *Trends in Ecology & Evolution*. **9:10**, pp.373-374.
- Moritz C. and Faith D.P.** (1998) Comparative Phylogeography and the Identification of Genetically Divergent Areas for Conservation. *Molecular Ecology*. **7:4**, pp.419-429
- Moura A.E.V.** (2011) Investigating the Relative Influence of Genetic Drift and Natural Selection in Shaping Patterns of Population Structure in Delphinids (*Delphinus delphis*; *Tursiops* spp.). PhD thesis, Durham theses, Durham University. Available at Durham E-Theses Online: <http://etheses.dur.ac.uk/755/>
- Moura A.E., Sillero N. and Rodrigues A.** (2012) Common Dolphin (*Delphinus delphis*) Habitat Preferences Using Data from Two Platforms of Opportunity. *Acta Oecologica*. **38**, pp.24-32
- Moura A.E., Nielsen S.C.A., Vilstrup J.T., Moreno-Mayar J.V., Gilbert M.T.P., Gray H.W.I., Natoli A., Möller L. and Hoelzel A.R.** (2013a) Recent Diversification of a Marine Genus (*Tursiops* spp.) Tracks Habitat Preference and Environmental Change. *Systematic Biology*. **62:6**, pp.865-77
- Moura A.E., Natoli A., Rogan E. and Hoelzel A.R.** (2013b) Atypical Panmixia in a European Dolphin Species (*Delphinus delphis*): Implications for the Evolution of Diversity Across Oceanic Boundaries. *Journal of Evolutionary Biology*. **26:1**, pp.63-75
- Moura A.E., Van Rensburg C.J., Pilot M., Tehrani A., Best P.B., Thornton M., Plön S., De Bruyn P.J.N., Worley K.C. and Gibbs R.A.** (2014) Killer Whale Nuclear Genome and mtDNA Reveal Widespread Population Bottleneck During the Last Glacial Maximum. *Molecular Biology and Evolution*.
- Moura A.E., Kenny J.G., Chaudhuri R.R., Hughes M.A., Reisinger R.R., De Bruyn P.J.N., Dahlheim M.E., Hall N. and Hoelzel A.R.** (2015) Phylogenomics of the Killer Whale Indicates Ecotype Divergence in Sympatry. *Heredity*. **114:1**, pp.48-55
- Mullen L.M. and Hoekstra H.E.** (2008) Natural Selection Along an Environmental Gradient: A Classic Cline in Mouse Pigmentation. *Evolution*. **62:7**, pp.1555-1570

- Murakami M., Shimada C., Hikida Y., Soeda Y. and Hirano H.** (2014) *Eodelphis kabatensis*, a New Name for the Oldest True Dolphin *Stenella kabatensis* Horikawa, 1977 (Cetacea, Odontoceti, Delphinidae), from the Upper Miocene of Japan, and the Phylogeny and Paleobiogeography of Delphinoidea. *Journal of Vertebrate Paleontology*. **34:3**, pp.491-511
- Murphy S., Herman J.S., Pierce G.J., Rogan E. and Kitchener A.C.** (2006) Taxonomic Status and Geographical Cranial Variation of Common Dolphins (*Delphinus*) in the Eastern North Atlantic. *Marine Mammal Science*. **22:3**, pp.573-599
- Murphy S., Winship A., Dabin W., Jepson P.D., Deaville R., Reid R.J., Spurrier C., Rogan E., López A., González A.F., Read F.L., Addink M., Silva M., Ridoux V., Learmonth J.A., Pierce G.J., Northridge S.P.** (2009) Importance of Biological Parameters in Assessing the Status of *Delphinus delphis*. *Marine Ecology Progress Series*. **388**, pp.273-291
- Murtagh F.** (1985) A Survey of Algorithms for Contiguity-Constrained Clustering and Related Problems. *The Computer Journal*. **28:1**, pp.82--88
- Murtagh F. and Legendre P.** (2014) Wards Hierarchical Agglomerative Clustering Method: Which Algorithms Implement Wards Criterion? *Journal of Classification*. **31:3**, pp.274-295
- Muss A., Robertson D.R., Stepien C.A., Wirtz P. and Bowen B.W.** (2001) Phylogeography of *Ophioblennius*: the Role of Ocean Currents and Geography in Reef Fish Evolution. *Evolution*. **55:3**, pp.561-572
- Naidu P.D. and Malmgren B.A.** (1999) Quaternary Carbonate Record from the Equatorial Indian Ocean and Its Relationship with Productivity Changes. *Marine Geology*. **161:1**, pp.49-62
- Nakagawa S. and Freckleton R.P.** (2008) Missing Inaction: the Dangers of Ignoring Missing Data. *Trends in Ecology and Evolution*. **23:11**, pp.592-6
- Natoli A., Peddemors V.M. and Rus Hoelzel A.** (2004) Population Structure and Speciation in the Genus *Tursiops* Based on Microsatellite and Mitochondrial DNA Analyses. *Journal of Evolutionary Biology*. **17:2**, pp.363-375
- Natoli A., Birkun A., Aguilar A., Lopez A. and Hoelzel A.R.** (2005) Habitat Structure and the Dispersal of Male and Female Bottlenose Dolphins (*Tursiops truncatus*). *Proceedings of the Royal Society of London. Series B, Biological Sciences*. **272:1569**, pp.1217-26
- Natoli A., Cañadas A., Peddemors V.M., Aguilar A., Vaquero C., Fernández-Piqueras P. and Hoelzel A.R.** (2006) Phylogeography and Alpha Taxonomy of the Common Dolphin (*Delphinus* sp.). *Journal of Evolutionary Biology*. **19:3**, pp.943-54
- Natoli A., Peddemors V.M. and Hoelzel A.R.** (2008a) Population Structure of Bottlenose Dolphins (*Tursiops aduncus*) Impacted by Bycatch Along the East Coast of South Africa. *Conservation Genetics*. **9:3**, pp.627-636

- Natoli A., Cañadas A., Concepción V., Politi E., Fernandez-Navarro P. and Hoelzel A.R.** (2008b) Conservation Genetics of the Short-Beaked Common Dolphin (*Delphinus delphis*) in the Mediterranean Sea and in the Eastern North Atlantic Ocean. *Conservation Genetics*. **9**, pp.1479-1487
- Nei M.** (1987) Molecular Evolutionary Genetics. Columbia University Press
- Neumann D.R.** (2001) Activity Budget of Free-Ranging Common Dolphins (*Delphinus delphis*) in the Northwestern Bay of Plenty, New Zealand. *Aquatic Mammals*. **27:2**, pp.121-136
- Nicolosi P. and Loy A.** (2010) Landmark Based Morphometric Variation in Common Dolphin (*Delphinus delphis* L., 1758). In: Nimis P.L. and Vignes Lebbe R. (Eds). *Tools for Identifying Biodiversity: Progress and Problems*. EUT Edizioni Università di Trieste. pp.263-268
- Nielsen R. and Wakeley J.** (2001) Distinguishing Migration from Isolation: A Markov Chain Monte Carlo Approach. *Genetics*. **158:2**, pp.885-896
- Nielsen E.E., Nielsen P.H., Meldrup D. and Hansen M.M.** (2004) Genetic Population Structure of Turbot (*Scophthalmus maximus* L.) Supports the Presence of Multiple Hybrid Zones for Marine Fishes in the Transition Zone Between the Baltic Sea and the North Sea. *Molecular Ecology*. **13:3**, pp.585-595
- Niemiller M.L., Fitzpatrick B.M. and Miller B.T.** (2008) Recent Divergence with Gene Flow in Tennessee Cave Salamanders (Plethodontidae: *Gyrinophilus*) Inferred from Gene Genealogies. *Molecular Ecology*. **17:9**, pp.2258-75
- Nowacek D.P.** (2002) Sequential Foraging Behaviour of Bottlenose Dolphins, *Tursiops truncatus* Sarasota Bay, Fl. *Behaviour*. **139:9**, pp.1125-1145
- Nowacek D.P.** (2005) Acoustic Ecology of Foraging Bottlenose Dolphins (*Tursiops truncatus*), Habitat-Specific Use of Three Sound Types. *Marine Mammal Science*. **21:4**, pp.587--602
- O'higgins P. and Jones N.** (1998) Facial Growth in *Cercocebus torquatus*: An Application of Three-Dimensional Geometric Morphometric Techniques to the Study of Morphological Variation. *Journal of Anatomy*. **193:2**, pp.251-272
- O'loughlin P.M., Paulay G., Davey N. and Michonneau F.** (2011) The Antarctic Region as a Marine Biodiversity Hotspot for Echinoderms: Diversity and Diversification of Sea Cucumbers. *Deep Sea Research Part II: Topical Studies in Oceanography*. **58:1**, pp.264-275
- Oremus M., Poole M., Steel D. and Baker C.** (2007) Isolation and Interchange Among Insular Spinner Dolphin Communities in the South Pacific Revealed by Individual Identification and Genetic Diversity. *Marine Ecology Progress Series*. **336**, pp.275-289
- Ott P.H. and Danilewicz D.** (1996) Southward Range Extension of *Steno bredanensis* in the Southwest Atlantic and New Records of *Stenella coeruleoalba* for Brazilian Waters. *Aquatic Mammals*. **22**, pp.185-189

- Owen K., Charlton-Robb K. and Thompson R.** (2011) Resolving the Trophic Relations of Cryptic Species: An Example Using Stable Isotope Analysis of Dolphin Teeth. *PLoS One*. **6:2**, e16457
- Pääbo S.** (1989) Ancient DNA: Extraction, Characterization, Molecular Cloning, and Enzymatic Amplification. *Proceedings of the National Academy of Sciences*. **86:6**, pp.1939-1943
- Pagel M.** (1997) Inferring Evolutionary Processes from Phylogenies. *Zoologica Scripta*. **26:4**, pp.331-348
- Pagel M.** (1999) Inferring the Historical Patterns of Biological Evolution. *Nature*. **401:6756**, pp.877-884
- Pagel M., Meade A. and Barker D.** (2004) Bayesian Estimation of Ancestral Character States on Phylogenies. *Systematic Biology*. **53:5**, pp.673-684
- Palsbøll P.J., Bérubé M. and Allendorf F.W.** (2007) Identification of Management Units using Population Genetic Data. *Trends in Ecology & Evolution*. **22:1**, pp.11-16
- Palumbi S.R.** (1992) Marine Speciation on a Small Planet. *Trends in Ecology & Evolution*. **7:4**, pp.114-118
- Palumbi S.R.** (1994) Genetic Divergence, Reproductive Isolation, and Marine Speciation. *Annual Review of Ecology and Systematics*. **25**, pp.547-572
- Palumbi S.R.** (2003) Population Genetics, Demographic Connectivity, and the Design of Marine Reserves. *Ecological Applications*. **13**, pp.146-158
- Papastavrou V. and Van Waerebeek K.** (1997) A Note on the Occurrence of Humpback Whales (*Megaptera novaeangliae*) in Tropical and Subtropical Areas: the Upwelling Link. *Annual Report to the International Whaling Commission*. **47**, pp.945-947
- Paradis E., Claude J. and Strimmer K.** (2004) APE: Analyses of Phylogenetics and Evolution in R Language. *Bioinformatics*. **20:2**, pp.289-290
- Pardo M.A., Jiménez-Pinedo C. and Palacios D.M.** (2009) The False Killer Whale (*Pseudorca crassidens*) in the Southwestern Caribbean: First Stranding Record in Colombian Waters. *Latin American Journal of Aquatic Mammals*. **7:1-2**, pp.63-67
- Park K.J., Sohn H., An Y.R., Moon D.Y., Choi S.G. and An D. H.** (2013) An Unusual Case of Care-Giving Behavior in Wild Long-Beaked Common Dolphins (*Delphinus capensis*) in the East Sea. *Marine Mammal Science*. **29:4**, pp.508-514.
- Parsons K.M., Durban J.W., Claridge D.E., Herzog D.L., Balcomb K.C., and Noble, L.R.** (2006) Population Genetic Structure of Coastal Bottlenose Dolphins (*Tursiops truncatus*) in the Northern Bahamas. *Marine Mammal Science*. **22:2**, pp.276-298.
- Parés-Casanova P.M. and Fabre L.** (2013) Size and Shape Variability in the Skull of the Bottlenose Dolphin, *Tursiops truncatus* (Montagu, 1821). *Anatomia Histologia Embryologia*. **42:5**, pp.379-83

- Patenaude N. and White B.** (1995) Skin Biopsy Sampling of Beluga Whale Carcasses: Assessment of Biopsy Darting Factors for Minimal Wounding and Effective Sample Retrieval. *Marine Mammal Science*. **11:2**, pp.163-171
- Patton J.L. and Brylcki P.V.** (1987) Pocket Gophers in Alfalfa Fields: Causes and Consequences of Habitat-Related Body Size Variation. *American Naturalist*. **130:4**, pp.493-506
- Paul J.R.** (1968) Risso's Dolphin, *Grampus griseus*, in the Gulf of Mexico. *Journal of Mammalogy*. **49:4**, pp.746-748
- Peddemors V.** (1999) Delphinids of Southern Africa: A Review of Their Distribution, Status and Life History. *Journal of Cetacean Research and Management*. **1:2**, pp.157-165
- Peddemors V., Best P., Cockcroft V. and Oosthuisen H.** (2002) Report on the Recent Categorization of South African Cetaceans According to the 2001 IUCN Red List Criteria (Ver. 3.1). IWC Scientific Committee Document. SC/54/O22.
- Peltier H., Dabin W., Daniel P., Van Canneyt O., Dorémus G., Huon M. and Ridoux V.** (2012) The Significance of Stranding Data As Indicators of Cetacean Populations at Sea: Modelling the Drift of Cetacean Carcasses. *Ecological Indicators*. **18**, pp.278-290
- Perrin W.F.** (1975) Variation of Spotted and Spinner Porpoise (Genus *Stenella*) in the Eastern Pacific and Hawaii. Bulletin of the Scripps Institution of Oceanography. University of California, San Diego, La Jolla, California Vol. 21
- Perrin W., Mitchell E., Mead J., Caldwell D., Caldwell M., Bree P.V. and Dawbin W.** (1987) Revision of the Spotted Dolphins, *Stenella* spp. *Marine Mammal Science*. **3:2**, pp.99-170
- Perrin W.** (1990) Subspecies of *Stenella longirostris* (Mammalia: Cetacea: Delphinidae). *Proceedings of the Biological Society of Washington*. **103:2**, pp.453-463
- Perrin W.F. and Heyning J.E.** (1993) Rostral Fusion as a Criterion of Cranial Maturity in the Common Dolphin, *Delphinus delphis*. *Marine Mammal Science*. **9:2**, pp.195-197
- Perrin W.F., Robertson K.M., van Bree P.J.H. and Mead J.G.** (2007) Cranial Description and Genetic Identity of the Holotype Specimen of *Tursiops aduncus* (Ehrenberg, 1832). *Marine Mammal Science*. **23(2)**, pp.343-357
- Perrin** (2009) Common Dolphins, *Delphinus delphis* and *D. capensis*. In: Leatherwood S. and Reeves R.R. (Eds). *The Bottlenose Dolphin*. Academic Press Limited 24-48 Oval Road, London NW1 7DX. pp.255-259
- Perrin W.F., Thieleking J.L., Walker W.A., Archer F.I. and Robertson K.M.** (2011) Common Bottlenose Dolphins (*Tursiops truncatus*) in California Waters: Cranial Differentiation of Coastal and Offshore Ecotypes. *Marine Mammal Science*. **27:4**, pp.769-792

- Pfenninger M. and Schwenk K.** (2007) Cryptic Animal Species Are Homogeneously Distributed Among Taxa and Biogeographical Regions. *BMC Evolutionary Biology*. 7, pp.121
- Photopoulou T., Best P., Hammond P. and Findlay K.** (2011) Movement Patterns of Coastal Bottlenose Dolphins in the Presence of a Fast-Flowing, Prevailing Current: Shore-Based Observations At Cape Vidal, South Africa. *African Journal of Marine Science*. 33:3, pp.393-401
- Pilleri G. and Gihl M.** (1972) Contribution to the Knowledge of the Cetaceans of Pakistan with Particular Reference to the Genera *Neomeris*, *Sousa*, *Delphinus* and *Tursiops* and Description of a New Chinese Porpoise (*Neomeris asiaeorientalis*). *Investigations on Cetacea*. 4, 107-162
- Pilot M., Dahlheim M.E. and Hoelzel A.R.** (2010) Social Cohesion Among Kin, Gene Flow Without Dispersal and the Evolution of Population Genetic Structure in the Killer Whale (*Orcinus orca*). *Journal of Evolutionary Biology*. 23:1, pp.20-31
- Pinela A.M., Aguilar A. and Borrell A.** (2008) Occurrence of Long-Beaked and Short-Beaked Forms of *Delphinus* spp. off NW Africa Appears to Reflect Differential Use of Habitat Rather Than Taxonomy. IWC Scientific Committee Document. SC/60/SM20.
- Pinela A.M., Borrell A. and Aguilar A.** (2011) Common Dolphin Morphotypes: Niche Segregation or Taxonomy? *Journal of Zoology*. 284:4, pp.239-247
- Poelstra J.W., Vijay N., Bossu C.M., Lantz H., Ryll B., Müller I., Baglione V., Unneberg P., Wikelski M., Grabherr M.G. and Wolf J.B.W.** (2014) The Genomic Landscape Underlying Phenotypic Integrity in the Face of Gene Flow in Crows. *Science*. 344:6190, pp.1410-1414
- Pomilla C., Collins T., Minton G., Findlay K., Leslie M.S., Ponnampalam L., Baldwin R. and Rosenbaum H.C.** (2010) Genetic Distinctiveness and Decline of a Small Population of Humpback Whales (*Megaptera novaeangliae*) in the Arabian Sea (Region X). IWC Scientific Committee Document SC/62/SH6
- Pomilla C., Amaral A.R., Collins T., Minton G., Findlay K., Leslie M.S., Ponnampalam L., Baldwin R. and Rosenbaum H.** (2014) The World's Most Isolated and Distinct Whale Population? Humpback Whales of the Arabian Sea. *Plos One*. 9:12, e114162
- Ponnampalam L.S.** (2009) Ecological Studies and Conservation of Small Cetaceans in the Sultanate of Oman, with Special Reference to Spinner Dolphins, *Stenella longirostris* (Gray, 1828). PhD thesis. University of London.
- Ponnampalam L.S., Collins T.J., Minton G., Schulz I., Gray H., Ormond R.F.G. and Baldwin R.M.** (2012) Stomach Contents of Small Cetaceans Stranded Along the Sea of Oman and Arabian Sea Coasts of the Sultanate of Oman. *Journal of the Marine Biological Association of the United Kingdom*. 92:8, pp.1699-1710

- Preen A.** (1991) Report on the Die-Off of Marine Mammals Associated with the Gulf War Oil Spill. Report Prepared for the National Commission for Wildlife Conservation and Development.
- Preen A.** (2004) Distribution, Abundance and Conservation Status of Dugongs and Dolphins in the Southern and Western Arabian Gulf. *Biological Conservation*. **118**, pp.205-218
- Prell W.L., Hutson W.H., Williams D.F., Bé A.W., Geitzenauer K. and Molfino B.** (1980) Surface Circulation of the Indian Ocean During the Last Glacial Maximum, Approximately 18,000 Yr Bp. *Quaternary Research*. **14:3**, pp.309-336
- Pritchard J.K., Stephens M. and Donnelly P.** (2000) Inference of Population Structure Using Multilocus Genotype Data. *Genetics*. **155:2**, pp.945-959
- Punt A.E. and Donovan G.P.** (2007) Developing Management Procedures that are Robust to Uncertainty: Lessons from the International Whaling Commission. *ICES Journal of Marine Science: Journal du Conseil*. **64:4**, pp.603-612.
- Pusineri C., Magnin V., Meynier L., Spitz J., Hassani S. and Ridoux V.** (2007) Food and Feeding Ecology of the Common Dolphin (*Delphinus delphis*) in the Oceanic North-east Atlantic and Comparison with Its Diet in Neritic Areas. *Marine Mammal Science*. **23:1**, pp.30-47
- Quartly G.D. and Srokosz M.A.** (2004) Eddies in the Southern Mozambique Channel. *Deep Sea Research Part II: Topical Studies in Oceanography*. **51:1**, pp.69-83
- Queller D.C. and Goodnight K.F.** (1989) Estimating Relatedness Using Genetic Markers. *Evolution*. **43:2**, pp.258-275
- Quérrouil S., Silva M.A., Freitas L., Prieto R., Magalhães S., Dinis A., Alves F., Matos J.A., Mendonça D., Hammond P.S. and Santos R.S.** (2007) High Gene Flow in Oceanic Bottlenose Dolphins (*Tursiops truncatus*) of the North Atlantic. *Conservation Genetics*. **8:6**, pp.1405-1419
- Querouil S., Freitas L., Cascao I., Alves F., Dinis A., Almeida J.R., Prieto R., Borrás S., Matos J.A., Mendonça D. and Santos R.S.** (2010) Molecular Insight Into the Population Structure of Common and Spotted Dolphins Inhabiting the Pelagic Waters of the Northeast Atlantic. *Marine Biology*. **157:11**, pp.2567-2580
- R Core Team** (2013) R: A Language and Environment for Statistical Computing. R Foundation for Statistical Computing, Vienna, Austria. <http://www.R-project.org>
- Rambaut A., Suchard M.A., Xie D. and Drummond A.J.** (2014) Tracer v1.6. Available from <http://beast.bio.ed.ac.uk/Tracer>
- Rasoloarison R.M., Goodman S.M. and Ganzhorn J.U.** (2000) Taxonomic Revision of Mouse Lemurs (*Microcebus*) in the Western Portions of Madagascar. *International Journal of Primatology*. **21:6**, pp.963-1019

- Ravaoarimanana I.B., Tiedemann R., Montagnon D. and Rumpler Y.** (2004) Molecular and Cytogenetic Evidence for Cryptic Speciation Within a Rare Endemic Malagasy Lemur, the Northern Sportive Lemur (*Lepilemur septentrionalis*). *Molecular Phylogenetics and Evolution*. **31:2**, pp.440-8
- Reeves R., Perrin W., Taylor B., Baker C. and Mesnick S.** (2004) Report of the Workshop on Shortcomings of Cetacean Taxonomy in Relation to Needs of Conservation and Management, April 30-May 2, 2004, La Jolla, California. US Department of Commerce, National Oceanic and Atmospheric Administration, National Marine Fisheries Service, Southwest Fisheries Science Center.
- Reid J.B., Evans P.G. and Northridge S.P.** (2003) Atlas of Cetacean Distribution in North-West European Waters. Joint Nature Conservation Committee.
- Reis-Filho J.S.** (2009) Next-Generation Sequencing. *Breast Cancer Research*. **11:Suppl 3**, pp.7
- Rice D.W.** (1998) Marine Mammals of the World: Systematics and Distribution. Society for Marine Mammalogy. Allen Press Inc.
- Ricklefs R.E., Schluter D.** (1993) Species Diversity in Ecological Communities: Historical and Geographical Perspectives.. University of Chicago Press.
- Rissler L.J. and Apodaca J.J.** (2007) Adding More Ecology Into Species Delimitation: Ecological Niche Models and Phylogeography Help Define Cryptic Species in the Black Salamander (*Aneides flavipunctatus*). *Systematic Biology*. **56:6**, pp.924-42
- Robinson B.W., Wilson D.S., Margosian A.S. and Lotito P.T.** (1993) Ecological and Morphological Differentiation of Pumpkinseed Sunfish in Lakes Without Bluegill Sunfish. *Evolutionary Ecology*. **7:5**, pp.451-464
- Robinson B.W. and Wilson D.S.** (1996) Genetic Variation and Phenotypic Plasticity in a Trophically Polymorphic Population of Pumpkinseed Sunfish (*Lepomis gibbosus*). *Evolutionary Ecology*. **10:6**, pp.631-652
- Rogers A.R. and Harpending H.** (1992) Population Growth Makes Waves in the Distribution of Pairwise Genetic Differences. *Molecular Biology and Evolution*. **9:3**, pp.552-569
- Rohlf F.J. and Marcus L.F.** (1993) A Revolution in Morphometrics. *Trends in Ecology and Evolution*. **8:4**, pp.129-132
- Rohlf F.J.J.** (2003) Bias and Error in Estimates of Mean Shape in Geometric Morphometrics. *Journal of Human Evolution*. **44:6**, pp.665-683
- Rohlf F.** (2005) TPSDIG, Version 2.04. Department of Ecology and Evolution, State University of New York, Stony Brook.
- Rohling E.J., Foster G.L., Grant K.M., Marino G., Roberts A.P., Tamisiea M.E. and Williams F.** (2014) Sea-Level and Deep-Sea-Temperature Variability Over the Past 5.3 Million Years. *Nature*. **508:7497**, pp.477-82

- Ronquist F.** (1996) DIVA Version 1.0. Computer Program for MacOS and Win 32. www.ebc.uu.se/systzoo/research/diva/diva.html.
- Ronquist F.** (1997) Dispersal-Vicariance Analysis: a New Approach to the Quantification of Historical Biogeography. *Systematic Biology*. **46:1**, pp.195-203
- Rooney A.P., Merritt D.B. and Derr J.N.** (1999) Microsatellite Diversity in Captive Bottlenose Dolphins (*Tursiops truncatus*). *Journal of Heredity*. **90:1**, pp.228-231
- Rosel P.E., Dizon A.E. and Heyning J.E.** (1994) Genetic Analysis of Sympatric Morphotypes of Common Dolphins (Genus *Delphinus*). *Marine Biology*. **119**, 159-167
- Rosel P.E., Hansen L. and Hohn A.A.** (2009) Restricted Dispersal in a Continuously Distributed Marine Species: Common Bottlenose Dolphins *Tursiops truncatus* in Coastal Waters of the Western North Atlantic. *Molecular Ecology*. **18:24**, pp.5030-5045
- Rosenbaum H.C., Collins T.J.Q., Minton G., Baldwin R., Glaberman S., Findlay K.P. and Best P.** (2002) Preliminary Analysis of mtDNA Variation Among Humpback Whales off the Coast of Oman and Their Relationships to Whales from Wintering Grounds in the Southwestern Indian Ocean. IWC Scientific Committee Document SC/54/H4.
- Rosenbaum H.C., Pomilla C., Leslie M., Best P.B., Collins T.J.Q., Engel M.H., Ersts P.J., Findlay K.P., Kotze P.J.H., Meyer M., Minton G., Barendse J., Van Waerebeek K., Razafindrakoto Y.** (2004) Mitochondrial DNA Diversity and Population Structure of Humpback Whales from Their Wintering Areas in the Indian and South Atlantic Oceans (Wintering Regions A, B, C, and X). IWC Scientific Committee Document SC/56/SH3.
- Rosenbaum H.C., Pomilla C.C., Leslie M.C., Mendez M.C., Best P.B., Collins T., Engel M.H., Ersts P.J., Findlay K.P., Bonatto S., Kotze P.G.H., Meyer M., Minton G., Barendse J., Thornton M., Razafindrakoto Y. and Ngouesso S.** (2006) Mitochondrial DNA Diversity and Population Structure of Humpback Whales from Their Wintering Areas (Breeding Stocks) in the Indian and South Atlantic Oceans (Wintering Regions A, B, C, and X). IWC Scientific Committee Document SC/A06/HW41.
- Rosenbaum H.C., Pomilla C., Mendez M., Leslie M.S., Best P.B., Findlay K.P., Minton G., Ersts P.J., Collins T., Engel M.H., Bonatto S.L., Kotze D.P.G.H., Meyer M., Barendse J., Thornton M., Razafindrakoto Y., Ngouesso S., Vely M. and Kiszka J.** (2009) Population Structure of Humpback Whales from Their Breeding Grounds in the South Atlantic and Indian Oceans. *Plos One*. **4:10**, e7318
- Ross G.J.** (1977) The Taxonomy of Bottlenosed Dolphins *Tursiops* Species in South African Waters, with Notes on Their Biology. *Annals of the Cape Provincial Museums, Natural History*. **11**, pp.259-327
- Ross G.J.** (1984) Smaller Cetaceans of the South East Coast of Southern Africa. *Annals of the Cape Provincial Museums, Natural History*. **15**, 173-410

- Ross G.J.B. and Cockcroft V.G.** (1990) Comments on Australian Bottlenose Dolphins and Taxonomic Stock of *Tursiops aduncus* (Ehrenberg 1832). *In*: Leatherwood S. and Reeves R.R. (Eds). *The Bottlenose Dolphin*. Academic Press Limited 24-48 Oval Road, London NW1 7DX. pp. 101-128
- Ross P.S.** (2000) Marine Mammals As Sentinels in Ecological Risk Assessment. *Human and Ecological Risk Assessment*. **6:1**, pp.29-46
- Ross K.G.** (2001) Molecular Ecology of Social Behaviour: Analyses of Breeding Systems and Genetic Structure. *Molecular Ecology*. **10:2**, pp.265-284
- Rosbach K.A. and Herzing D.L.** (1997) Underwater Observations of Benthic-Feeding Bottlenose Dolphins (*Tursiops truncatus*) Near Grand Bahama Island, Bahamas. *Marine Mammal Science*. **13:3**, pp.498-504
- Rumpler Y., Ravaoarimanana B., Hauwy M. and Warter S.P.** (2001) Cytogenetic Arguments in Favour of a Taxonomic Revision of *Lepilemur septentrionalis*. *Folia Primatologica*. **72:6**, pp.308--315
- Rundle H.D. and Nosil P.** (2005) Ecological Speciation. *Ecology Letters*. **8:3**, pp.336-352
- Russell R.J.** (1968) Revision of Pocket Gophers of the Genus *Pappogeomys*. University of Kansas Publications, Museum of Natural History. **16**, pp.581-776
- Saayman G. and Tayler C.** (1973) Social Organisation of Inshore Dolphins (*Tursiops aduncus* and *Sousa*) in the Indian Ocean. *Journal of Mammalogy*. **54:4**, pp.993-996
- Saayman G.S. and Tayler C.K.** (1979) The Socioecology of Humpback Dolphins (*Sousa* sp.). *In*: Winn H.E. and Olla B.L. (Eds). *Behaviour of Marine Animals*. pp.165-226
- Saetre R. and Da Silva A.J.** (1984) The Circulation of the Mozambique Channel. *Deep Sea Research Part A. Oceanographic Research Papers*. **31:5**, pp.485-508
- Salm R.V., Jensen R.A.C., Papastavrou V. and Oman** (1993) Marine Fauna of Oman: Cetaceans, Turtles, Seabirds, and Shallow Water Corals. Gland, Switzerland: IUCN in collaboration with the Sultanate of Oman.
- Sander N., Abel G.J., Bauer R. and Schmidt J.** (2014) Visualising Migration Flow Data with Circular Plot. Vienna Institute of Demography, Austrian Academy of Sciences.
- Sargeant B.L., Mann J., Berggren P. and Krützen M.** (2005). Specialization and Development of Beach Hunting, a Rare Foraging Behavior, by Wild Bottlenose Dolphins (*Tursiops* sp.). *Canadian Journal of Zoology*. **83:11**, pp.1400-1410.
- Särnblad A., Danbolt M., Dalén L., Amir O.A. and Berggren P.** (2011) Phylogenetic Placement and Population Structure of Indo-Pacific Bottlenose Dolphins (*Tursiops aduncus*) off Zanzibar, Tanzania, Based on mtDNA Sequences. *Marine Mammal Science*. **27:2**, pp.431-448

- Särnblad A., Dalén L., Kiszka J., Collins T., Amir O.A., Angerbjörn A., Berggren P.** (in review) Population Structure and Diversity of Indo-Pacific Bottlenose Dolphins (*Tursiops aduncus*) in the Western Indian Ocean.
- Savidge G., Lennon J. and Matthews A.J.** (1990) A Shore-Based Survey of Upwelling Along the Coast of Dhofar Region, Southern Oman. *Continental Shelf Research*. **10:3**, pp.259-275
- Savolainen V., Anstett M.C., Lexer C., Hutton I., Clarkson J.J., Norup M.V., Powell M.P., Springate D., Salamin N. and Baker W.J.** (2006) Sympatric Speciation in Palms on an Oceanic Island. *Nature*. **441:7090**, pp.210-213
- Schluter D.** (2001) Ecology and the Origin of Species. *Trends in Ecology and Evolution*. **16(7)**, pp.372-380
- Schott F.A. and McCreary Jr J.P.** (2001) The Monsoon Circulation of the Indian Ocean. *Progress in Oceanography*. **51:1**, pp.1-123
- Segura I., Rocha-Olivares A., Flores-Ramírez S. and Rojas-Bracho L.** (2006) Conservation Implications of the Genetic and Ecological Distinction of *Tursiops truncatus* Ecotypes in the Gulf of California. *Biological Conservation*. **133:3**, pp.336-346
- Segura-Garcia I.H.** (2011) Population Genetics of Species on the Genera *Tursiops* and *Delphinus* Within the Gulf of California and Along the Western Coast of Baja California. PhD thesis, Durham University. Available at Durham E-Theses Online: <http://etheses.dur.ac.uk/592/>.
- Sekiguchi K., Klages N. and Best P.** (1992) Comparative Analysis of the Diets of Smaller Odontocete Cetaceans Along the Coast of Southern Africa. *South African Journal of Marine Science*. **12:1**, pp.843-861
- Sellas A.B., Wells R.S. and Rosel P.E.** (2005) Mitochondrial and Nuclear DNA Analyses Reveal Fine Scale Geographic Structure in Bottlenose Dolphins (*Tursiops truncatus*) in the Gulf of Mexico. *Conservation Genetics*. **6:5**, pp.715-728
- Servedio M.R. and Kirkpatrick M.** (1997) The Effects of Gene Flow on Reinforcement. *Evolution*. **51:6**, pp.1764-1772
- Servedio M.R. and Noor M.A.** (2003) The Role of Reinforcement in Speciation: Theory and Data. *Annual Review of Ecology, Evolution, and Systematics*. **34**, pp.339-364
- Shackleton N.J.** (1987) Oxygen Isotopes, Ice Volume and Sea Level. *Quaternary Science Reviews*. **6:3**, pp.183-190
- Shane S.** (1980) Occurrence, Movements, and Distribution of Bottlenose Dolphin, *Tursiops truncatus*, in Southern Texas. *Fishery Bulletin*. **78:3**, pp.593-600
- Shaw P., Pierce G. and Boyle P.** (1999) Subtle Population Structuring Within a Highly Vagile Marine Invertebrate, the Veined Squid *Loligo forbesi*, Demonstrated with Microsatellite DNA Markers. *Molecular Ecology*. **8:3**, pp.407-417

- Sheppard C.R.C., Price A. and Roberts C.** (1992) Marine Ecology of the Arabian Region. Patterns and Processes in Extreme Tropical Climates. Academic Press, London.
- Shimodaira H.** (2002) An Approximately Unbiased Test of Phylogenetic Tree Selection. *Systematic Biology*. **51:3**, pp.492-508
- Shimodaira H.** (2004) Approximately Unbiased Tests of Regions Using Multistep-Multi-scale Bootstrap Resampling. *The Annals of Statistics*. **32:6**, pp.2616-2641
- Shinohara M., Domingo-Roura X. and Takenaka O.** (1997) Microsatellites in the Bottlenose Dolphin *Tursiops truncatus*. *Molecular Ecology*. **6:7**, pp.695-696
- Shirakihara M., Yoshida H. and Shirakihara K.** (2003) Indo-Pacific Bottlenose Dolphins *Tursiops aduncus* in Amakusa, Western Kyushu, Japan. *Fisheries Science*. **69:3**, pp.654-656
- Silva Jr J.M., Silva F.J. and Sazima I.** (2005) Two Presumed Interspecific Hybrids in the Genus *Stenella* (Delphinidae) in the Tropical West Atlantic. *Aquatic Mammals*. **31:4**, pp.468-472
- Simmonds M.P. and Isaac S.J.** (2007) The Impacts of Climate Change on Marine Mammals: Early Signs of Significant Problems. *Oryx*. **41:01**, pp.19-26
- Simmonds M.P. and Elliott W.J.** (2009) Climate Change and Cetaceans: Concerns and Recent Developments. *Journal of the Marine Biological Association of the United Kingdom*. **89:01**, pp.203-210
- Singh A.D., Jung S.J.A., Darling K., Ganeshram R., Ivanochko T. and Kroon D.** (2011) Productivity Collapses in the Arabian Sea During Glacial Cold Phases. *Paleoceanography*. **26:3**
- Singleton M.** (2002) Patterns of Cranial Shape Variation in the Papionini (Primates: Cercopithecinae). *Journal of Human Evolution*. **42:5**, pp.547-578
- Skulason S. and Smith T.B.** (1995) Resource Polymorphisms in Vertebrates. *Trends in Ecology and Evolution*. **10:9**, pp.366-370
- Slatkin M. and Excoffier L.** (1996) Maximization Algorithm. *Heredity*. **76**, pp.377-383
- Slice D.** (1998) MORPHEUS at al.: Software for Morphometric Research. Department of Ecology and Evolution, State University of New York, Stony Brook, New York.
- Smith B.D.** (1993) 1990 Status and Conservation of the Ganges River Dolphin *Platanista gangetica* in the Karnali River, Nepal. *Biological Conservation*. **66:3**, pp.159-169
- Smith B.D. and Reeves R.R.** (2012) River Cetaceans and Habitat Change: Generalist Resilience or Specialist Vulnerability? *Journal of Marine Biology*. **2012**, pp.1-11
- Sorenson M.D. and Franzosa E.A.** (2007) TREEROT, Version 3. Boston University, Boston.

- Stamatakis A.** (2014) RAXML Version 8: a Tool for Phylogenetic Analysis and Post-Analysis of Large Phylogenies. *Bioinformatics*. **30:9**, pp.1312-1313
- Steeman M.E., Hebsgaard M.B., Fordyce R.E., Ho S.Y.W., Rabosky D.L., Nielsen R., Rahbek C., Glenner H., S Martin V. and Willerslev E.** (2009) Radiation of Extant Cetaceans Driven by Restructuring of the Oceans. *Systematic Biology*. **58:6**, pp.573-585
- Stensland E., Berggren P., Johnstone R. and Jiddawi N.** (1998) Marine Mammals in Tanzanian Waters: Urgent Need for Status Assessment. *Ambio*. **27:8**, pp.771-774
- Stensland E., Carlen I., Sarnblad A., Bignert A. and Berggren P.** (2006) Population Size, Distribution, and Behavior of Indo-Pacific Bottlenose (*Tursiops aduncus*) and Humpback (*Sousa chinensis*) Dolphins off the South Coast of Zanzibar. *Marine Mammal Science*. **22:3**, pp.667-682
- Stephens M., Smith N.J. and Donnelly P.** (2001) A New Statistical Method for Haplotype Reconstruction from Population Data. *American Journal of Human Genetics*. **68:4**, pp.978-89
- Stephens M. and Donnelly P.** (2003) A Comparison of Bayesian Methods for Haplotype Reconstruction from Population Genotype Data. *American Journal of Human Genetics*. **73:5**, pp.1162-1169
- Stewart J.R., Lister A.M., Barnes I. and Dalén L.** (2010) Refugia Revisited: Individualistic Responses of Species in Space and Time. *Proceedings of the Royal Society of London. Series B, Biological Sciences*. **277:1682**, pp.661-71
- Stockin K.A. and Visser I.N.** (2005) Anomalously Pigmented Common Dolphins (*Delphinus* sp.) off Northern New Zealand. *Aquatic Mammals*. **31:1**, pp.43-51
- Stockin K.A., Amaral A.R., Latimer J., Lambert D.M. and Natoli A.** (2013) Population Genetic Structure and Taxonomy of the Common Dolphin (*Delphinus* sp.) at its Southernmost Range Limit: New Zealand Waters. *Marine Mammal Science*. **30:1**, pp.44-63
- Storz J.F. and Beaumont M.A.** (2002) Testing for Genetic Evidence of Population Expansion and Contraction: An Empirical Analysis of Microsatellite DNA Variation Using a Hierarchical Bayesian Model. *Evolution*. **56:1**, pp.154-166
- Sun X., Luo Y., Huang F., Tian J. and Wang P.** (2003) Deep-Sea Pollen from the South China Sea: Pleistocene Indicators of East Asian Monsoon. *Marine Geology*. **201:1-3**, pp.97-118
- Sundberg P.** (1989) Shape and Size Constrained Principal Components Analysis. *Systematic Zoology*. **38:2**, pp.166-168
- Suzuki R. and Shimodaira H.** (2006) PVCLUST: An R Package for Assessing the Uncertainty in Hierarchical Clustering. *Bioinformatics*. **22:12**, pp.1540-1542

- Swallow J.** (1984) Some Aspects of the Physical Oceanography of the Indian Ocean. *Deep Sea Research Part A. Oceanographic Research Papers*. **31:6**, pp.639-650
- Swofford D.L.L.** (2011) PAUP*: Phylogenetic Analysis Using Parsimony, Version 4.0B10.
- Tajima F.** (1989) Statistical Method for Testing the Neutral Mutation Hypothesis by DNA Polymorphism. *Genetics*. **123:3**, pp.585-95
- Tavares M., Moreno I.B., Siciliano S., Rodríguez D., De O. Santos M.C., Lailson-Brito Jr J. and Fabián M.E.** (2010) 'Biogeography of Common Dolphins (Genus *Delphinus*) in the Southwestern Atlantic Ocean', *Mammal Review*. **40:1**, pp.40-64
- Taylor B.L., Chivers S.J., Larese J. and Perrin W.F.** (2007) Generation Length and Percent Mature Estimates for IUCN Assessments of Cetaceans. Southwest Fisheries Science Center.
- Teacher A. and Griffiths D.** (2011) HAPSTAR: Automated Haplotype Network Layout and Visualization. *Molecular Ecology Resources*. **11:1**, pp.151-153
- Templeton A.R.** (2009) Statistical Hypothesis Testing in Intraspecific Phylogeography: Nested Clade Phylogeographical Analysis vs. Approximate Bayesian Computation. *Molecular Ecology*. **18:2**, pp.319-331
- Thiele K.** (1993) The Holy Grail of the Perfect Character: the Cladistic Treatment of Morphometric Data. *Cladistics*. **9**, pp.275-304
- Thoday J. and Boam T.** (1959) Effects of Disruptive Selection. II. Polymorphism and Divergence Without Isolation. *Heredity*. **13:2**, pp.205-218
- Thoday J. and Gibson J.** (1962) Isolation by Disruptive Selection. *Nature*. **193:4821**, pp.1164-1166
- Tieleman B. and Williams J.** (2002) Cutaneous and Respiratory Water Loss in Larks from Arid and Mesic Environments. *Physiological and Biochemical Zoology*. **75:6**, pp.590-599
- Tolley K.A., Read A.J., Wells R.S., Urian K.W., Scott M.D., Irvine A.B. and Hohn A.A.** (1995) Sexual Dimorphism in Wild Bottlenose Dolphins (*Tursiops truncatus*) from Sarasota, Florida. *Journal of Mammalogy*. **76:4**, pp.1190-1198
- Tolley K.A., Vikingsson G.A. and Rosel P.E.** (2001) Mitochondrial DNA Sequence Variation and Phylogeographic Patterns in Harbour Porpoises (*Phocoena phocoena*) from the North Atlantic. *Conservation Genetics*. **2:4**, pp.349-361
- Torres L.G., Rosel P.E., D'agrosa C. and Read A.J.** (2003) Improving Management of Overlapping Bottlenose Dolphin Ecotypes Through Spatial Analysis and Genetics. *Marine Mammal Science*. **19:3**, pp.502-514
- Torres L.G., Read A.J. and Halpin P.** (2008) Fine-Scale Habitat Modeling of a Top Marine Predator: Do Prey Data Improve Predictive Capacity. *Ecological Applications*. **18:7**, pp.1702-1717

- Torres L.G. and Read A.J.** (2009) Where to Catch a Fish? The Influence of Foraging Tactics on the Ecology of Bottlenose Dolphins (*Tursiops truncatus*) in Florida Bay, Florida. *Marine Mammal Science*. **25:4**, pp.797-815
- Tsai Y.J.J. and Mann J.** (2013). Dispersal, Philopatry, and the Role of Fission-Fusion Dynamics in Bottlenose Dolphins. *Marine Mammal Science*. **29:2**, pp.261-279.
- Tsao K.** (1978) Discovery of *Tursiops* Fossil from Sarchow, Kiangsu. *Vertebrata Palasiatica*. **16:4**, pp.264-266
- Untergasser A., Cutcutache I., Koressaar T., Ye J., Faircloth B., Remm M. and Rozen S.** (2012) Primer3-New Capabilities and Interfaces. *Nucleic Acids Research*. **40:15**, e115
- Valsecchi E. and Amos W.** (1996) Microsatellite Markers for the Study of Cetacean Populations. *Molecular Ecology*. **5**, pp.151-156
- van Bree P.** (1971) *Delphinus tropicalis*, a New Name for *Delphinus longirostris* G. Cuvier, 1829. *Mammalia*. **35:2**, pp.345-346
- Van Oosterhout C., Hutchinson W.F., Wills D.P.M. and Shipley P.** (2004) Micro-Checker: Software for Identifying and Correcting Genotyping Errors in Microsatellite Data. *Molecular Ecology Notes*. **4:3**, pp.535-538
- Van Waerebeek K., Reyes J.C., Read A.J. and Mckinnon J.S.** (1990) Preliminary Observations of Bottlenose Dolphins from the Pacific Coast of South America. *In: Leatherwood S. and Reeves R.R. (Eds). The Bottlenose Dolphin*. Academic Press Limited 24-48 Oval Road, London NW1 7DX. pp.143-154
- Van Waerebeek K.** (1993) Geographic Variation and Sexual Dimorphism in the Skull of the Dusky Dolphin, *Lagenorhynchus obscurus* (Gray, 1828). *Fishery Bulletin*. **91**, 754-774
- Van Waerebeek K., Gallagher M., Baldwin R., Papastavrou V. and Mustafa A.L.** (1999) Morphology and Distribution of the Spinner Dolphin, *Stenella longirostris*, Rough Toothed Dolphin, *Steno bredanensis* and Melon-Headed Whale, *Peponocephala electra* from Water off the Sultanate of Oman. *Journal of Cetacean Research and Management*. **1:2**, pp.167-177
- Vandergast A.G., Bohonak A.J., Weissman D.B. and Fisher R.N.** (2007) Understanding the Genetic Effects of Recent Habitat Fragmentation in the Context of Evolutionary History: Phylogeography and Landscape Genetics of a Southern California Endemic Jerusalem Cricket (Orthoptera: Stenopelmatidae: *Stenopelmatus*). *Molecular Ecology*. **16:5**, pp.977-92
- Venables W. and Ripley B.** (2002) 'Modern Applied Statistics with S-PLUS', Statistics and Computing. Springer Science & Business Media. pp.498
- Viarsdóttir U.S., O'Higgins P. and Stringer C.** (2002) A Geometric Morphometric Study Of Regional Differences in the Ontogeny of the Modern Human Facial Skeleton. *Journal Of Anatomy*. **201:3**, pp.211-229

- Viaud-Martinez K.A., Brownell R.L., Komnenou A. and Bohonak A.J.** (2008) Genetic Isolation and Morphological Divergence of Black Sea Bottlenose Dolphins. *Biological Conservation*. **141:6**, pp.1600-1611
- Vilstrup J.T., Ho S.Y., Foote A.D., Morin P.A., Krebs D., Krützen M., Parra G.J., Robertson K.M., De Stephanis R., Verborgh P., Willerslev E., Orlando L. and Gilbert M.T.P.** (2011) Mitogenomic Phylogenetic Analyses of the Delphinidae with An Emphasis on the Globicephalinae. *BMC Evolutionary Biology*. **11:65**, pp.10
- Viricel A., Strand A.E., Rosel P.E., Ridoux V. and Garcia P.** (2008). Insights on Common Dolphin (*Delphinus delphis*) Social Organization from Genetic Analysis of a Mass-Stranded Pod. *Behavioral Ecology and Sociobiology*. **63:2**, pp.173-185
- Vivekanandan E., Srinath M., Pillai V.N., Immanuel S. and Kurup K.N.** (2003) Marine Fisheries Along the Southwest Coast of India. Assessment, Management and Future Directions for Coastal Fisheries in Asian Countries. pp.757-792
- von Rad U. and Tahir M.** (1997) Late Quaternary Sedimentation on the Outer Indus Shelf and Slope (Pakistan): Evidence from High-Resolution Seismic Data and Coring. *Marine Geology*. **138:3**, pp.193-236
- Voris H.K.** (2000) Maps of Pleistocene Sea Levels in Southeast Asia: Shorelines, River Systems and Time Durations. *Journal of Biogeography*. **27:5**, pp.1153-1167
- Waddell V.G., Milinkovitch M.C., Bérubé M. and Stanhope M.J.** (2000) Molecular Phylogenetic Examination of the Delphinoidea Trichotomy: Congruent Evidence from Three Nuclear Loci Indicates That Porpoises (Phocoenidae) Share a More Recent Common Ancestry with White Whales (Monodontidae) Than They Do with True Dolphins (Delphinidae). *Molecular Phylogenetics and Evolution*. **15:2**, pp.314-318
- Walker W.A. and Southwest Fisheries Center (U.S.)** (1981) Geographical Variation in Morphology and Biology of Bottlenose Dolphins (*Tursiops*) in the Eastern North Pacific. National Oceanic and Atmospheric Administration, National Marine Fisheries Service, Southwest Fisheries Center.
- Wang L., Sarnthein M., Erlenkeuser H., Grimalt J., Grootes P., Heilig S., Ivanova E., Kienast M., Pelejero C. and Pflaumann U.** (1999a) East Asian Monsoon Climate During the Late Pleistocene: High-Resolution Sediment Records from the South China Sea. *Marine Geology*. **156:1**, pp.245-284
- Wang J.Y., Chou L.S. and White B.N.** (1999b) Mitochondrial DNA Analysis of Sympatric Morphotypes of Bottlenose Dolphins (Genus: *Tursiops*) in Chinese Waters. *Molecular Ecology*. **8:10**, pp.1603-1612
- Wang J.Y., Chou L.-S. and White B.N.** (2000) Osteological Differences Between Two Sympatric Forms of Bottlenose Dolphins (Genus *Tursiops*) in Chinese Waters. *Journal of Zoology*. **252:2**, pp.147-162

- Wang J.Y. and Yang S.C.** (2009) Indo-Pacific Bottlenose Dolphin *Tursiops aduncus*. In: Perrin W.F., Würsig B. and Thewissen, J.G.M. (Eds). *Encyclopedia of Marine Mammals*. pp.602-607
- Waples R.S., Punt A.E. and Cope J.M.** (2008) Integrating Genetic Data Into Management of Marine Resources: How Can We Do It Better? *Fish and Fisheries*. **9:4**, pp.423-449
- Webster M. and Sheets H.D.** (2010) A Practical Introduction to Landmark-Based Geometric Morphometrics. *Quantitative Methods in Paleobiology*. **16**, pp.168-188
- Weihls C., Ligges U., Luebke K. and Raabe N.** (2005) klaR Analyzing German Business Cycles. In: Baier D., Decker R. and Schmidt-Thieme L. (Eds). *Data Analysis and Decision Support*. Springer-Verlag, Berlin. pp.335-343
- Weir B.S. and Cockerham C.C.** (1984) Estimating F-Statistics for the Analysis of Population Structure. *Evolution*. **38:6**, pp.1358-1370
- Wells R. and Scott M.** (2009) Common Bottlenose Dolphin *Tursiops truncatus*. In: Perrin W.F., Würsig B. and Thewissen, J.G.M. (Eds). *Encyclopedia of Marine Mammals*. pp.249-255
- Wells R.S. and Scott M.D.** (1999) Bottlenose Dolphin *Tursiops truncatus* (Montagu, 1821), Handbook of Marine Mammals. **6**, pp.137-182
- Wells R.S., Rhinehart H.L., Cunningham P., Whaley J., Baran M., Koberna C. and Costa D.P.** (1999) Long Distance Offshore Movements of Bottlenose Dolphins. *Marine Mammal Science*. **15:4**, pp.1098-1114
- Wells R.S., Rhinehart H.L., Hansen L.J., Sweeney J.C., Townsend F.I., Stone R., Casper D.R., Scott M.D., Hohn A.A. and Rowles T.K.** (2004) Bottlenose Dolphins as Marine Ecosystem Sentinels: Developing a Health Monitoring System. *Ecohealth*. **1:3**, pp.246-254
- Wenzel F.W., Nicolas J.R., Larsen F. and Pace R.M.** (2010) Northeast Fisheries Science Center Cetacean Biopsy Training Manual. US Department of Commerce, National Oceanic and Atmospheric Administration, National Marine Fisheries Service, Northeast Fisheries Science Center. pp.20
- Westgate A.J.** (2007) Geographic Variation in Cranial Morphology of Short-Beaked Common Dolphins (*Delphinus delphis*) from the North Atlantic. *Journal of Mammalogy*. **88:3**, pp.678-688
- Whitmore F.** (1994) Neogene Climatic Change and the Emergence of the Modern Whale Fauna of the North Atlantic Ocean. In: Berta A. and Deméré T.A., Contributions in Marine Mammal Paleontology Honoring Frank C. Whitmore, Jr.. San Diego, California: San Diego Society of Natural History. pp.223-227
- Williams S.T. and Benzie J.A.H.** (1993) Genetic Consequences of Long Larval Life in the Starfish *Linckia laevigata* (Echinodermata: Asteroidea) on the Great Barrier Reef. *Marine Biology*. **117:1**, pp.71-77

- Williams S.T. and Benzie J.A.H.** (1998) Evidence of a Biogeographic Break Between Populations of a High Dispersal Starfish: Congruent Regions Within the Indo-West Pacific Defined by Color Morphs, mtDNA, and Allozyme Data. *Evolution*. **52:1**, pp.87-99
- Wilson B., Thompson P. and Hammond P.** (1997) Habitat Use by Bottlenose Dolphins: Seasonal Distribution and Stratified Movement Patterns in the Moray Firth, Scotland. *Journal of Applied Ecology*. **34**, pp.1365-1374
- Wilson G.A. and Rannala B.** (2003) Bayesian Inference of Recent Migration Rates Using Multilocus Genotypes. *Genetics*. **163:3**, pp.1177-1191
- Wright S.** (1943) Isolation by Distance. *Genetics*. **28:2**, pp.114-138
- Xie W., Lewis P.O., Fan Y., Kuo L. and Chen M.H.** (2011) Improving Marginal Likelihood Estimation for Bayesian Phylogenetic Model Selection. *Systematic Biology*. **60:2**, pp.150-60
- Xiong Y., Brandley M.C., Xu S.X., Zhou K.Y. and Yang G.** (2009) Seven New Dolphin Mitochondrial Genomes and a Time-Calibrated Phylogeny of Whales. *BMC Evolutionary Biology*. **9**, pp. 13
- Yan J., Zhou K. and Yang G.** (2005) Molecular Phylogenetics of 'River Dolphins' and the Baiji Mitochondrial Genome. *Molecular Phylogenetics and Evolution*. **37:3**, pp.743-750
- Yoder A.D., Rasoloarison R.M., Goodman S.M., Irwin J.A., Atsalis S., Ravosa M.J. and Ganzhorn J.U.** (2000) Remarkable Species Diversity in Malagasy Mouse Lemurs (Primates, *Microcebus*). *Proceedings of the National Academy of Sciences*. **97:21**, pp.11325-11330
- Young D.D. and Cockcroft V.** (1994) Diet of Common Dolphins (*Delphinus delphis*) off the South-East Coast of Southern Africa: Opportunism or Specialization? *Journal of Zoology*. **234:1**, pp.41-53
- Yu Y., Harris A.J. and He X.** (2010) S-DIVA (Statistical Dispersal-Vicariance Analysis): A Tool for Inferring Biogeographic Histories. *Molecular Phylogenetics and Evolution*. **56:2**, pp.848-50
- Zelditch M.L., Swiderski D.L. and Sheets H.D.** (2012) Geometric Morphometrics for Biologists: A Primer. Academic Press.
- Zerbini A.N. and Santos M.** (1997) First Record of the Pygmy Killer Whale *Feresa attenuata* (Gray, 1874) for the Brazilian Coast. *Aquatic Mammals*. **23**, pp.105-110
- Zerbini A.N., Waite J.M., Durban J.W., Leduc R., Dahlheim M.E. and Wade P.R.** (2007) Estimating Abundance of Killer Whales in the Nearshore Waters of the Gulf of Alaska and Aleutian Islands Using Line-Transsect Sampling. *Marine Biology*. **150:5**, pp.1033-1045